frontiers | Research Topics

Emerging zoonoses and transboundary infections

Edited by
Yashpal S. Malik, Lester J. Perez and Levon Abrahamyan

Published in
Frontiers in Veterinary Science

ISSN 1664-8714
ISBN 978-2-83251-669-0
DOI 10.3389/978-2-83251-669-0

About Frontiers

Frontiers is more than just an open access publisher of scholarly articles: it is a pioneering approach to the world of academia, radically improving the way scholarly research is managed. The grand vision of Frontiers is a world where all people have an equal opportunity to seek, share and generate knowledge. Frontiers provides immediate and permanent online open access to all its publications, but this alone is not enough to realize our grand goals.

Frontiers journal series

The Frontiers journal series is a multi-tier and interdisciplinary set of open-access, online journals, promising a paradigm shift from the current review, selection and dissemination processes in academic publishing. All Frontiers journals are driven by researchers for researchers; therefore, they constitute a service to the scholarly community. At the same time, the *Frontiers journal series* operates on a revolutionary invention, the tiered publishing system, initially addressing specific communities of scholars, and gradually climbing up to broader public understanding, thus serving the interests of the lay society, too.

Dedication to quality

Each Frontiers article is a landmark of the highest quality, thanks to genuinely collaborative interactions between authors and review editors, who include some of the world's best academicians. Research must be certified by peers before entering a stream of knowledge that may eventually reach the public - and shape society; therefore, Frontiers only applies the most rigorous and unbiased reviews. Frontiers revolutionizes research publishing by freely delivering the most outstanding research, evaluated with no bias from both the academic and social point of view. By applying the most advanced information technologies, Frontiers is catapulting scholarly publishing into a new generation.

What are Frontiers Research Topics?

Frontiers Research Topics are very popular trademarks of the *Frontiers journals series*: they are collections of at least ten articles, all centered on a particular subject. With their unique mix of varied contributions from Original Research to Review Articles, Frontiers Research Topics unify the most influential researchers, the latest key findings and historical advances in a hot research area.

Find out more on how to host your own Frontiers Research Topic or contribute to one as an author by contacting the Frontiers editorial office: frontiersin.org/about/contact

Emerging zoonoses and transboundary infections

Topic editors

Yashpal S. Malik — Indian Veterinary Research Institute (IVRI), India

Lester J. Perez — Abbott, United States

Levon Abrahamyan — Montreal University, Canada

Citation

Malik, Y. S., Perez, L. J., Abrahamyan, L., eds. (2023). *Emerging zoonoses and transboundary infections*. Lausanne: Frontiers Media SA.

doi: 10.3389/978-2-83251-669-0

Table of contents

06 ONE Health Approach to Address Zoonotic Brucellosis: A Spatiotemporal Associations Study Between Animals and Humans
Kun Zhou, Beibei Wu, Hang Pan, Narayan Paudyal, Jize Jiang, Le Zhang, Yan Li and Min Yue

16 Roles of MOV10 in Animal RNA Virus Infection
Feng Su, Xueming Liu and Yunliang Jiang

23 The "Bio-Crime Model" of Cross-Border Cooperation Among Veterinary Public Health, Justice, Law Enforcements, and Customs to Tackle the Illegal Animal Trade/Bio-Terrorism and to Prevent the Spread of Zoonotic Diseases Among Human Population
Paolo Zucca, Marie-Christin Rossmann, Jorge E. Osorio, Kevin Karem, Paola De Benedictis, Josef Haißl, Paola De Franceschi, Elisa Calligaris, Michaela Kohlweiß, Giulio Meddi, Wolfgang Gabrutsch, Horst Mairitsch, Oronzo Greco, Roberto Furlani, Marcello Maggio, Massimiliano Tolomei, Alessandro Bremini, Ingrid Fischinger, Paolo Zambotto, Peter Wagner, Yvonne Millard, Manlio Palei and Gianna Zamaro

36 Isolation and Identification of a Murine Norovirus Persistent Infection Strain in China
Zhao Na, Jiang Bo, Yang Yifei, Cao Fuyuan, He Bin, Zhang Yanshu, Jin Huan, Su Jingliang and Li Shuang

43 Small Mammals as Carriers/Hosts of *Leptospira spp*. in the Western Amazon Forest
Luciana dos Santos Medeiros, Susan Christina Braga Domingos, Maria Isabel Nogueira Di Azevedo, Rui Carlos Peruquetti, Narianne Ferreira de Albuquerque, Paulo Sérgio D'Andrea, André Luis de Moura Botelho, Charle Ferreira Crisóstomo, Anahi Souto Vieira, Gabriel Martins, Bernardo Rodrigues Teixeira, Filipe Anibal Carvalho-Costa and Walter Lilenbaum

52 The True Host/s of Picobirnaviruses
Souvik Ghosh and Yashpal S. Malik

61 Genomic Analysis of an Indian G8P[1] Caprine Rotavirus-A Strain Revealing Artiodactyl and DS-1-Like Human Multispecies Reassortment
Shubhankar Sircar, Yashpal Singh Malik, Prashant Kumar, Mohd Ikram Ansari, Sudipta Bhat, S. Shanmuganathan, Jobin Jose Kattoor, O.R. Vinodhkumar, Narayan Rishi, Nadia Touil, Souvik Ghosh, Krisztián Bányai and Kuldeep Dhama

72 Deltacoronavirus Evolution and Transmission: Current Scenario and Evolutionary Perspectives
Anastasia N. Vlasova, Scott P. Kenney, Kwonil Jung, Qiuhong Wang and Linda J. Saif

80 Identification of Dendritic Cell Maturation, TLR, and TREM1 Signaling Pathways in the *Brucella canis* Infected Canine Macrophage Cells, DH82, Through Transcriptomic Analysis
Woo Bin Park, Suji Kim, Soojin Shim and Han Sang Yoo

95 Serosurvey of Avian Influenza Viruses (H5, H7, and H9) and Associated Risk Factors in Backyard Poultry Flocks of Lahore District, Pakistan
Mamoona Chaudhry, Hamad Bin Rashid, Michael Thrusfield, Mark C. Eisler and Susan C. Welburn

104 Ecological and Socio-Economic Determinants of Livestock Animal Leptospirosis in the Russian Arctic
Olga I. Zakharova, Fedor I. Korennoy, Ivan V. Iashin, Nadezhda N. Toropova, Andrey E. Gogin, Denis V. Kolbasov, Galina V. Surkova, Svetlana M. Malkhazova and Andrei A. Blokhin

115 Aerosol Transmission of Coronavirus and Influenza Virus of Animal Origin
Jing Lv, Jing Gao, Bo Wu, Meiling Yao, Yudong Yang, Tongjie Chai and Ning Li

123 Whole Genome or Single Genes? A Phylodynamic and Bibliometric Analysis of PRRSV
Alba Frias-De-Diego, Manuel Jara, Brittany M. Pecoraro and Elisa Crisci

131 Reindeer Anthrax in the Russian Arctic, 2016: Climatic Determinants of the Outbreak and Vaccination Effectiveness
Elena A. Liskova, Irina Y. Egorova, Yuri O. Selyaninov, Irina V. Razheva, Nadezhda A. Gladkova, Nadezhda N. Toropova, Olga I. Zakharova, Olga A. Burova, Galina V. Surkova, Svetlana M. Malkhazova, Fedor I. Korennoy, Ivan V. Iashin and Andrei A. Blokhin

140 Deletion of the Transcriptional Regulator MucR in *Brucella* canis Affects Stress Responses and Bacterial Virulence
Jiali Sun, Hao Dong, Xiaowei Peng, Yufu Liu, Hui Jiang, Yu Feng, Qiaoling Li, Liangquan Zhu, Yuming Qin and Jiabo Ding

149 African Swine Fever in the Russian Far East (2019–2020): Spatio-Temporal Analysis and Implications for Wild Ungulates
Olga I. Zakharova, Ilya A. Titov, Andrey E. Gogin, Timofey A. Sevskikh, Fedor I. Korennoy, Denis V. Kolbasov, Levon Abrahamyan and Andrey A. Blokhin

162 A High-Throughput Method to Analyze the Interaction Proteins With p22 Protein of African Swine Fever Virus *In Vitro*
Xuejiao Zhu, Baochao Fan, Junming Zhou, Dandan Wang, Huiying Fan and Bin Li

173 Presence of Antibodies to SARS-CoV-2 in Domestic Cats in Istanbul, Turkey, Before and After COVID-19 Pandemic
Aysun Yilmaz, Abdullah Kayar, Nuri Turan, Onur Iskefli, Alper Bayrakal, Gleyder Roman-Sosa, Erman Or, Hasan Emre Tali, Bekir Kocazeybek, Ridvan Karaali, Dashzeveg Bold, Jean-Remy Sadeyen, Deimante Lukosaityte, Pengxiang Chang, Munir Iqbal, Juergen A. Richt and Huseyin Yilmaz

183 Evolution, Interspecies Transmission, and Zoonotic Significance of Animal Coronaviruses
Prapti Parkhe and Subhash Verma

212 Insight Into an Outbreak of Canine Distemper Virus Infection in Masked Palm Civets in China
Ning Shi, Le Zhang, Xiuhua Yu, Xiangyu Zhu, Shu Zhang, Daining Zhang and Ming Duan

218 Isolation and Phylogenetic Analysis of Reemerging Pseudorabies Virus Within Pig Populations in Central China During 2012 to 2019
Hui-Hua Zheng, Yi-Lin Bai, Tong Xu, Lan-Lan Zheng, Xin-Sheng Li, Hong-Ying Chen and Zhen-Ya Wang

226 Extension of Sylvatic Circulation of African Swine Fever Virus in Extralimital Warthogs in South Africa
Anthony F. Craig, Mathilde L. Schade-Weskott, Henry J. Harris, Livio Heath, Gideon J. P. Kriel, Lin-Mari de Klerk-Lorist, Louis van Schalkwyk, Peter Buss, Jessie D. Trujillo, Jan E. Crafford, Juergen A. Richt and Robert Swanepoel

237 Canine Leptospirosis Outbreak in Japan
Jun Saeki and Aki Tanaka

243 Experimental Susceptibility of North American Raccoons (*Procyon lotor*) and Striped Skunks (*Mephitis mephitis*) to SARS-CoV-2
Raquel Francisco, Sonia M. Hernandez, Daniel G. Mead, Kayla G. Adcock, Sydney C. Burke, Nicole M. Nemeth and Michael J. Yabsley

253 Climate Conditions During a Rift Valley Fever Post-epizootic Period in Free State, South Africa, 2014–2019
Assaf Anyamba, Richard Damoah, Alan Kemp, Jennifer L. Small, Melinda K. Rostal, Whitney Bagge, Claudia Cordel, Robert Brand, William B. Karesh and Janusz T. Paweska

266 High Occurrence Among Calves and Close Phylogenetic Relationships With Human Viruses Warrants Close Surveillance of Rotaviruses in Kuwaiti Dairy Farms
Mohammad A. Alotaibi, S. Al-Amad, Ali Chenari Bouket, H. Al-Aqeel, E. Haider, A. Bin Hijji, Lassaad Belbahri and Faizah N. Alenezi

274 Targeted sampling reduces the uncertainty in force of infection estimates from serological surveillance
Kiyeon Kim and Kimihito Ito

frontiers in Veterinary Science

SYSTEMATIC REVIEW
published: 02 September 2020
doi: 10.3389/fvets.2020.00521

ONE Health Approach to Address Zoonotic Brucellosis: A Spatiotemporal Associations Study Between Animals and Humans

Kun Zhou[1†], *Beibei Wu*[2†], *Hang Pan*[1†], *Narayan Paudyal*[3], *Jize Jiang*[4], *Le Zhang*[4], *Yan Li*[1,5*] *and Min Yue*[1,5*]

[1] Department of Veterinary Medicine & Institute of Veterinary Sciences, Zhejiang University College of Animal Sciences, Hangzhou, China, [2] Zhejiang Province Center for Disease Control and Prevention, Hangzhou, China, [3] Animal Health Research Division, Nepal Agricultural Research Council, Kathmandu, Nepal, [4] College of Computer Science, Sichuan University, Chengdu, China, [5] Zhejiang Provincial Laboratory of Preventive Veterinary Medicine, Hangzhou, China

OPEN ACCESS

Edited by:
Yashpal S. Malik,
Indian Veterinary Research Institute (IVRI), India

Reviewed by:
Vassilis Papatsiros,
University of Thessaly, Greece
Mohammed AbdelHameed AboElkhair,
University of Sadat City, Egypt

***Correspondence:**
Yan Li
yanli3@zju.edu.cn
Min Yue
myue@zju.edu.cn

[†]These authors have contributed equally to this work

Specialty section:
This article was submitted to Veterinary Infectious Diseases, a section of the journal Frontiers in Veterinary Science

Received: 18 May 2020
Accepted: 07 July 2020
Published: 02 September 2020

Citation:
Zhou K, Wu B, Pan H, Paudyal N, Jiang J, Zhang L, Li Y and Yue M (2020) ONE Health Approach to Address Zoonotic Brucellosis: A Spatiotemporal Associations Study Between Animals and Humans. Front. Vet. Sci. 7:521. doi: 10.3389/fvets.2020.00521

Background: Brucellosis is one of the most significant zoonosis over the world, threatening both veterinary and human public health. However, few studies were focused on nationwide animal brucellosis and made association with human brucellosis.

Methodology and Principal Findings: We conducted a bilingual literature search on *Brucella* or brucellosis in China on the two largest databases (China National Knowledge Infrastructure and PubMed) and conducted a systematic review. A total of 1,383 Chinese and 81 English publications, published between 1958 and 2018 were identified. From them, 357 publications presenting 692 datasets were subjected to the meta-analysis. The overall prevalence rate is 1.70% (95% CI: 1.66–1.74), with a declining (until the late 1990s) and rising trend (starting the early 2000s). Interestingly, the animal with highest prevalence rate is canine (8.35%, 95% CI: 7.21–9.50), and lowest in cattle (1.22%, 95% CI: 1.17–1.28). The prevalence of *Brucella* in animals was unequally distributed among the 24 examined regions in China.

Conclusions: Brucellosis is a reemerging disease for both humans and animals in China. The observed data suggests that dogs and yaks are the leading reservoirs for *Brucella*, and the provinces with highest prevalence rates in animals are Hubei, Sichuan, Inner Mongolia, Fujian, and Guizhou. Accordingly targeted intervention policy should be implemented to break the *Brucella* transmission chain between animals and humans in China.

Keywords: *Brucella*, brucellosis, China, spatial, temporal

INTRODUCTION

Zoonotic diseases are capable of infecting humans from animals by direct contact, or via food, water and environment, representing a significant public health problem. Brucellosis, caused by multiple species of the genera *Brucella*, is a textbook example of zoonotic disease prevalent all over the world. Brucellosis, recognized as the leading neglected zoonotic diseases by World Health Organization (WHO), remains a major epidemic, particularly in low- and

middle-income countries, including China (1–4). During the past decades, it was observed a significant increase in human brucellosis in China (5, 6). Given a broad range of animal reservoirs, and humans serving as an accidental host, the exact relationship between human brucellosis and its animal reservoirs remains elusive. This is one of the most pressing knowledge gaps to understand the dynamics of zoonotic *Brucella* in China.

The *Brucella* pathogens infect and invade the host via the mucous membranes, gastrointestinal tract, respiratory tract or abraded skin. In China, human infections are more often related to the occupation and consumption of foods of animal origin (7). Veterinary personnel, animal-farmers, and slaughterhouse workers are at the highest risk, usually acquiring infections through the mucous or abraded skin (8, 9). Respiratory tract infections are common in people inhaling contaminated airborne droplets or dust, for example, those working in the fur processing environment (10). People with no exposure to farm animals or animal-products are usually infected by contaminated food or water via gastrointestinal tract infections (11). The disease burden of human brucellosis infections is dynamic with respect to the endemic areas and time. Despite this dynamism, the only static component in the transmission chain is that the human incidences of brucellosis are always linked to certain animal reservoirs. Here, for the first time, we can address these key questions by using a "One Health" approach in an interconnected manner (6).

Farm animals, companion animals, and wild animals are well-known reservoirs for human *Brucella* infections (10). Farm animal brucellosis, with a wide range of clinical signs, is dependent on the infected animal hosts, age, sex, routes of exposure and organs involved (12). The hallmarks of infection include spontaneous abortion, undulant fever, and sometimes mastitis. Generally, animal brucellosis is sub-clinical but causes significant economic losses in the livestock industry. In companion animals, most of the infection cases are usually asymptomatic or mild (13). Therefore, farm and companion animal brucellosis are usually underappreciated due to their obscure syndrome and clinical presentations. Nevertheless, a systematic understanding the burden of animal brucellosis is largely lacking in China.

TABLE 1 | Inclusion/exclusion criteria for publication screening.

Inclusion criteria	Exclusion criteria
• Case report on brucellosis	• Literature review
• Epidemiological investigation of brucellosis	• Publication with no positive sample
• Study on biotype of *Brucella* strains	• Number of samples is uncertain
	• No Chinese strains or cases
	• Article with repeated data
	• Study not related to *Brucella* or brucellosis
	• Full text not available
	• Sample type and province are not available

In this study, we conducted a systematic review and meta-analysis of the spatiotemporal epidemiological feature of brucellosis in animals and humans from a nationwide One Health approach. A comprehensive review of animal brucellosis in China, with an integrated evidence-based result analysis of human brucellosis to address the parameters for potential transboundary infections, was also undertaken.

MATERIALS AND METHODS

Search Strategy

This review and systematic analysis included studies published in Chinese or English languages, between 1958 and 2018. The Chinese Publications were retrieved from China National Knowledge Infrastructure, CNKI (https://www.cnki.net/) and English papers were from PubMed with the same search string composed using keywords "*Brucella* or Brucellosis" and "China."

Selection Criteria

Publications were firstly screened based on their title and abstract followed by inclusion or exclusion criteria formulated by the authors (**Table 1**).

Data Extraction

Selected publications were perused for data extraction. Information on the title, author, journal, publication year, province, host (sheep and goat were grouped into one category because they were referred to as one single entity in Chinese literature), sampling year, type of samples, number of total samples, number of positive samples and number of *Brucella* strains and species wherever available, were determined. That information was extracted and arranged in an MS Excel spreadsheet formatted especially for this purpose.

Descriptive Analysis

Descriptive analysis was undertaken to calculate an approximately accurate epidemiologic picture of the disease and its causative agent. We analyzed the spatiotemporal relationship between human and animal brucellosis, where possible. We identified dominant species of *Brucella* in humans and some common animals including cattle, dog, pig, sheep & goat, and pointed out potentially high-risk infectious sources toward the human.

Meta-Analysis

A second step quality control screening of each record used for the descriptive analysis was applied using the exclusion criteria (**Table 2**). This was used to revise the data necessary for a meta-analysis of the prevalence of animal brucellosis.

TABLE 2 | Exclusion criteria for the second round of record screening.

1. No specific host or host mentioned is human
2. No specific sample types mentioned
3. Total number of samples is less than 100
4. No specific province reported in the study
5. No reporting of any specific sampling year

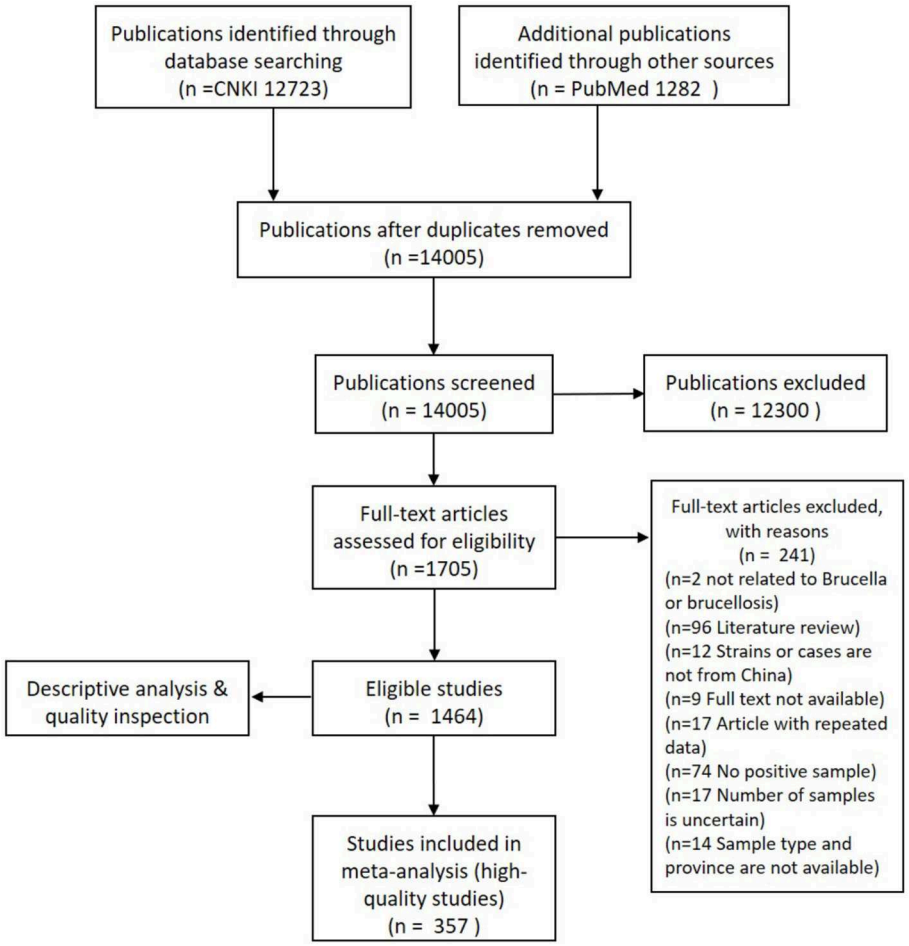

FIGURE 1 | A flow chart of literature research and data extraction.

The data extracted from hence selected publications were meta-analyzed in a binary random-effects model by DerSimonian-Laird method at 95% confidence level using OpenMeta-analysis, as described previously (14). The meta-analysis was performed according to the Preferred Reporting Items for Systematic Reviews and Meta-Analyses (PRISMA) guidelines to ensure the quality of the writing and presentation of this review (15). Three subgroup meta-analysis on the host, sampling year, and province were conducted simultaneously. The results obtained as the forest plots were projected with GraphPad Prism 7.

RESULTS

Literature Search and Data Extraction

A total of 1,464 bilingual publications, which included 1,383 in Chinese and 81 in English, were used for the descriptive analysis after a full-text screening of primary eligible studies. Only 357 publications, 350 in Chinese, and 7 in English, among the total of 692 eligible records, were deemed suitable for meta-analysis. A flow chart of literature research and data extraction is shown (**Figure 1**).

Descriptive Analysis

All provinces or municipality cities in China except Macao had reported positively for the prevalence of brucellosis. In mainland China, the largest number of records were from Inner Mongolia ($n = 431$), while there were only a few records from Tianjin ($n = 11$). Rose-Bengal Plate Agglutination Test (RBPT), Standard Tube Agglutination Test (SAT), Polymerase Chain Reaction (PCR), and Enzyme-Linked Immunosorbent Assay (ELISA) were the most common assays used for the detection of positive samples which were mostly blood. A total of 70,035,273 samples were tested in all these eligible studies, while 2,339,773 samples turned out to be positive, considered as the confirmed brucellosis cases or separated strains in these studies. There were more records on *Brucella* and brucellosis in northern China than in southern China. The number of samples tested in northern China was also much higher. The details are shown in **Table 3**

TABLE 3 | Characteristics of records from eligible studies.

	Total		Northern China*		Southern China#	
	Human	Animal	Human	Animal	Human	Animal
Number of records (%)	1,904	1,382	1,386 (73%)	939 (68%)	480 (25%)	409 (30%)
Number of total samples (%)	10,283,133	59,741,718	8,522,768 (83%)	55,531,284 (93%)	1,360,477 (13%)	2,668,094 (4%)
Number of positive samples (%)	1,037,606	1,293,024	919,372 (89%)	1,202,177 (93%)	24,156 (2%)	78,523 (6%)

*Northern China: Includes provinces such as Heilongjiang, Jilin, Liaoning, Inner Mongolia, Gansu, Xinjiang, Qinghai, Ningxia, Shanxi, Shaanxi, Hebei, Beijing, Tianjin, Shandong, Henan. #Southern China: Includes provinces such as Shanghai, Jiangsu, Anhui, Hubei, Chongqing, Sichuan, Yunnan, Guizhou, Hunan, Jiangxi, Zhejiang, Fujiang, Taiwan, Guangzhou, Hong Kong, Guangxi, Hainan, Tibet.

below (Some data are not counted into the table because they are lacking information either on host or on sampling places).

We also calculated the number of specific *Brucella* species mentioned in all these studies in human, sheep & goat, cattle, yak, dog and pig. Only five species, *B. melitensis, B. canis, B. abortus, B. suis,* and *B. ovis* were detected (**Figure 2**). Humans are most likely to be infected by all the four *Brucella* species from all kinds of animal host albeit in varying proportions. The proportion of presence of these pathogens in humans and sheep & goat are highly similar, illustrating that sheep & goat may be the likely source of infection for human brucellosis. *Brucella* serovars infecting yak, dog and pig are apparently highly species-specific, for example, *B. abortus* for yak, *B. canis* for dog, and *B. suis* for pig.

The average prevalence rates of all the records were calculated and the results are illustrated as the temporal (**Figure 3**) and spatial (**Figure 4**) prevalence rates in humans and animals in China. Prevalence rates of human and animal brucellosis both have a decreasing trend, until the late 1990s, followed by an increasing trend, starting the early 2000s. Interestingly, prevalence of brucellosis in animals was higher than that of humans before the year 1995, while after 1995 the prevalence of brucellosis in humans becomes higher.

Provinces in southern China had a higher prevalence rate before 1990, and currently, central Chinese provinces make the lead. There is always a higher rate of prevalence in the animals than in humans in most littoral areas, while things are on the contrary in the inwards areas. Regarding the geographic distribution, except in two municipal cities of Shanghai and Tianjin where only human cases were recorded, all other provinces had recorded an almost simultaneous increase or decrease in the prevalence in human and animal subjects. The analysis also reveals that the prevalence in hosts was high before 1990, then it started a downhill trend from 1991 to 2000, but again climbing up with a gradual increase after the 2000s at multiple geographical regions in mainland China. This spatiotemporal dynamism for human and animal brucellosis in China from 1951 to 2018 has been clearly shown (**Supplemental Figure 1**).

Prevalence of Brucellosis in Animals and Humans

A total of 357 publications screened twice (using the criteria as given in **Table 2**) were put into a meta-analysis, followed by a subgroup analysis on three variables including sampling year, geographical regions and host was also undertaken. Subgroups with less than five records were also put into meta-analysis but were not showed in the results below.

The overall prevalence rate among all animals in China from 1951 to 2018 was estimated to be 1.70% (95% CI: 1.66–1.74) (**Figure 5A**). As a factor of time, the largest number of records were for years between 2011 and 2015 ($n = 170$), whereas the smallest was for 1961–1965 ($n = 6$). There was an insufficient number of records (less than five) for the years 1951–1955, 1956–1960, 1966–1970, and 1971–1975 so these time frames were not shown. The result of subgroup analysis on the sampling year showed declining followed by a rising trend. Period with the lowest prevalence rate, irrespective of the host was 0.24% during 1996–2000 (63 records, 95% CI: 0.20–0.27), while the one with the highest prevalence was 12.44% during 1961–1965 (6 records, 95% CI: 7.70–17.19). In recent years, 2016–2018 the prevalence rate was 2.91% (29 records, 95% CI: 2.57–3.26), ∼10 times higher than the lowest one.

There were only 24 provinces/autonomous regions which had no less than five qualified datasets for meta-analysis (**Figure 5B**). Five provinces/autonomous with the highest rate were Hubei (5 records, 7.69%, 95% CI: 5.51–9.87), Sichuan (20 records, 6.86%, 95% CI: 5.68–8.04), Inner Mongolia (50 records, 4.44%, 95% CI: 4.04–4.85), Fujian (20 records, 4.25%, 95% CI: 3.58–4.92), and Guizhou (18 records, 3.89%, 95% CI: 3.18–4.59). In contrast, five lowest rates were for Jilin (16 records, 0.39%, 95% CI: 0.29–0.48), Gansu (55 records, 0.70%, 95% CI: 0.60–0.79), Jiangsu (15 records, 0.77%, 95% CI: 0.49–1.05), Shandong (37 records, 1.13%, 95% CI: 0.95–1.31), and Qinghai (112 records, 1.40%, 95% CI: 1.29–1.52).

Among the five different types of host groups analyzed (**Figure 5C**), dog possessed the highest prevalence rate (52 records, 8.35%, 95% CI: 7.21–9.50), followed by yak with 43 records and 8.22% prevalence rate (95% CI: 7.23–9.20), while cattle (228 records, 1.22%, 95% CI: 1.17–1.28), sheep & goat (277 records, 1.61%, 95% CI: 1.54–1.67), and lastly the pigs (63 records, 2.35%, 95% CI: 2.16–2.54). This preferably indicates that dogs and yaks could be the emerging host that possess some significant threat to *Brucella* transmission in China. The detailed results of subgroup analysis are shown as forest plots in **Figures 5A–C**.

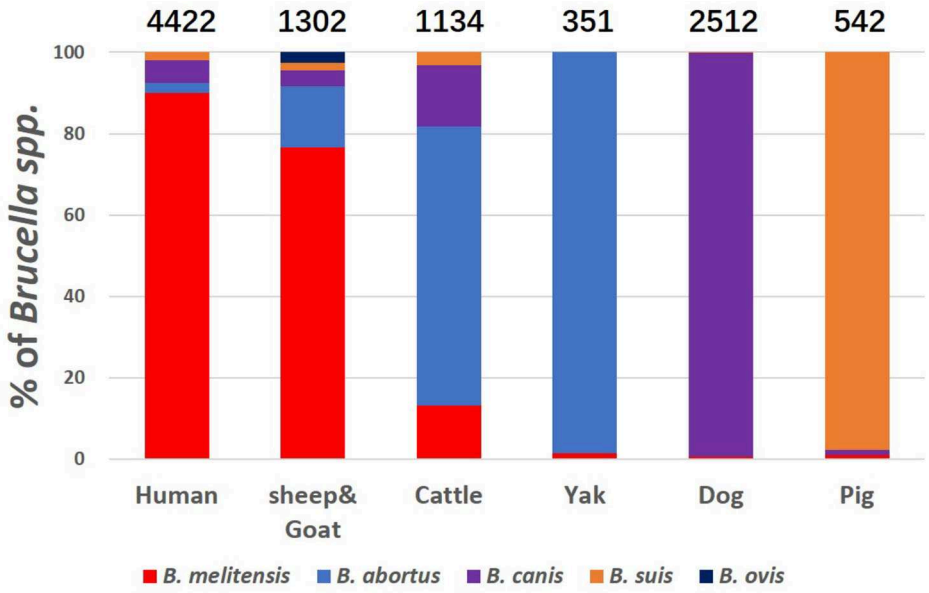

FIGURE 2 | Prevalence of various species of *Brucella* on different hosts. Height of the column in different color shows the proportion of *Brucella* species. Hosts are specified as human, sheep & goat, cattle, yak, dog, and pig at the base of each bar. Number above the bars indicates the number of positive samples.

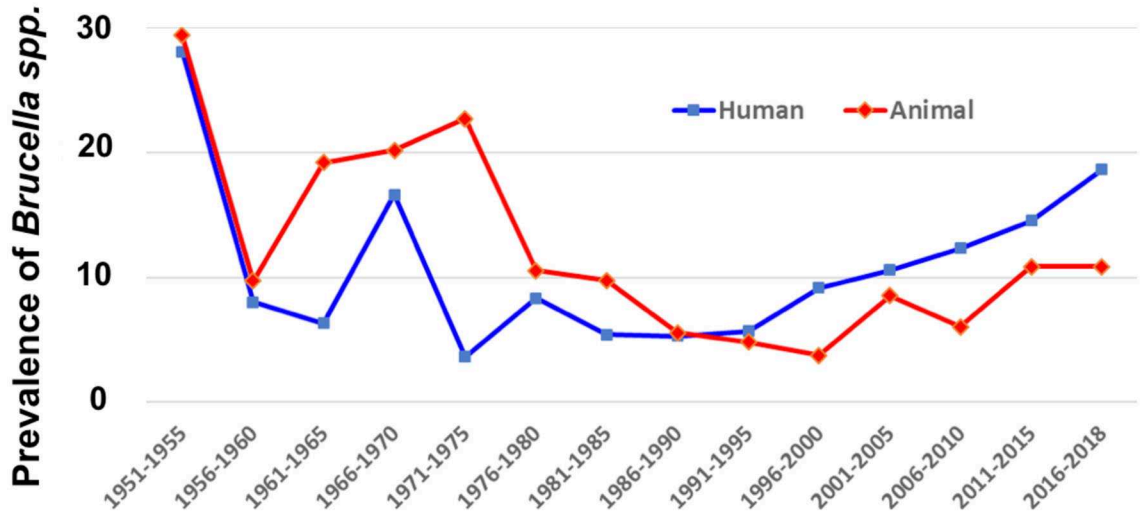

FIGURE 3 | Temporal distribution of human and animal brucellosis in China between 1951 and 2018.

DISCUSSION

Brucellosis is one of the most common zoonotic diseases worldwide, with a bioweapon potential, posing a significant public health concern (16). It not only causes considerable damages to public health but also significantly impairs veterinary public health and animal welfare. For example, reduced milk yield and contaminated dairy products due to animal brucellosis in America alone worth ∼400 million US dollars (17), and the annual economic losses of brucellosis in two counties in Jilin province, China was more than 2.3 million US dollars (18). Brucellosis had been well-controlled last century in China by a nationwide program for brucellosis control, as well as by a national campaign for preventing and controlling brucellosis (19). In China, it had been well-controlled by a national campaign for preventing and controlling brucellosis in the last century. However, the disease has reemerged during the last two decades (20). In certain regions of China, the number of cases of brucellosis reported is higher than that in the 1990s (21). Recently, a study on the epidemiology of human brucellosis was carried out with official data (6). Moreover, Ran and his group applied a meta-analysis on seroprevalence in dairy cows in China

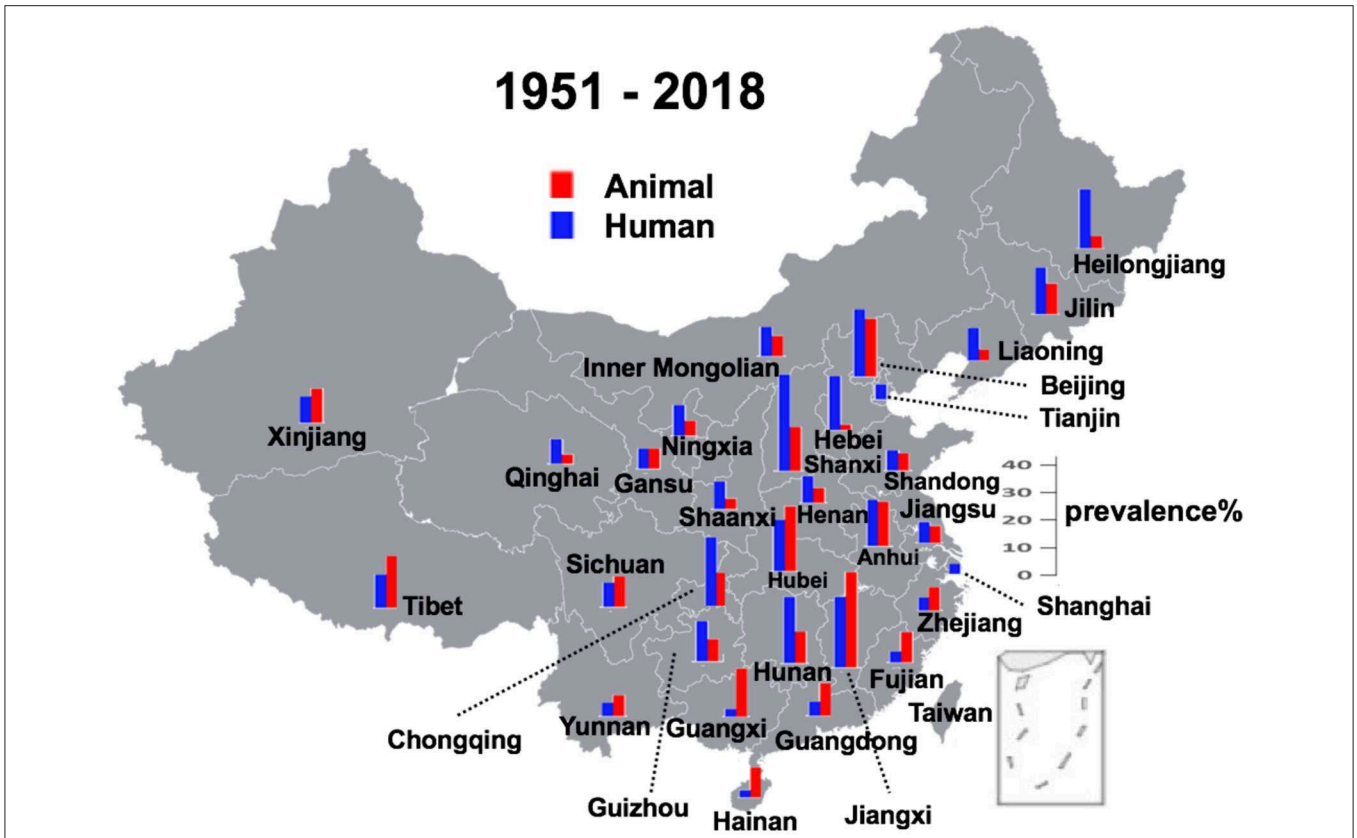

FIGURE 4 | Geographical distribution of brucellosis in animal reservoirs and humans. In two municipal cities Shanghai and Tianjin, only human cases were observed.

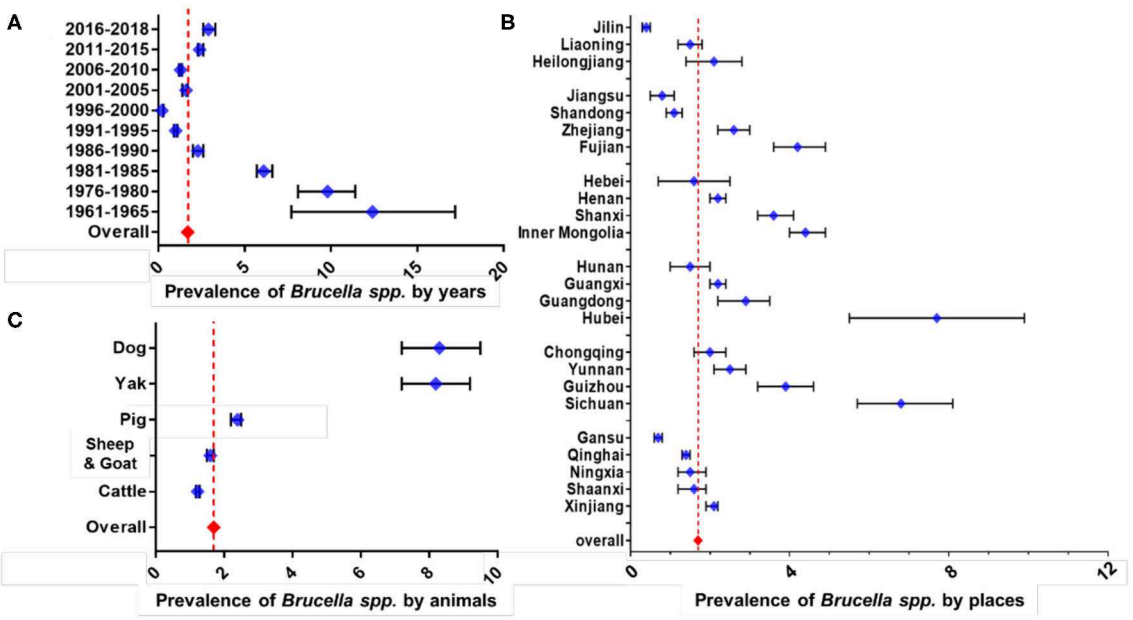

FIGURE 5 | Results of subgroup meta-analysis for different animal-related factors. Subgroup analysis on sampling year **(A)**, subgroup analysis on the province **(B)**, and subgroup analysis on the host **(C)**. The broken vertical line indicates the pooled summary estimate of prevalence for the selected variable.

(22). Despite these interesting and novel studies, information on the dominant biotype of *Brucella* in multiple kinds of hosts and prevalence within other animals is ambiguous. To a general extension, our unique One Health approach, combined with evidence-based meta-analysis, could be readily scaled to other zoonotic agents with significant public health importance.

In China, brucellosis was first recorded as Malta fever in two foreigners in Shanghai in 1905 (6). Until the 1990s, there was a high incidence of animal brucellosis, with relatively few human incidence (**Supplemental Figure 1**). Then after the 1990s, it started an uphill climb in most of the regions of mainland China. Brucellosis, previously thought to be frequently detected in northern China, is now increasingly seen in highly cosmopolitan parts of southern China (23). Our findings are in line with an earlier study which, using the notifiable reporting data for 1955–2014 based on the magnitude and distribution of human brucellosis in mainland China, had emphasized its recent re-emergence (6). Similar to the findings of our analysis, a previous study focusing only on the human incidence of brucellosis, showed some distinct temporal patterns, such as high incidence during 1955–1978, low incidence during 1979–1994, and dramatic accumulation incidences from 1995 onwards is consistent with the trend in *Brucella* seroprevalence from animal and human sero-surveys conducted in China during 1950–2014 (6). In general, where human prevalence of brucellosis is higher than prevalence of brucellosis in animals are mainly in southern China, including Hainan, Guangxi, Guangdong, Fujian, Jiangxi, Zhejiang, and Hubei (**Figure 4**). This might be because (1) a lack of animal surveillance capabilities in southern regions as a result of small population of large livestock; (2) the imported animal food contaminated with *Brucella* are responsible for the infections, which further support the multiple routes for disease transmission (24–28). These reasons might be lead to extreme cases in particular years and places where there is only human brucellosis without an indication of animal brucellosis (**Supplemental Figure 1**).

In China, 90% of brucellosis occurs in six northern agricultural provinces including Inner Mongolia, Shanxi, Heilongjiang, Hebei, Jilin, and Shaanxi. The Inner Mongolia Autonomous Region has the highest incidence rate of human and animal brucellosis throughout China (29). Human cases have been observed in those regions where animal farming is prevalent, particularly in areas with many poor rural farms and pastures in northwest China (30). However, it is suggested that there is a change in the epidemiology of brucellosis in China (23). Recent publications show that the areas of brucellosis endemicity gradually shifted from pasturing areas, i.e., Inner Mongolia, Xinjiang, Tibet, Qinghai, and Ningxia, to grassland and agricultural areas, i.e., Shanxi, Liaoning, Hebei, Shandong, and Jilin provinces, and the southern provinces became increasingly affected (6). Some analyses further revealed that patients from Guangdong province were more likely to have consumption of apparently exotic foods such as goat placenta (23), thereby manifesting as increased incidence of brucellosis. Although incidence appeared to increase in every province, Tibet seems to follow an inverse pattern and reported a few cases during the past 10 years (6). These hint on the probable movement of infected animals or contaminated food from northern to southern China and thus may explain the current change in the epidemiology of brucellosis in China (23).

Sheep and goats are the major herbivores in northwest China, and they are primarily kept by poor rural farmers in pastoral areas. In general, a considerable number of sheep and yaks are raised on the same grazing land on the Tibetan plateau, and these animals are considered to be the main hosts of *Brucella* (30). Brucellosis was recognized in Tibet in the 1980s as a disease of both livestock and humans. Some study indicates that bovine brucellosis is endemic among the yak population in the plateau region of China (31).

In the last 12 years, brucellosis has re-emerged in most regions of China, showing an annual accumulation in animal and human infections during this period (29). This is also evident in our meta-analysis which shows a general increasing trend in the prevalence, particularly for the recent past years. With regard to the geographic distribution, our investigation confirmed that sero-prevalence in eastern regions was higher than the central and western regions. This conclusion is also supported by the localized and dense clusters of small ruminants in those regions.

Our analysis has shown that most of the human cases of brucellosis were caused by *B. melitensis*. It is well-known that *B. melitensis* is a dominant epidemic strain in animal and *B. abortus* and *B. suis* can also infect sheep; *B. suis* biovar 3, especially emerged in Inner Mongolia (32). *B. melitensis* genotype ST8 was not only the predominant genotype in sheep but also responsible for human brucellosis (33). The results of seroprevalence assays have confirmed that *Brucella* spp. was mainly epidemic in sheep and dairy cows, whereas other animals had a very low incidence. These results also showed a strong host preference for certain *Brucella* species. Furthermore, this also indicates that small ruminants or cattle are the primary risk factors for human contagion. Human brucellosis in northwest China is closely related to infectious sheep. From an epidemiological perspective, the major causes of brucellosis in animals in China have been sheep infected by *B. melitensis* (34). Sheep and dairy cows with *Brucella* had higher infection trends, although the positive rates in dairy cows dipped to a downward trend between 2013 and 2014. Compared with this, in sheep and dairy cows, brucellosis in yellow cattle and dogs maintained sporadic onset, and no cases were found in swine (34).

A notable feature in our analysis is the presence of *B. canis* in all other hosts except for pig and yak. Human brucellosis caused by *B. suis* and *B. canis* in Guangxi, China (35) have also been reported earlier. An earlier study reports that *B. canis* is a rare source of human brucellosis in China (36), where *B. melitensis* has been the major pathogen associated with human brucellosis outbreaks. *B. canis* infection was first reported in China in 1983 (13), but now our data indicates that this has become the leading reservoir for emerging brucellosis. This scenario will be even more challenging, considering a significantly growing population in canine market. In a less frequent situation, *B. suis* can also be directly or indirectly transferred from swine to sheep, which could act as reservoirs for *B. suis* infection and later transmitted to humans (37). Therefore, an enhanced surveillance

system for companion animals in the densely populated cities is urgently needed.

Our data and subsequent analysis have thus revealed that brucellosis was a major concern for study and research in Northern China as compared to Southern China over time, for around three-quarters publications on brucellosis were carried out in North China. However, the meta-analysis showed that some areas in Southern China had even higher prevalence rates than northern ones, suggesting that brucellosis in the south is as severe as the north. It can be inferred from these analyses that human is likely to get infected with *Brucella* from all available transmission pathways, and various kinds of animals, among which the sheep and goat are possibly the highest risks because the formation of *Brucella* species in sheep and goat is similar with that of human. More alarmingly, canine brucellosis could be a top public health concern imposing a greater threat to human because pet dogs are playing a more and more important role in the current days of Chinese life. According to statistics, there have been over 740 million domestic dogs in China in 2019 (38), relationships between pet dogs and human are getting more and more close, which emphasizes that canine brucellosis is a pressing concern. An earlier study had shown that Chinese isolates of *B. suis* strains had unique genetic lineages at the global level whereas the isolates of *B. canis* were closely homologous to strains from Korea (35). Despite this disease being the most widespread zoonosis globally, it is also true that it remains severely neglected as a potential cause for chronic, debilitating maladies for multiple reasons such as its non-descript clinical presentation in human populations and its varying degree of clinical presentations (11).

Despite our updated largest analysis, there are some limitations to our analysis. Firstly, we only used two databases for bilingual publication research, so we might have missed some literatures. Second, most publications chose RBPT and SAT to detect positive blood samples, which have lower specificity and sensitivity than other recommended methods such as ELISA. Only 24 provinces in China had sufficient qualified data and thus were eligible for meta-analysis, leaving a quite large leak of animal brucellosis in remaining regions in China. Despite these, owing to a large number in the examined dataset, we believe that our meta-analysis is able to unravel a general situation and trend of animal brucellosis in China over time, thus attracting more attention to prevention and control of brucellosis in China.

CONCLUSION

Brucellosis is an important zoonosis in China, which was controlled well in the late twentieth century but re-emerged in the past two decades. Human may get infected from various domesticated animals, and most possibly sheep and goat. Canine brucellosis deserves more attention for the prevalence rate in dogs are quite high and the relationship between human and dogs is more and more close. Studies on brucellosis and *Brucella* were gaining more attention at northern provinces than those of southern region. However, our findings suggests that brucellosis among animals in the south is as equally serious as that in the north. Therefore, a nationwide comprehensive monitoring program must be reinitiated for both human and animals. In this perspective, brucellosis being a zoonotic disease, the One Health approach would be an ideal tool for alleviating the other diseases impacts on both humans and animals with the public health concerns.

AUTHOR SUMMARY

Brucellosis is a worldwide zoonosis caused by *Brucella* posing significant damage to both public health and agriculture. However, the report about animal brucellosis in China is scattered, unintegrated, and dominant species among each kind of animals remains unknown. Here, we aimed to present the nationwide evidence-based results by using the systematic review and meta-analytic approach.

EVIDENCE BEFORE THIS STUDY

After over 100 years in discovery of the agent of Malta fever by David Bruce, brucellosis remains one of the important zoonotic infections causing huge reproductive failure in livestock, and economic losses of the dairy industry in low and middle-income countries. Brucellosis is also a serious public health problem for humans, due to food-chain, and/or occupational exposure. It is estimated that over one-fifth of the 1.4 billion worldwide cattle population is currently infected by *Brucella*, and results in over half-million new human cases annually, representing the most common systemic bacterial zoonosis. As the world largest population (1.4 billion people and 500 million livestock units), even though numerous studies reported significant accumulation of human brucellosis in China, only scattered and unintegrated animal brucellosis datasets are available, leaving huge knowledge gap for the zoonotic control and measurement.

ADDED-VALUE OF THIS STUDY

We used the evidence-based studies, a meta-analysis, to build the most updated and comprehensive picture of brucellosis in China, including humans, livestock, and companion animals. The One Health approach indicates that the trend of human and animal brucellosis are closely associated with each other in China, with significant expansion from traditional northern farming areas to southern China. Importantly, we found that canine and yak could serve as the emerging reservoirs for human infections in China.

IMPLICATIONS OF ALL THE AVAILABLE EVIDENCE

The surveillance measurement for human brucellosis should be shifted from traditional northern China to southern regions. Policymakers should consider regional epidemiological data and risk factors to mitigate the zoonotic transmission from animals to humans. Our unique One Health approach, combined with evidence-based meta-analysis, could be readily scaled to other zoonotic agents with significant public health importance.

DATA AVAILABILITY STATEMENT

All datasets generated for this study are included in the article/**Supplementary Material**.

AUTHOR CONTRIBUTIONS

MY: conceptualization. KZ and BW: data curation. KZ and NP: formal analysis and visualization. MY, NP, and HP: methodology. MY and YL: project administration, and writing—review and editing. NP, HP, and JJ: software. MY, YL, and LZ: supervision. KZ: writing—original draft. All authors contributed to the article and approved the submitted version.

FUNDING

This study was supported by the National Program on Key Research Project of China (2019YFE0103900; 2018YFD0500501; and 2017YFC1600103) as well as European Union's Horizon 2020 Research and Innovation Programme under Grant Agreement No. 861917—SAFFI, Zhejiang Provincial Natural Science Foundation of China (LR19C180001), Zhejiang Provincial Key R&D Program of China (2020C02032), and National Science and Technology Major Project of China (No. 2018ZX10201002).

ACKNOWLEDGMENTS

We would like to thank the Veterinary Medicine students from Class of 2018 at ZJU, who participate in this data collection.

SUPPLEMENTARY MATERIAL

The Supplementary Material for this article can be found online at: https://www.frontiersin.org/articles/10.3389/fvets.2020.00521/full#supplementary-material

Supplemental Figure 1 | Spatiotemporal prevalence of human and animal brucellosis in China from 1951 to 2018.

REFERENCES

1. Rubach MP, Halliday JE, Cleaveland S, Crump JA. Brucellosis in low-income and middle-income countries. *Curr Opin Infect Dis.* (2013) 26:404–12. doi: 10.1097/QCO.0b013e3283638104
2. Pappas G, Papadimitriou P, Akritidis N, Christou L, Tsianos EV. The new global map of human brucellosis. *Lancet Infect Dis.* (2006) 6:91–9. doi: 10.1016/S1473-3099(06)70382-6
3. Musallam II, Abo-Shehada MN, Hegazy YM, Holt HR, Guitian FJ. Systematic review of brucellosis in the Middle East: disease frequency in ruminants and humans and risk factors for human infection. *Epidemiol Infect.* (2016) 144:671–85. doi: 10.1017/S0950268815002575
4. Cárdenas L, Awada L, Tizzani P, Cáceres P, Casal J. Characterization and evolution of countries affected by bovine brucellosis (1996-2014). *Transbound Emerg Dis.* (2019) 66:1280–90. doi: 10.1111/tbed.13144
5. Kong W. Brucellosis infection increasing in Southern China. *Eur J Intern Med.* (2018) 51:e16–8. doi: 10.1016/j.ejim.2018.03.004
6. Lai S, Zhou H, Xiong W, Gilbert M, Huang Z, Yu J, et al. Changing epidemiology of human brucellosis, China, 1955-2014. *Emerg Infect Dis.* (2017) 23:184–94. doi: 10.3201/eid2302.151710
7. Xiao Y, Zou G, Yin J, Tan W, Zhou J, Zhang H. Seroepidemiology of human *Brucella* infection in Yixing, China. *Trop Doc.* (2017) 47:165–7. doi: 10.1177/0049475516640191
8. Krueger WS, Lucero NE, Brower A, Heil GL, Gray GC. Evidence for unapparent *Brucella canis* infections among adults with occupational exposure to dogs. *Zoonoses Public Health.* (2014) 61:509–18. doi: 10.1111/zph.12102
9. Lytras T, Danis K, Dounias G. Incidence patterns and occupational risk factors of human brucellosis in Greece, 2004-2015. *Int J Occup Environ Med.* (2016) 7:221–6. doi: 10.15171/ijoem.2016.806
10. Mangalgi SS, Sajjan AG, Mohite ST, Gajul S. Brucellosis in occupationally exposed groups. *J Clin Diagn Res.* (2016) 10: Dc24–7. doi: 10.7860/JCDR/2016/15276.7673
11. Hull NC, Schumaker BA. Comparisons of brucellosis between human and veterinary medicine. *Infect Ecol Epidemiol.* (2018) 8:1500846. doi: 10.1080/20008686.2018.1500846
12. Deng Y, Liu X, Duan K, Peng Q. Research progress on brucellosis. *Curr Med Chem.* (2019) 26:5598–608. doi: 10.2174/0929867325666180510125009
13. Piao D, Wang H, Di D, Tian G, Luo J, Gao W, et al. MLVA and LPS characteristics of *Brucella canis* isolated from humans and dogs in Zhejiang, China. *Front Vet Sci.* (2017) 4:223. doi: 10.3389/fvets.2017.00223
14. Paudyal N, Pan H, Liao X, Zhang X, Li X, Fang W, et al. A meta-analysis of major foodborne pathogens in Chinese food commodities between 2006 and 2016. *Foodborne Pathog Dis.* (2018) 15:187–97. doi: 10.1089/fpd.2017.2417
15. Shamseer L, Moher D, Clarke M, Ghersi D, Liberati A, Petticrew M, et al. Preferred reporting items for systematic review and meta-analysis protocols (PRISMA-P) 2015: elaboration and explanation. *BMJ.* (2015) 350:g7647. doi: 10.1136/bmj.g7647
16. Ariza J, Bosilkovski M, Cascio A, Colmenero JD, Corbel MJ, Falagas ME, et al. Perspectives for the treatment of brucellosis in the 21st century: the ioannina recommendations. *PLoS Med.* (2007) 4:e317. doi: 10.1371/journal.pmed.0040317
17. Seleem MN, Boyle SM, Sriranganathan N. Brucellosis: a re-emerging zoonosis. *Vet Microbiol.* (2010) 140:392–8. doi: 10.1016/j.vetmic.2009.06.021
18. Liu F, Wang D, Wang J, Li T, Zhao Y, Jiang S. National brucellosis intervention pilot county survey on the economic losses. *Chin J Control Endemic Dis.* (2008) 23:424–5.
19. Shang D. 50-Year research on prevention and control of brucellosis in China. *Chin J Epidemiol.* (2000) 21:55–57.
20. Jia P, Joyner A. Human brucellosis occurrences in Inner Mongolia, China: a spatio-temporal distribution and ecological niche modeling approach. *BMC Infect Dis.* (2015) 15:36. doi: 10.1186/s12879-015-0763-9
21. Zhang J, Yin F, Zhang T, Yang C, Zhang X, Feng Z, et al. Spatial analysis on human brucellosis incidence in mainland China: 2004-2010. *BMJ Open.* (2014) 4:e004470. doi: 10.1136/bmjopen-2013-004470
22. Ran X, Cheng J, Wang M, Chen X, Wang H, Ge Y, et al. Brucellosis seroprevalence in dairy cattle in China during 2008-2018: a systematic review and meta-analysis. *Acta Trop.* (2019) 189:117–23. doi: 10.1016/j.actatropica.2018.10.002
23. Ye HY, Xing FF, Yang J, Lo SK, Lau RW, Chen JH, et al. High index of suspicion for brucellosis in a highly cosmopolitan city in southern China. *BMC Infect Dis.* (2020) 20:22. doi: 10.1186/s12879-019-4748-y
24. Pan H, Paudyal N, Li X, Fang W, Yue M. Multiple food-animal-borne route in transmission of antibiotic-resistant salmonella newport to humans. *Front Microbiol.* (2018) 9:23. doi: 10.3389/fmicb.2018.00023
25. Pan H, Zhou X, Chai W, Paudyal N, Li S, Zhou X, et al. Diversified sources for human infections by *Salmonella enterica* serovar newport. *Transbound Emerg Dis.* (2019) 66:1044–8. doi: 10.1111/tbed.13099
26. Wang X, Biswas S, Paudyal N, Pan H, Li X, Fang W, et al. Antibiotic resistance in salmonella typhimurium isolates recovered from the food chain through national antimicrobial resistance monitoring system between 1996 and 2016. *Front Microbiol.* (2019) 10:985. doi: 10.3389/fmicb.2019.00985

27. Elbediwi M, Pan H, Biswas S, Li Y, Yue M. Emerging colistin resistance in *Salmonella enterica* serovar Newport isolates from human infections. *Emerg Microbes Infect.* (2020) 9:535–8. doi: 10.1080/22221751.2020.1733439
28. Paudyal N, Pan H, Wu B, Zhou X, Zhou X, Chai W, et al. Persistent asymptomatic human infections by *Salmonella enterica* serovar newport in China. *mSphere.* (2020) 5:e00163-20. doi: 10.1128/mSphere.00163-20
29. Liu ZG, Wang M, Ta N, Fang MG, Mi JC, Yu RP, et al. Seroprevalence of human brucellosis and molecular characteristics of *Brucella* strains in Inner Mongolia autonomous region of China, from 2012 to 2016. *Emerg Microbes Infect.* (2020) 9:263–74. doi: 10.1080/22221751.2020.1720528
30. Cao X, Li Z, Liu Z, Fu B, Liu Y, Shang Y, et al. Molecular epidemiological characterization of *Brucella* isolates from sheep and yaks in northwest China. *Transbound Emerg Dis.* (2018) 65:e425–e33. doi: 10.1111/tbed.12777
31. Zeng J, Duoji C, Yuan Z, Yuzhen S, Fan W, Tian L, et al. Seroprevalence and risk factors for bovine brucellosis in domestic yaks (*Bos grunniens*) in Tibet, China. *Trop Anim Health Prod.* (2017) 49:1339–44. doi: 10.1007/s11250-017-1331-7
32. Liu ZG, Di DD, Wang M, Liu RH, Zhao HY, Piao DR, et al. MLVA genotyping characteristics of human *Brucella melitensis* isolated from Ulanqab of Inner Mongolia, China. *Front Microbiol.* (2017) 8:6. doi: 10.3389/fmicb.2017.00006
33. Piao DR, Liu X, Di DD, Xiao P, Zhao ZZ, Xu LQ, et al. Genetic polymorphisms identify in species/biovars of *Brucella* isolated in China between 1953 and 2013 by MLST. *BMC Microbiol.* (2018) 18:7. doi: 10.1186/s12866-018-1149-0
34. Cao X, Li S, Li Z, Liu Z, Ma J, Lou Z, et al. Enzootic situation and molecular epidemiology of *Brucella* in livestock from 2011 to 2015 in Qingyang, China. *Emerg Microb Infect.* (2018) 7:58. doi: 10.1038/s41426-018-0060-y
35. Liu ZG, Wang M, Zhao HY, Piao DR, Jiang H, Li ZJ. Investigation of the molecular characteristics of *Brucella* isolates from Guangxi Province, China. *BMC Microbiol.* (2019) 19:292. doi: 10.1186/s12866-019-1665-6
36. Ferreira Vicente A, Girault G, Corde Y, Souza Ribeiro Mioni M, Borges Keid L, Jay M, et al. The study of worldwide *Brucella canis* of phylogenetic groups by comparative genomics-based approaches. *China Biotechnol.* (2020) 40, 38–47. doi: 10.13523/j.cb.1907053
37. Liu ZG, Wang LJ, Piao DR, Wang M, Liu RH, Zhao HY, et al. Molecular investigation of the transmission pattern of *Brucella suis* 3 from inner Mongolia, China. *Front Vet Sci.* (2018) 5:271. doi: 10.3389/fvets.2018.00271
38. De-gui L. Current status, opportunities and challenges of pet industry in China. *Chin J Comp Med.* (2010) 20:13–6. doi: 10.3969/j.issn.1671/7856.2010.11.12.004

Conflict of Interest: The authors declare that the research was conducted in the absence of any commercial or financial relationships that could be construed as a potential conflict of interest.

frontiers in Veterinary Science

REVIEW
published: 16 September 2020
doi: 10.3389/fvets.2020.569737

Roles of MOV10 in Animal RNA Virus Infection

Feng Su, Xueming Liu and Yunliang Jiang**

Shandong Provincial Key Laboratory of Animal Biotechnology and Disease Control and Prevention, College of Animal Science and Veterinary Medicine, Shandong Agricultural University, Tai'an, China

Animal epidemic diseases caused by RNA viruses are the primary threat to the livestock industry, and understanding the mechanisms of RNA virus clearance from target cells is critical to establish an effective method to reduce economic losses. As an SF-1, ATP-dependent RNA helicase in the UPF1p family, MOV10 participates in the RNA degradation of multiple viruses mediated via miRNA pathways and therefore contributes to a decrease in the replication of RNA viruses. This review primarily focuses on the bioactivity of MOV10, the mechanism of RNA virus removal, and the potential roles of MOV10 in RNA virus clearance. In addition, clues are provided to reduce animal diseases caused by RNA viruses.

Keywords: animal RNA virus, antivirus mechanism, MOV10, miRNA pathways, mRNA

OPEN ACCESS

Edited by:
Lester J. Perez, University of Illinois at Urbana–Champaign, United States

Reviewed by:
Andrii Slonchak, The University of Queensland, Australia
Francisco Rivera-Benítez, Instituto Nacional de Investigaciones Forestales, Agrícolas y Pecuarias (INIFAP), Mexico

***Correspondence:**
Feng Su
suf@sdau.edu.cn
Yunliang Jiang
yljiang723@aliyun.com

Specialty section:
This article was submitted to Veterinary Infectious Diseases, a section of the journal Frontiers in Veterinary Science

Received: *04 June 2020*
Accepted: *14 August 2020*
Published: *16 September 2020*

Citation:
Su F, Liu X and Jiang Y (2020) Roles of MOV10 in Animal RNA Virus Infection. Front. Vet. Sci. 7:569737. doi: 10.3389/fvets.2020.569737

Animal epidemic diseases caused by RNA viruses are the primary threat to the livestock industry (1), and understanding the mechanisms of RNA virus clearance in target cells can lead to an effective method to reduce economic losses. Therefore, this review focuses on the current understanding of the mechanisms of viral resistance to RNA viruses that cause animal diseases.

DISEASES CAUSED BY RNA VIRUSES IN THE LIVESTOCK INDUSTRY

Animal epidemic diseases are the primary threat to the livestock industry. Of the veterinary pathogens that cause these diseases, viruses are responsible for approximately half of the most important animal diseases, according to the OIE's (Office of International Epizootic) classification of terrestrial and aquatic notifiable animal diseases (1). Animal viruses are divided into DNA and RNA viruses on the basis of the genetic materials, both the viruses are the dominate pathogens that affecting animal production in livestock industry (1, 2). The differences between DNA and RNA viruses include their lifetimes in target cells, how they attach to and enter host cells, and their biosynthesis, maturation, and release from cells (2, 3).

Compared with DNA viruses, RNA viruses have a higher mutation rate and cause more serious economic damage in the livestock industry (4). Lower mutation rates of DNA viruses were usually influence by the viral genome and DNA repairing protein that benefit for proofread and correct replication errors (5). Oppositely, offspring of RNA viruses are usually produced 1 ± 2 mutations compared with their parent. RNA virus usually producing a mutant cloud of descendants in extremely environment (5). RNA viruses are also divided into avian, mammalian, and zoonotic viruses in domestic animal industries. For example, the avian leukosis retrovirus causes great losses in the avian industry and many subgroups have been isolated in recent years (6–12). In mammals, more RNA viruses are also being reported, of which the classical swine fever virus and porcine reproductive and respiratory syndrome virus (PRRSV) are the main RNA viruses that cause great

losses in porcine industries. Because of their high mutation rates and the additional subgroups identified in recent years (13–17), both viruses are difficult to eliminate. Some RNA viruses not only infect animals but also humans, with the influenza virus the most typical RNA zoonotic virus. For example, H5N1 and H9N2 subgroups of the influenza virus are the main infectious pathogens affecting both humans and animals (18–23). To reduce economic losses in animal industries, the main approaches are to reduce the virus titer in animals and to improve their immunity. Thus, an understanding of the mechanism that clears RNA viruses from target cells is the most important step in controlling virus infection.

MIRNA PATHWAYS ARE IMPORTANT IN THE CLEARANCE OF ANIMAL RNA VIRUSES

RNA interference (RNAi) is an important mechanism in mediating the clearance of RNA viruses (24). Viral RNA can be degraded through the inhibition of viral replication by the binding effects between small interfering RNAs and viral nucleic acids (24, 25). Generally, the antiviral effects due to RNAi are typically found in invertebrates, and RNAi functioning as an antiviral effector has only been detected in undifferentiated stem cells (26, 27). RNAi also plays important roles in the activation of IFN-I (Type I interferon) and its antiviral effectors (IFN-stimulated genes), with those genes producing the main antiviral effects in differentiated vertebrate somatic cells (**Figure 1**) (28).

RNA virus replication and clearance are typically influenced by several factors, of which miRNAs produced in cells may play important roles in a regulated network. miRNAs usually bind to the miRNA binding sites within mRNAs and viral genomes to exert their regulatory function (29, 30). The number of miRNA binding sites within a viral genome affects the viral replication (**Figure 1**). Most miRNA binding sites are in the 5' and 3' non-translation regions (NTRs) of a viral genome (31), but the sites were also recently found in the translated regions (32, 33). An increase in the number of perfect complementary miRNA binding sites in the NTRs of RNA viruses causes strong translational repression *in vitro* and a decrease in virulence in mice (34). miRNA gene translation is also influenced by epigenetic and environmental conditions (34, 35). For example, compared with primary tissues, low levels of miRNAs are detected in cultural cells, especially in a high confluency (36). Furthermore, non-canonical miRNA target sites in specific cells are also potential factors that affect miRNA production and therefore RNA virus replication (25).

Direct inhibition effects of miRNAs on viruses were previous recognized as an effective way in invertebrates rather than in vertebrates, subsequent studies confirmed the anti-viral function of miRNAs in undifferential vertebrates' stem cells. But the direct viral inhibition effect of miRNAs was controversial in somatic Cells (37). Cullen's studies evaluated the directly viral genome targeting effects of miRNAs and his research revealed viruses induced miRNAs are hardly causing reduction of virus copy number (38–40). Recently study summarized the potential directly viral genome targeting effects of miRNAs. Trobaugh's review analyzed the direct inhibitory effects of miRNAs. And the review point out that direct inhibitory effects of miRNAs on viruses are primarily concentrated in the viral genome and in viral genome translation (**Figure 1**) (31, 41). There are so many reasons causing direct targeting reduction of miRNAs, of which viruses escaping mechanism, incomplete pairing of miRNA and viruses mutation are the important reasons. But the artificial application of miRNAs on viruses genome were reported as an important method to reduce viral replication copies recently.

Direct inhibitory effects of miRNAs on viruses mainly play its roles in viral genome and in viral genome translation. Positive-strand RNA viruses release their genomes into the cytoplasm after entering cells following recognition by receptors within the membrane surface (41). Similar to mRNA produced in a cell, the released viral RNA is either decayed or replicated when combined with miRNAs in the cytoplasm. For example, the expression of miR-181, miR-206, miR-23, and miR-378 in specific cells can inhibit the replication of PRRSV by binding to the viral genome (42, 43). By contrast, miR-17 and let-7c bind to the 3' NTR of the bovine viral diarrhea virus genome and cause virus genome translation and an increase in RNA stability rather than translational repression (41). Similar effects are also found in negative-strand viruses. The negative-stand RNA released in the cytoplasm is first translated into positive-stand RNA for protein synthesis and virus assembly. The translated positive RNA can recruit miRNA binding to the miRNA-recognized sites and ultimately influence virus replication and assembly (25). For example, the influenza PB1 gene recruits miR-323, miR-491, miR-485, miR-654, and miR-3145, which leads to RNA degradation in infected human and canine epithelial cell lines *in vitro* (33, 44, 45).

To determine the indirect effects of miRNAs on virus infection, the primary focus is on the level of miRNAs and the changes in host immunity response in target cells (**Figure 1**) (46). Specifically, an immune response initiated by a virus mediates viral-recognition receptors that lead to activation of translation factors and ultimately changes in the expression profiles of miRNAs (47, 48). For example, changes in the expression of specific miRNAs (miR-151-5p and miR-223-3p) determine whether the H5N2 influenza virus is pathogenic or is attenuated (49). Changes in specific miRNAs also affect miRNA-mediated protein expression (50). The IFN systems are a crucial mechanism in the removal of viral infection (25). Virus-mediated regulation of the IFN signaling cascade is controlled by miRNA levels in target cells (25). For example, miR-23 and miR-505 can increase IFN-α/β expression, which is useful in clearing PRRSV (42, 43). By contrast, with the expression of miR-23b, avian leukosis viral infection in chicken spleen downregulates IFN regulatory factor 1 levels and innate immune induction (51). Thus, the miRNAs that are involved in downregulating the innate immune response during RNA virus infections need to be identified in the future.

Though the indirect effects of miRNAs on RNA viral infection were widely confirmed and recognized, the direct effects of miRNAs were still controversial. This controversy was mainly concentrated on several factors. Firstly, miRNAs were reducible

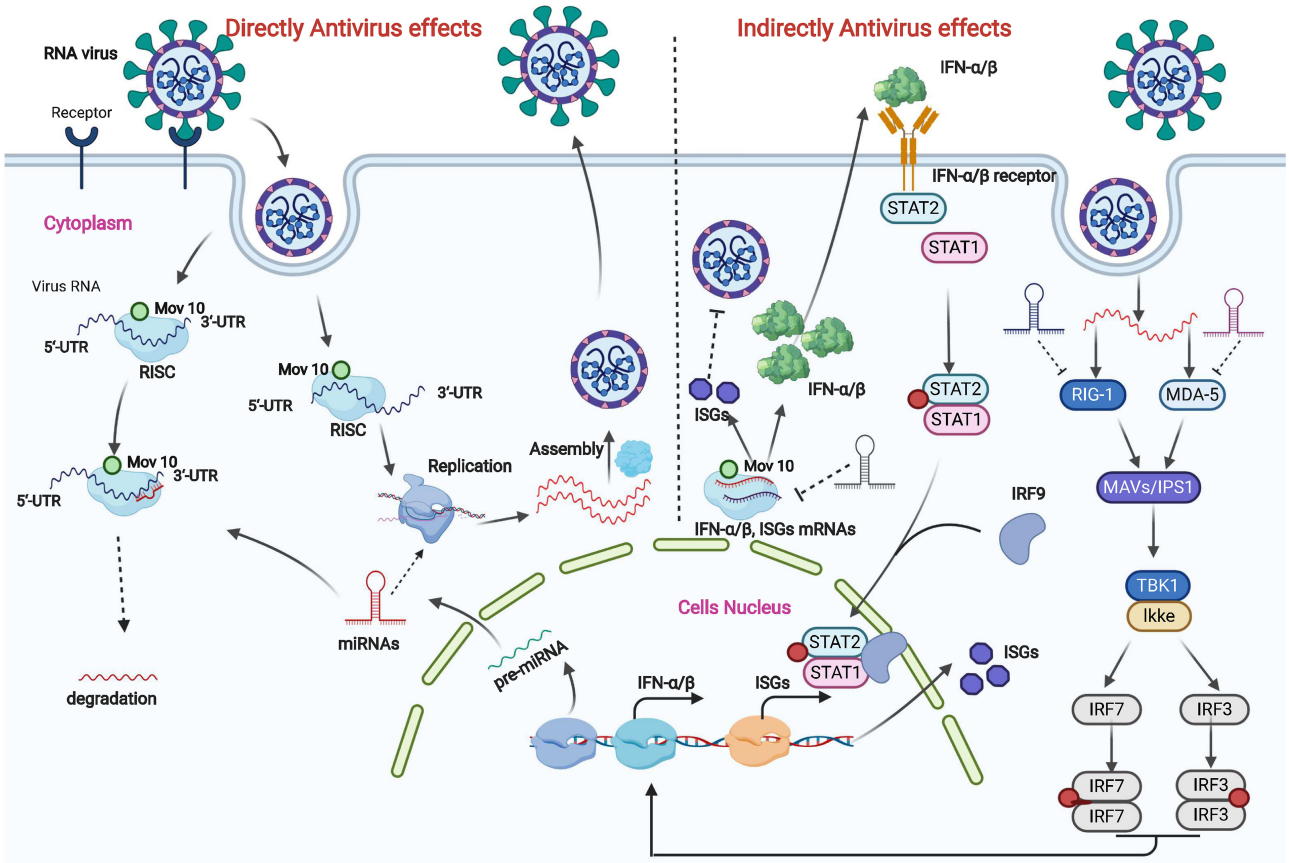

FIGURE 1 | Direct and indirect antivirus effects of miRNAs in target cells. Antivirus effects of miRNAs are divided into direct and indirect regulation in target cells. In direct regulation, host miRNAs participate in viral RNA degradation in a RISC within a P body in target cells and are also involved in viral RNA replication processes by targeting RNA replication components. Indirect antiviral effects are complex. First, host miRNAs participate in the RIG-1 and MDA-5 pathway-mediated IFN-α/β production. The production of IFN-α/β not only inhibits viral replication in cells but also activates the IFN signal pathway and ultimately causes the expression of IFN-stimulated genes (ISGs) to decrease virus replication. miRNAs also participate in this regulation process.

generated from the cells after the viruses infection, but these miRNAs were hardly presented its' directly target effects on viral genome because of the low level of miRNAs produced by the target cells. The other factor is the potential escaping mechanism of viral and the cells complex immune system. The mismatch of miRNAs and viral genome mutation also reduced its inhibition effects.

MOV10 IS AN IMPORTANT REGULATOR OF ANIMAL RNA VIRUS INVASION

MOV10 is an important SF-1, ATP-dependent RNA helicase in the UPF1p family (52–55), originally identified as a protein that prevents Moloney murine leukemia virus infection in mice. Two potential mechanisms can explain the antiviral bioactivity of MOV10: (1) regulating antiviral gene expression so as to achieve antiviral capacity (56) and (2) changing miRNA expression directly or indirectly so as to mediate viral clearance effects (46). The two mechanisms are discussed below in detail.

MOV10 Regulates Antiviral Gene Expression by Different Pathways

The antiviral activity of MOV10 has been evaluated and detected in many studies. The infectivity of different viruses is regulated by the MOV10 helicase, for example, human hepatitis delta virus (57), human immunodeficiency virus type 1 (HIV-1), and dengue virus (58). The same effect is also observed with PRRSV infection (59). Different genes and pathways are activated in specific virus-infected target cells. In HIV-infected cells, the antiviral activity of MOV10 is detected in multiple stages in original studies. MOV10 is efficiently incorporated into virions and reduces virus infectivity by inhibiting reverse transcription in the first stage (52). Overexpression of APOBEC3G and MOV10 reduces proteolytic processing of HIV-1 Gag, which effectively reduces HIV replication in the later stage (60). Recent studies show that MOV10 inhibits the degradation of APOBEC3G through interfering with the Vif-mediated (Vif: HIV-1-encoded virion infectivity factor protein) ubiquitin–proteasome pathway (61–63). MOV10 can also provide antiviral activity against RNA viruses by increasing the induction of RIG-I–MAVS-independent

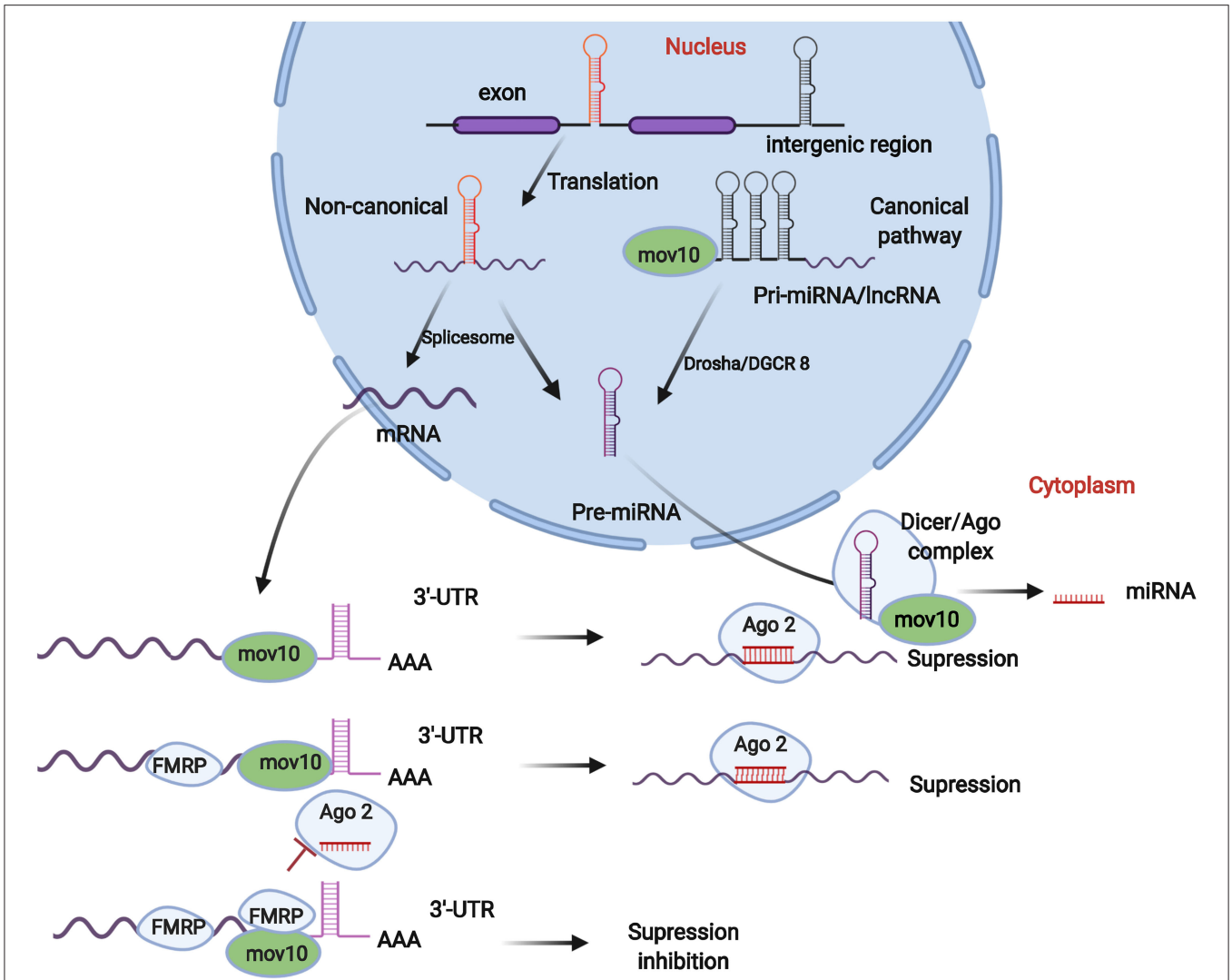

FIGURE 2 | Roles of MOV10 in miRNA generation and mRNA stability. The MOV10 gene regulates the generation of miRNAs. Pre-miRNAs produced in the cell nucleus are generated from pri-miRNAs. The production of pri-miRNAs typically occurs in intergenic and intronic regions of the genome, which are then spliced into pre-miRNAs by a spliceosome (non-canonical pathway) or Drosha/DGCR8 enzymes (canonical pathway). In this process, MOV10 participates in the generation and cleavage of pri-miRNAs. Subsequently, miRNAs mature in the Dicer/Ago complex in cytoplasm. MOV10 is an important factor affecting the composition of the Dicer/Ago complex and plays crucial roles in miRNA maturation. MOV10 is also stored in the P body in cytoplasm and plays crucial roles in mRNA maturation, degradation, and stabilization, which contribute to maintaining the balance in miRNA, lncRNA, and mRNA pools in cells.

IFN (56) and through IKKε and IRF3, the induction of IFN (**Figure 1**) (64). In influenza A virus-infected models, MOV10 with nucleoprotein (NP) promotes viral RNA degradation through the lysosomal pathway (65). In addition, MOV10 sequesters the ribonucleoprotein (RNP) of influenza A virus in the cytoplasm and is antagonized by viral influenza non-structural (NS1) protein (66).

In a recent study of MOV10 that focused on animal disease, MOV10 directly inhibited replication of the PRRSV by retaining the viral nucleocapsid protein in the cytoplasm of Marc-145 cells (59). MOV10 also inhibits replication of the murine leukemia virus (67). Many genes potentially activated by MOV10 exhibit strong antiviral bioactivity (58). IRAV (FLJ11286) is an interferon-stimulated gene with antiviral activity against dengue virus that interacts with MOV10 (58).

MOV10 Mediates Inhibition of RNA Viruses via miRNA Pathways

As mentioned above, MOV10 antiviral activity is expressed through the activation of different genes and pathways, of which miRNA pathway-mediated viral inhibition is important in restricting viral invasion. In the entire synthesis process of miRNAs, MOV10 not only functions in pri-miRNA production in the cell nucleus (68) but also has crucial roles in miRNA maturation and degradation (69). MOV10 also has crucial roles

in mRNA maturation and degradation via exposure of miRNA recognition sites within mRNAs (**Figure 2**) (70).

The generation of pri-miRNAs and pre-miRNAs is the first step in the production of miRNAs, which is regulated by Drosha and DGCR8 enzymes and is also controlled by the MOV10 gene (71). Generally, the original pool is composed of pri-miRNAs and pre-mRNAs. Pre-miRNAs are typically produced in the cell nucleus by two important pathways. In the canonical pathway, pre-miRNAs are generated from exonic, intronic, or intergenic regions, followed by Drosha/DGCR8 processing to transform pri-miRNA transcripts into pre-miRNAs (72, 73). In the non-canonical pathway, pre-miRNAs are formed by splicing, debranching, and trimming of short introns without Drosha processing (74). In this process to form pre-miRNAs, MOV10 typically binds splicing factors, such as SRSF1 and DDX5 (68, 75), forming a splicing complex, which completes the pre-mRNA and pri-miRNA splicing process after binding intronic regions (**Figure 2**).

The pre-miRNAs generated from the canonical and non-canonical pathways are exported from the nucleus via Exportin 5 and then cleavage by Dicer occurs within the RISC loading complex (RLC) (76). Then, the miRNA/miRNA duplex unwinds via the Argonaute complex. In this process, MOV10 typically combines with Dicer, Ago, and TRBP (transactivation response element RNA-binding protein) forming the RISC complex and finally promoting miRNA maturation (76). Thus, MOV10 deficiency could cause an imbalance in the pools of miRNA, mRNA, and lncRNA (long non-code RNA) (**Figure 2**).

MOV10 is also important in the regulation of mRNA degradation and stability. A MOV10 protein, typically in the cytoplasm, combines with an Argonaute protein to form a complex that was recognized as an important component stored in a mRNA processing body (the P body) (60). In a previous study (60, 66), MOV10 inhibited retrotransposition by binding cell ribonucleoprotein particles (RNPs). MOV10 can bind high GC regions of the 3′-UTR within mRNAs, exposing miRNA recognition sites and guiding Ago proteins in promoting mRNA degradation (60). MOV10 can also increase mRNA stability and maturity via enriching the Fragile X mental retardation protein (FMRP) in miRNA-recognized sites (**Figure 2**) (66).

The virulence and infectivity of RNA viruses are influenced by MOV10-mediated changes in miRNA/mRNA. In the third stage of HIV infection, HIV infectivity is weakened because of miRNA expression in target cells (63). MOV10 also serves as a cofactor of HIV-1 Rev to facilitate Rev/RRE-dependent nuclear export of viral mRNAs (77). The same influence of MOV10 is apparent in the replication of human hepatitis delta virus (57). MOV10 can also weaken influenza infectivity and inhibit influenza A virus replication via binding RNP (65, 78).

CONCLUSIONS

The antiviral activity of MOV10 during RNA virus infection is discussed in this review. Overall, the antiviral capacity of MOV10 is primarily reflected in two important mechanisms. First, MOV10 weakens viral virulence by binding the related protein, thereby activating IFN signal and cell autophagy pathways. Second, MOV10 functions as an RNA helicase during RNA virus infection. MOV10 regulates miRNA and mRNA generation, maturation, and degradation by miRNA pathways, which influence virus replication and packaging. The two mechanisms are typically coordinated in different virus infection stages. In addition, the number of studies is increasing that confirm MOV10 not only has important roles in infection by human viruses, such as HIV and human hepatitis delta virus, but also shows antiviral activity against animal RNA viruses. The antiviral ability of MOV10 and the related pathways during animal RNA virus infection are worthy of future attention. It is also can be used as an important tools for reduction of animal RNA viruses infection in future.

AUTHOR CONTRIBUTIONS

FS, XL, and YJ conceived the study and wrote the manuscript. All authors contributed to the article and approved the submitted version.

FUNDING

This work was supported by funds from the Shandong Agricultural Breeding project (2019LZGC019) and the Grant from China Scholarship Council.

REFERENCES

1. Alejandro B. Vaccines and vaccination for veterinary viral diseases: a general overview. In *Vaccine Technologies for Veterinary Viral Diseases*. New York, NY: Springer (2016). p. 1–24.
2. Roy P. Bluetongue virus proteins and particles and their role in virus entry, assembly, and release. *Adv Virus Res.* (2005) 64:69–123. doi: 10.1016/S0065-3527(05)64004-3
3. Steinhauer DA, Holland J. Rapid evolution of RNA viruses. *Annu Rev Microbiol.* (1987) 41:409–31. doi: 10.1146/annurev.mi.41.100187.002205
4. Lauring AS, Frydman J, Andino R. The role of mutational robustness in RNA virus evolution. *Nat Rev Microbiol.* (2013) 11:327–36. doi: 10.1038/nrmicro3003
5. Duffy S. Why are RNA virus mutation rates so damn high? *PLoS Biol.* (2018) 16:e3000003. doi: 10.1371/journal.pbio.3000003
6. Li D, Qin L, Gao H, Yang B, Liu W, Qi X, et al. Avian leukosis virus subgroup A and B infection in wild birds of Northeast China. *Vet Microbiol.* (2013) 163:257–63. doi: 10.1016/j.vetmic.2013.01.020
7. Zhou D, Xue J, Zhang Y, Wang G, Feng Y, Hu L, et al. Outbreak of myelocytomatosis caused by mutational avian leukosis virus subgroup J in China, 2018. *Transbound Emerg Dis.* (2019) 66:622–6. doi: 10.1111/tbed.13096
8. Li J, Meng F, Li W, Wang Y, Chang S, Zhao P, et al. Characterization of avian leukosis virus subgroup J isolated between 1999 and 2013 in China. *Poultry Sci.* (2018) 97:3532–9. doi: 10.3382/ps/pey241
9. Su Q, Li Y, Li W, Cui S, Tian S, Cui Z, et al. Molecular characteristics of avian leukosis viruses isolated from indigenous chicken breeds in China. *Poultry Sci.* (2018) 97:2917–25. doi: 10.3382/ps/pex367
10. Li Y, Fu J, Cui S, Meng F, Cui Z, Fan J, et al. Gp85 genetic diversity of avian leukosis virus subgroup J among different individual chickens from a native flock. *Poultr Sci.* (2017) 96:1100–7. doi: 10.3382/ps/pew407

11. Chen H, Wang Y, Zhao P, Li J, Cui Z. Acute fibrosarcomas caused by avian leukosis virus subgroup J associated with v-fps oncogene. *J Anim Vet Adv.* (2012) 11:2910–6. doi: 10.3923/javaa.2012.2910.2916
12. Zhao P, Dong X, Cui Z. Isolation, identification, and gp85 characterization of a subgroup A avian leukosis virus from a contaminated live newcastle disease virus vaccine, first report in China. *Poultr Sci.* (2014) 93:2168–74. doi: 10.3382/ps.2014-03963
13. Yu Y, Cai X, Wang G, Kong N, Liu Y, Xiao Y, et al. Anti-idiotypic antibodies reduce efficacy of the attenuated vaccine against highly pathogenic PRRSV challenge. *BMC Vet Res.* (2014) 10:39. doi: 10.1186/1746-6148-10-39
14. Wang X, Qiu H, Zhang M, Cai X, Qu Y, Hu D, et al. Distribution of highly pathogenic porcine reproductive and respiratory syndrome virus (HP-PRRSV) in different stages of gestation sows: HP-PRRSV distribution in gestation sows. *Vet Immunol Immunopathol.* (2015) 166:88–94. doi: 10.1016/j.vetimm.2015.06.002
15. Zhao P, Ma C-T, Cui Z-Z. Analysis of quasispecies diversity and mutations for highly pathogenic porcine reproductive and respiratory syndrome virus in china based on ORF 5 genes. *J Anim Vet Adv.* (2012) 11:2741–6. doi: 10.3923/javaa.2012.2741.2746
16. Gao J, Kong N, Xiao Y, Zhang A, Zhou E. Development of real-time PCR methods for the detection of CD163 and porcine reproductive and respiratory syndrome virus N genes in Marc-145 cell. *J Anim Vet Adv.* (2012) 11:4489–93. doi: 10.3923/javaa.2012.4489.4493
17. Zhang K, Li H, Dong S, Liu Y, Wang D, Liu H, et al. Establishment and evaluation of a PRRSV-sensitive porcine endometrial epithelial cell line by transfecting SV40 large T antigen. *BMC Vet Res.* (2019) 15:1. doi: 10.1186/s12917-019-2051-1
18. Xue R, Tian Y, Hou T, Bao D, Chen H, Teng Q, et al. H9N2 influenza virus isolated from minks has enhanced virulence in mice. *Transb Emerg Dis.* (2018) 65:904–10. doi: 10.1111/tbed.12805
19. Peng L, Chen C, Kai-yi H, Feng-xia Z, Yan-li Z, Zong-shuai L, et al. Molecular characterization of H9N2 influenza virus isolated from mink and its pathogenesis in mink. *Vet Microbiol.* (2015) 176:88–96. doi: 10.1016/j.vetmic.2015.01.009
20. Wei L, Cui J, Song Y, Zhang S, Han F, Yuan R, et al. Duck MDA5 functions in innate immunity against H5N1 highly pathogenic avian influenza virus infections. *Vet Res.* (2014) 45:66. doi: 10.1186/1297-9716-45-66
21. Lv J, Wei L, Yang Y, Wang B, Liang W, Gao Y, et al. Amino acid substitutions in the neuraminidase protein of an H9N2 avian influenza virus affect its airborne transmission in chickens. *Vet Res.* (2015) 46:44. doi: 10.1186/s13567-014-0142-3
22. Song Q-q, Zhang F-x, Liu J-j, Ling Z-s, Zhu Y-l, Jiang S-j, et al. Dog to dog transmission of a novel influenza virus (H5N2) isolated from a canine. *Vet Microbiol.* (2013) 161:331–3. doi: 10.1016/j.vetmic.2012.07.040
23. Yao M, Zhang X, Gao J, Chai T, Miao Z, Ma W, et al. The occurrence and transmission characteristics of airborne H9N2 avian influenza virus. *Berliner Munchener Tierarztliche Wochenschr.* (2011) 124:136–41.
24. Ding S-W, Voinnet O. Antiviral immunity directed by small RNAs. *Cell.* (2007) 130:413–26. doi: 10.1016/j.cell.2007.07.039
25. Trobaugh DW, Klimstra WB. MicroRNA regulation of RNA virus replication and pathogenesis. *Trends Mol Med.* (2017) 23:80–93. doi: 10.1016/j.molmed.2016.11.003
26. Maillard P, Ciaudo C, Marchais A, Li Y, Jay F, Ding S, et al. Antiviral RNA interference in mammalian cells. *Science.* (2013) 342:235–8. doi: 10.1126/science.1241930
27. Li Y, Lu J, Han Y, Fan X, Ding S-W. RNA interference functions as an antiviral immunity mechanism in mammals. *Science.* (2013) 342:231–4. doi: 10.1126/science.1241911
28. Schneider WM, Chevillotte MD, Rice CM. Interferon-stimulated genes: a complex web of host defenses. *Annu Rev Immunol.* (2014) 32:513–45. doi: 10.1146/annurev-immunol-032713-120231
29. Grimson A, Farh KK-H, Johnston WK, Garrett-Engele P, Lim LP, Bartel DP. MicroRNA targeting specificity in mammals: determinants beyond seed pairing. *Mol Cell.* (2007) 27:91–105. doi: 10.1016/j.molcel.2007.06.017
30. Teterina NL, Liu G, Maximova OA, Pletnev AG. Silencing of neurotropic flavivirus replication in the central nervous system by combining multiple microRNA target insertions in two distinct viral genome regions. *Virology.* (2014) 456:247–58. doi: 10.1016/j.virol.2014.04.001
31. Trobaugh DW, Gardner CL, Sun C, Haddow AD, Wang E, Chapnik E, et al. RNA viruses can hijack vertebrate microRNAs to suppress innate immunity. *Nature.* (2014) 506:245–8. doi: 10.1038/nature12869
32. Song L, Liu H, Gao S, Jiang W, Huang W. Cellular microRNAs inhibit replication of the H1N1 influenza A virus in infected cells. *J Virol.* (2010) 84:8849–60. doi: 10.1128/JVI.00456-10
33. Zheng Z, Ke X, Wang M, He S, Li Q, Zheng C, et al. Human microRNA hsa-miR-296-5p suppresses enterovirus 71 replication by targeting the viral genome. *J Virol.* (2013) 87:5645–56. doi: 10.1128/JVI.02655-12
34. Heiss BL, Maximova OA, Thach DC, Speicher JM, Pletnev AG. MicroRNA targeting of neurotropic flavivirus: effective control of virus escape and reversion to neurovirulent phenotype. *J Virol.* (2012) 86:5647–59. doi: 10.1128/JVI.07125-11
35. Davis-Dusenbery BN, Hata A. Mechanisms of control of microRNA biogenesis. *J Biochem.* (2010) 148:381–92. doi: 10.1093/jb/mvq096
36. Hwang H-W, Wentzel EA, Mendell JT. Cell–cell contact globally activates microRNA biogenesis. *Proc Natl Acad Sci USA.* (2009) 106:7016–21. doi: 10.1073/pnas.0811523106
37. Tenoever BR. RNA viruses and the host microRNA machinery. *Nat Rev Microbiol.* (2013) 11:169–80. doi: 10.1038/nrmicro2971
38. Cullen BR, Cherry S. Is RNA interference a physiologically relevant innate antiviral immune response in mammals? *Cell Host Microbe.* (2013) 14:374–8. doi: 10.1016/j.chom.2013.09.011
39. Cullen BR. How do viruses avoid inhibition by endogenous cellular microRNAs? *PLoS Pathog.* (2013) 9:e1003694. doi: 10.1371/journal.ppat.1003694
40. Bogerd HP, Skalsky RL, Kennedy EM, Furuse Y, Whisnant AW, Flores O, et al. Replication of many human viruses is refractory to inhibition by endogenous cellular microRNAs. *J Virol.* (2014) 88:8065–76. doi: 10.1128/JVI.00985-14
41. Scheel TK, Luna JM, Liniger M, Nishiuchi E, Rozen-Gagnon K, Shlomai A, et al. A broad RNA virus survey reveals both miRNA dependence and functional sequestration. *Cell Host Microbe.* (2016) 19:409–23. doi: 10.1016/j.chom.2016.02.007
42. Guo X-K, Zhang Q, Gao L, Li N, Chen X-X, Feng W-H. Increasing expression of microRNA 181 inhibits porcine reproductive and respiratory syndrome virus replication and has implications for controlling virus infection. *J Virol.* (2013) 87:1159–71. doi: 10.1128/JVI.02386-12
43. Zhang Q, Guo X-k, Gao L, Huang C, Li N, Jia X, et al. MicroRNA-23 inhibits PRRSV replication by directly targeting PRRSV RNA and possibly by upregulating type I interferons. *Virology.* (2014) 450:182–95. doi: 10.1016/j.virol.2013.12.020
44. Khongnomnan K, Makkoch J, Poomipak W, Poovorawan Y, Payungporn S. Human miR-3145 inhibits influenza A viruses replication by targeting and silencing viral PB1 gene. *Exp Biol Med.* (2015) 240:1630–9. doi: 10.1177/1535370215589051
45. Ingle H, Kumar S, Raut AA, Mishra A, Kulkarni DD, Kameyama T, et al. The microRNA miR-485 targets host and influenza virus transcripts to regulate antiviral immunity and restrict viral replication. *Sci Signal.* (2015) 8:ra126-ra. doi: 10.1126/scisignal.aab3183
46. Maillard PV, van der Veen AG, Poirier EZ, e Sousa CR. Slicing and dicing viruses: antiviral RNA interference in mammals. *EMBO J.* (2019) 38:e100941. doi: 10.15252/embj.2018100941
47. Wu J, Chen ZJ. Innate immune sensing and signaling of cytosolic nucleic acids. *Annu Rev Immunol.* (2014) 32:461–88. doi: 10.1146/annurev-immunol-032713-120156
48. Aguado LC, Schmid S, Sachs D, Shim JV, Lim JK. MicroRNA function is limited to cytokine control in the acute response to virus infection. *Cell Host Microbe.* (2015) 18:714–22. doi: 10.1016/j.chom.2015.11.003
49. Choi E-J, Kim HB, Baek YH, Kim E-H, Pascua PNQ, Park S-J, et al. Differential microRNA expression following infection with a mouse-adapted, highly virulent avian H5N2 virus. *BMC Microbiol.* (2014) 14:252. doi: 10.1186/s12866-014-0252-0
50. Beachboard DC, Horner SM. Innate immune evasion strategies of DNA and RNA viruses. *Curr Opin Microbiol.* (2016) 32:113–9. doi: 10.1016/j.mib.2016.05.015

51. Li Z, Chen B, Feng M, Ouyang H, Zheng M, Ye Q, et al. MicroRNA-23b promotes avian leukosis virus subgroup J (ALV-J) replication by targeting IRF1. *Sci Rep*. (2015) 5:10294. doi: 10.1038/srep10294
52. Furtak V, Mulky A, Rawlings SA, Kozhaya L, Lee K, KewalRamani VN, et al. Perturbation of the P-body component Mov10 inhibits HIV-1 infectivity. *PLoS ONE*. (2010) 5:e9081. doi: 10.1371/journal.pone.0009081
53. Saito K, Ishizu H, Komai M, Kotani H, Kawamura Y, Nishida KM, et al. Roles for the Yb body components armitage and Yb in primary piRNA biogenesis in *Drosophila*. *Genes Dev*. (2010) 24:2493–8. doi: 10.1101/gad.1989510
54. Haase AD, Fenoglio S, Muerdter F, Guzzardo PM, Czech B, Pappin DJ, et al. Probing the initiation and effector phases of the somatic piRNA pathway in Drosophila. *Genes Dev*. (2010) 24:2499–504. doi: 10.1101/gad.1968110
55. Fischer SE, Montgomery TA, Zhang C, Fahlgren N, Breen PC, Hwang A, et al. The ERI-6/7 helicase acts at the first stage of an siRNA amplification pathway that targets recent gene duplications. *PLoS Genet*. (2011) 7:e1002369. doi: 10.1371/journal.pgen.1002369
56. Cuevas RA, Ghosh A, Wallerath C, Hornung V, Coyne CB, Sarkar SN. MOV10 provides antiviral activity against RNA viruses by enhancing RIG-I–MAVS-independent IFN induction. *J Immunol*. (2016) 196:3877–86. doi: 10.4049/jimmunol.1501359
57. Haussecker D, Cao D, Huang Y, Parameswaran P, Fire AZ, Kay MA. Capped small RNAs and MOV10 in human hepatitis delta virus replication. *Nat struct Mol Biol*. (2008) 15:714–21. doi: 10.1038/nsmb.1440
58. Balinsky CA, Schmeisser H, Wells AI, Ganesan S, Jin T, Singh K, et al. IRAV (FLJ11286), an interferon-stimulated gene with antiviral activity against dengue virus, interacts with MOV10. *J Virol*. (2017) 91:e01606–16. doi: 10.1128/JVI.01606-16
59. Zhao K, Li L-W, Zhang Y-J, Jiang Y-F, Gao F, Li G-X, et al. MOV10 inhibits replication of porcine reproductive and respiratory syndrome virus by retaining viral nucleocapsid protein in the cytoplasm of Marc-145 cells. *Biochem Biophys Res Commun*. (2018) 504:157–63. doi: 10.1016/j.bbrc.2018.08.148
60. Burdick R, Smith JL, Chaipan C, Friew Y, Chen J, Venkatachari NJ, et al. P body-associated protein Mov10 inhibits HIV-1 replication at multiple stages. *J Virol*. (2010) 84:10241–53. doi: 10.1128/JVI.00585-10
61. Arjan S, Swanson C, Sherer N, Malim M. Mov10, an APOBEC3G-interacting RNA-binding protein, inhibits HIV-1 infection. *Retrovirology*. (2011) 8(Suppl. 2):P2. doi: 10.1186/1742-4690-8-S2-P2
62. Chen C, Ma X, Hu Q, Li X, Huang F, Zhang J, et al. Moloney leukemia virus 10 (MOV10) inhibits the degradation of APOBEC3G through interference with the Vif-mediated ubiquitin–proteasome pathway. *Retrovirology*. (2017) 14:56. doi: 10.1186/s12977-017-0382-1
63. Liu C, Zhang X, Huang F, Yang B, Li J, Liu B, et al. APOBEC3G inhibits microRNA-mediated repression of translation by interfering with the interaction between Argonaute-2 and MOV10. *J Biol Chem*. (2012) 287:29373–83. doi: 10.1074/jbc.M112.354001
64. Cuevas R, Hornung V, Coyne C, Sarkar S. MOV10 provides antiviral activity against RNA viruses by enhancing IFN induction through IKK? and IRF3 (INC8P. 441). *Am Assoc Immnol*. (2014) 196:3877–86.
65. Villalón-Letelier F, Reading PC. Unraveling the role of the MOV10 RNA helicase during influenza A virus infection. *Biochem J*. (2019) 476:1005–8. doi: 10.1042/BCJ20190018
66. Li J, Hu S, Xu F, Mei S, Liu X, Yin L, et al. MOV10 sequesters the RNP of influenza A virus in the cytoplasm and is antagonized by viral NS1 protein. *Biochem J*. (2019) 476:467–81. doi: 10.1042/BCJ20180754
67. Zhang Y, Hu S, Pang X, Li J, Guo F. Host factor Moloney leukemia virus 10 (MOV10) protein inhibits replication of the xenotropic murine leukemia virus-related virus (XMRV). *Bing Du Xue Bao*. (2014) 30:514–20.
68. Fu K, Tian S, Tan H, Wang C, Wang H, Wang M, et al. Biological and RNA regulatory function of MOV10 in mammalian germ cells. *BMC Biol*. (2019) 17:39. doi: 10.1186/s12915-019-0659-z
69. El Messaoudi-Aubert S, Nicholls J, Maertens GN, Brookes S, Bernstein E, Peters G. Role for the MOV10 RNA helicase in polycomb-mediated repression of the INK4a tumor suppressor. *Nat Struct Mol Biol*. (2010) 17:862. doi: 10.1038/nsmb.1824
70. Liu T, Sun Q, Liu Y, Cen S, Zhang Q. The MOV10 helicase restricts hepatitis B virus replication by inhibiting viral reverse transcription. *J Biol Chem*. (2019) 294:19804–13. doi: 10.1074/jbc.RA119.009435
71. Winter J, Jung S, Keller S, Gregory RI, Diederichs S. Many roads to maturity: microRNA biogenesis pathways and their regulation. *Nat Cell Biol*. (2009) 11:228–34. doi: 10.1038/ncb0309-228
72. Kawahara H, Imai T, Okano H. MicroRNAs in neural stem cells and neurogenesis. *Front Neurosci*. (2012) 6:30. doi: 10.3389/fnins.2012.00030
73. Li S, Wang L, Fu B, Dorf ME. Trim65: a cofactor for regulation of the microRNA pathway. *RNA Biol*. (2014) 11:1113–21. doi: 10.4161/rna.36179
74. Okamura K. Diversity of animal small RNA pathways and their biological utility. *Wiley Interdiscip Rev RNA*. (2012) 3:351–68. doi: 10.1002/wrna.113
75. Goodier JL, Cheung LE, Kazazian HH Jr. Mapping the LINE1 ORF1 protein interactome reveals associated inhibitors of human retrotransposition. *Nucleic Acids Res*. (2013) 41:7401–19. doi: 10.1093/nar/gkt512
76. Xie M, Li M, Vilborg A, Lee N, Shu M-D, Yartseva V, et al. Mammalian 5′-capped microRNA precursors that generate a single microRNA. *Cell*. (2013) 155:1568–80. doi: 10.1016/j.cell.2013.11.027
77. Huang F, Zhang J, Zhang Y, Geng G, Liang J, Li Y, et al. RNA helicase MOV10 functions as a co-factor of HIV-1 Rev to facilitate Rev/RRE-dependent nuclear export of viral mRNAs. *Virology*. (2015) 486:15–26. doi: 10.1016/j.virol.2015.08.026
78. Chang C-K, Chen C-J, Wu C-C, Chen S-W, Shih S-R, Kuo R-L. Cellular hnRNP A2/B1 interacts with the NP of influenza A virus and impacts viral replication. *PLoS ONE*. (2017) 12:e0188214. doi: 10.1371/journal.pone.0188214

Conflict of Interest: The authors declare that the research was conducted in the absence of any commercial or financial relationships that could be construed as a potential conflict of interest.

frontiers in Veterinary Science

HYPOTHESIS AND THEORY
published: 03 November 2020
doi: 10.3389/fvets.2020.593683

The "Bio-Crime Model" of Cross-Border Cooperation Among Veterinary Public Health, Justice, Law Enforcements, and Customs to Tackle the Illegal Animal Trade/Bio-Terrorism and to Prevent the Spread of Zoonotic Diseases Among Human Population

Paolo Zucca[1,2], Marie-Christin Rossmann[3,2], Jorge E. Osorio[4], Kevin Karem[5], Paola De Benedictis[6], Josef Haißl[7], Paola De Franceschi[8], Elisa Calligaris[8], Michaela Kohlweiß[9], Giulio Meddi[10], Wolfgang Gabrutsch[9], Horst Mairitsch[11], Oronzo Greco[12], Roberto Furlani[12], Marcello Maggio[13], Massimiliano Tolomei[14], Alessandro Bremini[1,2], Ingrid Fischinger[2,3], Paolo Zambotto[15], Peter Wagner[16], Yvonne Millard[17], Manlio Palei[1] and Gianna Zamaro[1]*

[1] Central Directorate for Health, Social Policies, and Disabilities, Trieste, Italy, [2] Bio-crime Veterinary Medical Intelligence Centre - c/o International Police and Custom Cooperation Centre, Thörl-Maglern, Austria, [3] Agriculture, Forestry, Rural areas Veterinary Department, Land Carinthia, Klagenfurt, Austria, [4] Department of Pathobiological Sciences, School of Veterinary Science, Madison, WI, United States, [5] Centre for Global Health Leadership, Centre for Disease Control and Prevention, Atlanta, GA, United States, [6] OIE Collaborating Centre and National Reference Centre for Infectious Diseases at the Animal-Human Interface, FAO and National Reference for Rabies, Istituto Zooprofilattico Sperimentale delle Venezie, Legnaro, Italy, [7] Public Prosecutor Office, Klagenfurt, Austria, [8] Public Prosecutor Office, Udine, Italy, [9] Police Direction of the Land Carinthia, Klagenfurt, Austria, [10] SCIP International Service of Police Cooperation, International Police and Custom Cooperation Centre, Thörl-Maglern, Austria, [11] Custom Office, Ministry of Finance, Klagenfurt, Austria, [12] Italian Financial Police, Regional Command Friuli Venezia Giulia Region, Trieste, Italy, [13] Italian Army, Regional Command Friuli Venezia Giulia Region, Trieste, Italy, [14] Smart Solution Mentor, Bologna, Italy, [15] Veterinary Services, Autonomous Province of South Tyrol, Bolzano, Italy, [16] Health and Care Management Department, Veterinary Services, Land Styria, Graz, Austria, [17] Veterinary Services, Land Burgenland, Eisenstadt, Austria*

OPEN ACCESS

Edited by:
Lester J. Perez, University of Illinois at Urbana–Champaign, United States

Reviewed by:
Jeanne Marie Fair, Los Alamos National Laboratory (DOE), United States
Irit Davidson, Kimron Veterinary Institute, Israel

***Correspondence:**
Paolo Zucca
zucca.paolo@regione.fvg.it

Specialty section:
This article was submitted to Veterinary Infectious Diseases, a section of the journal Frontiers in Veterinary Science

Received: *11 August 2020*
Accepted: *29 September 2020*
Published: *03 November 2020*

Citation:
Zucca P, Rossmann M-C, Osorio JE, Karem K, De Benedictis P, Haißl J, De Franceschi P, Calligaris E, Kohlweiß M, Meddi G, Gabrutsch W, Mairitsch H, Greco O, Furlani R, Maggio M, Tolomei M, Bremini A, Fischinger I, Zambotto P, Wagner P, Millard Y, Palei M and Zamaro G (2020) The "Bio-Crime Model" of Cross-Border Cooperation Among Veterinary Public Health, Justice, Law Enforcements, and Customs to Tackle the Illegal Animal Trade/Bio-Terrorism and to Prevent the Spread of Zoonotic Diseases Among Human Population. Front. Vet. Sci. 7:593683. doi: 10.3389/fvets.2020.593683

Illegal animal trade (pet, wildlife, animal products, etc.) is an example of transnational organized crime (T.O.C.) that generates a large business with huge profit margins. This criminal activity causes several negative effects on human health (zoonoses), animal health and welfare, market protection, consumer fraud and may be used as tool of agro/bio-terrorism. Illegal animal trade can facilitate the spread of zoonoses that are defined as diseases and infections that are transmitted by vertebrate animals to man. Humans are affected by more than 1,700 known pathogens: 60% of existing human infectious diseases are zoonotic and at least 75% of emerging infectious diseases of humans have an animal origin and 72% of zoonoses originate from wildlife or exotic animals. The Bio-Crime Project was developed in 2017 by Friuli Venezia Giulia Region (Italy) and Land Carinthia (Austria) together with other public institutions to combat illegal animal trade and to reduce the risk of disease transmission from animals to humans. Project partners agreed that a multi-agency approach was required to tackle

the illegal animal trade that was high value, easy to undertake and transnational crime. The Bio-crime model of cross-border cooperation introduces the novel approach of replicating the cooperative framework given by the triad of Veterinary Public Health, Justice and Law Enforcements/Customs across borders using the International Police and Custom Cooperation Centres (IPCCCs) as a connection link among public entities of the neighbor countries. This model has been recognized as a best practice at European level because it can be easily replicated and scaled up without any supplementary cost for Member States.

Keywords: bio-crime, veterinary services, law enforcements, medical intelligence, zoonoses, illegal animal trade, bio-terrorism, cooperation

INTRODUCTION

The European Union (EU) faces an increasing level of transnational crime where criminal conduct in one country has an impact on another or even on many others. Illegal animal trade (pet, wildlife, animal products, etc.) is an example of transnational organized crime (T.O.C.) that generates a large business with great profit margins. In 2015, the cat and dog trade involved 61 million dogs and 67 million cats in twelve EU Member States, representing €1.3 billion and generated a direct employment of about 300,000 workers (1, 2). This criminal activity and its negative impacts in terms of risks to human and animal health, are considered by the European Commission to be a real and emerging risk for Member States and the need to improve legislation at the EU and national level on the welfare of dogs and cats involved in commercial activities has been underlined since 2013 (2, 3). Illegal pet sellers do not pay taxes or bear any costs necessary for ethical breeding/transportation of pets and the impact on the EU market of this criminal activity generates several negative effects on human health (zoonoses), animal health and welfare, market protection, consumer fraud and agro/bio-terrorism (1, 4).

Zoonoses and Public Health

Illegal animal trade can facilitate a spread of zoonoses that are defined as diseases or infections that are transmitted by vertebrate animals to humans. In addition to being a public health problem, many of the major zoonoses prevent effective production of food of animal origin and create obstacles to the international trade in animal products (5). Humans are affected by more than 1,700 known pathogens: 60% of existing human infectious diseases are zoonotic. At least 75% of emerging infectious diseases of humans have an animal origin and 72% of zoonoses originate from wildlife or exotic animals. One factor leading to the emergence and spread of zoonotic infections is due to the increase of contacts between animals and humans that occurs for many disparate reasons (pets, food, population density, bush-meat, globalization and illegal animal trafficking) (6, 7). The trade in live animals and animal products is considered one of the major drivers of zoonotic disease emergence (8).

It is a mistake to think that the distribution and higher prevalence of zoonotic diseases is related to a higher density of mammalian hosts, meaning that the probability of contracting a zoonotic disease is higher in the tropical forests of the Old and New World. In fact, as reported by Han et al. (9) although major hotspots of mammalian hosts occur in the New and Old World tropics (South America and Eastern Africa, particularly), more zoonoses are concentrated in Northern latitudes, Eastern Africa, and Southeast Asia. According to these findings, it is very important to emphasize that zoonoses are not "exotic diseases" for North American and European citizens.

Bio-Terrorism and Public Health

Bio-terrorism can be defined as the use of biological agents to intentionally produce disease or intoxication in susceptible populations - humans, animals, or plants - to meet terrorist aims. Biological agents may be naturally occurring or genetically modified and generally, the types of agents used as biological weapons cause systemic diseases, haemorrhagic fevers, pneumonias, or involve toxins and biological poisons (6, 10, 11). Biological weapons suitable for terrorist attacks are easy to produce, conceal, and transport. Elaborate "weaponization" is not needed for attacks to cause considerable damage and they have potential for dissemination over large geographic areas. Some pathogens can survive to sunlight, drying, heat, and they can cause high morbidity, mortality, resulting in public panic. Person-to-person transmission is possible for some infectious agents, many of which are difficult to diagnose and/or treat (6, 10, 11).

Many naturally occurring pathogens could be used as well as genetically modified pathogens produced in a laboratory and this would make it difficult to discriminate between a naturally occurring outbreak and a bio-terrorist attack. In any case, regardless of whether the attack is related to a terroristic act or it is a naturally occurring outbreak, the damage caused by the biological agent is always significant for the affected country (see **Figure 1**).

Legal Framework Concerning Zoonoses and Public Health

The EU system for monitoring and collecting information on zoonoses is based on the Zoonoses Directive 2003/99/EC (12), which obliges European Union Member States to collect relevant and, when applicable, comparable data on zoonoses, zoonotic agents, antimicrobial resistance and food-borne outbreaks (FBO) (13). Data collection on human diseases from Member States is

FIGURE 1 | A truck with 2,615 parrots was confiscated on the Italian Austrian border of Tarvisio during a routine vehicle control by the Forestal Police of Friuli Venezia Giulia, December 2015. All the birds were infected with *Chlamydia psittaci* a zoonotic biosafety agent class III on IV of biosecurity level and recognized as a critical biological agent for public health. This agent can be transmissible by inhalation of contaminated dusts o contact with excretions but also by human-to-human infection (photos courtesy of Noava, Forestal Police of Friuli Venezia Giulia Region Italy).

conducted in accordance with Decision 1082/2013/EU (14) on serious cross-border threats to health. This Decision replaced Decision 2119/98/EC and identifies the fight against serious cross-border threats to health in response to planning and monitoring. Member States have to report data on infectious diseases to the European Centre for Disease Prevention and Control (ECDC) according to the Decision 2018/945/EU (15). Since 2008, data on human cases have been received by ECDC via The European Surveillance System.

The European Parliament Resolution 2019/2814 (16) of 12 February 2020 focuses on protecting the EU's internal market and consumer rights against the negative implications of illegal trade in companion animals. European Parliament Resolution P9 TA 0035 (17) approved on 14 February 2020 on a proposal from the Commission for the Environment, Public Health and Food Safety (SANI) indicates that profitable cooperation between Member States constitutes an urgent need and deems appropriate to promote and improve *ad hoc* training programs aimed at customs, medical and veterinary authorities in order to intercept pet illegal trade. This resolution underlines the importance of proposing training courses aimed at providing customs, medical and veterinary authorities with better tools for intercepting pet smuggling and highlights how Member States should ensure adequate staff training at borders.

The Bio-Crime Project and the Bio-Crime Center

The two Regions on the border between Italy and Austria, Friuli Venezia Giulia and Carinthia, are both transit routes as regions of destination for the illegal animal trade from Eastern European countries (mainly pet animals such as dogs, cats, birds, small mammals, and reptiles). The Bio-Crime Project (18) (www.biocrime.org) was developed in 2017 by Friuli Venezia Giulia Region and Land Carinthia together with other public institutions to combat illegal animal trade and to reduce the risk of disease transmission from animals to humans, following numerous criminal episodes and zoonotic infections that had occurred in both Regions. The objective of this joint action funded by the European Community by means of the Interreg V-A financial tool, is to protect the health and safety of citizens through health prevention strategies and repression of cross-border crime. One of the project output that will maintains the sustainability of the actions after the end of the project is represented by the Bio-crime veterinary medical intelligence center that has been created by Friuli Venezia Giulia Region and Land Carinthia (19). This cross-border joint center put together all the public entities involved in tackling Transnational Organised Crime (TOC) related to the illegal animal trade and it is based into the International Police and Custom Cooperation Centre (IPCCC) of Thörl-Maglern (Austria). It is the first Veterinary Medical Intelligence Centre based inside an IPCC Centre in Europe. From a symbolic point of view, it represents the first neuronal synapse among the Veterinary Public Health, Justice and Law Enforcement/Customs Networks at a downside horizontal level (see also **Figures 2**, **4**).

Public Entities Involved in Tackling TOC/Illegal Animal Trade and the Related Spread of Zoonoses

The public entities involved in tackling illegal animal trade and the related spread of zoonotic diseases among human population on the border between Italy and Austria, work within the framework of the Bio-crime project and belong to:

- Justice (Public Prosecutors Offices of Udine Italy and Klagenfurt Austria);
- Veterinary Services and Laboratories of Friuli Venezia Giulia Region Italy and Land Carinthia Austria;

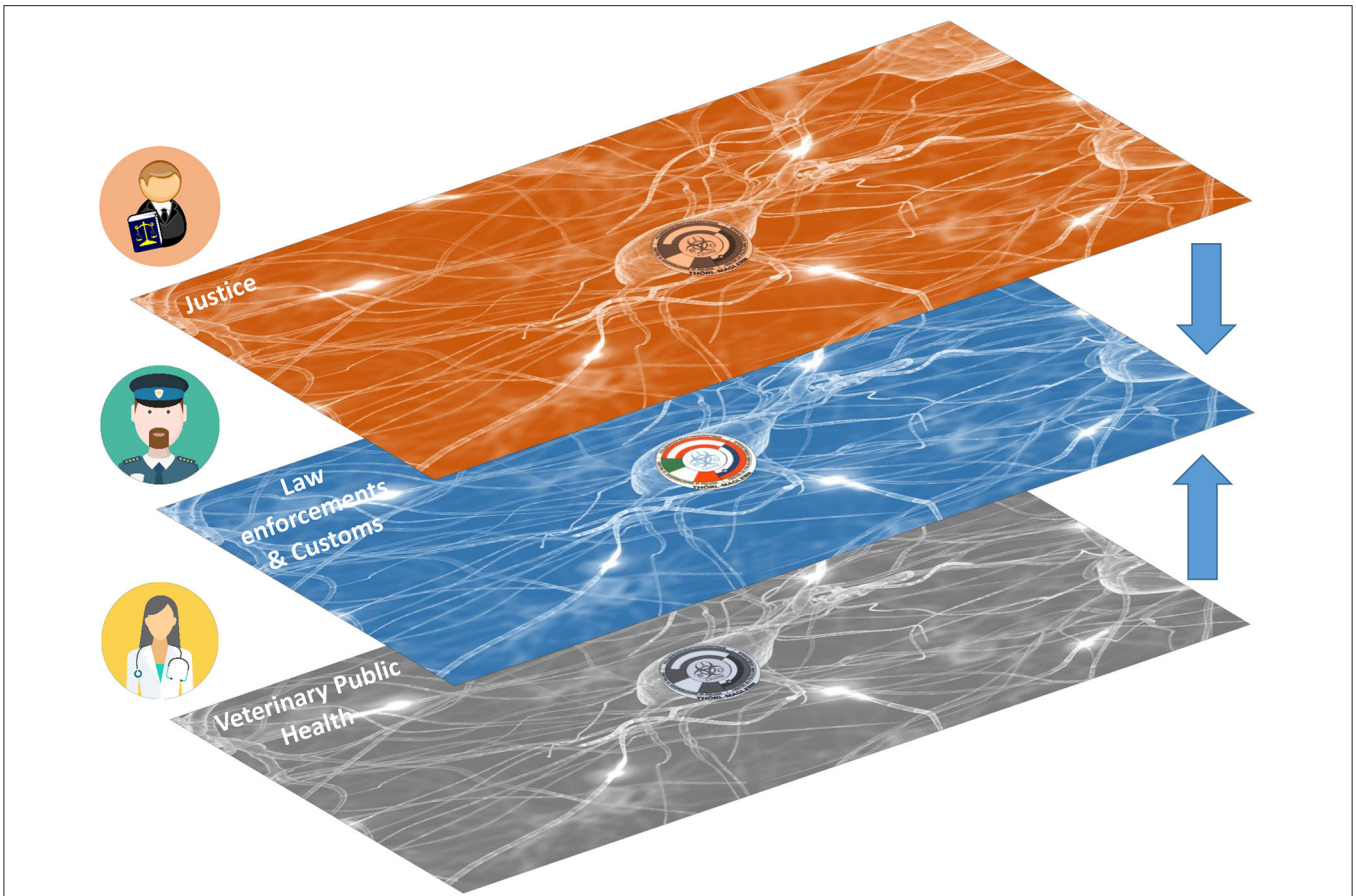

FIGURE 2 | The International Police and Custom Cooperation Centre (IPCCC) of Thörl-Maglern (Austria) is the first IPCCC in Europe that host a connection link (synapse) among the Veterinary Public Health, Justice, Law Enforcements and Customs Networks (icons of Veterinarian, Policeman and Judge from Wikimedia Commons, the free media repository; synapse layer's patterns from Internet, source unknown, modified).

- Law Enforcements and Customs of Italy and Austria;
- The International Police and Custom Cooperation Centre (IPCCC) of Thörl-Maglern.

An International Police and Custom Cooperation Centre (IPCCC) is an institution established by the EU national Police according to the Art. 39 of the Convention implementing the Schengen agreement for a better cross-border cooperation among the Law Enforcements and Customs of the Member States. In an International Police and Custom Cooperation Centre (IPCCC), officials from at least two, sometimes even several Member States, work together both in the office and in the field. On one hand, investigations by the security apparatuses of one State to another are processed directly by the respective officials in the cooperation center and allow efficient and rapid work, on the other hand a common field service is provided by patrolling the border area. The first International Police and Custom Cooperation Centre (IPCCC) among Austria, Italy and Slovenja was established in Thörl-Maglern in 2005 and it hosts the law enforcement representatives of Austria, Italy, Slovenja and Germany. At present there are more than 40 International Police and Custom Cooperation Centres (IPCCCs) distributed along the internal and external borders of the European Community.

The Organizational Sector of Public Entities Involved in Tackling Transnational Organized Crime (TOC) and Illegal Animal Trade

All the European public entities (Veterinary Public Health, Justice, Law Enforcements/Customs, IPCCCs) involved in tackling TOC/illegal animal trade are organized hierarchically top-down around vertical chains of command. This type of structure resembles a pyramid and gets wider as you move down. Roles are clearly defined within this structure, and every unit knows to whom it should report. However, on the downside, horizontal communication between different units may be poor, as the system is built around a vertical chain of command and furthermore all the different pyramid's layers of bureaucracy can slow down decision making and reduce the capability of the public entity to collaborate with other agencies and adapt to fast "environmental changes" (see **Figure 3**).

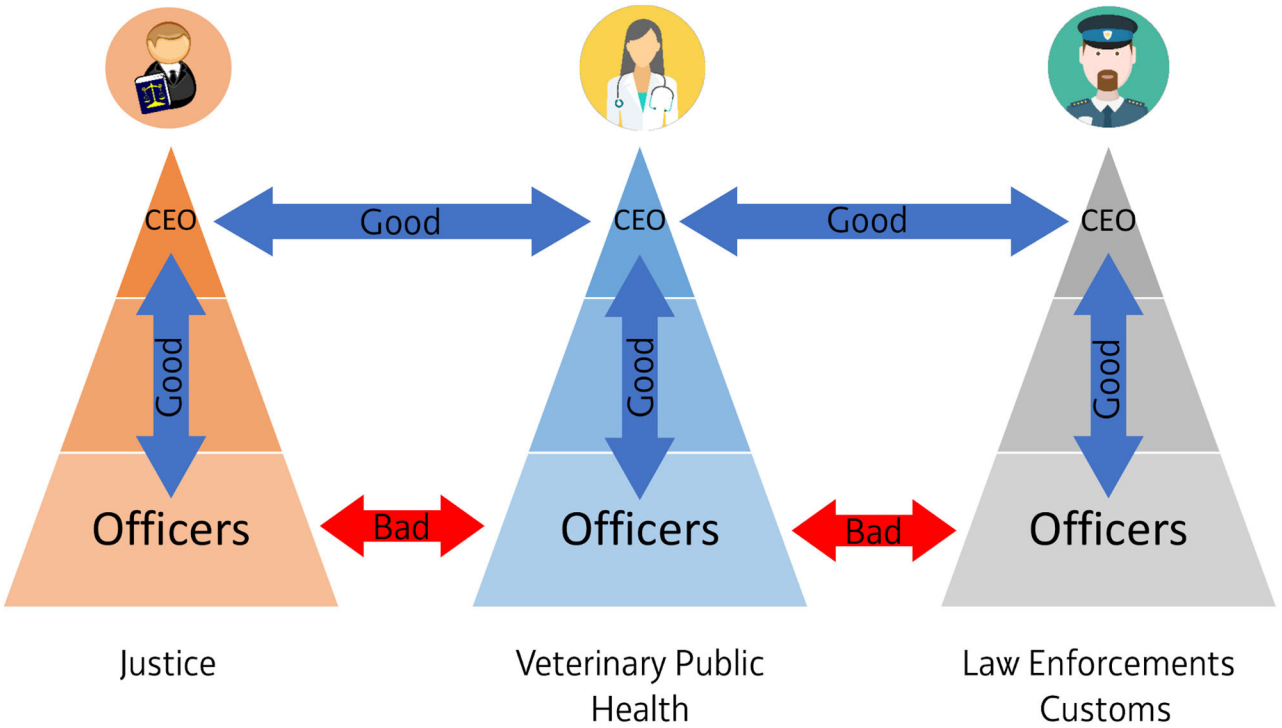

FIGURE 3 | Organizational communication within and among public entities involved in tackling Transnational Organized Crime/Illegal animal trade. Vertical communication within a pyramidal structure is good although is time spending and slow down decision making (blue arrows). Horizontal communication among top management of different structures is good (blue arrows) while on the downside level, horizontal communication among Officers of different structures is poor (red arrows) (icons of Veterinarian, Policeman and Judge from Wikimedia Commons, the free media repository).

MATERIALS AND METHODS

Public entities belonging to the Veterinary Public Health, Justice, Law Enforcements/Customs and IPCCC of both side of the Italian-Austria border agreed that a multi-agency approach was required to tackle the illegal animal trade that was high value, easy to undertake and transnational crime. Such trade is endangering human and animal health by facilitating the spread of diseases and threatening economic security and public safety. In order to be effectively countered, this illegal trade requires a coordinated transnational response as well defined by "Decision no. 1082/2013 of the European Parliament and of the European Council on serious cross-border threats to health" that explain how preparedness and response planning are essential elements for effective monitoring, early warning and the fight against serious threats to cross-border health.

The Bio-crime cooperation model has been developed through a process of refinement of cross-border cooperation procedures between Friuli Venezia Giulia and Carinthia started in 2017. Initially, the increase in the exchange of information and cooperation between public entities at regional cross-border level occurred only between Veterinary Public Health services of Friuli Venezia Giulia Region (Italy) and Carinthia (Austria) that analyzed the problem and decided to enlarge the stakeholder's participation. Subsequently, the other two main stakeholders of the Bio-crime cooperative model represented by Justice and Law Enforcements/Customs were involved since only a rapid and horizontal communication that could take place also at the downside and horizontal level guaranteed an effective response to the contrast of the Transnational Organized Crime (TOC) and at the same time allowed the implementation of health prevention procedures for staff and citizens of the two Regions. The main connection link of the cross-border cooperation procedure was identified as the International Police and Custom Cooperation Centre (IPCCC) of Thörl-Maglern on the Italian-Austrian border that since December 2019 hosts the joint Friuli Venezia Giulia Region and Land Carinthia Bio-crime Veterinary Medical Intelligence Centre.

RESULTS

Cross-Border Model of Cooperation

The structural and functional architecture of the "Bio-crime model" of cooperation is described in **Figure 4**. One Region institutional triad represented by Veterinary Public Health, Justice, Law Enforcements/Customs is replicated specular on the other side of the border and the International Police and Custom Cooperation Centre (IPCCC) of Thörl-Maglern acts as the main connection link of the cooperation system. The IPCCC of Thörl-Maglern hosts the Bio-crime center office and two local branches at the Central Veterinary Directorates of Friuli Venezia

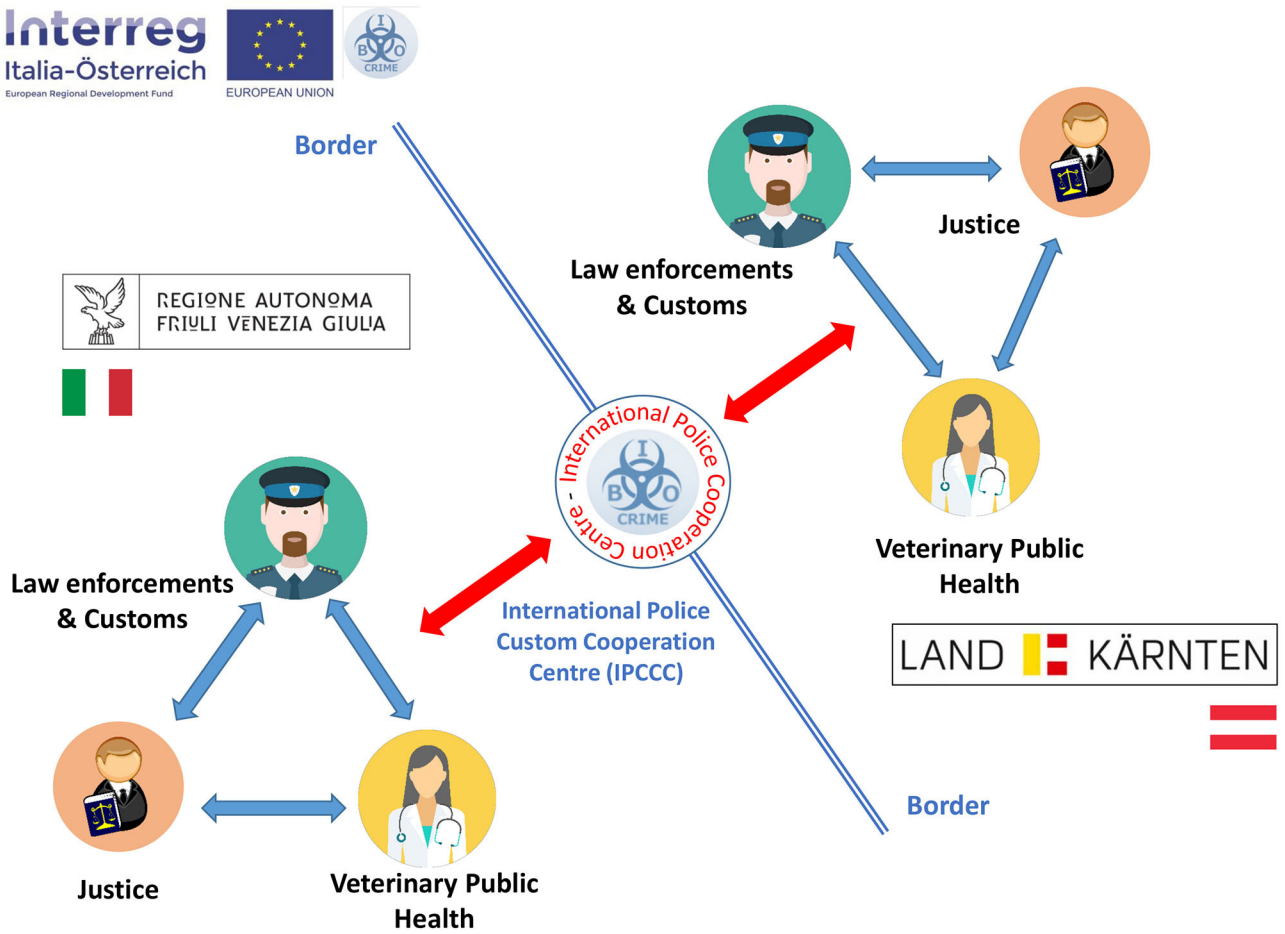

FIGURE 4 | Bio-crime model of cross-border cooperation among Veterinary Public Health, Justice and Law Enforcements/Customs. The International Police and Custom Cooperation Centre (IPCCC) of Thörl-Maglern acts as the link between the two specular triad of public entities (icons of Veterinarian, Policeman and Judge from Wikimedia Commons, the free media repository).

Giulia and Carinthia in Trieste and Klagenfurt, respectively, have been established.

Performance Indicators of Cross-Border Institutional Cooperation Before and After the Bio-Crime Program

The Bio-crime model has consolidated the institutional cooperation among five neighboring European Regions through the development of training programs for Law enforcements/Customs/Medical and Veterinary Officers, health prevention programs on biological risk/zoonoses in schools and development of Standard Operation Procedures (SOP) and best practices at a cross-border level. The different entities involved in the program exchange data directly during cross-border monthly meetings at the IPCCC of Thörl-Maglern or digitally via secure intranet institutional Share-Points. Furthermore, an alert system named "Bio-crime alert," for short and fast communications within the partner's network has been established via an institutional mailing list. The performance indicators of institutional cross-border cooperation before and after the establishment of the Bio-crime program are summarized in **Table 1**.

Illegal Pet Trade Cross-Border Data Collection and Analysis Before and After the Bio-Crime Program

Prior to the development of the Bio-crime program, a comprehensive shared database on illegal pet trade data at cross-border level was not available. Over the years, the Bio-crime alert data sharing platform has made it possible to share information on the (i) country of origin, (ii) number of events, (iii) pet species prevalence, (iv) absolute numbers of dog and cat puppies confiscated, (v) prevalence of sanitary quarantine on the total number of pets, (vi) number of pets tested every year, (vii) diseases that are looked for through laboratory testing and a tendency indicator of the increase or decrease of the illegal pet trade over time (**Table 2**).

TABLE 1 | Performance indicators of cross-border institutional cooperation before and after the Bio-crime program.

Public entities	**Units**	**Before**	**After**	**Note**
Institutional cooperation established among Justice, Law Enforcements, Customs and Veterinary Services	Number	0	13	n. 2 Public Prosecutor Offices, n. 6 Law enforcements, Customs and Army, n. 5 Regional Veterinary Services
Regions involved	Number	0	5	Friuli Venezia Giulia, Land Carinthia, South Tyrol Province of Bolzano, Land Styria, Land Burgenland
People	**Units**	**Before**	**After**	**Note**
Law Enforcements/Public Officers trained during the past 3 years	Number	0	1.072	Customs and Law enforcements belonging to several different specialties, Medical and Veterinary Officers
Students involved into the health prevention program	Number	0	656*	Age cluster 11–13 years-old
Standard Operation Procedures (SOP)	**Units**	**Before**	**After**	**Targets**
SOP Public Prosecutors Offices (procedure for the correct execution of investigative activities/reports)	number	0	1	Law Enforcements/Customs, Veterinary Officers
SOP for Vehicle inspections (procedure for the correct and safe inspection of vehicles that might transport pet animals)	Number	0	1	Law Enforcements, Customs and Veterinary Officers
SOP Veterinary Public Health (procedure for the correct management of the confiscated animals /zoonotic risk)	Number	0	1	Public Prosecutors, Law Enforcements/Customs, Medical and Veterinary Officers

**The school's program involved also students from Slovenja, Germany, Mauritius, and Japan.*

TABLE 2 | Illegal pet trade data collection and analysis at cross-border level.

Illegal pet trade data	**Units**	**Before**	**After**	**Note**
Countries of origin	Number	Unkonwn*	13	Ukraine, Hungary, Romania, Slovakia, Poland, Bulgaria, Austria, Slovenja, Czech Republic, Serbia, Bosnia, Russia, China.
Events caught (Dec 2017–July 2020)	Number	Unkonwn*	40	Two peaks with four events per month in May 2018 and Sept 2019.
Pet species prevalence (Dec 2017–July 2020)	%	Unkonwn*	Dogs, cats, birds	In order of decreasing prevalence.
Puppy's dogs and cats confiscated (Dec 2017–July 2020)	Number	Unkonwn*	652	Maltese, French bulldog, Golden retriever, Terriers and Chihuahua puppies for dog breeds while Scottish folds for cats breeds show the higher prevalence among confiscated pets.
Sanitary quarantine on the total number of pets	Number	Unkonwn*	77.5%	Health documents or identification or country of origin data were missing.
Number of pets tested every year	Number	Unkonwn*	All	Until Dec. 2020.
Diseases that are looked for through laboratory testing	Category	Unkonwn*	Zoonotic and notifiable diseases	Among zoonotic diseases laboratories are focusing especially on Salmonellosis, Chlamydiosis, Rabies, endo-ectoparasites, and other notifiable diseases.
Illegal pet trade tendency indicator	Trend	Unkonwn*	Light increase	Very difficult to assess because at present many illegal pet transactions are placed via Internet and many pets are delivered directly from traders to buyers without any intermediate.

**A comprehensive shared database at cross-border level was not available before the establishment of the Bio-crime program.*

Furthermore, this dataset cross-checked with data reported on the documents that accompany the animals, with particular reference to the presence of a transponder for individual identification, the pet passport, the valid rabies vaccination certificate, of a clinical examination by a veterinarian within 48 h prior to departure and of the TRACES certificate, if relevant, as shown in **Figure 5**.

The Cost-Benefit Ratio (CBR) of the Program Investments of the Bio-Crime Project

It is always complex to provide a quantitative analysis of the Cost-Benefit Ratio (CBR) applied to the areas of crime reduction and health prevention since the positive effects of preventive actions in these two areas are not easily quantifiable financially and they

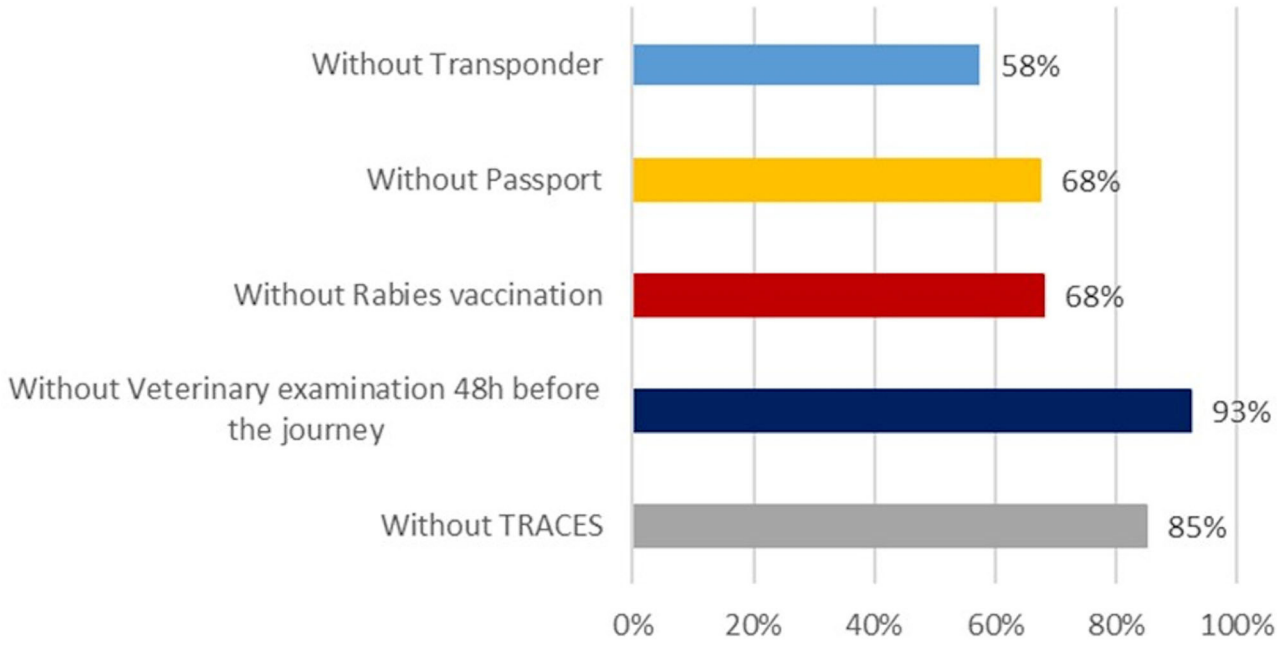

FIGURE 5 | Missing documents of confiscated pets (dog and cat puppies $n = 652$) in Friuli Venezia Giulia Region Italy, Autonomous Province of South Tyrol Bolzano Italy and Land Carinthia Austria (Dec 2017–July 2020).

are often difficult to link to a specific geographical area. In order to provide the clearest picture of the CBR relating to the Bio-crime program, the analysis will focus on two specific project scenarios represented by (i) Free training courses on biological risks/zoonoses and by (ii) Border controls on illegal pet trade.

The Cost-Benefit Ratio (CBR) of Free Training Courses on Biological Risks/Zoonoses

A total number of 1,072 law enforcements, customs, medical and veterinary officers have attended the free training courses over the past 3 years. The average cost on the market of a 2-day training course on these subject amount to about €2,300. and therefore the cost avoidance for the public system for 1,072 units of personnel is €2,465,600. As the budget of the Bio-crime project Working Package (WP) 4 allotted to training courses was €120,000. the CBR amount to 19.57 meaning that the benefit was almost twenty times the budget cost.

The Cost-Benefit Ratio (CBR) of Border Controls on Illegal Pet Trade

The border controls for tackling illegal animal trade are not part of a specific Working Package (WP) of the project as they include personnel, administrative, travel costs, health screenings on confiscated animals, and training courses for staff members; to avoid any overestimation of the CBR, it was decided to consider the entire budget of the project (€1,117,300) as the overall cost of the project program. Taking as an example the scenario of 2,615 parrots infected with *Chlamydia psittaci* confiscated at the Italian-Austrian border, if these animals were sold on the market and assuming the best epidemiological scenario a low transmission rate between parrots and humans with absence of human-to-human transmission of the infection, the costs of the outbreak for the public health system would approximately be €35 M. The worst epidemiological scenario includes in the model the possibility of a human-to-human transmission of the pathogen with a basic reproductive rate $R_0 = 10$ (20). The estimated costs of the outbreak for the health system could therefore rise up to €350 M (21). Assuming the best epidemiological scenario, the CBR would be 31.32 while for the worst it could reach 313.20.

DISCUSSION

Cross-Border Model of Cooperation

There are several examples of joint cooperation programs among veterinary services and law enforcement/customs agencies all over the world although these programs don't normally involve a third important actor, i.e., the judiciary system. The Bio-crime model includes in its cooperative framework also public prosecutors whose contribution is essential to tackle the illegal animal trade and reduce the related health risks for citizens. Furthermore, this model introduces the novel approach of replicating the cooperative framework across borders using the International Police and Custom Cooperation Centres

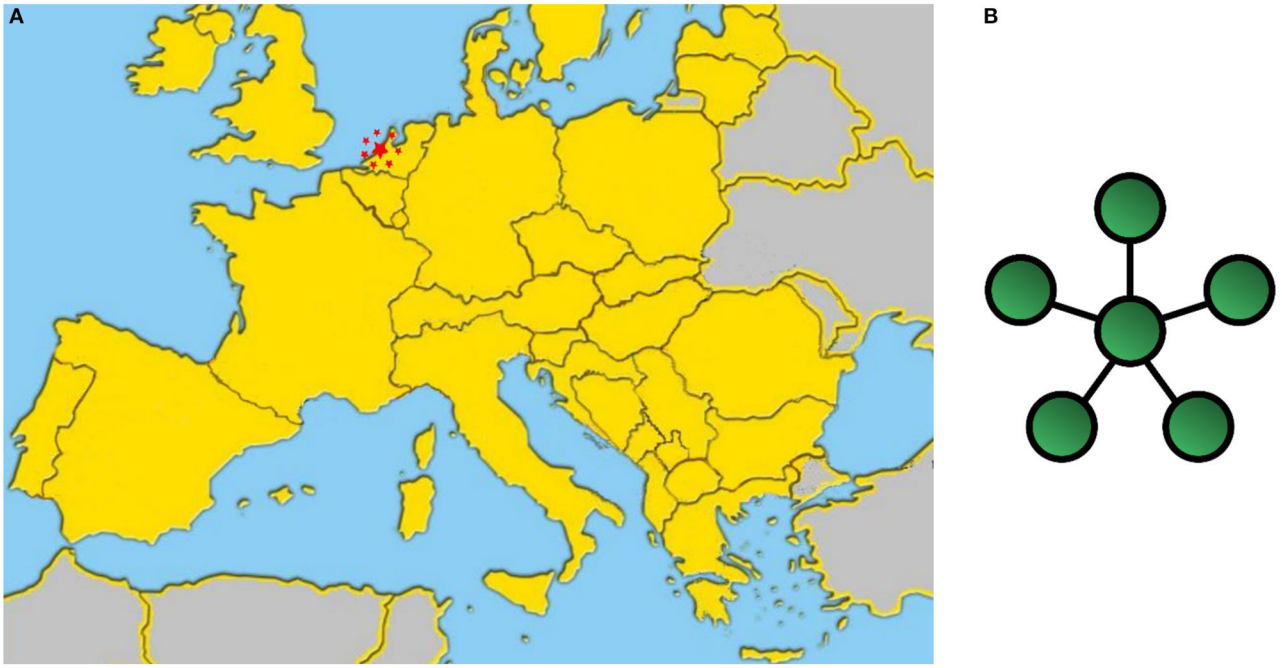

FIGURE 6 | (A) The "centralized star network" approach uses a single EU task force that brings together all the stakeholders of the EU Member States; **(B)** Network topology of a star network (icon 6B from Wikimedia Commons, the free media repository).

(IPCCCs) as a connection link among public entities of neighboring countries.

According to this new approach, at European level the "Bio-crime model" has been recognized as a best practice that can be easily replicated and scaled up without any supplementary cost for the Member States. In fact, the Veterinary Public Health, Justice, Law Enforcements/Customs and IPCCCs infrastructures already exist all over Europe. It is only a matter of involving all the public stakeholders and increasing the downside horizontal communication among different public entities of the framework. The model has been discussed during the conference "*Illegal pet trade: Game over*" organized by the Eurogroup for animals and the Croatian Presidency of the European Council (Bruxelles 21 April 2020) and it has been listed among the recommendations for the European Union as follows: "*Other enforcement projects should be funded under the European Regional Development Fund and Internal Security Fund based on the Bio-crime model at key borders crossed by the puppy trade using the links between animal and human health and the 43 IPCCCs*" (1).

There are at least two main approaches that could help to contrast the illegal animal trade and bio-terrorism. One "*centralized star network*" approach to solve the problem is to create a single EU task force, hosted by an existing European agency such as EUROPOL for instance, that brings together all the stakeholders of the EU Member States (see **Figures 6A,B**).

Another approach, represented by the "Bio-crime model" can easily be scaled at European level by means of a "*fully connected network*" perspective: the architecture of such model connecting Veterinary Public Health, Justice, Law Enforcements and Customs at a cross-border level as described in **Figure 5**, is replicated in every International Police and Custom Cooperation Centre (IPCCCs) of Europe that are already connected one to each other (see also **Figures 7A,B**).

Both approaches have advantages and disadvantages: a "*centralized star network*" provides a global view of what is happening all over Europe and allows the implementation of common strategies; however, at the same time its centralized architecture limits its connections with the fields. Furthermore, the fault/delay response of the central node (Central Agency) will stop the whole network activity. On the other hand, the "*fully connected network*" of the "Bio-crime model" is much more responsive and appropriate to investigate, and it guarantees more rapid decisions at local level. According to our experience, the "*centralized star network*" EU task force and the Bio-crime "*fully connected network*" models are not opposed but complementary because one node represented by a IPCCC of the Bio-crime model can acquire, even if temporarily, a higher hierarchical level and coordinate the activities of the others. In case of fault/slowdown of the lead node (Central Agency), the highest hierarchy level can be immediately shifted to an IPCCC, thus keeping the network always active and efficient.

Illegal Pet Trade Phenomena at Cross Border Level

The illegal pet trade data collected by the Bio-crime program allows us to have an exhaustive picture of this criminal activity that transports pets from Eastern countries to Europe and sells

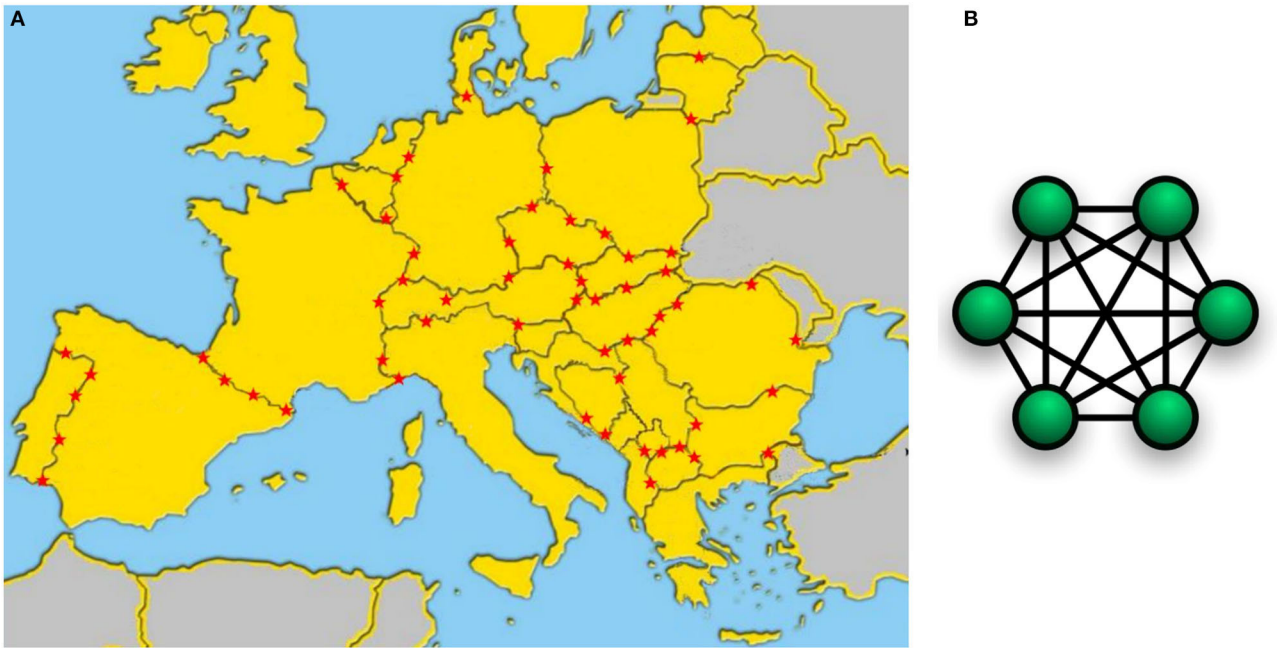

FIGURE 7 | (A) The "Bio-crime model" can easily be scaled at European level by means of a "fully connected network" approach: the architecture of the Bio-crime model that connects Veterinary Public Health, Justice, Law Enforcement and Customs at a cross-border level as described in **Figure 4**, is replicated in every International Police and Custom Cooperation Centre (IPCCCs) of Europe (identified with a red star). Each IPCCC is already connected one to each other; **(B)** (right) Network topology of the "fully connected network" used by the Bio-crime model where all nodes (IPCCCs) are interconnected (icon 7B from Wikimedia Commons, the free media repository).

them on black markets. Over time, the countries of origin of the illegal pet trade have changed their attitude and have become more involved, not only non-European countries relatively close to the EU borders such as Ukraine, but also countries such as Russia or even China. The number of events and the prevalence of the species are quite constant over time. Dog and cat puppies and birds are the pet species most subject to illegal pet trade. Most of the confiscated animals don't have an identification device, pet passport or valid rabies vaccination and they represent a serious health risk. In order to avoid the introduction of infectious diseases into the EU countries, 77.5% of the 652 puppies confiscated between December 2017 and July 2020 were placed in sanitary quarantine by the local Veterinary Officers. Thanks to the financial support from the Bio-crime project, it was possible to perform laboratory tests to all the confiscated animals and carry out necropsies on those that had died during transport or while in sanitary quarantine. It is difficult to briefly summarize the results of the laboratory survey performed on the confiscated animals although, it was surprising to discover that (i) almost 100% of the confiscated cat and dog puppies were positive for *Toxocara* sp., an intestinal zoonotic nematode transmissible to humans; (ii) about 5.5% of the dog and cat puppies were positive to *Salmonella* sp.; (iii) serological investigation displayed failure in post-rabies vaccination immunity in about 75% of total analyzed, a percentage even worse than previously described (22) while *Chlamydia psittaci*, Canine distemper and Parvovirus have been isolated quite frequently in the target species. Although most zoonoses evolve from wildlife hosts, most of them need an intermediate domestic/pet hosts transmission to be able to spread to human (23–25). For this reason, the choice of focusing the health monitoring procedures on confiscated pets coming from the illegal trade developed by the Bio-crime project can improve the effectiveness of human and animal health prevention procedures and reduce the risk of incursion of zoonotic and exotic animal diseases into the EU Member States (4, 26).

Illegal Pet Trade, On-Line Illegal Pet Trade and Bio-Terrorism

The economic impact of a zoonotic event (natural, accidental, or deliberate) is difficult to assess because it changes according to the different pathogen. However, small-scale events can generate high economical losses (21, 27) and the example of Chlamydia-infected parrots mentioned in the results section confirms how true this statement is. The total value of the parrots and the truck used to transport these animals did not exceed €5,000 while the damage they could have caused to the health system if they had been sold on the market ranged between €35 and €420 M. A single event of this kind, regardless of whether the introduction of the pathogen is natural, accidental or deliberate, can lead to a default of the health system in a whole Region.

Through the simultaneous use of different tools, the Bio-crime program has contributed to reduce the risk of natural, accidental or deliberate introduction of pathogens dangerous for human and animal health. First, suspicious transports were examined

with great attention posed to the species of animals transported, to the infectious isolated diseases and, in particular to the Cost-Benefit Ratio (CBR) between the value of the transported pets and the distance traveled by car. For instance, transporting only few puppies in a vehicle traveling for days from Asia to Europe is a suspicious behavior, as the sale value of the puppies on the market does not even cover the cost the fuel.

Furthermore, the online trade of dogs, cats and other pet species was monitored simultaneously with a veterinary medical intelligence approach. This trade, and digital technologies in general, can pose significant challenges for the competent authorities of the Member States operating within national boundaries, particularly as their systems of official controls may not be adequately adapted to deal with the rapidly evolving character and cross-boundary nature of internet commerce (28). Open Source Intelligence (OSINT) tools were also used to monitor the on-line illegal pet trade, while computational linguistic and sentiment analysis tools were used to profile illegal animal traders and to analyze bio-terroristic claims.

The Cost-Benefit Ratio (CBR) of the Program Investments of the Bio-Crime Project

The results of a 3 years cross-border cooperation extended also to the health sector confirm what has already been widely reported in the scientific literature, namely that local public health interventions are highly cost-saving. Free trainings generate a saving rate higher than the entire project budget with a Cost-Benefit Ratio that is almost 20 times the budget used while the cost avoidance related to the spread of infectious diseases transmissible from animals to humans can generate a Cost-Benefit Ratio that for a single criminal event can reach up to 313 times the whole budget of the project. Therefore, cuts to public health budgets in high income countries therefore represent a false economy, and are likely to generate billions of Euro of additional costs to health services and the wider economy (29).

CONCLUSIONS

The prevention and control of zoonotic diseases related to the illegal pet trade is not only a matter of the cooperation architecture model but requires a strong communication network and a continuous training education program for all the stakeholders involved. The public health infrastructure must look beyond passive surveillance of acute animal disease events to build capacity for active surveillance and intervention efforts to detect and control on-going outbreaks of disease in domestic and wild animal populations (30). In fact, there are no short cuts, because you can control disease only with laboratory capacity, workforce training (epidemiology, clinical, laboratory, IT, …), surveillance and network communications across political boundaries (31, 32). It will be more and more important to use a medical intelligence approach, including also social media content analysis, during the processes of data collection, data analysis and data sharing at cross-border level for a better prevention, monitoring and control of zoonotic diseases (21, 33).

"Although it is difficult to make predictions, especially those about the future" (quot. by Niels Bohr), the use of predictive models for risk assessment in veterinary medicine is becoming increasingly important as demonstrated for instance by the "spatial risk assessment model framework for incursion of exotic animal disease into the European Union Member States" by Simons et al. (34) and by the Handbook for the Assessment of Capacities at the Human-Animal Interface (35, 36). The Bio-crime model of cross-border cooperation is placed within the context of Organizational modeling that integrates organizational structure, goals, behavior and components and has been developed to improve the veterinary health prevention procedures at cross-border level. Such model proves that an increase in communication and data sharing on a horizontal level among public officers belonging to different disciplines like Justice, Law enforcements, Customs, Veterinary public health, improves the early-warning system, increasing the capacity to detect, report, assess and respond to the entry of zoonotic infectious diseases into the EU Member States according to the International Health Regulation standard (35, 36).

Despite that fact that 60% of existing human infectious diseases are zoonoses and most of the bioterrorism threat agents are zoonotic disease agents, veterinary medical expertise is scarcely present in biohazard training and education programs for law enforcement agencies and public officials. We hope that in the near future, collaboration and data sharing between Veterinary public health, Justice, Law Enforcements and Customs engaged in the fight against illegal animal trade and agro/bio-terrorism, will increase (21). In fact, "without data you're simply another person with an opinion" (quot. W.E. Deming).

DATA AVAILABILITY STATEMENT

The datasets generated for this study can be found in online repositories. The names of the repository/repositories and accession number(s) can be found at: https://www.biocrime.org/frontiers-data-repository.

ETHICS STATEMENT

Ethical review and approval was not required for the animal study because scientific data related to the pet animals mentioned in the article come from clinical and laboratory examinations performed by the Public Veterinary Health Authorities on confiscated pets. The only aim of these veterinary procedures was to diagnose diseases and treating ill confiscated pets as required by EU and national MS legislation for the protection and welfare of animals/zoonoses protection. Confiscated pets have not been subjected to any further procedures other than those required by law. According to current EU and MS legislation, routine public health veterinary procedures on confiscated pets from the illegal animal trade don't fall under the legislation on laboratory animals research and don't require the authorization of an ethical committee.

AUTHOR CONTRIBUTIONS

PZu, M-CR, MK, WG, GM, HM, PW, PDF, EC, and JH conceived of the idea of developing a cross-border model of cooperation. PZu wrote the manuscript proof. All authors discussed the results and contributed to the final version of the manuscript.

FUNDING

This study was supported by the European Regional Development Fund - Interreg V-A Italia-Österreich, Bio-crime Project, project Code ITAT3002 and by the Bio-crime centre of Friuli Venezia Giulia Region, Italy and Land Carinthia, Austria (www.biocrime.org).

ACKNOWLEDGMENTS

Authors would like to thank Dr. Roberto Balbo, World Organization for Animal Health, OIE, Sub-Regional Representative in Brussels and Dr. Tonie Rocke, USGS, National Wildlife Health Centre, Wisconsin for their useful comments on the manuscript and their long term support to the Bio-crime project. Dr. Antonio De Nicolo, Public Prosecutor, Public Prosecutor Office of Trieste, Italy for his long term support to the Bio-crime project. NOAVA, Forestal Police of Friuli Venezia Giulia Region, Italy, for providing photos of **Figure 1**. Monia Cocchi, Patrizia Danesi, Francesca Ellero and all the IZSVe staff contributing to the project. Angelika Foltin-Hoffmann of Land Burgenland Austria and Iwona Mertin of the Eurogroup for Animals Bruxelles for data and procedures sharing about illegal pet trade.

REFERENCES

1. Croatian Presidency of the Council of the European Union and Eurogroup for Animals. *Report of the conference "The Illegal Pet Trade: Game Over"*. Bruxelles: Croatian Presidency of the Council of the European Union and Eurogroup for Animals (2020). Available online at: https://www.eurogroupforanimals.org/sites/eurogroup/files/2020-06/Report_Illegal%20Pet%20Trade_%20Game%20Over_2020.pdf (accessed June 18, 2020).
2. SANCO. *Study on the Welfare of Dogs and Cats Involved Incommercial Practices*. SANCO (2015). SANCO contract 2013/12364. Available online at: https://ec.europa.eu/food/sites/food/files/animals/docs/aw_eu-strategy_study_dogs-cats-commercial-practices_en.pdf (accessed July 7, 2020).
3. *Regulation (EU) 2016/429 of the European Parliament and of the Council of 9 March 2016 on Transmissible Animal Diseases and Amending and Repealing Certain Acts in the Area of Animal Health* ('Animal Health Law'). Available online at: https://eur-lex.europa.eu/legal-content/EN/TXT/PDF/?uri=CELEX:32016R0429&from=EN (accessed July 7, 2020).
4. Zucca P. Biocrime alert procedure related to the illegal animal trade/zoonoses of the Veterinary Public Health Unit of Friuli Venezia Giulia Region, Italy. In: *Proceedings of Bio-crime Conference "The Integration of the One Health Approach in Veterinary Public Health and Education"*. Trieste: Area Science Park (2018).
5. FAO, OIE, WHO. *A Tripartite Guide to Addressing Zoonotic Diseases in Countries*. World Health Organization (WHO), Food and Agriculture Organization of the United Nations (FAO) and World Organisation for Animal Health (OIE) (2019). Available online at: http://www.fao.org/3/ca2942en/ca2942en.pdf (accessed June 18, 2020).
6. Friend M. *Disease Emergence and Resurgence: The Wildlife-Human Connection*. Reston, VA: US Geological Survey, Circular 1285 (2006). 400 p.
7. OIE. *OIE Biological Threat Reduction Strategy, Strengthening Global Biological Security*. (2015). Available online at: https://www.oie.int/fileadmin/Home/eng/Our_scientific_expertise/docs/pdf/A_Biological_Threat_Reduction_Strategy_jan2012.pdf (accessed July 2020).
8. van Roon A, Maas M, Toale D, Tafro N, van der Giessen J. Live exotic animals legally and illegally imported via the main Dutch airport and considerations for public health. *PLoS ONE*. (2019) 14:e0220122. doi: 10.1371/journal.pone.0220122
9. Han BA, Kramer AM, Drake JM. Global patterns of zoonotic disease in mammals. *Trends Parasitol*. (2016) 32:565–77. doi: 10.1016/j.pt.2016.04.007
10. Osorio J. Biodefense pathogens. In: *Proceedings of Bio-Crime Conference "The Integration of the One Health Approach in Veterinary Public Health and Education"*. Trieste: Area Science Park (2018).
11. Friend M. Biowarfare, bioterrorism, and animal diseases as bioweapons. In: Friend M, editor. *Disease Emergence and Resurgence: The Wildlife-Human Connection*. Reston, VA: U.S. Geological Survey, Circular 1285 (2006). 400 p.
12. *Directive 2003/99/EC of the European Parliament and of the Council of 17 November 2003 on the Monitoring of Zoonoses and Zoonotic Agents, Amending Council Decision 90/424/EEC and repealing Council Directive 92/117/EEC*. Available online at: https://eur-lex.europa.eu/legal-content/EN/TXT/PDF/?uri=CELEX:32003L0099&from=EN (accessed June 18, 2020).
13. EFSA and ECDC (European Food Safety Authority and European Centre for Disease Prevention and Control). The European Union One Health 2018 Zoonoses Report. *EFSA J*. (2019) 17:e05926. doi: 10.2903/j.efsa.2019.5926
14. *Decision No 1082/2013/EU of the European Parliament and of the Council of 22 October 2013 on Serious Cross-Border Threats to Health and Repealing Decision No 2119/98/EC*. Available online at: https://ec.europa.eu/health/sites/health/files/preparedness_response/docs/decision_serious_crossborder_threats_22102013_en.pdf (accessed June 18, 2020).
15. *Decision 2018/945/EU of 22 June 2018 on the Communicable Diseases and Related Special Health Issues to be Covered by Epidemiological Surveillance as well as Relevant Case Definitions*. Available online at: ehttps://eur-lex.europa.eu/legal-content/EN/TXT/PDF/?uri=CELEX:32018D0945 (accessed June 18, 2020).
16. RSP. *European Parliament Resolution 2019/2814 (RSP)*. (2020). Available online at: https://oeil.secure.europarl.europa.eu/oeil/popups/ficheprocedure.do?reference=2019/2814(RSP) (accessed June 18, 2020).
17. *European Parliament Resolution P9_TA (2020) 0035*. (2020). Available online at: https://www.europarl.europa.eu/doceo/document/TA-9-2020-0035_EN.pdf (accessed June 18, 2020).
18. *European Commission, Biocrime Project*. Available online at: https://ec.europa.eu/regional_policy/en/projects/italy/cross-border-cooperation-to-tackle-illegal-animal-trade-and-related-diseases-transmissible-to-humans (accessed June 18, 2020).
19. Land Kärnten and Regione Friuli Venezia Giulia. *Nutzungsvereinbarung Landespolizeidirektion Kärnten*. Klagenfurt: Amt Der Kärntner Landesregierung, Unterabteilung Veterinärwesen. Delibera di Giunta Regionale Regione Friuli Venezia Giulia n. 876 – Progetto Supporto Amministrativo Centro Bio-crime (2019).
20. Wallensten AH, Fredlund H, Runehagen A. Multiple human-to-human transmission from a severe case of psittacosis, Sweden, January-February 2013. *Eurosurveillance*. (2014) 19:20937. doi: 10.2807/1560-7917.ES2014.19.42.20937
21. Zucca and Meddi. Towards a stronger partnership between veterinary services and law enforcements. In: *Building Global Resilience Against Agro-Terrorism and Agro-Crime Project Conference, 28-30th July 2020 Paris*. The Biocrime Veterinary Medical Intelligence Centre. World Organization for Animal Health (OIE) and International Criminal Police Organization (INTERPOL), FAO (2020).
22. Rota Nodari E, Alonso S, Mancin M, De Nardi M, Hudson-Cooke S, Veggiato C, et al. Rabies vaccination: higher failure rates in imported dogs

that in those vaccinated in Italy. *Zoonoses Public Health.* (2016) 64:146–55. doi: 10.1111/zph.12268
23. Plowright RK, Eby P, Hudson PJ, Smith IL, Westcott D, Bryden WL, et al. Ecological dynamics of emerging bat virus spillover. *Proc R Soc.* (2015) B282:20142124. doi: 10.1098/rspb.2014.2124
24. Bailey ES, Choi JY, Fieldhouse JK, Borkenhagen LK, Zemke J, Zhang D, et al. (2018). The continual threat of influenza virus infections at the human–animal interface: what is new from a one health perspective? *Evol Med Public Health* 1:192–8. doi: 10.1093/emph/eoy013
25. Chua KB, Bellini WJ, Rota PA, Harcourt BH, Tamin A, Lam SK, et al. Nipah Virus: a recently emergent deadly paramyxovirus. *Science.* (2000) 288:1432–5. doi: 10.1126/science.288.5470.1432
26. De Benedictis P, Danesi P, Cocchi M. Challenges and knowledge after a two year of Bio-crime surveillance on illegal imported puppies. In: *Proceedings of the 1 One Health Bio-Crime Conference.* Thörl-Maglern: International Police and Custom Cooperation Centre (2019).
27. Kaufmann AF, Meltzer MI, Schmid GP. The economic impact of a bioterrorist attack: are prevention and post attack intervention programs justifiable? *Emerg Infect Dis*. (1997) 3:83–94. doi: 10.3201/eid0302.970201
28. Commission Recommendation. *On a Coordinated Control Plan for the Official Controls on Online Sales of Dogs and Cats*. (2018). Available online at: https://ec.europa.eu/food/sites/food/files/animals/docs/aw_other_euccp_recommend_2018-5488-f1_987143.pdf (accessed July 7, 2020).
29. Masters R, Anwar E, Collins B, Cookson R, Capewell S. Return on investment of public health interventions: a systematic review. *J Epidemiol Community Health.* (2017) 71:827–34. doi: 10.1136/jech-2016-208141
30. Rabinowitz P, Gordon Z, Chudnov D, Wilcox M, Odofin L, Liu A, et al. Animals as sentinels of bioterrorism agents. *Emerg Infect Dis.* (2006) 12:647. doi: 10.3201/eid1204.051120
31. Karem K. Response aspects of global health and laboratory operations used by CDC during zoonotic outbreaks. In: *Proceedings of Bio-Crime Conference "The Integration of the One Health Approach in Veterinary Public Health and Education"*. Trieste: Area Science Park (2018).
32. Rocke T. Zoonoses and alert management protocols/measures currently used in the USA. In: *Proceedings of Bio-crime conference "The Integration of the One Health Approach in Veterinary Public Health and Education"*. Trieste: Area Science Park (2018).
33. Di Minin E, Fink C, Hiippala T, Tenkanen H. A framework for investigating illegal wildlife trade on social media with machine learning. *Conserv Biol.* (2018) 33:210–3. doi: 10.1111/cobi.13104
34. Simons RR, Horigan V, Ip S, Taylor RA, Crescio MI, Maurella C, et al. A spatial risk assessment model framework for incursion of exotic animal disease into the European Union Member States. *Microbial Risk Anal.* (2019) 13:100075. doi: 10.1016/j.mran.2019.05.001
35. WHO. *International Health Regulations (IHR)*. 3rd ed. World Health Organization (2005). Available online at: https://apps.who.int/iris/bitstream/handle/10665/246107/9789241580496-eng.pdf;jsessionid=D16B3BF72881D1782D6505F0809AEC83?sequence=1 (accessed July 7, 2020).
36. WHO and World Organization for Animal Health – OIE. *Handbook for the Assessment of Capacities at the Human-Animal Interface.* Geneva: World Health Organization and World Organization for Animal Health – OIE (2015).

Conflict of Interest: The authors declare that the research was conducted in the absence of any commercial or financial relationships that could be construed as a potential conflict of interest.

frontiers in Veterinary Science

ORIGINAL RESEARCH
published: 01 December 2020
doi: 10.3389/fvets.2020.571730

Isolation and Identification of a Murine Norovirus Persistent Infection Strain in China

Zhao Na[1†], Jiang Bo[2†], Yang Yifei[3], Cao Fuyuan[1], He Bin[1], Zhang Yanshu[1], Jin Huan[2], Su Jingliang[4] and Li Shuang[1*]*

[1] The Experiment Animal Center, North China University of Science and Technology, Tangshan, China, [2] Institute of Animal Husbandry and Veterinary Medicine, Beijing Academy of Agricultural and Forestry Sciences, Beijing, China, [3] Institute of Chinese Materia Medica, China Academy of Chinese Medical Sciences, Beijing, China, [4] Key Laboratory of Animal Epidemiology and Zoonosis, Ministry of Agriculture, College of Veterinary Medicine, China Agricultural University, Beijing, China

OPEN ACCESS

Edited by:
Yashpal S. Malik,
Indian Veterinary Research Institute (IVRI), India

Reviewed by:
Ahmed Ali,
Beni-Suef University, Egypt
Alex Malogolovkin,
University of London, United Kingdom

***Correspondence:**
Su Jingliang
suzhang@cau.edu.cn
Li Shuang
lishuangdwzx@ncst.edu.cn

[†]These authors have contributed equally to this work and share first authorship

Specialty section:
This article was submitted to Veterinary Infectious Diseases, a section of the journal Frontiers in Veterinary Science

Received: 11 June 2020
Accepted: 02 November 2020
Published: 01 December 2020

Citation:
Na Z, Bo J, Yifei Y, Fuyuan C, Bin H, Yanshu Z, Huan J, Jingliang S and Shuang L (2020) Isolation and Identification of a Murine Norovirus Persistent Infection Strain in China. Front. Vet. Sci. 7:571730. doi: 10.3389/fvets.2020.571730

Murine Norovirus (MNV) is one of the most known viruses among viruses in mice. Because of the high prevalence of MNV in frequently used laboratory animals in biomedical researches, there is a significant impact of MNV. There may be different prevalence degrees and molecular characteristics of MNV in different regions around the world. Here, we reported an MNV strain "designated HBTS-1806" isolation from commercial mice's feces that caused a detectable cytopathic effect (CPE) in RAW264.7 cells. According to electron microscopy, the virus was 50–70 nm in diameter. The complete genome of HBTS-1806 is 7383 nucleotides with a structure similar to that of MNV reference strains. According to phylogenetic analysis on the basis of the whole genome, HBTS-1806 shared nucleotide sequence identities of 90.2–95.4% with other Chinese isolates reported. Analysis of amino acid sequence on the basis of ORF1 and ORF2 suggested that the isolated strain may be derived from recombination. Although no gross lesions or histopathological changes were found from mice infected with 5×10^5 $TCLD_{50}$ of MNV by oral gavage inoculation, the intestinal virus loads lasted 12 weeks, suggesting a persistent infection strain of MNV isolate in China.

Keywords: murine norovirus, virus isolate, persistent infection, laboratory animals, C57 (C57BL/6J)

INTRODUCTION

As single-stranded and positive-sense RNA viruses, noroviruses belong to the family *Caliciviridae* and the genus *Norovirus*. Recently, noroviruses are divided into five genogroups (GI to GV) (1). The GI and GII viruses are the causes of most cases of acute non-bacterial gastroenteritis among all ages worldwide of human, causing great burden to public health (2, 3). Due to the lack of cell culture and small animal model systems research on the virus replication and pathogenesis of noroviruses have been difficult to carry out (4). Nevertheless, murine noroviruses (MNVs), categorized as GV, were discovered in conventionally housed mice at Washington University in a screen for novel human pathogens capable of infecting mice (5). This MNV can propagate in the RAW 264.7 cell line originated from mouse macrophages (4, 6). Therefore, MNV has been considered as an alternative model of human norovirus.

The MNV is non-enveloped, non-segmented virus and has ∼7.5 kb pairs of bases that encode three open reading frames (ORFs): ORF1 encoding a large polyprotein cleaved to single non-structural proteins is encoded; ORF2 encoding the viral capsid protein (VP1) is encoded by ORF2; and ORF3 encoding a minor structural protein (VP2) (7–9). An additional ORF4 has also been found in the MNV genome (10). The original strain was called MNV-1, and then many MNV-1 strains have been isolated by different institutions around the world (11). The reports showed that all MNV strains isolated from laboratory mice around the world are of single genotype with ∼13% nt and ∼7% aa diversity in the ORF2 (VP1) region, indicating very limited genetic diversity when comparing with the human noroviruses (12).

The discovery of MNV-1 strain accelerated the development of assays for detection of antibody to MNV, so that serologic evidence is provided for a widespread distribution of this virus in laboratory mice (13, 14). Almost all mouse strains are liable to MNV infection (15, 16). In immunodeficient mice, MNV infection recapitulated various clinical symptoms such as hepatitis, focal interstitial pneumonia, and peritonitis (17–21). Propagateion could both wild-type and immunocompromised mice as an asymptomatic infection (22). Asymptomatically infected mice would cross-infect from institution to another and caused high prevalence of MNV among animal institutes (23–25). Undoubtedly, this infection is able to can cause detrimental effects to laboratory animals and bring biased experimental results. Therefore, the research on the epidemiology and etiology of MNV is of great particular importance. In this study, an MNV persistent infection strain from laboratory mice was identified and characterized in China.

MATERIALS AND METHODS

Sample Collection

Three laboratory animal production companies in Beijing, Shandong, and Liaoning province respectively provided 160 C57BL/6J mice between March and September 2018. After mixing the feces of 10 individual mice from the same company, it was made into 10% suspensions in phosphate buffer (PBS, pH 7.2) was prepared and stored at −80°C.

RT-PCR Detection of MNV

Detection of MNV in the samples of commercial laboratory mice were attempted with a MNV specific primer pair targeting a 396 bp region at the 5′ end of MNV ORF2 (VP1) (24). Briefly, 2 μl RNA as template was used in one step RT-PCR kit (Thermo Fisher Scientific) according to the manufacturer's protocol. Thermocycling conditions starts with reverse transcription at 42°C for 40 min (for the RT-PCR) followed by an initial incubation at 94°C for 2 min and 30 cycles of denaturation at 94°C for 40 s, annealing at 50°C or 40 s, and extension at 72°C for 10 min. PCR products were analyzed on 2% agarose gels in the presence of ethidium bromide.

Virus Isolation and Identification

Adopting Eagle's medium (DMEM, Gibco, USA) modified by Dulbecco as growth medium (GM), supplemented with 10% heat-inactivated fetal calf serum, penicillin (250 units/ml, Gibco, USA) and streptomycin (250 mg/ml, Gibco, USA) were supplemented. Maintenance medium (MM) consists of DMEM supplemented with 2% heat-inactivated fetal calf serum, penicillin (250 units/ml, Gibco, USA) and streptomycin (250 mg/ml, Gibco, USA). The murine macrophage-like cell line RAW264.7 was supplied by the Cell Ceter of Basic Medical Sciences, Institute of Basic Medical Sciences, Chinese Academy of Medical Sciences (3111C0001CCC000146), which was used to perform virus isolation as described previously (26). Briefly, a 0.22-μm syringe filter (Millipore, USA) was used to further filter feces samples that are positive by reverse transcription-polymerase chain reaction (RT-PCR). A RAW264.7 cell monolayers was added with the feces samples in a 6-well tissue culture plate (Costar, Corning Inc., Corning, NY). After 60-min adsorption at the temperature of 37°C, MM was added to wash cells. Cultures were incubated at 37°C with 5%CO_2, and its cytopathic effect (CPE) was checked every day. It was necessary to harvest and froze the cultures when CPE of the cells reaches 75%. A new RAW264.7 cell monolayer was infected by 20 ml of the resultant suspensio. According to the amount of associated CPE, the material was passed between 3 and 5 times. RT-PCR was used to test MNV in the cell culture supernatants.

Electron Microscopy

Virus-infected RAW264.7 cells were fixed in 2.5% glutaraldehyde at 24 and 48 h after infection. Uranyl acetate and leadcitrate were used to stain the ultrathin sections. Then, a Hitachi TEM H-7500 was used to examine the samples as described previously (27).

Animal Infection

Beijing Huafukang Bioscience Co., Ltd. (Beijing, China) which was certified MNV-free vendors provided female C57BL/6 mice. To investigate the efficiency of virus replication, the 6 week-old mice infected 5×10^5 $TCLD_{50}$ of MNV by oral gavage inoculation ($n = 60$), and the same volume of PBS (pH 7.2) was applied to treat the mice in the negative control group ($n = 10$). Food uptakes, body weight and clinical signs of infected mice were examined daily for 12 weeks. Ten infected mice were euthanized 2, 4, 6, 8, 10, and 12 weeks after infection. Heparinized blood and tissue samples from liver, spleen and appendix were collected from both infected and control mice. For each organ, one half was frozen at −80°C, and the other half was fixed in 10% neutral-buffered formalin. Paraffin-embedded tissue blocks were cut into 5 μm thick sections and stained with hematoxylin and eosin (HE) with standard methods.

Virus Gene Amplification and Genome Sequencing

E.Z.N.A.®Viral RNA Kit (Omega, USA) was used to extract viral RNAs from MNV-infected RAW264.7 culture supernatant according to the manufacturer's instructions. The SuperScript III First-Strand Synthesis System for RT-PCR (Invitrogen, USA) was adopted to synthesize DNA. Different regions of the

MNV genomes were amplified by applying 12 pairs of oligo nucleotide primers designed on basis of the sequence of MNV BJ 10-2062 strain (**Table 1**). After being purified and cloned into pMD18-T vector (TaKaRa, Japan), the PCR products were sequenced by Beijing Sunbiotech Co., Ltd. Lasergene software (DNAstar Inc., USA) was employed to assemble and analyze sequence data. Clustal X 2.1 was adopted to perform multiple sequence alignments. The MEGA 6 program was used to carry out phylogenetic analyses. The genome sequence of the isolated strain was registered in GenBank (the Accession Number MT358379).

Virus Quantitation by Real-Time PCR

The viral RNA detected by real-time PCR to monitor viral RNA in the organs and feces of mice. The primers used to detect MNV were MNV-S (5′-CCGCAGGAACGCTCAGCAG-3′) and R2 (5′-GGYTGAATGGGACGGCCTG-3′). The sequence of the TaqMan probe was 5′-FAM-ATGAGTGATGGCGCA-MGB-NFQ (28). A E.Z.N.A.®Total RNA Kit I (Omega, USA) was used to extract total RNA from different tissues and feces samples according to the manufacturer's instructions. A PrimeScript RT reagent Kit with gDNA Eraser (TaKaRa, Japan) was applied to conduct reverse transcription. A QuantiTect Probe PCR Kit (Qiagen, USA) was used for perform the quantitative real-time PCR in a 25 μl reaction volume. The thermal cycling profile below was made by an ABI 7500 Fast Real-Time PCR System (Applied Biosystems): initial denaturation at 95°C for 15 min, then 40 cycles of 95°C for 10 s and 60°C for 1 min.

Ethics Statement

The Experimental Animal Ethics Committee (North China University of Science and Technology) approved this animal infection experiment, and the animals were maintained in accordance with the guidelines issued by North China University of Science and Technology for the care and use of laboratory animals.

TABLE 1 | Oligonucleotide primers referred to in this study.

Name	Sequence(5′-3′)	Genomic postion*
1F	GTGAAATGAGGATGGCAACG	1-20
1282R	AGTTGGCACTCGTTCTTGAT	1263-1282
851F	AAACCTTCTGGCATCTGTGA	851-870
1985R	CAAGATGAAATTGATGTGGC	1966-1985
1790F	CATCATCATCACCACCAACC	1790-1809
3442R	ACCCAGGTGTTTCCTTTCTT	3423-3442
3229F	TTGTCGCTTCGGTCCTTGTT	3229-3248
4816 R	TGGTGATTGGGTCCTTTGGT	4797-4816
4388F	CCCTTCGCTGCTGGATGTTG	4368-4387
5967R	CACCTGACCCGTGCCTGATT	5948-5967
5454F	AGGGTCACTCACCACTGCTC	5454-5673
7382R	AAAATGCATCTAATTACTAC	7363-7382R

Location corresponds to position within the BJ 10-2062 (KM458057) genome.

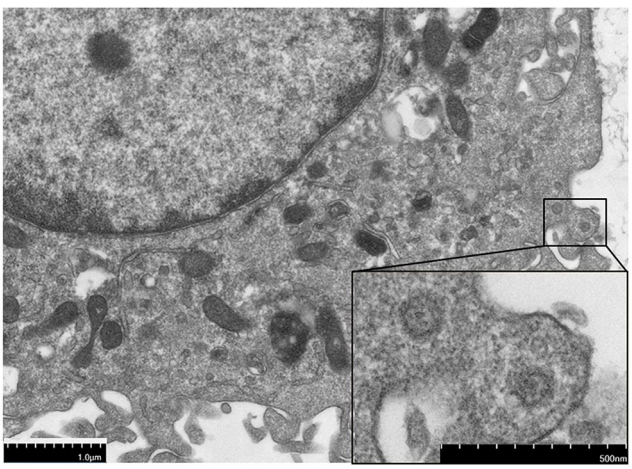

FIGURE 2 | The electron micrographs of virus particles. The section of the infected cell 24 h post-infection, showing dense particles and virions.

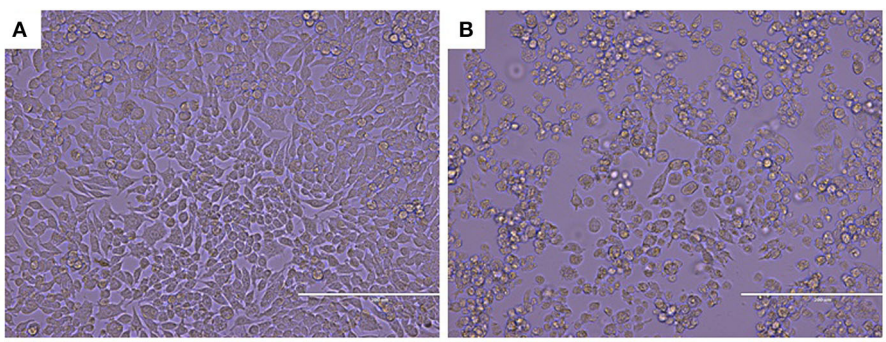

FIGURE 1 | CPE in MNV infected RAW264.7 cell (Original magnification × 200). **(A)** Non-infected RAW264.7 cell monolayer; **(B)** Infected Vero cells rounded up and focal detachment 48 h post-infection.

RESULTS

MNV Detection in Commercial Laboratory Mice

The presence of MNV was checked by testing fecal specimens from 170 C57BL/6J mice. Among 17 laboratory mice pooled samples, RT-PCR revealed 15 samples positive for MNV by RT-PCR (**Supplementary Table 1** and **Supplementary Figure 1**), and all of the mice pooled samples from Shandong and Liaoning Province were detected positive for MNV.

TABLE 2 | MNV RNA detection in tissues of 6 week-old C57BL/6J mice tissues sacrificed at various time-points.

Weeks	Tissues samples			
post-infection	Stomach	Appendix	Liver	Spleen
2	80% (10/10)	100% (10/10)	50% (5/10)	70% (7/10)
4	40% (4/10)	100% (10/10)	10% (1/10)	10% (1/10)
6	20% (2/10)	100% (10/10)	0% (0/10)	0% (0/10)
8	10% (1/10)	80% (8/10)	0% (0/10)	0% (0/10)
10	10% (0/10)	80% (8/10)	0% (0/10)	0% (0/10)
12	10% (0/10)	60% (6/10)	0% (0/10)	0% (0/10)

TABLE 3 | MNV strains investigated in this study.

Strain	GenBank no.	Country
Mu/NoV/GV/MNV1/2002/USA	AY228235	USA
GV/NIH-4431/2005/USA	JF320651	USA
GV/CR6/2005/USA	EU004676	USA
GV/CR18/2005/DEU	EU004683	USA
GV/WU24/2005/USA	EU004669	USA
CW3	EF014462	USA
GV/NIH-A114/2006/USA	JF320652	USA
MNV2	DQ223041	USA
GV/NIH-D220/2007/USA	JF320653	USA
Berlin/05/06/DE	EF531290	GER
MNV 3 K4	FJ446720	ROK
MNV 4 S18	FJ446719	ROK
Guangzhou/K162/09/CHN	HQ317203	CHN
MT30-2	AB601769	JPN
KHU-1	JX048594	CHN
O7	KF113526	GBR
BJ 10-2062	KM458057	CHN
SC/2014/USA	KM102450	USA
MuNoVIT1	KR349276	ITA

Isolation and Identification of the MNV

Since the virus could replicate in RAW264.7 cells, infected cells rounded up and drifted out of the flask surface and focal CPE appeared 48 h after infection (**Figure 1**). The newly isolated virus was named MNV HBTS-1806. 24 h after infection an ultrathin section of infected RAW cells was obtained. EM identified dense particles with the diameter of 50–70 nm within cytoplasmic vesicles (**Figure 2**). Human norovirus appeared similar morphology as ∼50 nm in diameter (29). All the passages of the cell cultures were tested positive for MNV by RT-PCR.

Persistent Infection With the Isolated Virus in Wild-Type Mice

All mice infected by the MNV HBTS-1806 strain *via* oral gavage inoculation at a dose of 5×10^5 $TCLD_{50}$/mouse exhibited no significant clinical signs until 12 weeks post-infection. There are no significant difference in food intake and body weight between two groups. To monitor viral RNA in some organs of all infected mice between 2 and 12 weeks after infection, the viral RNA was extracted and analyzed from stomach, appendix, liver, spleen, and feces at different time points (**Table 2**). Six of ten appendices were still positive12 weeks after infection. Tissues from mice sacrificed at 2, 4, and 12 weeks were examined histologically after infection. There is no apparent microscopic change in the liver, spleen and appendix (**Supplementary Figure 2**).

Genomic Sequencing and Phylogenetic Analysis

The entire genome of MNV HBTS-1806 strain was sequenced and compared with the full-length sequences of reference MNVs (**Table 3**). The HBTS-1806 contained 7383 nucleotides and had four ORFs, conforming to the genomic characteristics of MNV1. The genetic distances between the query strain and the reference MNV strains were drawn according to nucleotide position. The overall sequence similarity among these MNVs was 88.9–95.4%. Highest homology to isolates was the MNV BJ-2011-1 strain, which was isolated in Beijing of China. The glutamate at position 94 in the NS1/2 protein was critical for persistent replication and shedding (**Figure 3**).

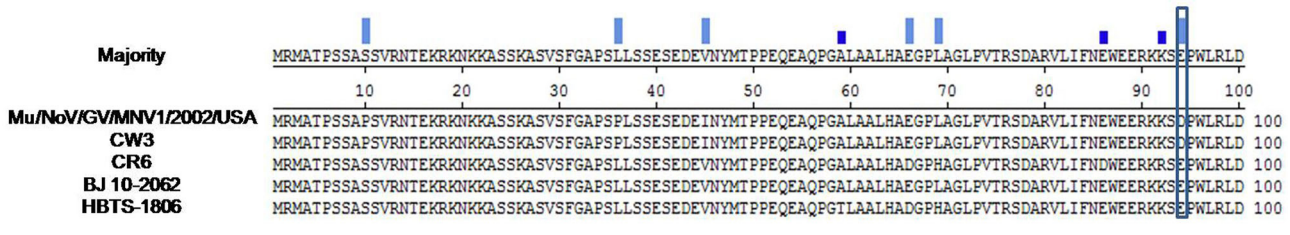

FIGURE 3 | Align sequencs of 1–100 domain of MNV NS1/2 protein construts. The presence of a glutamate at position 94 of the NS1/2 protein could played an essential role in persistent replication and shedding of MNV.

Phylogenetic analysis based on ORF1 sequences placed HBTS-1806 away from MNV1 (Mu/NoV/GV/MNV1/2002/USA) (**Figure 4B**), while the tree based on the whole genome and ORF2 showed close evolutional relationship between HBTS-1806 and MNV1 (Mu/NoV/GV/MNV1/2002/USA) (**Figures 4A,C**).

DISCUSSION

Murine noroviruses consist of a group of newly-recognized pathogens that are able to infect laboratory mice. The first reported MNV-1 generates a transient infection with a short duration of fecal shedding after infecting immunocompetent mice in laboratory (30). It is very likely that MNV infection can be widespread across the world (11). Besides, once infected the host, MNV is highly persistent and hard to be removed completely without an integrated eradication system (31). MNV isolates such as MNV-2, MNV-3, and MNV-4,have been extractedfrom laboratory mice in academic research institutes around the world (8). There are dramatic differences between these MNV strains and MNV-1 in pathogenicity because MNV-1 persistently infect tissues in experimentally inoculated immunocompetent mice (32). Therefore, it is necessary to screen laboratory animals for MNV frequently to prevent animal diseases and interfere in experiments (8, 33, 34). This stduy describes a novel strain of MNV isolated from feces samples of commercial laboratory mice. The virus was successfully propagates in RAW264.7 cell culture. And the size and morphological characteristics of this virus were similar to norovirus described previously by other investigators (35, 36).

In general, different MNV isolates show different pathogenicity. A recent research reported that an MNV strain (CR6) can cause intestinal pathology under a specific Crohn's disease genetic background, while another strain (MNV-1) cannot (37). In this work, MNV HBTS-1806 strain infection of immunocompetent C57BL/6J mice did not cause gross pathology. Moreover, no lesion was found in small intestine, liver or spleen of animals in this study. Although no significant pathological changes in immunocompetent mice were shown, it should be noted that infectious viral titers in tissues were continuously detected 2–12 weeks after infection. And even virus loads in the intestinal would last 12 weeks. Our data demonstrated that intestinal pathology cannot be predicted by MNV titers in wild-type mice, which could be potentially explained by that to the specificity of virus strains in either cell tropism relating to virulence or interactions with host cells (12). Since the biological significance of these observation is not completely understood yet, the situation that the prolonged viral load may be a major risk factor for large-scale MNV infection in the animal breeding and housing environment shall be recognized. Because the MNV was described as an acute infection with apparent mortality and morbidity in Stat1$^{-/-}$ mice, persistent subclinical infection in Rag$^{-/-}$ mice, the pathogenicity of isolates in immunodeficient mice requires further study (11).

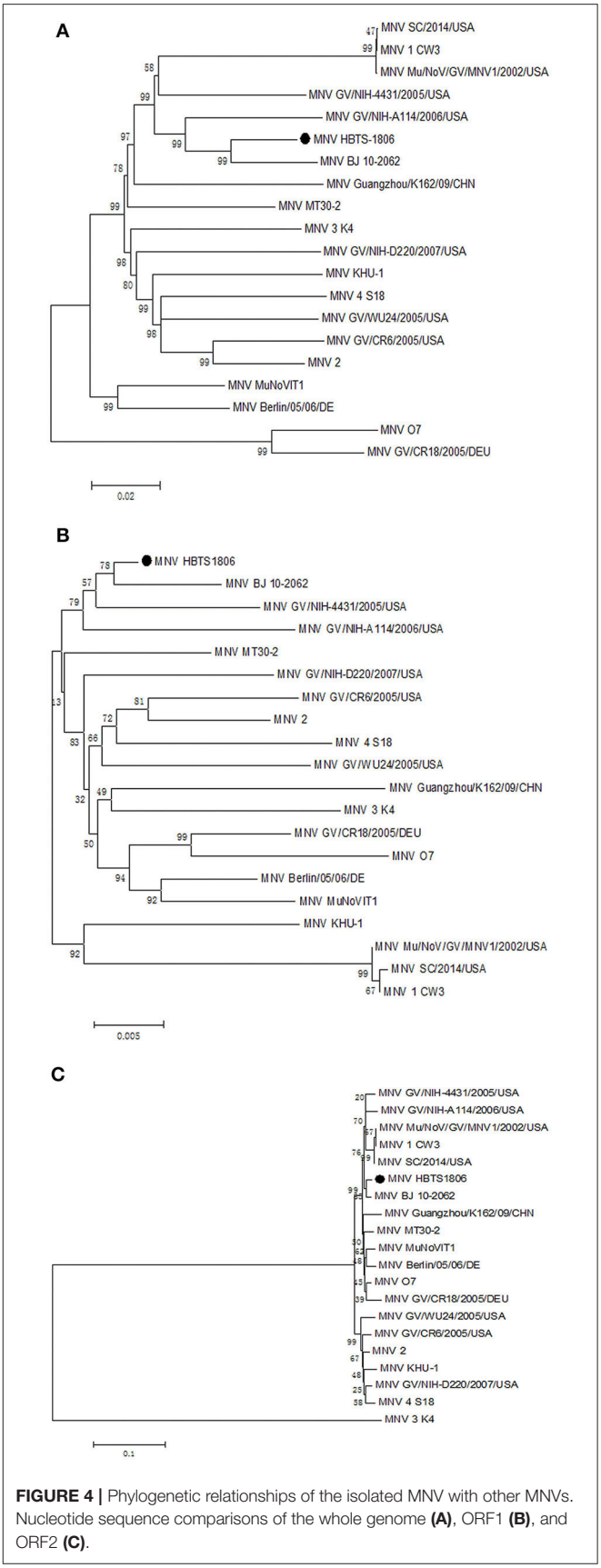

FIGURE 4 | Phylogenetic relationships of the isolated MNV with other MNVs. Nucleotide sequence comparisons of the whole genome **(A)**, ORF1 **(B)**, and ORF2 **(C)**.

How persistent MNV infection is maintained is unclear. During persistent infection, the mutations of MNV surface antigens were predicted to make viral progeny avoid the immune system (38). In addition, genetic elements in the NS1/2 protein causing persistence of the virus in the mouse determine the viral persistence in the intestinal tract. Residue 94, a critical factor determining persistence, was separated in a reverse turn after an α-helix in the folded domain (39). The presence of glutamate at position 94 of the NS1/2 protein from HBTS-1806 plays an essential role in persistent replication and shedding.

This study reported the complete genomic sequence of HBTS-1806 and analyzed the phylogenetic associations among MNV strains on basis of the genomic and individual gene levels, so as to characterize the novel isolated virus. Sequence homology and phylogenetic analysis of the MNV showed that the HBTS-1806 strain has high homology with MNV BJ-2011-1. The alignments of the whole genome, ORF1, and ORF2 nucleotide sequences of the HBTS-1806 strain and MNV1 (Mu/NoV/GV/MNV1/2002/USA) strain revealed considerable distinctions among the trees. The recombinantion of human noroviruses have been recognized as the cause of global norovirus outbreak (40–42). Nevertheless, the molecular mechanisms promoting norovirus recombination have not been determined experimentally (43). The report suggested that the recombination may occurred at several points of breakout within ORF2 in several MNV genomes, despite of the predominant break point detected in recombinant human norovirus genomes is at the ORF1-ORF2 junction (44). However, contribution of recombination to the evolution of the MNV strains is not known, and the effects of the recombination on MNV biology are to be elucidated in the future.

DATA AVAILABILITY STATEMENT

The datasets generated in this study can be found in online repositories. The names of the repository/repositories and Accession Number(s) can be found below: https://www.ncbi.nlm.nih.gov/, MT358379.

ETHICS STATEMENT

The animal study was reviewed and approved by the Experimental Animal Ethics Committee (North China University of Science and Technology).

AUTHOR CONTRIBUTIONS

LS and SJ performed experiments, analyzed data, and wrote the manuscript. ZN, JB, YY, and CF carried out the experiments. HB and JH participated in the design. ZY and JB participated in the design and analysis of data of sequence. JB and ZN participated in manuscript drafting. All authors contributed to the article and approved the submitted version.

FUNDING

This work was supported by the National Natural Science Foundation of China (31802194, 3170220) and Natural Science Foundation of Hebei Province of China (C2018209056).

SUPPLEMENTARY MATERIAL

The Supplementary Material for this article can be found online at: https://www.frontiersin.org/articles/10.3389/fvets.2020.571730/full#supplementary-material

REFERENCES

1. Zheng DP, Tamie A, Fankhauser RL, Beard RS, Glass RI, Monroe SS. Norovirus classification and proposed strain nomenclature. *Virology.* (2006) 346:312–23. doi: 10.1016/j.virol.2005.11.015
2. Blanton LH, Adams SM, Beard RS, Wei G, Bulens SN, Widdowson M A, et al. Molecular and epidemiologic trends of caliciviruses associated with outbreaks of acute gastroenteritisin the United States, 2000–2004. *J Infect Dis.* (2006) 193:413–21. doi: 10.1086/499315
3. Glass RI, Parashar UD, Estes MK. Norovirus gastroenteritis. *N Engl J Med.* (2009) 361:1776–85. doi: 10.1056/NEJMra0804575
4. Wobus CE, Karst SM, Thackray LB, Chang KO, Sosnovtsev SV, Belliot G, et al. Replication of norovirus in cell culture reveals a tropism for dendritic cells and macrophages. *PLoS Biol.* (2004) 2:e432. doi: 10.1371/journal.pbio.0020432
5. Karst SM, Wobus CE, Lay M, Davidson J, Virgin HW, IV. STAT1-dependentinnate immunity to a Norwalk-like virus. *Science.* (2003) 299:1575–8. doi: 10.1126/science.1077905
6. Wobus CE, Thackray LB, Virgin HW, IV. Murine norovirus: a model system to study norovirus biology and pathogenesis. *J Virol.* (2006) 80:5104–12. doi: 10.1128/JVI.02346-05
7. Jiang X, Wang M, Wang K, Estes MK. Sequence and genomic organization of Norwalk virus. *Virology.* (1993) 195:51–61. doi: 10.1006/viro.1993.1345
8. Hsu CC, Riley LK, Livingston RS. Molecular characterization of three novel murine noroviruses. *Virus Genes.* (2007) 34:147–55. doi: 10.1007/s11262-006-0060-1
9. Thorne LG, Goodfellow IG. Norovirus gene expression and replication. *J Gen Virol.* (2014) 95:278–91. doi: 10.1099/vir.0.059634-0
10. McFadden N, Bailey D, Carrara G, Benson A, Chaudhry Y, Shortland A, et al. Norovirus regulation of the innate immune response and apoptosis occurs *via* the product of the alternative open reading frame 4. *PLoS Pathog.* (2011) 7:e1002413. doi: 10.1371/journal.ppat.1002413
11. Henderson KS. Murine norovirus, a recently discovered and highly prevalent viral agent of mice. *Lab Anim (NY).* (2008) 37:314–20. doi: 10.1038/laban0708-314
12. Thackray LB, Wobus CE, Chachu KA, Liu B, Alegre ER, Henderson KS, et al. Murine noroviruses comprising a single genogroup exhibit biological diversity despite limited sequence divergence. *J Virol.* (2007) 81:10460–73. doi: 10.1128/JVI.00783-07
13. Hsu CC, Riley LK, Wills HM, Livingston RS. Persistent infection with and serologic cross-reactivity of three novel murine noroviruses. *Comp Med.* (2006) 56:247–51.
14. Ohsugi T, Matsuura K, Kawabe S, Nakamura N, Kumar JM, Wakamiya M, et al. Natural infection of murine norovirus in conventional and specific pathogen-free laboratory mice. *Front Microbiol.* (2013) 4:12. doi: 10.3389/fmicb.2013.00012
15. Pritchett-Corning KR, Cosentino J, Clifford CB. Contemporary prevalence of infectious agents in laboratory mice and rats. *Lab Anim.* (2009) 43:165–73. doi: 10.1258/la.2008.008009
16. Goto K, Hayashimoto N, Yasuda M, Ishida T, Kameda S, Takakura A, et al. Molecular detection of murine norovirus from experimentally

and spontaneously infected mice. *Exp Anim.* (2009) 58:135–40. doi: 10.1538/expanim.58.135
17. Ward JM, Wobus CE, Thackray LB, Erexson CR, Faucette LJ, Belliot G, et al. Pathology of immunodeficient mice with naturally occurring murine norovirus infection. *Toxicol Pathol.* (2006) 34:708–15. doi: 10.1080/01926230600918876
18. Mumphrey SM, Changotra H, Moore TN, Heimann-Nichols ER, Wobus CE, Reilly MJ, et al. Murine norovirus 1 infection is associated with histopathological changes in immunocompetent hosts, but clinical disease is prevented by STAT1-dependent interferon responses. *J Virol.* (2007) 81:3251–63. doi: 10.1128/JVI.02096-06
19. Shortland A, Chettle J, Archer J, Wood K, Bailey D, Goodfellow I, et al. Pathology caused by persistent murine norovirus infection. *J Gen Virol.* (2014) 95:413–22. doi: 10.1099/vir.0.059188-0
20. Patil K, Campbell LA, Rosenfeld ME, Paik J, Brabb T, O'brien KD, et al. Effects of murine norovirus on chlamydia pneumoniae-accelerated atherosclerosis in *apoE(-/-)* mice. *Comp Med.* (2016) 66:188–96.
21. Hsu CC, Piotrowski SL, Meeker SM, Smith KD, Maggio-Price L, Treuting PM. Histologic lesions induced by murine norovirus infection in laboratory mice. *Vet Pathol.* (2016) 53:754–63. doi: 10.1177/0300985815618439
22. Buxbaum LU, DeRitis PC, Chu N, Conti PA. Eliminating murine norovirus by cross-fostering. *J Am Assoc Lab Anim Sci.* (2011) 50:495–9.
23. Perdue KA, Green KY, Copeland M, Barron E, Mandel M, Faucette LJ, et al. Naturally occurring murine norovirus infection in a large research institution. *J Am Assoc Lab Anim Sci.* (2007) 46:39–45.
24. Kim JR, Seok SH, Kim DJ, Baek MW, Na YR, Han JH, et al. Prevalence of murine norovirus infection in Korean laboratory animal facilities. *J Vet Med Sci.* (2011) 73:687–91. doi: 10.1292/jvms.10-0226
25. Barron EL, Sosnovtsev SV, Bok K, Prikhodko V, Sandoval-Jaime C, Rhodes CR, et al. Diversity of murine norovirus strains isolated from asymptomatic mice of different genetic backgrounds within a single U.S. research Institute. *PLoS ONE.* (2011) 6:e21435. doi: 10.1371/journal.pone.0021435
26. Kitamoto T, Takai-Todaka R, Kato A, Kanamori K, Takagi H, Yoshida K, et al. Viral population changes during murine norovirus propagation in RAW 264.7 cells. *Front Microbiol.* (2017) 8:1091. doi: 10.3389/fmicb.2017.01091
27. Su J, Li S, Hu X, Yu X, Wang Y, Liu P, et al. Duck egg-drop syndrome caused by BYD virus, a new Tembusu-related flavivirus. *PLoS ONE.* (2011) 6:e18106. doi: 10.1371/journal.pone.0018106
28. Kitajima M, Oka T, Takagi H, Tohya Y, Katayama H, Takeda N, et al. Development and application of a broadly reactive real-time reverse transcription-PCR assay for detection of murine noroviruses. *J Virol Methods.* (2010) 169:269–73. doi: 10.1016/j.jviromet.2010.07.018
29. Jiang X, Wang M, Graham DY, Estes MK. Expression, self-assembly, and antigenicity of the Norwalk virus capsid protein. *J Virol.* (1992) 66:6527–32. doi: 10.1128/JVI.66.11.6527-6532.1992
30. Kastenmayer RJ, Perdue KA, Elkins WR. Eradication of murine norovirus from a mouse barrier facility. *J Am Assoc Lab Anim Sci.* (2008) 47:26–30.
31. Nice TJ, Robinson BA, Van Winkle JA. The role of interferon in persistent viral infection: insights from murine norovirus. *Trends Microbiol.* (2018) 26:510–24. doi: 10.1016/j.tim.2017.10.010
32. Arias A, Bailey D, Chaudhry Y, Goodfellow I. Development of a reverse-genetics system for murine norovirus 3: long-term persistence occurs in the caecum and colon. *J Gen Virol.* (2012) 93:1432–41. doi: 10.1099/vir.0.042176-0
33. Zorn J, Ritter B, Miller M, Kraus M, Northrup E, Brielmeier M. Murine norovirus detection in the exhaust air of IVCs is more sensitive than serological analysis of soiled bedding sentinels. *Lab Anim.* (2017) 51:301–10. doi: 10.1177/0023677216661586
34. Rodrigues DM, Moreira JCO, Lancellotti M, Gilioli R, Corat MAF. Murine norovirus infection in brazilian animal facilities. *Exp Anim.* (2017) 66:115–24. doi: 10.1538/expanim.16-0027
35. Warnes SL, Summersgill EN, Keevil CW. Inactivation of murine norovirus on a range of copper alloy surfaces is accompanied by loss of capsid integrity. *Appl Environ Microbiol.* (2014) 81:1085–91. doi: 10.1128/AEM.03280-14
36. Gilling DH, Kitajima M, Torrey JR, Bright KR. Mechanisms of antiviral action of plant antimicrobials against murine norovirus. *Appl Environ Microbiol.* (2014) 116:1149–63. doi: 10.1111/jam.12453
37. Nice TJ, Strong DW, McCune BT, Pohl CS, Virgin HW. A single-amino-acid change in murine norovirus NS1/2 is sufficient for colonic tropism and persistence. *J Virol.* (2013) 87:327–34. doi: 10.1128/JVI.01864-12
38. Robinson BA, Van Winkle JA, McCune BT, Peters AM, Nice TJ. Caspase-mediated cleavage of murine norovirus NS1/2 potentiates apoptosis and is required for persistent infection of intestinal epithelial cells. *PLoS Pathog.* (2019) 15:e1007940. doi: 10.1371/journal.ppat.1007940
39. Borin BN, Tang W, Nice TJ, McCune BT, Virgin HW, Krezel AM. Murine norovirus protein NS1/2 aspartate to glutamate mutation, sufficient for persistence, reorients side chain of surface exposed tryptophan within a novel structured domain. *Proteins.* (2014) 82:1200–9. doi: 10.1002/prot.24484
40. Phan TG, Kaneshi K, Ueda Y, Nakaya S, Nishimura S, Yamamoto A, et al. Genetic heterogeneity, evolution, and recombination in noroviruses. *J Med Virol.* (2017) 79:1388–400. doi: 10.1002/jmv.20924
41. Shen Q, Zhang W, Yang S, Chen Y, Shan T, Cui L, et al. Genomic organization and recombination analysis of human norovirus identified from China. *Mol Biol Rep.* (2012) 39:1275–81. doi: 10.1007/s11033-011-0845-8
42. Mathijs E, Muylkens B, Mauroy A, Ziant D, Delwiche T, Thiry E. Experimental evidence of recombination in murine noroviruses. *J Gen Virol.* (2010) 91:2723–33. doi: 10.1099/vir.0.024109-0
43. Ludwig-Begall LF, Mauroy A, Thiry E. Norovirus recombinants: recurrent in the field, recalcitrant in the lab -A scoping review of recombination and recombinant types of noroviruses. *J Gen Virol.* (2018) 99:970–88. doi: 10.1099/jgv.0.001103
44. Bull RA, Hansman GS, Clancy LE, Tanaka MM, Rawlinson WD, et al. Norovirus recombination in ORF1/ORF2 overlap. *Emerg Infect Dis.* (2005) 11:1079–85. doi: 10.3201/eid1107.041273

Conflict of Interest: The authors declare that the research was conducted in the absence of any commercial or financial relationships that could be construed as a potential conflict of interest.

frontiers in Veterinary Science

BRIEF RESEARCH REPORT
published: 02 December 2020
doi: 10.3389/fvets.2020.569004

Small Mammals as Carriers/Hosts of *Leptospira spp.* in the Western Amazon Forest

Luciana dos Santos Medeiros[1], Susan Christina Braga Domingos[1], Maria Isabel Nogueira Di Azevedo[2], Rui Carlos Peruquetti[1], Narianne Ferreira de Albuquerque[1], Paulo Sérgio D'Andrea[3], André Luis de Moura Botelho[4], Charle Ferreira Crisóstomo[4], Anahi Souto Vieira[2], Gabriel Martins[2], Bernardo Rodrigues Teixeira[3], Filipe Anibal Carvalho-Costa[5] and Walter Lilenbaum[2]*

[1] Laboratório de Microbiologia e Imunologia Veterinária, Universidade Federal do Acre, Rio Branco, Brazil, [2] Laboratório de Bacteriologia Veterinária, Universidade Federal Fluminense, Niterói, Brazil, [3] Laboratório de Biologia e Parasitologia de Mamíferos Silvestres Reservatórios, IOC, Fiocruz, Rio de Janeiro, Brazil, [4] Instituto Federal de Educação, Ciência e Tecnologia do Acre, Rio Branco, Brazil, [5] Laboratório de Epidemiologia e Sistemática Molecular, IOC, Fiocruz, Rio de Janeiro, Brazil

OPEN ACCESS

Edited by:
Lester J. Perez,
University of Illinois at Urbana–Champaign, United States

Reviewed by:
André Alex Grassmann,
University of Connecticut Health Center, United States
Sharon Yvette Angelina Manalo Villanueva,
University of the Philippines Manila, Philippines
Vanina Guernier,
USDA APHIS Veterinary Services, United States

***Correspondence:**
Luciana dos Santos Medeiros
lusmedeiros@yahoo.com.br

Specialty section:
This article was submitted to Veterinary Infectious Diseases, a section of the journal Frontiers in Veterinary Science

Received: 02 June 2020
Accepted: 31 August 2020
Published: 02 December 2020

Citation:
Medeiros LdS, Domingos SCB, Di Azevedo MIN, Peruquetti RC, de Albuquerque NF, D'Andrea PS, Botelho ALM, Crisóstomo CF, Vieira AS, Martins G, Teixeira BR, Carvalho-Costa FA and Lilenbaum W (2020) Small Mammals as Carriers/Hosts of Leptospira spp. in the Western Amazon Forest. Front. Vet. Sci. 7:569004. doi: 10.3389/fvets.2020.569004

Leptospira is a bacteria that causes leptospirosis and is transmitted through water, soil, or mud that is contaminated by the urine of infected animals. Although it is mainly associated with the urban environment, Leptospires also circulate in rural and wild environments. This study aimed to investigate the role of small mammals in leptospirosis epidemiology in the western Amazon, Brazil. In total, 103 animals from 23 species belonging to the orders Didelphimorphia and Rodentia were captured. Blood, kidney, and urine samples were collected and Microscopic Agglutination Test (MAT), *lip*L32 PCR, *sec*Y sequencing, and culturing were conducted. MAT was reactive on 1/15 sera, and no bacterial isolate was obtained. PCR yielded 44.7% positive samples from 16 species. Twenty samples were genetically characterized and identified as *L. interrogans* ($n = 12$), *L. noguchii* ($n = 4$), and *L. santarosai* ($n = 4$). No statistical association was found between the prevalence of infection by *Leptospira* spp. in small mammals within carrier/hosts species, orders, study area, and forest strata. Our results indicate a high prevalence of pathogenic *Leptospira* spp. in several rodent and marsupial species and report the first evidence of *Leptospira* spp. carrier/hosts in the Brazilian Western Amazon.

Keywords: marsupial, small mammal, Amazon, wild rodent, sylvatic leptospirosis

INTRODUCTION

Leptospirosis is a zoonotic infectious disease caused by the bacteria from the *Leptospira* genus (1) and transmitted through water, soil, or mud contaminated by the urine of infected animals. Although it is mainly reported in the urban environment, leptospirosis also circulates in rural and wild environments, with a wide variety of mammal species acting as carrier/hosts of the bacterium (2).

The Amazonian biome has the ideal conditions for maintaining and disseminating *Leptospira* spp. The high humidity and temperature along with the high diversity of mammals and potential renal carriers of the bacteria, creates a scenario that exposes the animals to different strains of *Leptospira* (3, 4). Besides the importance of small mammals in the maintenance of *Leptospira* spp.

in the wild and in the transmission to humans, the possibility of transmission between wild and domestic animals has been a major concern among conservationists and livestock authorities in many areas, especially in the Amazon (5–7). The emergence of zoonosis can greatly impact the abundance of some carrier/host populations, in some extreme cases leading to local extinctions (8).

Every mammal is a potential renal carrier of leptospires. Rodents have been described as the most essential maintenance/amplifier reservoirs in nature for several pathogenic *Leptospira* (9, 10). In Brazil, marsupials from the eastern Amazon (11), semi-arid regions (12), and the Atlantic Forest biome (13, 14) have also been reported with antibodies against *Leptospira* spp. The first report of *Leptospira* isolation in samples of *Didelphis albiventris* was from southern Brazil. These findings suggest marsupials may serve as important transmission reservoirs of pathogenic *Leptospira* spp. (15). Despite this, little is known about the role of wild small mammals as *Leptospira* carrier/hosts in the Amazon forest. Therefore, the objective of this study was to identify *Leptospira* infection in wild small mammals (rodents and marsupials) and investigate predictor variables related to infection in these animals in the Western Amazon, Brazil.

MATERIALS AND METHODS

Study Design

The following licenses were used to conduct the study: permanent license to collect zoological material number 13373 (SISBIO-ICMBIO) and CEUA LW-39/14 license (Ethics Committee on Animal Use, FIOCRUZ). The studied areas were forests in the state of Acre, Brazil, western Amazon on Acre river basin, and represented different levels of conservation and land use (**Figure 1**). These areas included: (1) Floresta do Seringal Cachoeira (FSC) (10°49′S, 68°21′W), in the municipality of Xapuri, a continuous and conserved primary forest with 24,200 ha, a medium anthropic impact and land use for eco-tourism and traditional activities of latex and castanha-do-Brasil extractions; (2) Reserva Florestal Humaitá (RFH) (9°43′S, 67°48′W), in the municipality of Porto Acre, is a wide fragment of ∼2,000 ha of primary and secondary rain forest, submitted to moderate anthropic action, surrounded by farms, roads and a large river. This area belongs to the Federal University of Acre (UFAC) and is a preserved area designated for research; (3) Floresta Experimental Catuaba (FEC) (10°04′S, 67°37′W), in the municipality of Senador Guiomard, comprising 900 ha of primary and secondary rain forest. This farm is used for research

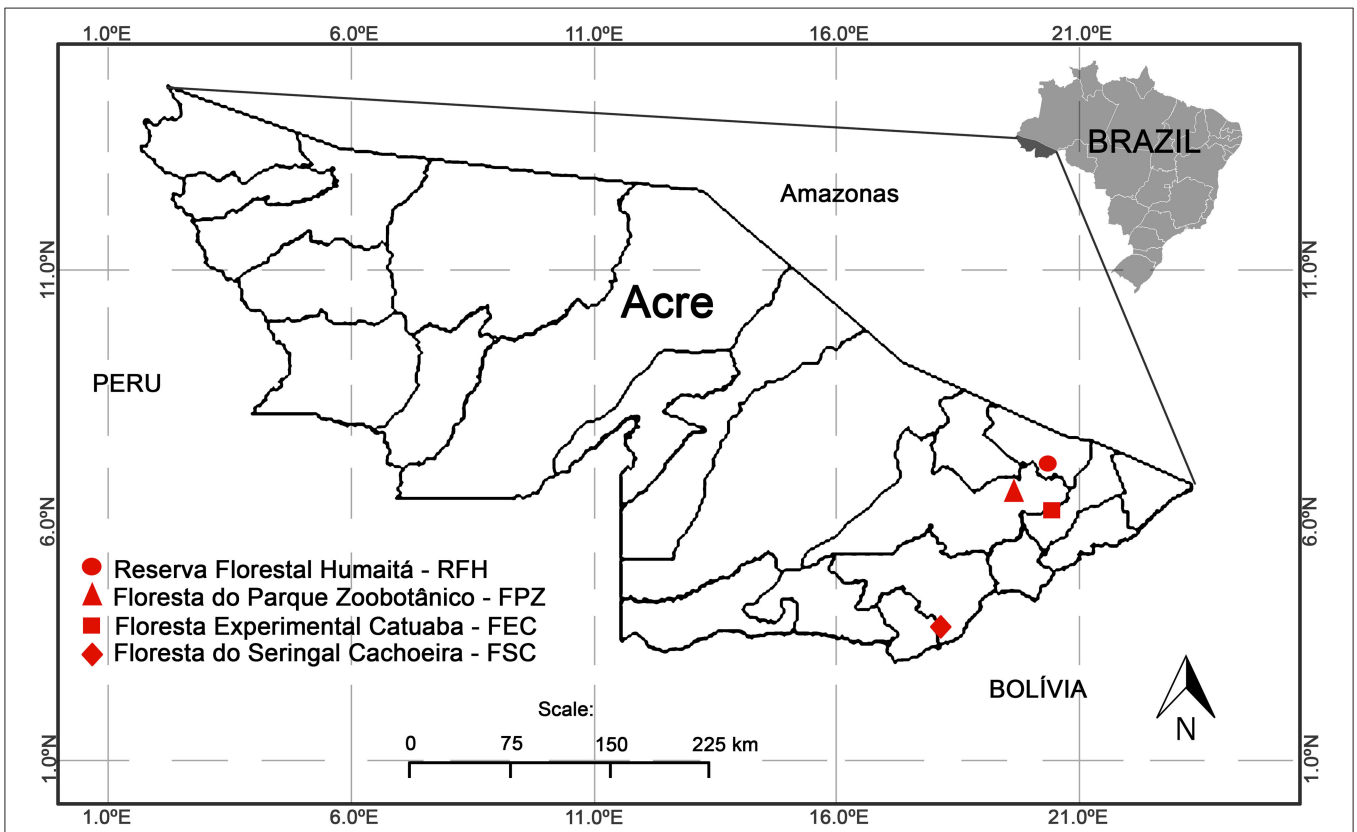

FIGURE 1 | The four study areas located in the state of Acre. Floresta do Seringal Cachoeira (FSC): a continuous and conserved primary forest, Reserva Florestal Humaitá (RFH): a wide fragment of a primary rain forest, Floresta do Parque Zoobotânico (FPZ): an urban small fragment, and Floresta Experimental Catuaba (FEC): a secondary forest with agriculture.

activities and also belongs to UFAC; and (4) Floresta do Parque Zoobotânico (FPZ) (9°57′S, 67°52′W), in the municipality of Rio Branco, an intense anthropized small fragment of approximately 140 ha in different succession stages. It is an urban park located on the UFAC campus, with land use destined to activities such as trekking, research, and recreation.

The field expeditions to capture small mammals and collect biological samples were conducted in the rainy seasons, between November and December 2015, at the RFH, FPZ, and FSC, and in FEC in December 2016.

Animal Capture

Trapping was conducted over five consecutive nights. In each study area, the animals were captured with live traps, Sherman® (30 × 8 × 9 cm) and Tomahawk® (40 × 12 × 12 cm), in five to ten linear transects with 15 trapping stations each. Sampling was conducted at three forest strata—soil level, understory (at a height of 2 m), and canopy (15 m). At the end of each transect, four pitfalls were installed, with a volume of 60 L. The bait used was a mixture of bacon, oat, banana, and peanut butter. The captured animals were transported to a field laboratory base, where they were anesthetized and euthanized following the procedures reported previously (16). Blood samples were collected by cardiac puncture. Immediately after euthanasia, the urinary bladder and kidneys were exposed, and urine and kidney fragments were collected using sterile instruments. The small mammals were identified by external and cranial morphology, karyotyping, and DNA sequencing of cytochrome b gene (17, 18). Specimens were deposited in the mammal collection of the Laboratório de Biologia e Parasitologia de Mamíferos Reservatórios Silvestres, Instituto Oswaldo Cruz (tagged as LBCE), Rio de Janeiro, Brazil.

Bacteriological Procedures

Individual urine samples were processed immediately in a mobile laboratory. Three to five drops of urine were inoculated to three different culture mediums: 5 mL of liquid EMJH medium (Difco, BD, Franklin Lakes, NJ, USA), 5 mL of semisolid Fletcher medium (Difco, BD, Franklin Lakes, NJ, USA), and 5 mL of liquid EMJH medium supplemented with an antibiotic cocktail named STAFF (19). Kidney fragment samples were macerated into EMJH using a 5 mL syringe. After inoculation, the tubes were maintained at room temperature and sent to the Reference Laboratory on Rio de Janeiro after 5 days due to Biosafety standards (4,000 km away from the initial collection site). There, tubes were incubated at 28°C and evaluated weekly for 4 months using dark-field optical microscopy. If contamination occurred, the liquid cultures were filtered or once again transferred to the EMJH and STAFF.

Serology

To detect anti-*Leptospira* antibodies, we conducted the MAT according to World Organization for Animal Health standards (20). Strains related to 22 serogroups were used as antigens, using the highest titer obtained to identify the infecting serogroup. Animals were considered seroreactive when titration was ≥50, as carrier/host animals tend to present low titers (21).

PCR

DNA was extracted from all individual kidney samples using the DNeasy® Blood & Tissue Kit (QIAamp, Qiagen, France) as recommended by the manufacturer. First, PCR was conducted using primers targeting a short region of the *lip*L32 gene (241 bp), reported to be present only in pathogenic leptospires (LipL32-45F: 5′-AAG CAT TAC CGC TTG TGG TG-3′ and LipL32-286R: 5′-GAA CTC CCA TTT CAG CGA TT-3′) (21). Second, *lip*L32 positive samples were subjected to a nested PCR targeting a partial region of *sec*Y gene. An initial reaction targeting a 549 bp region was conducted using the primers secY_outer_F (5′-ATGCCGATCATTTTTGCTTC-3′) and secY_outer_R (5′- CCGTCCCTTAATTTTAGACTTCTTC-3′). Finally, amplicons were included in a second reaction using the primers secY_inner_F (5′-CCTCAGACGATTATTCAATGGTTATC-3′) and secY_inner_R (5′- AGAAGAGAAGTTCCACCGAATG-3′) (Mathieu Picardeau, personal communication, November 27, 2019), providing an expected amplicon of 410 bp. In all reactions, for each set of samples, ultrapure water was used as negative control, while 10 fg of DNA extracted from *Leptospira interrogans* serovar Copenhageni (Fiocruz L1-130) was used as positive control. PCR products were analyzed by gel electrophoresis in 1.5–2% agarose and visualized under UV light, after GelRed® staining.

Sequencing and Phylogenetic Analysis

The *sec*Y amplicons were directly sequenced using the Big Dye Terminator v. 3.1 Cycle Sequencing Ready Reaction Kit (Applied Biosystems) in a 3100 Automated DNA Sequencer according to the manufacturer's instructions. The nucleotide sequences were deposited in GenBank under accession numbers MT361666-MT361685. Phylogenetic analysis was accomplished using Pairwise/Blast/NCBI, SeqMan v. 7.0, ClustalW v. 1.35 (22) and BioEdit v. 7.0.1 (23) software for editing and sequence analysis. A maximum likelihood (ML) tree was constructed using the Tamura-Nei model with the gamma distribution (TN + G) in MEGA X software (24), as it was determined to be the best-fitting model of DNA substitution using the Bayesian information criterion. Information about sequences used for phylogenetic analysis is shown in the **Supplementary Material**.

Statistics

We calculated the prevalence of infection by *Leptospira* sp., considering mammal carrier/host orders (rodents and marsupials), localities (FSC, RFH, FPZ, and FEC), forest strata (soil, understory, or canopy) and species. Prevalence of infection represents the proportion of PCR positive carrier/hosts by the total number of analyzed individuals.

Considering differences in conservation status among the study areas and differences among small mammal species in terms of their habits and habitat use, we tested the influence of carrier/host species, carrier/host orders, study area, and forest strata on the prevalence of infection by *Leptospira* spp. using generalized linear models (GLM). Best models were chosen using the corrected Akaike information criterion (AICc), where the suitable models presented Delta AICc ≤ 2. The GLM analysis followed a binomial distribution. The analyses were performed

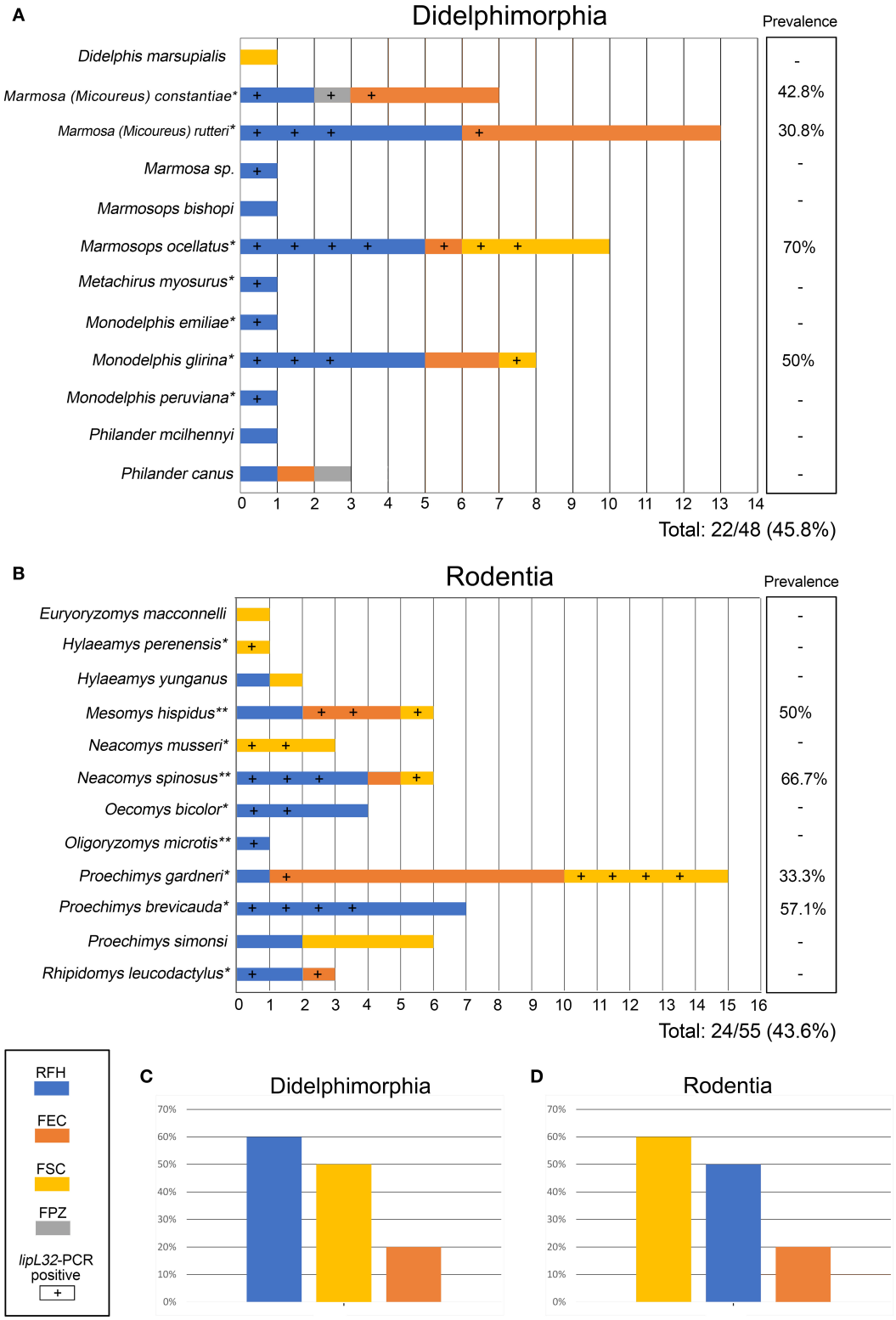

FIGURE 2 | Small mammals (**A**: Didelphimorphia; **B**: Rodentia) included in the present study according to study area (shown by different colors as indicated in the figure). Samples positive for pathogenic *Leptospira,* detected by *lipL32* gene amplification, are indicated by a (+) sign. Columns at right show prevelance values for each host. Pathogenic *Leptospira* prevalence on Didelphimorphia **(C)** and Rodentia **(D)** of each collection site are also presented. *Species with first *Leptospira* DNA detection. **Species already described as carrier hosts of *Leptospira* by Bunnell at al. (29) and Cortez et al. (30). Species for which all samples were negative for Leptospira have no asterisk. Study areas located in the state of Acre: Floresta do Seringal Cachoeira (FSC), Reserva Florestal Humaitá (RFH), Floresta do Parque Zoobotânico (PPZ), and Floresta Experimental Catuaba (FEC).

with R version 3.4.2 (25) using the vegan package (26). We also tested differences in *Leptospira* infection between two rodent families (Cricetidae and Echimyidae), with different evolutionary histories, using a chi-square test.

RESULTS

We analyzed 103 animals, including 55 wild rodents and 48 marsupials, belonging to 23 species (**Figures 2A,B**). Of 15 serum samples subjected to MAT, only one (6.6%) was positive, a sample from the marsupial *Marmosa (Micoureus) rutteri* that was reactive to two *L. interrogans* serogroups (Australis and Autumnalis) at a titer of 1:100 each. All kidney culture attempts were negative. The most important result was the high prevalence (44.7%) of the *lip*L32 gene confirmed by PCR. Of the 15 sera submitted to MAT, six were *lip*L32 positive and nine were negative by PCR (including the only positive in MAT). We detected leptospiral DNA in kidney samples from carrier/hosts representing 16 species ($n = 46/103$, overall prevalence of 44.7%) in all four study areas investigated. Of the 23 mammalian carrier/host species studied, 16 had at least one leptospiral DNA-positive specimen (**Figures 2A,B**). In the carrier/host *Marmosops ocellatus*, *Leptospira* was found in 7/10 (70%) specimens, the highest prevalence in marsupials (**Figure 2A**). In rodents, *Neacomys spinosus* showed the highest percentage of *lipL32*-PCR positives (4/6, 66.7%) (**Figure 2B**).

The prevalence by study area was 12/23 (52.2%) in FSC, 26/49 (53.1%) in RFH, 1/2 (50%) in FPZ and 7/29 (24.1%) in FEC. Considering mammal orders, 22/48 (45.8%) marsupials and 24/55 (43.6%) rodents were PCR-positive. The prevalence by forest strata were 13/29 (44.8%) in canopy, 26/59 (44.1%) in soil and 6/14 (42.9%) in understory. The prevalences for each species are shown in **Figures 2A,B**, and prevalances according to collection site are show on **Figure 2C** (marsupials) and **Figure 2D** (rodents).

Considering only the PCR positive samples, 12/46 (26.1%) were positive in FSC, 26/46 (56.5%) in RFH, 1/46(2.2%) in FPZ, and 7/46 (15.2%) in FEC. Among mammal orders, 22/46 (47.8%) marsupials and 24/46 (52.2%) rodents were PCR positive. Also, considering forest strata, 13/45 (28.9%) in canopy, 26/45 (57.8%) in soil, and 6/45 (13.3%) in understory were PCR positive.

According to GLM analyses, the model with study area was suitable; however, the null model was also suitable, indicating no relation between the prevalence of infection by *Leptospira* sp. in small mammals considering the studied variables (**Table 2**). There were no differences in *Leptospira* infection between Cricetidae (12/21 = 57.1%) and Echimyidae (12/34 = 35.3%) ($\chi^2 = 2.52$, $p = 0.1124$, df = 1).

DNA from 20 samples representing 13 carrier mammalian species was amplified and sequenced using the *sec*Y genetic marker (410 bp), providing a species-specific identification of leptospires. In three samples, it was not possible to perform phylogenetic analysis due to low sequence quality. Pairwise/Blast/NCBI comparisons with the GenBank *sec*Y gene dataset identified them as *L. interrogans* ($n = 12$), *L. noguchii* ($n = 4$) and *L. santarosai* ($n = 4$) (**Table 1**). Phylogenetic analysis based on ML TN+G tree including *sec*Y sequences from different carrier/hosts confirmed species identification (**Figure 3**). Sequence data included in phylogenetic analysis are shown in the **Supplementary Material**. Sequences of *L. interrogans* from the present study clustered together with sequences of *Leptospira* isolated from small mammals but also isolated from humans, swine, and dogs from different geographical locations (**Figure 3**) with high support value (98%). Two main *L. noguchii* clusters are observed, with all sequences from the present study grouping with high support value (99%) with sequences of *Leptospira* isolated from swine and opossum, from China and Peru, respectively, and distant from sequences from other carrier/hosts (**Figure 3**). A main cluster well-supported (98%) was observed with *L. santarosai* sequences from the present study and those from different carrier/hosts and geographical locations, including small mammals, humans, swine, and capybara, all from Americas (**Figure 3**).

TABLE 1 | Pathogenic *Leptospira* genetically identified through secY gene sequencing in small mammals of the western Amazon.

Carrier/Host	*Leptospira* species	Collection Site	Sample ID (LBCE)
DIDELPHIMORPHIA			
Marmosa (micoureus) constantiae	*L. interrogans*	RFH	19802
	L. noguchii	FPZ	19850
Marmosa (Micoureus) rutteri	*L. interrogans*	RFH	19826
Marmosops ocellatus	*L. interrogans*	RFH	19804
	L. interrogans	FEC	18063
Marmosops ocellatus	*L. santarosai*	FSC	19866
Metachirus myosurus	*L. santarosai*	FSC	19828
Monodelphis glirina	*L. interrogans*	RFH	19799
	L. santarosai	FSC	19871
Monodelphis peruviana	*L. santarosai*	RFH	19823
RODENTIA			
Mesomys hispidus	*L. noguchii*	FSC	19861
Neacomys spinosus	*L. interrogans*	RFH	19818
	L. interrogans	RFH	19845
	L. interrogans	FSC	19875
Neacomys musseri	*L. interrogans*	FSC	19881
Oligoryzomys microtis	*L. interrogans*	RFH	19817
Proechimys gardneri	*L. noguchii*	FSC	19882
Proechimys gardneri	*L. interrogans*	FEC	18052
Proechimys brevicauda	*L. interrogans*	RFH	19812
Rhipidomys leucodactylus	*L. noguchii*	RFH	19819

Study areas located in the state of Acre: FSC, Floresta do Seringal Cachoeira; RFH, Reserva Florestal Humaitá; PPZ, Floresta do Parque Zoobotânico; FEC, Floresta Experimental Catuaba.

DISCUSSION

To our knowledge, this is the first study that investigated the leptospiral infection in small mammals in the Brazilian Western Amazon forest. Only one sample (6.6%), originating from the marsupial *Marmosa (Micoureus) rutteri*, was reactive against two *L. interrogans* serogroups (Australis and Autumnalis) with

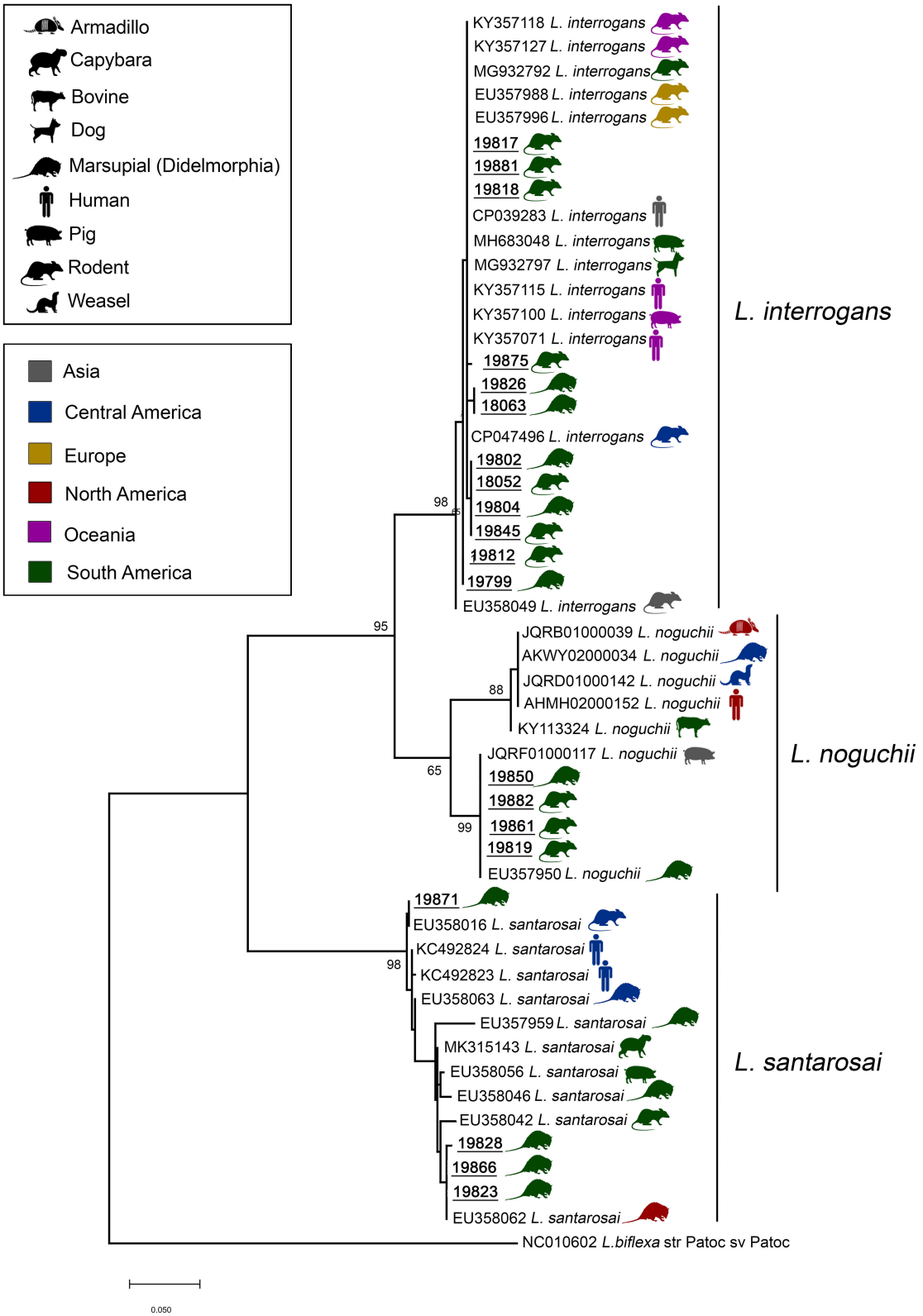

FIGURE 3 | Maximum likelihood phylogenetic tree inferred from partial *secY* gene sequences (410 bp) of *L. interrogans*, *L. noguchii,* and *L. santarosai* from this study (bold and underlined) and GenBank sequences from other carrier/hosts (accession numbers are shown). Hosts are indicated by vectors and geographical locations by colors, as indicated in the figure. Numbers at nodes are bootstrap values >50%. *Leptospira biflexa* strain "Patoc" is the outgroup taxa.

titers of 1:100 each. A limitation of this study was the small number of samples submitted to MAT, as obtaining sera from wild animals is not a trivial procedure. However, as reservoirs tend to show a seronegative response (27), the focus of this study was the identification of carriers/hosts by bacterial isolation and molecular techniques.

No bacterial isolate was obtained, possibly due to the expected low sensitivity of this technique. It is known that bacterial culturing of leptospires is fastidious, laborious, and difficult to perform (28). Additionally, the transport of samples from the field Laboratory on Acre State to the Reference Laboratory on Rio de Janeiro State delayed the filtration and reseeding of the samples, and consequently impaired bacterial isolation. Thus, the use of molecular techniques contributed for improving sensitivity of leptospiral detection, providing a broader understanding of the potential significance of infection.

We could identify, by PCR, seven Didelphimorphia and nine Rodentia species that could act as carriers of leptospires in the Amazon region. Our findings show, 13 new carrier/hosts (**Figures 2A,B**). Additionally, three species (*Mesomys hispidus*, *Neacomys spinosus* and *Oligoryzomys microtis*) were already described as leptospiral carriers in the Peruvian Amazon (29, 30) but described for the first time in the Brazilian region. Although the role of wild animals in the leptospirosis transmission cycle is unclear, the high diversity of carrier/host species found and the lack of correlation between a specific taxonomic level and a forest stratum with leptospiral infection suggest wide dissemination of the bacteria in those environments. Some studies found a higher occurrence of *Leptospira* infection in specific species of small mammals or a specific habitat/locality (9, 31). In our study, although we had observed differences in prevalence among study areas, the GLM model had no differences in relation to the null model (**Table 2**). Thus, there was no clear evidence of influence of those study areas with different land use and levels of conservation on the *Leptospira* prevalence.

Samples from the present study clustered in highly supported clades with *L. interrogans*, *L. noguchii*, and *L. santarosai*. Interestingly, sequences from the present study were similar (>98%) to sequences identified in rodents and marsupials from different locations, including all continents (**Figure 3**). Moreover, while *L. noguchii* sequences were closest to each other, forming a distinct clade almost exclusively with sequences from South America. *L. interrogans* and *L. santarosai* sequences were closely related to sequences from other carrier/hosts from different geographical locations, including dogs and humans. This reinforces that these strains are widespread geographically and between carrier/host species.

From the epidemiological perspective, the identification of the animal species that may act as carriers/hosts is crucial since each species has a particular habitat use and geographic distribution. Thus, our data comprise 16 new mammalian species, described in **Table 1**, that can be carrier/hosts in the Brazilian Western Amazon (10). Those species were found in all study areas and in all habitat strata, showing that *Leptospira* could be widely distributed. All of the 23 mammal species have a known geographic distribution in the Amazon (32, 33). Considering the 16 PCR positive species, the most tolerant species are often found in peri-urban and rural forest fragments, and therefore, the most in contact with humans are the marsupials, *D. marsupialis* and *P. canus,* and rodent species *Proechimys gardneri* (32). Regarding other carrier/host species, besides their potential role in the *Leptospira* transmission in the Amazon region, some of them could also have an epidemiological importance in other Brazilian regions since they have a wider geographic distribution.

TABLE 2 | Generalized linear models (GLM) for the prevalence of infection by *Leptospira* sp. in small mammals from Western Amazon, Acre, Brazil.

Models	AICc	Delta	Weight	K	Log-Likelihood
Locality	141.5	0	0.374	4	−66.535
Null	142	0.54	0.285	1	−69.993

AICc, corrected version of Akaike information criterion; Delta, Difference between the AICc value of a model and that of the best model; Weight, Akaike weights; K, number of parameters of the model.

Moreover, genetic analysis showed that *Leptospira* species are circulating in different ecosystems including humans and other animals as carrier/hosts. This finding confirms the importance of a One Health context to study leptospirosis. Finally, this study reports the first evidence of the diversity of small mammals as leptospiral carriers/hosts in the western Brazilian Amazon forest.

DATA AVAILABILITY STATEMENT

All datasets generated for this study are included in the article/**Supplementary Material**.

ETHICS STATEMENT

The animal study was reviewed and approved by The following licenses were used to conduct the study: permanent license to collect zoological material number 13373 (SISBIO–ICMBIO) and CEUA LW-39/14 license (Ethics Committee on animal use–FIOCRUZ).

AUTHOR CONTRIBUTIONS

LM paper writing, animal sampling, field work, PCR and MAT laboratory procedures, and project coordination. SB paper writing, bibliography research, field work, animal sampling, and data analysis. MD Leptospira sequencing, phylogenetic analysis, figures development, and paper writing. RP paper writing, bibliography research, and data analysis. NdA paper writing, field work, animal sampling, PCR procedures, and data analysis. PD'A paper writing, field work, animal sampling, animal identification by karyotyping, and DNA sequencing. AB paper writing, animal sampling, field work, animal identification by external, and cranial morphology. CC paper writing, field work, animal sampling, animal identification by external, and cranial morphology. AV PCR procedures, analysis, and paper writing. GM serological procedures, analysis, and paper writing. BT paper writing, animal identification by karyotyping, DNA sequencing, and statistical analysis. FC-C leptospira sequencing analysis and paper writing. WL project coordination and paper writing. All authors contributed to the article and approved the submitted version.

FUNDING

Field and lab work were supported by grants from Institutional Agreement IOC-Fiocruz/IFAC and from CNPq and FAPAC to Dr. LM (CNPq 428213/2016-2, CNPq 157533/2015-8 and PPSUS/FAPAC 001/2015), to Dr. PD'A (CNPq 439208/2018-1) to Dr. Elder Morato and to Dr. Marcus Silveira (PPBio/CNPq 457540/2012-5).

ACKNOWLEDGMENTS

We are grateful to the field team of Dr. LM (UFAC), à Instituto Federal de Educação, Ciência e Tecnologia do Acre. PPBIO/AC and LABPMR/Fiocruz, especially Sócrates Fraga da Costa Neto, Camila dos Santos Lucio and Fernando de Oliveira Santos for help in fieldwork. We are grateful to Drs. Thomas Wittum, Dixie Mollenkopf, Gregory Ballash, and Elizabeth Parker for the technical and English review and to the three referees for their helpful comments. We also thank UFAC for conceding the PIBIC scholarships. MD is a FAPERJ fellow. WL and PSA are CNPq fellows.

SUPPLEMENTARY MATERIAL

The Supplementary Material for this article can be found online at: https://www.frontiersin.org/articles/10.3389/fvets.2020.569004/full#supplementary-material

REFERENCES

1. Schneider MC, Najera P, Pereira MM, Machado G, Anjos CB, Rodrigues RO, et al. Leptospirosis in Rio Grande do Sul, Brazil : an ecosystem approach in the animal-human interface. *PLoS Negl Trop Dis.* (2015) 9:e0004095. doi: 10.1371/journal.pntd.0004095
2. Ellis WA. Animal leptospirosis. *Curr Top Microbiol Immunol.* (2015) 387:99–137. doi: 10.1007/978-3-662-45059-8_6
3. Haake DA. Molecular epidemiology of leptospirosis in the Amazon. *PLoS Med.* (2006) 3:e302. 10.1371/journal.pmed.0030302
4. Matthias MA, Ricaldi JN, Cespedes M, Diaz MM, Galloway RL. Human leptospirosis caused by a new, antigenically unique leptospira associated with a rattus species reservoir in the peruvian amazon. *PLoS Negl Trop Dis.* (2008) 2:e213. doi: 10.1371/journal.pntd.0000213
5. Guedes IB, Araújo SAA, de Souza GO, de Souza Silva SO, Taniwaki SA, Cortez A, et al. Circulating Leptospira species identified in cattle of the Brazilian Amazon. *Acta Trop.* (2019) 191:212–6. doi: 10.1016/j.actatropica.2019.01.011
6. Benavidez KM, Guerra T, Torres M, Rodriguez D, Veech JA, Hahn D, et al. The prevalence of Leptospira among invasive small mammals on Puerto Rican cattle farms. *PLoS Negl Trop Dis.* (2019) 13:e0007236. doi: 10.1371/journal.pntd.0007236
7. Ospina-Pinto C, Rincón-Pardo M, Soler-Tovar D, Hernández-Rodríguez P. Papel de los roedores en la transmission de Leptospira spp. en granjas porcinas. [The role of rodents in the transmission of *Leptospira spp*. in swine farms]. *Rev Salud Publica (Bogota).* (2017) 19:555–61. doi: 10.15446/rsap.v19n4.41626
8. Venter O, Fuller RA, Segan DB, Carwardine J, Brooks T, Butchart SHM, et al. Targeting global protected area expansion for imperilled biodiversity. *PLoS Biol.* (2014) 12:e1001891. doi: 10.1371/journal.pbio.1001891
9. Obiegala A, Woll D, Karnath C, Silaghi C, Schex S, Eßbauer S, et al. Prevalence and Genotype Allocation of Pathogenic *Leptospira* Species in Small Mammals from Various Habitat Types in Germany. *PLoS Negl Trop Dis.* (2016) 10:e0004501. doi: 10.1371/journal.pntd.0004501
10. Vieira AS, Pinto PS, Lilenbaum W. A systematic review of leptospirosis on wild animals in Latin America. *Trop Anim Health Pro.* (2017) 1125:1–10. doi: 10.1007/s11250-017-1429-y
11. Mesquita GSS, Rocha KS, Monteiro TRM, Rosário MKSD, Baia IWM, Pereira HS, et al. Detection of antibodies against Leptospira spp. in free-living marsupials caught in the Eastern Amazon. *Rev Soc Bras Med Trop.* (2018) 51:368–71. doi: 10.1590/0037-8682-0236-2017
12. dos Santos LF, Guimarães MF, de Souza GO, da Silva IWG, Santos JR, Azevedo SS, et al. Seroepidemiological survey on *Leptospira* spp. infection in wild and domestic mammals in two distinct areas of the semi-arid region of northeastern Brazil. *Trop Anim Health Prod.* (2017) 49:1715–22. doi: 10.1007/s11250-017-1382-9
13. Vieira AS, Di Azevedo MIN, D'Andrea PS, do Val Vilela R, Lilenbaum W. Neotropical wild rodents Akodon and Oligoryzomys (Cricetidae: Sigmodontinae) as important carriers of pathogenic renal Leptospira in the Atlantic forest, in Brazil. *Res Vet Sci.* (2019) 124:280–3. doi: 10.1016/j.rvsc.2019.04.001
14. Jorge S, Hartleben CP, Seixas FK, Coimbra MA, Stark CB, Larrondo AG, et al. *Leptospira borgpetersenii* from free-living white-eared opossum (*Didelphis albiventris*): first isolation in Brazil. *Acta Trop.* (2012) 124:147–51. doi: 10.1016/j.actatropica.2012.07.009
15. Fornazari F, Langoni H, Marson PM, Nóbrega DB, Teixeira CR. Leptospira reservoirs among wildlife in Brazil: Beyond rodents. *Acta Trop.* (2018) 178:205–12. doi: 10.1016/j.actatropica.2017.11.019
16. Lemos ERS, D'Andrea PS. *Trabalho de Campo Com Animais: Procedimentos, Riscos e Biossegurança*. Rio de Janeiro, Publisher: FIOCRUZ, Rio de Janeiro, RJ, Brazil. (2014). p. 180.
17. Bonvicino CR, Otazu IB, Vilela JF. Karyologic and molecular analysis of Proechimys Allen, 1899 (Rodentia, Echimyidae) from the Amazonian region. *Arq Mus Nac.* (2005) 63:191–200.
18. Gonçalves PR, Oliveira JA. An integrative appraisal of the diversification in the Atlantic Forest genus Delomys (Rodentia: Cricetidae: Sigmodontinae) with the description of a new species. *Zootaxa.* (2014) 1:1–38. doi: 10.11646/zootaxa.3760.1.1
19. Chakraborty A, Miyahara S, Villanueva SY, Saito M, Gloriani NG, Yoshida S. A novel combination of selective agents for isolation of *Leptospira* species. *Microbiol Immunol.* (2011) 55:494–501. doi: 10.1111/j.1348-0421.2011.00347
20. World Organisation for Animal Health, 2012: Leptospirosis. In: *Manual of Diagnostic Tests and Vacines for Terrestrial Animals.* World Organization for Animal Health, Paris. Available online at: http://www.oie.int/fileadmin/Home/eng/Health_standards/tahm/3.01.12_LEPTO.pdf
21. Vieira AS, Narduche L, Martins G, Schabib PIA, Zimmermann NP, Juliano RS, et al. Detection of wild animals as carriers of Leptospira by PCR in the Pantanal biome, Brazil. *Acta Tropica.* (2016) 163:87–9. doi: 10.1016/j.actatropica.2016.08.001
22. Thompson J, Higgins D, Gibson, T. CLUSTAL W: improving the sensitivity of progressive multiple sequence alignment through sequence weighting, positions-specific gap penalties and weight matrix choice. *Nuc Ac Res.* (1994) 22:4673–80.
23. Hall TA. BioEdit: a user-friendly biological sequence alignment editor and analysis program for Window 95/98/NT. *Nucleic Acids Symposium Series.* (1999) 41:95–8.
24. Kumar S, Stecher G, Li M, Knyaz C, Tamura K. MEGA X: molecular evolutionary genetics analysis across computing platforms. *Mol Biol Evol.* (2018) 35:1547–9. doi: 10.1093/molbev/msy096
25. R Core Team. *R: A Language and Environment for Statistical Computing. R Foundation for Statistical Computing, Vienna, Austria*. (Retrieved on February 10th, 2017 (2017). Available from: https://www.R-project.org/
26. Oksanen J, Blanchet FG, Kindt R, Legendre P, Minchin PR, O'Hara RB, et al. *Community Ecology Package*. (2017) R. package version. 2, 4–2.
27. de Albuquerque NF, Martins G, Medeiros L, Lilenbaum W, Ribeiro VMF. The role of capybaras as carriers of leptospires in periurban

and rural areas in the western Amazon. *Acta Trop.* (2017) 169:57–61. doi: 10.1016/j.actatropica.2017.01.018
28. Faine S, Adler B, Bolin C, Perolat P. *Leptospira and Leptospirosis*. (2nd ed). Melbourne, VIC: MedScience (2000). p. 272.
29. Bunnell JE, Hice CL, Watts VM, Montrueil V, Tesh RB, Vinetz, et al. Detection of pathogenic Leptospira spp. Infections among mammals captured in the Peruvian Amazon basin region. *Am J Trop Med Hyg.* (2000) 63:255–8. doi: 10.4269/ajtmh.2000.63.255
30. Cortez V, Canal E, Dupont-Turkowsky JC, Quevedo T, Albujar C, Chang TC, et al. Identification of Leptospira and Bartonella among rodents collected across a habitat disturbance gradient along the Inter- Oceanic Highway in the southern Amazon Basin of Peru. *PLoS ONE*. (2018) 13:e0205068. doi: 10.1371/journal.pone.0205068
31. Fischer S, Mayer-Scholl A, Imholt C, Spierling NG, Heuser E, Schmidt S, et al. *Leptospira* genomospecies and sequence type prevalence in small mammal populations in Germany. *Vect Borne Zoonotic Dis.* (2018) 4:188–99. doi: 10.1089/vbz.2017.2140
32. Faria MB, Lanes RO, Bonvicino CR. *Marsupiais do Brasil. Guia de identificação com base em caracteres morfológicos externos e cranianos*. 1. ed. São Caetano do Sul: Amélie Editorial (2019). v. 1. p.84.
33. Patton JL, Pardiñas UFJ, D'Elía G (editors). *Mammals of South America.* Volume 2: Rodents. Chicago, IL: University of Chicago Press (2015). p. xxvi + 1336.

Conflict of Interest: The authors declare that the research was conducted in the absence of any commercial or financial relationships that could be construed as a potential conflict of interest.

frontiers in Veterinary Science

MINI REVIEW
published: 20 January 2021
doi: 10.3389/fvets.2020.615293

The True Host/s of Picobirnaviruses

Souvik Ghosh[1]* *and Yashpal S. Malik*[2]

[1] Department of Biomedical Sciences, Ross University School of Veterinary Medicine, Basseterre, Saint Kitts and Nevis,
[2] College of Animal Biotechnology, Guru Angad Dev Veterinary and Animal Science University, Ludhiana, India

Picobirnaviruses (PBVs) are bisegmented double-stranded RNA viruses that have been detected in a wide variety of animal species including invertebrates and in environmental samples. Since PBVs are ubiquitous in feces/gut contents of humans and other animals with or without diarrhea, they were considered as opportunistic enteric pathogens of mammals and avian species. However, the virus remains to be propagated in animal cell cultures, or in gnotobiotic animals. Recently, the classically defined prokaryotic motif, the ribosomal binding site sequence, has been identified upstream of putative open reading frame/s in PBV and PBV-like sequences from humans, various animals, and environmental samples, suggesting that PBVs might be prokaryotic viruses. On the other hand, based on the detection of some novel PBV-like RNA-dependent RNA polymerase sequences that use the alternative mitochondrial genetic code (that of mold or invertebrates) for translation, and principal component analysis of codon usage bias for these sequences, it has been proposed that PBVs might be fungal viruses with a lifestyle reminiscent of mitoviruses. These contradicting observations warrant further studies to ascertain the true host/s of PBVs, which still remains controversial. In this minireview, we have focused on the various findings that have raised a debate on the true host/s of PBVs.

Keywords: picobirnavirus, true host/s, opportunistic animal pathogen, prokaryotic virus, fungal virus

OPEN ACCESS

Edited by:
Subhash Verma,
Chaudhary Sarwan Kumar Himachal Pradesh Krishi Vishvavidyalaya, India

Reviewed by:
Soma Chattopadhyay,
Institute of Life Sciences (ILS), India
Santhamani Ramasamy,
Public Health Research Institute (PHRI), United States

***Correspondence:**
Souvik Ghosh
souvikrota@gmail.com

Specialty section:
This article was submitted to Veterinary Infectious Diseases, a section of the journal Frontiers in Veterinary Science

Received: *08 October 2020*
Accepted: *24 December 2020*
Published: *20 January 2021*

Citation:
Ghosh S and Malik YS (2021) The True Host/s of Picobirnaviruses. Front. Vet. Sci. 7:615293. doi: 10.3389/fvets.2020.615293

INTRODUCTION

Picobirnaviruses (PBVs) are bisegmented double-stranded RNA viruses that belong to the sole genus *Picobirnavirus* within the family *Picobiraviridae* (1). Picobirnaviruses have been widely reported in fecal samples/gut contents of humans and various animal species with, or without diarrhea (1–3). Traditionally, PBVs are considered as opportunistic enteric pathogens of mammals and avian species (1–5). On the other hand, PBVs have also been detected in invertebrates and environmental samples (6–9). During the past few years, the whole genomes, or at least the complete/nearly complete gene segment-2 sequences of several PBV strains from humans, different animal species and environmental samples have been obtained using next generation sequencing technologies, or a modified non-specific primer-based amplification method (1, 4, 6–8, 10–20). Analyses of the expanded repertoire of diverse full-length/nearly full-length PBV sequences revealed remarkable features in the PBV genome including those that suggest that PBVs might be actually prokaryotic or fungal viruses (1, 4, 6–8, 10–21). In this minireview, we have discussed the various findings that have raised a debate on the true hosts of PBVs.

PICOBIRNAVIRUS MORPHOLOGY AND GENOME

Picobirnaviruses are spherical, non-enveloped viruses with a diameter of ∼33–37 nm (1). Since PBVs are non-cultivable, information on the virus capsid is based on those of recombinant virion-like particles (22). PBV possess a simple icosahedral capsid that is composed of 60 symmetric dimers (22). The PBV capsid contains two segments of dsRNA, designated as gene segment-1 (∼2.2–2.7 kb in size) and −2 (∼1.2–1.9 Kb in size) (**Figure 1**) (1–3, 5). Because of their small size ("*pico*" in Spanish) and bi-segmented ("*bi*" in Latin) nature of the viral genome, the viruses were named "Picobirnaviruses" (23). However, PBVs with monopartite genomes have also been reported in a few studies (6, 24, 25).

The gene segment-1 of PBVs consists of 2 or 3 open reading frames (ORFs), designated as ORF1, ORF2, and ORF3 from the 5′- end (**Figure 1**) (1, 13). The ORF3 codes for a precursor of the capsid protein which undergoes autocatalytic cleavage to generate the mature capsid protein, and a charged peptide that is believed to interact electrostatically with the viral RNA (22). The ORF2 encodes a protein characterized by repeats of the ExxRxNxxxE motif (1, 26). However, the function/s of this protein is not yet known. On the other hand, the functionality, or even the presence of ORF1 in gene segment-1 of PBVs remain to be elucidated (1, 13, 26). The PBV gene segment-2 possess a single large ORF that encodes the RNA-dependent RNA polymerase (RdRp) (**Figure 1**) (1–3, 5). The 5′- (GUAAA) and 3′- (ACUGC) termini sequences appear to be conserved in the gene segment 2 of PBVs (1, 10, 14–20). The PBV RdRp catalyzes RNA synthesis with both single-stranded RNA and dsRNA templates, and transcription occurs in a semi-conservation manner (27). During encapsidation, the RdRp is believed to form a complex with the viral genome (27).

Picobirnaviruses exhibit high genetic diversity within and between host species (1–5, 10–18, 24, 28–30). A viral metagenomics study in diarrheic free-ranging wolves has provided evidence for genetic reassortment events among PBVs (31). Most studies on genetic diversity of PBVs are based on gene segment-2/RdRp sequences (2–5). The phylogenetic analysis of PBV RdRp sequences has been shown in **Figure 2**. Majority of the PBV RdRp sequences reported so far use the standard genetic code for translation, whilst, recently, some novel PBV-like RdRp gene sequences that use an alternative mitochondrial genetic code have been detected in bats, humans, invertebrates, and a mongoose (6, 11, 12, 14). Picobirnaviruses using the standard genetic code cluster separately from PBVs using the alternative mitochondrial genetic code (12, 14). However, three PBV-like RdRp sequences (from a bat, a mongoose and a myriapod) that use an alternative mitochondrial genetic code were found to cluster with PBVs using the standard genetic code (12, 14). These unique PBV-like RdRp sequences have been discussed in the section "evidence that picobirnaviruses might infect fungi" of the review article. Within the cluster of PBV RdRp sequences using the standard genetic code, PBVs are further classified into two genogroups (genogroup-I (GI) and GII), although several PBVs that could not be classified into either genogroup have also been reported (1–5, 10–20, 24, 29, 30). Picobirnavirus GI strains have been more frequently detected compared to GII strains (2, 3, 5).

PICOBIRNAVIRUS INFECTION IN HUMANS AND ANIMALS

Picobirnavirus infection in humans and animals have been excellently reviewed by Ganesh et al. (2) and Malik et al. (3). Picobirnaviruses have been detected in sporadic cases of diarrhea as well as associated with outbreaks of gastroenteritis in humans and in a wide variety of animals (1–3, 5). They are often reported in coinfection with other enteric pathogens (1–5, 32–34). On the other hand, PBVs have also been frequently detected in apparently healthy humans and animals without diarrhea (1–3, 5, 14, 15, 18).

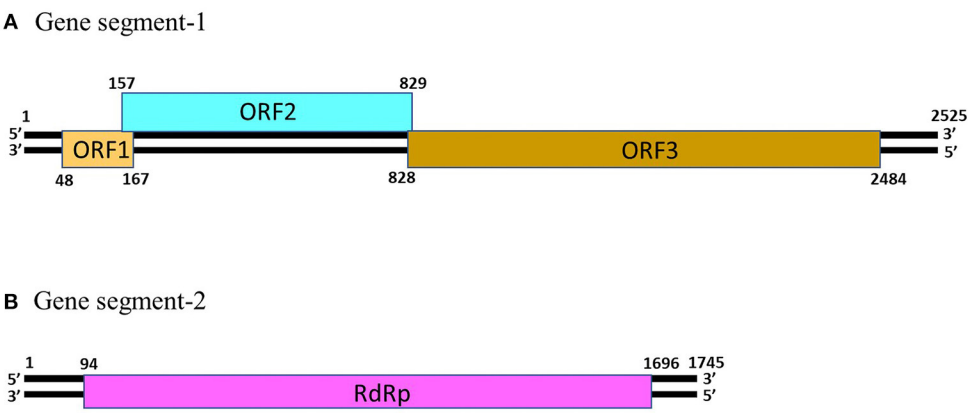

FIGURE 1 | The genomic organization of human picobirnavirus genogroup-I strain Hy005102. **(A)** Gene segment-1 (GenBank accession number AB186897) of PBV strain Hy005102 consists of 3 putative open reading frames (ORF), designated as ORF1, ORF2 and ORF3. The ORF3 codes for a precursor of the viral capsid protein. **(B)** Gene segment-2 (GenBank accession number AB186898) of PBV strain Hy005102 possess a single ORF that encodes the viral RNA-dependent RNA polymerase (RdRp).

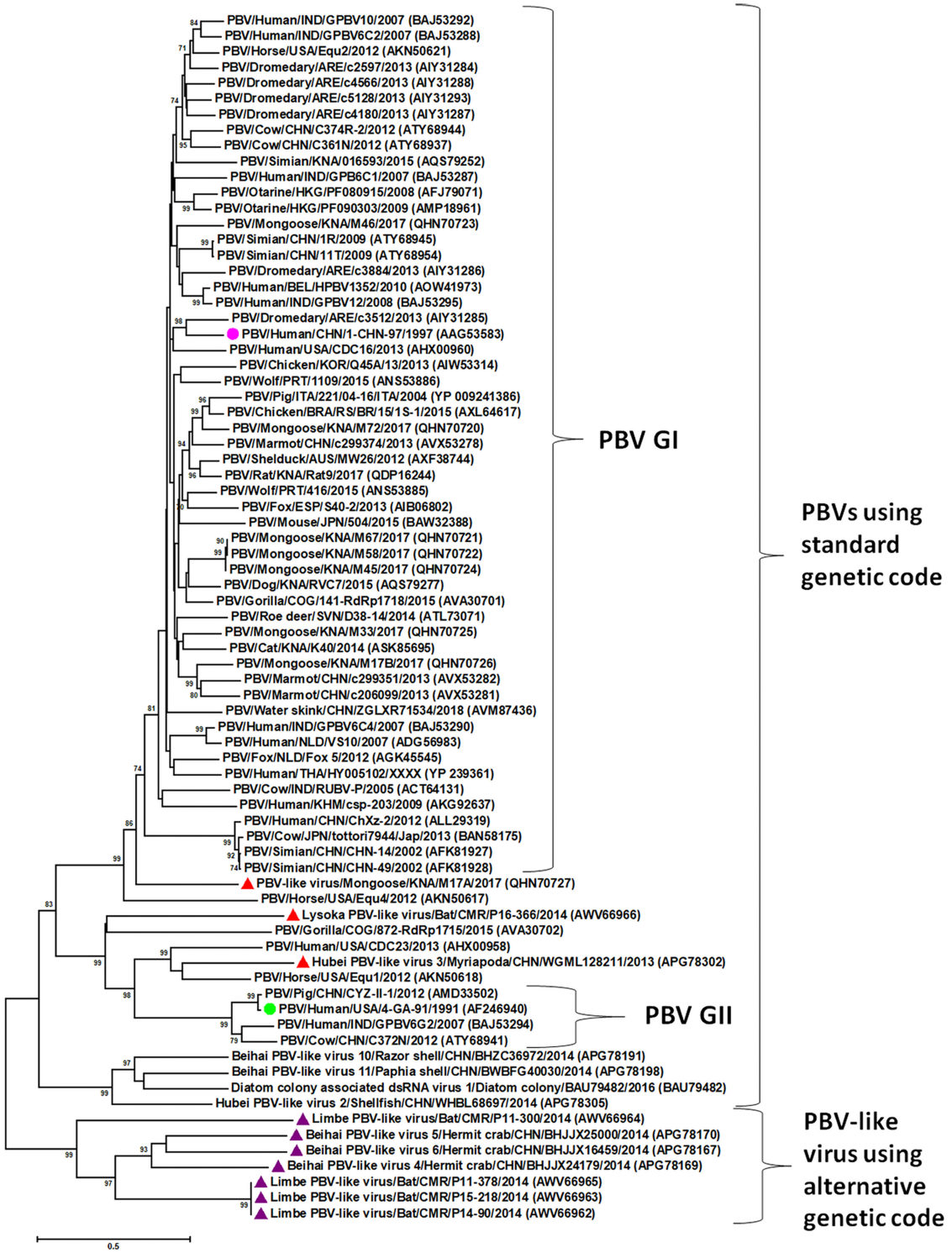

FIGURE 2 | Phylogenetic analysis of the picobirnavirus (PBV) and PBV-like RNA-dependent RNA polymerase (RdRp) sequences. The phylogenetic tree was constructed by the Maximum Likelihood method using the MEGA6 software. Phylogenetic distances were measured using the LG + G model of substitution. The tree was statistically supported by bootstrapping with 500 replicates. Bootstrap values <70% are not shown. Scale bar, 0.5 substitutions per amino acid. The name of the PBV strain includes virus/host of detection/country/common name/date of collection. GenBank accession numbers are shown in parentheses. Pink circle: prototype PBV genogroup-I (GI) strain; green circle: prototype PBV GII strain; purple triangles: PBV-like viruses that use an alternative mitochondrial genetic code to translate the RdRp and cluster separately from PBVs using the standard genetic code; red triangles: PBV-like strains that use an alternative mitochondrial genetic code to translate the RdRp, yet cluster within PBVs using standard genetic code.

Based on studies in immunocompromised and immunosuppressed humans, PBVs were considered as opportunistic enteric pathogens (2, 3). PBVs have been reported more frequently in HIV-infected patients with diarrhea than those without diarrhea (35–38), and in fecal samples from kidney transplant patients (39, 40). In organ transplant recipients, PBVs were predictive of the occurrence of severe enteric graft-vs.-host disease (GVHD), and correlated with the high levels of GVHD severity markers in feces (41). Recently, it was demonstrated that pregnant women with type 1 diabetes (T1D) are more likely to harbor PBVs than those without T1D (42).

Prolonged fecal shedding of PBVs, characterized by alternating periods of high-, low-, and no- virus detection, have been observed in asymptomatic animals, and in healthy and HIV-infected humans (35, 38, 43–50). Various factors, such as age, stress, physiological status and environmental conditions have been proposed to influence the PBV shedding patterns in infected humans and animals. In studies monitoring PBV shedding patterns in animals, highest excretion rates were observed during the lactogenic period in pigs and sheep, whilst increased viral shedding occurred at a young age in rabbits (weaned), broilers (aged 2–7 weeks) and rhea (∼3 weeks of age) (44, 46, 49, 51, 52). Based on these observations, it has been suggested that animals could acquire PBV infection early in life, followed by establishment of persistent infection, with infected adults serving as asymptomatic carriers (2, 3, 5).

Although mostly reported in feces/gut contents, PBVs have also been detected, albeit rarely, in the respiratory tract of humans (from individuals with unexplained respiratory disease in Netherlands and cases of severe acute respiratory infection in Uganda) and animals (asymptomatic cattle, monkeys and pigs) and in the plasma of a febrile horse, suggesting an expanded tissue tropism of the virus (10, 24, 53–55).

PBVs exhibit high genetic diversity between and within host species, and phylogenetically, species specific clustering patterns have not been observed so far (1, 4, 10–18, 24, 28–31). Nevertheless, based on sequence identities and phylogenetic analysis, interspecies transmission events including zoonoses have been proposed for PBVs, although several of these studies were based on partial gene segment-2 sequences and are not conclusive (2–5, 11, 40, 43, 53, 56–60).

EVIDENCE THAT PICOBIRNAVIRUSES MIGHT INFECT PROKARYOTES

One of the intriguing recent findings on PBVs has been the identification of a classically defined prokaryotic motif, the ribosomal binding site (RBS) sequence (also known as Shine-Dalgarno sequence), upstream of putative ORF/s in PBV gene segment-1 and−2 sequences (**Table 1**) (13, 21). In prokaryotes, the RBS sequence (AGGAGG), or its subset (4-, 5-, or 6- mer of AGGAGG) enables the mRNA to bind to ribosome, resulting in initiation of translation, and is mostly located anywhere between −18 and −4 nucleotides upstream from the start codon (21, 61–63). Certain viruses that infect prokaryotes have been shown to be highly enriched for RBS sequences, such as the bacteriophages with segmented dsRNA genomes of family *Cystoviridae* (13, 21, 64, 65). Similar to prokaryotic mRNAs and the cystoviruses, the RBS sequence, or its subset has been found to be conserved upstream of putative ORF/s (putative ORF1, 2 and 3 in gene segment-1 and putative ORF for RdRp in gene segment-2) in published PBV sequences from humans, animals and environmental samples (4, 7, 8, 11–18, 21). The presence of the conserved prokaryotic RBS sequence upstream of the putative start codon/s in representative PBV gene segment-1 sequences, gene segment-2 sequences of PBV GI and GII strains, and PBV-like RdRp sequences are shown in **Table 1**. In fact, PBVs exhibited an enrichment level for RBS sequences that was higher than those observed in any known prokaryotic viral family (21). Based on these observations, it has been proposed that PBVs might be actually prokaryotic viruses (13, 21). Since not all prokaryotic viruses appear to retain the prokaryotic RBS sequence, and not every bacterial phylum exhibits a high level of enrichment for RBS sequences, it has been hypothesized that viruses enriched for RBS sequences, such as PBVs, were more likely to infect bacteria that highly conserves the RBS sequences for its own genes (21).

Supporting the hypothesis on prokaryotic hosts, PBVs remain to be successfully propagated in eukaryotic cell cultures (1). However, previous experiences with adapting enteric viruses, especially noroviruses to cell culture have been extremely challenging (66). Furthermore, the lack of a cell culture platform in itself does not rule out the possibility that PBVs are animal viruses. Recently, attempts were made to cultivate PBVs in prokaryotic cells by inoculating 3% cloacal suspension from a PBV positive chicken into brain heart infusion broth (13). The *in vitro* cultures were maintained under aerobic and anaerobic conditions for 2 weeks, and regularly monitored for PBV RNA by RT-qPCR assay. There was no evidence for amplification of PBVs during the study period. Since the sample was collected and frozen long-term to analyze viral nucleic acid rather than maintain bacterial diversity or retain viral infectivity, it might have been possible that the number of cultivable, intact bacteria as well as the low initial infective particles were significantly decreased. However, in the same study, expression analysis in *Escherichia coli* using 6xHis-tagged recombinant PBV segment-1 and western blot assay revealed the *in vivo* functionality of PBV segment-1 sequences containing the RBS motif in a bacterial system (13). The ubiquitous nature of PBVs, especially high prevalence of the virus in environmental samples including sewage water and detection of viral RNA in feces/gut contents from a wide variety of animal species including atypical hosts such as reptiles and invertebrates, and persistent fecal shedding by asymptomatic animals, suggest that PBVs might be prokaryotic viruses of the gut microbiome (1–3, 6–9, 43–52).

On the other hand, certain observations with PBVs are reminiscent of eukaryotic viruses, such as (i) viremia in a sick horse and respiratory tract infections in cattle, humans, monkeys and pigs, (ii) immune response in a rabbit that was temporally associated with PBV excretion, and (iii) autoproteolytic processing of the PBV capsid protein and liposome-perforating capacity of viral particles (10, 22, 24, 53–55, 67). However, similar findings have also been reported for bacteriophages:(i) bacteriophages have been detected in blood

TABLE 1 | The location of the prokaryotic ribosomal binding site (RBS) sequence upstream of the putative open reading frame/s (ORF) in picobirnavirus (PBV) and PBV-like sequences.

Host/PBV strain	PBV gene segment-1			
	GenBank accession number	5′- UTR of putative ORF-1	5′ -UTR of putative ORF-2	5′ -UTR of putative ORF-3 (ORF3 codes for the Capsid)
(A) PBV GENE SEGMENT-1				
Human/Hy005102	AB186897	GAAGGAGAGATGTT**ATG**AA	AAAGGAGGTTATTTA**ATG**AC	GCAGGAGGTTTATC**ATG**AA
Pig/221/04-16/ITA/2004	KF861770	AAAGGAGAATGATCTAAC**ATG**AA	TAAGGAGGTGAAAGTT**ATG**CT	ATGGAGGCTAAT**ATG**AA
Otarine/PF090307	KU729753	AAAGGAGATGTGCATTTTTA**ATG**GA	AAAGGAGGAAATGT**ATG**AC	AAAGGAGTGTTTAAT**ATG**TC
Roe deer/SLO/D38-14/2014	NC_040752	GAAGGAGGAG**ATG**CT	AAAGGAGGACACAGTTTC**ATG**AC	TAAGGAGAATATTACAA**ATG**AA
Wolf/PRT/891/2015	KT934310	AAAGGAGGAACTT**ATG**TGTAGTAA	AAAGGAGGA**ATG**CA	AAAGGAGACCATTAATA**ATG**GC
Marmot/c130145_g1_i1 _libraryA_2712	KY928752	AAAGGAGGACTGTTGGA**ATG**TT	AAAGGAGGTC**ATG**TA	AAAGGATTTATTATC**ATG**AG
Rabbit/ R5-9	NC_038919	ATAGGAGGAAGTGCTTATGAAAC**ATG**CA	AAAGGAGGTGTCAATGGT**ATG**AC	CTAGGAGGTAAAAT**ATG**AA
Macaque/WUSTL	MG010886	AAAGGAGAACAGATC**ATG**GT	AAAGGAGGAAACGTTT**ATG**AC	CTGGAGAAAATT**ATG**AG
Chicken/ChPBV-S1-ctg289/2013-HUN	MH425579	AAAGGAGGAATCAGTGTTTT**ATG**GA	AAAGGAGGTATATA**ATG**AC	ATAGGAGGAATAAAT**ATG**AA
Turkey/USA/MN-1/2011	KJ495689	AAAGGAGGCGTACGTA**ATG**GT	CAAGAAAGGAAGTGACAAAC**ATG**AC	TTGGAGGAATTATCG**ATG**GG

Host/Genogroup/PBV strain	PBV gene segment-2		Host/Genogroup/PBV strain	PBV gene segment-2	
	GenBank accession number	5′-UTR of putative ORF (ORF codes for the RdRp)		GenBank accession number	5′ -UTR of putative ORF (ORF codes for the RdRp)
(B) PBV GENE SEGMENT-2					
Human/GI/Hy005102	AB186898	AAAGGAGGACTACTT**ATG**CA	Marmot/GI/c299351	KY928717	AAAGGAGGTTCACGTT**ATG**CC
Pig/GI/221/04-16/ITA/2004	KF861773	AAAGGAGGCTAAGCATT**ATG**CC	Rat/GI/Rat9	MH412924	AAAGGAGGCTTTTCTAT**ATG**CC
Otarine/GI/PF090307	KU729767	AAAGGAGGCCATTACA**ATG**CC	Shelduck/GI/MW26	MH453875	AAAGGAGGCTATCTTT**ATG**CC
Roe deer/GI/SLO/D38-14/2014	NC_040753	AAAGGAGGTTATCGTT**ATG**CC	Chicken/GI/ChPBV-S2-ctg1042/2013-HUN	MH425584	AAAGGAGGTAATGCTT**ATG**CT
Dog/GI/RVC7	KY399057	AAAGGAGGTTCACATT**ATG**CC	Turkey/GI/USA/MN-1/2011	KJ495690	AAAGGAGGTCATTCATGT**ATG**AA
Cat/GI/K40	MF071281	AAAGGAGGTCGCGTA**ATG**CC	Human/GII/4-GA-91	AF246940	AAAGGAGGTTTACT**ATG**AA
Cow/GI/RUBV-P	GQ221268	AAAGGAGGACTACAAA**ATG**TC	Cow/GII/C372N	KY120178	AAAGGAGGTTTACT**ATG**AA
Horse/GI/Equ2	KR902505	AAAGGAGGTTACGTT**ATG**CC	Pig/GII/CYZ-II-1	KP984805	AAAGGAGGTTTACT**ATG**AA
Water skink/GI/ZGLXR71534	MG600064	AAAGGAGGACATTAGAT**ATG**TC	*Mongoose/ND/M17A*	MN563302	TCAGGAGGTTAGTTTCTT**GTG**AT
Wolf/GI/PRT/1109/2015	KT934308	AAAGGAGGTCCGTT**ATG**CC	*Myriapoda/ND/WGML128211*	KX884187	AAAGGAGTTTTACT**ATG**AG
Simian/GI/016593	KY053143	AAAGGAGGCCATCATT**ATG**CC	*Bat/ND/P15-218*	MG693102	AAAGGAGGAAACAAGA**ATG**CC
Mongoose/GI/M17B	MN563301	AAAGGAGGTTCACGTT**ATG**CC	*Hermit crab/ND/BHJJX25000*	KX884060	AGAGAGGGATATCTA**ATG**AA

The RBS sequence is underlined, whilst the putative start codon is shown with bold font, respectively. The PBV-like sequences that use an alternative mitochondrial genetic code for translating the putative RNA-dependent RNA polymerase (RdRp) are shown with italics. UTR, untranslated region.

(phagemia) and respiratory samples, (ii) immune responses have been raised against prokaryotic viruses, and (iii) autoproteolytic capacities have been demonstrated for bacteriophages (68–72).

EVIDENCE THAT PICOBIRNAVIRUSES MIGHT INFECT FUNGI

The recent detection of unique PBV-like sequences that lack a putative ORF for RdRp using the standard genetic code, but use an alternative mitochondrial genetic code for translation has further complicated the ongoing debate on true hosts of PBVs (6, 11, 12, 14). These PBV RdRp-like sequences have been detected in bats, humans, invertebrates (crustaceans and myriapods), and a mongoose (6, 11, 12, 14). The human PBV-like RdRp sequences were closely related (99% sequence identities) to that of a bat PBV-like RdRp sequence detected in the same region (11). The PBV-like RdRp sequences were found to translate the putative RdRp using the invertebrate mitochondrial genetic code (transl_table=5, NCBI genetic codes, www.ncbi.nlm.nih.gov/Taxonomy/Utils/wprintgc.cgi#SG5) as well as the mold mitochondrial genetic

code (transl_table=4, NCBI genetic codes, www.ncbi.nlm.nih.gov/Taxonomy/Utils/wprintgc.cgi#SG4) (6, 11, 12, 14). Based on phylogenetic analysis of the PBV- and PBV-like RdRp sequences, except for three PBV-like strains (Lysoka PBV-like virus/Bat/CMR/P16-366/2014, Hubei PBV-like virus 3/Myriapoda/CHN/WGML128211/2013, and PBV-like virus/Mongoose/KNA/M17A/2017), the PBV-like RdRp sequences formed a separate cluster that was distinct from the PBVs using standard genetic code including PBV GI and GII strains (**Figure 2**) (6, 11, 12, 14). The metagenomics data pool reporting these PBV-like RdRp sequences did not reveal any PBV-like capsid sequences (6, 12). Based on these observations, it has been proposed that the PBV-like strains using the alternative mitochondrial genetic code might have a lifestyle that is reminiscent of mitoviruses (12).

Mitoviruses (genus *Mitovirus*, family *Narnaviridae*) are plus-stranded RNA virus-like elements that replicate in the fungal mitochondria, although they have also been reported in plants and invertebrates (thought to be derived from fungal symbionts) (73–75). Mitoviruses lack a capsid, and the viral genome consists of a single long ORF that encodes a deduced protein with the conserved motifs of a viral RdRp. Principal component analysis of the codon usage bias revealed close clustering of the PBV-like RdRp sequences from bats and invertebrates with those of mitoviruses using the mitochondrial genetic code, corroborating the hypothesis that PBVs might behave like mitoviruses (12). By phylogenetic analysis of RdRp sequences from different virus families, PBVs and partitiviruses (known to infect fungi and plants, and share similarities in capsid architecture and genome organization with PBVs) were found to constitute the partitivirus-picobirnavirus clade, which, interestingly, also consisted of some naked RNA replicons that reproduce in algae mitochondria or chloroplasts, translate using a mitochondrial genetic code, and exhibit mitovirus-like behavior (76). Taken together, these findings suggested that PBVs might be fungal viruses.

On the other hand, at least three PBV-like RdRp sequences (P16-366, WGML128211, and M17A from a bat, myriapod and mongoose, respectively) that use the alternative mitochondrial genetic code (that of mold or invertebrate) for translation were found to cluster within PBVs using the standard genetic code (**Figure 2**) (6, 12, 14). Furthermore, a capsid sequence was identified for the bat PBV-like strain P16-366 (12). Based on phylogenetic analysis of RdRp sequences, it has been hypothesized that the dsRNA viruses of the partitivirus-picobirnavirus clade might have evolved through reassortment events involving gene segments encoding, respectively, a dsRNA virus capsid protein related to those of the major clade of dsRNA viruses (cystoviruses, totiviruses, and reoviruses) and a positive sense RNA virus RdRp (possibly from a naked RNA replicon within the partitivirus-picobirnavirus clade) (76), which might offer a possible explanation for the origin of P16-366. Although the presence or absence of a capsid sequence could not be determined for the mongoose PBV-like strain M17A, the RdRp sequence of M17A retained the various features (5′- terminal nucleotide sequence and the three motifs (DFXKFD, SGSGGT and GDD) in putative RdRp) that are conserved in gene segment-2 of PBVs, and phylogenetically, clustered near PBV GI strains (14). Further analyses are required to decipher the complex evolution of these PBV-like strains.

LIMITATIONS AND FUTURE SCOPE OF RESEARCH

Studies so far could not establish a consistent association between PBV detection and diarrhea in humans and animals (1, 5). Moreover, there are a few reports on detection of PBVs in respiratory samples and in a serum sample from mammals (10, 24, 53–55). To date, PBVs remain to be successfully propagated in mammalian cell culture systems and/or gnotobiotic animal models (1). As a result, the tissue tropism and pathogenesis of PBVs in mammals remain to be elucidated so far, necessitating further research toward establishing mammalian cell culture systems, intestinal organoids, and/or gnotobiotic animal models that would support the propagation of the virus. On the other hand, the recent speculations that PBVs might actually infect bacteria or fungi were based on analyses of PBV and PBV-like sequences (7, 8, 12–14, 21, 76). To date, PBVs have not yet been isolated from cultured bacterial or fungal cells. In order to conclusively establish that PBVs are prokaryotic or mycoviruses, future research should focus on successful propagation of PBVs in various prokaryotic and fungal cell culture systems, especially those derived from the gut microbiome of mammals.

CONCLUSIONS

Since PBVs have been mostly detected in feces/gut contents of animals and humans with or without diarrhea, they were considered as opportunistic enteric pathogens of mammals (2, 3). However, the identification of the prokaryotic RBS sequence upstream of putative ORF/s in PBV and PBV-like sequences indicate that PBVs might actually infect bacteria (7, 8, 13, 21). Furthermore, by phylogenetic analysis of viral RdRp sequences, the partitivirus-picobirnavirus clade has been hypothesized to have originated in an as-yet-undiscovered lineage of prokaryotic RNA viruses (76). On the other hand, detection of some novel PBV-like RdRp sequences that use the alternative mitochondrial genetic code (that of mold or invertebrates) for translation has raised the speculation that PBVs might be fungal viruses with a mitovirus-like lifestyle (6, 12, 14). Based on these observations, it might be possible that PBVs actually infect the gut microbiome of mammals and not mammalian cells. Taken together, these contradicting findings warrant further studies to ascertain the true host/s of PBVs, which still remains controversial. Until the true host/s of PBVs are proven, caution should be exercised during interpretation of PBV-related data in animals and humans, especially those on interspecies transmission events.

AUTHOR CONTRIBUTIONS

All authors listed have made a substantial, direct and intellectual contribution to the work, and approved it for publication.

FUNDING

This work was funded by the One Health Center for Zoonoses and Tropical Veterinary Medicine, Ross University School of Veterinary Medicine, St. Kitts and Nevis.

REFERENCES

1. Delmas B, Attoui H, Ghosh S, Malik YS, Mundt E, Vakharia VN. Ictv virus taxonomy profile: picobirnaviridae. *J Gen Virol*. (2019) 100:133–4. doi: 10.1099/jgv.0.001186
2. Ganesh B, Masachessi G, Mladenova Z. Animal picobirnavirus. *VirusDisease*. (2014) 25:223–38. doi: 10.1007/s13337-014-0207-y
3. Malik YS, Kumar N, Sharma K, Dhama K, Shabbir MZ, Ganesh B, et al. Epidemiology, phylogeny, and evolution of emerging enteric picobirnaviruses of animal origin and their relationship to human strains. *Biomed Res Int*. (2014) 2014:780752. doi: 10.1155/2014/780752
4. Joycelyn SJ, Ng A, Kleymann A, Malik YS, Kobayashi N, Ghosh S. High detection rates and genetic diversity of picobirnaviruses (PBVs) in pigs on St. Kitts Island: identification of a porcine PBV strain closely related to simian and human PBVs. *Infect Genet Evol*. (2020) 84:102383. doi: 10.1016/j.meegid.2020.104383
5. Kumar N, Mascarenhas JDAP, Ghosh S, Masachessi G, da Silva Bandeira R, Nates S V, et al. Picobirnavirus. In: Malik YS, Singh RK, Dhama K, editors. *Animal-Origin Viral Zoonoses*. Singapore: Springer (2020). p. 291–312.
6. Shi M, Lin XD, Tian JH, Chen LJ, Chen X, Li CX, et al. Redefining the invertebrate RNA virosphere. *Nature*. (2016) 540:539–43. doi: 10.1038/nature20167
7. Guajardo-Leiva S, Chnaiderman J, Gaggero A, Díez B. Metagenomic insights into the sewage RNA virosphere of a large city. *Viruses*. (2020) 12:1050. doi: 10.3390/v12091050
8. Adriaenssens EM, Farkas K, Harrison C, Jones DL, Allison HE, McCarthy AJ. Viromic analysis of wastewater input to a river catchment reveals a diverse assemblage of RNA viruses. *mSystems*. (2018) 3:e00025-18. doi: 10.1128/msystems.00025-18
9. Bell N, Khamrin P, Kumthip K, Rojjanadumrongkul K, Nantachit N, Maneekarn N, et al. Molecular detection and characterization of picobirnavirus in environmental water in Thailand. *Clin Lab*. (2020) 66:855–8. doi: 10.7754/CLIN.LAB.2019.191013
10. Woo PCY, Teng JLL, Bai R, Tang Y, Wong AYP, Li KSM, et al. Novel picobirnaviruses in respiratory and alimentary tracts of cattle and monkeys with large intra-and inter-host diversity. *Viruses*. (2019) 11:574. doi: 10.3390/v11060574
11. Yinda CK, Vanhulle E, Conceição-Neto N, Beller L, Deboutte W, Shi C, et al. Gut virome analysis of cameroonians reveals high diversity of enteric viruses, including potential interspecies transmitted viruses. *mSphere*. (2019) 4:e00585-18. doi: 10.1128/msphere.00585-18
12. Yinda CK, Ghogomu SM, Conceição-Neto N, Beller L, Deboutte W, Vanhulle E, et al. Cameroonian fruit bats harbor divergent viruses, including rotavirus H, bastroviruses, and picobirnaviruses using an alternative genetic code. *Virus Evol*. (2018) 4: vey008. doi: 10.1093/ve/vey008
13. Boros Á, Polgár B, Pankovics P, Fenyvesi H, Engelmann P, Phan TG, et al. Multiple divergent picobirnaviruses with functional prokaryotic Shine-Dalgarno ribosome binding sites present in cloacal sample of a diarrheic chicken. *Virology*. (2018) 525:62–72. doi: 10.1016/j.virol.2018.09.008
14. Kleymann A, Becker AAMJ, Malik YS, Kobayashi N, Ghosh S. Detection and molecular characterization of picobirnaviruses (PBVs) in the mongoose: identification of a novel PBV using an alternative genetic code. *Viruses*. (2020) 12:99. doi: 10.3390/v12010099
15. Ghosh S, Shiokawa K, Aung MS, Malik YS, Kobayashi N. High detection rates of picobirnaviruses in free roaming rats (*Rattus* spp.): molecular characterization of complete gene segment-2. *Infect Genet Evol*. (2018) 65:131–5. doi: 10.1016/j.meegid.2018.07.024
16. Navarro R, Yibin C, Nair R, Peda A, Aung MS, Ketzis J, et al. Molecular characterization of complete genomic segment-2 of picobirnavirus strains detected in a cat and a dog. *Infect Genet Evol*. (2017) 54:200–4. doi: 10.1016/j.meegid.2017.07.006
17. Ghosh S, Kobayashi N, Nagashima S, Naik TN. Molecular characterization of full-length genomic segment 2 of a bovine picobirnavirus (PBV) strain: evidence for high genetic diversity with genogroup I PBVs. *J Gen Virol*. (2009) 90:2519–24. doi: 10.1099/vir.0.013987-0
18. Gallagher CA, Navarro R, Cruz K, Aung MS, Ng A, Bajak E, et al. Detection of picobirnaviruses in vervet monkeys (*Chlorocebus sabaeus*): molecular characterization of complete genomic segment-2. *Virus Res*. (2017) 230:13–8. doi: 10.1016/j.virusres.2016.12.021
19. Wakuda M, Pongsuwanna Y, Taniguchi K. Complete nucleotide sequences of two RNA segments of human picobirnavirus. *J Virol Methods*. (2005) 126:165–9. doi: 10.1016/j.jviromet.2005.02.010
20. Rosen BI, Fang ZY, Glass RI, Monroe SS. Cloning of human picobirnavirus genomic segments and development of an RT-PCR detection assay. *Virology*. (2000) 277:316–29. doi: 10.1006/viro.2000.0594
21. Krishnamurthy SR, Wang D. Extensive conservation of prokaryotic ribosomal binding sites in known and novel picobirnaviruses. *Virology*. (2018) 516:108–14. doi: 10.1016/j.virol.2018.01.006
22. Duquerroy S, Da Costa B, Henry C, Vigouroux A, Libersou S, Lepault J, et al. The picobirnavirus crystal structure provides functional insights into virion assembly and cell entry. *EMBO J*. (2009) 28:1655–65. doi: 10.1038/emboj.2009.109
23. Malik YS, Ghosh S. Etymologia: picobirnavirus. *Emerg Infect Dis*. (2020) 26:89. doi: 10.3201/eid2601.et2601
24. Li L, Giannitti F, Low J, Keyes C, Ullmann LS, Deng X, et al. Exploring the virome of diseased horses. *J Gen Virol*. (2015) 96:2721–33. doi: 10.1099/vir.0.000199
25. Shi M, Lin XD, Chen X, Tian JH, Chen LJ, Li K, et al. The evolutionary history of vertebrate RNA viruses. *Nature*. (2018) 556:197–202. doi: 10.1038/s41586-018-0012-7
26. Da Costa B, Duquerroy S, Tarus B, Delmas B. Picobirnaviruses encode a protein with repeats of the ExxRxNxxxE motif. *Virus Res*. (2011) 158:251–6. doi: 10.1016/j.virusres.2011.02.018
27. Collier AM, Lyytinen OL, Guo YR, Toh Y, Poranen MM, Tao YJ. Initiation of RNA polymerization and polymerase encapsidation by a small dsRNA virus. *PLoS Pathog*. (2016) 12:e1005523. doi: 10.1371/journal.ppat.1005523
28. Knox MA, Gedye KR, Hayman DTS. The challenges of analysing highly diverse picobirnavirus sequence data. *Viruses*. (2018) 10:685. doi: 10.3390/v10120685
29. Woo PCY, Lau SKP, Teng JLL, Tsang AKL, Joseph M, Wong EYM, et al. Metagenomic analysis of viromes of dromedary camel fecal samples reveals large number and high diversity of circoviruses and picobirnaviruses. *Virology*. (2014) 471–473:117–25. doi: 10.1016/j.virol.2014.09.020
30. Duraisamy R, Akiana J, Davoust B, Mediannikov O, Michelle C, Robert C, et al. Detection of novel RNA viruses from free-living gorillas, Republic of the Congo: genetic diversity of picobirnaviruses. *Virus Genes*. (2018) 54:256–71. doi: 10.1007/s11262-018-1543-6
31. Conceição-Neto N, Mesquita JR, Zeller M, Yinda CK, Álvares F, Roque S, et al. Reassortment among picobirnaviruses found in wolves. *Arch Virol*. (2016) 161:2859–62. doi: 10.1007/s00705-016-2987-4
32. Karte C, Platje N, Bullermann J, Beer M, Höper D, Blome S. Re-emergence of porcine epidemic diarrhea virus in a piglet-producing farm in northwestern Germany in 2019. *BMC Vet Res*. (2020) 16:329. doi: 10.1186/s12917-020-02548-4
33. Kylla H, Dutta TK, Roychoudhury P, Subudhi PK. Coinfection of diarrheagenic bacterial and viral pathogens in piglets of Northeast region of India. *Vet World*. (2019) 12:224–30. doi: 10.14202/vetworld.2019.224-230

34. Mahar JE, Shi M, Hall RN, Strive T, Holmes EC. Comparative analysis of RNA virome composition in rabbits and associated ectoparasites. J Virol. (2020) 94:e02119-19. doi: 10.1128/jvi.02119-19
35. Grohmann GS, Glass RI, Pereira HG, Monroe SS, Hightower AW, Weber R, et al. Enteric viruses and diarrhea in HIV-infected patients. Enteric Opportunistic Infections Working Group. *N Engl J Med*. (1993) 329:14–20.
36. Giordano MO, Martinez LC, Rinaldi D, Gúinard S, Naretto E, Casero R, et al. Detection of picobirnavirus in HIV-infected patients with diarrhea in Argentina. *J Acquir Immune Defic Syndr Hum Retrovirol.* (1998) 18:380–3. doi: 10.1097/00042560-199808010-00010
37. González GG, Pujol FH, Liprandi F, Deibis L, Ludert JE. Prevalence of enteric viruses in human immunodeficiency virus seropositive patients in Venezuela. *J Med Virol*. (1998) 55:288–92. doi: 10.1002/(SICI)1096-9071(199808)55:4<288::AID-JMV6>3.0.CO;2-X
38. Giordano MO, Martinez LC, Rinaldi D, Espul C, Martinez N, Isa MB, et al. Diarrhea and enteric emerging viruses in HIV-infected patients. *AIDS Res Hum Retroviruses.* (1999) 15:1427–32. doi: 10.1089/088922299309937
39. Valle MC, Martínez LC, Ferreyra LJ, Giordano MO, Isa MB, Paván JV, et al. Agentes virales asociados al sindrome diarreico en pacientes trasplantados renales [Viral agents related to diarrheic syndrome in kidney transplanted patients]. *Medicina (B Aires)*. (2001) 61:179–82.
40. Giordano MO, Martinez LC, Masachessi G, Barril PA, Ferreyra LJ, Isa MB, et al. Evidence of closely related picobirnavirus strains circulating in humans and pigs in Argentina. *J Infect*. (2011) 62:45–51. doi: 10.1016/j.jinf.2010.09.031
41. Legoff J, Resche-Rigon M, Bouquet J, Robin M, Naccache SN, Mercier-Delarue S, et al. The eukaryotic gut virome in hematopoietic stem cell transplantation: new clues in enteric graft-versus-host disease. *Nat Med*. (2017) 23:1080–5. doi: 10.1038/nm.4380
42. Kim KW, Allen DW, Briese T, Couper JJ, Barry SC, Colman PG, et al. Distinct gut virome profile of pregnant women with type 1 diabetes in the ENDIA study. *Open Forum Infect Dis*. (2019) 6: ofz025. doi: 10.1093/ofid/ofz025
43. Ganesh B, Bányai K, Martella V, Jakab F, Masachessi G, Kobayashi N. Picobirnavirus infections: viral persistence and zoonotic potential. *Rev Med Virol*. (2012) 22:245–56. doi: 10.1002/rmv.1707
44. Martínez LC, Masachessi G, Carruyo G, Ferreyra LJ, Barril PA, Isa MB, et al. Picobirnavirus causes persistent infection in pigs. *Infect Genet Evol*. (2010) 10:984–8. doi: 10.1016/j.meegid.2010.06.004
45. Masachessi G, Martínez LC, Giordano MO, Barril PA, Isa BM, Ferreyra L, et al. Picobirnavirus (PBV) natural hosts in captivity and virus excretion pattern in infected animals. *Arch Virol*. (2007) 152:989–98. doi: 10.1007/s00705-006-0900-2
46. Masachessi G, Martinez LC, Ganesh B, Giordano MO, Barril PA, Isa MB, et al. Establishment and maintenance of persistent infection by picobirnavirus in greater rhea (Rhea Americana). *Arch Virol*. (2012) 157:2075–82. doi: 10.1007/s00705-012-1400-1
47. Masachessi G, Ganesh B, Martinez LC, Giordano MO, Barril PA, Isa MB, et al. Maintenance of picobirnavirus (PBV) infection in an adult orangutan (*Pongo pygmaeus*) and genetic diversity of excreted viral strains during a three-year period. *Infect Genet Evol*. (2015) 29:196–202. doi: 10.1016/j.meegid.2014.11.019
48. Haga IR, Martins SS, Hosomi ST, Vicentini F, Tanaka H, Gatti MSV. Identification of a bisegmented double-stranded RNA virus (Picobirnavirus) in faeces of giant anteaters (*Myrmecophaga tridactyla*). *Vet J*. (1999) 158:234–6. doi: 10.1053/tvjl.1999.0369
49. Kunz AF, Possatti F, de Freitas JA, Alfieri AA, Takiuchi E. High detection rate and genetic diversity of picobirnavirus in a sheep flock in Brazil. *Virus Res*. (2018) 255:10–3. doi: 10.1016/j.virusres.2018.06.016
50. Kapusinszky B, Minor P, Delwart E. Nearly constant shedding of diverse enteric viruses by two healthy infants. *J Clin Microbiol*. (2012) 50:3427–34. doi: 10.1128/JCM.01589-12
51. Ludert JE, Abdul-Latiff L, Liprandi A, Liprandi F. Identification of picobirnavirus, viruses with bisegmented double stranded rna, in rabbit faeces. *Res Vet Sci*. (1995) 59:222–5. doi: 10.1016/0034-5288(95)90006-3
52. Tamehiro CY, Alfieri AF, Médici KC, Alfieri AA. Segmented double-stranded genomic RNA viruses in fecal samples from broiler chicken. *Brazilian J Microbiol*. (2003) 34:349–53. doi: 10.1590/s1517-838220030004 00013
53. Smits SL, Poon LLM, van Leeuwen M, Lau PN, Perera HKK, Peiris JSM, et al. Genogroup I and II picobirnaviruses in respiratory tracts of pigs. *Emerg Infect Dis*. (2011) 17:2328–30. doi: 10.3201/eid1712.110934
54. Smits SL, van Leeuwen M, Schapendonk CME, Schürch AC, Bodewes R, Haagmans BL, et al. Picobirnaviruses in the human respiratory tract. *Emerg Infect Dis*. (2012) 18:1539–40. doi: 10.3201/eid1809.120507
55. Cummings MJ, Tokarz R, Bakamutumaho B, Kayiwa J, Byaruhanga T, Owor N, et al. Precision surveillance for viral respiratory pathogens: virome capture sequencing for the detection and genomic characterization of severe acute respiratory infection in Uganda. *Clin Infect Dis*. (2019) 68:1118–25. doi: 10.1093/cid/ciy656
56. Li W, Qiang X, Qin S, Huang Y, Hu Y, Bai B, et al. Virome diversity analysis reveals novel enteroviruses and a human picobirnavirus in stool samples from African green monkeys with diarrhea. *Infect Genet Evol*. (2020) 82: 104279. doi: 10.1016/j.meegid.2020.104279
57. Bányai K, Martella V, Bogdán Á, Forgách P, Jakab F, Meleg E, et al. Genogroup I picobirnaviruses in pigs: evidence for genetic diversity and relatedness to human strains. *J Gen Virol*. (2008) 89:534–9. doi: 10.1099/vir.0.83134-0
58. Chen M, Sun H, Lan D, Hua X, Cui L, Yuan C, et al. Molecular detection of genogroup I and II picobirnaviruses in pigs in China. *Virus Genes*. (2014) 48:553–6. doi: 10.1007/s11262-014-1058-8
59. Wang Y, Bányai K, Tu X, Jiang B. Simian genogroup I picobirnaviruses: prevalence, genetic diversity, and zoonotic potential. *J Clin Microbiol*. (2012) 50:2779–82. doi: 10.1128/JCM.00634-12
60. Ganesh B, Banyai K, Masachessi G, Mladenova Z, Nagashima S, Ghosh S, et al. Genogroup i picobirnavirus in diarrhoeic foals: can the horse serve as a natural reservoir for human infection? *Vet Res*. (2011) 42:52. doi: 10.1186/1297-9716-42-52
61. Shine J, Dalgarno L. Determinant of cistron specificity in bacterial ribosomes. *Nature*. (1975) 254:34–8. doi: 10.1038/254034a0
62. Ma J, Campbell A, Karlin S. Correlations between Shine-Dalgarno sequences and gene features and operon structures. *J Bacteriol*. (2002) 184:5733–45. doi: 10.1128/jb.184.20.5733-5745.2002
63. Steitz JA. Polypeptide chain initiation: nucleotide sequences of the three ribosomal binding sites in bacteriophage R17 RNA. *Nature*. (1969) 224:957–64. doi: 10.1038/224957a0
64. Osterman IA, Evfratov SA, Sergiev PV, Dontsova OA. Comparison of mRNA features affecting translation initiation and reinitiation. *Nucleic Acids Res*. (2013) 41:474–86. doi: 10.1093/nar/gks989
65. Mindich L. Bacteriophage φ6: a unique virus having a lipid-containing membrane and a genome composed of three dsRNA segments. *Adv Virus Res*. (1988) 35:137–76. doi: 10.1016/S0065-3527(08)60710-1
66. Estes MK, Ettayebi K, Tenge VR, Murakami K, Karandikar U, Lin SC, Ayyar BV, et al. Human norovirus cultivation in nontransformed stem cell-derived human intestinal enteroid cultures: success and challenges. *Viruses*. (2019) 11:638. doi: 10.3390/v11070638
67. Gallimore C, Lewis D, Brown D. Detection and characterization of a novel bisegmented double-stranded RNA virus (picobirnavirus) from rabbit faeces. *Arch Virol*. (1993) 133:63–73. doi: 10.1007/BF01309744
68. Blanco-Picazo P, Fernández-Orth D, Brown-Jaque M, Miró E, Espinal P, Rodríguez-Rubio L, et al. Unravelling the consequences of the bacteriophages in human samples. *Sci Rep*. (2020) 10:6737. doi: 10.1038/s41598-020-63432-7
69. Dabrowska K, Switała-Jelen K, Opolski A, Weber-Dabrowska B, Gorski A. A review: bacteriophage penetration in vertebrates. *J Appl Microbiol*. (2005) 98:7–13. doi: 10.1111/j.1365-2672.2004.02422.x
70. Lee CK, Bent SJ. Uncovering the hidden villain within the human respiratory microbiome. *Diagnosis*. (2014) 1:203–12. doi: 10.1515/dx-2014-0039
71. Górski A, Kniotek M, Perkowska-Ptasińska A, Mróz A, Przerwa A, Gorczyca W, et al. Bacteriophages and transplantation tolerance. *Transplant Proc*. (2006) 38:331–3. doi: 10.1016/j.transproceed.2005.12.073
72. Wang S, Chang JR, Dokland T. Assembly of bacteriophage P2 and P4 procapsids with internal scaffolding protein. *Virology*. (2006) 348:133–40. doi: 10.1016/j.virol.2005.12.021
73. Nibert ML, Debat HJ, Manny AR, Grigoriev IV, De Fine Licht HH. Mitovirus and mitochondrial coding sequences from basal fungus entomophthora muscae. *Viruses*. (2019) 11:351. doi: 10.3390/v11040351

74. Shackelton LA, Holmes EC. The role of alternative genetic codes in viral evolution and emergence. *J Theor Biol*. (2008) 254:128–34. doi: 10.1016/j.jtbi.2008.05.024
75. Shahi S, Eusebio-Cope A, Kondo H, Hillman BI, Suzuki N. Investigation of host range of and host defense against a mitochondrially replicating mitovirus. *J Virol*. (2019) 93:e01503-18. doi: 10.1128/jvi.01503-18
76. Wolf YI, Kazlauskas D, Iranzo J, Lucía-Sanz A, Kuhn JH, Krupovic M, et al. Origins and evolution of the global RNA virome. *MBio*. (2018) 9:e02329-18. doi: 10.1128/mBio.02329-18

Conflict of Interest: The authors declare that the research was conducted in the absence of any commercial or financial relationships that could be construed as a potential conflict of interest.

frontiers in Veterinary Science

ORIGINAL RESEARCH
published: 27 January 2021
doi: 10.3389/fvets.2020.606661

Genomic Analysis of an Indian G8P[1] Caprine Rotavirus-A Strain Revealing Artiodactyl and DS-1-Like Human Multispecies Reassortment

Shubhankar Sircar[1,2], Yashpal Singh Malik[1,3], Prashant Kumar[2], Mohd Ikram Ansari[1], Sudipta Bhat[1], S. Shanmuganathan[1], Jobin Jose Kattoor[4], O.R. Vinodhkumar[5], Narayan Rishi[2], Nadia Touil[6], Souvik Ghosh[7], Krisztián Bányai[8] and Kuldeep Dhama[9]*

[1] Division of Biological Standardization, Indian Council of Agricultural Research-Indian Veterinary Research Institute, Bareilly, India, [2] Amity Institute of Virology and Immunology, J-3 Block, Amity University, Noida, India, [3] College of Animal Biotechnology, Guru Angad Dev Veterinary and Animal Sciences University, Ludhiana, India, [4] Animal Disease Diagnsotic Laboratory, Purdue University, West Lafayette, IN, United States, [5] Division of Epidemiology, Indian Council of Agricultural Research-Indian Veterinary Research Institute, Bareilly, India, [6] Laboratoire de Recherche et de Biosécurité, Hôpital Militaire d'instruction Med V de Rabat, Rabat, Morocco, [7] Department of Biomedical Sciences, One Health Center for Zoonoses and Tropical Veterinary Medicine, Ross University School of Veterinary Medicine, Basseterre, Saint Kitts and Nevis, [8] Centre for Agricultural Research, Institute for Veterinary Medical Research, Hungarian Academy of Sciences, Budapest, Hungary, [9] Division of Pathology, Indian Council of Agricultural Research-Indian Veterinary Research Institute, Bareilly, India

OPEN ACCESS

Edited by:
Subhash Verma,
Chaudhary Sarwan Kumar Himachal Pradesh Krishi Vishvavidyalaya, India

Reviewed by:
Martin M. Nyaga,
University of the Free State, South Africa
Frederick Joseph Fuller,
North Carolina State University, United States

***Correspondence:**
Yashpal Singh Malik
malikyps@gmail.com
orcid.org/0000-0002-2832-4854

Specialty section:
This article was submitted to Veterinary Infectious Diseases, a section of the journal Frontiers in Veterinary Science

Received: 15 September 2020
Accepted: 14 December 2020
Published: 27 January 2021

Citation:
Sircar S, Malik YS, Kumar P, Ansari MI, Bhat S, Shanmuganathan S, Kattoor JJ, Vinodhkumar OR, Rishi N, Touil N, Ghosh S, Bányai K and Dhama K (2021) Genomic Analysis of an Indian G8P[1] Caprine Rotavirus-A Strain Revealing Artiodactyl and DS-1-Like Human Multispecies Reassortment. Front. Vet. Sci. 7:606661. doi: 10.3389/fvets.2020.606661

The surveillance studies for the presence of caprine rotavirus A (RVA) are limited in India, and the data for the whole-genome analysis of the caprine RVA is not available. This study describes the whole-genome-based analysis of a caprine rotavirus A strain, RVA/Goat-wt/IND/K-98/2015, from a goat kid in India. The genomic analysis revealed that the caprine RVA strain K-98, possess artiodactyl-like and DS-1 human-like genome constellation G8P[1]-I2-R2-C2-M2-A3-N2-T6-E2-H3. The three structural genes (VP2, VP4, and VP7) were close to caprine host having nucleotide-based identity range between 97.5 and 98.9%. Apart from them, other gene segments showed similarity with either bovine or human like genes, ultimately pointing toward a common evolutionary origin having an artiodactyl-type backbone of strain K-98. Phylogenetically, the various genes of the current study isolate also clustered inside clades comprising Human-Bovine-Caprine isolates from worldwide. The current findings add to the knowledge on caprine rotaviruses and might play a substantial role in designing future vaccines or different alternative strategies combating such infections having public health significance. To the best of our knowledge, this is the first report on the whole-genome characterization of a caprine RVA G8P[1] strain from India. Concerning the complex nature of the K-98 genome, whole-genome analyses of more numbers of RVA strains from different parts of the country are needed to comprehend the genomic nature and genetic diversity among caprine RVA.

Keywords: rotavirus-A, goat, G8P[1] strain, whole-genome analysis, India, reassortment

INTRODUCTION

Rotaviruses (RVs) are the major viral pathogens that often leads to severe diarrhea in young neonates of animals as well as humans. It affects multiple livestock species, including newborn calves (1), pigs (2), foals (3), small ruminants (4), incurring significant economic losses (5). The virus is a non-enveloped, triple-layered, and the genome consists of 11 segmented dsRNA encoding for six structural genes and six non-structural proteins (6). Based on antigenic and genetic properties, RVs are further classified into eight recognized species *A-H* and two tentative species rotavirus *I* and rotavirus *J* (7, 8).

As per recommendations of the Rotavirus Classification Work Group (RCWG), nucleotide percent similarity cut-off values of all 11 viral gene segments are used to determine a genotypic scheme Gx–P[x]–Ix–Rx–Cx–Mx–Ax–Nx–Tx–Ex–Hx designating VP7–VP4–VP6–VP1–VP2–VP3–NSP1–NSP2–NSP3–NSP4–NSP5/6 genes, respectively (9, 10).

Globally, data regarding epidemiology, prevalence, and circulating genotypes of small ruminant RVA is scarce compared to other domesticated species. To date, three rotavirus species (RVA, RVB, and RVC) have been reported in the caprine population worldwide (11, 12). Association of RVs with diarrhea in the caprine population and their prevalence have been described from the United Kingdom (13), Italy (14), Spain (15), Japan (16), South Korea (16), Egypt (17), Bangladesh (18), Turkey (19), and Argentina (20). Apart from these published reports, a few GenBank sequence records of caprine RVA are available from Argentina (21), China (22), and India (23) but are unpublished. To best of our knowledge, there are only two reports from India describing the detection and characterization of caprine RVA (24, 25). Past studies reported G2, G3, G6, G8, G9, and G10 and with P[1], P[3], P[4], P[5], P[8], P[11], P[14] and P[15] genotype circulation in caprine and ovine population worldwide (26). To sum up the count of whole-genome reports available for caprine RVA, there are only four complete genomes published from Argentina (20), Bangladesh (18), China (22), and Uganda (27).

Based on the 20th livestock census, the combined cattle and buffalo population of India stands at 302.34 million (56.42%), and small ruminants constitute around 223.14 million (41.64%) in livestock, which are a notable species reared by the marginal farmers for their livelihood. Goats contribute around 27.8% (148.88 million) of livestock. India lacks epidemiological and molecular studies on caprine RVs. The proximity of the caprine population to human settlements is a matter of concern with regards to the interspecies transmission of caprine and human RVA between them (27, 28). Several studies have documented zoonotic as well as zooanthroponotic transmission of common RV genotypes between the caprine-bovine-human population (18, 29–32). We, for the first time characterized the whole-genome of a caprine isolate and studied its possible origin. The findings of this study contribute to the understanding of re-assortment events, interspecies transmission, and the emergence of unusual RVA isolates.

MATERIALS AND METHODS

Sampling, Screening, and Primers Designing

During an investigation of the outbreak of diarrhea in goat population located in an unorganized sector, reared by local people randomly, a sample K-98 was collected from a goat kid in the Northern state of Uttar Pradesh, India was found positive using an antigen-capture sandwich ELISA for RVA infection (33).

In the preliminary testing, RNA–polyacrylamide gel electrophoresis (34, 35) revealed eleven dsRNA bands of RVA with 4:2:3:2 pattern after silver staining.

The sample was processed by preparing 10% (w/v) fecal suspension in 1X PBS, followed by RNA extraction using Qiazol lysis reagent (Qiagen, Hilden, Germany). The extracted RNA was then reverse-transcribed using MuMLV RT (Promega, Wisconsin, USA). PCR for the detection/diagnosis of RVA was carried out using previously described primers based on the VP6 gene, the positive samples yielded a specific amplicon of 226 bp on agarose gel electrophoresis (36). Structural genes VP2, VP3, VP4, VP6, VP7, and non-structural genes NSP1, NSP2, NSP3, NSP4, and NSP5 were amplified using earlier reported primers (18, 37, 38) whereas two new pair of overlapping primers for VP1 gene were designed to amplify its partial gene for nearly ∼1,400 bp (**Supplementary Data 1**). Standalone software like MEGA 7.0 (39) and online primer designing tool IDTs Oligoanalyzer (https://eu.idtdna.com/calc/analyzer) were used to design and verify the primers sets (33).

Complete Genome Amplification—Cloning, Sequencing, and Genotyping

The PCR amplified products of all the gene segments were cloned in pDrive vector (Qiagen, Hilden, Germany) and sequenced bi-directionally with universal sequencing primer pairs T7 and SP6. The open reading frames (ORFs) along with respective untranslated regions (UTR) were located using the EditSeq tool, DNASTAR software (Lasergene, USA) for all the gene segments. The VP7 gene is responsible for eliciting neutralizing antibodies through its antigenic epitopes. The VP7 trimer consists of two structurally distinct antigenic epitopes: 7-1 and 7-2. The 7-1 epitope extends to the inter-subunit boundary and is further subdivided into 7-1a and 7-1b (40). Comparison between the amino acid residues that contains the 7-1a, 7-1b, and 7-2 epitopes of the strain K-98 and other G8 type VP7 genes from different species was conducted using the MegAlign tool of DNASTAR (**Figure 4**). All eleven gene segments were assigned a particular genotype by comparing them against the available reference sequences in NCBI GenBank using the nucleotide BLAST tool (BLASTn) search. Further, their genotype was also ascertained using the online Rotavirus A Genotype Determination tool (https://www.viprbrc.org). Nearest isolates to eleven gene segments were also determined and compared using the BLAST tool and RVA genotyping tool of ViPRBRC (https://www.viprbrc.org).

NCBI GenBank Submissions

Each gene segment for the caprine strain RVA/Goat-wt/IND/K-98/2015 was submitted to NCBI GenBank under the accession number MT501452 to MT501462.

Phylogenetic Analysis and Percent Identity Calculation

Phylogenetic analysis was conducted using MEGA 7.0 software (39) using the maximum likelihood (ML) method. Before applying the ML method, best substitution models were selected according to the individual datasets of all the 11 gene segment through "find model" program incorporated in MEGA 7.0. Based on the "find model" analysis, datasets of six genes (NSP1, NSP2, VP1, VP2, VP3, and VP7) were assigned the GTR+G+I substitution model, whereas four genes (NSP3, NSP4, VP3, and VP4) and one single gene (NSP5) were assigned GTR+G and HKY+G substitution models, respectively.

Recombination Detection

In silico study was performed to identify the possible chances of recombination in the virus genes using the recombination detection program 4 (RDP 4 v 4.95) (41). Following the detection of a "recombination signal" with BOOTSCAN (42), MAXCHI (43), CHIMERA (44), 3SEQ (45), GENECONV (46), LARD (47), and SISCAN (48), RDP4 determines approximate breakpoint positions using a Hidden Markov Model, BURT. It then identifies the recombinant sequence using the PHYLPRO (49), VISRD (50), and EEEP methods (51, 52). The RDP 4 program was used for all the 11 gene segments to find out any possible recombination.

Selection Pressure Analysis

The datamonkey web server (http://www.datamonkey.org/), was used to analyze the major genes (VP7, VP4, VP6, and NSP4) for selection pressure analysis to test the rate of non-synonymous to synonymous (dN/dS) ratio (53). Several codon-specific models like Fixed-Effect-Likelihood (FEL), Single Likelihood Ancestor Counting (SLAC), Mixed Effects Model of Evolution (MEME), and Fast, Unconstrained Bayesian AppRoximation were used for Inferring Selection (FUBAR) methods incorporated in the datamonkey web server. Sites identified significant by at least three models were considered under positive selection.

RESULTS

Whole-Genome Sequencing and Genotype Constellation

The 11 genes of the RVA including six structural genes VP1, VP2, VP3, VP4, VP6, VP7, and five non-structural genes NSP1, NSP2, NSP3, NSP4, and NSP5 for the strain K-98 were sequenced and compared with other RVA sequences available in the GenBank database. Nucleotide sequencing analysis in ViPR and BLASTn analysis of each gene revealed a genotype constellation G8P[1]-I2-R2-C2-M2-A13-N2-T6-E2-H3. The lengths of the nucleotide sequences obtained for each of the 11 genomic segments of strain K-98 are shown in **Table 1**.

All genotypes have been reported earlier, and its comparison to known genotype constellations of human, bovine, and small ruminant are shown in **Figure 1**. The genotype constellation of strain K-98 reveal a mixed backbone of RVA wherein five genes (VP1, NSP1, NSP3, NSP4, and NSP5) were derived from a bovine host, three genes (VP3, VP6, and NSP2) were derived from a human host, and three caprine gene segments (VP2, VP4, and VP7) were derived from caprine species (**Figure 1**). Based on the genotype constellation, it was observed that apart from NSP1, where an unusual bovine like A13 genotype was observed, all other genes exhibited genotypes that have been described in the caprine host in earlier studies. The genomic combination of G8P[1] has also been reported in the Argentinian caprine population earlier (20). Reports of G8P[1] genotype being diagnosed in small ruminants of Turkey emerged in 2012 and recently in 2020 (19, 54).

Phylogenetic and Percent Identity Analysis of Non-structural Proteins (NSP1-5)

In phylogenetic analysis, K-98 NSP1 gene clustered with A13 type bovine and bovine-like human (SI-R56) and Lapine (K1130027) RVA isolates (**Figure 2**). Rest all other small ruminant isolates from worldwide clustered inside a single clade of A11 genotype. The nucleotide sequence of the NSP1 gene for K-98 showed the maximum similarity of 95.7% with a bovine isolate from South Africa (KP752872) (**Supplementary Data 2**). Strain K-98 showed 94.2% nucleotide similarity with its next nearest neighbor, a bovine-like Lapine, and human RVA isolates.

In the phylogenetic analysis of the NSP2 gene, the isolate K-98 formed a separate cluster along with human RVA isolates MCS-KOL-383 and N-1 from India inside the N2 genotype clade (**Figure 2**). All major small ruminant strains from worldwide also clustered inside the same branch of the N2 genotype. It showed the highest percent nucleotide similarity of 98.1% with a human isolate (KU292526) from Kolkata, India. Further, the percent nucleotide similarity with the nearest human isolate was 94.7% (KX655458) from Uganda, whereas it was found to be 94.6% (JX040428) with a caprine isolate from Bangladesh, respectively (**Supplementary Data 2**).

The NSP3 gene of isolate K-98 clustered inside a clade comprising other small ruminant isolates belonging to the T6 genotype (**Figure 2**). The NSP3 gene of K-98 isolate showed 99.5% identity with a bovine isolate BR91 (JX442772) from India, which is an artiodactyl-like human RVA strain. Apart from BR91, the next nearest neighbor to the K-98 NSP3 gene was an Italian human isolate PR457 (KP198633), showing 98.6% similarity (**Supplementary Data 2**).

The NSP4 gene of K-98 isolate also grouped inside a clade comprising other E2 genotype isolates from bovine, human, and caprine species (**Figure 2**). Apart from E2 type NSP4, E12 genotype has been previously described in Argentinian caprine RVA isolate 0040. Notably, a camel RVA (JX968472) carrying E15 NSP4 genotype appeared inside the major clade of E2.

TABLE 1 | Size and accession number of 11 gene segments of caprine strain RVA/Goat-wt/IND/K-98/2015.

Sl No.	Gene name	Size (bp)	Accession no.	Nucleotide completeness	ORFs position
1	VP1	1,402	MT501452	Partial cds	12–1,402
2	VP2	2,663	MT501453	Complete cds	17–2,662
3	VP3	2,586	MT501454	Complete cds	9–2,516
4	VP4	2,087	MT501455	Partial cds	1–2,087
5	VP6	1,314	MT501456	Complete cds	9–1,202
6	VP7	981	MT501457	Complete cds	1–981
7	NSP1	1,515	MT501458	Complete cds	3–1,478
8	NSP2	1,060	MT501459	Complete cds	47–1,000
9	NSP3	1,074	MT501460	Complete cds	26–967
10	NSP4	739	MT501461	Complete cds	42–569
11	NSP5/NSP6	654	MT501462	Complete cds	14–610/72–368

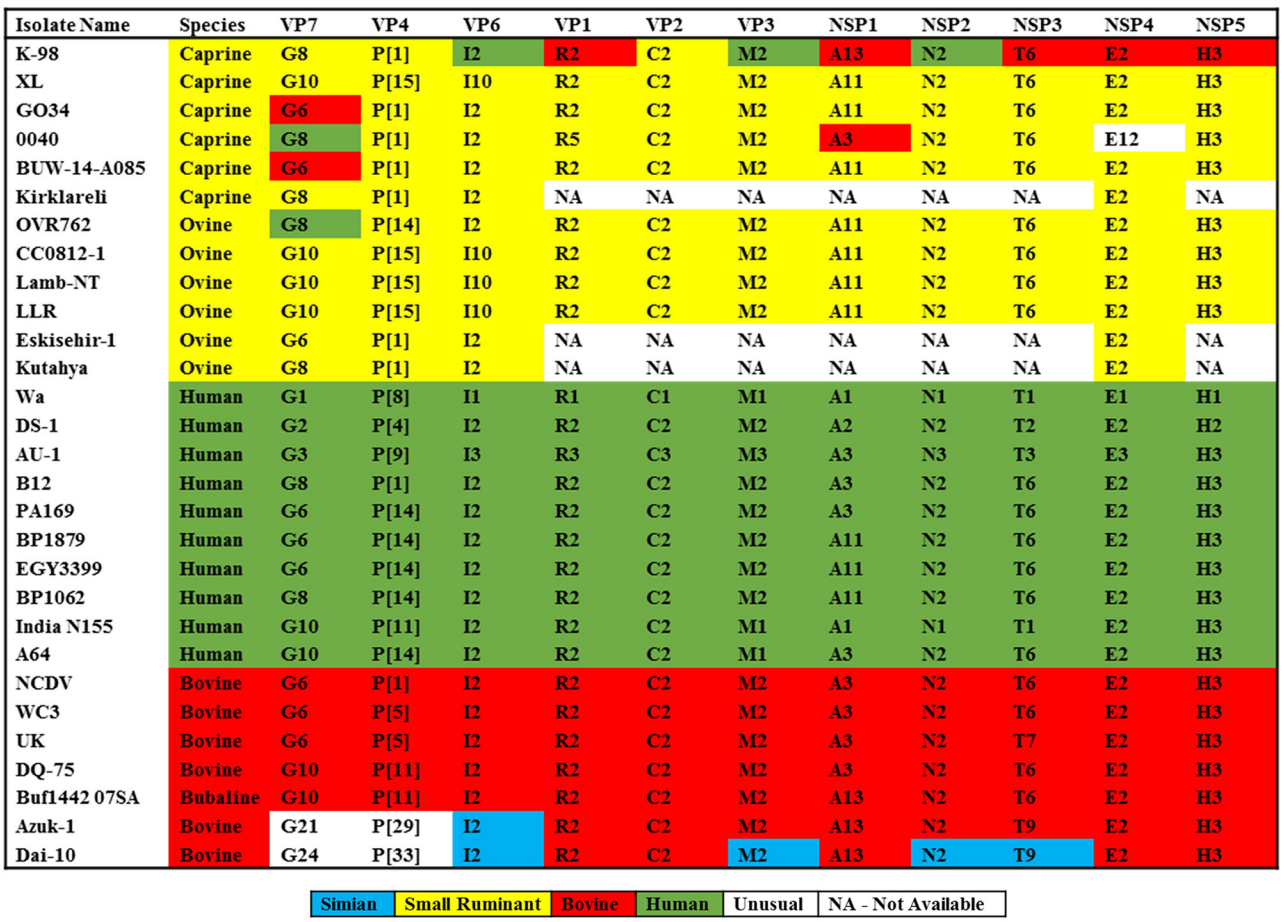

FIGURE 1 | Comparison of genomic constellations of RVA/Goat-wt/IND/K-98/2015 with those of selected human and animal RVA strains with known genomic constellations. Individual gene segments of all strains are color coded based on the maximum homology with the RVA strains available in the public domain.

The NSP4 gene of K-98 was closely related to a bovine isolate 86 (GU984765) of western India, sharing a nucleotide percent identity of 98.4% (**Supplementary Data 2**).

In the phylogenetic analysis of the NSP5 gene segment, K-98 clustered alongside humans, bovine, caprine, and ovine RVA isolates inside the major clade of the H3 genotype. It showed the highest percent nucleotide similarity of 99.0% with bovine isolate RUBV81 (EF200580) from India (**Supplementary Data 2**). The nearest caprine isolate was Ugandan BUW-14-085 (KY055437), with a nucleotide percent identity of 98.4% (**Figure 2**).

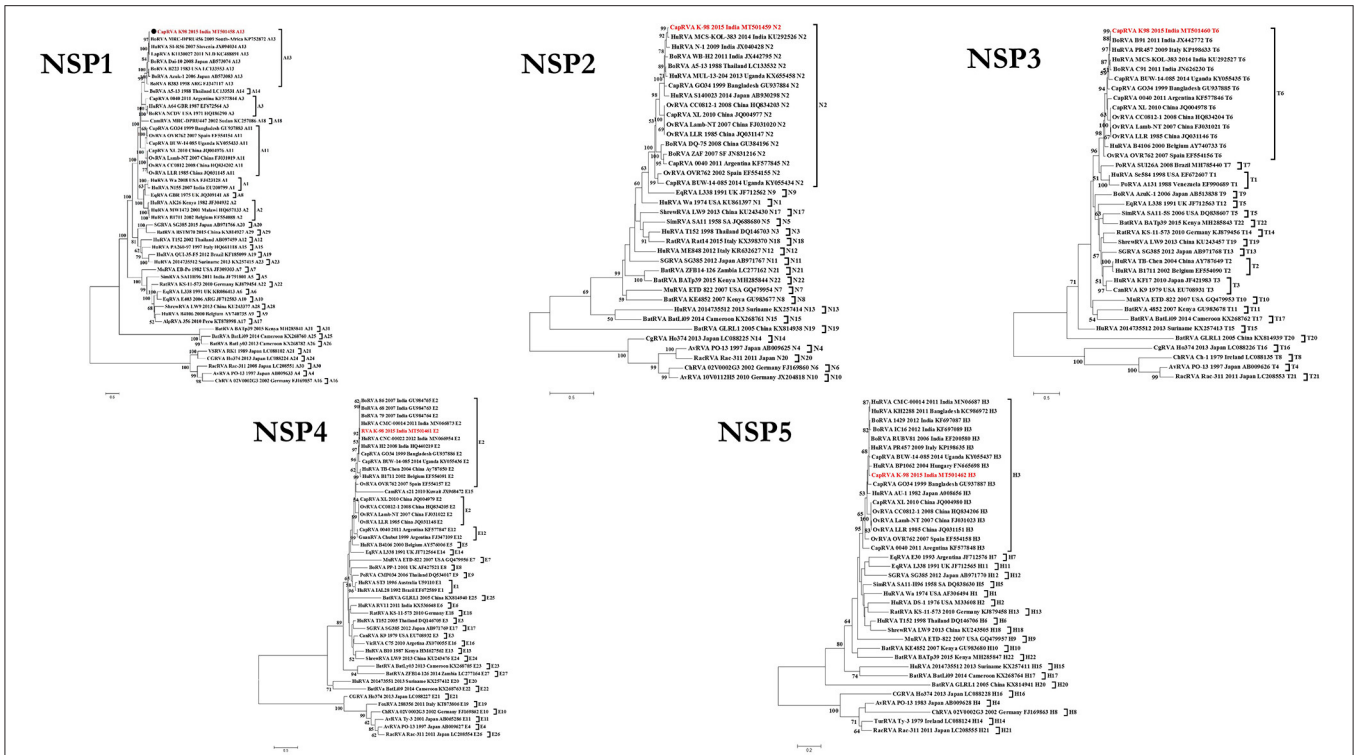

FIGURE 2 | Phylogenetic dendrograms of all non-structural gene segments of caprine strain RVA/Goat-wt/IND/K-98/2015/G8P[1] with those of representative RVA strains. Phylogenetic dendrogram was constructed by the maximum likelihood method using MEGA software version 7. Phylogenetic distances were statistically supported by bootstrapping with 1,000 replicates. In all the dendrograms, the position of strain K-98 is indicated by the red colored text. The scale bar indicates nucleotide substitutions per site. The genotypes are indicated at the right-hand side of each dendrogram.

Phylogenetic and Percent Identity Analysis of Structural Proteins (VP1-4 and VP6-7)

Phylogenetic analysis of the VP1 gene segment revealed that all the small ruminant RVA were found to fall in the R2 genotype clade except the Argentinian caprine strain 0040 (KF577838), which possessed the R5 genotype. The current study isolate K-98 clustered with an Indian bovine rotvairus A BoRVA isolate M1 (HQ440220), which also shared the highest similarity of 97.5% at the nucleotide level. The percent similarity with human, ovine, and caprine isolates ranged from 88.5 to 88.9%, belonging to group R2 genotype (**Figure 3** and **Supplementary Data 2**).

The VP2 gene of isolate K-98 is grouped within the C2 genotype clade with all other small ruminant strains worldwide (**Figure 3**). Caprine strain GO34 (GU937878) from Bangladesh was the nearest neighbor in the phylogeny having 97.5% nucleotide similarity (**Supplementary Data 2**). Apart from GO34, an Indian human RVA isolate having a 95.3% identity at the nucleotide level also appeared inside the same branch (**Figure 3**). The percent nucleotide similarity with other isolates like the prototype DS-1 human RVA isolate was 95.3%, whereas it ranged between 85.5 and 89.4% with small ruminant origin strains worldwide.

The phylogenetic analysis of the VP3 gene clustered the K-98 isolate close to two human isolates from Italy and India inside a major clade comprising the M2 genotype (**Figure 3**). Apart from PR457 human RVA isolate from Italy, it clustered alongside an Indian human RVA isolate CMC-00022 (MN066958) with a nucleotide similarity of 96.9%. The M2 genotype clade is also comprised of small ruminant origin isolates from worldwide sharing close relationships. The percent nucleotide identity of the VP3 gene of the K-98 isolate showed the highest similarity of 97.5% with a human RVA isolate PR457 (KP198630) from Italy (**Supplementary Data 2**).

In a phylogenetic analysis of the outer capsid VP6 gene, K-98 clustered alongside human RVA isolates from eastern and southern India within the I2 clade (**Figure 3**). The I2 clade also includes the caprine and ovine origin strains from China, Bangladesh, Uganda, Spain, and Argentina. The percent nucleotide similarity of K-98 showed the highest similarity of 97.4% with a human RVA isolate MCS-KOL-383 (KU292523) from India (**Supplementary Data 2**).

The phylogenetic analysis of the VP4 gene grouped the caprine RVA K-98 isolate with caprine and a human RVA isolate of P[1] genotype having the highest similarity of 97.4% at the nucleotide level with a caprine RVA isolate GO34 (GU937878) from Bangladesh (**Supplementary Data 2** and **Figure 3**). Apart from our study, P[1] genotype have been reported from Bangladesh, Argentina, and Ugandan caprine strains. Genotype P[1] has been the major P-type reported worldwide in small ruminant, whereas P[14] and P[15] has only been reported in Spain and China, respectively.

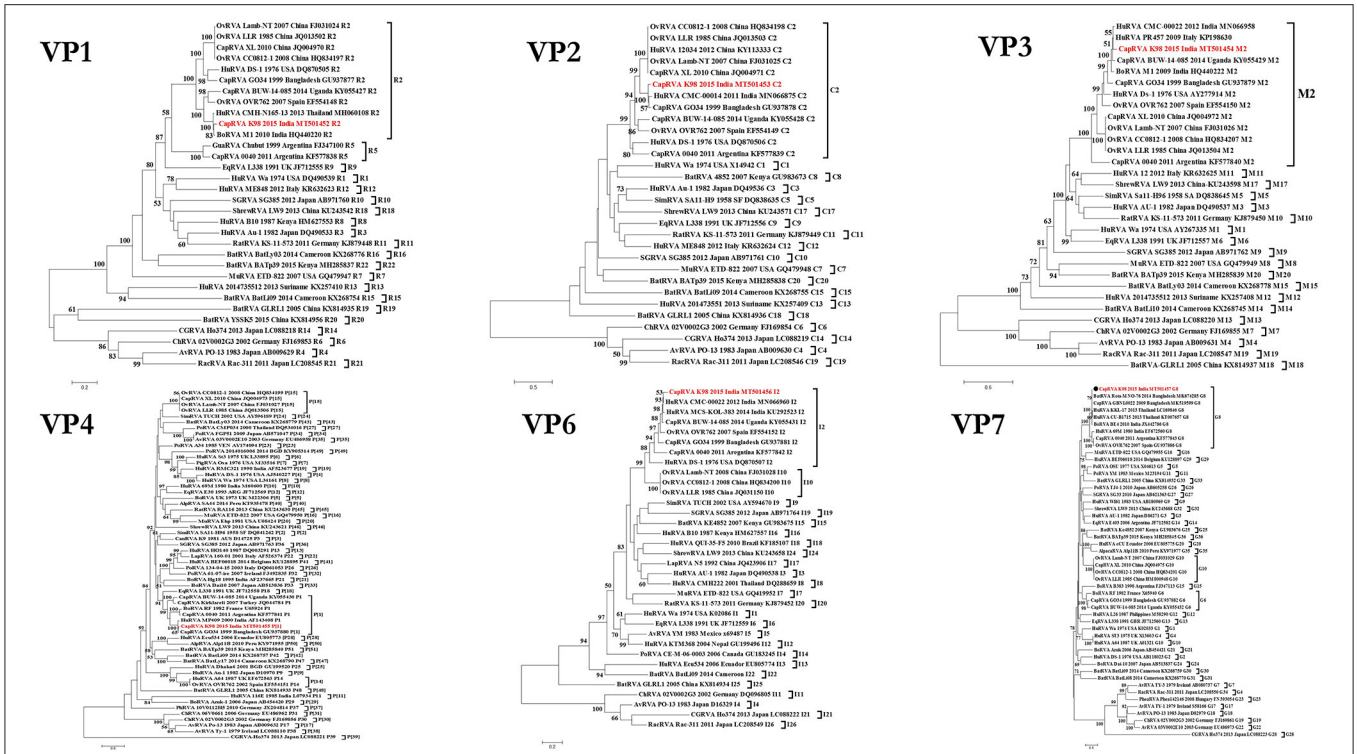

FIGURE 3 | Phylogenetic dendrograms of all structural gene segment of caprine strain RVA/Goat-wt/IND/K-98/2015/G8P(1) with those of representative RVA strains. Phylogenetic dendrogram was constructed by the maximum likelihood method using MEGA software version 7. Phylogenetic distances were statistically supported by bootstrapping with 1,000 replicates. In all the dendrograms, the position of strain K-98 is indicated by the red-colored text. The scale bar indicates nucleotide substitutions per site. The genotypes are indicated at the right-hand side of each dendrogram.

	7-1a													
	87	91	94	96	97	98	99	100	104	123	125	129	130	291
CapRVA_India_K-98_G8	T	T	A	S	S	W	K	D	Q	D	A	I	N	K
CapRVA_Argentina_0040_G8	V	T	S	S	S	W	K	D	Q	D	A	I	N	K
CapRVA_Turkey_Kirklareli_G8	V	T	S	S	S	W	K	D	Q	D	A	I	N	K
CapRVA_Turkey_Kutahya_G8	V	T	A	S	S	W	K	D	Q	N	A	I	N	M
OvRVA_Spain_OVR762_G8	T	T	A	S	S	W	K	D	Q	D	A	I	N	K
BoRVA_OAgent_G8	V	T	A	S	S	W	K	D	Q	D	A	I	N	K
BoRVA_Thailand_A5_G8	T	T	A	S	S	W	K	D	Q	D	A	I	N	K
BoRVA_Nigeria_NGRBg8_G8	A	T	A	S	S	W	K	D	Q	D	A	I	N	K
CamRVA_Sudan_MRCDPRU447_G8	T	T	A	N	S	W	K	E	Q	D	A	I	N	K
SimRVA_USA_PTRV_G8	A	T	A	S	S	W	K	D	Q	D	A	I	N	K
DogRVA_Germany_88977_G8	V	K	A	S	S	W	K	D	Q	D	A	I	N	K
GuaRVA_ARG_RioNegro_G8	V	T	A	S	S	W	K	D	Q	D	A	I	N	K
DeerRVA_USA_02218_G8	V	T	A	S	S	W	K	D	Q	D	A	I	N	K
HuRVA_IND_69M_G8	V	T	A	S	S	W	K	D	Q	D	A	I	N	K
HuRVA_Kenya_B12_G8	V	T	A	S	S	W	K	D	Q	D	A	I	N	K
HuRVA_Nigeria_HMG035_G8	A	T	A	S	S	W	K	D	Q	D	A	I	N	K
HuRVA_Paraguay_492SR_G8	T	T	A	S	S	W	K	D	Q	D	A	I	N	K
HuRVA_DRC_DRC86_G8	A	T	A	S	S	W	K	D	Q	D	A	I	N	K
HuRVA_Ghana_GH018_G8	A	T	A	S	S	W	K	D	Q	D	A	I	N	K
HuRVA_Hungary_BP1062_G8	T	T	A	S	S	W	K	D	Q	D	A	I	N	K
HuRVA_Italy_PR1300_G8	V	T	A	S	S	W	K	D	Q	D	A	I	N	K

	7-1b					
	201	211	212	213	238	242
CapRVA_India_K-98_G8	Q	D	T	T	N	T
CapRVA_Argentina_0040_G8	Q	D	T	T	N	T
CapRVA_Turkey_Kirklareli_G8	Q	D	T	T	N	T
CapRVA_Turkey_Kutahya_G8	Q	D	T	T	N	T
OvRVA_Spain_OVR762_G8	Q	D	T	T	N	T
BoRVA_OAgent_G8	Q	D	T	T	N	T
BoRVA_Thailand_A5_G8	Q	D	T	T	N	A
BoRVA_Nigeria_NGRBg8_G8	Q	D	T	T	N	T
CamRVA_Sudan_MRCDPRU447_G8	Q	D	T	T	N	T
SimRVA_USA_PTRV_G8	Q	D	T	T	N	T
DogRVA_Germany_88977_G8	Q	D	T	T	N	T
GuaRVA_ARG_RioNegro_G8	Q	D	T	T	N	T
DeerRVA_USA_02218_G8	Q	D	T	T	N	T
HuRVA_IND_69M_G8	Q	D	T	T	N	T
HuRVA_Kenya_B12_G8	Q	D	T	T	N	T
HuRVA_Nigeria_HMG035_G8	Q	D	T	T	N	T
HuRVA_Paraguay_492SR_G8	Q	D	T	T	D	A
HuRVA_DRC_DRC86_G8	Q	D	T	T	N	T
HuRVA_Ghana_GH018_G8	Q	D	T	T	N	T
HuRVA_Hungary_BP1062_G8	Q	D	T	T	N	T
HuRVA_Italy_PR1300_G8	Q	D	T	T	N	T

	7-2								
	143	145	146	147	148	190	217	221	264
CapRVA_India_K-98_G8	K	N	A	N	S	S	E	A	G
CapRVA_Argentina_0040_G8	K	N	A	N	S	S	E	A	G
CapRVA_Turkey_Kirklareli_G8	K	N	A	N	S	S	E	A	G
CapRVA_Turkey_Kutahya_G8	K	D	A	N	S	S	E	A	G
OvRVA_Spain_OVR762_G8	K	N	A	N	S	S	E	A	G
BoRVA_OAgent_G8	K	N	A	N	S	S	E	A	G
BoRVA_Thailand_A5_G8	K	N	A	N	A	S	E	A	G
BoRVA_Nigeria_NGRBg8_G8	K	N	A	N	S	S	E	A	G
CamRVA_Sudan_MRCDPRU447_G8	K	S	A	N	S	S	E	A	G
SimRVA_USA_PTRV_G8	K	N	A	N	S	S	E	A	G
DogRVA_Germany_88977_G8	K	N	A	N	S	S	E	A	G
GuaRVA_ARG_RioNegro_G8	K	N	A	N	S	S	E	A	G
DeerRVA_USA_02218_G8	K	N	A	N	S	S	E	A	G
HuRVA_IND_69M_G8	K	N	A	N	S	S	E	A	G
HuRVA_Kenya_B12_G8	K	N	A	N	S	S	E	A	G
HuRVA_Nigeria_HMG035_G8	K	N	A	N	S	S	E	A	G
HuRVA_Paraguay_492SR_G8	K	D	A	N	S	S	E	A	G
HuRVA_DRC_DRC86_G8	K	N	T	N	S	S	E	A	G
HuRVA_Ghana_GH018_G8	K	N	A	N	S	S	E	A	G
HuRVA_Hungary_BP1062_G8	K	N	A	N	S	S	E	T	G
HuRVA_Italy_PR1300_G8	K	N	A	N	S	S	E	A	G

FIGURE 4 | The VP7 antigenic epitopes analysis of caprine strain RVA/Goat-wt/IND/K-98/2015 with selected G8 strains. The alignment of residues in VP7 is divided into three antigenic epitopes (7-1a, 7-1b, and 7-2). Residues that differ from the strain K-98 caprine strain are highlighted by yellow color. Majority of the residues were observed to be in consensus with the caprine strain K-98 except the site 87 where extensive variation was observed throughout the species.

In the phylogenetic analysis, VP7 gene of the K-98 isolate clustered into a clade comprising G8 genotype strains (**Figure 3**). Apart from the current study, small ruminant origin G8 genotype strains have been reported from Argentinian caprine strain 0040, Spanish, and Turkish ovine strain OVR762 and Kutahya, respectively. Other G-types of small ruminants that clustered separately in the phylogenetic tree include G6 and G10. The VP7 gene of the K-98 isolate shows the highest percent nucleotide identity with bat isolate Rota_MNO_76 (MK674285) from Bangladesh. The next nearest neighbor to isolate K-98 is a Bangladeshi caprine RVA isolate GBNL0022. Moreover, the maximum nucleotide identity with other G8 type RVA species like caprine, human, bovine, and the ovine isolate was 98.9, 98.6, 98.1, and 85.5%, respectively (**Supplementary Data 2**). The major antigenic epitopes of the VP7 gene were also analyzed with those of other reported G8 genotypes of different species worldwide (**Figure 4**). Among all the 29 antigenic epitopes, residues number 87 showed

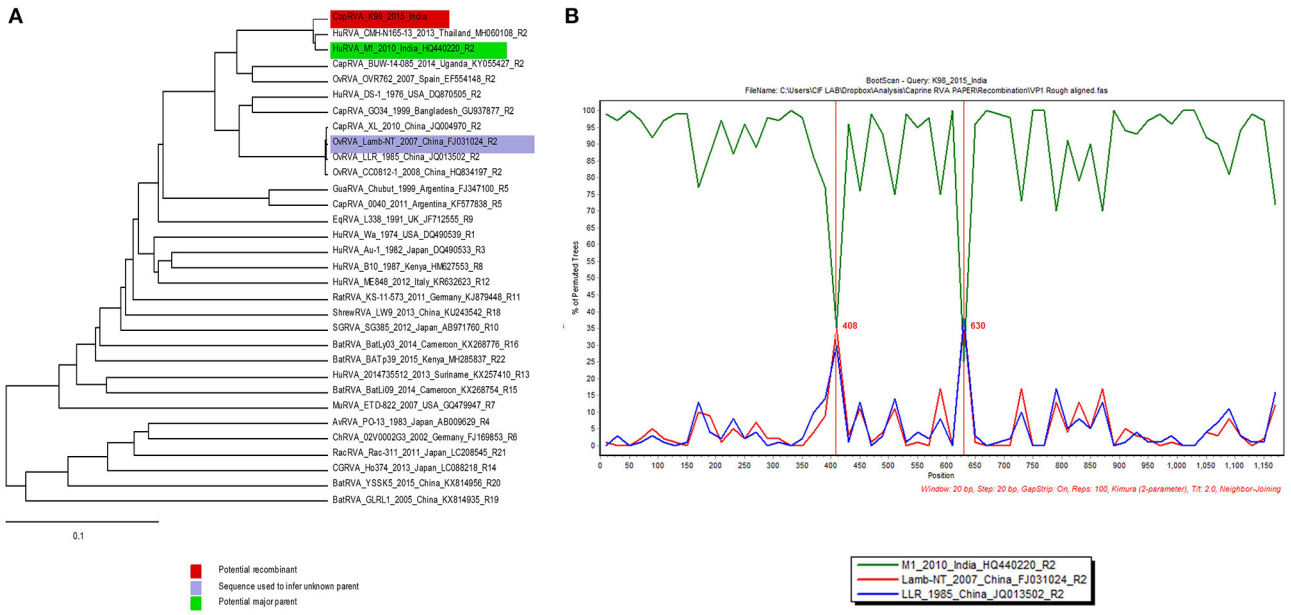

FIGURE 5 | SimPlot output for VP1 gene segment of caprine RVA strain K-98. **(A)** The image shows RDP 4.0 output depicting the major and minor parents by blue and green color on a phylogenetic tree. **(B)** The right-side window in the image generated using SimPlot analysis shows the recombination crossover points (408 and 630) in the gene depicted by a green and blue color line across them.

extensive change concerning other G8 genotype reported in different species.

Recombination Detection by RDP 4.0

Analysis of all the genes from K-98 isolate for any possible recombination revealed recombination events in segment 1 (VP1) gene. The statistical results supported that K-98 (isolated in this study), HuRVA_M1_2010 (GenBank no. HQ440220), and OvRVA_Lamb-NT_2007 (GenBank no. FJ031024) are three recombinants exhibiting unique genetic recombination patterns (recombinant score >0.68, $P < 0.001$) (**Supplementary Data 1**). Recombination events were further confirmed by SimPlot analysis (55). SimPlot analysis detected recombination breakpoints at position number 408 and 630 (**Figure 5**).

Selection Pressure Analysis

Using the datamonkey web server, site by site-selective pressure analysis by FEL, SLAC, MEME, and FUBAR methods were tried with no positively selected sites in any of the four genes chosen for the analysis. For each of the four genes, either one or two models gave positive selection sites, but as per the thumb rule, those sites which are identified as significant by at least three models are only considered positively selected. In the current study, none of the genes showed a positive selection at least by three models.

DISCUSSION

RVs are the major diarrheic pathogens which causes severe diarrhea in humans as well as domesticated animals. There have been ample reports regarding RVA infection in large ruminants from different parts of the world, but data concerning RVA infections in small ruminants (sheep and goats) is very scarce. We aimed to investigate RVA associated diarrhea in the goat population of India. In India, only few studies have been done on RVA infection in goat population (24, 25). Apart from these two previous studies, there is only an NCBI GenBank submission for a partial length VP7 gene segment (KC416965) of the G8 genotype from India in the year 2011. Following a shortage in reports of RVA infection status in goat population of India, the data on its characterization is also less. The scarcity of well-characterized caprine RVA strains in NCBI GenBank from goat species India also needs to be addressed. This report characterizes the first whole-genome of a caprine isolate RVA/Goat-wt/IND/K-98/2015 from India.

Upon characterization of the caprine RVA isolate K-98, it possessed the genotype constellation of G8P[1]-I2-R2-C2-M2-A13-N2-T6-E2-H3, which is exhibited by RVA strains human and artiodactyl (bovine, caprine, and ovine) type species (9, 28, 56). Human G8P[1], G10P[11], G6P[14], G8P[14], and G10P[14] strains also display this type of consensus genotype constellation (29, 57–60). Previously, whole-genome caprine RVA strains reported from China, Bangladesh, Argentina and Uganda showed multi-reassortant backbone wherein few genes were also found to have been derived from human. Majority, of the previously described caprine RVA backbones, were showing closeness to artiodactyl-type species where they were not significantly associated with any other rotavirus strains known till date.

In the phylogenetic analysis of non-structural protein gene segments of K98, NSP1, NSP3, NSP4, and NSP5 were found clustering with bovine isolates, whereas only NSP2 is branching alongside a human RVA isolate. Gene segment NSP1 and NSP5

of K-98 clustered with bovine RVA isolates from South Africa (MRC-DPRU456) and India (RUBV81) having 95.7% and 99.0% of nucleotide similarity, respectively. It was observed that these two bovine RVA isolates from South Africa (61) and India (62) are only NCBI GenBank records for which no publications were found. Therefore, their origin and association with a particular species could not be determined. Gene segment NSP2 was located closer to Indian human RVA isolate KOL-383 (KU292526) having a close identity with Indian human rotavirus A HuRVA strain N-1 and Bangladeshi caprine RVA strain GO34 possessing human origin (63). Thus, NSP2 reflects a true human-origin having 98.2% nucleotide similarity with HuRVA isolate KOL-383 (KU292526). Gene segment NSP3 was found closer to a bovine RVA isolate HR-B91 in phylogenetic analysis having an artiodactyl-like backbone with 99.5% of nucleotide similarity (32). Similarly, gene segment NSP4 shared a high nucleotide similarity of 98.4% with a bovine RVA isolate 86 (GU984765) clustering alongside three human-like bovine RVA isolates from western India (64).

In the structural protein gene analysis, the VP1 gene of the current study isolate K-98 clustered with an Indian BoRVA isolate M1 (HQ440220) (65) within the R2 clade sharing the highest similarity of 97.5% at the nucleotide level. This particular bovine RVA isolate M1 has been described to be close to Italian human strains. The VP2 gene of isolate K-98 grouped with caprine GO34 (GU937878) and human CMC-00014 isolates from Bangladesh (18) and India (66) inside the C2 genotype clade having 97.5 and 95.3% nucleotide similarity, respectively. The study regarding the caprine isolate GO34 indicated its closeness to a Chinese lamb isolate Lamb-NT (67), which suggests it to be of small ruminant origin. Similarly, the VP4 gene was also found closer to caprine GO34 isolate in the phylogenetic analysis, which also shared a high nucleotide-based identity of 97.4%. The GO34 VP4 gene sequence was found closer to a bovine isolate A5 from Thailand. Two gene segments VP3 and VP6 also clustered close to human RVA isolates in phylogeny having 97.5% and 97.4% nucleotide-based identity. Moreover, the human RVA isolate PR457 close to VP3 K-98 had been described to possess a bovine-like VP3 gene in its respective publication. Similarly, the human RVA isolate KOL-383 from Kolkata, India also contained a porcine/bovine like VP6 gene. In a phylogenetic analysis of the VP7 gene of the K-98 isolate clustered into a clade comprising G8 genotype strains. It showed the highest percent nucleotide identity with bat isolate Rota_MNO_76 (MK674285) from Bangladesh (68). This caprine RVA VP7 G8 isolate from Bangladesh was described to have transmitted from human or livestock to bats. It shared high a high similarity to human, bovine as well as porcine RVA strains. As reported in the recently concluded study, the closeness of VP7 gene of K-98 to this bat RVA isolate from Bangladesh points toward the possibility that bats may have acquired the RVA infection as they share the water bodies while drinking which lie in close proximity to livestock as well as humans (68). The next nearest neighbor to isolate K-98 is a Bangladeshi caprine RVA isolate GBNL0022, which also appeared to be a GenBank submission (69).

Phylogenetic and percent identity analysis indicated that five gene segments (NSP1, NSP3, NSP4, NSP5, and VP1) and three gene segments (NSP2, VP3, and VP6) out of the eleven gene segments of caprine strain K-98 were derived from a heterologous host species, bovine and human, respectively. Notably, the RNA binding protein VP2 and the two surface protein genes VP4 and VP7, which are responsible for stimulating the production of neutralizing antibodies, were found to be of caprine origin. Cumulatively, it was observed that out of the eleven gene segments, 4 NSPs (NSP1, NSP3, NSP4, NSP5) and 6 VPs (VP1-VP7) were found having their origin from artiodactyl-like RVA strains.

In the antigenic epitope analysis of VP7, apart from the residue number 87, all other residues in the three putative antigenic regions showed that the VP7 gene of strain K-98 might have shared origin with human, bovine, and small ruminant origin G8 genotype. There were very few sporadic changes in the antigenic epitope regions, which point toward the conservation of pivotal epitopes that are responsible for attachment of the virus to the host.

Upon analyzing the two major neutralizing genes VP4 and VP7, along with the background data, we observed that G8P[1] is quite a common genotype circulating in caprine and ovine population, which is also found in humans, cattle, monkey, guanaco, goats, dogs, and other hosts (19, 54, 60, 70, 71). In Asia, Central America and Europe, this G8P[1] genotype combination has also been described to possess bovine-like gene segments in different mammalian species (72–75). In India, a partial G8 genotype has also been reported from North India in the year 2011, which had been submitted to NCBI GenBank (ca/KRR81/IVRI). The G8 genotype has been published worldwide in artiodactyl type species (ruminants and camelids) (20, 71). It was also described earlier in Hungary, where a zoonotic RVA strain had spread from goat and sheep to human (76). Although G8 genotype is quite commonly found in humans (77), the close proximity of humans and goats to each other may be responsible for the host switching of G8 genotype. Moreover, the finding of genotype A13 of NSP1, which is usually a common bovine genotype also sheds lights toward the interspecies transmission of artiodactyl-type genes among different farm animals.

Recombination analysis by RDP and Simplot software revealed putative recombination events in gene segment VP1. It was observed to have recombined with an Indian human-like bovine and a Chinese lamb RVA strains. These *in-silico* based analyses suggest the continuous recombination tendency of RVA strains having zoonosis potential between human and caprine origin RVA strains.

CONCLUSION

The first full-length genome sequencing of a K-98 caprine isolate from India revealed a complex bovine or a human reassortant RVA strain backbone. In total, the strain K-98 possessed an artiodactyl type genomic constellation, which seems to have acquired the majority of genes from bovine, porcine, or caprine host. Due to these conjectures, it is tough to determine the particular RVA backbone's exact ancestral origin. Diarrheal diseases due to rotavirus have been a significant burden to the

large ruminant industry. Still, the burden of such etiologies in the small ruminant industry has not been explored widely in previous studies from India.

Due to the simultaneous circulation of identical RVA genotypes in humans, large and small ruminants, the utmost importance for the surveillance studies targeting these three species is needed in the future. The full genomic analysis of strain K-98 has provided significant insights into the whole genetic makeup of caprine RVA strain from India and its genetic relatedness to different RVA from other host species. Concerning the complex nature of the K-98 genome, whole-genome analyses of RVA strains from different parts of the country are needed to comprehend the genomic nature and genetic diversity of caprine RVA. The current study's findings add to the knowledge on caprine rotaviruses and might play a substantial role in designing future vaccines or other alternative strategies combating such infections having public health significance.

DATA AVAILABILITY STATEMENT

The datasets generated in this study can be found in online repositories. The names of the repository/repositories and accession number(s) can be found in the article/**Supplementary Material**.

ETHICS STATEMENT

The study involves non-invasive methods of sample collection therefore no ethical issues were involved.

AUTHOR CONTRIBUTIONS

SSi and YM involved in the conceptualization of work. SSi, MA, SB, and OV involved in the analysis of data and manuscript drafting. SSh and JJK helped in sampling and drafting of initial manuscript. PK performed the computational studies, and did manuscript drafting. NT helped in reviewing the manuscript, SG and KB helped in writing and reviewing of the manuscript. YM and KD worked on final draft check and finalization of submission. All authors contributed to the article and approved the submitted version.

FUNDING

This work was supported by ICAR-National Fellow Scheme to YM.

ACKNOWLEDGMENTS

All the authors acknowledge and thank their respective Institutes and Universities. YM acknowledges the Education Division, ICAR, GoI for National Fellowship.

SUPPLEMENTARY MATERIAL

The Supplementary Material for this article can be found online at: https://www.frontiersin.org/articles/10.3389/fvets.2020.606661/full#supplementary-material

REFERENCES

1. Saif L, Jiang B. Nongroup A rotaviruses of humans and animals. *Curr Top Microbiol Immunol*. (1994) 185:339–71. doi: 10.1007/978-3-642-78256-5_11
2. Malik Y, Kumar N, Sharma K, Sircar S, Dhama K, Bora DP, et al. Rotavirus diarrhea in piglets: a review on epidemiology, genetic diversity and zoonotic risks. *Indian J Anim Sci*. (2014) 84:1035–42.
3. Conner ME, Darlington R. Rotavirus infection in foals. *Am J Vet Res*. (1980) 41:1699–703.
4. Martella V, Decaro N, Buonavoglia C. Enteric viral infections in lambs or kids. *Vet Microbiol*. (2015) 181:154–60. doi: 10.1016/j.vetmic.2015.08.006
5. Dhama K, Chauhan R, Mahendran M, Malik S. Rotavirus diarrhea in bovines and other domestic animals. *Vet Res Commun*. (2009) 33:1–23. doi: 10.1007/s11259-008-9070-x
6. Estes M, Kapikian A. *Fields Virology*. Philadelphia, PA: Lippencott, Williams and Wilkins (2007).
7. Bányai K, Kemenesi G, Budinski I, Földes F, Zana B, Marton S, et al. Candidate new rotavirus species in Schreiber's bats, Serbia. *Infect Genet Evol*. (2017) 48:19–26. doi: 10.1016/j.meegid.2016.12.002
8. Mihalov-Kovács E, Gellért Á, Marton S, Farkas SL, Fehér E, Oldal M, et al. Candidate new rotavirus species in sheltered dogs, Hungary. *Emerg Infect Dis*. (2015) 21:660. doi: 10.3201/eid2104.141370
9. Matthijnssens J, Ciarlet M, Rahman M, Attoui H, Bányai K, Estes MK, et al. Recommendations for the classification of group A rotaviruses using all 11 genomic RNA segments. *Arch Virol*. (2008) 153:1621–9. doi: 10.1007/s00705-008-0155-1
10. RCWG. *Rotavirus Classification Working Group: Newly Assigned Genotypes: RCWG*. (2019). Available online at: https://rega.kuleuven.be/cev/viralmetagenomics/virus-classification/rcwg (accessed September 27, 2020).
11. Munoz M, Alvarez M, Lanza I, Carmenes P. Role of enteric pathogens in the aetiology of neonatal diarrhoea in lambs and goat kids in Spain. *Epidemiol Infect*. (1996) 117:203–11. doi: 10.1017/S0950268800001321
12. Kaminjolo J, Adesiyun A. Rotavirus infection in calves, piglets, lambs and goat kids in Trinidad. *Br Vet J*. (1994) 150:293–9. doi: 10.1016/S0007-1935(05)80009-0
13. Scott A, Luddington J, Lucas M, Gilbert F. Rotavirus in goats. *Vet Rec*. (1978) 103:145. doi: 10.1136/vr.103.7.145-b
14. Legrottaglie R, Volpe A, Rizzi V, Agrimi P. Isolation and identification of rotaviruses as aetiological agents of neonatal diarrhoea in kids. Electrophoretical characterization by PAGE. *New Microbiol*. (1993) 16:227–35.
15. Munoz M, Alvarez M, Lanza I, Carmenes P. An outbreak of diarrhoea associated with atypical rotaviruses in goat kids. *Res Vet Sci*. (1995) 59:180–2. doi: 10.1016/0034-5288(95)90057-8
16. Lee J-B, Youn S-J, Nakagomi T, Park S-Y, Kim T-J, Song C-S, et al. Isolation, serologic and molecular characterization of the first G3 caprine rotavirus. *Arch Virol*. (2003) 148:643–57. doi: 10.1007/s00705-002-0963-7
17. Khafagi M, Mahmoud M, Habashi A. Prevalence of rotavirus infections in small ruminants. *Global Vet*. (2010) 4:539–43.
18. Ghosh S, Alam MM, Ahmed MU, Talukdar RI, Paul SK, Kobayashi N. Complete genome constellation of a caprine group A rotavirus strain reveals common evolution with ruminant and human rotavirus strains. *J Gen Virol*. (2010) 91:2367–73. doi: 10.1099/vir.0.022244-0
19. Alkan F, Gulyaz V, Timurkan MO, Iyisan S, Ozdemir S, Turan N, et al. A large outbreak of enteritis in goat flocks in Marmara, Turkey, by G8P [1] group A rotaviruses. *Arch Virol*. (2012) 157:1183–7. doi: 10.1007/s00705-012-1263-5
20. Uriarte ELL, Badaracco A, Matthijnssens J, Zeller M, Heylen E, Manazza J, et al. The first caprine rotavirus detected in Argentina displays genomic features

resembling virus strains infecting members of the Bovidae and Camelidae. *Vet Microbiol*. (2014) 171:189–97. doi: 10.1016/j.vetmic.2014.03.013
21. de Beer M, Steele D. *Characterization of the VP7 and VP4 Genes of a South African Group A Caprine Rotavirus (GenBank Record)*. Bethesda, MD: NCBI (2002).
22. Liu F, Xie JX, Liu CG, Wang KG, Zhou BJ, Wen M. *Full Genomic Sequence and Phylogenetic Analyses of a Caprine G10P[15] Rotavirus A Strain XL Detected in 2010 (GenBank Record)*. Huaxi, GZ: NCBI (2010).
23. Kaur S, Bhilegaonkar KN, Dubal ZB, Rawat S, Lokesh KM. *Caprine Rotavirus A Isolate Ca/KRR81/IVRI/India/2011/G8 Outer Capsid Protein (VP7) Gene, Partial cds (GenBank Record)*. Bethesda, MD: NCBI (2013).
24. Reddy G, Kumari A, Mishra A, Shivashanarappa N, Paul S, Gupta V, et al. Prevalence of groupa rotavirus in diarrhoeic goat kids from organized goat farms. *Indian J Comp Immunol Microbiol Infect Dis*. (2014) 35:9–12.
25. Singh U, Singh R, Singh AP, Yadav SK, Sircar S, Malik YS. Detection and characterization of caprine and ovine rotaviruses, India. *Indian J Anim Sci*. (2017) 87:1358–61.
26. Papp H, Malik YS, Farkas SL, Jakab F, Martella V, Bányai K. Rotavirus strains in neglected animal species including lambs, goats and camelids. *Virusdisease*. (2014) 25:215–22. doi: 10.1007/s13337-014-0203-2
27. Bwogi J, Jere KC, Karamagi C, Byarugaba DK, Namuwulya P, Baliraine FN, et al. Whole genome analysis of selected human and animal rotaviruses identified in Uganda from 2012 to 2014 reveals complex genome reassortment events between human, bovine, caprine and porcine strains. *PLoS ONE*. (2017) 12:e0178855. doi: 10.1371/journal.pone.0178855
28. Matthijnssens J, Potgieter CA, Ciarlet M, Parreño V, Martella V, Bányai K, et al. Are human P [14] rotavirus strains the result of interspecies transmissions from sheep or other ungulates that belong to the mammalian order Artiodactyla? *J Virol*. (2009) 83:2917–29. doi: 10.1128/JVI.02246-08
29. Ghosh S, Varghese V, Samajdar S, Sinha M, Naik TN, Kobayashi N. Evidence for bovine origin of VP4 and VP7 genes of human group A rotavirus G6P [14] and G10P [14] strains. *J Clin Microbiol*. (2007) 45:2751–3. doi: 10.1128/JCM.00230-07
30. Rajendran P, Kang G. Molecular epidemiology of rotavirus in children and animals and characterization of an unusual G10P [15] strain associated with bovine diarrhea in south India. *Vaccine*. (2014) 32:A89–94. doi: 10.1016/j.vaccine.2014.03.026
31. Doro R, Farkas SL, Martella V, Bányai K. Zoonotic transmission of rotavirus: surveillance and control. *Expert Rev Anti Infect Ther*. (2015) 13:1337–50. doi: 10.1586/14787210.2015.1089171
32. Kumar N, Malik Y, Sharma K, Dhama K, Ghosh S, Bányai K, et al. Molecular characterization of unusual bovine rotavirus A strains having high genetic relatedness with human rotavirus: evidence for zooanthroponotic transmission. *Zoonoses Public Health*. (2018) 65431–42. doi: 10.1111/zph.12452
33. Kumar N, Malik YS, Kumar S, Sharma K, Sircar S, Saurabh S, et al. Peptide-recombinant VP6 protein based enzyme immunoassay for the detection of group a rotaviruses in multiple host species. *PLoS ONE*. (2016) 11:e0159027. doi: 10.1371/journal.pone.0159027
34. Laemmli UK. Cleavage of structural proteins during the assembly of the head of bacteriophage T4. *Nature*. (1970) 227:680–5. doi: 10.1038/227680a0
35. Malik YS, Sharma K, Vaid N, Chakravarti S, Chandrashekar K, Basera SS, et al. Frequency of group A rotavirus with mixed G and P genotypes in bovines: predominance of G3 genotype and its emergence in combination with G8/G10 types. *J Vet Sci*. (2012) 13:271–8. doi: 10.4142/jvs.2012.13.3.271
36. Mondal A, Sharma K, Malik YS, Joardar SN. Detection of group a rotavirus in faeces of diarrhoeic bovine porcine and human population from eastern India by reverse transcriptase-polymerase chain reaction. *Adv Anim Vet Sci*. (2013) 1:18–9.
37. Gentsch JR, Glass R, Woods P, Gouvea V, Gorziglia M, Flores J, et al. Identification of group A rotavirus gene 4 types by polymerase chain reaction. *J Clin Microbiol*. (1992) 30:1365–73. doi: 10.1128/JCM.30.6.1365-1373.1992
38. Ghosh S, Kobayashi N, Nagashima S, Chawla-Sarkar M, Krishnan T, Ganesh B, et al. Full genomic analysis and possible origin of a porcine G12 rotavirus strain RU172. *Virus Genes*. (2010) 40:382–8. doi: 10.1007/s11262-010-0454-y
39. Kumar S, Stecher G, Tamura K. MEGA7: molecular evolutionary genetics analysis version 7.0 for bigger datasets. *Mol Biol Evol*. (2016) 33:1870–4. doi: 10.1093/molbev/msw054
40. Aoki ST, Settembre EC, Trask SD, Greenberg HB, Harrison SC, Dormitzer PR. Structure of rotavirus outer-layer protein VP7 bound with a neutralizing Fab. *Science*. (2009) 324:1444–7. doi: 10.1126/science.1170481
41. Martin DP, Murrell B, Golden M, Khoosal A, Muhire B. RDP4: detection and analysis of recombination patterns in virus genomes. *Virus Evol*. (2015) 1:vev003. doi: 10.1093/ve/vev003
42. Salminen MO, Carr JK, Burke DS, McCutchan FE. Identification of breakpoints in intergenotypic recombinants of HIV type 1 by bootscanning. *AIDS Res Hum Retroviruses*. (1995) 11:1423–5. doi: 10.1089/aid.1995.11.1423
43. Smith JM. Analyzing the mosaic structure of genes. *J Mol Evol*. (1992) 34:126–9. doi: 10.1007/BF00182389
44. Posada D, Crandall KA. Evaluation of methods for detecting recombination from DNA sequences: computer simulations. *Proc Natl Acad Sci USA*. (2001) 98:13757–62. doi: 10.1073/pnas.241370698
45. Boni MF, Posada D, Feldman MW. An exact nonparametric method for inferring mosaic structure in sequence triplets. *Genetics*. (2007) 176:1035–47. doi: 10.1534/genetics.106.068874
46. Padidam M, Sawyer S, Fauquet CM. Possible emergence of new geminiviruses by frequent recombination. *Virology*. (1999) 265:218–25. doi: 10.1006/viro.1999.0056
47. Holmes EC, Worobey M, Rambaut A. Phylogenetic evidence for recombination in dengue virus. *Mol Biol Evol*. (1999) 16:405–9. doi: 10.1093/oxfordjournals.molbev.a026121
48. Gibbs MJ, Armstrong JS, Gibbs AJ. Sister-scanning: a Monte Carlo procedure for assessing signals in recombinant sequences. *Bioinformatics*. (2000) 16:573–82. doi: 10.1093/bioinformatics/16.7.573
49. Weiller GF. Phylogenetic profiles: a graphical method for detecting genetic recombinations in homologous sequences. *Mol Biol Evol*. (1998) 15:326–35. doi: 10.1093/oxfordjournals.molbev.a025929
50. Lemey P, Lott M, Martin DP, Moulton V. Identifying recombinants in human and primate immunodeficiency virus sequence alignments using quartet scanning. *BMC Bioinformatics*. (2009) 10:126. doi: 10.1186/1471-2105-10-126
51. Beiko RG, Hamilton N. Phylogenetic identification of lateral genetic transfer events. *BMC Evol Biol*. (2006) 6:15. doi: 10.1186/1471-2148-6-15
52. Heath L, Van Der Walt E, Varsani A, Martin DP. Recombination patterns in aphthoviruses mirror those found in other picornaviruses. *J Virol*. (2006) 80:11827–32. doi: 10.1128/JVI.01100-06
53. Weaver S, Shank SD, Spielman SJ, Li M, Muse SV, Kosakovsky Pond SL. Datamonkey 2.0: a modern web application for characterizing selective and other evolutionary processes. *Mol Biol Evol*. (2018) 35:773–7. doi: 10.1093/molbev/msx335
54. Timurkan MÖ, Alkan F. Identification of rotavirus A strains in small ruminants: first detection of G8P [1] genotypes in sheep in Turkey. *Arch Virol*. (2020) 165:425–31. doi: 10.1007/s00705-019-04476-7
55. Lole KS, Bollinger RC, Paranjape RS, Gadkari D, Kulkarni SS, Novak NG, et al. Full-length human immunodeficiency virus type 1 genomes from subtype C-infected seroconverters in India, with evidence of intersubtype recombination. *J Virol*. (1999) 73:152–60. doi: 10.1128/JVI.73.1.152-160.1999
56. Matthijnssens J, Ciarlet M, Heiman E, Arijs I, Delbeke T, McDonald SM, et al. Full genome-based classification of rotaviruses reveals a common origin between human Wa-Like and porcine rotavirus strains and human DS-1-like and bovine rotavirus strains. *J Virol*. (2008) 82:3204–19. doi: 10.1128/JVI.02257-07
57. Ramani S, Iturriza-Gomara M, Jana AK, Kuruvilla KA, Gray JJ, Brown DW, et al. Whole genome characterization of reassortant G10P [11] strain (N155) from a neonate with symptomatic rotavirus infection: identification of genes of human and animal rotavirus origin. *J Clin Virol*. (2009) 45:237–44. doi: 10.1016/j.jcv.2009.05.003
58. Bányai K, Papp H, Dandár E, Molnár P, Mihály I, Van Ranst M, et al. Whole genome sequencing and phylogenetic analysis of a zoonotic human G8P [14] rotavirus strain. *Infect Genet Evol*. (2010) 10:1140–4. doi: 10.1016/j.meegid.2010.05.001
59. El Sherif M, Esona MD, Wang Y, Gentsch JR, Jiang B, Glass RI, et al. Detection of the first G6P [14] human rotavirus strain from a child with diarrhea in Egypt. *Infect Genet Evol*. (2011) 11:1436–42. doi: 10.1016/j.meegid.2011.05.012
60. Ghosh S, Gatheru Z, Nyangao J, Adachi N, Urushibara N, Kobayashi N. Full genomic analysis of a G8P [1] rotavirus strain isolated from an asymptomatic

infant in Kenya provides evidence for an artiodactyl-to-human interspecies transmission event. *J Med Virol*. (2011) 83:367–76. doi: 10.1002/jmv.21974
61. Das SR, Halpin RA, Stucker KM, Akopov A, Fedorova N, Puri V, et al. *Rotavirus A Strain RVA/Cow-wt/ZAF/MRC-DPRU456/2009/G6P[11] Segment 5 Non-Structural Protein 1 (NSP1) Gene—KP752872 (Genbank Record)*. Bethesda, MD: NCBI (2015).
62. Ghosh S, Naik TN. *NSP5-Encoding Gene of a Bovine Group A Rotavirus Strain—EF200580 (GenBank Record)*. Bethesda, MD: NCBI (2006).
63. Mandal P, Mullick S, Nayak MK, Mukherjee A, Ganguly N, Niyogi P, et al. Complete genotyping of unusual species A rotavirus G12P [11] and G10P [14] isolates and evidence of frequent *in vivo* reassortment among the rotaviruses detected in children with diarrhea in Kolkata, India, during 2014. *Arch Virol*. (2016) 161:2773–85. doi: 10.1007/s00705-016-2969-6
64. Chitambar SD, Arora R, Kolpe AB, Yadav MM, Raut CG. Molecular characterization of unusual bovine group A rotavirus G8P[14] strains identified in western India: emergence of P[14] genotype. *Vet Microbiol*. (2011) 148:384–8. doi: 10.1016/j.vetmic.2010.08.027
65. Malik YS, Kumar N, Sharma K, Saurabh S, Dhama K, Prasad M, et al. Multispecies reassortant bovine rotavirus strain carries a novel simian G3-like VP7 genotype. *Infect Genet Evol*. (2016) 41:63–72. doi: 10.1016/j.meegid.2016.03.023
66. Tan G, Pickett B, Fedorova N, Amedeo P, Hu L, Christensen J, et al. *Rotavirus A Strain RVA/Human-wt/IND/CMC_00014/2011/G6P[X] Segment 2 Core Capsid Protein VP2 (VP2) Gene, Complete cds—MN066875 (Genbank Record)*. Bethesda, MD: NCBI (2011).
67. Chen Y, Zhu W, Sui S, Yin Y, Hu S, Zhang X. Whole genome sequencing of lamb rotavirus and comparative analysis with other mammalian rotaviruses. *Virus Genes*. (2009) 38:302–10. doi: 10.1007/s11262-009-0332-7
68. Islam A, Hossain ME, Rostal MK, Ferdous J, Islam A, Hasan R, et al. Epidemiology and molecular characterization of rotavirus A in fruit bats in Bangladesh. *EcoHealth*. (2020) 17:398–405. doi: 10.1007/s10393-020-01488-7
69. Hossain MB, Rahman MS, Hasan R, Hossain ME, Rahman MZ, Rahman M. *Rotavirus in ruminants of Bangladesh: epidemiology and molecular characterization—MK519599 (GenBank Record)*. Bethesda, MD: NCBI (2009).
70. Jere KC, Mlera L, O'Neill HG, Peenze I, van Dijk AA. Whole genome sequence analyses of three African bovine rotaviruses reveal that they emerged through multiple reassortment events between rotaviruses from different mammalian species. *Vet Microbiol*. (2012) 159:245–50. doi: 10.1016/j.vetmic.2012.03.040
71. Komoto S, Adah MI, Ide T, Yoshikawa T, Taniguchi K. Whole genomic analysis of human and bovine G8P [1] rotavirus strains isolated in Nigeria provides evidence for direct bovine-to-human interspecies transmission. *Infect Genet Evol*. (2016) 43:424–33. doi: 10.1016/j.meegid.2016.06.023
72. Jagannath M, Vethanayagam RR, Reddy BY, Raman S, Rao CD. Characterization of human symptomatic rotavirus isolates MP409 and MP480 having 'long'RNA electropherotype and subgroup I specificity, highly related to the P6 [1], G8 type bovine rotavirus A5, from Mysore, India. *Arch Virol*. (2000) 145:1339–57. doi: 10.1007/s007050070094
73. Martinez M, Phan TG, Galeano ME, Russomando G, Parreno V, Delwart E, et al. Genomic characterization of a rotavirus G8P [1] detected in a child with diarrhea reveal direct animal-to-human transmission. Infect Genet Evol. 2014;27:402-7. doi: 10.1016/j.meegid.2014.08.015
74. Sieg M, Rückner A, Köhler C, Burgener I, Vahlenkamp TW. A bovine G8P [1] group A rotavirus isolated from an asymptomatically infected dog. *J Gen Virol*. (2015) 96:106–14. doi: 10.1099/vir.0.069120-0
75. Taniguchi K, Urasawa T, Pongsuwanna Y, Choonthanom M, Jayavasu C, Urasawa S. Molecular and antigenic analyses of serotypes 8 and 10 of bovine rotaviruses in Thailand. *J Gen Virol*. (1991) 72:2929–37. doi: 10.1099/0022-1317-72-12-2929
76. Marton S, Dóró R, Fehér E, Forró B, Ihász K, Varga-Kugler R, et al. Whole genome sequencing of a rare rotavirus from archived stool sample demonstrates independent zoonotic origin of human G8P [14] strains in Hungary. *Virus Res*. (2017) 227:96–103. doi: 10.1016/j.virusres.2016.09.012
77. Agbemabiese CA, Nakagomi T, Doan YH, Nakagomi O. Whole genomic constellation of the first human G8 rotavirus strain detected in Japan. *Infect Genet Evol*. (2015) 35:184–93. doi: 10.1016/j.meegid.2015.07.033

Conflict of Interest: The authors declare that the research was conducted in the absence of any commercial or financial relationships that could be construed as a potential conflict of interest.

frontiers in Veterinary Science

MINI REVIEW
published: 10 February 2021
doi: 10.3389/fvets.2020.626785

Deltacoronavirus Evolution and Transmission: Current Scenario and Evolutionary Perspectives

Anastasia N. Vlasova, Scott P. Kenney, Kwonil Jung, Qiuhong Wang and Linda J. Saif**

Food Animal Health Research Program, Ohio Agricultural Research and Development Center, Department of Veterinary Preventive Medicine, The Ohio State University, Wooster, OH, United States

Deltacoronavirus (DCoV)–the only coronavirus that can infect multiple species of mammals and birds–was initially identified in several avian and mammalian species, including pigs, in China in 2009–2011. Porcine DCoV has since spread worldwide and is associated with multiple outbreaks of diarrheal disease of variable severity in farmed pigs. In contrast, avian DCoV is being reported in wild birds in different countries without any evidence of disease. The DCoV transboundary nature and the recent discovery of its remarkably broad reactivity with its cellular receptor–aminopeptidase N (APN)–from different species emphasize its epidemiological relevance and necessitate additional research. Further, the ability of porcine DCoV to infect and cause disease in chicks and turkey poults and gnotobiotic calves is suggestive of its increased potential for interspecies transmission or of its avian origin. Whether, porcine DCoVs were initially acquired by one or several mammalian species from birds and whether avian and porcine DCoVs continue co-evolving with frequent spillover events remain to be major unanswered questions. In this review, we will discuss the current information on the prevalence, genetic diversity, and pathogenic potential of porcine and avian DCoVs. We will also analyze the existing evidence of the ongoing interspecies transmission of DCoVs that may provide novel insights into their complex evolution.

Keywords: deltacoronoviruses, diarrhea, epidemiology, evolution, recombination, pigs, birds

OPEN ACCESS

Edited by:
Lester J. Perez, University of Illinois at Urbana–Champaign, United States

Reviewed by:
Dongbo Sun, Heilongjiang Bayi Agricultural University, China
Jianqiang Zhang, Iowa State University, United States

****Correspondence:***
Anastasia N. Vlasova
vlasova.1@osu.edu
Linda J. Saif
saif.2@osu.edu

Specialty section:
This article was submitted to Veterinary Infectious Diseases, a section of the journal Frontiers in Veterinary Science

Received: *06 November 2020*
Accepted: *31 December 2020*
Published: *10 February 2021*

Citation:
Vlasova AN, Kenney SP, Jung K, Wang Q and Saif LJ (2021) Deltacoronavirus Evolution and Transmission: Current Scenario and Evolutionary Perspectives. Front. Vet. Sci. 7:626785. doi: 10.3389/fvets.2020.626785

INTRODUCTION

Coronaviruses (CoVs) infect humans and a wide variety of animals causing respiratory, enteric, hepatic, and neurological diseases and peritonitis of highly variable severity. Based on genetic and antigenic characterization, known CoVs were recently classified into four genera: *Alphacoronavirus*, *Betacoronavirus*, *Gammacoronavirus*, and *Deltacoronavirus* (1).

The unique mechanism of viral replication (that involves the synthesis of nested subgenomic RNAs), relatively low fidelity of RNA polymerases, and high frequency of recombination contribute to the remarkably high genetic diversity of CoVs (2). Their tendency for recombination and the inherently high mutation rates allow for rapid expansion of their host and geographic range, as emphasized by the recent [severe acute respiratory syndrome (SARS) CoV, Middle East respiratory syndrome (MERS) CoV] and ongoing (SARS-CoV-2) pandemics, emergence of new genogroup of highly virulent porcine epidemic diarrhea virus (PEDV) and porcine deltacoronavirus (PDCoV) in Asia, and its subsequent spread to the US (3–7).

Recently discovered bulbul CoV HKU11 (BuCoV HKU11), thrush CoV HKU12 (ThCoV HKU12), munia CoV HKU13 (MunCoV HKU13) (8), porcine CoV HKU15 (PDCoV HKU15), white-eye CoV HKU16 (WECoV HKU16), sparrow CoV HKU17 (SpCoV HKU17), magpie robin CoV HKU18 (MRCoV HKU18), night heron CoV HKU19 (NHCoV HKU19), wigeon CoV HKU20 (WiCoV HKU20), common moorhen CoV HKU21 (CMCoV HKU21) (9), falcon CoV HKU27 (FalCoV UAE-HKU27), houbara bustard CoV HKU28 (HouCoV UAE-HKU28), pigeon CoV HKU29 (PiCoV UAE-HKU29), and quail CoV HKU30 (QuaCoV UAE-HKU30) (10) are the best characterized DCoV species that form the *Deltacoronavirus* genus (1) (**Table 1**). Of interest, PDCoV HKU15, SpCoV HKU17, and QuaCoV HKU30 share more than 90% amino acid identity, indicating that these three CoVs may be subspecies of the same species (9, 10). While DCoVs were also detected in Asian leopard cats, Chinese ferret-badgers, green-cheeked Amazon parrot, and several other avian species, the complete genomes could not be recovered, which warrants further studies to determine whether DCoVs can replicate in these species (9, 11, 12, 26).

Deltacoronavirus (DCoV) genomes are the smallest known CoV genomes (25,400–26,689 bases) with the genomic organization similar to that of other CoVs: 5′-replicase ORF1ab, spike (S), envelope (E), membrane (M), and nucleocapsid (N)-3′ (9). Both 5′ and 3′ ends contain short untranslated regions. The replicase ORF1ab occupies up to 18,887 nt and encodes a number of proteins, including nsp3 [putative papain-like protease (PLpro)], nsp5 [putative chymotrypsin-like protease (3CLpro)], nsp12 (putative RdRp), and nsp13 (putative helicase), as well as some proteins with unknown function (9).

Although PDCoV was originally identified in pig fecal samples collected in 2009 in Hong Kong (9), its etiological role was not recognized until 2014 when it emerged as a significant source of diarrheal disease in baby pigs in the US (15, 28) (**Table 1**). However, a retrospective reverse transcription (RT)-PCR analysis demonstrated that PDCoV was present in the US swine as early as August 2013 (29). In contrast, a surveillance study in Asia and the Middle East demonstrated a high prevalence and frequent interspecies transmission of avian DCoVs (ADCoVs) in healthy aquatic birds (9, 10, 13).

PORCINE DELTACORONAVIRUS

PDCoV is a newly recognized enteropathogenic CoV that causes acute enteric disease in younger pigs (15). The disease is often manifested by diarrhea, vomiting, rapid dehydration, weight loss/decrease of weight gain, and lethargy and can lead to death in seronegative neonatal piglets, and these clinical signs generally subside within 10 days (28, 30). In older animals, including weaned pigs and sows, morbidity remains high, but the disease severity and mortality rates are low.

PDCoV diarrhea was first confirmed in the US (Ohio and Indiana) in early 2014, which coincided with the emergence of PEDV (15, 28). The latter as well as the lack of large-scale PDCoV outbreaks interfered with the comprehensive evaluation of PDCoV pathogenic and epidemic potential in the field and the exact time of its emergence. The PDCoV HKU15-OH1987 strain first identified in the US (GenBank accession no. KJ462462) has a 99% nucleotide identity to the prototype Chinese strains PDCoV HKU15-44 and HKU15-155. While it is considered that PDCoV was introduced around the same time as PEDV (2013/2014), molecular analysis of the US PDCoV strains traced back to a common ancestor between August 2010 and September 2012 (31). Recent serological data confirm the presence of swine PDCoV IgG antibodies as early as 2010 (32). The fact that the diversity of PDCoV in US swine is restricted (≥99.7% nucleotide identity) (31, 33, 34) is also consistent with the relatively recent introduction of the virus. While the exact route of emergence of PDCoV in the US is unknown, Asia is considered to be the area of PDCoV origin, where no association of this pathogen with significant clinical disease was reported (28). The latter might indicate that PDCoV could have been circulating in pigs in that geographical region for some time inducing partial immunity. In agreement with this hypothesis, a recent study has confirmed PDCoV presence in diarrheic pigs in mainland China as early as 2004 (35).

Relatively low prevalence and decreased pathogenicity of PDCoV vs. PEDV/transmissible gastroenteritis virus may indicate that PDCoV has only recently emerged in swine and is incompletely adapted to this host species, which may result in its decreased replication and spread and pathogenicity in pigs. Although BEAST analysis results suggested that PDCoV (HKU15) and SpCoV (HKU17) have shared the last common ancestor ∼523 years ago (9), this analysis does not account for recombination events (36) and for an evolutionary route that involves other (unknown) intermediate hosts. Lau et al. suggested that PDCoV (HKU15) could have resulted from recombination between HKU17 and bulbul CoV HKU11 (10). Thus, the actual time of PDCoV divergence from its ADCoV ancestor(s) could have been substantially more recent than estimated.

To date, PDCoV has been detected in most swine producing states (at least 20) within the United States (31), where it still occurs at an apparent low number of reported cases according to the Swine Health Information Center. PDCoV presence was also confirmed in Canada (16), South Korea (17), Japan (37), China (18, 38), Thailand (19), Lao People's Democratic Republic (22), Vietnam (20), and Mexico (24), posing a significant threat to the global swine industry (**Table 1**).

He et al. have recently demonstrated the presence of at least four distinct phylogenetic lineages of PDCoV that differ in their geographic circulation patterns (34). Of interest, more frequent intra- and inter-lineage recombination events (resulting in higher virus genetic diversity) were observed among PDCoV strains of the Chinese lineage than among those of the US lineage. This may be a result of different farming systems and ecological environments or more prolonged circulation of PDCoV in China and the presence of selective pressure due to partial immunity of the Chinese swine population. Surprisingly, PDCoV strains recently identified in South Korea were more closely related to the US and not the Chinese strains (17). Since there is currently no evidence that PDCoV was introduced into South Korea from the USA, this may suggest that PDCoV variants cluster according to the time of their emergence rather than geographical origin.

TABLE 1 | Summary of geographical locations and times of identification of known DCoVs.

DCoV species	Year of detection/ characterization	Host species	Location	Evidence of disease	References*
Green-cheeked Amazon parrot** CoV	1999/2006	Avian—green-cheeked Amazon parrot	Unknown, possibly England	Yes, similar to psittacine proventricular dilatation disease	(11)
Asian leopard cat DCoV Chinese ferret-badger DCoV	2005/2007	Mammalian—Asian leopard cat, Chinese ferret-badger	China	No	(12)
Bulbul CoV HKU11 Thrush CoV HKU12 Munia CoV HKU13	2006–2007/2009	Avian—bulbul, thrush, munia	Hong Kong	No	(8)
Aquatic bird (*Ciconiiformes*, *Pelecaniformes*, and *Anseriformes*) DCoVs	2009–2010/2011	Avian—gray herons, pond herons, great cormorants, black-faced spoonbills, and several duck species and other waterfowl/wading/shorebird species	Hong Kong	No	(13)
Porcine CoV HKU15 White-eye CoV HKU16 Sparrow CoV HKU17 Magpie robin CoV HKU18 Night heron CoV HKU19 Wigeon CoV HKU20 Common moorhen CoV HKU21	2007–2011/2012	Mammalian—pig Avian—white-eye, sparrow, magpie robin, night heron, wigeon, common moorhen	China, Hong Kong	No	(9)
Quail CoV HKU30	2013/2016	Avian—quail	Brazil	No	(14)
Porcine CoV HKU15	2014/2014	Mammalian—pig	USA	Yes, diarrhea	(15, 16)
Porcine CoV HKU15	2014/2014	Mammalian—pig	Canada	Unknown	(16)
Porcine CoV HKU15	2013–2015/2016	Mammalian—pig	South Korea	Yes, sporadic diarrhea	(17)
Porcine CoV HKU15	2015/2015	Mammalian—pig	China	Yes, sporadic diarrhea	(18)
Porcine CoV HKU15	2015/2016	Mammalian—pig	Thailand	Yes, diarrhea	(19)
Porcine CoV HKU15	2015/2018	Mammalian—pig	Vietnam	Yes, sporadic diarrhea	(20)
Quail CoV HKU30	2015/2019	Avian—quail	Poland	Yes, acute enteritis	(21)
Falcon CoV HKU27 Houbara bustard CoV HKU28 Pigeon CoV HKU29 Quail CoV HKU30	2013–2016/2018	Avian—falcon, houbara bustard, pigeon, quail	UAE	No	(10)
Porcine CoV HKU15	2016/2016	Mammalian—pig	Lao PDR	Yes, diarrhea	(22)
Australian duck and heron DCoVs	2016/2018	Avian—Australian duck and heron	Australia	No	(23)
Porcine CoV HKU15	2015–2017/2019	Mammalian—pig	Mexico	Yes, sporadic diarrhea	(24)
Sparrow CoV HKU17	2017/2018	Avian—sparrow	USA	No	(25)
"Novel" avian DCoVs	2009–2017/2020	Avian—a broad range of bird species including a broad range of host species, such as gulls, shorebirds, penguins, passerines, and even bustards	Poland	No	(26)
Blue-winged teal, mallard, snow goose, northern shoveler (HKU20-like), and red-tailed hawk DCoVs	2015–2018/2019	Avian—blue-winged teal, mallard, snow goose, northern shoveler, red-tailed hawk	USA	No	(27)

**If multiple references are available, only the earliest are cited. **Avian DCoVs are shown in red, and mammalian DCoVs are shown in blue.*

Similarly, we found that the emerging genogroup 2 PEDV strains from South Korea and Japan were genetically closer to the US PEDV strains than the Chinese strains (39).

AVIAN DELTACORONAVIRUS

CoVs are important pathogens of poultry and other birds (40). For decades, two gammacoronaviruses (GCoVs), infectious bronchitis virus and turkey CoV, have been recognized causes of respiratory and enteric diseases in chickens and turkeys, respectively (41–43). However, less is known about their pathogenesis in wild birds. The first ADCoV was identified by Gough and colleagues in a green-cheeked Amazon parrot in 2006 (11). The parrot had died in 1999 after having a history of anorexia, regurgitation, and passing undigested food, a suspect psittacine proventricular dilatation disease (formerly Macaw wasting disease). A CoV, distinct from all known CoVs, including GCoVs was isolated and confirmed to be the etiological agent. While its complete genomic sequence has not been determined, BLASTn analysis of the available sequence (DQ233651) indicated that it is a DCoV that shares 92% nt identity with MunCoV HKU13. This discovery was followed by identification of additional avian and mammalian DCoVs in Hong Kong, Guangdong Province of China, and the Middle East in apparently healthy wildlife species (8–10). Another recent study demonstrated that apparently healthy wild aquatic birds in Hong Kong and Cambodia serve as major reservoirs of a wide range of GCoVs and DCoVs, at a prevalence of 15 and 10%, respectively (13). Of interest, the latter findings indicated that GCoVs and DCoVs had distinct host species preference, and that GCoVs were associated with more frequent interspecies transmission among these hosts. Unlike DCoVs in pigs and GCoVs in poultry, these ADCoVs had no apparent association with clinical signs in the aquatic bird species. Further, similar to birds in Hong Kong and Cambodia, birds in the Middle East host a diversity of DCoVs with a reported prevalence of 3.7% (10). Moreover, Western blotting detected FalCoV UAE-HKU27-specific antibodies in 75% of the serum samples tested, supporting a high prevalence and likely productive DCoV infection in falcons. Recent studies that sampled wild birds in the US identified substantially lower prevalence of GCoVs and DCoVs (27, 44). Of interest, an earlier study did not identify any DCoV-positive samples among those collected from wild aquatic birds sampled in 2010–2011 in the Central and Eastern USA (44). However, we recently demonstrated that 4.99 and 1.14% of wild (aquatic and terrestrial) birds in the Mississippi and Atlantic flyways sampled between 2015 and 2018 were positive for GCoVs and DCoVs, respectively (27). The only DCoV-positive sample from terrestrial birds in our study was one from a red-tailed hawk, a predatory bird species, whereas 13 DCoV-positive samples were identified in aquatic or wading bird species and shared high nt identity with HKU20. Phylogenetic analysis demonstrated that the latter clustered with other DCoVs from aquatic/wading birds, whereas PDCoVs and SpCoVs formed a distinct lineage (27). Another study identified and characterized SpDCoVs from 10 samples collected from healthy sparrows at the sites of their commingling with pigs (swine farms in Illinois and Minnesota) (25); however, DCoV prevalence in sparrows has not been evaluated. Additionally, DCoVs have been confirmed in quail in Brazil (14) and in various wild birds in Australia (23), suggesting the global circulation of ADCoVs. Identification of DCoVs in farmed quail provides the first evidence of DCoV (highly similar to PDCoVs) circulation in poultry species (14). Interestingly, a recent study described a DCoV-associated disease in farmed quail in Poland, providing evidence of DCoV pathogenic potential in poultry species (21).

Overall, these findings suggest that unlike in Asia, ADCoVs may not be endemic in the US and may still be in the process of emergence. Collectively, these studies indicate that aquatic birds may represent a natural reservoir for DCoVs, whereas terrestrial birds and mammalian species may serve as spillover hosts. Terrestrial birds, such as sparrows, can facilitate DCoV spread through common pig–bird commingling in high-pig-traffic sites, and birds of prey (including red-tailed hawks, falcons, and other species) may play an important role in DCoV epidemiology due to their feeding habits: acquiring DCoVs from their prey and facilitating viral recombination and further spread.

DELTACORONAVIRUS INTERSPECIES TRANSMISSION

The great diversity and host specificity of bat and bird CoVs are hypothesized to be due to the large variety of bat/avian species, providing a large variety of cell types and receptors for the different CoVs (45, 46). Further, due to their flocking behavior and abilities to fly long distances, birds can play a role in the generation of novel CoV variants and their dissemination among avian species and other animals (9).

There is growing evidence of remarkable diversity and complex ecology of DCoVs from various host species (23, 34). Previously, avian DCoVs were suggested to have more stringent host specificities than GCoVs (13); however, emerging evidence provides numerous examples of the ability of DCoV to efficiently cross interspecies barriers under field or experimental conditions. These examples include: (1) evidence of circulation of "novel" avian DCoVs in a broad range of host species, such as gulls, shorebirds, penguins, passerines, and even bustards (26); (2) emergence of FalCoV UAE-HKU27, HouCoV UAE-HKU28, and PiCoV UAE-HKU29 through recombination between WECoV HKU16 and MRCoV HKU18; (3) emergence of QuaCoV UAE-HKU30 through recombination between PDCoV HKU15/SpCoV HKU17 and MunCoV HKU13; and (4) emergence of PDCoV HKU15 from recombination between SpCoV HKU17 and BuCoV HKU11 (10) (**Figure 1**). Additionally, it was demonstrated that PDCoV can infect chicks and turkey poults and gnotobiotic calves under experimental conditions (48–50) (**Figure 1**). In addition, of interest, while PDCoV infection was associated with diarrhea chicks and turkey poults, gnotobiotic calves infected with PDCoV-OH had fecal viral RNA shedding and seroconversion, but did not develop lesions or disease (48). In contrast, some DCoV species, such as CMCoV HKU21 and WiCoV HKU27, have only been described

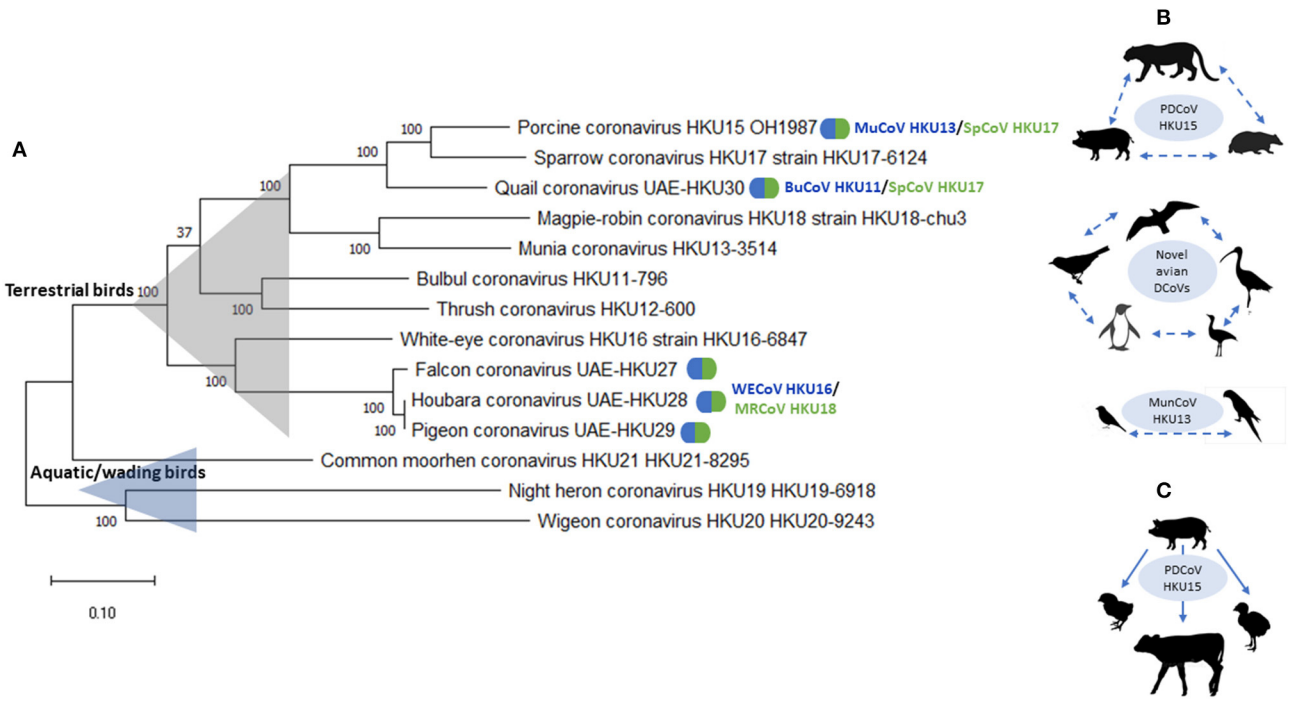

FIGURE 1 | (A) Phylogenetic analysis of complete genomic sequences of HKU11–HKU30 DCoVs. The evolutionary history was inferred by using the Maximum Likelihood method and General Time Reversible model. The tree with the highest log likelihood (−268,106.59) is shown. The tree is drawn to scale, with branch lengths measured in the number of substitutions per site. This analysis involved 14 nucleotide sequences. Evolutionary analyses were conducted in MEGA X (47). Natural recombinant variants are marked with. **(B)** Natural suggested host ranges are shown for PDCoV HKU15, MunCoV HKU13, and "novel" avian DCoVs. Dashed lines/arrows are used when the fact and direction of transmission cannot be confirmed due to the lack of complete genomic sequence and/or experimental evidence. **(C)** Experimental transmission and disease reproduction in chicks and poults using PDCoV HKU15.

in a single avian species, or within a single host order, such as BuCoV HKU11 and MunCoV HKU13 in passerines. These patterns are likely formed following the ecological traits of their avian host species: including bird feeding patterns and occupation of distinct ecological niches with or without frequent commingling with other avian or mammalian species.

A recent study demonstrated that PDCoV employs host aminopeptidase N (APN) as an entry receptor, whereby its S protein (S1 domain) interacts with an interspecies conserved domain allowing for virus entry (51–54). Moreover, in one of these studies, PDCoV was capable of infecting cell lines of porcine, human, and chicken origins, and transient expression of porcine, feline, human, and chicken APN rendered normally non-permissive cells susceptible to PDCoV infection (51). However, permissiveness of cell lines of human origin to PDCoV does not imply that this virus is readily transmissible to humans. Similarly, most bovine CoVs are capable of replication in human rectal tumor (HRT-18) cells (55), but are not known to infect humans with only a few exceptions (such as HECoV-4408) (56). Of interest, PDCoV infection of porcine cells was diminished, but not abolished, by APN knockout (KO) suggesting that it can utilize some other unknown receptor(s) in the absence of APN. This is further emphasized by the recent data demonstrating that APN absence in porcine alveolar macrophages (PAMs) from APN KO pigs made them resistant to PDCoV, whereas lung fibroblast-like cells, derived from the above PAM cultures, supported PDCoV infection to high levels (54). A possible promiscuity in PDCoV receptor usage is further corroborated by the fact that susceptibility of turkey poults and chicks to PDCoV infection cannot be explained by APN similarity between pigs and chickens/turkeys that only reaches 62.9/63.99%. In contrast, APN sequence identity between humans/domestic cats and pigs is 81.89/82.56%, but there is no evidence that PDCoV is transmissible to these species. Thus, the existing evidence highlights some molecular mechanisms that may contribute to DCoV interspecies transmission and suggests the existence of additional unknown cellular receptors as well as the importance of some additional host and possibly environmental factors.

FINAL PERSPECTIVES AND FUTURE RESEARCH

Recent pandemics of human CoVs of zoonotic origin (SARS-CoV, MERS-CoV, and SARS-CoV-2) emphasize the importance of avian and mammalian species as wild-life CoV reservoirs and intermediate hosts. This has given a tremendous boost to research on animal CoVs and generated significant amounts of novel knowledge on CoV diversity and ecology. Nevertheless, studying DCoV emergence and epidemiology remains exceptionally challenging. Current evidence indicates that aquatic avian species that carry highly diverse DCoVs and yet do not develop

DCoV-associated disease can be considered the natural host reservoir. Nevertheless, species definition of avian DCoVs remains challenging due to their relatively low global prevalence (compared with that of GCoVs) and often low amounts of virus found in the host species (26). This hinders the generation of complete genomic sequences of these viruses, preventing their proper classification by the International Committee on Taxonomy of Viruses (ICTV). The latter, in turn, impedes the accurate and comprehensive assessment of DCoV diversity in wild birds and limits our ability to study DCoV interspecies transmission among wild birds, between the latter and important poultry species, as well as between avian and mammalian species.

Further, numerous species of terrestrial birds including raptors and various migratory birds may promote genetic diversity and facilitate the spread of DCoVs. Consistent with this notion, a higher frequency of recombinant events was reported for DCoVs circulating in terrestrial birds including bulbuls, sparrows, munias, falcons, pigeons, houbara bustards, and white-eyes (10), whereas DCoVs from aquatic/wading birds seemed to have more stringent species specificities (9, 13). This signifies that terrestrial birds may serve as mixing vessels and means for DCoV spread. Finally, small migratory birds (such as sparrows) that commonly commingle with swine on farms and other high-pig-traffic sites may represent the intermediate host or viral vehicle that introduced DCoV into the swine population (25). Similar scenarios may occur in nature in different geographical locations.

One of the most intriguing unanswered questions is whether avian and porcine (and possibly other unknown mammalian) DCoVs co-evolve with frequent spillover events (similar to influenza A virus) or they evolve independently from one another in different geographic regions. This question cannot be fully answered without knowing the times of emergence of PDCoV in swine and avian DCoVs in different geographic regions. As discussed above, while it is considered that PDCoV was introduced around the time of PEDV emergence in the US, a time-scaled Bayesian phylogenetic analysis and recent serological data suggest that PDCoV could have been present in the US as early as 2010 (31, 32). Similarly, while the highest prevalence and diversity of ADCoVs were noted in earlier studies in several Asian countries (8, 9, 13), the first ADCoV was identified prior to that from another region (11). Because global studies evaluating the prevalence of ADCoVs are scarce, it is still unknown whether ADCoVs are endemic in many geographic regions or only in Asia. The lack of large-scale outbreaks in pigs and acute clinical disease in most avian hosts as well as the unavailability of comprehensive epidemiological data from different geographic regions and timeframes preclude the accurate evaluation of DCoV origins and emergence routes.

Additionally, the prevalence of DCoVs in birds worldwide is lower than that of GCoVs or other enteric CoVs in pigs during the epidemic phase in a given swine population. The reasons for the apparently lower prevalence are unknown; however, it may be an indication of incomplete adaptation of DCoVs to their hosts. The ability of PDCoV to utilize APN of numerous species origin for cell entry may be one of the key factors regulating the virus's increased potential for interspecies transmission, but it can also be associated with decreased virus–swine host fitness.

In conclusion, additional studies evaluating the genetic diversity of DCoVs in birds and mammalian hosts are needed to better understand their epidemiology and evolution. In addition, seroprevalence studies in various avian species (poultry and wild birds) can provide useful information highlighting the actual prevalence of DCoVs globally. Finally, experimental studies on DCoV interspecies transmission, host adaptation, and identification of additional cellular receptors are needed to carefully evaluate its pathogenicity in various hosts and its zoonotic potential. If indeed DCoVs have just recently emerged in most known highly diverse avian and mammalian hosts, their epidemic potential, including the possible spillover into humans, can be tremendous and should not be underestimated.

AUTHOR CONTRIBUTIONS

AV drafted the manuscript. AV, SK, KJ, QW, and LS critically revised the manuscript. All authors contributed to the article and approved the submitted version.

REFERENCES

1. De Groot R, Baker S, Baric R, Enjuanes L, Gorbalenya A, Holmes K, et al. Coronaviridae. In: King AMQ, Adams MJ, Carstens EB, Lefkowitz EJ, editors. *Virus Taxonomy: Ninth Report of the International Committee on Taxonomy of Viruses, International Union of Microbiological Societies, Virology Division*. London: Elsevier Academic Press (2011). p. 806–28.
2. Sawicki SG, Sawicki DL, Siddell SG. A contemporary view of coronavirus transcription. *J Virol*. (2007) 81:20–9. doi: 10.1128/JVI.01358-06
3. Ksiazek TG, Erdman D, Goldsmith CS, Zaki SR, Peret T, Emery S, et al. A novel coronavirus associated with severe acute respiratory syndrome. *N Engl J Med*. (2003) 348:1953–66. doi: 10.1056/NEJMoa030781
4. Rota PA, Oberste MS, Monroe SS, Nix WA, Campagnoli R, Icenogle JP, et al. Characterization of a novel coronavirus associated with severe acute respiratory syndrome. *Science*. (2003) 300:1394–9. doi: 10.1126/science.1085952
5. Drosten C, Muth D, Corman VM, Hussain R, Al Masri M, Hajomar W, et al. An observational, laboratory-based study of outbreaks of middle East respiratory syndrome coronavirus in Jeddah and Riyadh, kingdom of Saudi Arabia, 2014. *Clin Infect Dis*. (2015) 60:369–77. doi: 10.1093/cid/ciu812
6. Wang Q, Vlasova AN, Kenney SP, Saif LJ. Emerging and re-emerging coronaviruses in pigs. *Curr Opin Virol*. (2019) 34:39–49. doi: 10.1016/j.coviro.2018.12.001
7. Ralph R, Lew J, Zeng T, Francis M, Xue B, Roux M, et al. 2019-nCoV (Wuhan virus), a novel Coronavirus: human-to-human transmission, travel-related cases, and vaccine readiness. *J Infect Dev Ctries*. (2020) 14:3–17. doi: 10.3855/jidc.12425
8. Woo PC, Lau SK, Lam CS, Lai KK, Huang Y, Lee P, et al. Comparative analysis of complete genome sequences of three avian coronaviruses reveals a novel group 3c coronavirus. *J Virol*. (2009) 83:908–17. doi: 10.1128/JVI.01977-08
9. Woo PC, Lau SK, Lam CS, Lau CC, Tsang AK, Lau JH, et al. Discovery of seven novel Mammalian and avian coronaviruses in the genus deltacoronavirus supports bat coronaviruses as the gene source of alphacoronavirus and betacoronavirus and avian coronaviruses as the gene source of gammacoronavirus and deltacoronavirus. *J Virol*. (2012) 86:3995–4008. doi: 10.1128/JVI.06540-11

10. Lau SKP, Wong EYM, Tsang CC, Ahmed SS, Au-Yeung RKH, Yuen KY, et al. Discovery and sequence analysis of four deltacoronaviruses from birds in the middle east reveal interspecies jumping with recombination as a potential mechanism for avian-to-avian and avian-to-mammalian transmission. *J Virol*. (2018) 92:e00265-18. doi: 10.1128/JVI.00265-18
11. Gough RE, Drury SE, Culver F, Britton P, Cavanagh D. Isolation of a coronavirus from a green-cheeked Amazon parrot (Amazon viridigenalis Cassin). *Avian Pathol*. (2006) 35:122–6. doi: 10.1080/03079450600597733
12. Dong BQ, Liu W, Fan XH, Vijaykrishna D, Tang XC, Gao F, et al. Detection of a novel and highly divergent coronavirus from asian leopard cats and Chinese ferret badgers in Southern China. *J Virol*. (2007) 81:6920–6. doi: 10.1128/JVI.00299-07
13. Chu DK, Leung CY, Gilbert M, Joyner PH, Ng EM, Tse TM, et al. Avian coronavirus in wild aquatic birds. *J Virol*. (2011) 85:12815–20. doi: 10.1128/JVI.05838-11
14. Torres CA, Hora AS, Tonietti PO, Taniwaki SA, Cecchinato M, Villarreal LY, et al. Gammacoronavirus and Deltacoronavirus in Quail. *Avian Dis*. (2016) 60:656–61. doi: 10.1637/11412-032316-Reg.1
15. Wang L, Byrum B, Zhang Y. Porcine coronavirus HKU15 detected in 9 US states, 2014. *Emerg Infect Dis*. (2014) 20:1594–5. doi: 10.3201/eid2009.140756
16. Marthaler D, Raymond L, Jiang Y, Collins J, Rossow K, Rovira A. Rapid detection, complete genome sequencing, and phylogenetic analysis of porcine deltacoronavirus. *Emerg Infect Dis*. (2014) 20:1347–50. doi: 10.3201/eid2008.140526
17. Lee JH, Chung HC, Nguyen VG, Moon HJ, Kim HK, Park SJ, et al. Detection and phylogenetic analysis of porcine Deltacoronavirus in Korean Swine Farms, 2015. *Transbound Emerg Dis*. (2016) 63:248–52. doi: 10.1111/tbed.12490
18. Song D, Zhou X, Peng Q, Chen Y, Zhang F, Huang T, et al. Newly emerged porcine deltacoronavirus associated with diarrhoea in swine in china: identification, prevalence and full-length genome sequence analysis. *Transbound Emerg Dis*. (2015) 62:575–80. doi: 10.1111/tbed.12399
19. Madapong A, Saeng-Chuto K, Lorsirigool A, Temeeyasen G, Srijangwad A, Tripipat T, et al. Complete genome sequence of Porcine Deltacoronavirus isolated in Thailand in 2015. *Genome Announc*. (2016) 4:e00408-16. doi: 10.1128/genomeA.00408-16
20. Le VP, Song S, An BH, Park GN, Pham NT, Le DQ, et al. A novel strain of porcine deltacoronavirus in Vietnam. *Arch Virol*. (2018) 163:203–7. doi: 10.1007/s00705-017-3594-8
21. Domanska-Blicharz K, Kuczkowski M, Sajewicz-Krukowska J. Whole genome characterisation of quail deltacoronavirus detected in Poland. *Virus Genes*. (2019) 55:243–7. doi: 10.1007/s11262-019-01639-1
22. Lorsirigool A, Saeng-Chuto K, Temeeyasen G, Madapong A, Tripipat T, Wegner M, et al. The first detection and full-length genome sequence of porcine deltacoronavirus isolated in Lao PDR. *Arch Virol*. (2016) 161:2909–11. doi: 10.1007/s00705-016-2983-8
23. Chamings A, Nelson TM, Vibin J, Wille M, Klaassen M, Alexandersen S. Detection and characterisation of coronaviruses in migratory and non-migratory Australian wild birds. *Sci Rep*. (2018) 8:5980. doi: 10.1038/s41598-018-24407-x
24. Perez-Rivera C, Ramirez-Mendoza H, Mendoza-Elvira S, Segura-Velazquez R, Sanchez-Betancourt JI. First report and phylogenetic analysis of porcine deltacoronavirus in Mexico. *Transbound Emerg Dis*. (2019) 66:1436–41. doi: 10.1111/tbed.13193
25. Chen Q, Wang L, Yang C, Zheng Y, Gauger PC, Anderson T, et al. The emergence of novel sparrow deltacoronaviruses in the United States more closely related to porcine deltacoronaviruses than sparrow deltacoronavirus HKU17. *Emerg Microbes Infect*. (2018) 7:105. doi: 10.1038/s41426-018-0108-z
26. Wille M, Holmes EC. Wild birds as reservoirs for diverse and abundant gamma- and deltacoronaviruses. *FEMS Microbiol Rev*. (2020) 44:631–44. doi: 10.1093/femsre/fuaa026
27. Paim FC, Bowman AS, Miller L, Feehan BJ, Marthaler D, Saif LJ, et al. Epidemiology of Deltacoronaviruses (delta-CoV) and Gammacoronaviruses (gamma-CoV) in Wild Birds in the United States. *Viruses*. (2019) 11:897. doi: 10.3390/v11100897
28. Ma Y, Zhang Y, Liang X, Lou F, Oglesbee M, Krakowka S, et al. Origin, evolution, and virulence of porcine deltacoronaviruses in the United States. *mBio*. (2015) 6:e00064. doi: 10.1128/mBio.00064-15
29. Sinha A, Gauger P, Zhang J, Yoon KJ, Harmon K. PCR-based retrospective evaluation of diagnostic samples for emergence of porcine deltacoronavirus in US swine. *Vet Microbiol*. (2015) 179:296–8. doi: 10.1016/j.vetmic.2015.06.005
30. Jung K, Hu H, Saif LJ. Porcine deltacoronavirus infection: etiology, cell culture for virus isolation and propagation, molecular epidemiology and pathogenesis. *Virus Res*. (2016) 226:50–9. doi: 10.1016/j.virusres.2016.04.009
31. Homwong N, Jarvis MC, Lam HC, Diaz A, Rovira A, Nelson M, et al. Characterization and evolution of porcine deltacoronavirus in the United States. *Prev Vet Med*. (2016) 123:168–74. doi: 10.1016/j.prevetmed.2015.11.001
32. Thachil A, Gerber PF, Xiao CT, Huang YW, Opriessnig T. Development and application of an ELISA for the detection of porcine deltacoronavirus IgG antibodies. *PLoS ONE*. (2015) 10:e0124363. doi: 10.1371/journal.pone.0124363
33. Zhang J. Porcine deltacoronavirus: overview of infection dynamics, diagnostic methods, prevalence and genetic evolution. *Virus Res*. (2016) 226:71–84. doi: 10.1016/j.virusres.2016.05.028
34. He WT, Ji X, He W, Dellicour S, Wang S, Li G, et al. Genomic epidemiology, evolution, and transmission dynamics of porcine deltacoronavirus. *Mol Biol Evol*. (2020) 37:2641–54. doi: 10.1093/molbev/msaa117
35. Dong N, Fang L, Zeng S, Sun Q, Chen H, Xiao S. Porcine Deltacoronavirus in Mainland China. *Emerg Infect Dis*. (2015) 21:2254–5. doi: 10.3201/eid2112.150283
36. Bouckaert R, Vaughan TG, Barido-Sottani J, Duchene S, Fourment M, Gavryushkina A, et al. BEAST 2.5: an advanced software platform for Bayesian evolutionary analysis. *PLoS Comput Biol*. (2019) 15:e1006650. doi: 10.1101/474296
37. Suzuki T, Shibahara T, Imai N, Yamamoto T, Ohashi S. Genetic characterization and pathogenicity of Japanese porcine deltacoronavirus. *Infect Genet Evol*. (2018) 61:176–82. doi: 10.1016/j.meegid.2018.03.030
38. Liu C, Zhang X, Zhang Z, Chen R, Zhang Z, Xue Q. Complete genome characterization of novel Chinese Porcine Deltacoronavirus strain SD. *Genome Announc*. (2017) 5:e00930-17. doi: 10.1128/genomeA.00930-17
39. Lin CM, Saif LJ, Marthaler D, Wang Q. Evolution, antigenicity and pathogenicity of global porcine epidemic diarrhea virus strains. *Virus Res*. (2016) 226:20–39. doi: 10.1016/j.virusres.2016.05.023
40. Cavanagh D. Coronaviruses in poultry and other birds. *Avian Pathol*. (2005) 34:439–48. doi: 10.1080/03079450500367682
41. Guy JS. Turkey coronavirus is more closely related to avian infectious bronchitis virus than to mammalian coronaviruses: a review. *Avian Pathol*. (2000) 29:207–12. doi: 10.1080/03079450050045459
42. Cavanagh D. Coronavirus avian infectious bronchitis virus. *Vet Res*. (2007) 38:281–97. doi: 10.1051/vetres:2006055
43. Jackwood MW. Review of infectious bronchitis virus around the world. *Avian Dis*. (2012) 56:634–41. doi: 10.1637/10227-043012-Review.1
44. Jordan BJ, Hilt DA, Poulson R, Stallknecht DE, Jackwood MW. Identification of avian coronavirus in wild aquatic birds of the central and eastern USA. *J Wildl Dis*. (2015) 51:218–21. doi: 10.7589/2014-03-070
45. Milek J, Blicharz-Domanska K. Coronaviruses in avian species - review with focus on epidemiology and diagnosis in wild birds. *J Vet Res*. (2018) 62:249–55. doi: 10.2478/jvetres-2018-0035
46. Banerjee A, Kulcsar K, Misra V, Frieman M, Mossman K. Bats and Coronaviruses. *Viruses*. (2019) 11:41. doi: 10.3390/v11010041
47. Kumar S, Stecher G, Li M, Knyaz C, Tamura K. MEGA X: Molecular Evolutionary Genetics Analysis across computing platforms. *Mol Biol Evol*. (2018) 35:1547–9. doi: 10.1093/molbev/msy096
48. Jung K, Hu H, Saif LJ. Calves are susceptible to infection with the newly emerged porcine deltacoronavirus, but not with the swine enteric alphacoronavirus, porcine epidemic diarrhea virus. *Arch Virol*. (2017) 162:2357–62. doi: 10.1007/s00705-017-3351-z
49. Liang Q, Zhang H, Li B, Ding Q, Wang Y, Gao W, et al. Susceptibility of chickens to Porcine Deltacoronavirus infection. *Viruses*. (2019) 11:573. doi: 10.3390/v11060573
50. Boley PA, Alhamo MA, Lossie G, Yadav KK, Vasquez-Lee M, Saif LJ, et al. Porcine Deltacoronavirus infection and transmission in poultry, United States. *Emerg Infect Dis*. (2020) 26:255–65. doi: 10.3201/eid2602.190346

51. Li W, Hulswit RJG, Kenney SP, Widjaja I, Jung K, Alhamo MA, et al. Broad receptor engagement of an emerging global coronavirus may potentiate its diverse cross-species transmissibility. *Proc Natl Acad Sci USA*. (2018) 115:E5135–43. doi: 10.1073/pnas.1802879115
52. Wang B, Liu Y, Ji CM, Yang YL, Liang QZ, Zhao P, et al. Porcine deltacoronavirus engages the transmissible gastroenteritis virus functional receptor Porcine Aminopeptidase N for infectious cellular entry. *J Virol*. (2018) 92:e00318-18. doi: 10.1128/JVI.00318-18
53. Zhu X, Liu S, Wang X, Luo Z, Shi Y, Wang D, et al. Contribution of porcine aminopeptidase N to porcine deltacoronavirus infection. *Emerg Microbes Infect*. (2018) 7:65. doi: 10.1038/s41426-018-0068-3
54. Stoian A, Rowland RRR, Petrovan V, Sheahan M, Samuel MS, Whitworth KM, et al. The use of cells from ANPEP knockout pigs to evaluate the role of aminopeptidase N (APN) as a receptor for porcine deltacoronavirus (PDCoV). *Virology*. (2020) 541:136–40. doi: 10.1016/j.virol.2019.12.007
55. Laporte J, Bobulesco P, Rossi F. A cell line particularly susceptible to bovine enteric Coronavirus replication: HRT 18 cells. *C R Seances Acad Sci D*. (1980) 290:623–6.
56. Zhang XM, Herbst W, Kousoulas KG, Storz J. Biological and genetic characterization of a hemagglutinating coronavirus isolated from a diarrhoeic child. *J Med Virol*. (1994) 44:152–61. doi: 10.1002/jmv.1890440207

Conflict of Interest: The authors declare that the research was conducted in the absence of any commercial or financial relationships that could be construed as a potential conflict of interest.

frontiers in Veterinary Science

ORIGINAL RESEARCH
published: 19 March 2021
doi: 10.3389/fvets.2021.619759

Identification of Dendritic Cell Maturation, TLR, and TREM1 Signaling Pathways in the *Brucella canis* Infected Canine Macrophage Cells, DH82, Through Transcriptomic Analysis

Woo Bin Park[1,2], *Suji Kim*[1,2], *Soojin Shim*[1†] *and Han Sang Yoo*[1,2,3,4*]

[1] Department of Infectious Diseases, College of Veterinary Medicine, Seoul National University, Seoul, South Korea, [2] BK21 Four Future Veterinary Medicine Leading Education and Research Center, Seoul National University, Seoul, South Korea, [3] Research Institute for Veterinary Science, Seoul National University, Seoul, South Korea, [4] BioMax/N-Bio Institute, Seoul National University, Seoul, South Korea

OPEN ACCESS

Edited by:
Lester J. Perez,
University of Illinois at Urbana–Champaign, United States

Reviewed by:
Erika Sousa Guimarães,
Federal Institute of Minas Gerais, Brazil
Fengyang Wang,
Hainan University, China

***Correspondence:**
Han Sang Yoo
yoohs@snu.ac.kr

†Present address:
Soojin Shim,
Department of Mechanical and Biofunctional Systems, Institute of Industrial Science, University of Tokyo, Tokyo, Japan

Specialty section:
This article was submitted to Veterinary Infectious Diseases, a section of the journal Frontiers in Veterinary Science

Received: 21 October 2020
Accepted: 08 February 2021
Published: 19 March 2021

Citation:
Park WB, Kim S, Shim S and Yoo HS (2021) Identification of Dendritic Cell Maturation, TLR, and TREM1 Signaling Pathways in the Brucella canis Infected Canine Macrophage Cells, DH82, Through Transcriptomic Analysis. Front. Vet. Sci. 8:619759. doi: 10.3389/fvets.2021.619759

Research has been undertaken to understand the host immune response to *Brucella canis* infection because of the importance of the disease in the public health field and the clinical field. However, the previous mechanisms governing this infection have not been elucidated. Therefore, *in vitro* models, which mimic the *in vivo* infection route using a canine epithelial cell line, D17, and a canine macrophage, DH82, were established to determine these mechanisms by performing an analysis of the transcriptomes in the cells. In this study, a coculture model was constructed by using the D17 cell line and DH82 cell line in a transwell plate. Also, a single cell line culture system using DH82 was performed. After the stimulation of the cells in the two different systems infected with *B. canis*, the gene expression in the macrophages of the two different systems was analyzed by using RNA-sequencing (RNA-seq), and a transcriptomic analysis was performed by using the Ingenuity Pathway Analysis (IPA). Gene expression patterns were analyzed in the DH82 cell line at 2, 12, and 24 h after the stimulation with *B. canis*. Changes in the upregulated or downregulated genes showing 2-fold or higher were identified at each time point by comparing with the non-stimulated group. Differentially expressed genes (DEGs) between the two culture models were identified by using the IPA program. Generally, the number of genes expressed in the single cell line culture was higher than the number of genes expressed in the coculture model for all-time points. The expression levels of those genes were higher in the single cell line culture ($p < 0.05$). This analysis indicated that the immune response-related pathways, especially, the dendritic cell maturation, Triggering receptor expression on myeloid cells 1 (TREM1) signaling, and Toll-like receptor (TLR) signaling pathway, were significantly induced in both the culture systems with higher *p*-values and *z*-scores. An increase in the expression level of genes related to the pathways was observed over time. All pathways are commonly associated with a manifestation of pro-inflammatory cytokines and early immune responses. However, the Peroxisome proliferator-activation

receptor (PPAR) signaling and Liver X Receptor/Retinoid X Receptor (LXR/RXR) signaling associated with lipid metabolism were reduced. These results indicate that early immune responses might be highly activated in *B. canis* infection. Therefore, these results might suggest clues to reveal the early immune response of the canine to *B. canis* infection, particularly TLR signaling.

Keywords: *Brucella canis*, RNA-Seq, transcriptomic analysis, TLR signaling, early immune response

INTRODUCTION

Brucellosis is a reemerging worldwide zoonotic disease caused by the genus *Brucella*. *Brucella* spp. such as *Brucella melitensis* and *Brucellar suis*, are the facultative intracellular pathogens that are commonly able to overcome the host innate immunity during the early infection. *Brucella* spp. affecting not only the immune response but also the killing action of macrophages migrate within phagocytic vacuoles and replicate in cell vesicles, causing chronic infection (1). Among these species, *Brucella canis* is known as a cause of canine brucellosis and, similar to the other *Brucella* spp., is also a cause of the zoonotic disease that can occur in humans. The host of *B. canis* is mainly dogs, and granulomatous lesions are identified in various organs during the infection and are characterized by reproductive disorders such as abortion in females and epididymitis and prostatitis in male dogs (2). When an infection occurs in a human, mild and non-specific symptoms usually occur and then antibiotic therapy is usually applied. Infection with *B. canis* can occur through the conjunctival or oronasal route or along the venereal route, and can also occur through contaminated milk, urine, aborted fetuses, vaginal secretion, and semen (3–5). Human infection with *B. canis* is known to occur very rarely, but the frequency has been increasing in recent years. The prevalence has been increasing due to the increase in unsanitary kennel facilities, companion dogs, and stray dogs. *B. canis* is currently reported in many parts of the world, and is considered endemic in the USA, Latin America, and Mexico (6–11). Infections of *B. canis* have also been reported in Asian countries, such as China and Japan, in Africa, and in European countries, such as Germany, the United Kingdom, and Italy (12–18). The prevalence of *B. canis* infection in 2,394 dogs, including the companion and the stray dogs in Korea was examined. The prevalence was found to be significantly higher in dogs older than 6 years and in female dogs (19).

Immunological studies of *B. canis* infection have also been conducted. Usually, research has focused on the expression of cytokines following the infection of various cell lines with *B. canis* (20–23). Previous studies have shown that the immune responses of humans to brucellosis are similar to those of animals to brucellosis (21). In addition, the immune response of human and canine dendritic cells to *B. canis* infection has been compared based on the expression of cytokines (22). Many attempts have been made to understand the immunopathological mechanism of *B. canis* infection because of the importance of the disease in recent public and clinical realms (2, 21). To date, however, the mechanisms governing *B. canis* infection have not been elucidated.

Therefore, in this study, an *in vitro* coculture model was established by using the D17, a canine epithelial cell line, and the DH82, a canine macrophage cell line. The coculture model is designed to observe the host response to the pathogen by interaction between epithelial cells and immune cells in comparison to the single cell line culture model. The coculture model was applied to investigate the host immune response to *B. canis* infection through a transcriptomic analysis of the DH82 cells using total RNA-sequencing (RNA-seq).

MATERIALS AND METHODS

Cell Culture and Stimulation

Brucella canis QE13, from the College of Veterinary Medicine of Gyeongsang National University, was cultured on *Brucella* broth (BD, NJ, USA) at 37°C under aerobic conditions. For the stimulation of the D17 cell line and DH82 cell line, the bacteria were cultured up to the exponential growth phase, reaching 3.06E + 09 CFU.

In the coculture model, $\sim 5.0 \times 10^5$ cells/well of the D17 cell line (ATCC CCL-183) were seeded onto the apical side of a Transwell insert (Transwell permeable support; Corning, MA, USA) and incubated for 3 h in DMEM (Gibco, NY, USA) containing 15% fetal bovine serum (FBS; Gibco, NY, USA) at 37°C in a humidified chamber containing 5% CO_2. After the D17 cell line was stabilized, 5.0×10^5 cells/well of the DH82 cell line (ATCC CRL-10389) were seeded onto the Transwell plate well with DMEM containing 15% FBS. After the DH82 cells were stabilized, the D17 cell line where the apical side of Transwell insert was stimulated by using Dulbecco's Phosphate-Buffered Saline (DPBS; negative control) and *B. canis* at an multiplicity of infection (MOI) of 10:1.

In the single cell line culture model, 5.0×10^5 cells/well of the DH82 cell line were seeded onto one well of a 12-well plate (Corning, MA, USA) with DMEM containing 15% FBS. After the DH82 cell line was stabilized, it was stimulated by using DPBS (negative control) and *B. canis* at an MOI of 10:1.

Each experiment was conducted three times.

The D17 cell line and DH82 cell line were purchased through ATCC (https://atcc.org/).

Invasion Assay

The infection of *B. canis* to the DH82 cell line was performed at MOI of 1:10. After the infection, it was incubated for 12 h at 37°C in a humidified chamber containing 5% CO_2. Each well was thoroughly washed with PBS after the incubation. For the quantification of intracellular bacteria, the infected monolayer was cultured at a place with 100 μg/ml of gentamicin

(Sigma, St. Louis, USA) for 2 h to kill extracellular bacteria. After the antibiotics treatment, the cells were washed out with PBS to remove residual antibiotics and lysed with 0.2% Triton-X100 at 2, 12, and 24 h after the removal. Lysates were plated on agar after a serial dilution and measured colony-forming units (CFUs) after 48 h at 37°C in a humidified chamber containing 5% CO_2. These experiments were triplicated.

RNA Extraction

After 2, 12, and 24 h of the incubation, total RNA was extracted from the DH82 cell line using the RNeasy Mini Kit (Qiagen, Hilden, Germany) according to the instructions of the manufacturer. RNA purity and integrity were evaluated by determining the OD 260/280 ratio and an analysis using the Agilent 2100 Bioanalyzer (Agilent Technologies, CA, USA). The total RNA concentration was measured by using the Quant-IT Ribogreen (Invitrogen, CA, USA). To determine the integrity of the total RNA, the TapeStation RNA Screen Tape system (Agilent Technologies, CA, USA) was used. Only high-quality RNA preparation, with RNA integrity numbers (RINs) > 7.0, was used for the RNA library construction.

Transcriptomic Analysis

The libraries were prepared for 100-bp paired-end sequencing using a TruSeq Stranded mRNA Sample Preparation Kit (Illumina, CA, USA). Specifically, mRNA molecules were purified and fragmented from 1 μg of total RNA using oligo (dT) magnetic beads. The fragmented mRNAs were synthesized as a single-stranded complementary DNA (cDNA) using a Random Hexamer Primer (Kapa Biosystems, MA, USA). By applying cDNA as a template for the second strand synthesis, a double-stranded cDNA was prepared. After sequential end repair, A-tailing, and adapter ligation, the cDNA libraries were amplified by using a PCR. The quality of these cDNA libraries was evaluated using the Agilent 2100 Bioanalyzer (Agilent, CA, USA). These values were quantified using the KAPA library quantification kit (Kapa Biosystems, MA, USA) according to the library quantification protocol of the manufacturer. Following the cluster amplification of denatured templates, sequencing was progressed as paired end (2 × 150 bp) by using an Illumina platform sequencer (Illumina, CA, USA). Each gene was compared with the results of 0 h to proceed with the analysis.

Filtering

Low-quality reads were filtered according to the following criteria: reads containing more than 10% of the skipped base reads (marked as "N"s'), reads containing more than 40% of the bases whose quality score was < 20, and reads whose average quality scores are per read was < 20. The whole filtering process was performed using the in-house scripts.

Sequencing Alignment

The filtered reads were mapped to the reference genome species using the aligner TopHat (24).

Gene Expression Estimation

The gene expression level was measured by Cufflinks v2.1.1 (25) using the human gene annotation database. To improve the accuracy of the measurement, the multi-read-correction option and the frag-bias-correct option were applied. All other options were set to default values.

Differentially Expressed Gene Analysis

Differentially expressed gene (DEG) analysis was performed by using Cuffdiff (26). To enhance the analysis accuracy, the multi-read-correction option and the frag-bias-correct option were applied. All other options were set to default values. DEGs were identified based on a q-value threshold < 0.05 for correcting the errors caused by multiple testing (27).

Gene Ontology Analysis

The gene ontology (GO) database classifies the genes according to the three categories, such as biological process (BP), cellular component (CC), and molecular function (MF), and provides information on the functions of genes. To characterize the identified genes from the DEG analysis, a GO-based trend test was carried out using the Fisher's exact test (28).

Biological System Analysis

The data were analyzed using IPA (Qiagen, Hilden, Germany, https://www.qiagenbioinformatics.com/products/ingenuityphathway-analysis). DEGs with adjusted values of p < 0.05 were obtained by using the IPA program. Each gene was mapped to its corresponding gene gain using the Ingenuity Knowledge Base. Biological function analysis was performed using IPA to compare DEG associated with the disease and function, the molecular and cellular function, and physiological system function in DH82 cells treated with *B. canis* at each time point. The canonical pathway for the *B. canis*-treated DH82 cells was also identified through the canonical pathway of the IPA library (29).

Comparison Analysis

The data were analyzed by using IPA (Qiagen Inc., Hilden, Germany, https://www.qiagenbioinformatics.com/products/ingenuityphathway-analysis). Using the data, a comparative analysis was conducted according to each time and each culture model. However, the difference in DEGs with respect to time was confirmed, and the difference in DEGs according to the model type was confirmed.

Expression Analysis of Selected Genes by Using Quantitative Real-Time PCR

The expression of levels of five genes, IL6, CCL5, CXCL10, CXCL8, and IL1B, in RNA-seq at 2, 12, and 24 time points were compared with those from the quantitative real-time PCR (qRT-PCR) of the two different experiments. The qRT-PCR was performed by using 1 μl of cDNA, a Rotor-Gene SYBR Green PCR Kit (Qiagen Inc., Hilden, Germany), and a Rotor-Gene Q real-time PCR cycler (Qiagen, Hilden, Germany) (**Table 1**). The cycling condition is as follows: 95°C for 3 min, followed by 45 cycles of 95°C for 15 s, 30 s at 60°C, and 30 s at 72°C with a fluorescence detected during the extension phase. The expression level was determined by the $2^{-\Delta\Delta Ct}$ method using glyceraldehyde-3-phosphate dehydrogenase (GAPDH) as

TABLE 1 | Canine forward and reverse primers for validation by quantitative real-time PCR.

Target	Forward primer	Reverse primer	Accession number
IL-6	5′-CTGGCAGGAGATTCCAAGGAT-3′	5′-TCTGCCAGTGCCTCTTTGC-3′	NM_001003301
CCL5	5′-CAGAAGAAATGGGTGCGGGAGTA-3′	5′-CAAGAAGCAGTAGGAAAGTTTGCATG-3′	NM_001003010
CXCL10	5′-TCCTGCAAGTCCATCGTGTC-3′	5′-ATTGCTTTCACTAAACTCTTGATGGTC-3′	NM_001010949
CXCL8	5′-GACAGTGGCCCACAATGTGAAAACTC-3′	5′-GTTGTTTCACGGATCTTGTTTCTCAGC-3′	NM_001003200
IL1β	5′-GGAAATGTGAAGTGCTGCTGCCAA-3′	5′-GCAGGGCTTCTTCAGCTTCTCCAA-3′	NM_001037971

a reference gene. The relative expression levels were compared to the results of the control cells to determine expression $\log_2$ (fold change) for each gene.

Statistical Analysis

Statistical significance of internalization was analyzed by using the Student's *t*-test or repeated measures ANOVA using Graphpad Prism version 7.00 (Graphpad Software, San Diego, CA, USA, https://www.graphpad.com). All genes were considered to be differentially regulated when the value was $p < 0.05$. In the case where the difference was found to be significant, the fold change value was expressed as the control condition and it is mentioned as follows: fold change = the mean ratio of gene expression in the bacteria-treated cells/the mean ratio of gene expression in the DPBS-treated cells.

RESULTS

Invasion Assay

The invasibility of the *B. canis* was evaluated *in vitro* using the DH82 cell line. It has been confirmed that intracellular bacteria increase over time (**Supplementary Figure 1**). These results suggest that the changes of gene expression in the DH82 cell line were caused by *B. canis,* not by other external causes. Also, the results indicate that intracellular *B. canis* might induce immune responses in the host cells through the intracellular survival of the bacterium.

Differentially Expressed Genes

Each gene was analyzed for a change in the expression through the fold change value compared to 0 h. By stimulating cells with *B. canis*, DEGs with changes higher than 2-fold in the coculture model were 191, 634, and 2,112 at 2, 12, and 24 h, respectively, while DEGs in the single cell line culture model were identified as 515, 1,314, and 2,658 at different time points, respectively. The number of genes with altered expression in the single cell line culture model was higher than the coculture model. The results were compared with the two models in each time period and compared with respect to each model time period. About 87 and 267 DEGs were commonly identified at all-time points in the coculture and single cell line culture model, respectively. In comparison of the two models at the same time point, 137, 301, and 1,664 DEGs were commonly identified in 2, 12, and 24 h, respectively (**Figure 1**). From 2 or more samples, 30 genes were selected from the highest alternation in gene expression at each time period and each culture model. In five or more samples, 17 DEGs (ACOD1, CCL3L3, CCL4, CCL5, CXCL5, CXCL8, CXCL10, FST, GPR84, IL1A, IL1B, IL6, IL23A, OLR1, PTGS2, RASSF6, and SAA1) were upregulated, three DEGs (CACNA2D1, FHIT, and TSHZ2) were upregulated only in the coculture models, and six DEGs (FCRL2, INHBA, MMP3, MMP10, MMP13, SERPINB2, and SMPDL3A) were upregulated only in the single cell line culture models. Two DEGs (TNFAIP2 and STEAP4) were upregulated at the 2-h results in both the culture models, and three DEGs (SRGN, OSM, and F3) were upregulated at the 24-h results in both the culture models (**Table 2**). In four or more samples, nine DEGs (ADGRF1, CD180, FGFR2, FMN2, HUNK, MRVI1, SERTAD4, SLC27A6, and TRPM2) were found to be downregulated. The expression of five DEGs (ANKRD66, MLLT11, SORBS2, TMEM273, and WDR31) was downregulated only in the coculture models, and the two DEGs (CAVIN1 and TRIM72) were downregulated in the single cell line culture models. Only one DEG (SIRPB1) showed a downregulated expression only in the 2-h results of both the culture models, and the three DEGs (FZD1, PADI4, and SYPL2) showed a downregulated expression only in the 24-h results of both the culture models (**Table 3**).

Raw files and normalized data sets are available from the Gene Expression Omnibus (GEO) https://www.ncbi.nlm.nih.gov/geo under the accession number GSE134331 (https://www.ncbi.nlm.nih.gov/geo/query/acc.cgi?acc=GSE134331).

Canonical Pathway Analysis

Of all DEGs that mapped to the Ingenuity Knowledge Base and passed the data set filter (*p*-value), 191, 634, 2,112, 515, 1,314, and 2,658 DEGs of the DH82 cells treated with *B. canis* at 2, 12, and 24 h and each culture model, respectively, were analyzed. All DEGs were used in a core analysis, which was carried out by using Ingenuity® Pathways Analysis (IPA, Ingenuity Systems, https://www.ingenuity.com). Canonical pathways were identified for the DEGs of the DH82 cells treated with *B. canis* at each time point and each culture model. The canonical pathway was analyzed for each time period and each culture model, and was compared with the same time period of different culture models using a comparative analysis according to the passage of time for each model. In most cases, immunity-related pathways were predominantly identified (**Table 4**).

Signaling related to dendritic cell maturation, which is involved in the host innate immunity, was generally high in all models (**Figure 2**, **Supplementary Figures 2**, **3**). Overall, the signaling of dendritic cell maturation was found to be higher with *z*-score values of 3.742, 2.714, and 4.564 in the 2-, 12-,

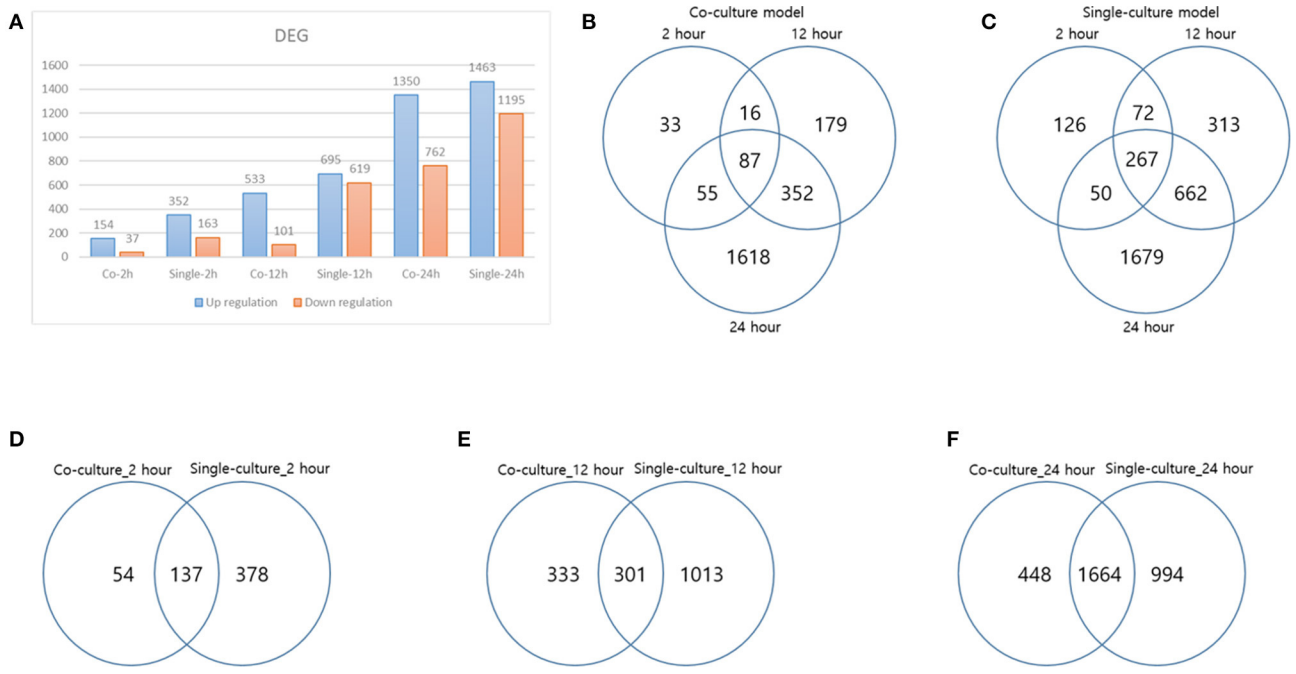

FIGURE 1 | Differentially expressed genes (DEGs) result. **(A)** DEG result over each time of each model, **(B)** DEG distribution over time in a coculture model, **(C)** DEG distribution over time in a single-culture model, **(D)** DEG comparison of each model at 2 h, **(E)** DEG comparison of each model at 12 h, and **(F)** DEG comparison of each model at 24 h.

and 24-h results in the coculture models. In the single cell line models, the *z*-score values were determined as high as 4.359, 4.041, and 4.333 at 2-, 12-, and 24-h results. In the coculture model, the *z*-score value shows a tendency to increase the expression with respect to the time, but in the single cell line culture model, the *z*-score value is maintained at a high value regardless of the time. The increase in expression with respect to the time in this canonical pathway, especially in the Fc gamma receptor- (FcγR-) associated pathways, was evident in the coculture model. The expression of DEGs associated with CD40, MYD88, Toll-like receptor (TLR), IL-1, TNF-α, and TNF-β associated with this pathway was found to be increased. In addition, TLR signaling, which is closely related to dendritic cell maturation and plays an important role in antigen presentation, has also been shown to increase expression at all-time points.

In both the models, the expression of TLR signaling was observed to increase with time, and the expression was more pronounced in the single cell culture model (**Figure 3**, **Supplementary Figures 4, 5**). In the coculture model, the *z*-scores of 2, 12, and 24 h were measured as 1.663, 2.121, and 2.668 and gradually increased with time period. In the single cell line model, the *z*-scores of the 2-, 12-, and 24-h results were 2.333, 2.887, and 2.887, respectively, which were higher than those of the coculture model. A distinct change in the gene expression was observed in the TRAP6-related pathway, and the coculture model confirmed that the expression of the related genes was gradually increasing. On the other hand, in the single cell line culture model, it was found that the expression of the TRAF6-related pathway decreased in 24 h. However, the trend of increasing expression with time period was found to be similar. This pathway shows that the stimuli of the pathogen induce the expression of pro-inflammatory cytokines in the host. DEGs associated with TLR, MYD88, TRAF6, IL-1, TNF-α, and NF-κB pathwyas were identified. TREM1 signaling, which is related to the TLR and closely related to the host immune response to the pathogen, has also been shown to increase the expression.

TREM1 signaling, similar to the other pathways, was found to increase gradually over time in both the models, especially in the 24-h results of the coculture model (**Figure 4**, **Supplementary Figures 6, 7**). In the coculture model, the *z*-score values were 3.207, 3.606, and 5.112 at 2, 12, and 24 h, and increased with time. In addition, the *z*-score value was largely measured at the 24-h result. In the single-culture model, *z*-score values were measured as 3.771, 3.578, and 4.315 at 2, 12, and 24 h, respectively. Both the models have been identified in this pathway, particularly on the pathways of TREM1 signaling with an association to TLR, increasing over time. This result, similar to that observed with the coculture model, showed a tendency to increase over time, but was found to be a more gentle trend. The TREM1-associated pathway has also been activated to induce the expression of pro-inflammatory cytokines, similar to the TLR signaling pathway. An increased expression of DEGs, such as TREM1, TLR, IL-8, TNF-α, and DAP12 associated with this pathway was found.

In the comparison analysis, the 2-h results of both the culture models identified the pathways that are closely related to the cell immune responses, such as dendritic cell maturation,

TABLE 2 | Differentially expressed genes (DEGs) identified for each model and each time.

Gene symbol	Fold changes in coculture model			Fold changes in single-culture model		
	2 h	12 h	24 h	2 h	12 h	24 h
FHIT	89.264	83.286	86.223	–	–	–
ACOD1	64.445	18.126	53.446	156.498	71.012	–
CXCL10	55.330	26.723	–	168.897	95.010	–
CCL4	45.887	13.642	410.148	149.086	184.823	302.334
OLR1	33.128	28.840	270.597	49.522	36.504	57.282
FFAR2	29.243	9.646	88.035	99.044	–	–
CCL5	22.943	18.636	63.119	63.558	81.572	85.627
SAA1	22.471	28.051	198.088	95.010	436.549	826.001
CCL3L3	20.393	22.316	719.076	60.969	286.026	588.134
IL1A	19.427	13.454	704.277	84.449	337.794	608.874
SAA1	17.388	21.407	116.970	74.028	328.557	481.036
NEURL3	16.679	13.086	54.569	27.284	–	–
IL1B	16.679	13.929	1002.926	77.708	1351.176	1144.102
SAA1	16.223	24.251	116.970	86.223	354.588	398.932
IL6	14.026	12.126	202.251	54.569	421.679	471.136
CXCL8	12.295	–	89.884	34.060	138.141	181.019
GPR84	12.042	10.556	88.035	19.562	52.346	–
FST	10.056	–	–	25.634	43.111	–
CXCL5	8.456	10.483	97.681	16.450	174.853	138.141
TNFAIP2	7.516	–	–	19.293	–	–
STEAP4	7.062	–	–	23.425	–	–
RASSF6	6.409	–	–	18.126	45.887	–
PTGS2	6.320	–	272.479	21.857	95.670	396.177
IL1RN	5.242	–	58.081	17.030	–	–
EGLN3	–	25.813	110.661	−3.182	–	108.383
TSHZ2	–	7.621	56.493	–	–	–
IL23A	–	–	1009.902	29.041	76.639	1418.352
SRGN	–	–	91.139	–	–	56.103
OSM	–	–	88.035	–	–	237.207
F3	–	–	48.840	–	–	75.061
LIF	–	–	48.503	–	38.586	–
INHBA	–	–	–	–	134.364	240.518
MMP3	–	–	–	–	54.569	247.280
MMP13	–	–	–	–	44.324	83.865
MMP10	–	–	–	–	38.854	168.897
FCRL2	–	–	–	–	36.252	64.000
SMPDL3A	–	–	–	–	33.359	53.446
SERPINB2	–	–	–	–	31.341	59.714

The main DEGs in which upregulation occurred in each experiment.

TABLE 3 | DEGs identified for each model and each time.

Gene symbol	Fold changes in coculture model			Fold changes in single-culture model		
	2 h	12 h	24 h	2 h	12 h	24 h
SIRPB1	−4.823			−10.126		
HTR1D	−2.657	−5.464	−19.293		−27.096	
MLLT11	−2.297	−3.506				
SORBS2	−2.219	−5.856				
TMEM273	−2.189					–
GRIA4	−2.144	−3.605				
ADGRD1		−4.724			−6.727	
ANKRD66		−4.347	−7.062			
MRVI1		−4.141	−9.849			−12.381
WDR31		−4.000	−11.158			
FMN2		−3.580	−9.254			−17.388
LGR6		−3.531		−3.294	−8.340	
FGFR2		−3.506	−18.507			−12.126
DHRS3		−3.387		−3.227	−9.448	
SLC27A6		−3.053	−9.254			−12.817
SERTAD4			−33.359		−7.516	−49.867
ADGRF1			−26.909		−7.516	−170.072
FZD1			−15.562			−15.032
CD180			−13.929		−19.973	−38.055
SMAD6			−12.906		−6.916	
SYPL2			−11.876			−13.929
HUNK			−11.392		−6.964	−16.679
TRPM2			−10.411		−8.515	−24.761
PADI4			−10.267			−12.729
RAB36			−7.210		−7.413	
NIPAL1			−7.013		−10.339	
CAVIN1				−3.160	−6.964	
TRIM72					−7.210	−40.224

The main DEGs in which downregulation occurred in each experiment.

HMGB1 signaling, TREM1 signaling, IL-1 signaling, acute-phase response, the role of pattern recognition receptors (PRRs) in the recognition of bacteria and viruses, B-cell receptor signaling, and the IL-8 signaling pathway. Gene expression related to a communication between the innate and the adaptive immune cell was confirmed. At the 2- and 12-h time points of the early infection stage, the expression of acute-phase response signaling was high. The 12-h and the 24-h culture model also showed similar results to the 2-h culture model, but in the case of TNFR2 signaling, a differential regulation of the cytokine production in macrophage and T-helper cells by IL-17A and an acute-phase response, the 24-h model showed no high expression. In each model, the expression of canonical pathways with respect to time was commonly observed. In a single-culture model, the expression of genes associated with an acute-phase response was identified at all-time points. In the coculture model, the expression of genes was confirmed up to 12 h, but no expression was observed in the 24-h result. Most of the results showed the expression of the osteoarthritis pathway and neuroinflammation signaling pathway among the pathways that are not related to the cell immune response (**Figure 5**).

Changes in various DEGs related to dendritic cell maturation were identified. In FcγR, a difference in the expression was clearly observed according to the model. In the coculture model, the expression of FcγR was inhibited at the 2-h time point, but the expression was increased at 12- and 24-h time

TABLE 4 | Major canonical pathways related to immune response.

Pathway	Coculture model						Single cell culture model					
	2 h		12 h		24 h		2 h		12 h		24 h	
	p-value	*z*-score	*p*-value	*z*-score	*p*-value	*z*-score	*p*-value	*z*-score	*p*-value	*z*-score	*p*-value	*z*-score
Communication between adaptive immune cells and innate immune cells	1.10E-15	NaN	4.74E-11	NaN	1.17E-09	NaN	1.98E-11	NaN	3.52E-08	NaN	7.77E-07	NaN
Acute phase responses	5.49E-08	2.714	2.15E-04	3.317	5.77E-06	2.828	2.76E-10	2.683	1.87E-09	2.556	3.69E-04	2.828
Dendritic cell maturation	2.64E-12	3.742	1.61E-03	2.714	1.07E-06	4.564	5.82E-09	4.359	1.59E-07	4.041	1.86E-05	4.333
Toll-like receptor signaling	1.02E-09	1.633	1.56E-06	2.121	3.38E-09	2.668	2.30E-09	2.333	7.04E-08	2.887	1.79E-04	2.887
TREM1 signaling	1.18E-15	3.207	9.47E-08	3.606	3.83E-13	5.112	3.35E-14	3.771	3.42E-09	3.578	8.24E-08	4.315
Role of pattern of recognition receptors of bacteria and viruses	4.03E-10	2.828	2.48E-11	2.887	1.65E-12	3.838	9.08E-09	2.530	3.81E-12	2.500	8.01E-11	3.000
NF-κB signaling	4.44E-10	2.138	1.37E-05	2.500	4.08E-12	2.480	7.09E-09	1.147	3.83E-12	2.000	2.69E-07	3.429
IL-6 signaling	9.64E-10	3.464	2.68E-04	3.317	1.55E-08	4.352	1.72E-12	4.025	1.62E-12	3.772	1.04E-05	4.596
Role of cytokines in mediating communication between immune cells	1.41E-08	NaN	1.47E-05	NaN	8.89E-03	NaN	2.99E-06	NaN	2.05E-04	NaN	1.86E-02	NaN
HMGB1 signaling	9.79E-11	3.464	6.58E-07	3.606	6.45E-09	3.528	2.08E-11	3.638	8.80E-14	3.286	3.20E-06	3.528

List of canonical pathways organized according to z-score and p-value. Pathway with z-score value NaN means the pathway that has not been identified in the data contained within the IPA program but has been significantly expressed through p-value in the results of this study.

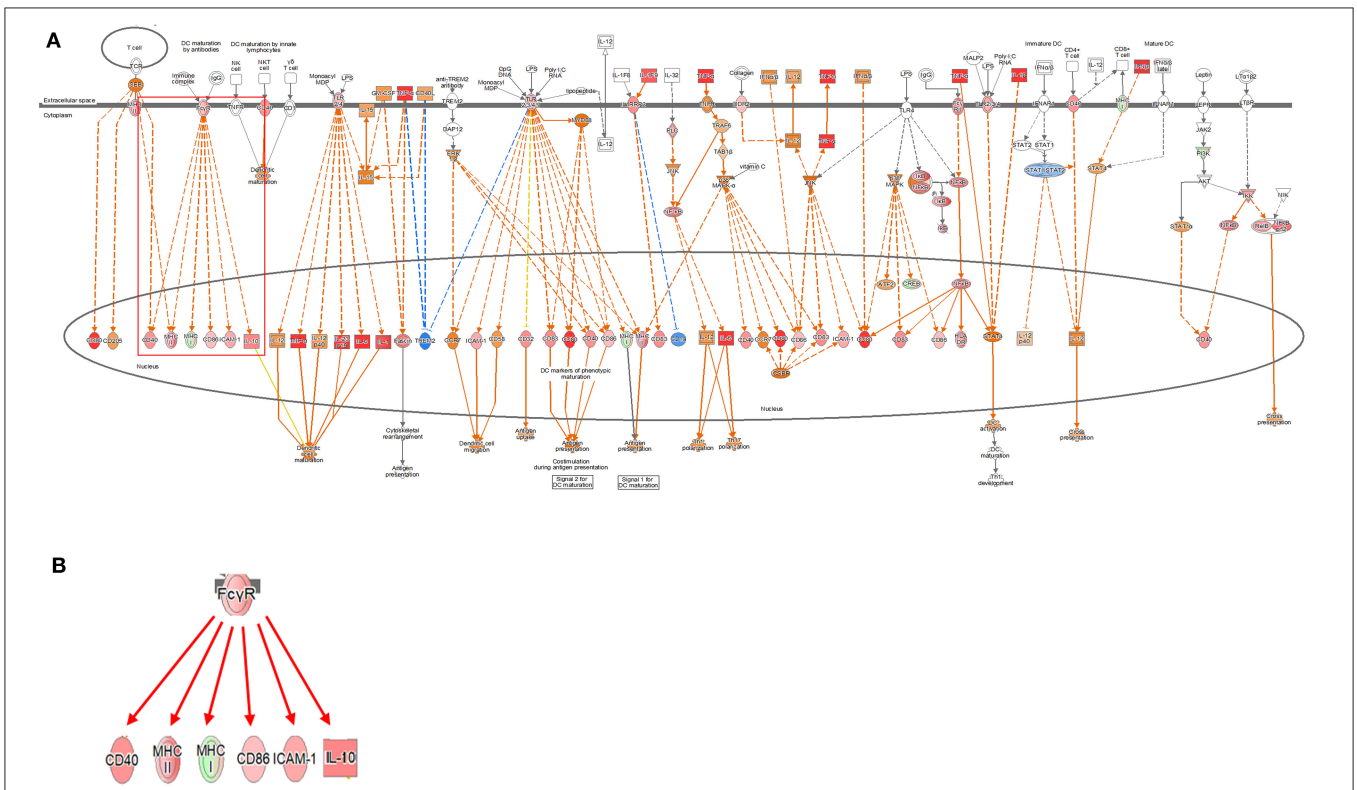

FIGURE 2 | Ingenuity pathway analysis of the dendritic cell maturation signaling pathway in the DH82 cell line treated with *Brucella canis*. **(A)** Dendritic cell maturation pathway in a 24 h on coculture model **(B)** Fc gamma receptor- (FcγR-) associated pathway on dendritic cell maturation pathway, **(B)** is enlarged from a rectangle of **(A)**. Genes with upregulation are shown in red, and genes with downregulation are shown in green. Orange indicates predicted activated genes, blue indicates predicted inhibited genes, and an uncolored node indicates that the genes were not differentially expressed in this pathway. The IPAs were produced using QIAGEN's IPA (https://www.qiagenbioinformatics.com/products/ingenuity-pathway-analysis). The increase in expression over time in this canonical pathway, especially in the FcγR-associated pathways, was evident in the coculture model.

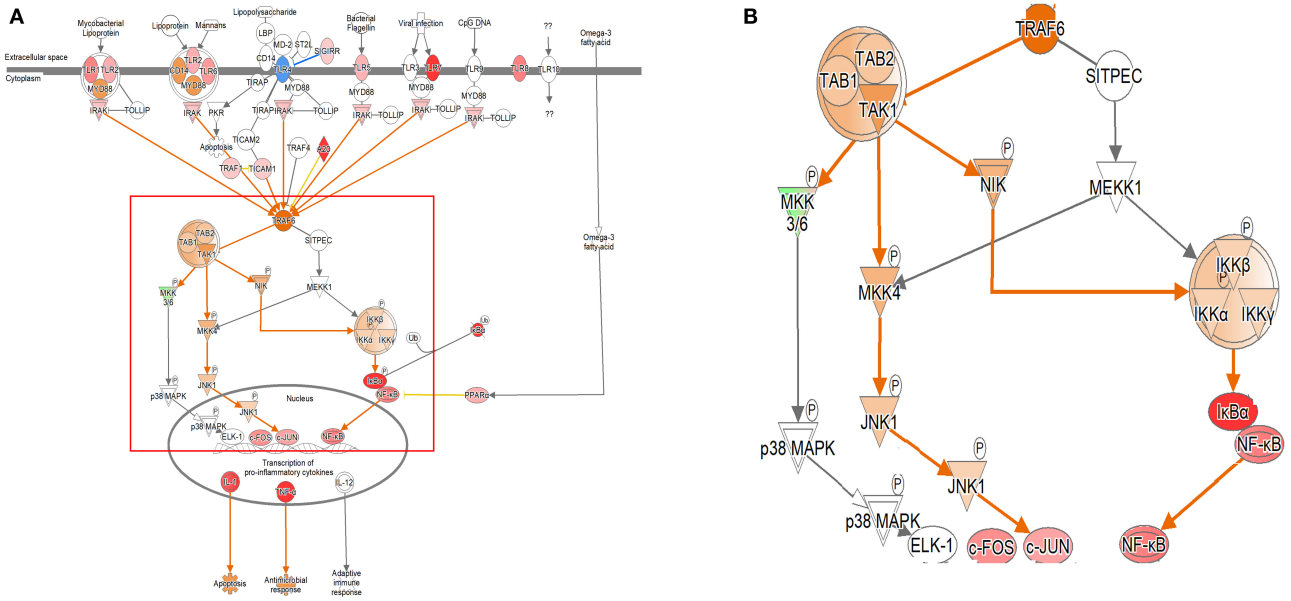

FIGURE 3 | Ingenuity pathway analysis of the Toll-like receptor (TLR) signaling pathway in the DH82 cell line treated with *B. canis*. **(A)** TLR signaling pathway in 24 h on coculture model, **(B)** TRAF6-associated pathway on TLR signaling pathway, **(B)** is enlarged from a rectangle of **(A)** genes with upregulation are shown in red, and genes with downregulation are shown in green. Orange indicates the predicted activated genes, blue indicates the predicted inhibited genes, and an uncolored node indicates that the genes were not differentially expressed in this pathway. The IPAs were produced using QIAGEN's IPA (https://www.qiagenbioinformatics.com/products/ingenuity-pathway-analysis). A distinct change in gene expression was observed in the TRAP6-related pathway, and the coculture model confirmed that the expression of the related genes was increasing gradually.

points. This finding is observed because the expression of two DEGs, except for FCGR1A, among FCGR1A, FCGR2B, and FCGR3A, which are related to FcγR and exhibit expression, is reduced (fold change value, FCGR1A: 1.240, FCGR2B:−2.099, and FCGR3A:−1.257). In contrast, in the single cell line culture model, the expression of FcγR increased at the 2-h result, but it was difficult to determine the expression pattern at 12- and 24-h results. This difficulty was due to the increase in FCGR1A at 2 h, but an increase in FCGR1A but a decrease in FCGR2B at 12 h (fold change value at 2 h, FCGR1A: 1.828, fold change values at 12 h, FCGR1A: 3.411, FCGR2B: −2.888). The 24-h results of the single cell line culture model were similar to the 12-h results, but the expression of FCGR1A increased but the expression of FCGR2B decreased (fold change value at 24 h, FCGR1A: 4.993, FCGR2B: −4.627).

Among the TREM1 signaling pathways, differences in pathways related to phagocytosis and apoptosis in the host were found. The 2-h results in the coculture model did not confirm the expression of TREM1- and TLR-related genes in relation to DEGs. However, at 12 h, the expression increased as the expression of TLR-related DEGs was confirmed. At 24 h, the expression of the pathway increased significantly, as the expression of not only TLR-related DEGs but also TREM1 increased. In the single cell culture model, the expression of TLR-related DEGs in the pathway associated with phagocytosis and apoptosis decreased by 2 h. However, as TLR-related DEGs increased at 12 and 24 h, the expression of related pathways also increased significantly.

In the case of TLR signaling, the differences were observed depending on the model. In the coculture model, the expression was reduced in the center of the TRAP6 gene for the 2- and 12-h results. However, the 24-h results showed an overall increase in the expression. When looking at the pattern over time, it was confirmed that the expression of TLR-associated DEGs gradually increased. The expression of TLR-related DEGs was not confirmed in the 2-h results, but the expression of TLR-related DEGs was confirmed in the subsequent results. The fold change values of TLR 1, 2, 3, 4, 6, 7, and 8 DEGs at 12 h were 1.602, 1.329, 3.531, 1.257, 1.474, 8.877, and 2.585, respectively. The expression of TLR 1, 2, 4, 5, 6, 7, and 8 DEGs was confirmed at 24 h, and the fold change values were 5.278, 2.990, 1.580, 2.751, 3.864, 42.224, and 5.426. All expression levels of TLR-related DEGs, which are commonly expressed, increased over time. In the single cell line culture model, TLR signaling was found to have an overall increase. When fold change values were confirmed at the genetic level, it was confirmed that the 2-h result was downregulated in some TLR-related DEGs (fold change values, TLR 1: −1.753, TLR 2: −1.301, TLR 4: 1.301, TLR 6: −2.395, and TLR 8: 1.347). The fold change values of DEGs increased over the 12-h period. The fold change value of TLR 2, TLR 7, and TLR 8 was 2.250, 22.785, and 3.272, respectively. The expression of more diverse TLR-related DEGs was observed to increase at 24 h. The expression of the TLR 1, 2, 4, 6, 7, and 8 DEGs was increased, and the fold change value of each was 4.141, 2.732, 1.223, 2.329, 29.651, and 4.563, respectively.

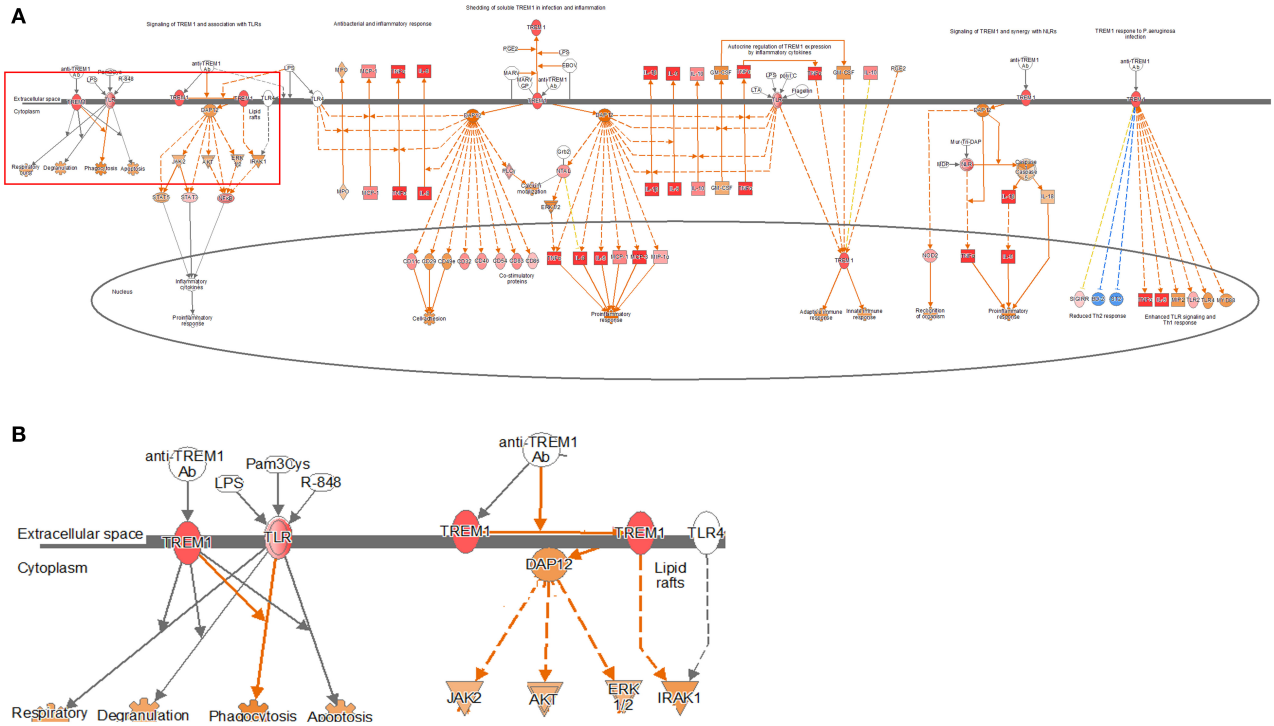

FIGURE 4 | Ingenuity pathway analysis of the TREM1 signaling pathway in the DH82 cell line treated with *B. canis*. **(A)** TREM1 signaling pathway in 24 h on coculture model, **(B)** TREM1 and TLR-associated pathway on TREM1 signaling pathway, **(B)** is enlarged from rectangle of **(A)** genes with upregulation are shown in red, and genes with downregulation are shown in green. Orange indicates the predicted activated genes, blue indicates the predicted inhibited genes, and an uncolored node indicates that the genes were not differentially expressed in this pathway. The IPAs were produced using QIAGEN's IPA (https://www.qiagenbioinformatics.com/products/ingenuity-pathway-analysis). Both the models have been identified in this pathway, particularly on the pathways of TREM1 signaling with association to TLR, increasing over time.

In addition, the expression of the "role of macrophages, fibroblast, and endothelial cells in rheumatoid arthritis," "role of osteoblasts, osteoclasts, and chondrocytes in rheumatoid arthritis," and the "neuroinflammation signaling pathway" associated with arthritis and neurological symptoms caused by the known *Brucella* species has been also observed (24, 30–33).

Validation of RNA-Sequencing Results by Using Quantitative Real-Time PCR

The RNA-seq results were verified following a qRT-PCR with samples from the two different experiments. The results of the five selected genes from the two analytic methods were highly correlated (**Figure 6**).

DISCUSSION

In this study, gene expressions were analyzed in the DH82 cell line treated with *B. canis* in the coculture model and the single cell line culture model. Most of the various signaling pathways identified as a result of DEGs were related to the host immune response. These pathways were commonly identified in the two models, and the degree of differences in the amount of expression in the related genes was identified. In particular, the expression of genes such as *CCL4, CCL5, CCL3L3, IL1A, IL1B,* and *SAA1* has been found to increase significantly in both the models in common. Genes such as *CCL4*, *CCL5,* and *CCL3L3* are all closely related to the activation of NF-κB, which is involved in the expression of cytokines related to the immune response. They are secreted by macrophages and play an important role in pro-inflammatory cytokines (34, 35). *SAA1* is a gene associated with serum amyloid A (SAA), an acute-phase protein, and is known to play a role in inflammatory reaction (36). This increase in the gene expression can be predicted to induce an early immune response from the host. Among the results, the expression of signaling pathways related to "adaptive immunity" was clearly observed. In particular, the signaling pathways related to IL-6, TLR, NF-κB, and TNFR2 signaling, which are related to dendritic cell maturation, were also markedly changed. The changes in DEGs related to immune response mechanisms associated with "cellular immune response" were also identified. In addition to HMGB1 signaling, these changes were also associated with the IL-6, NF-κB, IL-1α, IL-1β, and TNF-α signaling pathways. In addition, the expression of the innate immunity pathways that recognize and present antigens, such as pathogens, includes dendritic cell maturation, PRR signaling, and TLR signaling.

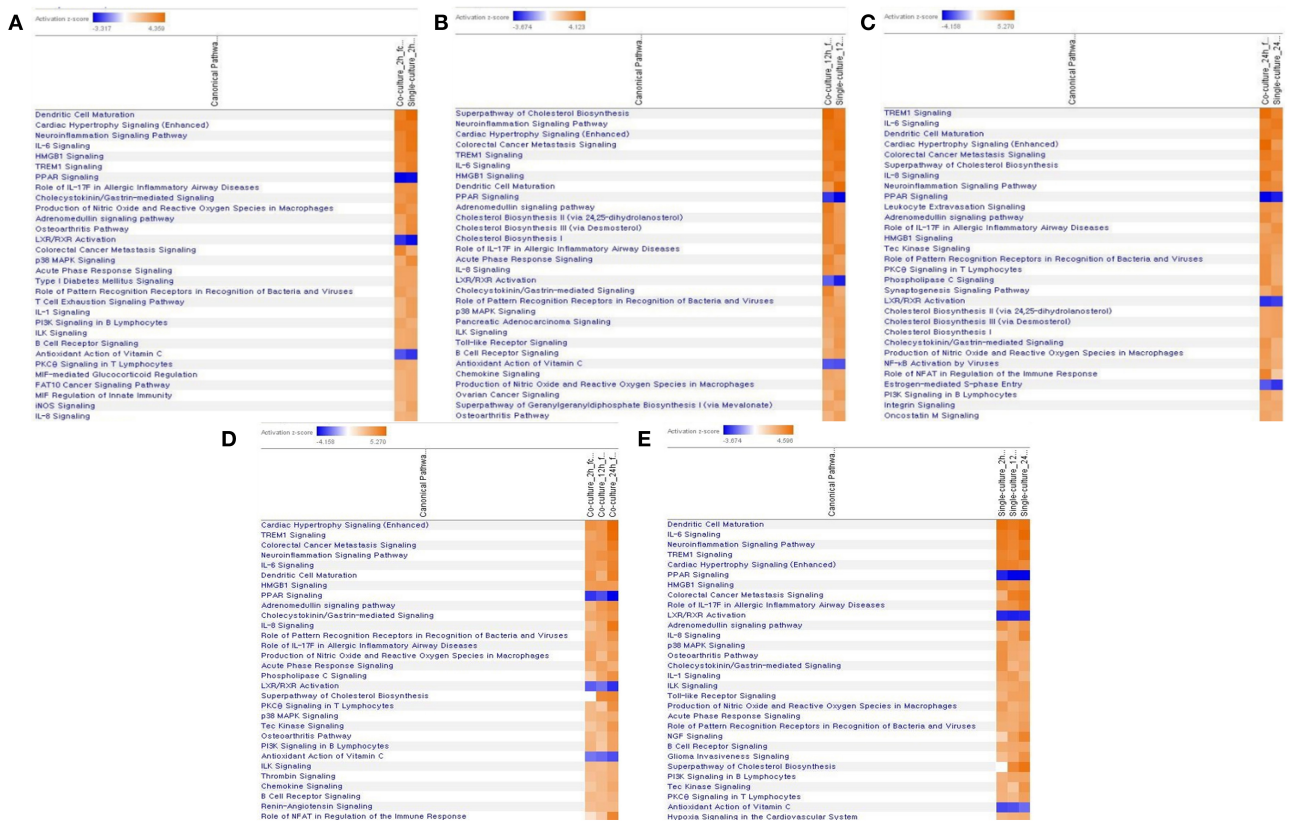

FIGURE 5 | Comparative analysis of canonical pathway by each model and time period by *z*-score value. **(A)** In a 2-h top 30 canonical pathway comparison analysis of each model, **(B)** in a 12-h top 30 canonical pathway comparison analysis of each model, **(C)** in a 24-h top 30 canonical pathway comparison analysis of each model, **(D)** comparative analysis of the canonical pathway over time in a coculture model, **(E)** comparative analysis of the canonical pathway over time in a single-culture model.

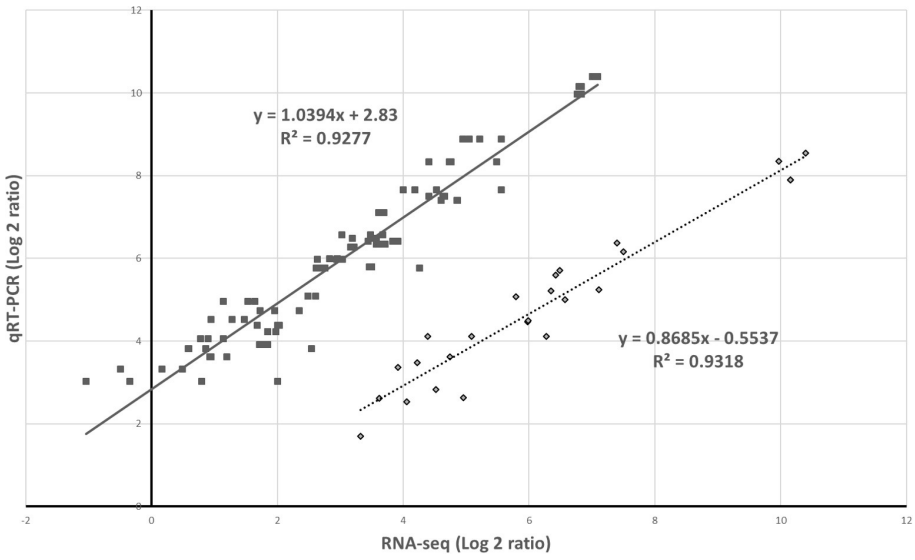

FIGURE 6 | Validation of gene expression by RNA-sequencing (RNA-seq) and quantitative real-time PCR. The relative expression was compared to that observed in the controls to determine the fold change in the expression for each gene. This indicates the two independent experiments.

In the aforementioned pathways, the expression of pathways, such as "communication between the innate and the adaptive immune cell," has been confirmed based on the same pathway, which suggests that the host immune mechanism is closely related to the innate immunity and the activity of the adaptive immunity following pathogen invasion. It can be observed that signaling related to acute-phase response is clearly expressed at 2 and 12 h in both the models by a comparison analysis. This finding suggests that *B. canis* usually develops chronically, but when the infection actually occurs, the host immune response is clear. The role of PRRs in the recognition of bacteria was also confirmed through the activity of TLR signaling in the cell membrane and NF-κB signaling, which induces pro-inflammatory cytokines.

In addition, this effect is known to be closely related to TREM1 signaling. TREM1 signaling is associated with pro-inflammatory cytokine activation. TREM1 activation triggers signals such as JAK2 and STAT3 and affects signals, such as NF-κB. TREM1 signaling is closely related to TLR signaling, and the synergy of the two produces neutrophil degranulation, phagocytosis, and the respiratory burst but also produces pro-inflammatory cytokines (37–39).

Dendritic cells are among the most efficient antigen-presenting cells (APCs) of the immune response system. Immature dendritic cells are responsible for capturing and processing antigens and for presenting major histocompatibility complex (MHC)-specific antigens in secondary lymphoid organs. After antigen capture, dendritic cells mature, antigen capture capacity is downregulated, and costimulatory molecules and MHC class I and II molecules are upregulated to enhance the antigen presentation. Matured dendritic cells have the ability to produce the cytokines that can enhance the innate and the adaptive immune response and have the ability to cross exogenous antigens to cytotoxic lymphocytes (40). In most APCs, peptides derived from exogenous antigens introduced from the extracellular environment are preferentially present in CD4+ T cells in MHC class II molecules. However, the antigens that are internalized in dendritic cells are also present in CD8+ T cells through a cross-presentation (41). The interaction between the peptide-loaded MHC class I molecules and the T-cell receptor alone is not sufficient to initiate the T-cell response. Therefore, an induction of CD8+ T-cell responses *in vivo* by antigens internalized by dendritic cells is achieved. Additional signaling of costimulatory molecules and cytokines is also essential for the development of effective T-cell responses. The pathogen is detected through a pattern of recognition receptors such as TLRs, present on dendritic cells, and activated TLRs trigger the mitogen-activated protein kinase (MAPK) pathway to induce the activation of transcription factors such as NF-κB (42, 43). This effect increases the expression of costimulatory molecules, including CD40 and CD80, and promotes the release of various inflammatory cytokines and chemokines (44). The FcγR of dendritic cell maturation pathway is closely related to the phagocytosis of microbes and is associated with a combination of the IgG molecule.

In many situations, dendritic cells are simultaneously stimulated by antigens and danger signals. This stimulation occurs, the release of the TLR ligand occurs and the innate sensor is associated with the endosomes and phagocytosis. In fact, the expression of various TLR DEGs was increased in the dendritic cell maturation signaling pathway identified in this study, and the expression of CD40 and MAPK pathways was increased. Changes in various DEGs related to dendritic cell maturation were identified. The expression of DEGs for related cytokines, such as IL-1, IL-6, IL-10, and IL-12, was found to be increasing in all the results, which induced dendritic cell maturation. FcγR is commonly known to be associated with the activation of dendritic cells, and this study has identified the expression of MHC I, II, and CD40 with the actual expression of FcγR (45). This result may be evident that dendritic cell maturation plays an important role in early *B. canis* infection and induces the host immune response. However, previous reports on *Brucella abortus* or *B. melitensis* suggested the suppression of host dendritic cell maturation signaling by the stimulation of *Brucella* spp. (46, 47). Those disagree with our results showing the activation of the dendritic cell maturation signaling. The disagreement might be due to a difference in structural components of the bacterium, which is used in each experiment. Opposite direction of the expression of the signaling could be related to the different chemical inducers of cell components because they used a smooth form of *Brucella* spp. (46, 47). However, the reality of the difference should be revealed in future studies.

TREM1, a triggering receptor expressed on myeloid cell 1, is an activation receptor expressed on myeloid cells included in the Ig superfamily (48). TREM1 plays an important regulatory role in the innate immune response, and early research has focused primarily on the role of TREM1 in lipopolysaccharide-induced sepsis (49). This gene is known to be induced at high levels in neutrophils, monocytes, and macrophages, which intensify the secretion of pro-inflammatory cytokines and chemokines in response to bacterial infections, further amplifying the TLR initiation response to microorganisms (49, 50). The effects of TREM1 signal transduction on microbial control are controversial. Infections with *Leishmania major* or influenza virus did not affect removal but were known to have been effective in *Klebsiella pneumonia* and *Pseudomonas aeruginosa* clearance (51, 52). Especially in the case of infection with *P. aeruginosa*, TREM1 contributed to this through mechanisms involved in the migration of neutrophils for the removal of pathogens (53). In addition, animal experiments confirmed that the mortality of Gram-positive or Gram-negative bacteria-infected TREM-1/3-deficient mice was significantly increased compared to wild-type mice (53, 54). In the TREM1 signaling pathway, DAP12 plays an important role. DAP12 is responsible for inducing intracellular signaling within the TREM1 signaling pathway, leading to the production of chemokines and cytokines through the phosphorylation of DAP12 (55). In this study, the expression of TLR as well as DAP12 was confirmed with the expression of TREM1, and the associated genes were also identified, resulting in the activation of TREM1 signaling pathway. This finding shows that TREM1 signaling plays an important role in the innate immune response. However, to date, the study of TREM1 has not thoroughly elucidated whether this protein participates in and regulates innate immune responses against other pathogenic

microbial groups. In this study, the expression of TREM1 signaling exhibited high *z*-scores in all the models, and it was confirmed that the expression showed an overall increase with respect to time. The results of this study confirmed that the dendritic cell maturation and TLR signaling pathways were activated and TREM1 signaling was also activated. This finding may be the reason why there is a close association between the activation of TLR and TREM1 signaling. The expression of the IL-6 and IL-8 signaling pathways occurred, which may be closely related to the activation of TREM1 signaling.

The TLR family is a part of the widely studied PRR class. TLRs have been identified in 10 humans and 12 murines, which play a role in recognizing intracellular and extracellular pathogen-associated molecular patterns (PAMPs). TLRs 1, 2, 4, 5, 6, and 11 are expressed in cell membranes, and TLRs 3, 7, 8, and 9 are present in endosomes in cells (43, 56). These receptors are found in a broad range of cell types, such as dendritic cells, macrophages, NK cells, B cells, and T cells. TLR2 usually recognizes a wide range of microbial molecules, such as peptidoglycans, lipoproteins, and yeast polysaccharides (57). TLR4 recognizes LPS and several viral envelope proteins, and TLR5 plays a role in recognizing flagella, the pathogenic factor of motility bacteria (58, 59). TLR3, -7, -8, and -9 recognize nucleic acids produced in viruses and bacteria, and all TLRs achieve the recognition of endogenous ligands according to inflammatory and autoimmune diseases (43). The role of TLRs in *Brucella* infection has been studied in mouse models using *B. abortus, B. melitensis, Brucella ovis, and Brucella microti,* and is known to play a key role in immune function (60–63). TLR signaling is closely related to dendritic cell maturation and TREM1 signaling pathways.

The pathways characterized by a manifestation in major canonical pathways are mostly associated with pro-inflammatory cytokines, which are known to be associated with the early immune response of a host. These results show that the infection of *B. canis* induces the early immune response from a host and is linked to phagocytosis.

As dendritic cell maturation is performed, the TLR signaling expression is increased to play an antigen-presenting role. In this study, the expression of TLR signaling gradually increased as dendritic cell maturation increased in both models. In particular, TLR7 was found to change the fold change value up to 40 times, unlike other TLR-related DEGs. Recent studies on TLR3 and TLR7 have shown that they are involved in the detection of *Brucella* RNA by the host. The production of cytokines, such as IL-6, IL-12, and TNF-α, induced by *B. abortus* RNA is known to be TLR-dependent and occurs through the signaling of MAPK and NK-κB signaling (64). Furthermore, a previous study showed the increase in TLR2 and TNF-α as the host immune responses to the infection of *B. abortus* through the host immune response to pathogen infection (65). When infected with the other *Brucella* spp. infections, TLR2, 4, 5, and 9 were mainly expressed, and these were the main concerns (60, 61). TLR7 expression was significantly increased in our study with *B. canis*. Usually, TRAF6 is identified primarily in the signaling pathway *via* CD40, but it has been confirmed that the TLR stimulates the activation of the TRAF6 pathway, and in this study, the activation of the TRAF6 pathway also confirms the activation of IKK and NF-κB (66). The increase in the expression of TLR7 led to an increase in the expression of TRAF6, which in turn induced the expression of NF-κB. This translates the expression of pro-inflammatory cytokines. Our results suggested the importance of the role of TLR7 in the early stage of infection of *B. canis*. However, the role of TLR7 in the infection of *Brucella* spp. seem to be not completely recognized, yet even though the results of this study suggest that TLR7 plays an important role in the infection of *B. canis*.

As is well-known, *B. canis* infection is likely to be closely associated with TLR as the other *Brucella* species. In addition, the expression of pathways, such as dendritic cell maturation, acute-phase response signaling, and TREM1 signaling, associated with early immunity suggests that *B. canis* has been active in the host since early infection. Through these pathways, the expression of pro-inflammatory cytokines, such as TNF-α, IL-1, and IL-6 signaling, was confirmed. In this study, high expression patterns of the pathways that interact with innate immunity, such as dendritic cell maturation, TREM1, and TLR signaling, were identified. Dendritic cell maturation and TLR signaling provide an immune response to pathogen invasion into the host, as well as continuous antigen recognition, while dendritic cell maturation and TREM signaling complement each other to induce a more effective immune response. These effects are well-known to recognize pathogens in the host and play a very important role in the initial immune response.

Based on the RNA-seq analysis, the host immune response to the infection of *B. canis* was analyzed at the transcriptomic level. No significant differences were identified in the pathways expressed between the two models, but the differences were identified in the degree of genes expressed in the pathways. These results suggest that, although *Brucella* infections generally occur chronically, they respond to active host immune activity in the early stage of infection. This effect may be an important indicator of *B. canis* infection. Dendritic cell maturation and TREM1 signaling are all closely related to the TLR signaling, all of which are closely related to the host early immune response. In addition, dendritic cell maturation confirmed that the communication between the innate and the adaptive immunity to the infection is not only the innate immunity of the host immune response but also the promotion of the adaptive immunity and the achievement of the immune response.

By using the coculture model, a model similar to the *in vivo* environment through the interaction between the epithelial cells and the macrophage was established. Gene expressions at the transcriptomic level were similarly identified in the two models, but a difference was found in the amount of expression. Despite the same proportion of pathogens, this difference in expression level has been identified, possibly where a preemptive defense function may have been activated as the pathogen undergo an epithelial cell. It is thought to be the host defense system that minimizes the infection damage through the primary protection against the pathogen infection in epithelial cells. However, further research on the role of epithelial cells in the infection should be considered to reveal the underlining mechanism of these models.

The results of this study have been analyzed at the genetic level of the host immune response, free from the investigation of the host simple immune response, isolation, and epidemiology. High expression of pathways, such as dendritic cell maturation, TREM1 signaling, and TLR signaling, provided more specific evidence of the host early immune response to *B. canis* infection, and the changes in the gene expression contained in these pathways may be useful references for the early diagnosis of *B. canis*.

DATA AVAILABILITY STATEMENT

The datasets presented in this study can be found in online repositories. The names of the repository/repositories and accession number(s) can be found at: https://www.ncbi.nlm.nih.gov/geo/query/acc.cgi?acc=GSE134331, GSE134331.

ETHICS STATEMENT

All experiments were reviewed and approved by the Seoul National University Institutional Biosafety Committee (protocol: SNUIBC-R180912-3).

AUTHOR CONTRIBUTIONS

WP conceived and designed the experiments, data curation, formal analysis, software, and writing the original draft. SK data curation, formal analysis, and software. SS data curation and formal analysis. HY conceptualization, project administration, supervision, and writing—review and editing. All authors contributed to the article and approved the submitted version.

FUNDING

This study was carried out with the support of the Cooperative Research Program of Center for Companion Animal Research (Project No. PJ01398501) Rural Development Administration, Republic of Korea.

ACKNOWLEDGMENTS

The authors would like to thank the BK21 PLUS and the Veterinary Research Institute of the College of Veterinary Medicine, Seoul National University for their assistance in the research.

SUPPLEMENTARY MATERIAL

The Supplementary Material for this article can be found online at: https://www.frontiersin.org/articles/10.3389/fvets.2021.619759/full#supplementary-material

REFERENCES

1. Martirosyan A, Gorvel JP. Brucella evasion of adaptive immunity. *Future Microbiol*. (2013) 8:147–54. doi: 10.2217/fmb.12.140
2. Hollett RB. Canine brucellosis: outbreaks and compliance. *Theriogenology*. (2006) 66:575–87. doi: 10.1016/j.theriogenology.2006.04.011
3. Carmichael LE, Kenney RM. Canine abortion caused by *Brucella canis*. *J Am Vet Med Assoc*. (1968) 152:605–16.
4. Moore JA, Kakuk TJ. Male dogs naturally infected with *Brucella canis*. *J Am Vet Med Assoc*. (1969) 155:1352–8.
5. Carmichael LE, Joubert JC. Transmission of *Brucella canis* by contact exposure. *Cornell Vet*. (1988) 78:63–73.
6. Flores-Castro R, Suarez F, Ramirez-Pfeiffer C, Carmichael LE. Canine brucellosis: bacteriological and serological investigation of naturally infected dogs in Mexico City. *J Clin Microbiol*. (1977) 6:591–7.
7. Brower A, Okwumabua O, Massengill C, Muenks Q, Vanderloo P, Duster M, et al. Investigation of the spread of *Brucella canis* via the U. S. interstate dog trade. *Int J Infect Dis*. (2007) 11:454–8. doi: 10.1016/j.ijid.2006.12.009
8. Cadmus SIB, Adesokan HK, Ajala OO, Odetokun WO, Perrett LL, Stack JA. Seroprevalence of Brucella abortus and *B. canis* in household dogs in southwestern Nigeria: a preliminary report. *J S Afr Vet Assoc*. (2011) 82:56–7. doi: 10.4102/jsava.v82i1.35
9. de Paula Dreer MK, Gonçalves DD, da Silva Caetano IC, Gerônimo E, Menegas PH, Bergo D, et al. Toxoplasmosis, leptospirosis, and brucellosis in stray dogs housed at the shelter in Umuarama municipality, Paraná, Brazil. *J Venom Anim Toxins Incl Trop Dis*. (2013) 19:23. doi: 10.1186/1678-9199-19-23
10. Krueger WS, Lucero NE, Brower A, Heil GL, Gray GC. Evidence for unapparent *Brucella canis* infections among adults with occupational exposure to dogs. *Zoonoses Public Health*. (2014) 61:509–18. doi: 10.1111/zph.12102
11. Chinyoka S, Dhliwayo S, Marabini L, Dutlow K, Matope G, Pfukenyi DM. Serological survey of *Brucella canis* in dogs in urban harare and selected rural communities in Zimbabwe. *J S Afr Vet Assoc*. (2014) 85:e1–5. doi: 10.4102/jsava.v85i1.1087
12. Di D, Cui B, Wang H, Zhao H, Piao D, Tian L, et al. Genetic polymorphism characteristics of *Brucella canis* isolated in China. *PLoS ONE*. (2014) 9:e84862. doi: 10.1371/journal.pone.0084862
13. Yoak AJ, Reece JF, Gehrt SD, Hamilton IM. Disease control through fertility control: secondary benefits of animal birth control in Indian street dogs. *Prev Vet Med*. (2014) 113:152–6. doi: 10.1016/j.prevetmed.2013.09.005
14. Keid LB, Chiebao DP, Batinga MCA, Faita T, Diniz JA, Oliveira TMFS, et al. *Brucella canis* infection in dogs from commercial breeding kennels in Brazil. *Transbound Emerg Dis*. (2017) 64:691–7. doi: 10.1111/tbed.12632
15. Cosford KL. *Brucella canis*: an update on research and clinical management. *Can Vet J*. (2018) 59:74–81.
16. Taylor DJ, Peplinksi G, Spence S, Bruce C, Cedersmyg M, Hallgren G, et al. Serological evidence for the presence of *Brucella canis* infection in dogs in Britain. *Vet Rec*. (1980) 106:102–4. doi: 10.1136/vr.106.5.102
17. Corrente M, Franchini D, Decaro N, Greco G, D'Abramo M, Greco MF, et al. Detection of *Brucella canis* in a dog in Italy. *New Microbiol*. (2010) 33:337–41.
18. Morgan J,Wake T, Pintos V, Rys H, Grace K, Perret L, et al. *Brucella canis* in a dog in the UK. *Vet Rec*. (2017) 180:384–5. doi: 10.1136/vr.j1811
19. Jung J.-Y, Yoon S.-S, Lee S.-H, Park J.-W, Lee J.-J, Her M, et al. Prevalence state of canine brucellosis in South Korea during 2015 and 2016. *Korean J Vet Res*. (2018) 58:125–9. doi: 10.14405/kjvr.2018.58.3.125
20. Chacon-Diaz C, Altamirano-Silva P, Gonzalez-Espinoza G, Medina MC, Alfaro-Alarcon A, Bouza-Mora L, et al. *Brucella canis* is an intracellular pathogen that induces a lower proinflammatory response than smooth zoonotic counterparts. *Infect Immun*. (2015) 83:4861–70. doi: 10.1128/IAI.00995-15
21. Cannella AP, Tsolis RM, Liang L, Felgner PL, Saito M, Sette A, et al. Antigen-specific acquired immunity in human brucellosis: implications for

diagnosis, prognosis, and vaccine development. *Front Cell Infect*. (2012) 2:1. doi: 10.3389/fcimb.2012.00001
22. Pujol M, Castillo F, Alvarez C, Rojas C, Borie C, Ferreira A, et al. Variability in the response of canine and human dendritic cells stimulated with *Brucella canis*. *Vet Res*. (2017) 48:72. doi: 10.1186/s13567-017-0476-8
23. Trapnell C, Pachter L, Salzberg SL. TopHat: discovering splice junctions with RNA-Seq. *Bioinformatics*. (2009) 25:1105–11. doi: 10.1093/bioinformatics/btp120
24. Pujol M, Borie C, Montoya M, Ferreira A, Vernal R. *Brucella canis* induces canine CD4+ T cells multi-cytokine Th1/Th17 production *via* dendritic cell activation. *Comp Immunol Microbiol Infect Dis*. (2019) 62:68–75. doi: 10.1016/j.cimid.2018.11.017
25. Trapnell C, Williams BA, Pertea G, Mortazavi A, Kwan G, van Baren MJ, et al. Transcript assembly and quantification by RNA-Seq reveals unannotated transcripts and isoform switching during cell differentiation. *Nat Biotechnol*. (2010) 28:511–5. doi: 10.1038/nbt.1621
26. Trapnell C, Roberts A, Goff L, Pertea G, Kim D, Kelley DR, et al. Differential gene and transcript expression analysis of RNA-seq experiments with TopHat and Cufflinks. *Nat Protoc*. (2012) 7:562–78. doi: 10.1038/nprot.2012.016
27. Benjamini Y, Hochberg Y. Controlling the false discovery rate: a practical and powerful approach to multiple testing. *J R Stat Soc Series B Stat Methodol*. (1995) 57:289–300. doi: 10.1111/j.2517-6161.1995.tb02031.x
28. Fisher RA. On the interpretation of $\chi 2$ from contingency tables, the calculation of P. *J R Stat Soc*. (1922) 85:87–94. doi: 10.2307/2340521
29. Krämer, A, Green J, Pollard J Jr, Tuqendreich S. Causal analysis approaches in ingenuity pathway analysis. *Bioinformatics*. (2014) 30:523–30. doi: 10.1093/bioinformatics/btt703
30. Lacey CA, Keleher LL, Mitchell WJ, Brown CR, Skyberg JA. CXCR2 mediates brucella-induced arthritis in interferon γ-deficient mice. *J Infect Dis*. (2016) 214:151–60. doi: 10.1093/infdis/jiw087
31. Colmenero JD, Reguera JM, Fernandez-Nebro A, Cabrera-Franquelo F. Osteoarticular complications of brucellosis. *Ann Rheum Dis*. (1991) 50:23–6. doi: 10.1136/ard.50.1.23
32. Rajapakse CN. Bacterial infections: osteoarticular brucellosis. *Baillieres Clin Rheumatol*. (1991) 9:161–77. doi: 10.1016/S0950-3579(05)80153-0
33. Zheng N, Wang W, Zhang JT, Cao Y. Neurobrucellosis. *Int J Neurosci*. (2018) 128:55–62. doi: 10.1080/00207454.2017.1363747
34. Kawai T, Akira S. Signaling to NF-kappaB by toll-like receptors. *Trends Mol Med*. (2007) 13:460–9. doi: 10.1016/j.molmed.2007.09.002
35. Liou CJ, Huang YL, Huang WC, Yeh KW, Huang TY, Lin CF. Water extract of Helminthostachys zeylanica attenuates LPS-induced acute lung injury in mice by modulating NF-κB and MAPK pathways. *J Ethnophamacol*. (2017) 6:30–8. doi: 10.1016/j.jep.2017.01.043
36. Olsen HG, Skovgaard K, Nielsen OL, Leifsson PS, Jensen HE, Iburg T, et al. Organization and biology of the porcine serum amyloid A (SAA) gene cluster: isoform specific responses to bacterial infection. *PLoS ONE*. (2013) 8:e76695. doi: 10.1371/journal.pone.0076695
37. Nguyen-Lefebvre AT, Ajith A, Portik-Dobos V, Horuzsko DD, Arbab AS, Dzutsev A, et al. The innate immune receptor TREM-1 promotes liver injury and fibrosis. *J Clin Invest*. (2018) 128:4870–83. doi: 10.1172/JCI98156
38. Alflen A, Stadler N, Aranda Lopez P, Teschner D, Theobald M, Heß G, et al. Idelalisib impairs TREM-1 mediated neutrophil inflammatory responses. *Sci Rep*. (2018) 8:5558. doi: 10.1038/s41598-018-23808-2
39. Fan D, He X, Bian Y, Guo Q, Zhenq K, Zhao Y, et al. Triptolide modulates TREM-1 signal pathway to inhibit the inflammatory response in rheumatoid arthritis. *Int J Mol Sci*. (2016) 17:498. doi: 10.3390/ijms17040498
40. Savina A, Amigorena S. Phagocytosis and antigen presentation in dendritic cells. *Immunol Rev*. (2007) 219:143–56. doi: 10.1111/j.1600-065X.2007.00552.x
41. Joffre OP, Segura E, Savina A, Amigorena S. Cross-presentation by dendritic cells. *Nat Rev Immunol*. (2012) 12:557–69. doi: 10.1038/nri3254
42. Medzhitov R. Toll-like receptors and innate immunity. *Nat Rev Immunol*. (2001) 1:135–45. doi: 10.1038/35100529
43. Akira S, Uematsu S, Takeuchi O. Pathogen recognition and innate immunity. *Cell*. (2006) 124:783–801. doi: 10.1016/j.cell.2006.02.015
44. Reis e Sousa C. Dendritic cells in mature age. *Nat Rev Immunol*. (2006) 6:476–83. doi: 10.1038/nri1845
45. Regnault A, Lankar D, Lacabanne V, Rodriguez A, Théry C, et al. Fcgamma receptor-mediated induction of dendritic cell maturation and major histocompatibility complex class I-restricted antigen presentation after immune complex internalization. *J Exp Med*. (1999) 189:371–80. doi: 10.1084/jem.189.2.371
46. Heller MC, Watson JL, Blanchard MT, Jackson KA, Stott JL, Tsolis RM. Characterization of *Brucella abortus* infection of bovine monocyte-derived dendritic cells. *Vet Immunol Immunopathol*. (2012) 149:255–61. doi: 10.1016/j.vetimm.2012.07.006
47. Salcedo S, Marchesini M, Lelouard H, Fugier E, Jolly G, Balor S, et al. Brucella control of dendritic cell maturation is dependent on the TIR-containing protein Btp1. *PLoS Pathog*. (2008) 4:e21. doi: 10.1371/journal.ppat.0040021
48. Boushon A, Dietrich J, Coloman M. Cutting edge: inflammatory responses can be triggered by TREM-1, a novel receptor expressed on neutrophils and monocytes. *J Immunol*. (2000) 164:4991–5. doi: 10.4049/jimmunol.164.10.4991
49. Gibot S, Kolopp-Sarda MN, Béné MC, Bollaert PE, Lozniewski A, Mory F, et al. A soluble form of the triggering receptor expressed on myeloid cells-1 modulates the inflammatory response in murine sepsis. *J Exp Med*. (2004) 200:1419–26. doi: 10.1084/jem.20040708
50. Colonna M, Facchetti F. TREM-1 (trigger receptor expressed on myeloid cells): a new player in acute inflammatory responses. *J Infect Dis*. (2003) 187(Suppl. 2):S397–401. doi: 10.1086/374754
51. Weber B, Schuster S, Zysset D, Rihs S, Dickqreber N, Schürch C, et al. TREM-1 deficiency can attenuate disease severity without affecting pathogen clearance. *PLoS Pathog*. (2014) 10:e1003900. doi: 10.1371/journal.ppat.1003900
52. Lin YT, Tseng KY, Yeh YC, Yang FC, Funq CP, Chen NJ. TREM-1 promote survival during Klebsiella pneumoniae liver abscess in mice. *Infect Immun*. (2014) 82:1335–42. doi: 10.1128/IAI.01347-13
53. Klesney-Tait J, Keck K, Li X, Gilfillan S, Otero K, Baruah S, et al. Transepithelial migration of neutrophils into the lung requires TREM-1. *J Clin Invest*. (2013) 123:138–49. doi: 10.1172/JCI64181
54. Homme TJ, Hoogendijk AJ, Dessing MC, Van't Veer, Florquin S, Colonna M, et al. Triggering receptor expressed on myeloid cells-1 (TREM-1) improves host defence in pneumococcal pneumonia. *J Pathol*. (2014) 233:357–67. doi: 10.1002/path.4361
55. Bleharski JR, Kiessler V, Buonsanti C, Sieling PA, Stenger S, Colonna M, et al. A role for triggering receptor expressed on myeloid cells-1 in host defense during the early-induced and adaptive phases of the immune response. *J Immunol*. (2003) 170:3812–8. doi: 10.4049/jimmunol.170.7.3812
56. Kawaii T, Akira S. Toll-like receptors and their crosstalk with other innate receptors in infection and immunity. *Immunity*. (2011) 34:637–50. doi: 10.1016/j.immuni.2011.05.006
57. Lewis DH, Chan DL, Pinheiro D, Armitage-Chan E, Garden OA. The immunopathology of sepsis: pathogen recognition, systemic inflammation, the compensatory anti-inflammatory response, and regulatory T cells. *J Vet Intern Med*. (2012) 26:458–82. doi: 10.1111/j.1939-1676.2012.00905.x
58. Takeda K, Akira S. Toll-like receptors in innate immunity. *Int Immunol*. (2005) 17:1–14. doi: 10.1093/intimm/dxh186
59. Andersen-Nissen E, Smith KD, Bonneau R, Strong RK, Aderm A. A conserved surface on toll-like receptor 5 recognizes bacterial flagellin. *J Exp Med*. (2007) 204:393–403. doi: 10.1084/jem.20061400
60. Campos MA, Rosinha GM, Almeida IC, Salgueiro XS, Jarvis BW, Splitter GA, et al. Role of Toll-like receptor 4 in induction of cell-mediated immunity and resistance to Brucella abortus infection in mice. *Infect Immun*. (2004) 72:176–86. doi: 10.1128/IAI.72.1.176-186.2004
61. Copin R, De Baetselier P, Carlier Y, Letesson JJ, Muraille E. MyD88-dependent activation of B220-CD11b+LY-6C+ dendritic cells during *Brucella melitensis* infection. *J Immunol*. (2007) 178:5182–91. doi: 10.4049/jimmunol.178.8.5182
62. Vieira AL, Silva TM, Mol JP, Oliveira SC, Santos RL, Paixão TA. MyD88 and TLR9 are required for early control of *Brucella ovis*

infection in mice. *Res Vet Sci*. (2013) 94:399–405. doi: 10.1016/j.rvsc.2012.10.028
63. Arias MA, Santiago L, Costas-Ramon S, Jaime-Sánchez P, Freudenberg M, Jiménez De Bagüés MP, et al. Toll-like receptors 2 and 4 cooperate in the control of the emerging pathogen *Brucella microti*. *Front Cell Infect Microbiol*. (2017) 6:205. doi: 10.3389/fcimb.2016.00205
64. Campos PC, Gomes MT, Guimarães ES, Guimarães G, Oliveira SC. TLR7 and TLR3 sense brucella abortus RNA to induce proinflammatory cytokine production but they are dispensable for host control of infection. *Front Immunol*. (2017) 8:28. doi: 10.3389/fimmu.2017.00028
65. Giambartolomei GH, Zwerdling A, Cassataro J, Bruno L, Fossati CA, Philipp MT. Lipoproteins, not lipopolysaccharide, are the key mediators of the proinflammatory response elicited by heat-killed *Brucella abortus*. *J Immunol*. (2004) 173:4635–42. doi: 10.4049/jimmunol.173.7.4635
66. Lomaga MA, Yeh WC, Sarosi I, Duncan GS, Furlonger C, Ho A, et al. TRAF6 deficiency results in osteopetrosis and defective interleukin-1, CD40, and LPS signaling. *Genes Dev*. (1999) 13:1015–24. doi: 10.1101/gad.13.8.1015

Conflict of Interest: The authors declare that the research was conducted in the absence of any commercial or financial relationships that could be construed as a potential conflict of interest.

frontiers in Veterinary Science

ORIGINAL RESEARCH
published: 24 March 2021
doi: 10.3389/fvets.2021.631164

Serosurvey of Avian Influenza Viruses (H5, H7, and H9) and Associated Risk Factors in Backyard Poultry Flocks of Lahore District, Pakistan

Mamoona Chaudhry[1,2*], *Hamad Bin Rashid*[3], *Michael Thrusfield*[4], *Mark C. Eisler*[5†] and *Susan C. Welburn*[1,6†]

[1] Infection Medicine, Deanery of Biomedical Sciences, Edinburgh Medical School, College of Medicine & Veterinary Medicine, The University of Edinburgh, Edinburgh, United Kingdom, [2] Deptarment of Epidemiology and Public Health, University of Veterinary and Animal Sciences, Lahore, Pakistan, [3] Deptarment of Surgery and Pet Sciences, University of Veterinary and Animal Sciences, Lahore, Pakistan, [4] Royal (Dick) School of Veterinary Studies, College of Medicine and Veterinary Medicine, University of Edinburgh-Easter Bush Campus, Roslin, United Kingdom, [5] Bristol Veterinary School, University of Bristol, Bristol, United Kingdom, [6] Zhejiang University-University of Edinburgh Institute, Zhejiang University School of Medicine, Zhejiang University, Haining, China

OPEN ACCESS

Edited by:
Lester J. Perez,
University of Illinois at Urbana–Champaign, United States

Reviewed by:
Mohammed AbdelHameed AboElkhair,
University of Sadat City, Egypt
Yogesh Chander,
Varigen Biosciences Corporation, United States

***Correspondence:**
Mamoona Chaudhry
mamoona.chaudhry@uvas.edu.pk

[†] These authors have contributed equally to this work

Specialty section:
This article was submitted to Veterinary Infectious Diseases, a section of the journal Frontiers in Veterinary Science

Received: 19 November 2020
Accepted: 08 February 2021
Published: 24 March 2021

Citation:
Chaudhry M, Rashid HB, Thrusfield M, Eisler MC and Welburn SC (2021) Serosurvey of Avian Influenza Viruses (H5, H7, and H9) and Associated Risk Factors in Backyard Poultry Flocks of Lahore District, Pakistan. Front. Vet. Sci. 8:631164. doi: 10.3389/fvets.2021.631164

Rural poultry constitutes 56% of the total poultry population in Pakistan; however, epidemiological information about avian influenza viruses (AIVs) in backyard poultry flocks is lacking. A cross-sectional survey of villages of Lahore district was conducted from July 2009 to August 2009 using two-stage cluster sampling and probability proportional to size (PPS) sampling to estimate seroprevalence and its associated risk factors. A random selection of 35 clusters from 308 villages of Lahore were considered, and from each cluster, six chickens aged >2 months were selected. A total of 210 serum samples were collected and examined by the hemagglutination inhibition (HI) test for specific antibodies against AIV subtypes H5, H7, and H9. Overall weighted seroprevalence for AIVs was 65.2% (95% CI: 55.6–74.8%), and for subtype H5, H7 & H9 was 6.9% (95% CI: 10.8–23.0%), 0% (95% CI: 0–1.7%), and 62.0% (95% CI: 52.2–71.8%) respectively. However, none of the samples were positive for H7. The average flock size was 17.3 birds, and the main purpose of keeping poultry was for eggs/meat (70.6%, 95% CI: 59.7–81.4). A majority of them were reared in a semi-caged system (83%, 95% CI: 74.5–91.3). Backyard birds were received from different sources, that is, purchased from the market or received as a gift from friends or any NGO, and were 5.7 times more likely to become avian influenza (AI) seropositive than those that were not exposed to these sources (CI 95%: 2.0–716.0). Backyard birds which were received from different sources, that is, purchased from the market or received from friends or any NGO, were 5.7 times more likely to become AI seropositive compared to those that were not (CI 95%: 2.5–18.7). To reduce the risk of AIV in Pakistan, continuous surveillance of backyard poultry would be needed.

Keywords: avian influenza, backyard, poultry, H9, sero-prevalence, risk factors, Pakistan, zoonosis

INTRODUCTION

With the introduction of intensive poultry production, new breeds, improved biosecurity, and preventive health measures, poultry production has undergone drastic changes globally. In developing countries, however, the adoption of intensive production has been more restricted due to the cost of infrastructure to maintain biosecurity for birds, the cost of rearing quality hybrid chicks, and the cost of providing balanced feed and quality veterinary care (1). In these countries, most poultry is categorized as "family poultry," small-scale poultry kept by households using family labor and locally available feed resources when available. Poultry may run freely within the household/compound and scavenge much of their food while getting supplementary food from the householder. Flock size rarely exceeds 100 birds of unimproved or improved breeds. Labor is unsalaried and drawn from the family household (2). In developing countries, poultry keeping makes a major contribution toward the provision of both income and livelihood for many rural households (3). Backyard poultry is rarely the sole means of livelihood for the family; it is a complementary farming activity that contributes to the overall wellbeing of the household. Poultry keeping is a major income-generating activity and provides a valuable source of protein in the diet. Poultry also play an important sociocultural role in many societies. Women have an important role in the development of family poultry production (4), and almost all rural and peri-urban families keep a small flock of 5–20 adult chickens, mostly managed by women and children. Profits are normally low, and products are used for home consumption, given as gifts, or offered for religious purposes (1, 3, 5).

The majority of backyard poultry owners may be ignorant of basic biosecurity measures and the potential risk posed by zoonotic diseases to humans. Sick birds may be handled, sold, slaughtered, and consumed without consideration that the infection in cooked chicken could be potentially harmful to humans (3). Avian influenza virus (AIV) appears to affect all sectors of the poultry population in most Asian countries, but its presence in free-range commercial ducks, village poultry, live bird markets, and fighting cockerels seems to be especially significant in the spread of the virus (6, 7).

In Pakistan, every rural family and every fifth family in urban areas are associated with poultry production activities in some manner (8). The average flock size for backyard poultry is 22 birds. Investment in the poultry sector in Pakistan is estimated at 1 billion US$, but the industry faces various management problems such as infectious diseases (AIV). Rural poultry contributes 56% of the total egg production and 25% of the poultry meat. There is a strong preference for eggs and meat from rural poultry, and their market prices are high compared with the commercially produced eggs and meat (9). Although rural poultry constitutes up to 56% of the total egg production and 25% of the poultry meat and there are reports of various outbreaks of AIV subtypes H5, H7, and H9 in commercial poultry from the different parts of the country, the detailed epidemiology of the diseases in backyard poultry is largely unknown (10, 11). The main objective of the current study was to provide accurate estimates of the seroprevalence of AIVs, specifically subtypes H5, H7, and H9, which have been reported in commercial poultry, to identify high risk areas or villages for future surveillance and progressive control of AIV in Pakistan and to characterize the backyard production system in Pakistan.

MATERIALS AND METHODS

Study Design

A cross-sectional survey of backyard poultry in 35 clusters (30 villages) in different union councils (UCs) of Lahore district was conducted from July 2009 to August 2009. The total number of villages/rural settlements is 308 in 150 UCs of Lahore district (12). The target population included all chickens kept as backyard poultry in the villages/rural settlements of the Lahore district of Pakistan. The study population included healthy chickens of >2 months of age that were reared in backyards of village households of Lahore district for egg or meat production, and the outcome of interest was whether any chicken was diagnosed as either positive or negative for AIV (H5, H7, and H9) by the hemagglutination inhibition (HI) assay. A complete list of enumerating units (the total number of birds in households) in different villages of Lahore was unfortunately not available. Only a list of villages with an estimated total population of backyard birds was available. This information was gathered by the Department of Livestock and Dairy Development, Punjab, for a livestock census survey of Lahore district, in 2000 (12). The census data were used as the basic data frame to draw samples for the current study, and two-stage cluster sampling with probability proportional to size (PPS) with replacement (WR) was selected since no sampling frame of enumerating units was available (13). Villages were included as clusters or a primary sampling unit (PSU) at the first stage, and chickens of >2 months of age were taken as elementary units at the second stage of the two-stage cluster sampling method.

Sample Size

The sample size was calculated using the C-Survey software, version 2.0 (14). To determine the sample size, the estimated proportion with an attribute was conservatively kept as 50% (13). The precision of the prevalence estimate was set at ±10% at the 95% level of confidence, and the value of design effect (DE) was 2 based on the estimates reported by Bennett et al. (13) and Otte and Gumm (15). Thus, the total number of clusters required for this survey was 35. The elementary units required per cluster were fixed, i.e., six birds per cluster were selected systematically without replacement. The total sample size for the proposed study, therefore, was 210 backyard birds from 35 clusters (30 villages). Four villages (Chung, Dhullam Kurd, Dhullam Jullian, and Kungh Sharif) of Lahore district were sampled more than once, and each selection from each village was considered as the PSU, as the sampling method was WR (**Supplementary Table 1**). All birds in a village were treated as a single flock since they were kept under similar conditions. Blood samples were collected from the captured birds that were systematically selected. The central point of the village (e.g., mosque) was selected as a starting point, and survey sampling was started on a random side by using the "Spin the Pen" method (16). While moving through the village,

every fifth healthy bird observed was selected, and permission was requested from the owner to collect blood from the brachial vein (17) until the desired number of samples was obtained.

Laboratory Analysis

Blood, collected from the brachial vein of the selected birds, was immediately transferred to serum separator tubes, and serum samples were allowed to clot by slightly inclining the tubes at room temperature (22–25°C) before refrigeration. The separated sera were transferred to labeled screw-capped cryotubes and stored at −20°C. Serum samples were thawed once and examined within 1 month post-collection by the HI test for specific antibodies to AIV subtypes H9, H5, and H7 according to the OIE Diagnostic Manual (18). The circulation of these subtypes of AIV has been reported from Pakistan previously; therefore, the samples were only screened for these subtypes (10, 11). The HI test was performed using four hemagglutinin units of virus antigen (4HAU) and 1% chicken erythrocytes diluted in phosphate buffer saline (PBS). Serial 2-fold serum dilutions in PBS were mixed with 25 μl of the virus (4HAU), and then, 25 μl of washed chicken red blood cells were added and mixed well. After that, the plates were incubated for 30 min at room temperature (20–25°C). The HI titer was calculated as the reciprocal of the highest dilution of serum that inhibited the hemagglutination of the chicken erythrocytes. Samples with titers ≥1:16 were considered as positive. Reference antigens [A/turkey/wisconsin/68 (H5N9); A/Chicken/Italy/1067/99 (H7N1); H9N2 (Middle East origin), Merial Italia S.p.A., Noventa, Italy] and antibodies (VLDIA042 HAR-INFH5, VLDIA043 HAR-INFH7, VLDIA150 HAR-INFH9, GD, Animal health service, Deventer, The Netherlands) for H5, H7, and H9 were used to test the serum samples. All hypodermics and biological waste were disposed of properly. The work was done at the Grand Parent Poultry Laboratory, Lahore, Pakistan and the University of Veterinary and Animal Sciences, Lahore, Pakistan.

Data Collection

A questionnaire was designed based on an extensive review of the previous literature and biological plausibility of the risks (19–27) and was pretested in five villages with 10 respondents in the same area in which the sampling was to be undertaken. The questionnaire included 34 closed and semi-closed questions. Information on flock size and type, the purpose of keeping backyard birds, qualifications and profession of the owner, other animals maintained with the backyard birds, and management practice (questionnaire in **Supplementary Material**) was collected from the owner of each selected bird in a face-to-face interview after receiving their consent. All owners permitted to collect blood samples from their birds and answered all questions in the questionnaire. Permission to conduct the survey was obtained from the Livestock and Dairy Development Department of Punjab, Pakistan.

Statistical Analysis

Locations of the villages and households owning the selected birds were recorded with a hand-held global positioning system (GPS; Garmin, Olathe, KS, USA). The data collected during the survey from questionnaires were stored in EpiData Entry version 3.1 (28) and were validated by rechecking the computerized data and by matching it to the hard copy. The stored data were exported in dBase and the Excel format for further processing and analysis in ArcGIS 10 (Geographical Information System, ESRI System, Redlands, CA, USA), and a statistical analysis was undertaken in the R-statistical computing environment version 2.14.0 (29).

The weighted proportion estimates with 95% CIs of the overall seroprevalence were computed by the svy function using the survey package in R (30). Point estimates of the weighted means, percentages for each characteristic of interest, and 95% CIs were also calculated (30). Within each village, prevalence point estimates were computed by the epi.conf function in the epiR package using an exact method for CI calculation.

About 34 potential risk factors were analyzed for association with an outcome by measuring the odds ratio (OR) (31). The survey-weighted logistic regression model was used to fit into the univariable and multivariable models, and seroprevalence ORs with 95% CI for each explanatory variable were calculated using the survey package in the R software (30). All independent variables associated with the seroprevalence of AIV were initially screened with the chi-square test in univariable analysis, and all variables with $p < 0.25$ were included in the multivariable logistic regression model by using a forward stepwise variable selection strategy (31, 32). For building the final model, variables with $p \leq 0.05$ based on the Wald statistic (or the log-likelihood ratio test for categorical variables with 3 or more levels) were retained in the model. Collinearity among the selected variables was tested using the Spearman's rank correlation (33). If there was a strong positive correlation ($\rho > 0.5$) between the variables, the more clinically important and biologically plausible variable from pairs of correlated variables was chosen for the multivariable model.

Spatial Data and Analysis

A paper map of the rural settlements of Pakistan (scale 1:5,000,000) was digitally scanned from the Atlas of Survey of Pakistan published in 2002 by the Survey of Pakistan Office, Rawalpindi (34), and a map showing town boundaries and UC boundaries of Lahore district was downloaded from the website of the City District (http://www.lahore.gov.pk/city-government/lahore-map.aspx). These maps were georeferenced using ArcGIS 10. Point (dot or location) maps and graduated pie maps of the spatial distribution of villages and premises of backyard poultry birds in different UCs of Lahore district were generated (35, 36).

RESULTS

A total of 144 sera were positive for AIVs (H5, H9, or both) using the HI test from 210 samples and, among these, 134 serum samples were positive for subtype H9, 38 were positive for subtype H5 A, and 27 samples had antibodies to both subtypes (**Figure 1**). The distribution of HI titer against subtypes H9 and H5 are presented in **Table 1**. There were no positive samples for the H7 subtype.

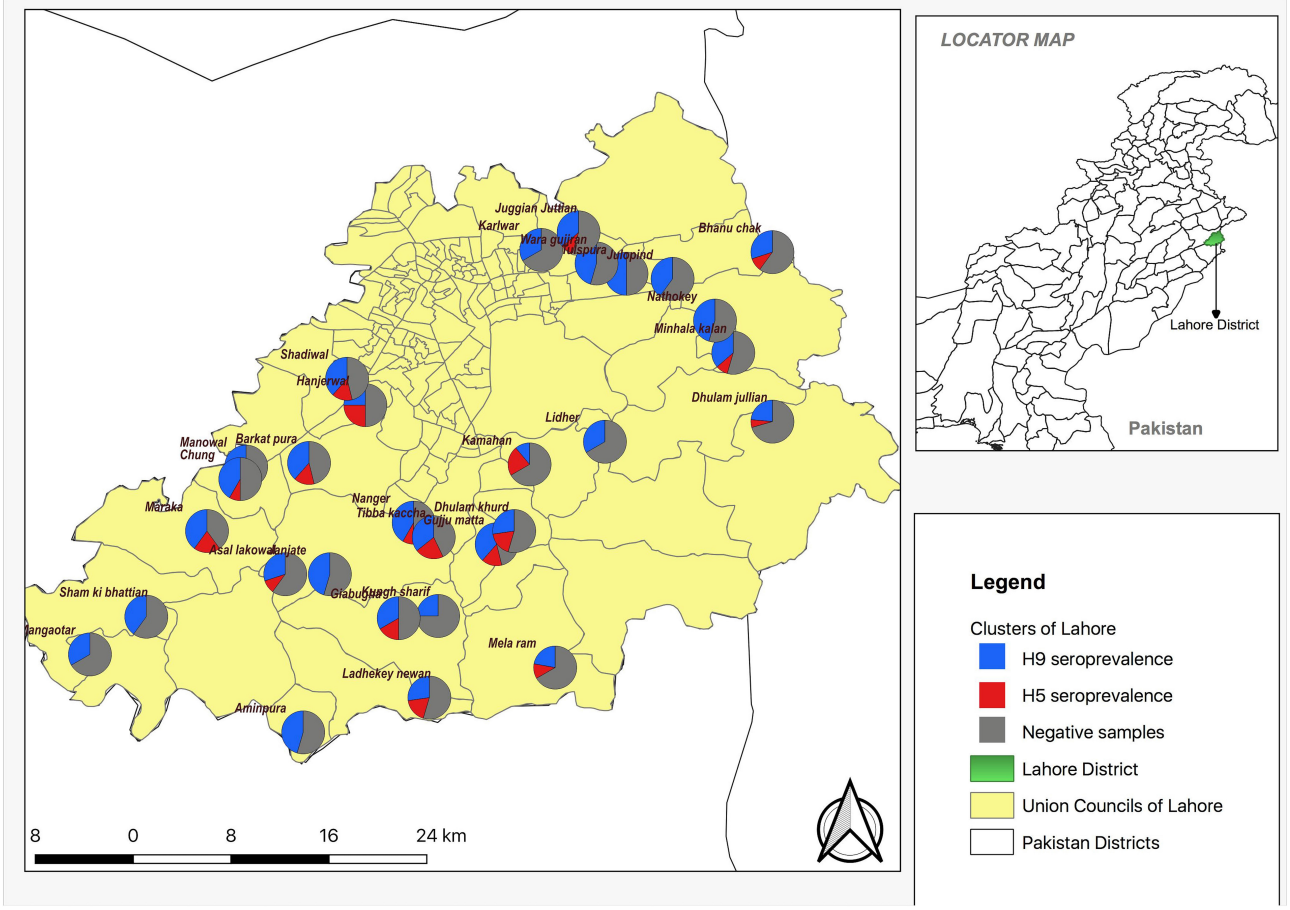

FIGURE 1 | Spatial distribution and village (cluster) level seroprevalence of H9 and H5 in backyard poultry in Lahore district.

The spatial distribution of positive samples indicated that all 30 villages were seropositive for H9 antibodies while 21 villages were seropositive for H5. Coinfection with H9 and H5 occurred in 18 villages (**Figure 1**). The overall seroprevalence of AIVs, subtypes H5, H7, and H9, was 65.2% (95% CI: 55.6–74.8%); 16.9% (95% CI: 10.8–23.0%), 0% (95% CI: 0–1.7%), and 62.0% (95% CI: 52.2–71.8%), respectively, calculated by a two-stage cluster analysis with PPS (**Table 2**). The highest seroprevalence of H5 was in Manowal, Maraka, Hanjarwal, and Tibba Kaccha (50.0%, 95% CI: 11.8–83.2) and the lowest was 0% (95% CI: 0–26.5) in Kungh Sharif, and 0% (95% CI: 0–45.9) in Aminpura, Wara Gujjran, Karlwar, Sham ki Bhattian, Mangaotar, Janjate, Lidher, and Nathokey. The highest seroprevalence for H9 was observed in the Maraka village (100%, 95% CI: 54.1–100), while the lowest seroprevalence for H9 was in Kamahan (16.7%, 95% CI: 0.42–64.1).

The average flock size was 17.3 birds (range 1–922 birds), and the main purpose of keeping poultry was for eggs/meat (70.6%, 95% CI: 59.7–81.4). The average number of chickens reared as layers was 3.4 (range 0–50). The most common breed of poultry in the backyard was indigenous Desi (94.0%, 95% CI: 89.2–99.0), followed by a mixture of different breeds (6%, 95% CI: 1.0–10.8). The majority of the birds (83%) were reared in a semi-caged system (95% CI: 74.5–91.3), while 17% of them were kept completely outdoors (95% CI: 8.7–25.5). Most farmers fed their flock with leftover food from home (74.8%, 95% CI: 58.4–91.2), while 25.2% of backyard poultry were fed on leftover food and also scavenged outside the house (95% CI: 8.8–41.6).

The most common source of water intake for birds was both tap water at home and street channel drainage water (60.6%, 95% CI: 41.4–79.8). Some farmers (20.0%, 95% CI: 8.2–31.9) provided only tap water to poultry, while 19.4% of backyard birds used street channels as the main source of water intake (95% CI: 3.3–35.4).

Out of 34 potential risk factors, six variables (the profession of farmers, buying adult birds, the source of birds, selling birds or eggs, disposal of dead birds by the farmer, disinfection of backyard) were excluded from analysis due to insufficient (zero cell value) values in a 2×2 table. A total of nine variables showed an association ($p < 0.25$) with the seroprevalence of AIVs in backyard poultry in univariable logistic analysis using the chi-square test. However, two variables (the presence of wild birds in the vicinity and pet animals visiting neighboring commercial farms) were excluded due to collinearity ($\rho > 0.5$), and seven

TABLE 1 | Distribution of antibody titers against avian influenza virus (AIV) subtypes H5 and H9 in the hemagglutination inhibition (HI) test.

HI dilution	No (%) [95% CI]	
	Subtype H5	Subtype H9
≤1:8	172 (81.90)	76 (36.19)
1:16	26 (12.38)	10 (4.76)
1:32	8 (3.80)	23 (10.95)
1:64	3 (1.42)	28 (13.33)
1:128	1 (0.47)	23 (10.95)
1:256	0 (0)	15 (7.14)
1:512	0 (0)	21 (10)
1:1,024	0 (0)	9 (4.28)
1:2,048	0 (0)	5 (2.38)
≥1:16	38 [16.9% (10.8–23.0)]	134 [62.0% (52.2–71.8)]

TABLE 2 | Overall seroprevalence of H5 and H9 estimated from 210 backyard birds in villages of Lahore district (in %).

AIV subtype	Seroprevalence ($n = 210$)		Design effect (DE)
	Point estimate	95% CI	
AIVs	65.20	55.6–74.8	2.22
H5	16.9	10.8–23.0	1.27
H9	62.0	52.2–71.8	2.08

variables, which were biologically more plausible, were retained in the analysis (**Table 3**). The final weighted logistic regression model identified two variables out of the initial seven as potential risk factors for AIV in these backyard birds (**Table 4**). The source of birds (hatched at home vs. other sources) was identified as a risk factor (OR: 5.7; CI 95%: 2.0–16.0, $p = 0.019$). Backyard birds kept in close vicinity of live poultry retail shops were 6.9 times more likely to be AIV seropositive compared to those that were not (CI 95%: 2.5–18.7, $p = 0.003$).

DISCUSSION

Backyard poultry infected with AIV can pose a risk for the introduction of AI into commercial poultry (19). In the current study, we estimated the seroprevalence of AIVs in backyard poultry flocks of Lahore district. The overall weighted seroprevalence of AIVs was 65.2% (95% CI: 55.6–74.8%). The present study estimate is higher than an estimate from Bangladesh (23% of flocks and 20% of chickens). This difference in the estimate may be due to a sampling strategy or low circulation of AIVs in Bangladesh (20).

All villages sampled were seropositive for H9, and the overall weighted seroprevalence of H9 was 62% (95% CI: 52.2–71.8%). Various studies from neighboring countries have reported slightly higher estimates of seroprevalence (73 and 81.6% in Iran) in backyard poultry, which suggests endemicity of H9N2 viruses in the region (37, 38). In the current study, the seroprevalence of H5 was 16.9% (95% CI: 10.8–23.0%), which is close to the seroprevalence estimates reported from Bangladesh (9.82%) and Vietnam (17.5%) (26, 39). Backyard birds had not been vaccinated against AI, and the antibody titers represented previous exposure to naturally circulating virus and confirmed that low pathogenic AIVs, H9 and H5, are circulating in backyard poultry in villages of Lahore, Pakistan. The variation in the estimates of seroprevalence of H9, H5, and H7 in our survey could be attributed to the pathogenicity of these subtypes. H5 and H7 have high mortality (40) and chicken infected with these subtypes usually die; hence, the number of seropositive birds was low. On the contrary, H9 is a low pathogenic subtype with endemic status in Pakistan (41), enabling repeated reinfections of the same birds and increasing seroprevalence (42). Furthermore, due to extensive biosecurity measures and the presence of inactivated vaccines in commercial poultry (11, 43), subtypes H5 and H7 have not been reported in commercial poultry in Pakistan since their last outbreak in 2008 (44), which might be attributed to their low or negligible seroprevalence in our survey.

Our results showed that the coinfection of H5 and H9 was present in 18 villages. A total of 27 samples from the backyard birds had antibodies to both the subtypes. The co-circulation of H9N2 and HPAI H5N1 viruses, along with their ability to mutate through antigenic shift and drift, may produce novel viruses with pandemic potential (45). Inter-subtype reassortment between the co-circulating H9N2 virus and the highly pathogenic H5N1 virus has been detected in China (46), Pakistan (47), Bangladesh (48), and Cambodia (49).

Most surveys were conducted to estimate the seroprevalence of AI in Pakistan and have not been incorporated due to lack of adequate study design to avoid bias. In the present study, PPS sampling was used to ensure that unbiased prevalence estimates were obtained. Recently, Henning et al. (26) also reported that bird-level prevalence using a multi-stage sampling design accounts for clustering and sampling fractions.

Characteristics of the backyard poultry production system vary with the socioeconomic and cultural heritages of the developing countries, but most are essentially similar. The major purpose of rearing birds was to get eggs and meat for personal use (70.6%). It has been observed globally that in more than 90% of the cases, backyard birds are kept for egg production for household consumption (25, 27). However, in Bangladesh, farmers reported the purpose of keeping birds as a cash source and as a protein source (50). Contrary to this data, the data from other countries with high income showed that the farmer ranked hobby/fun as the highest reason for keeping backyard birds (22).

In Pakistan, the most common breed is indigenous Desi. Farooq et al. (51) reported that the indigenous Desi birds dominated the flocks (10.2 birds) followed by Fayoumi (6.76) in Pakistan. This study also showed that the common breed in the backyard was indigenous Desi (94%). Farmers prefer to keep the indigenous Desi breed due to its greater capacity to survive and adapt to scavenging management systems (51). The average size of flock reported in the current study (17.3 birds/flock) is very close to estimates of the livestock census. Various studies from Pakistan have reported a varying size of flock ranging from 22 to 26 birds (51, 52), while other studies from Thailand, Bangladesh,

TABLE 3 | Results of univariable analysis with potential risk factors associated with the seroprevalence of AIVs in backyard poultry of villages of Lahore district.

Potential risk factors	Response level	AIVs result		Odds ratio (OR)	95% confidence interval for OR	*P*-value
		Negative	Positive			
Source of birds	Hatched at home	18	16	1.16	0.86–1.56	0.02
	Other/gift etc.	48	128			
Access to veterinary hospital	No	58	139	0.36	0.17–0.77	0.013
	Yes	8	5			
Decreased production in birds (eggs & weight)	No	39	61	2.31	1.17–4.57	0.022
	Yes	27	83			
Sharing feed with wild birds	No	9	6	3.96	1.25–12.62	0.027
	Yes	57	138			
Poultry farm workers visiting village	No	34	96	0.49	0.24–0.99	0.057
	Yes	32	48			
Farm vehicle visiting farm	No	28	88	0.44	0.22–0.86	0.024
	Yes	38	56			
Proximity of backyard to live bird retail shops	No	60	112	3.53	1.10–11.32	0.043
	Yes	6	32			

TABLE 4 | Results of final model with potential risk factors associated with the seroprevalence of AIVs in backyard poultry of villages of Lahore district.

Potential risk factors	Response level	Odds ratio (OR)	95% confidence interval for OR
Source of birds	Hatched at home	5.7	2.0–16.0
	Others/gift etc.		
Proximity of backyard to live bird retail shops	No	6.9	2.5–18.7
	Yes		

and Chile reported a flock size ranging from 10 to 37 birds (25, 50, 53).

In this study, the majority of farmers reared their backyard birds in a semi-caged system (83%, 95% CI: 74.5–91.3). Other studies also observed that the majority of farmers prefer to rear birds in semi-caged facilities (25, 27, 51). Outdoor backyard flocks may be more at risk for the introduction of AI strains of either high or low pathogenicity (54). Nooruddin et al. (39) also reported that chickens reared under a semi-scavenging system in Bangladesh were allowed to scavenge with ducks in the yard and in the crop fields near to water reservoirs where domestic ducks, wild ducks, and migratory birds were also present. This may contribute to the natural infection of the native chickens. Terregino et al. (55) indicated the backyard poultry farming system as being high risk for AI introduction, primarily due to many free-range holdings. The availability of food attracts wild birds and results in intermingling and in the deposition of droppings.

The results of a logistic regression analysis confirmed that the main risk factors for the infection of backyard flocks with AI were the "source of bird," i.e., hatched at home vs. other sources and birds that were kept in a backyard vs. close to a live poultry retail shop. Usually, farmers keep birds that are hatched at home; very few purchase birds from local markets or receive them as a gift from friends, and sometimes private NGOs provide free birds to women in villages. Birds purchased from local live bird markets have been previously identified as a risk to backyard poultry for infection with AIVs (56).

Our study showed that backyard poultry birds are usually raised in a unit with a semi-caged system, i.e., they roam around the village area and have access to live bird retail stalls in their vicinity, which may increase the risk of infection in backyard poultry. Contact of backyard birds with live bird markets and wild birds has been identified as a potential risk factor of AIV in backyard poultry (19, 27, 57). Live bird retail stalls pose a continuous threat due to the mixing of birds from various sources and poor sanitary conditions in stalls (58). Awareness of the owners to reduce the free-range rearing of poultry can limit the spread of AIV among backyard poultry. Current findings can be generalized to similar poultry rearing systems in other low- and middle-income countries.

The main limitation is that our study was a cross-sectional survey which only estimates a parameter at a certain point in time. The second limitation was that a more precise sample design (simple random sample) could not be defined due to the lack of a sampling frame. Another limitation of this survey was that only the serological status of the birds was tested; this can only detect antibodies against any previous exposure of the bird to the virus and does not detect live virus. A more detailed longitudinal study for the detection of live virus would better monitor the subtype of live virus circulating in the backyard birds. Neuraminidase subtyping of samples was not done due to financial constraints.

In conclusion, the result of the current study confirmed the presence of antibodies to H9 and H5 in villages, which demonstrate the exposure of chickens to circulating AIV viruses. Based on these results, regular surveillance in villages or peri-urban areas is recommended. To reduce the risk of the spread of AIV in Pakistan, continuous surveillance of backyard poultry would be needed because these birds are at a higher risk of

contracting infection due to the free-range system. The presence of AIV in these birds also poses a threat to human health because these birds are in frequent contact with farmers/handlers and interspecies transmission can occur (59). Backyard birds are a vital protein resource for the rural population of Pakistan; it might not be possible to prevent the rearing of these birds. The knowledge and status of AIV in these birds can be used to help devise control strategies for the containment of the spread of AIV in the poultry production system.

DATA AVAILABILITY STATEMENT

The raw data supporting the conclusions of this article will be made available by the authors, without undue reservation.

ETHICS STATEMENT

Ethical review and approval was not required for the animal study because informed consent for all participating owners of backyard poultry was taken prior to the sampling and data collection. Briefly the objectives of the study and voluntarily participation were explained and they were invited to participate. Only farmers who consented voluntarily were included and interviewed. A trained veterinarian or para veterinarian collected the blood samples from birds. The manuscript does not contain any clinical studies or patient data.

AUTHOR CONTRIBUTIONS

SW, ME, MT, and MC contributed conception and design of the study, data analysis, interpretation, read, revised, and approved the submitted version of the manuscript. MC and HR collected the data, organized and carried out statistical analysis, and prepared the manuscript. SW, ME, and MT supervized the proposal preparation, presentation, and data collection. ME and SW contributed equally. All authors contributed to the article and approved the submitted version.

FUNDING

The current study was conducted under the HEC scholarship scheme (10% overseas) awarded to MC by the Higher Education Commission of Pakistan. The University of Edinburgh also provided financial support for this study.

ACKNOWLEDGMENTS

The authors thank the owners of selected backyard birds in selected villages of Lahore district for providing samples and data. The authors are also grateful to the Livestock & Dairy Development Department, Punjab for providing logistic and technical support for sampling for the survey of villages in Lahore district. We are also thankful to the Grand Parent Poultry Laboratory, Lahore, for providing technical support for laboratory analysis of samples.

SUPPLEMENTARY MATERIAL

The Supplementary Material for this article can be found online at: https://www.frontiersin.org/articles/10.3389/fvets.2021.631164/full#supplementary-material

REFERENCES

1. Permin A, Pedersen G. The need for a holistic view on disease problems in free-range chickens. In: *Charateristics and Parameters of Family Production System in Africa*. Vienna: International Atomic Energy Agency (2002).
2. Sonaiya EB, editor. Poultry as a Tool in poverty eradication and promotion of gender equality. In: *ANRPD Proceedings International Network for Family Poultry Development (INFPD): Origins, Activities, Objectives and Visions* Tune (1990).
3. Iqbal M. Controlling avian influenza infections: the challenge of the backyard poultry. *J Mol Genet Med.* (2009) 3:119–20. doi: 10.4172/1747-0862.1000022
4. FAO. *Small-scale Poultry Production: Technical Guide.* Rome: Food and Agriculture Organization of United Nations. (2004). Available online at http://www.smallstock.info/reference/FAO/008/y5169e/y5169e00.pdf
5. Riise JC, Permin A, McAinsh CV, Frederiksen L. *Keeping Village Poultry: A Technical Manual on Small-Scale Poultry Production*. Copenhagen: Network for smallholder poultry development. (2004).
6. Sims LD, Domenech J, Benigno C, Kahn S, Kamata A, Lubroth J, et al. Origin and evolution of highly pathogenic H5N1 avian influenza in Asia. *Vet Rec.* (2005) 157:159–64. doi: 10.1136/vr.157.6.159
7. Martin V, Sims L, Lubroth J, Kahn S, Domenech J, Begnino C. History and evolution of HPAI viruses in southeast Asia. *Ann N Y Acad Sci.* (2006) 1081:153–62. doi: 10.1196/annals.1373.017
8. Sadiq M. Pakistan poultry sector still on upward swing. *World Poult.* (2004) 20:10–1. Available online at: https://www.poultryworld.net/PageFiles/23350/001_boerderij-download-WP6436D01.pdf
9. Afzal M. Pakistan country paper. In: Thomson EF, von Kaufmann R, Pun HL, Treacher T, von Houton H, editor. *Global Agenda for Livestock Research International Centre for Agricultural Research in Dry Area*. Aleppo: Food and Agriculture Organization (1998). p. 120–6.
10. Abbas MA, Spackman E, Swayne DE, Ahmed Z, Sarmento L, Siddique N, et al. Sequence and phylogenetic analysis of H7N3 avian influenza viruses isolated from poultry in Pakistan 1995-2004. *Virol J.* (2010) 7:137. doi: 10.1186/1743-422X-7-137
11. Naeem K, Siddique N, Ayaz M, Jalalee MA. Avian influenza in Pakistan: outbreaks of low- and high-pathogenicity avian influenza in Pakistan during 2003-2006. *Avian Dis.* (2007) 51 (1 Suppl):189–93. doi: 10.1637/7617-042506R.1
12. Anonymous. *Punjab Livestock Census 2000 Showing District-wise Livestock Number: Lahore District*. Punjab: Livestock and Dairy Development Department (2001).
13. Bennett S, Woods T, Liyanage WM, Smith DL. A simplified general method for cluster-sample surveys of health in developing countries. *World Health Stat Q.* (1991) 44:98–106.
14. Farid MN, Frerichs RR. *CSurvey.* 2.0 ed. Los Angeles, CA: Department of Epidemiology, University of California, Los Angeles (2007).
15. Otte MJ, Gumm ID. Intra-cluster correlation coefficients of 20 infections calculated from the results of cluster-sample surveys. *Prev Vet Med.* (1997) 31:147–50. doi: 10.1016/S0167-5877(96)01108-7
16. Abramson JH, Abramson ZH. *Research Methods in Comunity Medicine: Survey, Epidemiological Research, Programme Evalustion, Clinical Trials*. 6th ed. West Sussex: John Wiley & Sons Ltd (2008).

17. FAO. Wild birds and avian influenza: an introduction to applied field research and disease sampling techniques. In: Whitworth D, Newman SH, Mundkur T, Harris P, editors. *FAO Animal Production and Health Manual, No 5*. Rome: Food and Agrivulture Organization of the United Nation (2007).
18. OIE. *Manual of Diagnostic Tests and Vaccines for Terrestrial Animals*. Paris: OIE; Avian Influenza: World Organization for Animal Health (2009). Available online at: http://www.oie.int/fileadmin/Home/eng/Health_standards/tahm/2.03.04_AI.pdf
19. Biswas PK, Christensen JP, Ahmed SSU, Das A, Rahman MH, Barua H, et al. Risk for infection with highly pathogenic avian influenza virus (H5N1) in backyard chickens, Bangladesh. *Emerge Infect Dis.* (2009) 15:1931–6. doi: 10.3201/eid1512.090643
20. Biswas PK, Barua H, Uddin GM, Biswas D, Ahad A, Debnath NC. Serosurvey of five viruses in chickens on smallholdings in Bangladesh. *Prev Vet Med.* (2009) 88:67–71. doi: 10.1016/j.prevetmed.2008.06.018
21. McQuiston JH, Garber LP, Porter-Spalding BA, Hahn JW, Pierson FW, Wainwright SH, et al. Evaluation of risk factors for the spread of low pathogenicity H7N2 avian influenza virus among commercial poultry farms. *J Am Vet Med Assoc.* (2005) 226:767–72. doi: 10.2460/javma.2005.226.767
22. Garber L, Hill G, Rodriguez J, Gregory G, Voelker L. Non-commercial poultry industries: surveys of backyard and gamefowl breeder flocks in the United States. *Prev Vet Med.* (2007) 80:120–8. doi: 10.1016/j.prevetmed.2007.01.012
23. Garber L, Voelker L, Hill G, Rodriguez J. Description of live poultry markets in the United States and factors associated with repeated presence of H5/H7 low-pathogenicity avian influenza virus. *Avian Dis.* (2007) 51 (1 Suppl):417–20. doi: 10.1637/7571-033106R.1
24. Bulaga LL, Garber L, Senne D, Myers TJ, Good R, Wainwright S, et al. Descriptive and surveillance studies of suppliers to New York and New Jersey retail live-bird markets. *Avian Dis.* (2003) 47 (3 Suppl):1169–76. doi: 10.1637/0005-2086-47.s3.1169
25. Hamilton-West C, Rojas H, Pinto J, Orozco J, Herve-Claude LP, Urcelay S. Characterization of backyard poultry production systems and disease risk in the central zone of Chile. *Res Vet Sci.* (2011) 93:121–4. doi: 10.1016/j.rvsc.2011.06.015
26. Henning J, Henning KA, Morton JM, Long NT, Ha NT, Vu le T, et al. Highly pathogenic avian influenza (H5N1) in ducks and in-contact chickens in backyard and smallholder commercial duck farms in Viet Nam. *Prev Vet Med.* (2011) 101:229–40. doi: 10.1016/j.prevetmed.2010.05.016
27. Zheng T, Adlam B, Rawdon TG, Stanislawek WL, Cork SC, Hope V, et al. A cross-sectional survey of influenza A infection, and management practices in small rural backyard poultry flocks in two regions of New Zealand. *N Z Vet J.* (2010) 58:74–80. doi: 10.1080/00480169.2010.65086
28. Lauritsen JM. *EpiData: Data Entry, Data Management and Basic Statistical Analysis System*. Mortensen J, editor. 3.1 ed. Odense: EpiData Association, 2000–2006 (2006).
29. Team RDC. *R: A Language and Environment for Statistical Computing*. R 2.14.0 GUI 1.42. Vienna: R Foundation for Statistical Computing (2011).
30. Lumley T. *Survey Package: Analysis of Complex Survey Samples*. 3.28 ed. R Package (2011). Available online at http://faculty.washington.edu/tlumley/survey/
31. Hosmer DW, Lemeshow S. *Applied Logistic Regression*. New York, NY: John Wiley & Sons, Inc (2000). doi: 10.1002/0471722146
32. Dohoo I, Martin W, Stryhn H. *Veterinary Epidemiologic Research*. Charlottetown, PE: AVC Inc (2003).
33. Rayward-Smith VJ. Statistics to measure correlation for data mining application. *Comput Stat and Data Analy.* (2007) 51:3969–82. doi: 10.1016/j.csda.2006.05.025
34. Anonymous. *Atlas of Pakistan*. Rawalpindi: Director map publication, Survey of Pakistan (1997).
35. Thrusfield M. *Veterinary Epidemiology*. 3rd ed. Oxford: Blackwell Science (2007) 1–593p.
36. ESRI. *About Symbolizing Data to Represent Quantity*. Environmental System Research Institute (2008). Available online at http://webhelp.esri.com/arcgisdesktop/9.3/index.cfm?TopicName=About_symbolizing_data_to_represent_quantity (accessed January 10, 2012).
37. Hadipour MM, Habibi G, Vosoughi A. Prevalence of antibodies to H9N2 avian influenza virus in backyard chicken around Maharlou lake in Iran. *Pak Vet J.* (2011) 31:192–4. Available online at: http://www.pvj.com.pk/pdf-files/31_3/192-194.pdf
38. Hadipour MM. Seroprevalence survey of H9N2 avian influenza virus in backyard chickens around the Caspian Sea in Iran. *Braz J Poult Sci.* (2010) 12:53–5. doi: 10.1590/S1516-635X2010000100008
39. Nooruddin GM, Hossain MT, Mohammad M, Rahman, MM. Sero-epidemiology of avian influenza virus in native chicken in Bangladesh. *Int J Poult Sci.* (2006) 5:1029–33. doi: 10.3923/ijps.2006.1029.1033
40. Swayne DE. *Avian Influenza*. 1st ed. Oxford: Blackwell Publishing Ltd (2008) 587p. doi: 10.1002/9780813818634
41. Chaudhry M, Rashid HB, Angot A, Thrusfield M, Welburn SC, de CBBM, et al. Avian influenza A in poultry stalls of Lahore District, Pakistan in 2009-2010. *J Infect.* (2017) 74:609–11. doi: 10.1016/j.jinf.2017.03.008
42. Peacock THP, James J, Sealy JE, Iqbal M. A global perspective on H9N2 avian influenza virus. *Viruses.* (2019) 11:620. doi: 10.3390/v11070620
43. Abbas MA, Spackman E, Fouchier R, Smith D, Ahmed Z, Siddique N, et al. H7 avian influenza virus vaccines protect chickens against challenge with antigenically diverse isolates. *Vaccine.* (2011) 29:7424–9. doi: 10.1016/j.vaccine.2011.07.064
44. Tahir MF, Abbas MA, Ghafoor T, Dil S, Shahid MA, Bullo MMH, et al. Seroprevalence and risk factors of avian influenza H9 virus among poultry professionals in Rawalpindi, Pakistan. *J Infect Public Health.* (2019) 12:482–5. doi: 10.1016/j.jiph.2018.11.009
45. Fusaro A, Monne I, Salviato A, Valastro V, Schivo A, Amarin NM, et al. Phylogeography and evolutionary history of reassortant H9N2 viruses with potential human health implications. *J Virol.* (2011) 85:8413–21. doi: 10.1128/JVI.00219-11
46. Guan Y, Shortridge KF, Krauss S, Chin PS, Dyrting KC, Ellis TM, et al. H9N2 influenza viruses possessing H5N1-like internal genomes continue to circulate in poultry in southeastern China. *J Virol.* (2000) 74:9372–80. doi: 10.1128/JVI.74.20.9372-9380.2000
47. Iqbal M, Yaqub T, Reddy K, McCauley JW. Novel genotypes of H9N2 influenza A viruses isolated from poultry in Pakistan containing NS genes similar to highly pathogenic H7N3 and H5N1 viruses. *PLoS ONE.* (2009) 4:e5788. doi: 10.1371/journal.pone.0005788
48. Parvin R, Begum JA, Chowdhury EH, Islam MR, Beer M, Harder T. Co-subsistence of avian influenza virus subtypes of low and high pathogenicity in Bangladesh: challenges for diagnosis, risk assessment and control. *Sic Rep.* (2019) 9:8306. doi: 10.1038/s41598-019-44220-4
49. Horwood PF, Horm SV, Suttie A, Thet S, Y P, Rith S, et al. Co-circulation of Influenza A H5, H7, and H9 Viruses and Co-infected Poultry in Live Bird Markets, Cambodia. *Emerge Infect Dis.* (2018) 24:352–5. doi: 10.3201/eid2402.171360
50. Khan MSI, Akbar SMF, Hossain ST, Mahatab M, Hossain MM, Idrus Z. Possible route of transmission of highly pathogenic avian influenza virus type H5N1 in family poultry at rural Bangladesh. *Pak Vet J.* (2012) 32. Available online at: http://pvj.com.pk/pdf-files/32_1/112-116.pdf
51. Farooq M, Gul N, Chand N, Durrani FR, Khurshid A, Ahmed J, et al. Production performance of backyard chicken under the care of women in Charsadda, Pakistan. *Livestock Res Rural Devel.* (2002) 14. Available online at: http://www.lrrd.org/lrrd14/1/faro141.htm
52. Javed K, Farooq M, Mian MA, Durrani FR, Mussawar S. Flock size and egg production performance of backyard chicken reared by rural woman in Peshawar, Pakistan. *Livestock Res Rural Devel.* (2003) 15. Available online at: https://www.lrrd.org/lrrd15/11/jave1511.htm
53. Otte J, Pfeiffer D, Tiensin T, Price L, Silbergeld, E. Highly pathogenic avian influenza risk, biosecurity and smallholder adversity. *Livestock Res Rural Devel.* (2007) 19. Available online at: https://www.lrrd.org/lrrd19/7/otte19102.htm
54. Bavinck V, Bouma A, van Boven M, Bos ME, Stassen E, Stegeman JA. The role of backyard poultry flocks in the epidemic of highly pathogenic avian

influenza virus (H7N7) in the Netherlands in 2003. *Prev Vet Med.* (2009) 88:247–54. doi: 10.1016/j.prevetmed.2008.10.007
55. Terregino C, De Nardi R, Guberti V, Scremin M, Raffini E, Martin AM, et al. Active surveillance for avian influenza viruses in wild birds and backyard flocks in Northern Italy during 2004 to 2006. *Avian Pathol.* (2007) 36:337–44. doi: 10.1080/03079450701488345
56. Wang XX, Cheng W, Yu Z, Liu SL, Mao HY, Chen EF. Risk factors for avian influenza virus in backyard poultry flocks and environments in Zhejiang Province, China: a cross-sectional study. *Infect Dis Poverty.* (2018) 7:65. doi: 10.1186/s40249-018-0445-0
57. Wang Y, Jiang Z, Jin Z, Tan H, Xu B. Risk factors for infectious diseases in backyard poultry farms in the Poyang lake area, China. *PLoS ONE.* (2013) 8:e67366. doi: 10.1371/journal.pone.0067366
58. Chaudhry M, Rashid HB, Angot A, Thrusfield M, Bronsvoort BMd, Capua I, et al. Risk factors for avian influenza H9 Infection of chickens in live bird retail stalls of Lahore district, Pakistan 2009–2010. *Sci Rep.* (2018) 8:5634. doi: 10.1038/s41598-018-23895-1
59. Chaudhry M, Webby R, Swayne D, Rashid HB, DeBeauchamp J, Killmaster L, et al. Avian influenza at animal-human interface: one-health challenge in live poultry retail stalls of Chakwal, Pakistan. *Influenza Other Respir Viruses.* (2020) 14:257–65. doi: 10.1111/irv.12718

Conflict of Interest: The authors declare that the research was conducted in the absence of any commercial or financial relationships that could be construed as a potential conflict of interest.

frontiers in Veterinary Science

ORIGINAL RESEARCH
published: 12 April 2021
doi: 10.3389/fvets.2021.658675

Ecological and Socio-Economic Determinants of Livestock Animal Leptospirosis in the Russian Arctic

Olga I. Zakharova[1†], Fedor I. Korennoy[1,2*†], Ivan V. Iashin[1], Nadezhda N. Toropova[1], Andrey E. Gogin[3], Denis V. Kolbasov[3], Galina V. Surkova[4], Svetlana M. Malkhazova[4] and Andrei A. Blokhin[1]*

[1] Federal Research Center for Virology and Microbiology, Nizhny Novgorod Research Veterinary Institute-Branch of Federal Research Center for Virology and Microbiology, Nizhny Novgorod, Russia, [2] Federal Center for Animal Health (FGBI ARRIAH), Vladimir, Russia, [3] Federal Research Center for Virology and Microbiology, Pokrov, Russia, [4] Faculty of Geography, Lomonosov Moscow State University, Moscow, Russia

OPEN ACCESS

Edited by:
Yashpal S. Malik, Indian Veterinary Research Institute (IVRI), India

Reviewed by:
Giovanni Cilia, Council for Agricultural and Economics Research (CREA), Italy
Satparkash Singh, Guru Angad Dev Veterinary and Animal Sciences University, India

***Correspondence:**
Olga I. Zakharova
olenka.zakharova.1976@list.ru
Fedor I. Korennoy
korennoy@arriah.ru

†These authors share first authorship

Specialty section:
This article was submitted to Veterinary Epidemiology and Economics, a section of the journal Frontiers in Veterinary Science

Received: *26 January 2021*
Accepted: *15 March 2021*
Published: *12 April 2021*

Citation:
Zakharova OI, Korennoy FI, Iashin IV, Toropova NN, Gogin AE, Kolbasov DV, Surkova GV, Malkhazova SM and Blokhin AA (2021) Ecological and Socio-Economic Determinants of Livestock Animal Leptospirosis in the Russian Arctic. Front. Vet. Sci. 8:658675. doi: 10.3389/fvets.2021.658675

Leptospirosis is a re-emerging zoonotic infectious disease caused by pathogenic bacteria of the genus *Leptospira*. Regional differences in the disease manifestation and the role of ecological factors, specifically in regions with a subarctic and arctic climate, remain poorly understood. We here explored environmental and socio-economic features associated with leptospirosis cases in livestock animals in the Russian Arctic during 2000–2019. Spatial analysis suggested that the locations of the majority of 808 cases were in "boreal" or "polar" climate regions, with "cropland," "forest," "shrubland," or "settlements" land-cover type, with a predominance of "Polar Moist Cropland on Plain" ecosystem. The cases demonstrated seasonality, with peaks in March, June, and August, corresponding to the livestock pasturing practices. We applied the Forest-based Classification and Regression algorithm to explore the relationships between the cumulative leptospirosis incidence per unit area by municipal districts (G-rate) and a number of socio-economic, landscape, and climatic factors. The model demonstrated satisfactory performance in explaining the observed disease distribution ($R^2 = 0.82$, $p < 0.01$), with human population density, livestock units density, the proportion of crop area, and budgetary investments into agriculture per unit area being the most influential socio-economic variables. Climatic factors demonstrated a significantly weaker influence, with nearly similar contributions of mean yearly precipitation and air temperature and number of days with above-zero temperatures. Using a projected climate by 2100 according to the RCP8.5 scenario, we predict a climate-related rise of expected disease incidence across most of the study area, with an up to 4.4-fold increase in the G-rate. These results demonstrated the predominant influence of the population and agricultural production factors on the observed increase in leptospirosis cases in livestock animals in the Russian Arctic. These findings may contribute to improvement in the regional system of anti-leptospirosis measures and may be used for further studies of livestock leptospirosis epidemiology at a finer scale.

Keywords: Arctic, climate change, forest-based classification and regression algorithm, G-rate, leptospirosis, livestock, Russia, ArcGIS

INTRODUCTION

Animal leptospirosis is a re-emerging focal infectious disease (zoonosis) that is common in humans and animals globally (1–5). Over the past decades, inadequate attention has been directed toward the study of the disease and its impact on public health (6), particularly in countries with a temperate climate (7, 8). However, in recent years many reports and reviews of health organizations worldwide have highlighted leptospirosis as a growing problem as evidenced by the markedly increasing rates of mortality and incidence in both humans and animals in all continents (9, 10).

Apart from acute and chronic forms (11), genital leptospirosis is considered a specific syndrome unrelated to a systemic leptospirosis disease (12, 13) and caused by weakened leptospires that colonize urogenital organs. The transmission of pathogenic leptospires from animals to humans, and among animals within a population is influenced by numerous factors, including environmental (landscape and climatic) (14, 15) and anthropogenic (socio-economic) factors (14, 16, 17). According to some studies (18–20), climatic factors rank first among the common causes of endemicity and persistence of leptospirosis in tropical and subtropical countries (5, 21, 22). Globally, the prevalence of the disease varies from region to region depending on the geographic location. Regions and countries with high endemicity are characterized by hot humid weather, and tropical and subtropical climates, which contribute to the survival of pathogenic *Leptospira* in the external environment (23–25). In addition to the tropical climatic zones where environmental conditions are most favorable for survival of pathogenic *Leptospira*, the disease is also quite widespread among livestock in the temperate latitudes of the Eurasian continent (7, 8, 10). In the temperate zone, climatic changes (i.e., warming) could be one of the factors increasing the ability of *Leptospira* to survive in the environment (10, 25–27). Other factors contributing to the spread of infection among both humans and animals in these temperate zones are socio-economic phenomena, such as urbanization (17, 28), agricultural intensification (17, 29), as well as changes in the economic status of people, including poverty, homelessness, and even the presence of individual communities in poorly or sparsely populated urban areas (30), which may result in poor hygiene and rodent-borne infections (31–33).

Humans and animals carrying leptospires are direct sources of infection. The factors mediating transmission among livestock and humans, as well as the natural reservoirs of pathogenic *Leptospira*, are wild animals, including rodents, and the environment itself (34–36).

Scientific literature suggests that the etiological structure of the livestock with leptospirosis in Russia had not changed significantly over the last 40 years with the following prevailing serovars (37):

- In cattle: *Hebdomadis* - 34.13%, *Sejroe* - 27.25%, *Tarassovi* - 10.96%, *Pomona* - 6.65%, and *Grippotyphosa* - 6.03%;
- In pigs: *Pomona* - 41.60%, *Icterohaemorrhagiae* - 31.58%, and *Tarassovi*—14.44%;
- In small ruminants: *Icterohaemorrhagiae* - 35.62%, *Pomona*—17.75%, *Grippotyphosa*—14.84%, *Sejroe* - 7.48%, *Hebdomadis* - 6.68%, and *Tarassovi*- 6.31%;
- In equine: *Icterohaemorrhagiae* - 27.07%, *Grippotyphosa* - 22.67%, *Pomona*- 10.65%, *Tarassovi* - 10.12%, and *Canicola*—9.69%;
- In dogs: *Canicola* - 51.07% and *Icterohaemorrhagiae* - 26.86%.

This study aimed to gain a better understanding of the epidemiology of leptospirosis, particularly in the Arctic where there is a less dense livestock population and severe climate. Leptospirosis emergence under these conditions has been understudied. In this study, we analyzed the relationships between the cumulative leptospirosis incidence in livestock animals per unit area of the Russian Arctic and a number of potentially influential socio-economic and climatic factors. We also assessed the Forest-based Classification and Regression tool for predicting possible areas with an increased risk of an epidemic.

MATERIALS AND METHODS

Study Area

We studied the manifestation of leptospirosis in livestock animals in the regions located in the Arctic zone of the Russian Federation. The Russian Federation is administratively divided into 85 regions that are subdivided into secondary administrative units, which are the municipal and urban districts (hereinafter termed "districts"). The zone under consideration includes nine regions whose territories are crossed by the Arctic Circle: Arkhangelsk Oblast, Murmansk Oblast, Republic of Karelia, Republic of Komi, Yamalo-Nenets Autonomous Okrug, Nenets Autonomous Okrug, Krasnoyarsk Krai, Republic of Sakha (Yakutia), and Chukotka Autonomous Okrug. These regions are subdivided into 199 districts with areas varying from 4 to 798,000 km^2, while the population density varies from 0 to 2,896 people per km^2 (https://rosstat.gov.ru/free_doc/new_site/region_stat/arc_zona.html). Due to the high heterogeneity of population density, we excluded those areas with a population density exceeding the mean plus three standard deviations (i.e., representing outliers in population density) from further analysis. Such areas are represented by small but densely populated urban territories with a scarcity of agricultural livestock. Additionally, all the other districts with no livestock population were excluded. Thus, the total number of territorial units suitable for the analysis was 166. The majority of the study area lies north of 60°N; however, some of the Krasnoyarsk Krai districts extend southward, up to 52°N (**Figure 1**).

Leptospirosis Data

Data on the livestock leptospirosis cases for the 2000 to 2019 period were obtained from the regional veterinary services. Herein, a case is defined as a registered, laboratory-confirmed detection of leptospirosis in a geo-referenced population of animals (a herd or a farm). Cases were detected both by herd owners and during routine government monitoring. Under the state standard GOST 25386-91 (http://docs.cntd.ru/document/

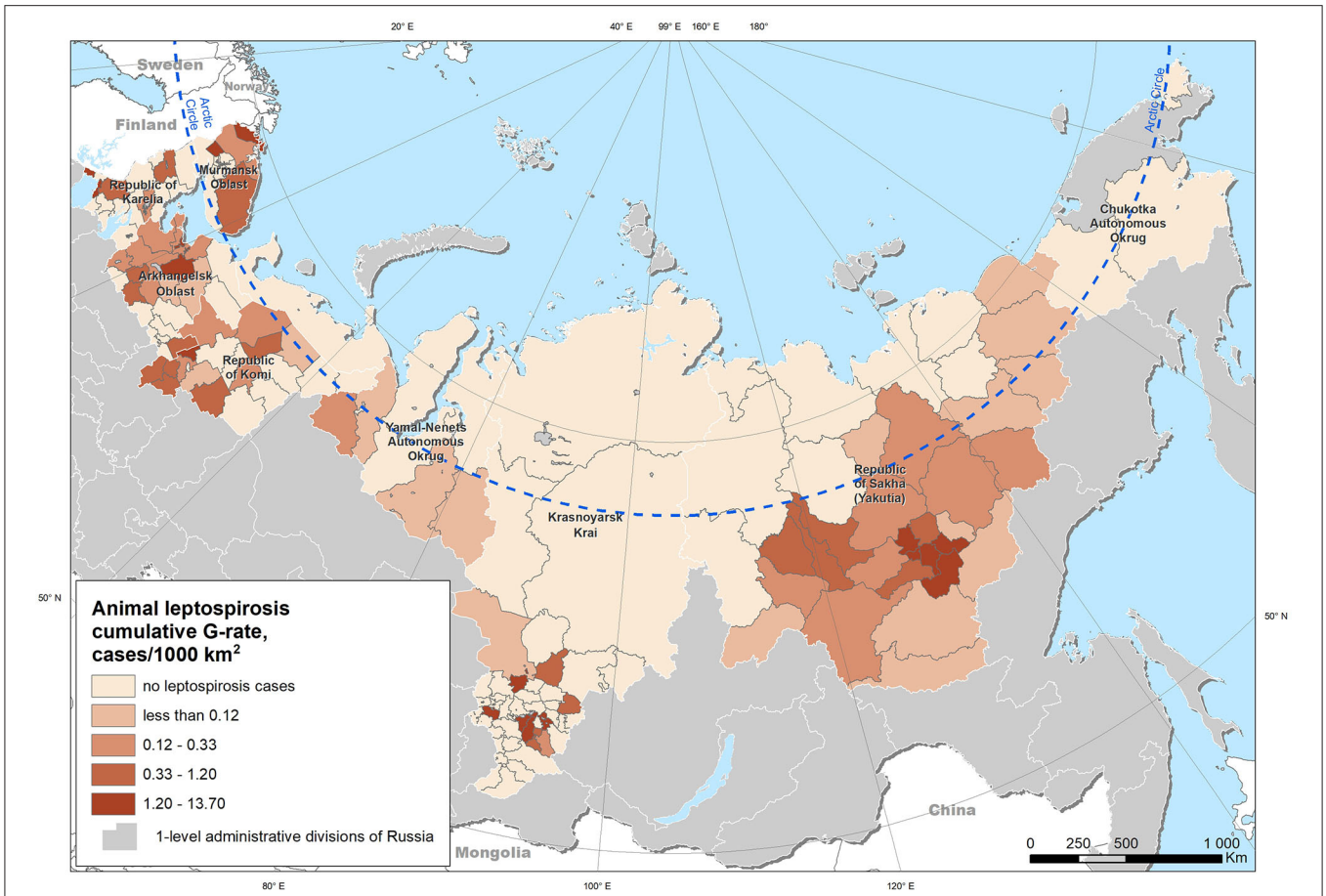

FIGURE 1 | Study area and cumulative leptospirosis G-rate in livestock (cases per 1,000 km^2) for the period from 2000 to 2019.

gost-25386-91), laboratory confirmation was performed using the microscopic agglutination test (MAT) method with a set of 7 reference cultures: *Pomona*, *Tarassovi*, *Canicola*, *Hebdomadis*, *Sejroe*, *Grippotyphosa*, and *Icterohaemorrhagiae* with preliminary testing on a reference culture previously identified as typical for the specific region. The reaction was evaluated with a positive cut-off using a serum dilution of 1:50 for unvaccinated animals and 1:100 for vaccinated animals with dark-field microscopy. For previously vaccinated animals, testing was conducted at least 3 months following the vaccination. In the case of a positive MAT result with no clinical signs, confirmatory testing using real-time polymerase chain reaction was conducted (38). After excluding data with inaccurate information or a lack of geographic coordinates, the database counted 808 cases among livestock animals. Most of them were cattle (398, 49%) and horses (314, 39%). **Figure 2** shows the distribution of cases by years. Leptospirosis location data were converted into a shape-file format for further modeling and processing.

Environmental and Socio-Economic Determinants

Several socio-economic, landscape, and climatic factors acting as geospatial explanatory variables were considered as potential determinants associated with the incidence of leptospirosis in the livestock according to an extensive literature search. The factors were as follows:

a. Socio-economic factors:

   1) *LSU_dens*—Livestock Unit Density index (units per 1 km^2), calculated according to the European Union methodology [https://ec.europa.eu/eurostat/statistics-explained/index.php?title=Glossary:Livestock_unit_(LSU)]
   2) *Pop_dens*—population density, people per km^2
   3) *Rural_prop*—the proportion of the rural population
   4) *Crop_prop*—the proportion of crop area in the total area of the region, as a factor presumably associated with the number of synanthropic rodents that are carriers of pathogenic *Leptospira*
   5) The volume of budgetary investments into the development of agriculture as a proxy for the level of financing of agriculture; relative indicators were considered: per unit area of the district (*Inv_area*) and per capita (*Inv_pop*).

b. Landscape factors:

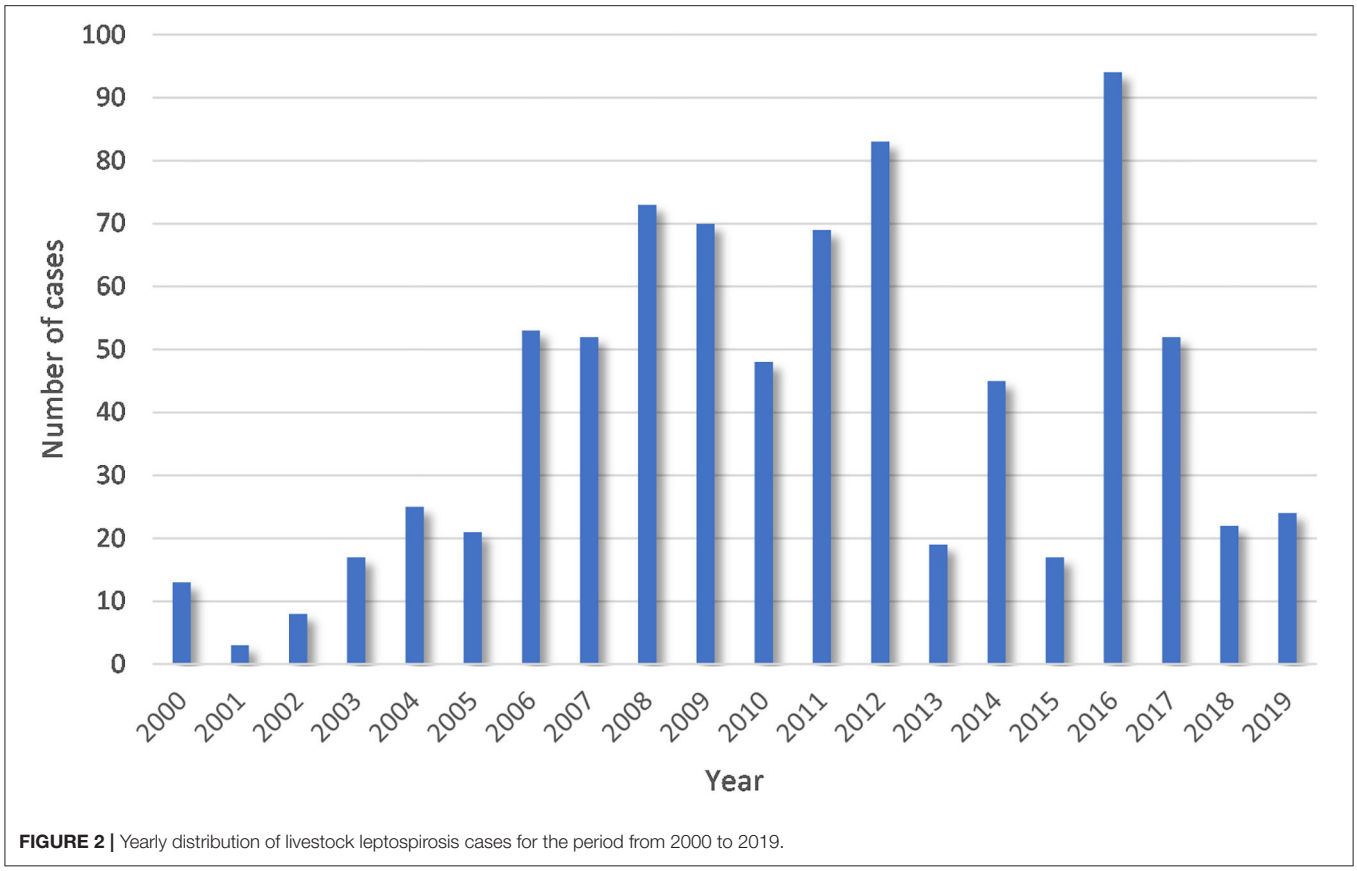

FIGURE 2 | Yearly distribution of livestock leptospirosis cases for the period from 2000 to 2019.

1) *Alt*—altitude, m
2) *Soil_pH*—soil pH
3) *Water_prop*—the proportion of water bodies in the total area of the region
4) *Swamp_prop*—the proportion of swamps in the total area of the region.

c. Climatic factors:

1) *Tasgod*—mean yearly air temperature, °C
2) *Tasamplit*—mean yearly amplitude of daily air temperature, °C
3) *Ndaytg0*—mean yearly number of days with the air temperature above 0°C, days
4) *Prgod*—yearly precipitation, mm
5) *Pr_tg0*—yearly precipitation for the period with the air temperature above 0°C, mm
6) *Pr_tl0*—yearly precipitation for the period with the air temperature below 0°C, mm.

The Federal State Statistics Service Rosstat (https://eng.gks.ru/) was used as a data source for socio-economic indicators. The altitude was calculated based on the GTOPO30 digital elevation model with a spatial resolution of 30" (https://earthexplorer.usgs.gov/). The soil pH data at zero depth were taken from the ISRIC World Soil Information digital database with a spatial resolution of 250 m (39). The water bodies and swamp areas were calculated using a land-cover dataset based on the Proba-V satellite system data with an initial spatial resolution of 100 × 100 m for the 2000 to 2018 period (40).

The climatic indicators were calculated based on the data of long-term observations at meteorological stations in the Russian Federation (41, 42) for the 1981 to 2015 ("current climate") period. Point data were interpolated and rasterized using the Kriging tool with a spatial resolution of 1 km^2 in ArcGIS software environment. To assess the possible change in the epidemiological situation for leptospirosis due to the expected climate change for the 2081 to 2100 period, a predictive set of the same parameters was also calculated based on 14 climate models included in the international CMIP5 project (43). The climate change scenario RCP8.5 was used, which represents the "most severe" projecting, with climate forcing due to both natural processes and anthropogenic impacts (44).

Additionally, we assessed the relationship of the leptospirosis cases to a particular ecosystem using the World Terrestrial Ecosystems map, which represents a dataset with a spatial resolution of 250 × 250 m consisting of 431 classes based on the unique combinations of temperature, precipitation, landforms, and vegetation/land-cover layers (45). A circular buffer with a radius of 2.5 km was created around the location of each leptospirosis case to account for potential inaccuracy of geolocation based on the veterinary services information that provided the data. The prevailing categories of the ecosystems

within the buffer zone were calculated using zonal statistics (ArcGIS, Esri).

Assessment of the Relationship Between Leptospirosis Incidence and Geospatial Factors

The cumulative number of leptospirosis cases for the entire observation period per unit area by the districts (G-rate) was chosen as a measure for the intensity of the leptospirosis epidemic within the study area (46–49). The Forest-based Classification and Regression method was applied to identify the relationships between the log-transformed G-rate and a set of potential explanatory factors (50, 51). This method is a supervised machine learning approach that uses a set of decision trees built using the observed values and variables in order to create a classification (in case of categorical variables) or a regression (for numeral variables). The method is based on the construction of a large number of decision trees, each resulting from a sample obtained from the initial training sample using bootstrapping (52). The final model was selected based on a majority vote. The regression estimation was performed by averaging the regression scores of all the individual trees. The advantage of this method is the ability to work with both continuous and categorical variables (in our study, only continuous variables were used), as well as elimination of overfitting of the model. In the present study, we used 1,000 decision trees for model training, with four randomly sampled variables per decision tree, and 1,000 decision trees for validation, with 25% of the input data randomly selected for validation. The initial training and validation of the model were performed for areas with non-zero cases of leptospirosis and with non-zero livestock units number ($N = 71$). The quality of the regression model was assessed using the coefficient of determination (R^2), which shows the proportion of data variation explained by the model. The R^2 was reported for: (1) training data, (2) validation data, and (3) the overall model prediction for the training districts. The model returns explanatory variables' importance metrics providing the "importance" and "percent" values. The former is based on the sum of all Gini coefficients, which could be assumed as the number of times a variable is responsible for a split, and the impact of that split divided by the number of decision trees, while the latter represents as the percentage of a given variable's Gini coefficients of the total sum of Gini coefficients (53, 54).

The absence of spatial clustering of regression residuals was verified using Global Moran's I index. The values of this index, which are near zero at a high p-value, confirm the null hypothesis of a random spatial distribution of the residuals. Furthermore, the model was used to predict the values in the rest of the study area, both using the parameters of the current climate and the projected climate. To provide accuracy of predictions, only those districts of the study area with the values of the primary explanatory factors within the range defined by the training districts ($N = 151$) were used. To visualize the expected change in the G-rate under a future climate, a map was created, which showed the ratio of its predicted to its current value for the training and predictive regression model.

Assessment of the Seasonality of Leptospirosis Emergence

To determine the seasonality of leptospirosis emergence, the seasonality index S was used and was calculated as the number of cases for a given month averaged over several years divided by the average annual number of cases for the corresponding year (55, 56). Additionally, seasonality was visualized using a radar chart.

Statistical Analysis

The statistical analysis of data was carried out using MS Office Excel (Microsoft, Redmond, WA, USA) with the @Risk v 4.5 simulation analysis package (Palisade Inc., Ithaca, NY, USA). The Forest-based Classification and Regression analysis as well as other spatial data processing and visualization were performed using the geographic information systems ArcGIS Pro 2.6.1 and ArcMap 10.8.1 (Esri, Redlands, CA, USA).

RESULTS

Epidemiological Analysis

Between 2000 and 2019, 808 cases of leptospirosis in livestock were recorded in the subarctic and Arctic regions of Russia. Based on the distribution of the detected cases by year (**Figure 2**), there appears to be three periods during which an increase in incidence was observed: 2000 to 2005, 2006 to 2013, and 2014 to 2019.

The calculation of the seasonality index revealed the prevalence of the relative number of cases in March as S = 1.53 (95% CI: 0–4.00), in June as S = 2.27 (0–5.76), and in August as S = 1.73 (0–9.6).

Spatial Analysis and Regression Modeling

An analysis of location of the leptospirosis cases, considering a 2.5-km buffer zone reflecting the possible uncertainty in geolocation, showed that all cases occurred in the polar or boreal climatic regions, with a predominance of croplands, forests, shrublands, and settlements as land-cover types. Most of the cases occurred in the "Polar Moist Cropland on Plains" ecological zone (**Figure 3**). Thus, even the most southern of the analyzed cases may still be considered as having an Arctic climate.

Training of a model based on the Forest-based Classification and Regression algorithm using known data on the leptospirosis incidence (G-rate) showed a high model fit to the training data ($R^2 = 0.94 \pm 0.03$; p-value ≤ 0.001) and an acceptable fit to the validation data ($R^2 = 0.53 \pm 0.10$; p-value ≤ 0.001). The relative importance of the variables based on the simulation results is shown in **Table 1**. The results clearly demonstrated that socio-economic factors (population density, the proportion of cropland, the density of agricultural livestock, and financial investments in agriculture per unit area) were of the greatest importance for explaining the observed distribution of leptospirosis cases, while the role of climatic and landscape factors was less significant. The test of regression residuals for spatial autocorrelation showed no tendency for residual clustering (Moran's I = −0.003; z-score = −0.227; p-value = 0.820). Comparison of the predicted and observed log G-rate

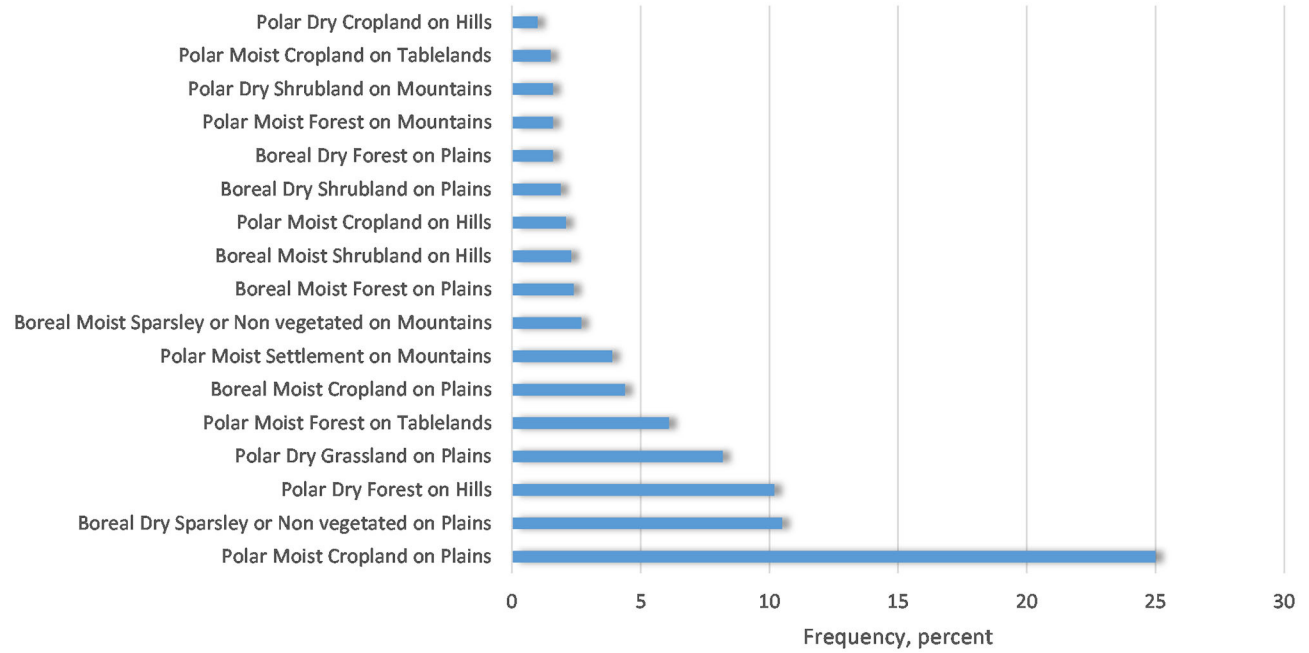

FIGURE 3 | Distribution of the leptospirosis cases in relation to ecosystems.

TABLE 1 | Relative importance of variables based on random forest-based classification and regression analysis results.

Variable	Importance	%
Population density	24.3	21
The proportion of crop area in the total area of the region	15.71	14
Livestock Unit Density index	14.55	13
Budgetary investments into the development of agriculture per unit area	12.99	11
Yearly precipitation for the period with the air temperature above 0°C	5.04	4
Mean yearly air temperature	4.97	4
Yearly precipitation	4.52	4
Mean yearly number of days with the air temperature above 0°C	4.45	4
Proportion of the rural population	4.13	4
Altitude	4.08	4
Mean yearly amplitude of daily air temperature	4.04	4
Proportion of swamps in the total area of the region	4.01	4
Soil PH	3.89	3
Proportion of water bodies in the total area of the region	3.87	3
Yearly precipitation for the period with the air temperature below 0°C	2.7	2

demonstrates a satisfactory model fit to the training data with $R^2 = 0.82$, p-value < 0.05 (**Figure 4**).

Extrapolation of the model obtained from the entire study area under the "current" climatic conditions yielded a map of the expected case density (**Figure 5**). Modeling using climatic indicators for the projected climate for the period up to 2100 demonstrated an expected increase in the risk of leptospirosis in most of the study area (**Figure 6**). The greatest increase in the leptospirosis risk was observed in the northern part of European Russia and Western Siberia. In some of these areas, the climate-dependent risk of leptospirosis was predicted to increase by more than 4-fold.

DISCUSSION

In this study, we investigated the epidemiology of leptospirosis in livestock in the Arctic zone. We demonstrated the utility of the Forest-based Classification and Regression method as a tool for obtaining valuable information on the significance of factors contributing to the occurrence of leptospirosis, as well as their possible changes under various climate scenarios in the Arctic and subarctic regions of Russia. Despite the formal discrepancy between the southern part of the model region and the concept of the "Arctic zone," our analysis demonstrates that all the considered cases of leptospirosis occurred in the polar and boreal climatic zones. Considering the selected scale of the study, socio-economic factors including population density of this region and the intensity of agricultural activity were associated with leptospirosis in this territory. In terms of landscape and climatic factors, the precipitation and temperature regime, including the mean yearly number of days with temperatures above 0°C, were identified as predominant climatic determinants, although they provided significantly lower contributions as compared to the above socio-economic variables. We also show the possible risk of future changes in

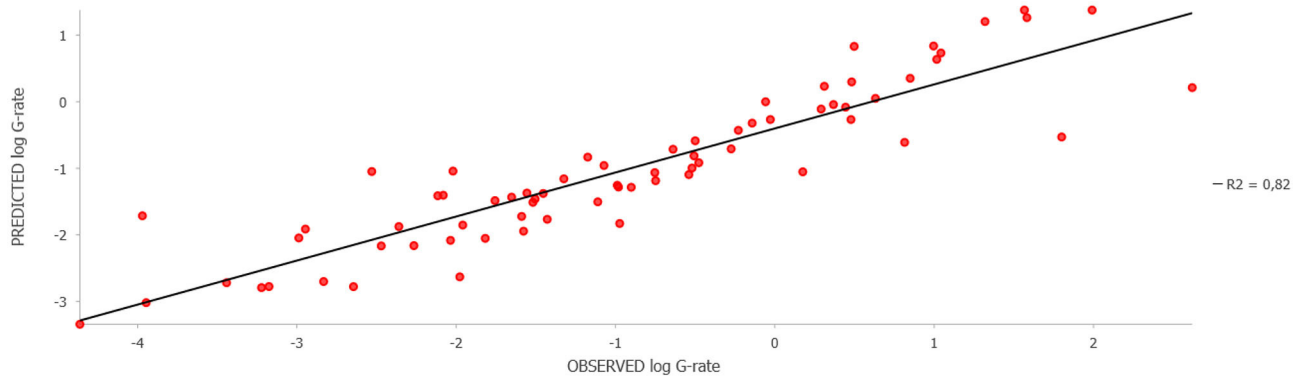

FIGURE 4 | Observed vs. Predicted animal leptospirosis log G-rate as per the model fit to the training districts.

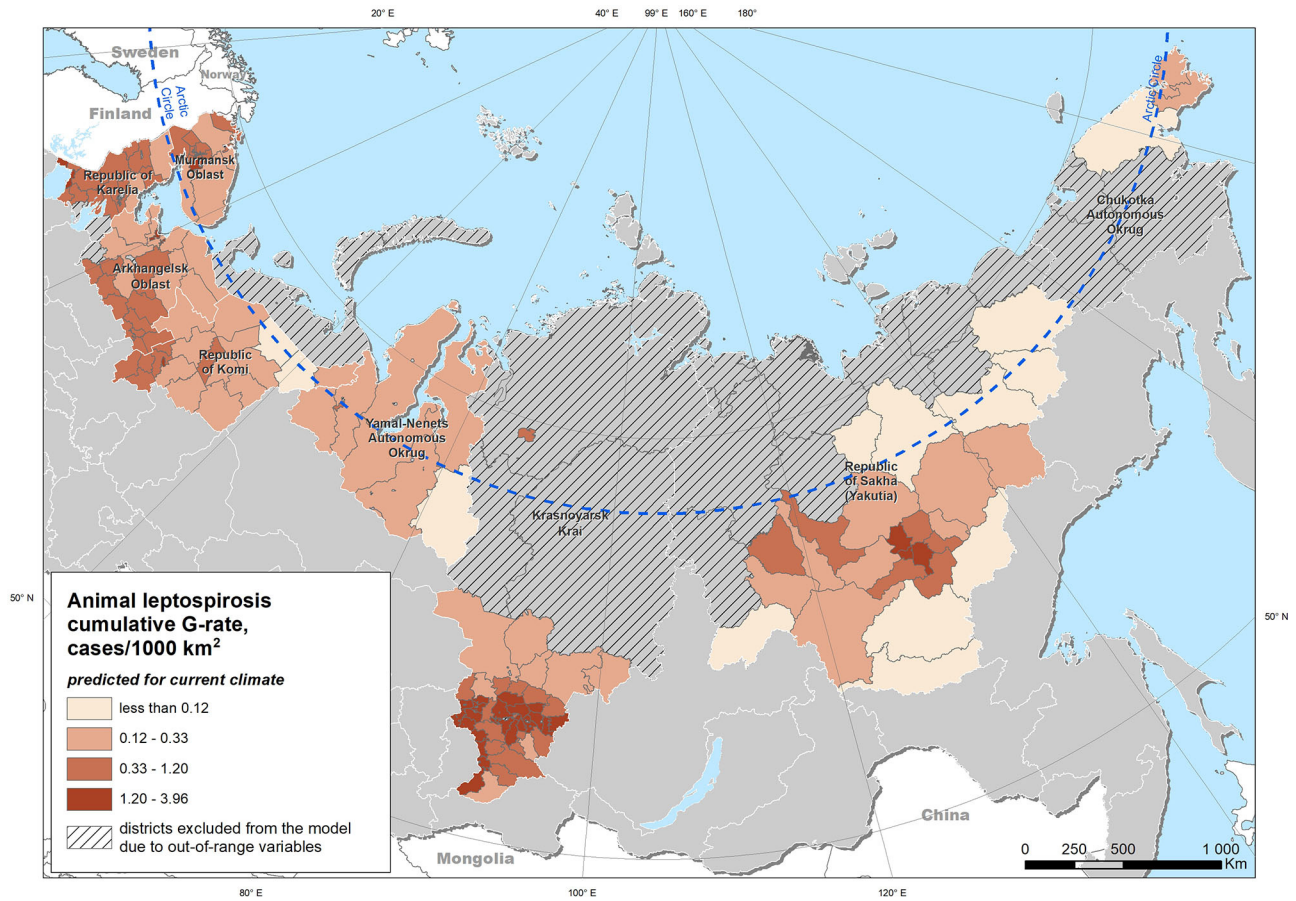

FIGURE 5 | Distribution of the predicted density of leptospirosis cases (G-rate) under the current climate conditions.

the leptospirosis epidemic situation under the most unfavorable climate change scenario.

Our results support previous reports that agricultural intensification may increase the outbreaks of zoonotic diseases, such as leptospirosis (57–62). However, while the high density of commercial dairy farms similarly increased the risk of infection in both urban and rural areas, investment (insufficient fund infusions) in agriculture has an equally significant impact on the formation of risk zones.

Leptospirosis is characterized by seasonality to some extent, although individual cases of the disease do occur throughout the year. By some accounts (10, 25), in temperate climates, the

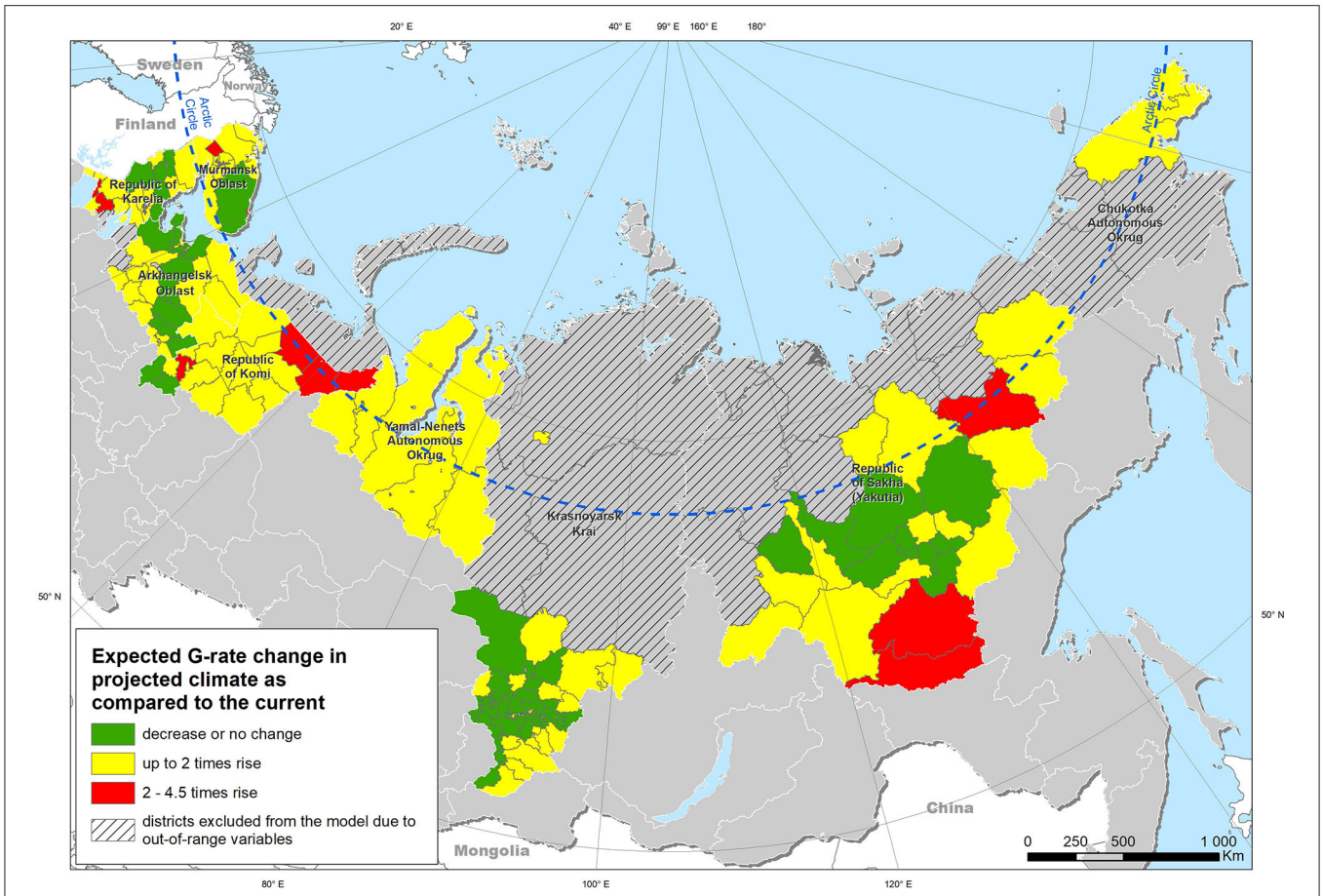

FIGURE 6 | Expected change in the density of leptospirosis cases under projected climate conditions in comparison with the current climate, based on modeled changes in climatic factors.

summer seasonality of leptospirosis is expressed as disease in cattle, which is explained by animals being on pastures more often in this season leading to a wider contact with leptospirosis carriers and alimentary transmission of the pathogen through fodder and water from open reservoirs (26, 27, 63). Based on the epidemiological analysis of monthly data throughout the year, we observed a pronounced seasonality of the disease in the spring–summer period. This pattern is regularly repeated over the years due to changes in climatic conditions, faunistic, and economic-organizational factors, which leads to activation of the mechanism of pathogenic transmission from their source to susceptible animals. The seasonality analysis suggests that the incidence of leptospirosis in livestock has two peaks—it starts in January and gradually increases to March (15.13%) and then declines until May. The peak incidence in March may be associated with the active migration of synanthropic rodents from natural wintering areas, where food supplies are depleted, to human habitats and livestock keeping areas, which entails an increase in contact with livestock animals. The second peak in incidence is observed in June (18.32%), which may be associated with climatic factors favorable to the accumulation of the causative agent in the external environment and the active interaction of the susceptible livestock with leptospirosis carriers.

Based on our results, climatic factors showed a significantly lower correlation with the areas showing an increased concentration of leptospirosis cases. This could be explained, firstly, by the selected scale of the study implying that the socio-economic variables have a predominant influence on the scale of the whole region, determining the intensity of the epidemic manifestation of the disease. Nevertheless, the most significant indicator among climatic factors was the mean yearly number of days with air temperatures above 0°, which was in good agreement with the previous studies' results (63–66). The next most important climatic factors were also indicators related to air temperature: the mean yearly amplitude of daytime temperature and the mean yearly air temperature. A significant relationship was also revealed with the proportion of swamps in the total area of the region, which is consistent with previously recognized environmental factors conducive to leptospirosis (57, 63, 67).

A total number of 808 leptospirosis cases over the whole study period of 20 years yields relatively small average yearly numbers

per study district (<1) that makes it difficult to implement space-time regression models. Hence, in our study we considered the aggregated number of cases per unit area throughout the whole study period, which provides response variable values more suitable for modeling.

The Forest-based Classification and Regression method is a popular machine learning method used in classification and forecasting. This tool allows analysts to easily incorporate tabular attributes, features, and explanatory rasters when building predictive models, and expands predictive modeling capabilities to be accessible to all geographic information system (GIS) users. Our research demonstrated the effectiveness of the spatial Forest-based Classification and Regression algorithm for analyzing results under various climate change scenarios. The integration of the Forest-based Classification and Regression tool as a spatial algorithm for exploring these factors makes it easier to consider different scenarios than using traditional regression methods due to reduced demands on the input data distribution and format.

Nevertheless, the study had some limitations in terms of the method used. First, there were a limited number of spatial units available for analysis. As a data-driven method, the Forest-based Classification and Regression tool performs better with large datasets [at least several hundred input analysis units according to the method guidance provided by the software producer (68), while in our study, we used 71 districts for model training and 151 districts for prediction]. However, some studies have reported successful implementation of this approach on relatively small datasets (69, 70). Increased number of trees (1,000 in our study) allows reducing out-of-bag errors, which represent portions of data not participating in trees' construction. Second, there is uncertainty regarding the binding of specific values to a territorial unit, as the variation in climatic parameters presented in raster form within the districts can be significant. The socio-economic factors, expressed as density indicators over the entire territory of the region, may also inadequately reflect the true significance of the factor in the places of actual registration of leptospirosis.

It should also be noted that our forecast is based only on the expected changes in climate in the future, which according to our model has a significantly smaller effect on the concentration of leptospirosis cases than the socio-economic determinants. Thus, a change in the structure of animal farming, expansion of cultivated areas, financial support for agriculture, and the occupation of new territories could collectively have a much stronger impact on the leptospirosis incidence outweighing the influence of climatic factors.

CONCLUSIONS

Our study provided empirical evidence that the factors involved in transmission of leptospirosis in the Arctic and subarctic regions of Russia are complex and include environmental and socio-demographic indicators. The assessment of the significance of the main factors (socio-economic and climatic) when using the Forest-based Classification and Regression method indicated that the main contribution to the increased incidence of leptospirosis is from socio-economic conditions related to the population agricultural activity. Indicators of precipitation and temperature regime were the predominant contributors among the climatic factors.

The information obtained in this study on the risk factors for livestock leptospirosis outbreaks supports the One Health approach to animal disease prevention and control, which takes into account anthropogenic factors, animal density distribution factors, and the environment. Future research should be specifically designed to assess the impact of interventions under different scenarios.

DATA AVAILABILITY STATEMENT

The raw data supporting the conclusions of this article will be made available by the authors, without undue reservation.

AUTHOR CONTRIBUTIONS

OZ, AB, and FK: conceptualization. FK and OZ: methodology, software, writing—original draft preparation, and visualization. AB and FK: validation. FK, OZ, and GS: formal analysis. OZ and NT: investigation. NT, SM, and GS: resources. FK and AG: data curation. FK, AB, OZ, and SM: writing—review and editing. AB, II, and AG: supervision. AB, FK, and DK: project administration. All authors have read and agree to the published version of the manuscript.

FUNDING

The work was supported by the Federal Research Center for Virology and Microbiology (FRCVM) for government assignment; research project #FGNM-2021-0004.

REFERENCES

1. Breneva NV, Balakhonov SV. Endemicity and enzooticity aspects of leptospirosis. *J Microbiol Epidemiol Immunobiol.* (2019) 0:118–25. doi: 10.36233/0372-9311-2019-5-118-125
2. Bolin C. Leptospirosis. In: Brown C, Bolin C, editors. *Emerging Diseases of Animals*. Washington, DC: ASM Press. p. 185–200.
3. Ellis WA. Animal leptospirosis. *Curr Top Microbiol Immunol.* (2015) 387:99–137. doi: 10.1007/978-3-662-45059-8_6
4. Guglielmini J, Bourhy P, Schiettekatte O, Zinini F, Brisse S, Picardeau M. Genus-wide Leptospira core genome multilocus sequence typing for strain taxonomy and global surveillance. *PLoS Negl Trop Dis.* (2019) 13:e0007374. doi: 10.1371/journal.pntd.0007374
5. Guernier V, Goarant C, Benschop J, Lau CL. A systematic review of human and animal leptospirosis in the Pacific Islands reveals pathogen and reservoir diversity. *PLoS Negl Trop Dis.* (2018) 12:e0006503. doi: 10.1371/journal.pntd.0006503
6. Guerra MA. Leptospirosis: public health perspectives. *Biologicals*. (2013) 41:295–7. doi: 10.1016/j.biologicals.2013.06.010
7. Wasiński B. [Leptospirosis–current problems]. *Przeglad Epidemiol.* (2011) 65:471–476.

8. Wasiński B, Dutkiewicz J. Leptospirosis – current risk factors connected with human activity and the environment. *Ann Agric Environ Med.* (2013) 20:239–44.
9. Costa F, Hagan JE, Calcagno J, Kane M, Torgerson P, Martinez-Silveira MS, et al. Global morbidity and mortality of leptospirosis: a systematic review. *PLoS Negl Trop Dis.* (2015) 9:e0003898. doi: 10.1371/journal.pntd.0003898
10. Dufour B, Moutou F, Hattenberger AM, Rodhain F. Global change: impact, management, risk approach and health measures–the case of Europe. *Rev Sci Tech.* (2008) 27:529–50. doi: 10.20506/rst.27.2.1817
11. OIE Terrestrial Manual. *Chapter 3.1.12. Leptospirosis* (2018). Available online at: https://www.oie.int/fileadmin/Home/eng/Health_standards/tahm/3.01.12_LEPTO.pdf (accessed February 02, 2021).
12. Cilia G, Bertelloni F, Piredda I, Ponti MN, Turchi B, Cantile C, et al. Presence of pathogenic leptospira spp. In the reproductive system and fetuses of wild boars (sus scrofa) in Italy. *PLoS Negl Trop Dis.* (2020) 14:e0008982. doi: 10.1371/journal.pntd.0008982
13. Loureiro AP, Lilenbaum W. Genital bovine leptospirosis: a new look for an old disease. *Theriogenology.* (2020) 141:41–7. doi: 10.1016/j.theriogenology.2019.09.011
14. Mwachui MA, Crump L, Hartskeerl R, Zinsstag J, Hattendorf J. Environmental and behavioural determinants of leptospirosis transmission: a systematic review. *PLoS Negl Trop Dis.* (2015) 9:e0003843. doi: 10.1371/journal.pntd.0003843
15. Rood EJJ, Goris MGA, Pijnacker R, Bakker MI, Hartskeerl RA. Environmental risk of leptospirosis infections in the Netherlands: Spatial modelling of environmental risk factors of leptospirosis in the Netherlands. *PLoS ONE.* (2017) 12:1–11. doi: 10.1371/journal.pone.0186987
16. Gottdenker NL, Streicker DG, Faust CL, Carroll CR. Anthropogenic land use change and infectious diseases: a review of the evidence. *Ecohealth.* (2014) 11:619–32. doi: 10.1007/s10393-014-0941-z
17. Slingenbergh J, Gilbert M, De Balogh K, Wint W. Ecological sources of zoonotic diseases. *OIE Rev Sci Tech.* (2004) 23:467–84. doi: 10.20506/rst.23.2.1492
18. Lau CL, Smythe LD, Craig SB, Weinstein P. Climate change, flooding, urbanisation and leptospirosis: fuelling the fire? *Trans R Soc Trop Med Hyg.* (2010) 104:631–8. doi: 10.1016/j.trstmh.2010.07.002
19. Hedlund C, Blomstedt Y, Schumann B. Association of climatic factors with infectious diseases in the Arctic and subarctic region - a systematic review. *Glob Health Action.* (2014) 7:1–6. doi: 10.3402/gha.v7.24161
20. Mayfield HJ, Lowry JH, Watson CH, Kama M, Nilles EJ, Lau CL. Use of geographically weighted logistic regression to quantify spatial variation in the environmental and sociodemographic drivers of leptospirosis in Fiji: a modelling study. *Lancet Planet Heal.* (2018) 2:e223–32. doi: 10.1016/S2542-5196(18)30066-4
21. Karnad DR, Richards GA, Silva GS, Amin P. Tropical diseases in the ICU: A syndromic approach to diagnosis and treatment. *J Crit Care.* (2018) 46:119–26. doi: 10.1016/j.jcrc.2018.03.025
22. Schneider MC, Jancloes M, Buss DF, Aldighieri S, Bertherat E, Najera P, et al. Leptospirosis: a silent epidemic disease. *Int J Environ Res Public Health.* (2013) 10:7229–34. doi: 10.3390/ijerph10127229
23. Garba B, Bahaman AR, Bejo SK, Zakaria Z, Mutalib AR, Bande F. Major epidemiological factors associated with leptospirosis in Malaysia. *Acta Trop.* (2018) 178:242–7. doi: 10.1016/j.actatropica.2017.12.010
24. Wójcik-Fatla A, Zajac V, Wasinski B, Sroka J, Cisak E, Sawczyn A, et al. Occurrence of Leptospira DNA in water and soil samples collected in eastern Poland. *Ann Agric Environ Med.* (2014) 21:730–2. doi: 10.5604/12321966.1129924
25. Henry RA, Johnson RC. Distribution of the genus Leptospira in soil and water. *Appl Environ Microbiol.* (1978) 35:492–9. doi: 10.1128/AEM.35.3.492-499.1978
26. Revich B, Tokarevich N, Parkinson AJ. Climate change and zoonotic infections in the Russian Arctic. *Int J Circumpolar Health.* (2012) 71:18792. doi: 10.3402/ijch.v71i0.18792
27. Fedorov EI, Haglov VA, Chepiga LP, Shvarsalon KN, Shumkova MS. Morfologiia prirodnogo ochaga leptospiroza Pomona stepnoi zony. *Zh Mikrobiol Epidemiol Immunobiol.* (1986) 32–35.
28. White RJ, Razgour O. Emerging zoonotic diseases originating in mammals: a systematic review of effects of anthropogenic land-use change. *Mamm Rev.* (2020) 50:336–52. doi: 10.1111/mam.12201
29. Miyama T, Watanabe E, Ogata Y, Urushiyama Y, Kawahara N, Makita K. Herd-level risk factors associated with Leptospira Hardjo infection in dairy herds in the southern Tohoku, Japan. *Prev Vet Med.* (2018) 149:15–20. doi: 10.1016/j.prevetmed.2017.11.008
30. Rajala EL, Sattorov N, Boqvist S, Magnusson U. Bovine leptospirosis in urban and peri-urban dairy farming in low-income countries: a "One Health" issue? *Acta Vet Scand.* (2017) 59:83. doi: 10.1186/s13028-017-0352-6
31. Cosson J-F, Picardeau M, Mielcarek M, Tatard C, Chaval Y, Suputtamongkol Y, et al. Epidemiology of leptospira transmitted by rodents in Southeast Asia. *PLoS Negl Trop Dis.* (2014) 8:e2902. doi: 10.1371/journal.pntd.0002902
32. Denipitiya DTH, Chandrasekharan N V., Abeyewickreme W, Hartskeerl RA, Hapugoda MD. Identification of cattle, buffaloes and rodents as reservoir animals of Leptospira in the District of Gampaha, Sri Lanka. *BMC Res Notes.* (2017) 10:134. doi: 10.1186/s13104-017-2457-4
33. Moseley M, Rahelinirina S, Rajerison M, Garin B, Piertney S, Telfer S. Mixed leptospira infections in a diverse reservoir host community, Madagascar, 2013–2015. *Emerg Infect Dis.* (2018) 24:1138–40. doi: 10.3201/eid2406.180035
34. Grimm K, Rivera NA, Fredebaugh-Siller S, Weng HY, Warner RE, Maddox CW, et al. Evidence of leptospira serovars in wildlife and leptospiral dna in water sources in a natural area in East-Central Illinois, USA. *J Wildl Dis.* (2020) 56:316–27. doi: 10.7589/2019-03-069
35. Cilia G, Bertelloni F, Angelini M, Cerri D, Fratini F. Leptospira survey in wild boar (Sus scrofa) hunted in tuscany, central italy. *Pathogens.* (2020) 9:377. doi: 10.3390/pathogens9050377
36. Vincent AT, Schiettekatte O, Goarant C, Neela VK, Bernet E, Thibeaux R, et al. Revisiting the taxonomy and evolution of pathogenicity of the genus Leptospira through the prism of genomics. *PLoS Negl Trop Dis.* (2019) 13:e0007270. doi: 10.1371/journal.pntd.0007270
37. Soboleva GL. *Prevalence, Etiological Structure and Specific Prophylactics of Leptospirosis in Animals* (Doctoral thesis in biology) (2001). Available online at: http://medical-diss.com/docreader/66243/d?#?page=6 (accessed 25.02.2021) [in Russian].
38. Zakharova OI, Korennoy FI, Toropova NN, Burova OA, Blokhin AA. Environmental risk of leptospirosis in animals: the case of the Republic of Sakha (Yakutia), Russian Federation. *Pathogens.* (2020) 9:504. doi: 10.3390/pathogens9060504
39. Hengl T, Mendes de Jesus J, Heuvelink GBM, Ruiperez Gonzalez M, Kilibarda M, Blagotić A, et al. SoilGrids250m: Global gridded soil information based on machine learning. *PLoS ONE.* (2017) 12:e0169748. doi: 10.1371/journal.pone.0169748
40. Egorov VA, Bartalev SA, Kolbudaev PA, Plotnikov DE, Khvostikov SA. Land cover map of Russia derived from Proba-V satellite data. *Sovrem Probl Distantsionnogo Zo Zemli izKosmosa.* (2018) 15:282–6. doi: 10.21046/2070-7401-2018-15-2-282-286
41. *Daily Temperature and Precipitation Data from 223 Former-USSR Stations*. Available online at: https://cdiac.ess-dive.lbl.gov/ndps/ndp040.html (accessed October 24, 2020).
42. Bulygina ON, Razuvaev VN, Aleksandrova TM. *Description of the Data Array of Daily Air Temperature and the Quantity of Precipitation at Meteorological Stations in Russia and the Former USSR (TTTR) "Certificate of state registration of the database No. 2014620942.* Available online at: http://meteo.ru/data/162-temperature-precipitation#описание-массива-данных (accessed October 24, 2020).
43. Taylor KE, Stouffer RJ, Meehl GA. An overview of CMIP5 and the experiment design. *Bull Am Meteorol Soc.* (2012) 93:485–98. doi: 10.1175/BAMS-D-11-00094.1
44. Moss R, Babiker M, Brinkman S, Calvo E, Carter T, Edmonds J, et al. Towards new scenarios for analysis of emissions, climate change, impacts, and response strategies. *Intergovernmental Panel on Climate Change* (Geneva), 132. Available online at: https://archive.ipcc.ch/pdf/supporting-material/expert-meeting-report-scenarios.pdf

45. Pisut D, A New Map of World Terrestrial Ecosystems. ArcGIS Blog. Esri (2020). URL: https://www.esri.com/arcgis-blog/products/arcgis-living-atlas/mapping/world-ecosystems/ (accessed 24.10.2020)
46. Chen K, Horton RM, Bader DA, Lesk C, Jiang L, Jones B, et al. Impact of climate change on heat-related mortality in Jiangsu Province, China. *Environ Pollut.* (2017) 224:317–25. doi: 10.1016/j.envpol.2017.02.011
47. Chen X, Wang K. Geographic area-based rate as a novel indicator to enhance research and precision intervention for more effective HIV/AIDS control. *Prev Med Rep.* (2017) 5:301–7. doi: 10.1016/j.pmedr.2017.01.009
48. Kanankege KST, Abdrakhmanov SK, Alvarez J, et al. Comparison of spatiotemporal patterns of historic natural Anthrax outbreaks in Minnesota and Kazakhstan. *PLoS ONE.* (2019) 14:e0217144. doi: 10.1371/journal.pone.0217144
49. Kanankege KST, Alvarez J, Zhang L, Perez AM. An introductory framework for choosing spatiotemporal analytical tools in population-level eco-epidemiological research. *Front Vet Sci.* (2020) 7:339. doi: 10.3389/fvets.2020.00339
50. Breiman L. Random forests. *Mach Learn.* (2001) 45:5–32. doi: 10.1023/A:1010933404324
51. Breiman L, Friedman JH, Olshen RA, Stone CJ. *Classification and Regression Trees 1, Breiman, Leo - Amazon.com* (2017). Available online at: https://www.amazon.com/Classification-Regression-Trees-Leo-Breiman-ebook/dp/B076M7QKC6 (accessed October 28, 2020).
52. Chistyakov SP. Random forests-overview: review. *Proc Karelian Sci Cent Russ Acad Sci.* (2013) 1:117–136. [In Russian]. Available online at: http://resources.krc.karelia.ru/transactions/doc/trudy2013/trudy_2013_1_117-136.pdf
53. Loh WY, Shih YS. Split selection methods for classification trees. *Stat Sin.* (1997) 7:815–40.
54. Grömping U. Variable importance assessment in regression: linear regression versus random forest. *Am Stat.* (2009) 63:308–19. doi: 10.1198/tast.2009.08199
55. Seasonal Index. *The Concise Encyclopedia of Statistics*. New York, NY: Springer. p. 476–9.
56. Abdrakhmanov SK, Tyulegenov SB, Korennoy FI, Sultanov AA, Sytnik II, Beisembaev KK, et al. Spatiotemporal analysis of foot-and-mouth disease outbreaks in the Republic of Kazakhstan, 1955 – 2013. *Transbound Emerg Dis.* (2018) 65:1235–45. doi: 10.1111/tbed.12864
57. Goarant C. Leptospirosis: risk factors and management challenges in developing countries. *Res Rep Trop Med.* (2016) 7:49–62. doi: 10.2147/RRTM.S102543
58. Jones BA, Grace D, Kock R, Alonso S, Rushton J, Said MY, et al. Zoonosis emergence linked to agricultural intensification and environmental change. *Proc Natl Acad Sci U S A.* (2013) 110:8399–404. doi: 10.1073/pnas.1208059110
59. Riley LW, Ko AI, Unger A, Reis MG. Slum health: diseases of neglected populations. *BMC Int Health Hum Rights.* (2007) 7:1–6. doi: 10.1186/1472-698X-7-2
60. Vlahov D, Freudenberg N, Proietti F, Ompad D, Quinn A, Nandi V, et al. Urban as a determinant of health. *J Urban Heal.* (2007) 84:16–26. doi: 10.1007/s11524-007-9169-3
61. Reis RB, Ribeiro GS, Felzemburgh RDM, Santana FS, Mohr S, Melendez AXTO, et al. Impact of environment and social gradient on Leptospira infection in urban slums. *PLoS Negl Trop Dis.* (2008) 2:228. doi: 10.1371/journal.pntd.0000228
62. Scovronick N, Lloyd SJ, Kovats RS. Climate and health in informal urban settlements. *Environ Urban.* (2015) 27:657–78. doi: 10.1177/0956247815596502
63. Nichols G, Lake I, Heaviside C. Climate change and water-related infectious diseases. *Atmosphere.* (2018) 9:385. doi: 10.3390/atmos9100385
64. Chadsuthi S, Modchang C, Lenbury Y, Iamsirithaworn S, Triampo W. Modeling seasonal leptospirosis transmission and its association with rainfall and temperature in Thailand using time-series and ARIMAX analyses. *Asian Pac J Trop Med.* (2012) 5:539–46. doi: 10.1016/S1995-7645(12)0095-9
65. Sumi A, Telan EFO, Chagan-Yasutan H, Piolo MB, Hattori T, Kobayashi N. Effect of temperature, relative humidity and rainfall on dengue fever and leptospirosis infections in Manila, the Philippines. *Epidemiol Infect.* (2017) 145:78–86. doi: 10.1017/S095026881600203X
66. Joshi YP, Kim E-H, Cheong H-K. The influence of climatic factors on the development of hemorrhagic fever with renal syndrome and leptospirosis during the peak season in Korea: an ecologic study. *BMC Infect Dis.* (2017) 17:406. doi: 10.1186/s12879-017-2506-6
67. Ghneim GS, Viers JH, Chomel BB, Kass PH, Descollonges DA, Johnson ML. Use of a case-control study and geographic information systems to determine environmental and demographic risk factors for canine leptospirosis. *Vet Res.* (2007) 38:37–50. doi: 10.1051/vetres:2006043
68. *How Forest Based Classification and Regression Works*. Esri ArcGIS Pro online help, v.2.7 (2021). Available online at: https://pro.arcgis.com/ru/pro-app/latest/tool-reference/spatial-statistics/how-forest-works.htm (accessed February 27, 2021).
69. Shaikhina T, Lowe D, Daga S, Briggs D, Higgins R, Khovanova N. Decision tree and random forest models for outcome prediction in antibody incompatible kidney transplantation. *Biomed Signal Process Control.* (2019) 52:456–62. doi: 10.1016/j.bspc.2017.01.012
70. Robinson GA, Peng J, Dönnes P, Coelewij L, Naja M, Radziszewska A, et al. Disease-associated and patient-specific immune cell signatures in juvenile-onset systemic lupus erythematosus: patient stratification using a machine-learning approach. *Lancet Rheumatol.* (2020) 2:e485–96. doi: 10.1016/S2665-9913(20)30168-5

Conflict of Interest: The authors declare that the research was conducted in the absence of any commercial or financial relationships that could be construed as a potential conflict of interest.

frontiers in Veterinary Science

REVIEW
published: 13 April 2021
doi: 10.3389/fvets.2021.572012

Aerosol Transmission of Coronavirus and Influenza Virus of Animal Origin

Jing Lv[1,2†], *Jing Gao*[3†], *Bo Wu*[1], *Meiling Yao*[1], *Yudong Yang*[1], *Tongjie Chai*[1*] *and Ning Li*[1*]

[1] Shandong Provincial Key Laboratory of Animal Biotechnology and Disease Control and Prevention, Sino-German Cooperative Research Center for Zoonosis of Animal Origin Shandong Province, Shandong Provincial Engineering Technology Research Center of Animal Disease Control and Prevention, College of Animal Science and Veterinary Medicine, Shandong Agricultural University, Taian, China, [2] Center for Disease Control and Prevention, Taian, China, [3] Taian Central Hospital, Taian, China

Coronavirus disease 2019 (COVID-19) caused by severe acute respiratory syndrome coronavirus 2 (SARS-CoV-2) has caused great harm to global public health, resulting in a large number of infections among the population. However, the epidemiology of coronavirus has not been fully understood, especially the mechanism of aerosol transmission. Many respiratory viruses can spread via contact and droplet transmission, but increasing epidemiological data have shown that viral aerosol is an essential transmission route of coronavirus and influenza virus due to its ability to spread rapidly and high infectiousness. Aerosols have the characteristics of small particle size, long-time suspension and long-distance transmission, and easy access to the deep respiratory tract, leading to a high infection risk and posing a great threat to public health. In this review, the characteristics of viral aerosol generation, transmission, and infection as well as the current advances in the aerosol transmission of zoonotic coronavirus and influenza virus are summarized. The aim of the review is to strengthen the understanding of viral aerosol transmission and provide a scientific basis for the prevention and control of these diseases.

Keywords: coronavirus, influenza virus, aerosol transmission, epidemiology, public health

OPEN ACCESS

Edited by:
Levon Abrahamyan, Université de Montréal, Canada

Reviewed by:
Erika R. Schwarz, Montana Department of Livestock, United States
Venkatramana D. Krishna, University of Minnesota Twin Cities, United States

***Correspondence:**
Ning Li
SDTaianlining@126.com
Tongjie Chai
chaitj117@163.com

[†] *These authors share first authorship*

Specialty section:
This article was submitted to Veterinary Infectious Diseases, a section of the journal Frontiers in Veterinary Science

Received: *12 June 2020*
Accepted: *26 January 2021*
Published: *13 April 2021*

Citation:
Lv J, Gao J, Wu B, Yao M, Yang Y, Chai T and Li N (2021) Aerosol Transmission of Coronavirus and Influenza Virus of Animal Origin. Front. Vet. Sci. 8:572012. doi: 10.3389/fvets.2021.572012

INTRODUCTION

As human production and activities continue to infringe on the territory of wildlife by illegally capturing and consuming wild animals, the contact between humans and wild animals becomes more frequent, and the opportunities for unknown pathogenic microorganisms entering the human living environment have greatly increased. Coupled with changes in livestock and poultry feeding modes and adverse changes in climate and ecological environment in recent years, the prevalence and variation of pathogenic microorganisms, especially viruses, are accelerating, and the ability to spread across species is increasing, largely boosting the risk of zoonotic diseases in humans.

Coronavirus, as a main zoonotic virus, has caused three pandemics worldwide since the beginning of the twenty-first century. In 2003, severe acute respiratory syndrome (SARS) raged in China and 29 other countries and regions (1). In 2014, Middle East respiratory syndrome (MERS) spread through Middle East (2). The ongoing coronavirus disease 2019 (COVID-19) pandemic caused by severe acute respiratory syndrome coronavirus 2 (SARS-CoV-2) was first reported in Wuhan, China in 2019 (3–5), but as of now, the original source of SARS-CoV-2 is unclear and

studies are continuing. COVID-19 is still rapidly spread around the world, and this disease is a rare major public health event in human history. As of December 29, 2020, there are over 79 million global confirmed cases and over 1.7 million deaths in 200 countries according to WHO COVID-19 situation report (6).

Many zoonotic diseases of animal origin, such as H5 and H7 subtype avian influenza, SARS, MERS, and other respiratory infectious diseases, can spread by airborne transmission, leading to rapid outbreaks within a short period of time (7–9). In March 2020, the National Health Commission of China successively released the sixth and seventh editions of the Protocol on Diagnosis and Treatment for COVID-19, in which it has stated the probability of aerosol transmission of SARS-CoV-2 under the conditions of long-term exposure to high-concentration aerosols in a relatively closed setting (10). The United States Centers for Disease Control and Prevention (CDC) also acknowledged that airborne transmission of SARS-CoV-2 could occur within enclosed space that had inadequate ventilation (11). These results reflect the continuous deepening of the understanding of COVID-19 transmission.

In this review, based on the research progress of aerosol transmission of zoonotic coronavirus and influenza virus, we summarized the characteristics of viral aerosol generation, transmission, and infection, as well as the experimental and clinical data of the human-to-human and animal-to-animal aerosol transmission. The aim of the review is to strengthen the understanding of viral aerosol transmission and provide a scientific basis for the development of rational protective measures for the prevention and control of COVID-19, including wearing masks, safety goggles, and face shields for healthcare workers (HCWs); strict isolation; and environmental disinfection measures.

VIRUS AEROSOL

Definition and Characteristics of Virus Aerosol

Microbial aerosol refers to the stable colloidal system of microorganisms floating in air in the state of a single cell suspension or fused with dry solid or liquid particles. If the microorganism is a virus, it is called a virus aerosol (12, 13). The aerodynamic diameter of virus aerosol particle is generally considered to be $<5\,\mu m$; virus aerosol transmission is fundamentally different from droplet transmission in terms of their colloidal and aerodynamic mechanisms. Droplets are often emitted when patients cough, sneeze, and talk, with larger particles $>5\,\mu m$. However, large droplets can produce smaller aerosol particles through water evaporation; the latter can travel deeply into the respiratory tract (alveoli) and have a strong ability of penetration, increasing the pathogenicity of the enclosed pathogen (14). Although viruses suspended in aerosol do not have the conditions for growth, virus aerosol can act as an important spread carrier to increase the infection risk of diseases.

Virus aerosols have the following four characteristics: (1) Instability: virus aerosol is unstable from the beginning of its formation. Virus survival is affected by many factors, including viral structure, suspension medium, and environmental factors. Generally, viral activity decreases with time. (2) Irregular motion: viral particles undergo Brownian motion in the air, that is, they can move up and down, left and right, and back and forth in the three-dimensional space, leading to a longer suspension time and transmission distance. (3) Regenerability of deposited aerosols: once aerosol particles settled on the surface of environmental objects encounter airflow, vibration, or other mechanical forces, they can be raised again to produce a regenerated aerosol. (4) Extensive infection: viral aerosols can also invade the body through the conjunctiva, damaged skin, and digestive tract in addition to the respiratory tract (15). Therefore, in the treatment of patients with COVID-19, in addition to masks, additional protective measures including safety goggles and face shields are also necessary for HCWs to avoid contact with SARS-CoV-2. It is reported that the infectious dose of SARS-CoV-2 is believed to be low ($1 \times 10^2 - 1 \times 10^3$ particles) (16); we speculate this may partly be due to the structural and physiological characteristics of the respiratory tract, the amount of pathogens required to cause respiratory infections is significantly lower than that of the digestive tract, especially the emerging pathogen SARS-CoV-2, and humans and animals are more susceptible to it in the absence of immune resistance. The susceptibility of the respiratory tract and the frequency of human or animal exposure to virus aerosols determine the widespread infection.

Generation of Virus Aerosol

Virus aerosols in hospitals mainly come from the exhaled gas, respiratory secretions, and feces of patients. Studies have shown that a person can produce about 3,000 droplets per cough and as many as 40,000 droplets per sneeze (17). As shown in **Figure 1**, in an enclosed ward, aerosol plumes produced by patient (a) when coughing or sneezing contain many droplets and particles with different sizes (<5 or $>5\,\mu m$). Nurse (b) who is close to the patient is exposed to the droplets and inhales them into the upper respiratory tract. The suspension time of a droplet is short, and its transmission distance is generally within 2 m, which is considered as a short-range transmission route, and at this moment, doctor (c) at a longer distance is not affected (**Figure 1A**). When the droplets are discharged into air, the larger droplets begin to settle on the surface of environmental objects (floor, walls, bed sheet, etc.) due to gravity, and meanwhile, the droplets begin to evaporate to form droplet nuclei with a diameter $<5\,\mu m$, which is aerosol. Over time, the droplets will form more aerosols, and virus can be independently suspended or attached to the aerosol particles. Aerosols with small sizes and weights are diffused and suspended in the indoor air for a long time. These particles are too small to settle because of gravity; the smaller the aerosols, the further the distance they can travel (18).

In the example illustrated in **Figure 1**, the doctor has gone through the process from no exposure to virus aerosol to inhales a large amount of viral particles, which can enter the lower respiratory tract or alveoli, increasing the risk of inhalation infection (**Figures 1B,C**). With further extension of time, virus aerosol particles will gradually deposit on ward floor, walls, bed sheet, clothing, and equipment, and the concentration of aerosols in the air will be reduced

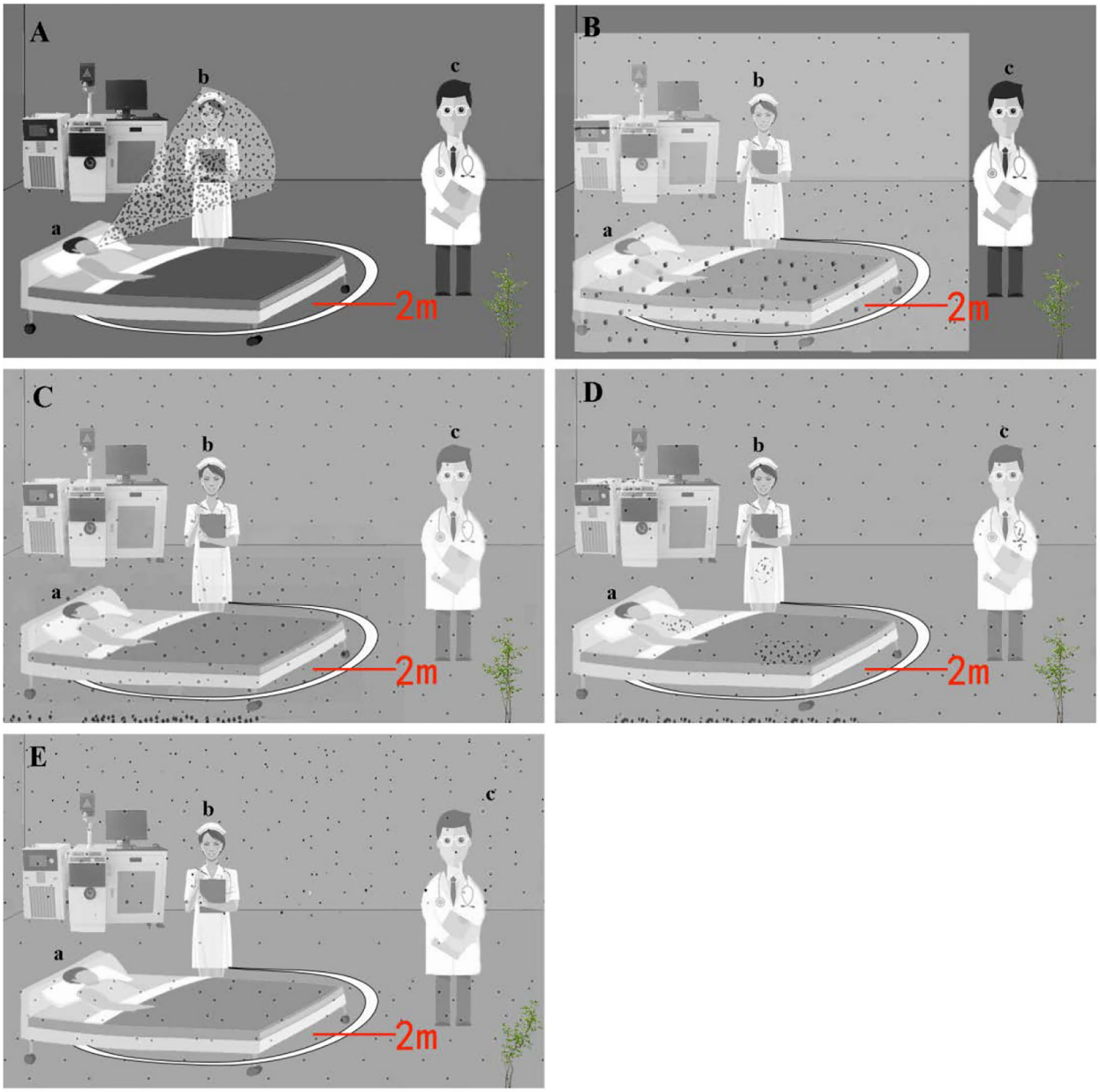

FIGURE 1 | Schematic of aerosol emission, dispersion, and regeneration over time. The larger circles represent droplet, and the smaller circles represent aerosol particles. **(A)** At time = 0, microbiology aerosol and droplet are generated by patient (a); nurse (b) standing near him is exposed to and inhales a large amount of particles, but the doctor (c) has no exposure. **(B)** At time = 1, the aerosol is dispersing, and droplets are setting within 2 m; nurse inhales particles, and the doctor has no exposure. **(C)** At time = 2, the aerosol dispersed throughout the ward, and droplets have been deposited on the floor. Nurse and doctor inhale particles. **(D)** At time = 3, the aerosol particles have deposited on the bed, floor, equipment, etc. **(E)** At time = 4, airflow or aerosol-generating procedure (AGP) re-aerosolizes the tiny particles that have been deposited.

(**Figure 1D**). However, the airflow caused by people activity can cause the re-suspension of the aerosols that have been deposited, which increases the infection risk (**Figure 1E**). Besides, the implementation of aerosol-generating procedure (AGP) operations in hospitals, such as tracheal intubation, increased the concentration of the virus aerosols and risk of SARS and MERS infection (19–21). Therefore, virus aerosols can be deposited, suspended, re-deposited, re-suspended, and continue to spread until the virus particles become inactive. As mentioned above, when people enter special circumstances containing virus aerosols without protection, especially confined spaces such as hospital intensive care units (ICU) and elevators, they are susceptible to COVID-19. This explains why one can get COVID-19 without direct contact with an infected patient. The

simple mode of infection is from pathogen to environment and then to humans.

Microbial aerosols of animal origin mainly come from respiratory secretions and feces of diseased or infected livestock and poultry and their contaminated feed, drinking water, and litter undergoing weathering, corrosion, and abrasion (15).

Survival of Virus Aerosol

The air environment does not provide the ideal conditions for the survival of pathogens. Viruses in aerosols are affected by various factors, and once inactivated, they generally lose their infectivity. The decay of virus in an aerosol usually includes two stages. In the first stage, about half of the virus is inactivated in the first few seconds after aerosol formation; in the second stage, the mortality slows down and is affected by the viral characteristics and environmental factors such as temperature, relative humidity (RH), ultraviolet rays, and electromagnetic radiation (17). To date, the survival time of the virus under different conditions has not been extensively investigated. One study shows that SARS coronavirus (SARS-CoV) can maintain its infectivity for 14 days at 4°C in hospital's sewer systems, but only for 2 days when the temperature rises to 20°C (22). SARS-CoV can survive for 2 weeks in a dry environment, but can only survive for 5 days at 22–25°C and 40–50% RH. Thereafter, the viral infectivity gradually decreases. At 38°C and 80–90% RH, the vitality of SARS-CoV gradually decreases after 24 h (23). MERS coronavirus (MERS-CoV) can survive in aerosols at 20°C and 40% RH for 10 min and on the surface of non-adsorbed objects for 8–48 h (24). SARS-CoV-2 remained viable in aerosols for 3 h with a reduction in infectious titer from $10^{3.5}$ to $10^{2.7}$ median tissue culture infective dose ($TCID_{50}$)/l air at 21–23°C and 65% RH; it was stable on plastic and stainless steel and survived for 2–3 days at 21–23°C and 40% RH (25). In addition, the deposited virus aerosol is susceptible to secondary aerosolization caused by human or environmental factors.

These results above indicate that the virus aerosol can exist for a long time in a polluted environment. It should be noted that although most viruses are easily diluted after long-time and long-distance transmission, and some have even died, it is undeniable that aerosols can be transmitted as long-term vectors and cause infections of the viruses.

AEROSOL TRANSMISSION OF CORONAVIRUS AND INFLUENZA VIRUS

Coronavirus

SARS-CoV-2

In the early stage of the COVID-19 outbreak, Huang et al. (26) clearly pointed out that this disease may be transmitted efficiently through human-to-human transmission, and it is strongly recommended to take measures to prevent airborne infections, such as the use of N95 masks. It is generally accepted that SARS-CoV-2 can spread via respiratory droplets during close contact and less commonly through contact with contaminated surfaces, but increasing evidences show that aerosols are strongly suspected to play a significant role in the rapid spread of COVID-19. A typical superspreading event reported in China involved 10 people from three families in the same air-conditioned restaurant. Authors found that the SARS-CoV-2 was able to propagate far enough to infect other members of the three families. The outbreak of COVID-19 cannot be explained by respiratory droplet transmission alone and aerosol transmission may be involved (27). Additionally, many studies have confirmed that SARS-CoV-2 can be detected in hospital air. Guo et al. (28) collected the air samples of ICU and general COVID-19 ward (GW) and found that 35% (14/40) and 12.5% (2/16) of samples tested positive for SARS-CoV-2 in ICU and GW, respectively. Moreover, air outlet swab samples also tested positive. Air samples in patient areas, medical staff areas, and public areas of two Wuhan hospitals were gathered during the COVID-19 outbreak in February and March 2020, and detection results showed that the highest concentration of SARS-CoV-2 RNA was 113 copies/m^3 in ICU in patient areas; some medical staff areas initially had high virus concentrations in aerosols, and aerodynamic diameters of most SARS-CoV-2 were <2.5 μm (29).

Recently, Lednicky et al. (30) reported that viable SARS-CoV-2 was isolated from air samples gathered 2–4.8 m away from patients, with concentrations ranging from 6 to 74 $TCID_{50}$ units/l of air. Patients with COVID-19 do not always cough and sneeze, so how is the viral aerosol produced? A recent study suggested that COVID-19 patients upon the onset of the disease were shown to emit about 10^5 viruses per min (31). Given that a study demonstrated that SARS-CoV-2 remained infective with undiminished virion integrity for up to 16 h in aerosol droplets (32), aerosol transmission of SARS-CoV-2 is undoubtedly plausible (33). High concentrations of SARS-CoV-2 have been detected in patients' toilet without ventilation (29), and the virus can also be isolated from urine and feces (34). Therefore, the aerosol is very likely from patients' feces and urine in the toilet; COVID-19 may also be transmitted through fecal–oral route (35). SARS-CoV-2 is present not only in indoor air but also in outdoor environments. Researchers tested 34 samples of outdoor/airborne PM_{10} from Bergamo Province, Italy, and found that SARS-CoV-2 RNA can be present on outdoor particulate matter (36).

Since the outbreak of COVID-19, research on the relationship between SARS-CoV-2 and animal infection has been increasing. Several cases of human-to-animal transmission have been reported, such as dogs, cats, minks, etc., and they have different susceptibility to SARS-CoV-2 (37–39). The available animal models for SARS-CoV-2 have been extensively explored, including mice, cats, ferrets, and primates, which are of great significance for understanding the susceptibility of animal species to the SARS-CoV-2, the viral transmission route, and pathogenicity (40). Although the infectivity of aerosolized SARS-CoV-2 has not been explored, as mentioned above, we must pay close attention to the formation, survival, and propagation characteristics of SARS-CoV-2 aerosols, especially in hospital wards, confined spaces, and the surrounding outdoor environments.

SARS-CoV

SARS caused by SARS-CoV was first detected in Guangdong, China in 2002, and then quickly spread to Southeast Asia and

other parts of the world. A large number of studies have found that SARS can spread through direct contact and droplets (41). However, clinical observation and analysis also suggest that SARS can be transmitted through aerosols. Studies have shown that 49% of SARS cases are related to hospitals, most likely caused by AGP for seriously ill patients (42–44). Tsai et al. (45) collected air samples near hospital beds (about 1 m) within 8 h after tracheal intubation and extubation for 11 SARS patients, and all samples tested positive for SARS-CoV. In a ward where a SARS patient lives, SARS-CoV is detected in air samples and swab samples on the surface of objects that are in frequent contact, although no live virus has been isolated in these samples (46, 47). Epidemiological investigations have pointed out that the infection in the Amoy Gardens in Hong Kong better shows that SARS is an opportunistic airborne transmission. Dense SARS-CoV aerosol plumes have been observed in contaminated sewers from index cases, which have spread to other buildings in the community, leading to 321 confirmed cases of infection. This outbreak of SARS also indicates that SARS-CoV aerosols can remain viable long enough to be transmitted to susceptible individual (48). Afterwards, hydraulic aerosol experiments, combined with epidemiological models, clearly indicate that the SARS outbreak in this community was transmitted by aerosol (9).

MERS-CoV

Since the first MERS case was confirmed in 2012 in Saudi Arabia, there have been a total of 858 patients who died from the infection and related complications in 27 countries (49). As a zoonotic virus, it has been reported that humans with MERS have been associated with direct or indirect contact with infected dromedary camels (50, 51). Human-to-human transmission of MERS has been documented, and it appears to be more frequent in health care settings than in the household (52, 53). Among the infection cases of MERS-CoV, 31% are related to hospitals (2, 42, 54). MERS-CoV can be detected from the bed sheets and medical and ventilation equipment contaminated by patients, and viruses can be isolated from some samples, indicating the presence of contact or contaminated fomites transmission (55). Of note, MERS-CoV has been detected and isolated from air samples in patient wards, toilets, and corridors, suggesting that this virus also has a great risk of airborne transmission (8).

In order to further understand the aerosol transmission of MERS-CoV, recently, several animal models of MERS-CoV aerosol infection have been established. In the mice infection model, hDPP4 transgenic mice were infected with MERS-CoV by an animal nose-only exposure device, and the results demonstrated that high viral loads were detected in lungs of MERS-CoV aerosol-infected mice, and they exhibited obvious diffuse interstitial pneumonia on day 7; moreover, the lung lesions more closely resembled those observed in humans (56). In primate model of MERS, African green monkeys were exposed to aerosolized MERS-CoV with different doses (10^3,10^4, and 10^5 PFU), and all animals in the 10^5 PFU group displayed overt respiratory disease signs, including chest congestion, rales, and wheezing, and a dose-dependent increase of respiratory disease signs was observed (57). As mentioned above, these experimental data confirm that MERS-CoV can spread through aerosols.

Influenza A Virus

Influenza A virus is a well-known respiratory virus, including the 2009 swine influenza H1N1, seasonal influenza viruses, highly pathogenic avian influenza virus (HPAI) H5N1 and H7N9, and low pathogenic avian influenza virus (LPAI) H9N2, and many strains can be transmitted by aerosols (7, 58–61). In special circumstances, such as households with poor ventilation, the aerosols can be the main transmission route of influenza virus (62), which sufficiently indicates the key role of aerosols in influenza virus spread.

A large number of studies have proved that influenza virus aerosols can be detected in air samples from health care settings. Recently, Zhao et al. (63) collected 91 air samples daily from hospital outpatient hall, clinical laboratory, fever clinic, children's ward, and adult ward, during January and April 2018, and found that air samples collected from the children's ward, adult ward, and fever clinic were positive for airborne influenza viruses, including epidemic strain H1N1. Influenza virus can be detected in the air up to 3.7 m away from patients with the majority of viral RNA contained in aerosols (64). About 50% of the influenza viral RNA detected by Blachere et al. (65) in the emergency department of a hospital are from aerosols (aerodynamic diameter $<4\,\mu$m). Quantitative analyses show that the highest load of the influenza virus is 13,426 median tissue culture infective dose ($TCID_{50}$), and the median infective dose (EID_{50}) of influenza virus aerosols (1–3 μm) in humans is about 0.6–3 $TCID_{50}$ (66), which is significantly higher than the EID_{50} for humans.

Further studies have shown that influenza virus aerosols are released when influenza patients cough, sneeze, and breathe normally. Lindsley et al. (67) reported influenza viral RNA was detected in coughs. Twenty-three percent of the influenza RNA was contained in particles 1–4 μm in aerodynamic diameter, and 42% was in particles $<1\,\mu$m. Viable influenza virus was detected in cough aerosols from 2 of 21 subjects with influenza. Fabian et al. (68) reported that, among 12 influenza patients, the virus was directly detected in the exhaled breath of four patients through qPCR. The generation rate can reach as high as 20 RNA copies per minute. Further analysis indicates that exhaling 20 RNA copies per minute is equivalent to excreting 4 $TCID_{50}$ viruses per hour, suggesting that one is also at risk of infection during normal conversation with an influenza patient. Furthermore, aerosol particles emitted by patients contained viable influenza virus (69, 70). In the environment of a poultry farm, Lv et al. (15) collected 18 air samples from 6 chicken farms in different areas of Shandong Province and found that the concentration of H9 subtype influenza aerosol is about 1.25×10^4-6.92×10^4 copies/m^3 air. These results indicate that influenza virus can naturally form aerosols, and more importantly, aerosols act as an important carrier for viral transmission.

In addition to the epidemiologic evidences of influenza viruses' aerosol transmission, mammals and poultry are used to perform experimental infection studies of influenza virus. Influenza infection has been documented by aerosol exposure in the guinea pig model. In this animal model, Lowen et al. (71) demonstrated that influenza virus was transmitted from

infected guinea pigs to non-infected guinea pigs housed in an adjacent cage separated by 91 cm. Subsequently, they described a stronger experimental evidence for influenza aerosol transmission, and they documented the instance of transmission with the distance between cages increasing to 107 cm (72). Additionally, transmission of HPAI H5N1 by aerosols from geese to quails has been demonstrated in experimental infections (73). Airborne transmission of HPAI viruses can occur among poultry and from poultry to humans who are exposed to infected poultry (61). HPAI H9N2 infection experiment of SPF chickens via aerosol and nasal and digestive tract infusion routes was conducted by Yao et al. (74), and it was found that the aerosol route requires the lowest dose of the virus. The viruses required for nasal and digestive tract routes are 2 and 113 times those for aerosol, respectively, indicating that the virus aerosol infection efficiency is very high.

Notably, not all influenza virus strains can form aerosols, and different strains differ significantly in their capacity for aerosol transmission (72). Further study confirmed that amino acid mutations (D368E, S370L, E313K, and G381D) in the neuraminidase gene of H9N2 subtype AIV can significantly affect their aerosol transmission and viral replication ability in the respiratory tract (60). The H5N1 strain (Indonesia/5/2005) acquired mutations [four amino acid substitutions in the hemagglutinin (HA) gene and one in the polymerase complex protein basic polymerase 2 gene] during passage in ferrets, and ultimately, it was able to spread via aerosols among ferrets (7). The molecular mechanism of HA amino acid mutation that enables the H5N1 to transmit in ferrets by aerosols is the change of the complex structures of viral protein and the decreased affinities for receptors (75). These epidemiologic observations and infection experiments strongly support the view that influenza infections can occur via the aerosol route (76).

DISCUSSION

With the outbreak of COVID-19, the aerosol transmission of pathogens has once again become a hot topic. In this article, we mainly reviewed the aerosol transmission of several important zoonotic viruses, including influenza virus and coronavirus. Through direct examination of patients' exhaled breath and air samples in hospital wards, influenza virus is found in the air, which can infect the susceptible population. More importantly, in the household environment, the main transmission route of influenza virus among family members is aerosols (62). SARS-CoV, SARS-CoV-2, and MERS-CoV are severe respiratory pathogens, which are generally believed to be transmitted through contact and droplets. Because in practice it is very difficult to completely rule out contributions of a given mode of transmission, the relative contribution of each mode is usually difficult to establish by epidemiologic studies alone (76). Airborne transmission is the main route for efficient transmission between humans (59). However, there is an argument that viral RNA detectable in air samples is circumstantial and correlated with disease state rather than direct evidence of causality; therefore, it is very necessary to establish an animal model of viral aerosol infection for actual experimental demonstration. All in all, although SARS-CoV-2 has not yet been used to conduct aerosol generation and infection experiments, experimental data, epidemiological investigation, and protective measures against airborne infection have proven the likelihood of aerosol transmission of SARS-CoV-2. Therefore, measures such as protective clothing, masks, safety goggles, face shields, room ventilation, and strict disinfection are necessary to cut off the chain of infection.

The crucial role of aerosols in the transmission of respiratory infectious diseases cannot be denied, although not all pathogens solely depend on aerosol transmission. Especially under special environmental conditions, there is no reason to underestimate the importance of viral aerosol transmission. Studies should be focused on clarifying the mechanism of viral aerosol generation and survival and fully understanding the transmission mechanism of infectious diseases, so as to formulate prevention and control strategies for the COVID-19 pandemic and other newly emerging pathogens.

AUTHOR CONTRIBUTIONS

JL and JG wrote the manuscript. JL, BW, and MY performed the relative experiments of H9N2 AIV aerosol. NL and TC designed, revised, and approved the review. All authors contributed to the article and approved the submitted version.

FUNDING

This research is supported by the National Natural Science Foundation of China (31470258), Chinese International Cooperation Program Monitoring of Zoonotic Infectious Diseases Originated in Animals (2009DFA32890), and Sino-German Technology Cooperation Research [(2010)6066], and High-level Scientific Research Foundation for the introduction of talent of Shandong Agricultural University.

REFERENCES

1. WHO. *Summary of Probable SARS Cases With Onset of Illness From 1 November 2002 to 31 July 2003.* WHO (2015). Available online at: http://www.who.int/csr/sars/country/table~2004_04_21/en/index.html
2. Oboho I, Tomczyk S, Al-Asmari A, Banjar A, Al-Mugti H, Aloraini M, et al. 2014 MERS-CoV outbreak in jeddah — a link to health care facilities. *N Engl J Med.* (2015) 372:846–54. doi: 10.1056/NEJMoa1408636
3. Gorbalenya AE, Baker SC, Baric RS, Groot RJd, Drosten C, Gulyaeva AA, et al. The species severe acute respiratory syndrome-related coronavirus: classifying 2019-nCoV and naming it SARS-CoV-2. *Nat Microbiol.* (2020) 5:536–44. doi: 10.1038/s41564-020-0695-z
4. Wang C, Horby P, Hayden F, Gao G. A novel coronavirus outbreak of global health concern. *Lancet.* (2020) 395:470–3. doi: 10.1016/S0140-6736(20)30185-9

5. Zhu N, Zhang D, Wang W, Li X, Yang B, Song J, et al. A novel coronavirus from patients with pneumonia in China, 2019. *N Engl J Med.* (2020) 382:727–33. doi: 10.1056/NEJMoa2001017
6. WHO. *Weekly Epidemiological Update—29 December 2020.* WHO (2020). Available online at: https://www.who.int/publications/m/item/weekly-epidemiological-update-$-$29-december-2020
7. Herfst S, Schrauwen EJA, Linster M, Chutinimitkul S, Wit Ed, Munster VJ, et al. Airborne transmission of influenza A/H5N1 virus between ferrets. *Science.* (2012) 336:1534–41. doi: 10.1126/science.1213362
8. Kim S, Chang S, Sung M, Park J, Bin Kim H, Lee H, et al. Extensive viable middle east respiratory syndrome (MERS) coronavirus contamination in air and surrounding environment in MERS isolation wards. *Clin Infect Dis.* (2016) 63:363–9. doi: 10.1093/cid/ciw239
9. Yu I, Li Y, Wong T, Tam W, Chan A, Lee J, et al. Evidence of airborne transmission of the severe acute respiratory syndrome virus. *N Engl J Med.* (2004) 350:1731–9. doi: 10.1056/NEJMoa032867
10. National Health Commission of the People's Republic of China. *Protocol on Prevention and Control of COVID-19 (Edition 6).* (2020). Available online at: https://www.chinadaily.com.cn/pdf/2020/2.\hboxCOVID-19.Prevention.and.Control.Protocol.V6.pdf
11. CDC. *How COVID-19 Spreads.* CDC (2020). Available online at: https://www.cdc.gov/coronavirus/2019-ncov/prevent-getting-sick/how-covid-spreads.html
12. Che F, Li J, Chai T. *Principle and Application of Aerobiology.* Beijing: Science Press (2004).
13. Langmuir A. Epidemiology of airborne infection. *Bacteriol Rev.* (1961) 25:173–81. doi: 10.1128/BR.25.3.173-181.1961
14. Tellier R. Aerosol transmission of influenza A virus: a review of new studies. *J R Soc Interface.* (2009) 6:S783–90.doi: 10.1098/rsif.2009.0302.focus
15. Lv J. *Detecting Airborne Transmission Determinants of H9N2 Avian Influenza Virus by Reverse Genetic and Monitoring its Transmission*. Taian: Shandong Agricultural University (2012).
16. Guzman MI. An overview of the effect of bioaerosol size in coronavirus disease 2019 transmission. *Int J Health Plann Manage.* (2021) 36: 257–66. doi: 10.1002/hpm.3095
17. Cole E, Cook C. Characterization of infectious aerosols in healthcare facilities: an aid to effective engineering controls and preventive strategies. *Am J Infect Control.* (1998) 26:453–64. doi: 10.1016/S0196-6553(98)70046-X
18. Liu L, Wei J, Li Y, Ooi A. Evaporation and dispersion of respiratory droplets from coughing. *Indoor Air.* (2017) 27:179–90. doi: 10.1111/ina.12297
19. Chen W, Ling W, Lu C, Hao Y, Lin Z, Ling L, et al. Which preventive measures might protect healthcare workers from SARS? *BMC Public Health.* (2009) 9:81. doi: 10.1186/1471-2458-9-81
20. Hui DS. Epidemic and emerging coronaviruses (severe acute respiratory syndrome and middle east respiratory syndrome). *Clin Chest Med.* (2017) 38:71–86. doi: 10.1016/j.ccm.2016.11.007
21. Tran K, Cimon K, Severn M, Pessoa-Silva CL, Conly J. Aerosol generating procedures and risk of transmission of acute respiratory infections to healthcare workers: a systematic review. *PLoS ONE.* (2012) 7:e35797. doi: 10.1371/journal.pone.0035797
22. Wang X, Li J, Guo T, Zhen B, Kong Q, Yi B, et al. Concentration and detection of SARS coronavirus in sewage from Xiao Tang Shan Hospital and the 309th Hospital. *J Virol Methods.* (2005) 128:156–61. doi: 10.1016/j.jviromet.2005.03.022
23. Chan KH, Peiris JSM, Lam S, Poon LLM, Seto WH. The effects of temperature and relative humidity on the viability of the SARS coronavirus. *Adv Virol.* (2011) 2011:734690. doi: 10.1155/2011/734690
24. van Doremalen N, Bushmaker T, Munster V. Stability of middle east respiratory syndrome coronavirus (MERS-CoV) under different environmental conditions. *Euro Surveill.* (2013) 18:20590. doi: 10.2807/1560-7917.ES2013.18.38.20590
25. van Doremalen N, Bushmaker T, Morris DH, Holbrook MG, Gamble A, Williamson BN, et al. Aerosol and surface stability of SARS-CoV-2 as compared with SARS-CoV-1. *N Engl J Med.* (2020) 382:1564–7. doi: 10.1056/NEJMc2004973
26. Huang C, Wang Y, Li X, Ren L, Zhao J, Hu Y, et al. Clinical features of patients infected with 2019 novel coronavirus in Wuhan, China. *Lancet.* (2020) 395:497–506. doi: 10.1016/S0140-6736(20)30183-5
27. Lu J, Gu J, Li K, Xu C, Su W, Lai Z, et al. COVID-19 outbreak associated with air conditioning in restaurant, Guangzhou, China, 2020. *Emerg Infect Dis.* (2020) 26:1628–31. doi: 10.3201/eid2607.200764
28. Guo ZD, Wang ZY, Zhang SF, Li X, Li L, Li C, et al. Aerosol and surface distribution of severe acute respiratory syndrome coronavirus 2 in Hospital wards, Wuhan, China, 2020. *Emerg Infect Dis.* (2020) 26:1583–91. doi: 10.3201/eid2607.200885
29. Liu Y, Ning Z, Chen Y, Guo M, Liu Y, Gali NK, et al. Aerodynamic analysis of SARS-CoV-2 in two Wuhan hospitals. *Nature.* (2020) 582:557–60. doi: 10.1038/s41586-020-2271-3
30. Lednicky JA, Lauzardo M, Fan ZH, Jutla A, Tilly TB, Gangwar M, et al. Viable SARS-CoV-2 in the air of a hospital room with COVID-19 patients. *IntJ Infect Dis.* (2020) 100:476–82. doi: 10.1016/j.ijid.2020.09.025
31. Ma JX, Qi X, Chen HX, Li XY, Zhang Z, Wang HB, et al. Coronavirus disease 2019 patients in earlier stages exhaled millions of severe acute respiratory syndrome coronavirus 2 per hour. *Clin Infect Dis.* (2020). doi: 10.1093/cid/ciaa1283. [Epub ahead of print].
32. Fears AC, Klimstra WB, Duprex P, Hartman A, Weaver SC, Plante KS, et al. Persistence of severe acute respiratory syndrome coronavirus 2 in aerosol suspensions. *Emerg Infect Dis.* (2020) 26:2168–71. doi: 10.3201/eid2609.201806
33. Morawska L, Milton DK. It is time to address airborne transmission of coronavirus disease 2019 (COVID-19). *Clin Infect Dis.* (2020) 71:2311–3. doi: 10.1093/cid/ciaa939
34. Peng L, Liu J, Xu W, Luo Q, Chen D, Lei Z, et al. SARS-CoV-2 can be detected in urine, blood, anal swabs, and oropharyngeal swabs specimens. *J Med Virol.* (2020) 92:1676–80. doi: 10.1002/jmv.25936
35. Yeo C, Kaushal S, Yeo D. Enteric involvement of coronaviruses: is faecal-oral transmission of SARS-CoV-2 possible? *Lancet Gastroenterol Hepatol.* (2020) 5:335–7. doi: 10.1016/S2468-1253(20)30048-0
36. Setti L, Passarini F, Gennaro GD, Baribieri P, Perrone MG, Borelli M, et al. SARS-Cov-2 RNA found on particulate matter of bergamo in northern italy: first preliminary evidence. *Environ Res.* (2020) 188:109754. doi: 10.1016/j.envres.2020.109754
37. Zhang Q, Zhang H, Gao J, Huang K, Yang Y, Hui X, et al. A serological survey of SARS-CoV-2 in cat in Wuhan. *Emerg Microbes Infect.* (2020) 9:2013–9. doi: 10.1080/22221751.2020.1817796
38. Oreshkova N, Molenaar RJ, Vreman S, Harders F, Oude Munnink BB, Hakze-van der Honing RW, et al. SARS-CoV-2 infection in farmed minks, the Netherlands, April and May 2020. *Euro Surveill.* (2020) 25:2001005. doi: 10.2807/1560-7917.ES.2020.25.23.2001005
39. Loeb J. Pet dog confirmed to have coronavirus. *Vet Rec.* (2020) 186:265. doi: 10.1136/vr.m892
40. Mahdy MAA, Younis W, Ewaida Z. An overview of SARS-CoV-2 and animal infection. *Front Vet Sci.* (2020) 7:596391. doi: 10.3389/fvets.2020.596391
41. Seto WH, Tsang D, Yung R, Ching TY, Ng TK, Ho M, et al. Effectiveness of precautions against droplets and contact in prevention of nosocomial transmission of severe acute respiratory syndrome (SARS). *Lancet.* (2003) 361:1519–20. doi: 10.1016/S0140-6736(03)13168-6
42. Chowell G, Abdirizak F, Lee S, Lee J, Jung E, Nishiura H, et al. Transmission characteristics of MERS and SARS in the healthcare setting: a comparative study. *BMC Med.* (2015) 13:210. doi: 10.1186/s12916-015-0450-0
43. Lee N, Hui D, Wu A, Chan P, Cameron P, Joynt GM, et al. A major outbreak of severe acute respiratory syndrome in Hong Kong. *N Engl J Med.* (2003) 348:1986–1994. doi: 10.1056/NEJMoa030685
44. Ofner M, Lem M, Sarwal S, Vearncombe M, Simor A. cluster of severe acute respiratory syndrome cases among protected health care workers-Toronto, April 2003. *Can Commun Dis Rep.* (2003) 29:93–97.
45. Tsai YH, Wan GH, Wu YK, Tsao KC. *Airborne Severe Acute Respiratory Syndrome Coronavirus Concentrations in a Negative-Pressure Isolation Room. Infect Control Hosp Epidemiol.* (2006) 27:523–5. doi: 10.1086/504357
46. Booth TF, Bill K, Nathalie B, Jim H, Darwyn K, Laurie S, et al. Detection of airborne severe acute respiratory syndrome (SARS) coronavirus and environmental contamination in SARS outbreak units. *J Infect Dis.* (2005) 191:1472–7. doi: 10.1086/429634
47. Xu Q, Fan Q, Duan N, Wang W, Chen J. Airborne spread pathway in Intensive Care Unit (ICU) of specialized SARS hospital. *Chin J Nosocomiol.* (2005) 15:1380–2. doi: 10.3321/j.issn:1005-4529.2005.12.019

48. Li Y, Duan S, Yu IT, Wong TW. Multi-zone modeling of probable SARS virus transmission by airflow between flats in block E, amoy gardens. *Indoor Air.* (2005) 15:96–111. doi: 10.1111/j.1600-0668.2004.00318.x
49. WHO. *Middle East Respiratory Syndrome Coronavirus (MERS-CoV).* Available onine at: https://www.who.int/health-topics/middle-east-respiratory-syndrome-coronavirus-mers#tab=tab_1
50. Haagmans BL, Al Dhahiry SH, Reusken CB, Raj VS, Galiano M, Myers R, et al. Middle East respiratory syndrome coronavirus in dromedary camels: an outbreak investigation. *Lancet Infect Dis.* (2014) 14:140–5. doi: 10.1016/S1473-3099(13)70690-X
51. Reusken CB, Messadi L, Feyisa A, Ularamu H, Godeke GJ, Danmarwa A, et al. Geographic distribution of MERS coronavirus among dromedary camels, Africa. *Emerg Infect Dis.* (2014) 20:1370–4. doi: 10.3201/eid2008.140590
52. Assiri A, McGeer A, Perl TM, Price CS, Al Rabeeah AA, Cummings DA, et al. Hospital outbreak of middle east respiratory syndrome coronavirus. *N Engl J Med.* (2013) 369:407–16. doi: 10.1056/NEJMoa1306742
53. Azhar EI, Lanini S, Ippolito G, Zumla A. The middle east Respiratory Syndrome Coronavirus - A Continuing Risk to Global Health Security. *Adv Exp Med Biol.* (2017) 972:49–60. doi: 10.1007/5584_2016_133
54. Hunter J, Nguyen D, Aden B, Al Bandar Z, Al Dhaheri W, Abu Elkheir K, et al. Transmission of middle east respiratory syndrome coronavirus infections in healthcare settings, Abu Dhabi. *Emerg Infect Dis.* (2016) 22:647–56. doi: 10.3201/eid2204.151615
55. Yu BS, Yeon HJ, Min-Suk S, Lee J, Eun-Ha K, Su-Jin P, et al. Environmental contamination and viral shedding in MERS patients during MERS-CoV outbreak in South Korea. *Clin Infect Dis.* (2015) 62:755–60. doi: 10.1093/cid/civ1020
56. Hao XY, Lv Q, Li FD, Xu YF, Gao H. The characteristics of hDPP4 transgenic mice subjected to aerosol MERS coronavirus infection via an animal nose-only exposure device. *Animal Model Exp Med.* (2019) 2:269–81. doi: 10.1002/ame2.12088
57. Totura A, Livingston V, Frick O, Dyer D, Nichols D, Nalca A. Small particle aerosol exposure of african green monkeys to MERS-CoV as a model for highly pathogenic coronavirus infection. *Emerg Infect Dis.* (2020) 26:2835–43. doi: 10.3201/eid2612.201664
58. Munster VJ, Wit Ed, van den Brand JMA, Herfst S, Schrauwen EJA, Bestebroer TM, et al. Pathogenesis and transmission of swine-origin 2009 A(H1N1) influenza virus in ferrets. *Science.* (2009) 325:481–3. doi: 10.1126/science.1177127
59. Richard M, Schrauwen E, de Graaf M, Bestebroer T, Spronken M, van Boheemen S, et al. Limited airborne transmission of influenza A/H7N9 virus between ferrets. *Nature.* (2013) 501:560–3. doi: 10.1038/nature12476
60. Lv J, Wei L, Yang Y, Wang B, Liang W, Gao Y, et al. Amino acid substitutions in the neuraminidase protein of an H9N2 avian influenza virus affect its airborne transmission in chickens. *Vet Res.* (2015) 46:44. doi: 10.1186/s13567-014-0142-3
61. Bertran K, Balzli C, Kwon YK, Tumpey TM, Clark A, Swayne DE. Airborne transmission of highly pathogenic influenza virus during processing of infected poultry. *Emerg Infect Dis.* (2017) 23:1806–14. doi: 10.3201/eid2311.170672
62. Cowling BJ, Ip DKM, Fang VJ, Suntarattiwong P, Olsen SJ, Levy JW, et al. Aerosol transmission is an important mode of influenza A virus spread. *Nat Commun.* (2013) 4:1935. doi: 10.1038/ncomms2922
63. Zhao X, Nie W, Zhou C, Cheng M, Wang C, Liu Y, et al. Airborne transmission of influenza virus in a hospital of qinhuangdao during 2017-2018 flu season. *Food Environ Virol.* (2019) 11:427–39. doi: 10.1007/s12560-019-09404-1
64. Lednicky JA, Loeb JC. Detection and isolation of airborne influenza A H3N2 virus using a sioutas personal cascade impactor sampler. *Influenza Res Treat.* (2013) 2013:656825. doi: 10.1155/2013/656825
65. Blachere FM, Lindsley WG, Pearce TA, Anderson SE, Fisher M, Khakoo R, et al. Measurement of airborne influenza virus in a hospital emergency department. *Clin Infect Dis.* (2009) 48:438–40. doi: 10.1086/596478
66. Alford R, Kasel J, Gerone P, Knight V. Human influenza resulting from aerosol inhalation. *Proc Soc Exp Biol Med.* (1966) 122:800–4. doi: 10.3181/00379727-122-31255
67. Lindsley WG, Blachere FM, Thewlis RE, Vishnu A, Davis KA, Cao G, et al. Measurements of airborne influenza virus in aerosol particles from human coughs. *PLoS ONE.* (2010) 5:e15100. doi: 10.1371/journal.pone.0015100
68. Fabian P, Mcdevitt J, Dehaan W, Fung R, Cowling B, Chan K, et al. Influenza virus in human exhaled breath: an observational study. *PLoS ONE.* (2008) 3:e2691. doi: 10.1371/journal.pone.0002691
69. Lindsley W, Noti J, Blachere F, Thewlis R, Martin S, Othumpangat S, et al. Viable influenza a virus in airborne particles from human cough. *J Occup Environ Hyg.* (2015) 12:107–13. doi: 10.1080/15459624.2014.973113
70. Lindsley WG, Blachere FM, Beezhold DH, Thewlis RE, Noorbakhsh B, Othumpangat S, et al. Viable influenza A virus in airborne particles expelled during coughs versus exhalations. *Influenza Other Respir Viruses.* (2016) 10:404–13. doi: 10.1111/irv.12390
71. Lowen AC, Mubareka S, Tumpey TM, García-Sastre A, Palese P. The guinea pig as a transmission model for human influenza viruses. *Proc Natl Acad Sci USA.* (2006) 103:9988–92. doi: 10.1073/pnas.0604157103
72. Mubareka S, Lowen AC, Steel J, Coates AL, García-Sastre A, Palese P. Transmission of influenza virus via aerosols and fomites in the guinea pig model. *J Infect Dis.* (2009) 199:858–65. doi: 10.1086/597073
73. Webster RG, Guan Y, Peiris M, Walker D, Krauss S, Zhou NN, et al. Characterization of H5N1 influenza viruses that continue to circulate in geese in southeastern China. *J Virol.* (2002) 76:118–26. doi: 10.1128/JVI.76.1.118-126.2002
74. Yao M, Zhang X, Gao J, Chai T, Miao Z, Ma W, et al. The occurrence and transmission characteristics of airborne H9N2 avian influenza virus. *Berl Munch Tierarztl Wochenschr.* (2011) 124:136–41.
75. Zhang W, Shi Y, Lu X, Shu Y, Qi J, Gao GF. An airborne transmissible avian influenza H5 hemagglutinin seen at the atomic level. *Science.* (2013) 340:1463–7. doi: 10.1126/science.1236787
76. Tellier, R. Review of aerosol transmission of influenza A virus. *Emerg Infect Dis.* (2006) 12:1657–62. doi: 10.3201/eid1211.060426

Conflict of Interest: The authors declare that the research was conducted in the absence of any commercial or financial relationships that could be construed as a potential conflict of interest.

frontiers in Veterinary Science

ORIGINAL RESEARCH
published: 24 June 2021
doi: 10.3389/fvets.2021.658512

Whole Genome or Single Genes? A Phylodynamic and Bibliometric Analysis of PRRSV

*Alba Frias-De-Diego, Manuel Jara, Brittany M. Pecoraro and Elisa Crisci**

Department of Population Health and Pathobiology, College of Veterinary Medicine, North Carolina State University, Raleigh, NC, United States

Diversity, ecology, and evolution of viruses are commonly determined through phylogenetics, an accurate tool for the identification and study of lineages with different pathological characteristics within the same species. In the case of PRRSV, evolutionary research has divided into two main branches based on the use of a specific gene (i.e., ORF5) or whole genome sequences as the input used to produce the phylogeny. In this study, we performed a review on PRRSV phylogenetic literature and characterized the spatiotemporal trends in research of single gene vs. whole genome evolutionary approaches. Finally, using publicly available data, we produced a Bayesian phylodynamic analysis following each research branch and compared the results to determine the pros and cons of each particular approach. This study provides an exploration of the two main phylogenetic research lines applied for PRRSV evolution, as well as an example of the differences found when both methods are applied to the same database. We expect that our results will serve as a guidance for future PRRSV phylogenetic research.

Keywords: bibliometrics, phylodynamics, pig, PRRSV, ORF5, whole genome

OPEN ACCESS

Edited by:
Lester J. Perez, University of Illinois at Urbana–Champaign, United States

Reviewed by:
Moh A. Alkhamis, Kuwait University, Kuwait
Rafael Zardoya, National Museum of Natural Sciences (MNCN), Spain

****Correspondence:***
Elisa Crisci
ecrisci@ncsu.edu

Specialty section:
This article was submitted to Veterinary Infectious Diseases, a section of the journal Frontiers in Veterinary Science

Received: *25 January 2021*
Accepted: *21 May 2021*
Published: *24 June 2021*

Citation:
Frias-De-Diego A, Jara M, Pecoraro BM and Crisci E (2021) Whole Genome or Single Genes? A Phylodynamic and Bibliometric Analysis of PRRSV. Front. Vet. Sci. 8:658512. doi: 10.3389/fvets.2021.658512

INTRODUCTION

Viral diseases affecting livestock are a major problem because of their rapid spread, negative impact in animal health, potential spillover to humans, and detrimental effect on economic systems (1, 2). In 2019, international commerce of livestock and swine products surpassed $20 billion worldwide, from which the U.S. alone reached over $7 billion as reported by the United States Department of Agriculture (USDA) (3). For those reasons, controlling infectious diseases affecting swine is an ever-growing challenge, shaped by the constant race between the potential of pathogens to evolve and spread, and the ability of researchers to elucidate mechanisms and to develop effective prophylactic and therapeutic measures to reduce their impact on the swine population.

Viruses in general are one of the infectious agents with the highest mutation rates, which hinders the ability of researchers to predict their evolution and spread due to their ever-changing genome (4, 5). This is particularly common in the case of RNA viruses such as Porcine Reproductive and Respiratory Syndrome Virus (PRRSV), currently one of the most deleterious diseases for the swine industry worldwide, reaching up to 60% prevalence in growing-finishing herds (1, 2, 6, 7). PRRSV is an enveloped positive sense single-stranded RNA virus in the family Arteriviridae (8) with a

genome of ∼15 kb that encodes at least nine open reading frames (ORFs) (9). ORF5 in particular is widely used for phylogenetic analysis, since its structure encompasses both hypervariable and conserved segments, allowing the classification of strains in a reasonably accurate way (10–12). Based on its genetic diversity and antigenic properties, PRRSV is classified into two distinct genotypes with different species (13): Type 1 and Type 2, that are mostly circulating in Europe and North America respectively (11, 14). Due to its genetic nature, its recombination ability is one of the main shapers of PRRSV evolution and diversity (15, 16), along with its mutation rate, that was recently estimated at 0.00672 (16).

Over the last decade, the concept and application of interdisciplinary sciences have improved infectious disease control measures by the combination of the genetic, geographic, and historical data of pathogens (17–20), providing a much deeper understanding of their evolutionary trajectory and therefore allowing the application of targeted control strategies and treatments based on this new information (16). However, due to the multiple possibilities that interdisciplinary approaches offer, there is often an open discussion to determine the most accurate method to apply in a given scientific scenario.

Early molecular studies of PRRSV applied RT-PCR to detect virus, leading to the first PRRSV phylogenetic reconstruction based on ORF-5 and ORF-7 sequences that was able to differentiate the European and American clades (21). This paper was followed by numerous phylogenetic studies using ORF-5 given the compromise of sites evolving at different rates, which generated well-resolved trees during a period where whole genome sequencing was particularly challenging. However, despite the increasing availability of whole genome sequences, scientists are still divided by the support of the use of whole genomes or single genes (22), particularly for evolutionary analyses of organisms like PRRSV, that is an exceptionally diverse virus (23).

Multiple factors have a key role in this decision, especially for research analyzing field isolates and samples that need to be sequenced, since the economic effort needed, along with the requirement of specialized laboratories, equipment and skilled personnel is remarkably higher to perform whole genome sequencing than single genes (24). In the case of whole genome defenders, they advocate the consideration of all nucleotides to identify all changes between genomes, rather than the changes in specific and usually conserved genes (caused for example by horizontal gene transfer) (25, 26). On the other hand, opinions of scientists supporting the use of single genes or multi-gene approaches (but not whole genome application) (27, 28) argue that by considering whole genomes, there is the possibility to detect changes in non-coding genes that could misclassify sequences.

The goal of this study is to evaluate and compare the different patterns and trends on PRRSV research in relation to the application of whole genomes or single genes, and assess the potential variations observed on the same analyses when one of the two approaches is applied using the same genetic database.

MATERIALS AND METHODS

Bibliometric Analyses

The bibliometric search for the available publications was performed in Scopus, using the search criteria "TITLE-ABS-KEY [(PRRSV AND [whole AND genome OR ORF5]) OR (porcine AND reproductive AND respiratory AND syndrome AND [whole AND genome OR ORF5]) OR (PRRSV AND [phylogeny OR phylogenetics OR evolution])]" and downloaded the obtained results in bib format. Using the R package Bibliometrix (29), the journal, year of publication, title, abstract, author names, and author affiliations of all resulting publications were extracted. From this initial database, a manual screening was performed: original or literature reviews, the study area (global vs. country level), and the use of whole genome or ORF5 gene were extracted.

Genetic Databases

All PRRSV whole genome sequences available were downloaded from Genbank as a.gb file and ran the python package "gbmunge" (https://github.com/sdwfrost/gbmunge) to retrieve the available metadata for each sequence. From that database, 765 sequences, for which geographic and temporal information was available, were selected for subsequent analyses. Sequences were aligned using MEGA X (30). Using this updated database, the sequences were aligned along with three PRRSV ORF5 sequences, EU556220, DQ405282, and DQ405279, to identify the region of the whole genome in which ORF5 was located. Then, ORF5 region of the sequences was manually identified and saved in a second database used for analyses.

Recombination Analyses

The recombination detection program (RDP) v5.3 was used to search for recombination within our data set (31). The alignment was screened using five methods (BootScan, Chimaera, MaxChi, RDP, and SiScan).

Phylogeny

To find the best substitution model for each database, the ModelFinder tool (32) built into IQ-Tree version 1.6.1 (33) was used. The marginal likelihood value supported the use of the general time-reversible model (GTR) with gamma-distributed rate heterogeneity plus a proportion of invariable sites (GTR+G+I) (34) for both databases (**Supplementary Table 1**). To determine the best fitting node-age and branch-rate model, each combination of molecular clock and branch rate was run to compare the marginal likelihood estimated by the stepping-stone and path-sampling methods, supporting the use of uncorrelated relaxed molecular clock model and coalescent logistic growth as the tree prior for both ORF-5 and whole genome databases. Both phylogenies were then estimated by Bayesian inference through Markov chain Monte Carlo (MCMC), implemented in BEAST v2.6.0 (35). The model was run for 100 million generations, sampling every 10,000th generation and removing 10% of the chain as burn-in in both cases. The probabilities of ancestral states were inferred from the Bayesian discrete-trait analysis and

visualized as pie charts on each node. Visualization of the trees was performed using FigTree v1.4.4 (Rambaut[1]).

Phylodynamics

The spatiotemporal spread patterns observed for both databases were performed via Bayesian continuous phylogeographic analysis, following the model selection described in the phylogeny section. An uncorrelated relaxed molecular clock model with lognormal distribution (36) and the Bayesian SkyGrid with covariates as the coalescent tree prior (37) were also applied. To ensure an effective sample size (ESS) value over 200, analyses were run for 200 million generations, sampling every 10,000th generation and removing 10% of the chain as burn-in. To determine the relative genetic diversity over time of each database we used Bayesian SkyGrid, as this approach relies on a non-parametric coalescent model to estimate the effective population size over time (38).

RESULTS

Bibliometric Analyses and Genetic Databases

The bibliometric search recognized 374 articles under our search criteria, from which only 49 were global studies. From that total, 23 literature reviews and 351 original articles, from which 190 of them applied whole genome analyses, and 155 used single genes, were identified. Detailed information about the 6 remaining articles was not available at the time of the screening (October 2020). One hundred and twenty five of the publications using single genes chose ORF5, leaving only 30 articles with a different genome section [i.e., ORF7 (10), Nsp2 (39)].

For both whole genome sequences (WGS) and ORF5 sequences, the countries with the highest scientific productivity were China (WGS = 295, ORF5 = 141), the United States (WGS = 89, ORF5 = 88), and South Korea (WGS = 55, ORF5 = 50) (**Figure 1A**). Overall, PRRSV research (whole and partial genome studies) evidenced higher scientific productivity per year up to 2018, with a rapid decrease maintained until our search was performed (October 2020) (**Figure 1B**, **Supplementary Figure 1**). In addition, 12 countries only evidenced articles using WGS, while 8 countries only produced articles related to ORF5 sequences (**Supplementary Table 2**).

In relation to the produced genetic databases, the starting point after running the gbmunge package was of 765 whole genome PRRSV sequences with most of the necessary metadata available (**Supplementary Table 1**). To avoid sampling bias, a similar number of sequences was chosen from different locations to reach a total of 100. The ORF5 database consisted of the exact same sequences from which the ORF5 section of the genome was manually identified and isolated.

Recombination Analyses

From the total number of sequences with metadata we obtained (765), the Recombination Detection Program (RDP) detected 491 recombinant sequences from the whole genome database, and 393 from the ORF5 database (**Figure 1**), making a difference of 98 between the two (data available upon request).

Phylogeny and Ancestral Reconstruction

Phylogenetic results for the whole genome database showed that the most likely center of origin for the PRRSV sequences analyzed was Belarus with a root state posterior probability (RSPP) = 10%. This original lineage then diverged into two groups likely driven by geographical distance and independent subsequent evolution, one with a higher probability of being originated in China (RSPP = 26%), and a second one likely originated in Hungary (RSPP = 16%) (**Figure 2A**). The amount of lineages present over time showed an overall increase in the number of different lineages with two main periods of growth from 1600 to 1750 and from 1950 to the present day (**Figure 2B**).

When the ORF5 sequence database was analyzed, the ancestral reconstruction also evidenced Belarus as the most likely country of origin (RSPP = 11%) (**Figure 3**). Similarly to the pattern shown by WGS, the analysis showed that this ancestral lineage diverged into two clearly defined groups, both of them with a higher probability of being originated in Denmark (RSPP = 45, and 26% respectively). In the case of the number of lineages through time, this database showed no new lineages appearing until after 1,800 when it presented two clear isolated diversification events that maintained the number of lineages until ∼1,900, which was the starting point of a rapid exponential increase in the number of lineages up to the day of the screening (**Figure 3B**). Finally, the 95% highest probability density (HPD) values of both trees showed similar uncertainty patterns, with the most recent nodes showing less uncertainty than the ancestral (**Supplementary Figure 2**). However, based on these HPD values the ORF-5 database showed less accuracy to reconstruct the ancestral nodes, suggesting whole genome as the most robust approach for this type of studies.

Phylodynamics

When the genetic diversity obtained for the analysis of whole genome vs. ORF5 databases was compared over time, SkyGrid plot revealed an overall higher genetic diversity exhibited by the ORF5 sequences. In addition, there is a noticeable difference in the pattern of diversity increase, where the ORF5 database showed constant growth while the whole genome database started to experience an increase in diversity from 1983, with a sharp decrease in 2009 that was not detected by the ORF5 result (**Figure 4**).

Finally, when we compared the dispersal velocity of PRRSV based on each database, we observed that ORF5 sequences showed higher spread velocity (2948.7 km/year) than whole genome sequences (1956.4 km/year) (**Supplementary Table 3**).

DISCUSSION

Our bibliometric screening detected an overall higher number of articles considering the use of whole genomes than single genes. However, this happened only after 2010, when the increase in the amount of whole genome related publications started to grow

[1]Rambaut, A. "Figtree v1.4.4. Available online at: http://tree.bio.ed.ac.uk/software/figtree/".

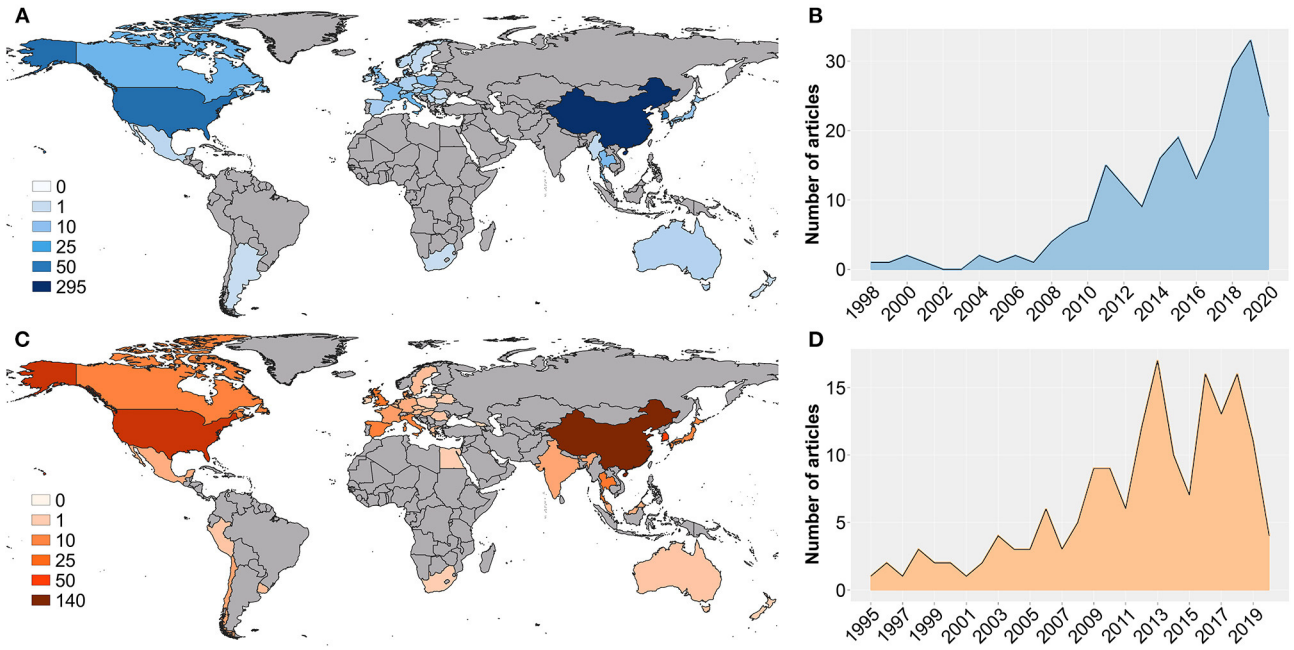

FIGURE 1 | Global annual scientific production involving whole genome sequences (blue) and single genes (orange) where **A** represents the number of publications per country of whole genome-related research, **B** represents the global annual scientific production of whole genome-related research, **C** represents the number of publications per country of single genes-related research, and **D** represents the global annual scientific production of single genes-related research.

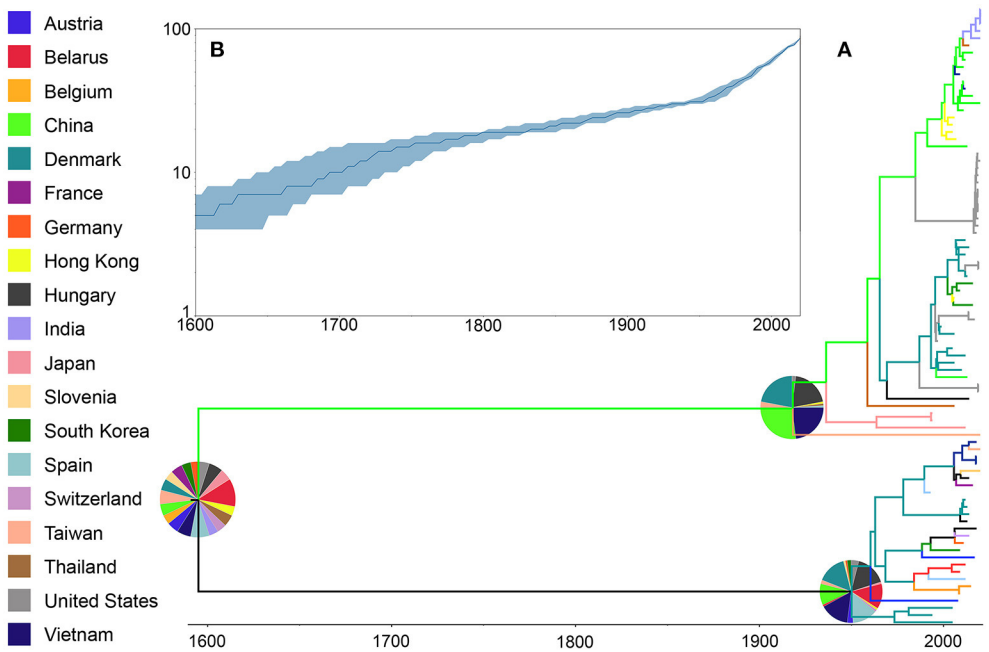

FIGURE 2 | Phylogenetic history of PRRSV inferred using whole genome sequences. **(A)** Maximum clade credibility (MCC) phylogeny, colored according to the country of origin of each sequence. The probabilities of ancestral states (inferred from the Bayesian discrete-trait analysis) are shown in pie charts on each node. **(B)** Spatiotemporal patterns represented through lineages through time plot.

and surpassed the application of ORF5 that had been applied in the previous years. The decrease in productivity observed around 2018 could be the result of the detection of an outbreak of African Swine Fever in China (40), which would likely trigger

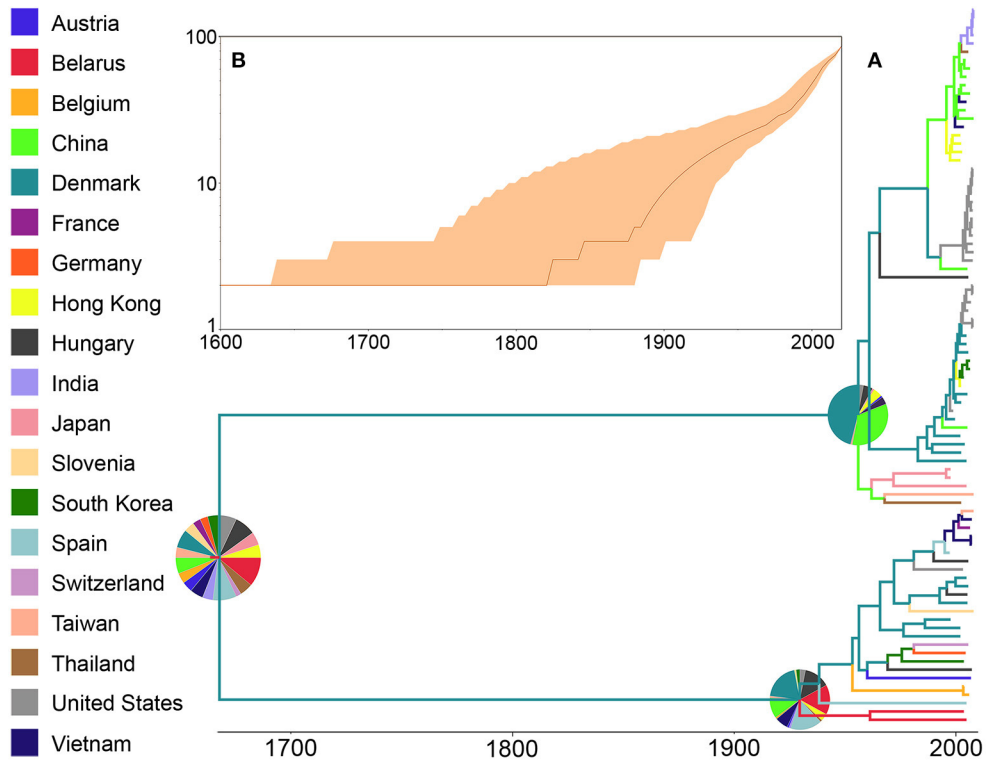

FIGURE 3 | Phylogenetic history of PRRSV inferred using ORF5 sequences. **(A)** Maximum clade credibility (MCC) phylogeny, colored according to the country of origin of each sequence. The probabilities of ancestral states (inferred from the Bayesian discrete-trait analysis) are shown in pie charts on each node. **(B)** Spatiotemporal patterns represented through lineages through time plot.

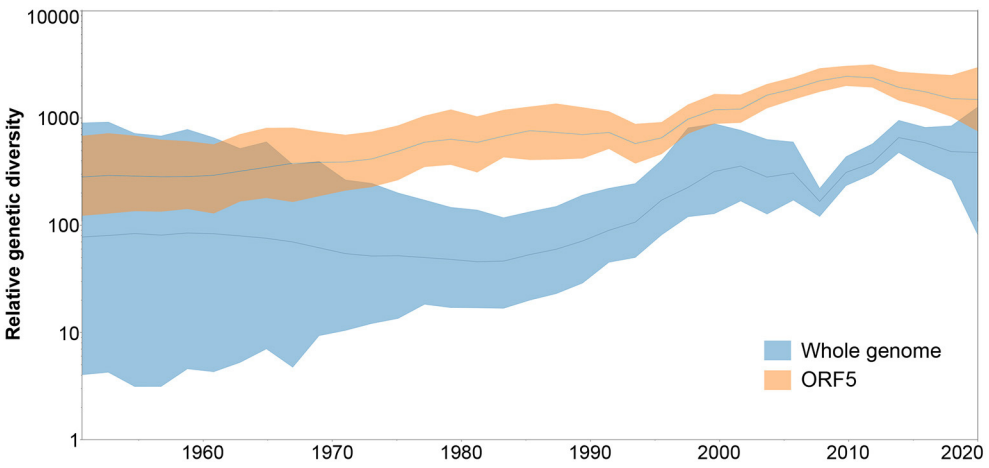

FIGURE 4 | Spatiotemporal patterns in the relative genetic diversity represented through the Bayesian SkyGrid plot, where dark lines represent the mean values, while shaded light regions correspond to the 95% highest posterior density (HPD).

a deviation on research efforts toward that disease. This growth in whole genome sequence application could have been triggered by the increase in the availability and affordability of RNA-seq technology once it became more accessible for general research, surpassing the levels of the use of ORF5 sequences, that had been posed as the standard gene applied to study PRRSV evolution due to their high variability (11). This hypothesis would also fit with our observation on country productivity, where countries with access to sequencing are leading scientific production for both whole genome studies and single genes. Not surprisingly, these increased publication rates are linked to wealthy economies with high pig production given the elevated cost of sequencing

studies, although not every country presented publications in both areas.

The bibliographic search was performed using the Scopus database, as it is a large, multidisciplinary database that includes MEDLINE and has been described to combine the characteristics of both Web of Science and PubMed, allowing an improved service for educational and academic needs, also favoring Natural Science and Biomedical research literature (41). Furthermore, previous research compared the amount of publications retrieved by those three different databases, obtaining a more extensive number of detected publications using Scopus (42).

Another expected result was the number of recombinant sequences detected on each database. Recombinant sequences should be considered when choosing between whole genomes or single genes, particularly in RNA viruses such as PRRSV (12, 43, 44). A common claim between scientists supporting the use of single genes for evolutionary analysis relies on the presence of numerous non-coding regions (introns) that could interfere with those analyses and cause bias on the results. However, we observed that the whole genome database detected a higher number of recombinants. Although there are no studies assessing the proportion of recombinant sequences detected due to non-coding regions, numerous publications have mentioned the implications and importance of considering these non-coding sequences on recombination, evolution, and chromosomal stability assessments (45–47).

The shape of the phylogenetic trees obtained for both databases was similar. This suggests that for analyses focusing on the evolutionary patterns as well as the identification and taxonomy of this virus, both approaches could fulfill the needs of the study. However, in the case of the ancestral reconstruction studies, as well as in the reconstruction of phylodynamic patterns, we observed numerous differences between the two datasets, showing that the choice between whole genome or single genes should be considered carefully depending on the study performed. Particularly in the case of ancestral reconstruction studies, where our whole genome database showed more accuracy on the estimated ancestral nodes (measured as HPD values) than our ORF-5 database. It is important to keep in mind that the main goal of this project was not to perform a phylodynamic study of PRRSV or to determine its ancestral origin, but to identify the similarities and differences observed when identical evolutionary analyses were performed in the same sequences of our database using the whole genome or only its ORF5 segment. Interestingly, with the set of sequences used in our analyses, the evolutionary trends and shape of the trees obtained coincide with previously published studies in PRRSV evolutionary history (11, 16), suggesting that even though higher number of sequences will generally produce more robust analyses, inferences and patterns can be identified with reduced amounts of data as a baseline for subsequent and more elaborated studies.

We faced some limitations during the development of this study. Firstly, the affiliation information extracted by the Bibliometrix R package did not necessarily correspond to the country where the initial research was developed. This is a common limitation in bibliometric studies that has been previously assessed via sensitivity analyses with no significant changes on the obtained results (48). In addition, publications using whole genome sequencing are generally complex and include wide collaboration networks where authors from different locations share resources and data. Therefore, one single article may be detected by bibliometric measurements in more than one country. Likewise, our search only included papers that were already published and available by October 2020. Therefore, the productivity of this year must not be considered final, because papers submitted but not yet published before our search day are likely to get published after our search was done or even in 2021.

Finally, this study represents a comparison of the most commonly applied evolutionary analyses in PRRSV research using whole genome or single gene sequences as an input. Here, we show the similarities and differences on the results driven by the use of the whole genome or the ORF-5 section of the same set of genes, analyze the evolution and patterns of research on each area over time and highlight the need to take these differences into consideration when deciding the most appropriate approach to apply depending on the specific aim of the research performed, particularly in analyses that involve ancestral reconstruction.

DATA AVAILABILITY STATEMENT

The original contributions generated for the study are included in the article/**Supplementary Material**, further inquiries can be directed to the corresponding author.

AUTHOR CONTRIBUTIONS

EC and AF-D-D were responsible for the conception of the study and manuscript writing and revisions. AF-D-D was responsible for the acquisition of data and data analysis. AF-D-D and MJ were responsible for data analysis and interpretation, manuscript editing, and revisions. BP was responsible for manual data screening and revision of the manuscript. EC was responsible for project supervision and administration. All authors have read and agreed to the published version of the manuscript.

FUNDING

This work was partially supported by the USDA National Institute of Food and Agriculture, Animal Health project 1021578.

ACKNOWLEDGMENTS

Authors would like to thank Dr. Rocio Crespo and Dr. Glen Almond for her insightful comments and suggestions that helped improved our manuscript.

SUPPLEMENTARY MATERIAL

The Supplementary Material for this article can be found online at: https://www.frontiersin.org/articles/10.3389/fvets.2021.658512/full#supplementary-material

REFERENCES

1. Holtkamp DJ, Kliebenstein JB, Neumann E, Zimmerman JJ, Rotto H, Yoder TK, et al. Assessment of the economic impact of porcine reproductive and respiratory syndrome virus on United States pork producers. *J Swine Health Prod.* (2013) 21:72. doi: 10.31274/ans_air-180814-28
2. Fablet C, Marois-Crehan C, Grasland B, Simon G, Rose N. Factors associated with herd-level PRRSV infection and age-time to seroconversion in farrow-to-finish herds. *Vet Microbiol.* (2016) 192:10–20. doi: 10.1016/j.vetmic.2016.06.006
3. USDA. *Pork 2019 Export Highlights.* U.S. Department of Agriculture (2019).
4. Malpica JM, Fraile A, Moreno I, Obies CI, Drake JW, García-Arenal F. The rate and character of spontaneous mutation in an RNA virus. *Genetics.* (2002) 162:1505–11. doi: 10.1093/genetics/162.4.1505
5. Pal C, Maciá MD, Oliver A, Schachar I, Buckling A. Coevolution with viruses drives the evolution of bacterial mutation rates. *Nature.* (2007) 450:1079–81. doi: 10.1038/nature06350
6. Neumann EJ, Kliebenstein JB, Johnson CD, Mabry JW, Bush EJ, Seitzinger AH, et al. Assessment of the economic impact of porcine reproductive and respiratory syndrome on swine production in the United States. *J Am Vet Med Assoc.* (2005) 227:385–92. doi: 10.2460/javma.2005.227.385
7. Pileri E, Mateu E. Review on the transmission porcine reproductive and respiratory syndrome virus between pigs and farms and impact on vaccination. *Vet Res.* (2016) 47:108. doi: 10.1186/s13567-016-0391-4
8. Cavanagh D, Brian D, Enjuanes L, Holmes K, Lai M, Laude H, et al. Recommendations of the coronavirus study group for the nomenclature of the structural proteins, mRNAs, and genes of coronaviruses. *Virology.* (1990) 176:306–307. doi: 10.1016/0042-6822(90)90259-T
9. Dokland T. The structural biology of PRRSV. *Virus Res.* (2010) 154:86–97. doi: 10.1016/j.virusres.2010.07.029
10. Pesente P, Rebonato V, Sandri G, Giovanardi D, Ruffoni LS, Torriani S. Phylogenetic analysis of ORF5 and ORF7 sequences of porcine reproductive and respiratory syndrome virus (PRRSV) from PRRS-positive Italian farms: a showcase for PRRSV epidemiology and its consequences on farm management. *Vet Microbiol.* (2006) 114:214–24. doi: 10.1016/j.vetmic.2005.11.061
11. Shi M, Lam TT-Y, Hon C-C, Hui K-H, Faaberg KS, Wennblom T, et al. Molecular epidemiology of PRRSV: a phylogenetic perspective. *Virus Res.* (2010) 154:7–17. doi: 10.1016/j.virusres.2010.08.014
12. Martín-Valls G, Kvisgaard LK, Tello M, Darwich L, Cortey M, Burgara-Estrella A, et al. Analysis of ORF5 and full-length genome sequences of porcine reproductive and respiratory syndrome virus isolates of genotypes 1 and 2 retrieved worldwide provides evidence that recombination is a common phenomenon and may produce mosaic isolates. *J Virol.* (2014) 88:3170–81. doi: 10.1128/JVI.02858-13
13. Kuhn JH, Lauck M, Bailey AL, Shchetinin AM, Vishnevskaya TV, Bào Y, et al. Reorganization and expansion of the nidoviral family Arteriviridae. *Arch Virol.* (2016) 161:755–68. doi: 10.1007/s00705-015-2672-z
14. Mardassi H, Mounir S, Dea S. Identification of major differences in the nucleocapsid protein genes of a Quebec strain and European strains of porcine reproductive and respiratory syndrome virus. *J Gen Virol.* (1994) 75:681–5. doi: 10.1099/0022-1317-75-3-681
15. Linhares D, Cano J, Torremorell M, Morrison RB. Comparison of time to PRRSv-stability and production losses between two exposure programs to control PRRSv in sow herds. *Prev Vet Med.* (2014) 116:111–9. doi: 10.1016/j.prevetmed.2014.05.010
16. Jara M, Rasmussen DA, Corzo CA, Machado G. Porcine reproductive and respiratory syndrome virus dissemination across pig production systems in the United States. *Transboundary Emerg Dis.* (2021) 68:667–83. doi: 10.1101/2020.04.09.034181
17. Frias-De-Diego A, Jara M, Escobar LE. Papillomavirus in wildlife. *Front Ecol Evol.* (2019) 7:406. doi: 10.3389/fevo.2019.00406
18. Jara M, Escobar LE, Rodriges RO, Frias-De-Diego A, Sanhueza J, Machado G. Spatial distribution and spread potential of sixteen *Leptospira serovars* in a subtropical region of Brazil. *Transboundary Emerg Dis.* (2019) 66:2482–95. doi: 10.1111/tbed.13306
19. Jara M, Frias-De-Diego A, Machado G. Phylogeography of equine infectious anemia virus. *Front Ecol Evol.* (2020) 8:127. doi: 10.3389/fevo.2020.00127
20. Krasteva S, Jara M, Frias-De-Diego A, Machado G. Nairobi Sheep Disease Virus: A Historical and Epidemiological Perspective. *Fron Vet Sci.* (2020) 7:419. doi: 10.3389/fvets.2020.00419
21. Suárez P, Zardoya R, Martín MJ, Prieto C, Dopazo J, Solana A, et al. Phylogenetic relationships of European strains of porcine reproductive and respiratory syndrome virus (PRRSV) inferred from DNA sequences of putative ORF-5 and ORF-7 genes. *Virus Res.* (1996) 42:159–65. doi: 10.1016/0168-1702(95)01305-9
22. Dudas G, Bedford T. The ability of single genes vs full genomes to resolve time and space in outbreak analysis. *BMC Evol Biol.* (2019) 19:1–17. doi: 10.1186/s12862-019-1567-0
23. Stadejek T, Oleksiewicz M, Potapchuk D, Podgorska K. Porcine reproductive and respiratory syndrome virus strains of exceptional diversity in eastern Europe support the definition of new genetic subtypes. *J Gen Virol.* (2006) 87:1835–41. doi: 10.1099/vir.0.81782-0
24. Schwarze K, Buchanan J, Fermont JM, Dreau H, Tilley MW, Taylor JM, et al. The complete costs of genome sequencing: a microcosting study in cancer and rare diseases from a single center in the United Kingdom. *Genet Med.* (2020) 22:85–94. doi: 10.1038/s41436-019-0618-7
25. Snel B, Bork P, Huynen MA. Genome phylogeny based on gene content. *Nat Genet.* (1999) 21:108–10. doi: 10.1038/5052
26. Du W, Cao Z, Wang Y, Sun Y, Blanzieri E, Liang Y. Prokaryotic phylogenies inferred from whole-genome sequence and annotation data. *BioMed Res Int.* (2013) 2013:409062. doi: 10.1155/2013/409062
27. Spatafora JW, Sung, G.-H., Johnson D, Hesse C, O'rourke B, et al. A five-gene phylogeny of Pezizomycotina. *Mycologia.* (2006) 98:1018–28. doi: 10.1080/15572536.2006.11832630
28. Vitorino L, Chelo IM, Bacellar F, Ze-Ze L. Rickettsiae phylogeny: a multigenic approach. *Microbiology.* (2007) 153:160–8. doi: 10.1099/mic.0.2006/001149-0
29. Aria M, Cuccurullo C. Bibliometrix: an R-tool for comprehensive science mapping analysis. *J Informetrics.* (2017) 11:959–75. doi: 10.1016/j.joi.2017.08.007
30. Kumar S, Stecher G, Li M, Knyaz C, Tamura K. MEGA X: molecular evolutionary genetics analysis across computing platforms. *Mol Biol Evol.* (2018) 35:1547–9. doi: 10.1093/molbev/msy096
31. Martin DP, Murrell B, Golden M, Khoosal A, Muhire B. RDP4: Detection and analysis of recombination patterns in virus genomes. *Virus Evol.* (2015) 1:vev003. doi: 10.1093/ve/vev003
32. Kalyaanamoorthy S, Minh BQ, Wong TK, Von Haeseler A, Jermiin LS. ModelFinder: fast model selection for accurate phylogenetic estimates. *Nat Methods.* (2017) 14:587–9. doi: 10.1038/nmeth.4285
33. Nguyen L-T, Schmidt HA, Von Haeseler A, Minh BQ. IQ-TREE: a fast and effective stochastic algorithm for estimating maximum-likelihood phylogenies. *Mol Biol Evol.* (2015) 32:268–74. doi: 10.1093/molbev/msu300
34. Tavaré S. Some probabilistic and statistical problems in the analysis of DNA sequences. *Lect Math Life Sci.* (1986) 17:57–86
35. Bouckaert R, Heled J, Kühnert D, Vaughan T, Wu CH, Xie D, et al. BEAST 2: a software platform for Bayesian evolutionary analysis. *PLoS Comput Biol.* (2014) 10:e1003537. doi: 10.1371/journal.pcbi.1003537
36. Drummond AJ, Ho SY, Phillips MJ, Rambaut A. Relaxed phylogenetics and dating with confidence. *PLoS Biol.* (2006) 4:e88. doi: 10.1371/journal.pbio.0040088
37. Gill MS, Lemey P, Bennett SN, Biek R, Suchard MA. Understanding past population dynamics: bayesian coalescent-based modeling with covariates. *Syst Biol.* (2016) 65:1041–56. doi: 10.1093/sysbio/syw050
38. Hill V, Baele G. Bayesian estimation of past population dynamics in BEAST 1.10 using the Skygrid coalescent model. *Mol Biol Evol.* (2019) 36:2620–8. doi: 10.1093/molbev/msz172
39. Wang C, Wu B, Amer S, Luo J, Zhang H, Guo Y, et al. Phylogenetic analysis and molecular characteristics of seven variant Chinese field isolates of PRRSV. *BMC Microbiol.* (2010) 10:1–11. doi: 10.1186/1471-2180-10-146
40. Fekede RJ, Van Gils H, Huang L, Wang X. High probability areas for ASF infection in China along the Russian and Korean borders. *Transboundary Emerg Dis.* (2019) 66:852–64. doi: 10.1111/tbed.13094

41. Mongeon P, Paul-Hus A. The journal coverage of web of science and scopus: a comparative analysis. *Scientometrics.* (2016) 106:213–28. doi: 10.1007/s11192-015-1765-5
42. Frias-De-Diego A, Posey R, Pecoraro BM, Fernandes Carnevale R, Beaty A, Crisci E. A century of swine influenza: is it really just about the pigs? *Vet Sci.* (2020) 7:189. doi: 10.3390/vetsci7040189
43. Alkhamis MA, Perez AM, Murtaugh MP, Wang X, Morrison RB. Applications of bayesian phylodynamic methods in a recent US porcine reproductive and respiratory syndrome virus outbreak. *Front Microbiol.* (2016) 7:67. doi: 10.3389/fmicb.2016.00067
44. Yu F, Yan Y, Shi M, Liu, H.-Z., Zhang, H.-L., Yang, Y.-B., et al. Phylogenetics, genomic recombination, and NSP2 polymorphic patterns of porcine reproductive and respiratory syndrome virus in China and the United States in 2014–2018. *J Virol.* (2020) 94:e01813-19. doi: 10.1128/JVI.01813-19
45. Hall DH, Liu Y, Shub DA. Exon shuffling by recombination between self-splicing introns of bacteriophage T4. *Nature.* (1989) 340:574–6. doi: 10.1038/340574a0
46. Comeron JM, Kreitman M. The correlation between intron length and recombination in *Drosophila*: dynamic equilibrium between mutational and selective forces. *Genetics.* (2000) 156:1175–90. doi: 10.1093/genetics/156.3.1175
47. Duret L. Why do genes have introns? Recombination might add a new piece to the puzzle. *Trends Genet.* (2001) 17:172–5. doi: 10.1016/S0168-9525(01)02236-3
48. Nafade V, Nash M, Huddart S, Pande T, Gebreselassie N, Lienhardt C, et al. A bibliometric analysis of tuberculosis research, 2007–2016. *PLoS ONE.* (2018) 13:e0199706. doi: 10.1371/journal.pone.0199706

Conflict of Interest: The authors declare that the research was conducted in the absence of any commercial or financial relationships that could be construed as a potential conflict of interest.

frontiers in Veterinary Science

ORIGINAL RESEARCH
published: 24 June 2021
doi: 10.3389/fvets.2021.668420

Reindeer Anthrax in the Russian Arctic, 2016: Climatic Determinants of the Outbreak and Vaccination Effectiveness

Elena A. Liskova[1], Irina Y. Egorova[2], Yuri O. Selyaninov[2], Irina V. Razheva[1], Nadezhda A. Gladkova[1], Nadezhda N. Toropova[1], Olga I. Zakharova[1], Olga A. Burova[1], Galina V. Surkova[3], Svetlana M. Malkhazova[3], Fedor I. Korennoy[1,4], Ivan V. Iashin[1] and Andrei A. Blokhin[1]**

[1] Federal Research Center for Virology and Microbiology, Nizhny Novgorod Research Veterinary Institute - Branch of Federal Research Center for Virology and Microbiology, Nizhny Novgorod, Russia, [2] Federal Research Center for Virology and Microbiology (FRCVM), Pokrov, Russia, [3] Faculty of Geography, Lomonosov Moscow State University, Moscow, Russia, [4] FGBI Federal Centre for Animal Health (FGBI ARRIAH), Vladimir, Russia

OPEN ACCESS

Edited by:
Lester J. Perez,
University of Illinois at Urbana–Champaign, United States

Reviewed by:
Krishna Thakur,
University of Prince Edward Island, Canada
Brianna R. Beechler,
Oregon State University, United States

***Correspondence:**
Elena A. Liskova
liskovaea@mail.ru
Andrei A. Blokhin
and.bloxin2010@yandex.ru

Specialty section:
This article was submitted to Veterinary Epidemiology and Economics, a section of the journal Frontiers in Veterinary Science

Received: 16 February 2021
Accepted: 19 April 2021
Published: 24 June 2021

Citation:
Liskova EA, Egorova IY, Selyaninov YO, Razheva IV, Gladkova NA, Toropova NN, Zakharova OI, Burova OA, Surkova GV, Malkhazova SM, Korennoy FI, Iashin IV and Blokhin AA (2021) Reindeer Anthrax in the Russian Arctic, 2016: Climatic Determinants of the Outbreak and Vaccination Effectiveness. Front. Vet. Sci. 8:668420. doi: 10.3389/fvets.2021.668420

The Yamal Peninsula in the Russian Federation experienced a massive outbreak of anthrax in reindeer (*Rangifer tarandus*) in July–August 2016, with 2,650 (6.46% of the total susceptible population) animals infected, of which 2,350 died (case fatality rate of 88.67%). In our study, we analyzed climatic and epidemiological factors that could have triggered the outbreak. The cancelation of reindeer vaccination against anthrax in 2007 resulted in an increase in population susceptibility. In response to the outbreak, total vaccination of all susceptible animals was resumed. To assess the vaccination effectiveness, we tested 913 samples of blood serum taken from vaccinated reindeer using an antigenic erythrocyte diagnostic kit to detect specific anti-anthrax antibodies via an indirect hemagglutination assay (IHA) 9 months after vaccination. We found that 814 samples had sufficiently high levels of anti-anthrax antibodies to indicate a protection level of 89% (95% confidence interval: 87–91%) of the whole reindeer population. Abnormally high ambient temperature in the summer of 2016 contributed to the thawing of permafrost and viable *Bacillus anthracis* spores could have become exposed to the surface; the monthly average air temperatures in June, July, and August 2016 were 20–100% higher than those of the previous 30-year period, while the maximum air temperatures were 16–75% higher. Using the projected climate data for 2081–2100 according to the "worst case" RCP8.5 scenario, we demonstrated that the yearly air temperature may average above 0°C across the entire Yamal Peninsula, while the yearly number of days with a mean temperature above 0°C may rise by 49 ± 6 days, which would provide conditions for reactivation of soil anthrax reservoirs. Our results showed that the outbreak of anthrax occurred under conditions of a significant increase in air temperature in the study area, underlined the importance of vaccination for controlling the epidemic process, and demonstrated the effectiveness of monitoring studies using the IHA diagnostic kit for detecting erythrocyte anthrax antigens.

Keywords: anthrax, arctic, climate, outbreak, reindeer, vaccination, Russia, indirect hemagglutination assay

INTRODUCTION

Anthrax is a bacterial disease affecting humans and other mammals, caused by the gram-positive, spore-forming, rod-shaped bacterium *Bacillus anthracis*. The main feature of this microorganism, which largely determines its epidemiological potential and population structure, is the ability to form endospores that are extremely resistant to unfavorable environmental conditions and are able to remain viable for a long time (1–3). Anthrax spores persist in the soil for a long time, and not only survive, but also become part of the soil biocenosis due to a combination of natural conditions. These include the structure of the natural soil cover, the chemical properties of the soil and its layers, and alternating floods and droughts, which increase leaching from the soil, drying, and dispersion of spores. The survival time of spores is unpredictable, which creates favorable conditions for the formation of natural foci (3–5).

The zoonotic potential of anthrax is well-known worldwide. Sheep, goats, cattle, buffaloes, horses, deer, donkeys, and other animals, including wild species, are known to be highly susceptible to anthrax, while pigs are less susceptible. Under natural conditions, rodents can also contract the disease (5). Currently, anthrax cases are extremely rare in most European countries, but the disease remains endemic in Russia, where it causes sporadic cases in animals and rare cases in the human population. The epidemic process usually involves grazing livestock becoming infected via the alimentary route, by ingesting *B. anthracis* spores while eating soil-contaminated plants or by drinking from water sources with a high concentration of spores (3, 4, 6, 7). The epidemiology of anthrax is characterized by summer–autumn seasonality, caused by grazing of animals on pastures that usually have sparse and dry grass. In the winter–spring (stall) period, infection is associated with the use of infected feed.

The prerequisites for the functioning of the anthrax biosystem are a constantly high level of soil contamination by *B. anthracis* spores, free grazing, and transhumance and semi-nomadic animal pasturing practice, which is typical for reindeer husbandry in the Far North of Russia (3). In Russia, the presence of large territories inhabited by populations of wild animals and livestock creates favorable conditions for outbreaks of epidemic diseases, and the low population density in most of the country makes it difficult to implement anti-epidemic measures and record the burial sites of animals that have died of anthrax correctly. Historical anthrax burials are often undocumented, and sometimes corpses are not buried properly. These burial grounds, as well as entire territories of historical epidemics, may be involved in economic activities, which may lead to new disease outbreaks given the marked preservation of spores in a cold climate.

Of particular interest in this regard is the tundra zone of Russia, located between 55 and 68 degrees North. The 1941 penultimate outbreak of anthrax in the Yamal Peninsula reindeer population resulted in the death of 6,700 reindeer. The last outbreak in 2016 killed more than 2,000 reindeer and led to the hospitalization of 90 local residents, as well as the death of one child (8–10).

Currently, in the northern regions of Russia, there is a risk of occurrence (revival) of soil foci of anthrax due the Yana, Indigirka, and Kolyma rivers flooding pastures and settlements, as well as large-scale earthworks (mining of diamonds, gold, oil, and gas; other types of subsurface use). This requires permanent preventive measures among livestock animals regardless of the current status of known anthrax foci, particularly in conditions where climate changes affect the habitat of macro- and microorganisms.

One important component of such preventive measures is the annual vaccination of susceptible animals, which is aimed at generating herd immunity against the disease in the population of livestock animals, including reindeer. The effectiveness of active immunization is monitored by evaluating the titer of anthrax antibodies (10–14). In 2007, the vaccination of reindeer in the Yamal Peninsula was canceled, which may have led to an increase in population susceptibility. In response to the 2016 outbreak, total vaccination of all susceptible animals was resumed.

The aims of the present study were (1) to evaluate the effectiveness of reindeer vaccination against anthrax performed as a response to the 2016 outbreak in the Yamal Peninsula, (2) to explore climate conditions in summer 2016 and their potential role in that outbreak, and (3) to assess the expected climate change on the Yamal Peninsula and its potential influence on the risk of anthrax resurgence.

MATERIALS AND METHODS

An ethical review was not required for this study, according to local and national legislation, because this work does not contain any experiments on animals. Blood samples for the study of anthrax immunity were collected by certified veterinarians using standard procedures to avoid the suffering of animals and followed the guidelines of the State Veterinary Service of the Russian Federation.

Study Area

Our study assessed the anthrax epidemic situation in the Yamalo-Nenets Autonomous Okrug (YaNAO), which is one of the 85 regions included in the Russian Federation. The YaNAO is located in the Arctic zone of Russia, partly on the Yamal Peninsula. Most of its territory is located beyond the Arctic Circle (**Figure 1**). The area comprises 769,250 km^2, and has a population density of about 0.7 persons/km^2. The region is characterized by permafrost, a large number of rivers and lakes, and Arctic and subarctic climates in most of the territory. The total reindeer population in the YaNAO is estimated to be more than 700,000 head (15).

Data Sources and Methods

Anthrax Data

The epidemiological analysis of the 2016 anthrax outbreak in reindeer in the YaNAO was based on official data by the Federal Service for Veterinary and Phytosanitary Surveillance ("Rosselkhoznadzor," https://fsvps.gov.ru/fsvps/iac/rf/operative-

FIGURE 1 | Study area, anthrax outbreaks in 2016, and the area of anthrax immunity monitoring in reindeer.

messages.html) that were notified by Russia to OIE (https://wahis.oie.int/#/dashboards/country-or-disease-dashboard). The data contained information on the infected species, exact location of the outbreaks, and the number of infected and dead animals. This information was represented as a shapefile to enable mapping and spatial analysis in a geographic information system (GIS).

Climate Data

Meteorological data for the assessment of monthly mean and maximum air temperatures in the study area (the Tazovsky district of the YaNAO) from 1987–2016 were extracted from the official website of the Federal Service for Hydrometeorology and Environmental Monitoring (16) and from the Weather Archive web portal (http://pogoda-service.ru/archive_gsod.php) for the stationary weather station Antipayuta (synoptic index 23058; geographical coordinates 69°6′13″N, 76°51′28″E). We compared monthly mean and maximum air temperatures in May, June, July, and August for 2016 (the 2 months with recorded anthrax outbreaks and the two preceding months) with corresponding indicators for the entire 30-year period. Assessment of the statistical significance of differences between the temperature ranges was performed using the two-sample *t*-test with unequal variances.

The expected future change in the study area climate regime was assessed by comparing the average annual air temperature and the average annual number of days with an air temperature above 0°C for the current climate and for the projected climate for the period 2081–2100. To quantify the expected changes in both indicators, we averaged the calculated differences over the whole study area.

As a "current" climate, we used the indicators obtained by averaging the daily air temperature observations at meteorological stations in the Arctic zone of Russia from 1981–2015 (17), which were interpolated using a kriging[1] (18–20) GIS technique with a spatial resolution of 1 km^2.

The projected indicators for the period 2081–2100 were calculated by an ensemble of 13 climate models included in the international Coupled Model Intercomparison Project 5 (21) according to the RCP8.5 experimental scenario (22). The RCP8.5 scenario accounts for a high level of greenhouse gas-related climate forcing and assumes "no change" in humans' current behavior regarding anthropogenic atmosphere emissions. This scenario provides the most statistically significant models'

[1]Kriging is a procedure of spatial interpolation that allows obtaining a predictive geostatistical surface based on a sparse set of sample data (18, 19). This is a most widely used geostatistical technique to convert point weather station climate observations into a smooth raster surface (20).

response to climate forcing and may be used as a "worst case," but still plausible, climate change scenario.

Climate data processing and visualization of results were performed with ArcMap 10.8.1 software including the Spatial Analyst extension (Esri, USA).

Study on Post-vaccine Immunity

Reindeer were immunized in the Tazovsky district of the YaNAO in September and October 2016 with a dry live vaccine against animal anthrax from the strain 55-VNIVVIM, which was produced by the Oryol Biological Factory (Oryol, Russia) according to the instructions (http://www.biofabrika.com/catalog.html?cid=13). About 15,000 head were vaccinated.

Blood samples were then taken by veterinarians from 913 vaccinated reindeer in July 2017 within the framework of standard veterinary procedures. Blood sampling was performed from the jugular vein and samples were collected in disposable sterile test tubes. Blood serum was obtained by settling the blood, followed by aliquoting 1–2 ml of serum into Eppendorf test tubes. The blood serum was stabilized with boric acid.

Detection of specific anthrax antibodies in the blood serum of animals was performed with the indirect hemagglutination (IHA) test reaction with an anti-anthrax erythrocyte diagnostic kit. Due to the lack of commercial test systems in Russia (14), we produced an antigenic erythrocyte diagnostic kit in accordance with the "Temporary instruction for the manufacture and control of antigenic erythrocyte diagnostic kit for the indirect hemagglutination test reaction (IHA test reaction) (1979)" (23). The method for developing the kit was obtained from the State Scientific Institution for Veterinary Virology and Microbiology of the Russian Agricultural Academy, and the effectiveness of the kit has been confirmed in similar studies (14, 24, 25).

The IHA test reaction was carried out in accordance with the generally accepted procedure (26). The initial blood serum was diluted in a ratio of 1:40 with saline solution (taken as the first serum dilution), after which double dilutions were made and assayed using the erythrocyte diagnostic kit. The preliminary registration of the reaction was carried out after 2–3 h, and the final one after 18 h. The reaction result was assessed visually according to the following scheme:

++++: erythrocytes cover the entire bottom of the well in an even layer; sometimes, an "umbrella" pattern with uneven edges is observed;
+++: red blood cells cover 3/4 of the bottom of the well, and the "umbrella" is smaller;
++: the "umbrella" is small and is located in the very center of the well;
+: in the center of a small "umbrella," the erythrocyte sediment is clearly visible ("buttons").
–: negative reaction, erythrocytes settle on the bottom of the well in the form of a "button" or a small ring with even, well-defined edges.

The reaction results were considered positive when erythrocyte antigen agglutination was detected, starting with a dilution of 1:80 and higher by 3–4 crosses.

To assess the proportion of the whole reindeer population with specific immunity, the testing was considered as a hypergeometric process, where n samples were taken from a population M with a protection level p, of which s were positive (i.e., with a protective titer detected above 1:80). Since the sample size n was much lower than the whole population M, a binomial approximation of the hypergeometric process was used, and the expected protection level p was calculated using the beta distribution: $p = \text{Beta}(s + 1; n - s + 1)$ (27). The calculations were performed using 10,000 Monte Carlo simulations in the Microsoft Excel add-in @RISK v.4.5 (www.palisade.com).

RESULTS

YaNAO Anthrax Outbreak Descriptive Analysis

The anthrax epidemic in the Russian Arctic occurred in July–August 2016 in three territories: the area of Lake Pisoto, the Novoportovskaya tundra, and the area of the Evayakha River. The regions are located at a distance of up to 250 km from each other, and they include two water barriers: the Ob Bay (width: 30–80 km) and the mouth of the Taz River (average width of 25 km). The boundaries of six outbreaks were determined (**Figure 1**), and the susceptible reindeer population was estimated as 41,001 head. Out of the total number of animals, 2,650 (6.46%) animals developed clinical signs, of which 2,350 died (case fatality rate of 88.67%). The outbreak was characterized by the involvement of the human population in the epidemic process, which was manifested by the infection of 36 people with one estimated fatal outcome (28).

An analysis of official reports and directives showed that animals had not been vaccinated in the region of anthrax origin since 2007.

Climate Data Analysis

The analysis of the mean and maximum monthly air temperatures in the spring and summer months of 2016 demonstrated no statistically significant differences between temperatures in May with corresponding values from 1987–2016, while mean temperatures for June, July, and August were found to be 16–100% higher in 2016 (**Table 1**). In general, a rise in summer air temperatures was observed in 2007–2016, reaching peak values of 15.4, 22.1, and 15.0°C in June, July, and August of 2016, respectively.

Modeling of the current and projected climate indicators showed that, in the "worst case" scenario of warming by 2100, the average annual air temperature within the study area is expected to increase by 8.3 ± 0.5°C and will be positive in most parts of the YaNAO, while the yearly number of days with air temperatures above 0°C may rise by 49 ± 6 days (**Figure 2**). Such climate changes may result in further thawing of permafrost over the whole study area and could aggravate the situation with thawing of the soil containing anthrax spores.

Vaccination Effectiveness Assessment

In 2007, the government discontinued routine vaccination of reindeer on the Yamal Peninsula, which was considered free of

TABLE 1 | The results of air temperature comparison in May, June, July, and August 2016 with corresponding indicators for 1987–2016 based on weather station Antipayuta data.

		Mean ± Standard deviation, °C		Difference of mean, °C	Difference of mean, %	*t*-test *p*-value
		1987–2016	2016			
Monthly mean air temperature	May	−4.4 ± 4.7	−4.4 ± 5.1	0	0	>0.1
	June	5.5 ± 5.4	11.0 ± 5.6	5.5	100%	<0.001
	July	13.0 ± 4.8	17.4 ± 4.7	4.4	34%	<0.001
	August	9.5 ± 3.3	11.5 ± 3.2	2.0	21%	<0.001
Monthly maximum air temperature	May	−1.9 ± 4.3	−2.2 ± 4.5	−0.3	−16%	>0.1
	June	8.8 ± 6.6	15.4 ± 6.6	6.6	75%	<0.001
	July	17.0 ± 5.5	22.1 ± 5.4	5.1	30%	<0.001
	August	12.9 ± 3.8	15.0 ± 3.6	2.1	16%	<0.001

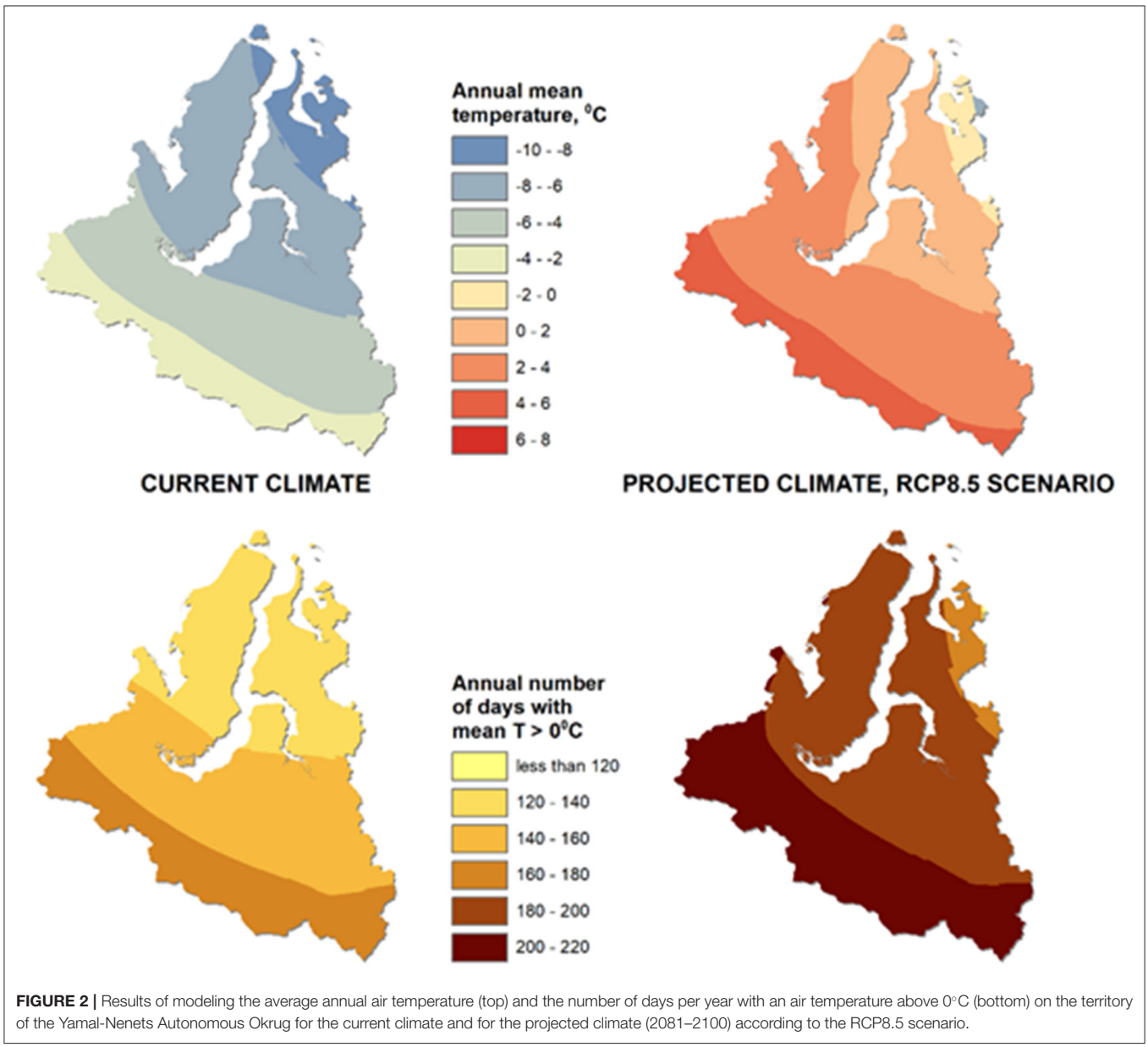

FIGURE 2 | Results of modeling the average annual air temperature (top) and the number of days per year with an air temperature above 0°C (bottom) on the territory of the Yamal-Nenets Autonomous Okrug for the current climate and for the projected climate (2081–2100) according to the RCP8.5 scenario.

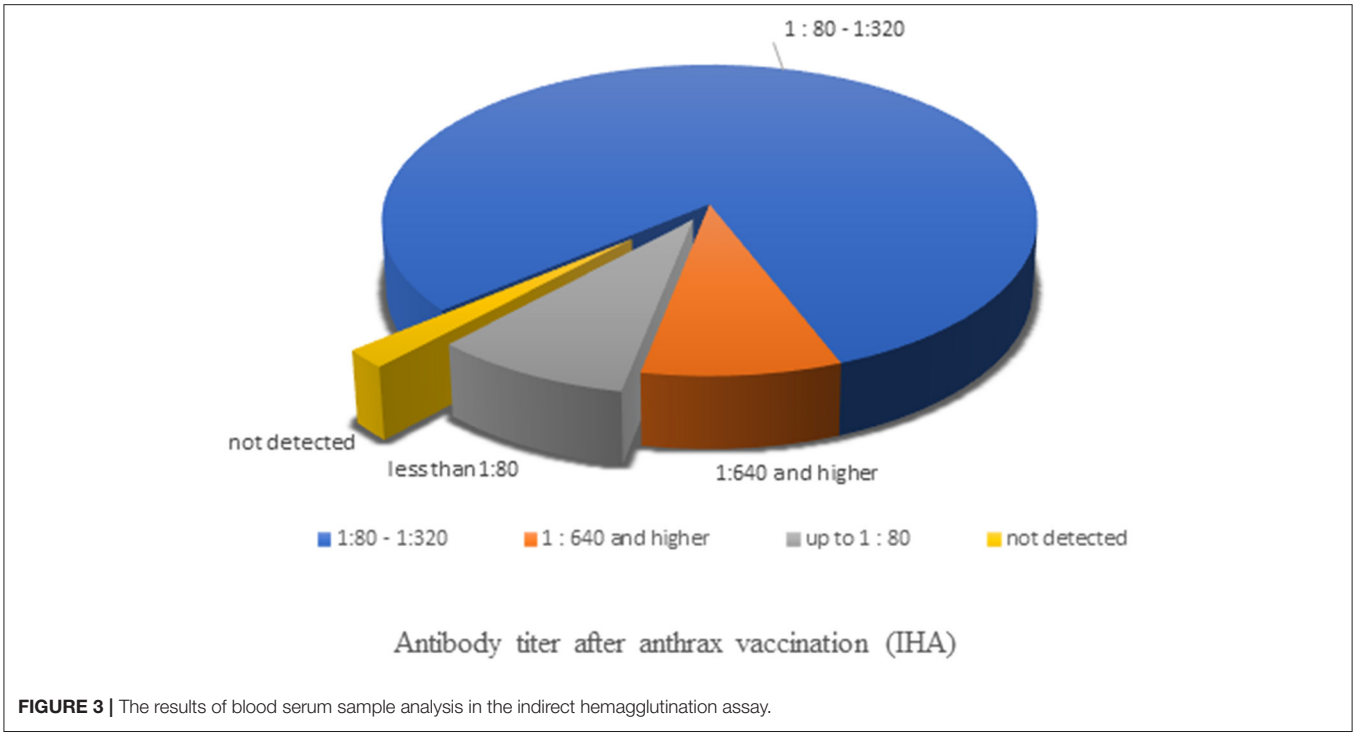

FIGURE 3 | The results of blood serum sample analysis in the indirect hemagglutination assay.

anthrax. Given the time span between the last vaccination in 2007 and the outbreak in 2016, it is likely that the vast majority of animals were not vaccinated prior to exposure to the anthrax bacterium in 2016. Such a naïve population is fertile ground for the spread of an infectious agent, as all or most animals would not have had immunity to anthrax.

The strength of immunity against anthrax after resumption of the vaccine in 2016 was determined in the IHA blood serum results (**Figure 3**). Screening of 913 samples of reindeer blood sera for anthrax antibodies by this assay showed that 1.97% of samples (18 head) did not contain anthrax antibodies. In 8.87% of samples (81 head), anthrax antibodies were detected at a titer of 1:80, which is lower than the protective level. In 89.16% of the samples (814 head), the level of specific antibodies at 9 months after vaccination was ≥1:80, of which 9.0% of the samples (82 head) had a serum anthrax antibody titer of ≥1:640. The data obtained indicate the creation of an immune proportion of 89% (95% confidence interval: 87–91%) of the reindeer population in the Tazovsky district of the YaNAO.

DISCUSSION

In this study, we evaluated the effectiveness of the reindeer vaccination against anthrax performed as a response to the 2016 outbreak in the Yamal Peninsula, explored the contribution of climate conditions in the summer of 2016 to that outbreak, and assessed the expected climate change in this region and its potential effect on the anthrax resurgence risk. We found that the vaccination led to a protection level of 89% of the whole reindeer population. Moreover, an abnormally high ambient temperature in summer 2016 contributed to the thawing of permafrost and the reactivation of soil reservoirs of *B. anthracis*. Using the projected climate data for 2081–2100 according to the "worst case" RCP8.5 scenario, we demonstrated that the expected climate change would provide conditions for reactivation of soil anthrax reservoirs.

Vaccination-based anthrax prevention in many developed countries has led to a decrease in the number of registered disease cases (29–36). However, the risk of anthrax remains high in sub-Saharan Africa, Southeast Asia, and parts of Russia and the former Soviet Union countries (37–40). Serological testing is necessary to determine the effectiveness of vaccination programs and obtain epidemiological information in anthrax-endemic areas. In Russia, the effectiveness of the vaccination of reindeer against anthrax has not previously been evaluated; therefore, no data exist on the levels of antibodies in reindeer during 2007–2017. To the best of our knowledge, this research is the first in the field to investigate this in reindeer specifically. However, data from studies on the effectiveness of anthrax vaccination in livestock animals demonstrated high levels of antibodies in cows and sheep for about 1.5 years (41). This suggests that at the time of the 2016 outbreak, there could be no immunity among reindeer. In this study, we demonstrated the usefulness of anthrax vaccination by screening reindeer herds in the Tazovsky district of the YaNAO for anthrax antibodies using an IHA. In 89.16% of the samples, the level of specific antibodies by 9 months after vaccination was ≥1:80, of which 9.0% of the samples had a serum anthrax antibody titer of ≥1:640. This indicates the establishment of immunity in 89% of the reindeer

population. No new anthrax outbreaks have been observed in the YaNAO since 2016. Based on the concept of herd immunity, the number of immune individuals in the population needed to prevent the spread of infection should be at least $1 - 1/R_0$, where R_0 is the basic reproductive ratio of the disease (42). Accepting the R_0 value for anthrax as 1.251–1.292 according to previous studies (43, 44), we obtained a minimum herd immunity threshold of 20–23%. Thus, the immune proportion achieved as a result of vaccination can be considered sufficient to prevent the spread of anthrax in the reindeer population. The absence or low levels of anthrax antibodies in a part of the population may indicate omission of anthrax vaccinations or violations of vaccination rules (vaccination of pregnant, weakened, and emaciated animals, etc.), or it could be related to the characteristics of some individuals.

Currently, climate change is more pronounced in the Russian Arctic than in any other part of the country. The fastest rates of environmental changes on the Earth are observed in this region, including a decrease in the extent of sea ice, melting of glaciers and ice sheets, lengthening of the growing season, melting of permafrost, and strengthening of the hydrological cycle. The average annual air temperature in the Russian North increased by 1.28°C from 1905–2000 (40). The global temperature of the Earth's surface warmed by 0.89°C from 1901–2012 (45). Permafrost is any ground that remains completely frozen below 0°C for at least 2 consecutive years (46). Permafrost may reach a base depth of more than 1,000 m and remain frozen for thousands of years.

In permafrost conditions, microorganisms are well-preserved and the permafrost acts as an accumulator of microbiota. The preservation of *B. anthracis* spores in permafrost conditions is not doubted (10). Permafrost temperatures increased by 0.29 ± 0.12°C worldwide following the increase in air temperature in the Arctic (47). Permafrost in the Russian Arctic has thus become a reservoir for anthrax that can preserve viable spores for a long time. The high air temperature in the studied region could lead to the thawing of permafrost and the opening of soil anthrax reservoirs, as well as an increase in the number of blood-sucking insects that may carry the anthrax pathogen (10, 48). Consequently, global warming in the Arctic could become one of the risk factors for the occurrence and spread of anthrax due to thawing of the permafrost (49, 50). Under changed climatic and soil-hydrological conditions, these spores could have appeared on the soil surface and consequently infected animals. Our modeling has shown that in the case of an unfavorable climate change scenario, the average annual air temperature on the territory of the YaNAO will exceed 0°C, creating conditions for widespread permafrost thawing.

The second risk factor for epidemic anthrax is the discontinuation of vaccination. The Yamal tundra is the largest center of reindeer husbandry in the Arctic; for example, 254,000 head of reindeer were grazed in the Yamal district of YaNAO in 2015 (51). Thus, the epidemic and economic risks are very high in this region. Retrospective analysis of climate data and modeling indicated the effectiveness of anthrax prevention by annual vaccination of reindeer.

To assess the extent of coverage of the animal population and the effectiveness of vaccination, serological monitoring should be carried out, including the use of the IHA diagnostic kit for detecting erythrocyte anthrax antigens.

CONCLUSIONS

This study showed that the factors that caused the 2016 anthrax epidemic in the Russian Arctic may include the increase in summer air temperatures, the climate change-induced thawing of permafrost, and the discontinuation of vaccination of reindeer against anthrax. This led to the creation of an anthrax epidemic chain. Moreover, the expected climate change according to the most unfavorable scenario may contribute to marked warming in the YaNAO territory, creating conditions for widespread thawing of permafrost and reactivation of anthrax foci in soil. The level of post-vaccination immunity in reindeer detected in our study can be considered sufficient to prevent anthrax outbreaks, including under conditions of thawing permafrost in the Russian Arctic. In the period 2017–2020, no new outbreaks of anthrax were recorded in the Yamal Peninsula, which can be ascribed to the traditional practice of annual vaccination against anthrax. Moreover, the IHA developed here is an effective tool that will be useful for monitoring the effectiveness of reindeer vaccination in the context of an increasing epidemic risk of anthrax in the Arctic.

DATA AVAILABILITY STATEMENT

The data analyzed in this study is subject to the following licenses/restrictions: The datasets of climatic variables as well as reindeer blood samples data cannot be publicly shared due to confidentiality. They can be obtained on reasonable request from the corresponding authors. Requests to access these datasets should be directed to Elena A. Liskova, liskovaea@mail.ru.

AUTHOR CONTRIBUTIONS

EL, AB, and FK: conceptualization, validation, and formal analysis. IE, EL, AB, GS, and SM: methodology. FK and OZ: software. IR, OZ, and NT: investigation. NG, OB, and GS: resources. EL and AB: data curation and supervision. EL, IR, OZ, and AB: writing—original draft preparation. EL, YS, FK, and AB: writing—review and editing. OZ and FK: visualization. IE and II: project administration. All authors have read and agree to the published version of the manuscript.

FUNDING

The work was supported by the Federal Research Center for Virology and Microbiology (FRCVM) for government assignment.

REFERENCES

1. Gomez JP, Nekorchuk DM, Mao L, Ryan SJ, Ponciano JM, Blackburn JK. Decoupling environmental effects and host population dynamics for anthrax, a classic reservoir-driven disease. *PLoS ONE.* (2018) 13:e0208621. doi: 10.1371/journal.pone.0208621
2. Rovid Spickler A. *Anthrax*. (2003). Available online at: www.cfsph.iastate.edu (accessed October 1, 2020).
3. Elvander M, Persson B, Sternberg Lewerin S. Historical cases of anthrax in Sweden 1916–1961. *Transbound Emerg Dis.* (2017) 64:892–8. doi: 10.1111/tbed.12456
4. Dixon TC, Meselson M, Guillemin J, Hanna PC. Anthrax. *N Engl J Med.* (1999) 341:815–26. doi: 10.1056/NEJM199909093411107
5. WHO. *Anthrax in Humans and Animals*. Available online at: https://www.who.int/csr/resources/publications/AnthraxGuidelines2008/en/ (accessed October 1, 2020).
6. Hugh-Jones ME, De Vos V. Anthrax and wildlife. *Rev Sci Tech l'OIE.* (2002) 21:359–83. doi: 10.20506/rst.21.2.1336
7. Eremenko EI, Ryazanova AG, Buravtseva NP. The current situation on anthrax in Russia and in the world main trends and features. *Probl Part Danger Infect.* (2017) 1:65–71. doi: 10.21055/0370-1069-2017-1-65-71
8. Revich BA, Podolnaya MA. Thawing of permafrost may disturb historic cattle burial grounds in East Siberia. *Glob Health Action.* (2011) 4:8482. doi: 10.3402/gha.v4i0.8482
9. Selyaninov YO, Egorova IY, Kolbasov DV, Listishenko AA. Anthrax in Yamal: re-emergence causes and diagnostic issues. *Veterinariya.* (2016) 10:3–7. Available online at: https://www.elibrary.ru/item.asp?id=27297097
10. Timofeev V, Bahtejeva I, Mironova R, Titareva G, Lev I, Christiany D, et al. Insights from *Bacillus anthracis* strains isolated from permafrost in the tundra zone of Russia. *PLoS ONE.* (2019) 14:e0209140. doi: 10.1371/journal.pone.0209140
11. Peterson MJ, Davis DS, Templeton JW. An enzyme-linked immunosorbent assay for detecting anthrax antibody in white-tailed deer (Odocoileus virginianus): evaluation of anthrax vaccination and sera from free-ranging deer. *J Wildl Dis.* (1993) 29:130–5. doi: 10.7589/0090-3558-29.1.130
12. Kazanovskiy ES. Veterinary problems of northern reindeer breeding and improvement of technology of carrying out of mass treatment-and-prophylactic actions. *Agric Sci Euro-North-East.* (2017) 59:44–8. doi: 10.30766/2072-9081.2017.59.4.44-48
13. Barkov AM, Barkova IA, Alekseev VV, Lipnitskiy AV, Kulakov MY. Detection of antibodies to protective antigen of bacillus anthracis using indirect hemagglutination test and enzime-linked immunosorbent assay. *Probl Part Danger Infect.* (2010) 52:42–5. doi: 10.21055/0370-1069-2010-3(105)-42-45
14. Vasina NK, Selyaninov YO, Egorova IY. *Serological Monitoring of the Efficiency of Specific Prevention of the Siberian Ulcer in the Cfd Rf.* (2012). Available online at: https://booksc.org/book/36540006/ee6fa4 (accessed October 7, 2020)
15. Yuzhakov AA. Northern reindeer breeding in the twenty-first century: genetic resource, cultural heritage and business. *Arct Ecol Econ.* (2017) 4:131. doi: 10.25283/2223-4594-2017-2-131-137
16. Russ Fed Serv Hydrometeorol Environ Monit. *A Report on Climate Features on the Territory of the Russian Federation in 2018*. (2019). Available online at: https://meteoinfo.ru/images/media/climate/rus-clim-annual-report.pdf (accessed October 11, 2020)
17. Bulygina ON, Razuvaev VN, Aleksandrova TM. *Description of the Data Array of Daily Air Temperature and the Quantity of Precipitation at Meteorological Stations in Russia and the FORMER USSR (TTTR) "Certificate of State Registration of the Database No. 2014620942*. Available online at: http://meteo.ru/data/162-temperature-precipitation#описание-массива-данных (accessed October 24, 2020).
18. Oliver MA. Kriging: a method of interpolation for geographical information systems. *Int J Geographic Inform Syst.* (1990) 4:313–32. doi: 10.1080/02693799008941549
19. Oliver MA. The variogram and kriging. In: Fischer MM, Business Vienna University of Economics and GIScience, editors. *Handbook of Applied Spatial Analysis*. Berlin; Heidelberg: Springer (2010). p. 319–52. doi: 10.1007/978-3-642-03647-7_17
20. Hofstra N, Haylock M, Jones MNP, Frei C. Comparison of six methods for the interpolation of daily, European climate data. *J Geophys Res Atmos.* (2008) 113:D21110. doi: 10.1029/2008JD010100
21. Taylor KE, Stouffer RJ, Meehl GA. An overview of CMIP5 and the experiment design. *Bull Am Meteorol Soc.* (2012) 93:485–98. doi: 10.1175/BAMS-D-11-00094.1
22. *Towards New Scenarios for Analysis of Emissions, Climate Change, Impacts, and Response Strategies. Technical Summary*. Available online at: https://www.researchgate.net/publication/236487152_Towards_New_Scenarios_for_Analysis_of_Emissions_Climate_Change_Impacts_and_Response_Strategies_Technical_Summary (accessed October 24, 2020)
23. *Temporary instructions for the Manufacture and Control of the Anthrax Dry Antigenic Erythrocyte Diagnosticum for Staging the Indirect Hemagglutination Reaction (RNGA)*. VNIIVViM (Pocrov). Pokrov (1979). Protocol #16, September 19, 1979.
24. Bakulov IA, Gavrilov VA, Seliverstov VV. *Anthrax. New Pages in the Study of the "old disease." Posad*. Vladimir (2001).
25. Ivanova SV, Melnikova LA, Rodionov AP, Makaev KhN. The use of erythrocyte diagnostic in assessing the effectiveness of cattle immunoprophylaxis against anthrax. *Veterinariya.* (2019) 11:25–8. doi: 10.30896/0042-4846.2019.22.11.25-29
26. Birger MO. *Handbook of Microbiological and Virological Research Methods*. Moscow: Medicina Moscow. (1982). 133–135.
27. Vose D. *Risk Anaysis - A Quantitative Guide*. Chichester: John Wiley & Sons (2008). p. 729.
28. Ryazanova AG, Semenova O V., Eremenko EI, Aksenova LY, Buravtseva NP, Golovinskaya TM, et al. Epidemiological and epizootiological situation on anthrax in 2017, Forecast for 2018. *Probl Part Danger Infect.* (2018) 1:63–5. doi: 10.21055/0370-1069-2018-1-63-65
29. Carlson CJ, Getz WM, Kausrud KL, Cizauskas CA, Blackburn JK, Bustos Carrillo FA, et al. Spores and soil from six sides: interdisciplinarity and the environmental biology of anthrax (*Bacillus anthracis*). *Biol Rev.* (2018) 93:1813–31. doi: 10.1111/brv.12420
30. Cross AR, Baldwin VM, Roy S, Essex-Lopresti AE, Prior JL, Harmer NJ. Zoonoses under our noses. *Microbes Infect.* (2019) 21:10–19. doi: 10.1016/j.micinf.2018.06.001
31. Dragon DC, Bader DE, Mitchell J, Woollen N. Natural dissemination of *Bacillus anthracis* spores in Northern Canada. *Appl Environ Microbiol.* (2005) 71:1610–5. doi: 10.1128/AEM.71.3.1610-1615.2005
32. Gates CC, Elkin BT, Dragon DC. Investigation, control and epizootiology of anthrax in a geographically isolated, free-roaming bison population in northern Canada. *Can J Vet Res.* (1995) 59:256–264.
33. Lewerin SS, Elvander M, Westermark T, Hartzell LN, Norström AK, Ehrs S, et al. Anthrax outbreak in a Swedish beef cattle herd - 1st case in 27 years: case report. *Acta Vet Scand.* (2010) 52:7. doi: 10.1186/1751-0147-52-7
34. Hueffer K, Drown D, Romanovsky V, Hennessy T. Factors contributing to anthrax outbreaks in the circumpolar North. *Ecohealth.* (2020) 17:174–80. doi: 10.1007/s10393-020-01474-z
35. Williamson ED, Dyson EH. Anthrax prophylaxis: Recent advances and future directions. *Front Microbiol.* (2015) 6:1009. doi: 10.3389/fmicb.2015.01009
36. World Health Organization. *Anthrax in Humans and Animals. Fourth Edition Food and Agriculture Organization of the United Nations World Organisation for Animal Health*. (2008). Available online at: https://www.who.int/csr/resources/publications/AnthraxGuidelines2008/en/ (accessed February 5, 2021).
37. Fasanella A, Garofolo G, Galante D, Quaranta V, Palazzo L, Lista F, et al. Severe anthrax outbreaks in Italy in 2004: considerations on factors involved in the spread of infection. *New Microbiol.* (2010) 33:83–86.
38. Kasradze A, Echeverria D, Zakhashvili K, Bautista C, Heyer N, Imnadze P, et al. Rates and risk factors for human cutaneous anthrax in the country of Georgia: National surveillance data, 2008–2015. *PLoS ONE.* (2018) 13:e0192031. doi: 10.1371/journal.pone.0192031
39. Kracalik I, Abdullayev R, Asadov K, Ismayilova R, Baghirova M, Ustun N, et al. Changing patterns of human anthrax in azerbaijan during the post-soviet and preemptive livestock vaccination eras. *PLoS Negl Trop Dis.* (2014) 8:e2985. doi: 10.1371/journal.pntd.0002985

40. Revich B, Tokarevich N, Parkinson AJ. Climate change and zoonotic infections in the Russian arctic. *Int J Circumpolar Health.* (2012) 71:18792. doi: 10.3402/ijch.v71i0.18792
41. Ipatenko NG, Gavrilov VA, Manichev AA. Experience in the prevention of anthrax in animals in Russia. *Veterinary*. (1995) 5:27–30.
42. Anderson RM, May RM. *Infectious Diseases of Humans: Dynamics and Control*. Oxford: Oxford University Press (1992). 757. p.
43. van den Driessche P. Reproduction numbers of infectious disease models. *Infect Dis Model.* (2017) 2:288–303. doi: 10.1016/j.idm.2017.06.002
44. Saad-Roy CM, van den Driessche P, Yakubu AA. A mathematical model of anthrax transmission in animal populations. *Bull Math Biol.* (2017) 79:303–24. doi: 10.1007/s11538-016-0238-1
45. Zhou Z, Shi H, Fu Q, Li T, Gan TY, Liu S, et al. Is the cold region in Northeast China still getting warmer under climate change impact? *Atmos Res.* (2020) 237:104864. doi: 10.1016/j.atmosres.2020.104864
46. Oliva M, Fritz M. Permafrost degradation on a warmer Earth: Challenges and perspectives. *Curr Opin Environ Sci Heal.* (2018) 5:14–18. doi: 10.1016/j.coesh.2018.03.007
47. Biskaborn BK, Smith SL, Noetzli J, Matthes H, Vieira G, Streletskiy DA, et al. Permafrost is warming at a global scale. *Nat Commun.* (2019) 10:264. doi: 10.1038/s41467-018-08240-4
48. Turell MJ, Knudson GB. Mechanical transmission of *Bacillus anthracis* by stable flies (Stomoxys calcitrans) and Mosquitoes (Aedes aegypti and Aedes taeniorhynchus). *Infect Immun.* (1987) 55:1859–61. doi: 10.1128/IAI.55.8.1859-1861.1987
49. Park H, Sherstiukov AB, Fedorov AN, Polyakov IV, Walsh JE. An observation-based assessment of the influences of air temperature and snow depth on soil temperature in Russia. *Environ Res Lett.* (2014) 9:064026. doi: 10.1088/1748-9326/9/6/064026
50. Government of the Yamalo-Nenets Autonomous Okrug. *Elimination of the Outbreak of Anthrax in the Yamal Region.*. Available online at: https://www.yanao.ru/activity/2833/?filter_p_type=current&nav-projects=page-1 (accessed October 8, 2020)
51. Bogdanov V, Golovatin M. Anthrax in Yamal: an ecological look at traditional reindeer husbandry. *Ecology.* (2017) 2:1–6. doi: 10.1134/S1067413617020059

Conflict of Interest: The authors declare that the research was conducted in the absence of any commercial or financial relationships that could be construed as a potential conflict of interest.

frontiers in Veterinary Science

ORIGINAL RESEARCH
published: 25 June 2021
doi: 10.3389/fvets.2021.650942

Deletion of the Transcriptional Regulator MucR in *Brucella canis* Affects Stress Responses and Bacterial Virulence

Jiali Sun[1†], Hao Dong[2,3†], Xiaowei Peng[1†], Yufu Liu[1†], Hui Jiang[1], Yu Feng[1], Qiaoling Li[1], Liangquan Zhu[1], Yuming Qin[1] and Jiabo Ding[1*]*

[1] National Reference Laboratory for Animal Brucellosis, China Institute of Veterinary Drug Control, Beijing, China, [2] Veterinary Diagnostic Laboratory, China Animal Disease Control Center, Beijing, China, [3] Institute for Laboratory Animal Resources, National Institutes for Food and Drug Control, Beijing, China

OPEN ACCESS

Edited by:
Lester J. Perez,
University of Illinois at Urbana–Champaign, United States

Reviewed by:
Huanying Pang,
Guangdong Ocean University, China
Shaohui Wang,
Chinese Academy of Agricultural Sciences (CAAS), China

***Correspondence:**
Yuming Qin
qinyuming73@163.com
Jiabo Ding
dingjiabo@126.com

[†] These authors share first authorship

Specialty section:
This article was submitted to Veterinary Infectious Diseases, a section of the journal Frontiers in Veterinary Science

Received: 08 January 2021
Accepted: 31 May 2021
Published: 25 June 2021

Citation:
Sun J, Dong H, Peng X, Liu Y, Jiang H, Feng Y, Li Q, Zhu L, Qin Y and Ding J (2021) Deletion of the Transcriptional Regulator MucR in Brucella canis Affects Stress Responses and Bacterial Virulence. Front. Vet. Sci. 8:650942. doi: 10.3389/fvets.2021.650942

The transcriptional regulator MucR is related to normal growth, stress responses and *Brucella* virulence, and affects the expression of various virulence-related genes in smooth-type *Brucella* strains. However, the function of MucR in the rough-type *Brucella canis* remains unknown. In this study, we discovered that MucR protein was involved in resistance to heat stress, iron-limitation, and various antibiotics in *B. canis*. In addition, the expression level of various bacterial flagellum-related genes was altered in *mucR* mutant strain. Deletion of this transcriptional regulator in *B. canis* significantly affected *Brucella* virulence in RAW264.7 macrophage and mice infection model. To gain insight into the genetic basis for distinctive phenotypic properties exhibited by *mucR* mutant strain, RNA-seq was performed and the result showed that various genes involved in translation, ribosomal structure and biogenesis, signal transduction mechanisms, energy production, and conversion were significantly differently expressed in Δ*mucR* strain. Overall, these studies have not only discovered the phenotype of *mucR* mutant strain but also preliminarily uncovered the molecular mechanism between the transcriptional regulator MucR, stress response and bacterial virulence in *B. canis*.

Keywords: *Brucella canis*, MucR, virulence, RNA-Seq, stress responses

INTRODUCTION

In 1966, *Brucella canis* was first isolated from aborted tissues and vaginal discharge of beagles (1). In dogs, *B. canis* causes reproductive failure, while it causes fever, chills, malaise, peripheral lymphadenomegaly, and splenomegaly in humans (2). Recent studies have demonstrated that the intracellular trafficking route of *B. canis* was indistinguishable from that of *B. abortus* and a less robust response was observed in mice infected with *B. canis* compared with *B. abortus* in terms of proinflammatory cytokines, interferon-gamma levels, splenic inflammation, and hepatic granulomas (3). Another study indicated that only a dose of *B. canis* (up to 10^9 CFU) could induce splenomegaly in infected mice at 1 and 2 weeks post-inoculation and the suitable challenge dose (1×10^7 CFU) for investigating vaccine safety for *B. canis* seemed to be about 10^3-fold higher than that of smooth-type *Brucella* strains (4). It seems that *B. canis* is less pathogenic than other smooth-type *Brucella* species in this murine model.

Due to the low prevalence of brucellosis caused by *B. canis*, which is less pathogenic than other *Brucella* species, most countries have not established clear protocols for its prevention and the public risk of this pathogen is usually ignored. Additionally, comparatively little is known about the pathogenic mechanism and virulence factors of *B. canis* strains.

Brucella strains do not produce classical virulence factors, such as cytolisins, exotoxin, exoenzymes, fimbria, plasmids, and drug-resistant forms. Lipopolysaccharide (LPS), T4SS secretion system, and BvrR/BvrS system have been considered to be major virulence factors allowing interaction with the host cell surface, the formation of an early, late BCV (*Brucella* Containing Vacuole) and interaction with the endoplasmic reticulum (ER) when the bacteria multiply (5). Besides, some transcription regulators have been proved to be involved in *Brucella* virulence, such as the well-studied LuxR-type regulator VjbR (6).

The virulence-related transcriptional regulator MucR, which is a member of the Ros/MucR family, is considered to control the expression of various genes involved in the successful interaction of α-proteobacteria with their eukaryotic hosts (7–9). In *B. melitensis* and *B. abortus*, the transcriptional regulator MucR is an extensively studied virulence factor and *mucR* mutant strain has been considered to be a promising vaccine candidate in mice model against both intraperitoneal and aerosol challenge (10). In *Brucella* strains, previous studies have also demonstrated that MucR protein is involved in resistance to environmental stresses, such as acidic stress, oxidative stress, detergent, cationic peptide, and iron deficiency (9, 11). Additionally, previous transcriptomic and microarray analyses have revealed that MucR could directly and indirectly affect the expression of hundreds of genes involved in metabolism, cell wall/envelope biogenesis, replication, and translation (9, 12). In recent studies, various target genes, which were directly regulated by MucR protein, were also identified, such as *babR*, *virB* genes, *bab1_0746*, *bab1_1035*, *bab1_1605,* and *bab1_1893* (12, 13). Compared to the well-studied MucR protein in smooth-type *Brucella* strains, no study has been carried out so far to demonstrate the function of MucR protein in *B. canis* strains.

Herein, we constructed *mucR* in-frame deleted mutant strain and complemented strain in *B. canis*. Then, we assessed the phenotypes of *mucR* mutant strain, such as growth characteristics and bacterial virulence in both macrophages and mice infection models. Moreover, the sensitivity of Δ*mucR* under various stress conditions was determined. Finally, RNA-seq analysis was performed to investigate the changes of the transcriptional profile of gene expression in *mucR* mutant strain compared with its parent strain RM6/66.

MATERIALS AND METHODS

Construction of *mucR* Deletion Mutant Strain

Construction of the suicide plasmid was performed as previously reported (14). Specifically, for *B. canis* RM6/66 *mucR* gene mutant, a 433-bp upstream fragment and a 500-bp downstream fragment of *mucR* gene were amplified using D-mucR-UF/UR and D-mucR-DF/DR primers, respectively (**Supplementary Table 1**). The two fragments were then used as templates for the second round of overlap polymerase chain reaction (PCR). The purified PCR product was digested with *Kpn*I and *Hind*III restriction enzymes and cloned into the puc19-*sacB* plasmid, which was verified using PCR and sequencing.

The *B. canis* RM6/66 *mucR* gene unmarked in-frame deletion mutant was constructed with allelic replacement using a two-step method (14). The suicide plasmid was transformed into the wild-type *B. canis* RM6/66 strain by electro transformation. Single crossover integrates were then selected on tryptic soy agar (TSA) supplemented with ampicillin (100 μg/ml). The second crossover selection was conducted by plating the bacteria on TSA containing 5% sucrose. Ampicillin sensitive colonies were selected and verified by PCR and sequencing.

Construction of *mucR* Complemented Strain

The *mucR* fragment, including the promoter sequence (500-bp of the intergenic region upstream of *mucR* start codon), was amplified with C-mucR-F/R primers (**Supplementary Table 1**). The PCR products were ligated to pMR11 plasmid, which was then referred to as the complementation plasmid pMR-*mucR*. To construct the complemented strain (C*mucR*), pMR-*mucR* was electroporated into *mucR* deletion mutant and then the cells were plated onto TSA containing ampicillin to detect the presence of pMR-*mucR* in the complemented strain. The resulting strains were verified by PCR and sequencing. For determination of minimum inhibitory concentrations (MICs) of antibiotics, the complemented strain (C*mucR*1) with chloramphenicol resistance was constructed using pBBR1MCS-1 plasmid using the same primers (C-mucR-F/R) as previously reported (15).

RNA Isolation

For RNA-seq assay, *Brucella* strains (RM6/66 and Δ*mucR*) were grown in three different tubes with TSB at 37°C from a single colony until the log phase was reached. Total RNA was isolated using TRIzol according to the manufacturer's instructions. Residual DNA in the samples was removed using DNase I. RNA concentration and purity were determined spectrophotometrically using an ND 1000 spectrophotometer (Thermo Scientific, Wilmington, USA).

RNA-Sequencing

The sequencing library of each RNA sample was prepared using NEB Next Ultra Directional RNA Library Prep Kit for Illumina as recommended by the manufacturer. Briefly, RNA fragments were reverse-transcribed and amplified to double-stranded cDNA and then ligated with an adaptor. The amplified cDNA was purified using the magnetic bead-based method and the molar concentration was determined for each cDNA library. The HiSeq X Ten platform was used to perform transcriptome sequencing. Sequencing and subsequent bioinformatics analysis were completed at Novel Bioinformatics Co., Ltd (Shanghai, China).

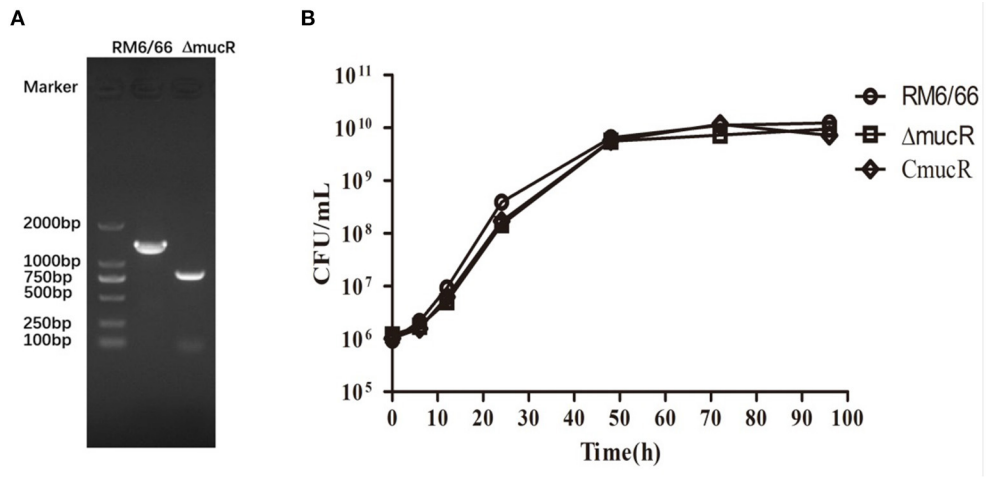

FIGURE 1 | Characterization of *mucR* in-frame deleted mutant strain Δ*mucR*. **(A)** PCR amplification confirmed deletion of the *mucR* gene in Δ*mucR*. Lane M: DNA marker DL2000 (Takara, Dalian, China). *B. canis* RM6/66: a 1429-bp fragment was amplified using primer pair D-mucR-UF/D-mucR-DR. Δ*mucR*: an 846-bp fragment was amplified using primer pair D-mucR-UF/D-mucR-DR. Primer sequences are provided in **Supplementary Table 1**. **(B)** Deletion of *mucR* in *B. canis* RM6/66 did not affect bacterial growth. *Brucella* strains (initial density of 1×10^6 CFU/mL) were grown in TSB at 37°C with continuous shaking for 96 h. The CFUs of *B. canis* RM6/66 and Δ*mucR* were measured at different time intervals. Statistical significance was determined using the unpaired Student's *t*-test. ns, no significance.

Quantitative RT-PCR

qRT-PCR was performed as previously described (16). Differentially expressed genes (DEGs) were verified by qRT-PCR using different samples like that in RNA-seq. Samples were amplified in a 20-μl reaction containing 10-μl 2 × SYBR® Premix Ex TaqTMII (TAKARA), 100 nM forward and reverse primers and 1-μl 10-fold diluted cDNA sample. 16S rRNA, which is constantly transcribed in bacteria, was chosen as the housekeeping gene. For each gene, qRT-PCR was performed in triplicate and relative transcription levels were determined using the $2^{-\Delta\Delta Ct}$ method. Primers used for qRT-PCR are provided in **Supplementary Table 1**.

Cell Infections

The multiplication of *B. canis* RM6/66 and its derived strains in RAW264.7 macrophages were evaluated to determine the ability of Δ*mucR* mutant strain to survive intracellularly. The assays were performed as previously described (14). Briefly, in a permissive culture condition, *B. canis* strains were cultured in a flask with 0.2 μM vent cap for 12 h. RAW264.7 cells were seeded in 24-well plates (Corning, NY, USA) and then infected with *Brucella* strains at a multiplicity of infection (MOI) of 100. After 1 h of incubation, cells were washed thrice with phosphate buffer saline (PBS) and incubated in Dulbecco's Modified Eagle Medium (DMEM) containing gentamycin (50 μg/ml) to eliminate extracellular bacteria. At 1, 24, and 48 h post-infection (hpi), cells were washed and lysed with 500 μl 0.1% (v/v) Triton X-100 water solution, and then the bacteria count was determined by plating on TSA. The assays were run in triplicate and repeated at least twice.

Mouse Infections

Virulence assay was performed using BALB/c mice as previously reported (14) with some modifications. Mice were inoculated intraperitoneally with 0.1 ml (1×10^7 CFU) of *B. canis* RM6/66 and its derived strains. On the 7th and 28th day post-infection (dpi), mice were euthanized *via* asphyxiation ($n = 4$ per group), after which the spleens were removed, weighed, and homogenized in 1 ml of PBS. The bacterial colonies were counted by the TSA plate method and CFUs per spleen were calculated.

Stress Assays

To test the susceptibility of *Brucella* strains under different stress conditions, modified stress assays were performed as previously reported (9, 15). *Brucella* strains (with an initial density of 1×10^6 CFU/mL) were, respectively, cultured in an acidic tryptic soy broth (TSB) medium (pH 4.5) for 2 h. Afterward, the concentration of bacteria was measured by plate count and the survival rate (%) calculated as surviving bacteria relative to the TSB control.

To determine the sensitivity of Δ*mucR* mutant to heat shock stress and hypertonic environments, 5 μl gradient dilution of bacterial cultures (1×10^9 CFU/mL) were cultured on TSA medium at 42°C or TSA medium containing 200 mM sodium chloride (NaCl) at 37°C for 72 h, respectively.

To compare the growth of *B. canis* RM6/66, Δ*mucR* and the complemented strain in low iron medium, the TSB medium was limited in iron by adding different concentrations of the iron chelator, 2,2-dipyridyl (2.5, 5, and 10 mM). The bacteria were cultured in this medium at the same initial density (1×10^6 CFU/ml) and the CFUs were determined at 48 h for each strain.

Determination of MICs of Antibiotics

MIC values of the antibiotics from both β-lactam (Ampicillin, Amoxycillin, and Carbenicillin) and non-β-lactam (Ciprofloxacin, Gentamicin, and Tetracycline) were determined as previously reported (16).

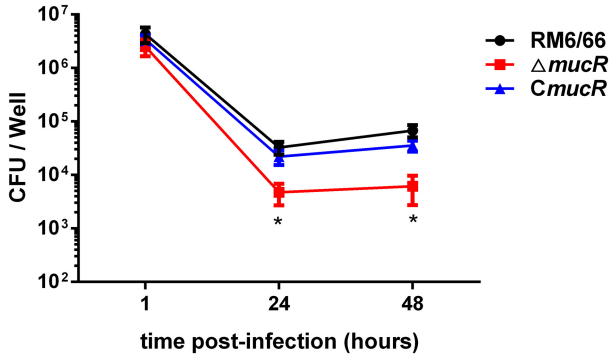

FIGURE 2 | Role of mucR in the intracellular behavior of *B. canis* RM6/66 in RAW264.7 macrophages. Intracellular survival of *B. canis* RM6/66, Δ*mucR*, and C*mucR* strains in RAW264.7 macrophages. The MOI was 100:1. Data represent the means of three experiments performed in duplicate and error bars indicate the SD. *$p < 0.05$.

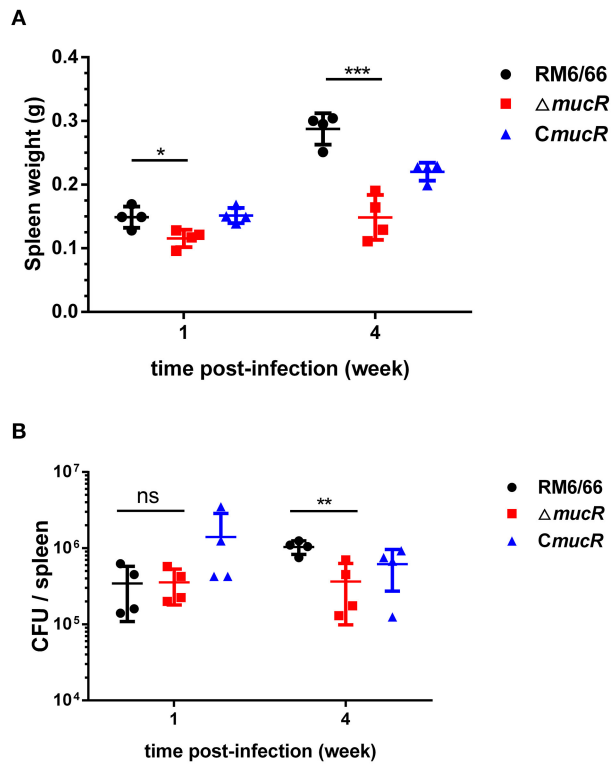

FIGURE 3 | Evaluation of the residual virulence of *B. canis* RM6/66, Δ*mucR* and C*mucR* in BALB/c mice model. **(A)** Spleen weight of *B. canis* RM6/66, Δ*mucR*, and C*mucR* infected mice at 1 and 4 weeks post-infection. **(B)** Splenic CFUs of *B. canis* RM6/66, Δ*mucR*, and C*mucR* infected mice at 1 and 4 weeks post-infection. *$p < 0.05$, **$p < 0.01$, ***$p < 0.001$.

Statistical Analysis

Differences between the means of the experimental and the control groups were analyzed using the independent-samples *t*-test using SPSS 17.0 program. The differences were considered to be significant at $p < 0.05$.

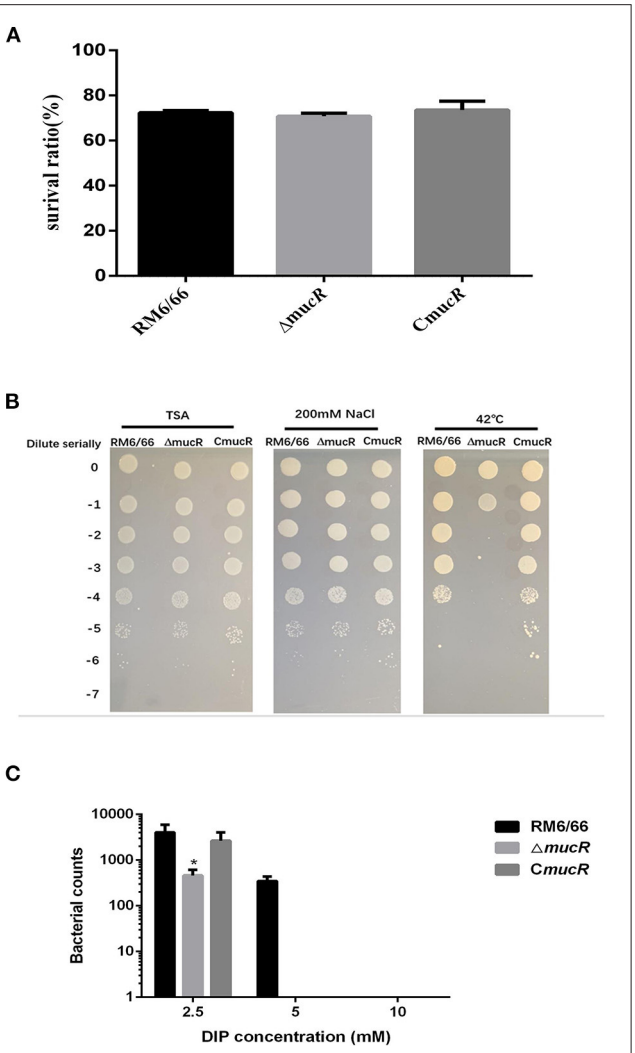

FIGURE 4 | Growth behavior of *B. canis* RM6/66, Δ*mucR*, and C*mucR* strains under various stress conditions. **(A)** *Brucella* strains (initial density of 1 × 10^6 CFU/ml) were grown in TSB (pH 4.5) at 37°C for 2 h. Viable counts were taken 2 h after the challenge. Values represent the mean from three independent experiments performed in duplicate. **(B)** 5-μl gradient dilution of bacterial cultures were, respectively, cultured on TSA medium at 42°C or TSA medium containing 200 mM NaCl at 37°C for 72 h. These experiments were independently repeated thrice. **(C)** Survival of *B. canis* RM6/66, Δ*mucR*, and C*mucR* strains in TSB medium containing various concentrations of 2,2-dipyridyl (iron chelator) was determined. The graph represents the average data from at least three independent experiments. Statistical analysis was performed with a *t*-test.

RESULTS

Construction of Δ*mucR* Mutant Strain and the Complementary Strain C*mucR*

B. canis RM6/66 *mucR* deletion mutant was constructed *via* a double recombination event and confirmed by PCR (**Figure 1A**). *mucR* complement strain C*mucR* was constructed by restoring the *mucR* gene using the broad-range plasmid pMR11. The resultant strains were verified by PCR and sequencing.

TABLE 1 | MIC of β-lactam and non β-lactam antimicrobials for *B. canis* RM6/66 and mutants.

Drug	MIC (μg/ml) for *B. canis*		
	RM6/66	Δ*mucR*	C*mucR*
β-lactam antibiotics			
Ampicillin	4	2	4
Amoxycillin	0.5	0.25	0.5
Carbenicillin	16	8	16
Non β-lactam antibiotics			
Tetracycline	0.25	0.25	0.25
Ciprofloxacin	0.25	0.25	0.25
Gentamicin	0.5	0.5	1

TABLE 2 | MucR affected the transcription level of the flagellar genes.

Gene	Locus tag	Log_2FC (Δ*mucR* vs. RM6/66)
ftcR	DK60_2824	8.96
fliC	DK60_2831	4.91
fliL	DK60_3013	−0.94
flgA	DK60_3033	−0.46
flgC	DK60_3030	2.86
flgE	DK60_2823	−1.34
fliN	DK60_3007	0.9
flhA	DK60_2816	3.93
flgB	DK60_3029	3.65
fliP	DK60_3038	1.23
fliQ	DK60_2817	0.17
fliR	DK60_2815	0.30
flgK	DK60_2822	4.90
fliF	DK60_2830	5.08
flgG	DK60_3032	−0.83

Deletion of *mucR* Showed No Difference in Growth

To characterize the cell growth rate of Δ*mucR* strain, the bacterial strains were analyzed in TSB medium at 37°C with the same initial density of 1×10^6 CFU/ml. The result showed that the growth rate of Δ*mucR* was almost the same as its parent strain RM6/66 and the complementation strain C*mucR* at different time points (**Figure 1B**).

Loss of MucR Impairs Survival of *B. canis* in Macrophages and Alters Virulence in BALB/c Mice

To assess the virulence of Δ*mucR* strain, the ability of Δ*mucR* to multiply within the cultured macrophage RAW264.7 was tested. As shown in **Figure 2**, the intracellular bacterial load of Δ*mucR* strain was almost the same as that of RM6/66 and C*mucR* at 1 h post-infection, while the bacterial load of Δ*mucR* was significantly reduced at 24 and 48 h (both with $p < 0.05$) in murine macrophage compared to RM6/66 and C*mucR* strains.

TABLE 3 | Transcriptional level of 12 randomly selected genes by RNA-seq and RT-qPCR.

Locus tag	Log_2FC (Δ*mucR* vs. RM6/66)		Function
	qPCR	RNA-seq	
DK60_1789	−1.167	−2.025	ATP synthase F1, epsilon subunit
DK60_1816	−1.777	−2.092	Signal recognition particle protein
DK60_2150	−2.397	−2.923	Opacity porin family protein
DK60_3002	1.47	1.173	HTH-type quorum sensing-dependent transcriptional regulator vjbR
DK60_2832	7.563	7.421	Autotransporter-associated beta strand repeat family protein
DK60_2794	4.103	6.656	PemK-like family protein
DK60_291	4.393	6.577	Bacterial regulatory s, luxR family protein
DK60_2276	−2.517	−2.165	Bacterioferritin
DK60_1531	2.933	7.728	Bacterial SH3 domain protein
DK60_2952	0.612	0.889	P-type DNA transfer protein VirB5
DK60_2949	−0.49	−0.077	Type IV secretion system protein virB8
DK60_647	−6.287	−8.581	Transcriptional regulatory protein ros
DK60_1976	6.183	7.005	Aquaporin Z 2

To assess the virulence of Δ*mucR* strain, the behaviors of Δ*mucR* and RM6/66 strains in an infected mouse model at 1 and 4 weeks were also analyzed. The spleen weight of the mice infected by the Δ*mucR* mutant infection group was significantly lighter than that of the RM6/66 infection group at both 1 ($p < 0.05$) and 4 ($p < 0.001$) weeks post-infection (**Figure 3A**). In addition, the CFU of Δ*mucR* mutant recovered from mice spleens was almost the same as that of RM6/66 at 1-week post-infection. However, the CFU number of *mucR* mutant recovered from the mice spleens was significantly lower at 4 weeks post-infection ($p < 0.01$) (**Figure 3B**).

mucR Deletion Strain Was Sensitive to Heat Stress and Iron Limitation

As shown in **Figure 4A**, the survival ratio of Δ*mucR* strain was not significantly affected in acidic TSB medium compared with RM6/66 strain and the complemented strain C*mucR* (**Figure 4A**). When exposed to a hypertonic environment, the survival ratio of Δ*mucR* was similar to that of the parental strain RM6/66 and C*mucR* (**Figure 4B**). However, when Δ*mucR* strain was cultured at 42°C for 72 h, the survival ratio of the mutant strain was significantly reduced than that of RM6/66 and C*mucR* (**Figure 4B**).

The growth patterns of Δ*mucR*, *B. canis* RM6/66, and the complemented strain in the low iron medium were also

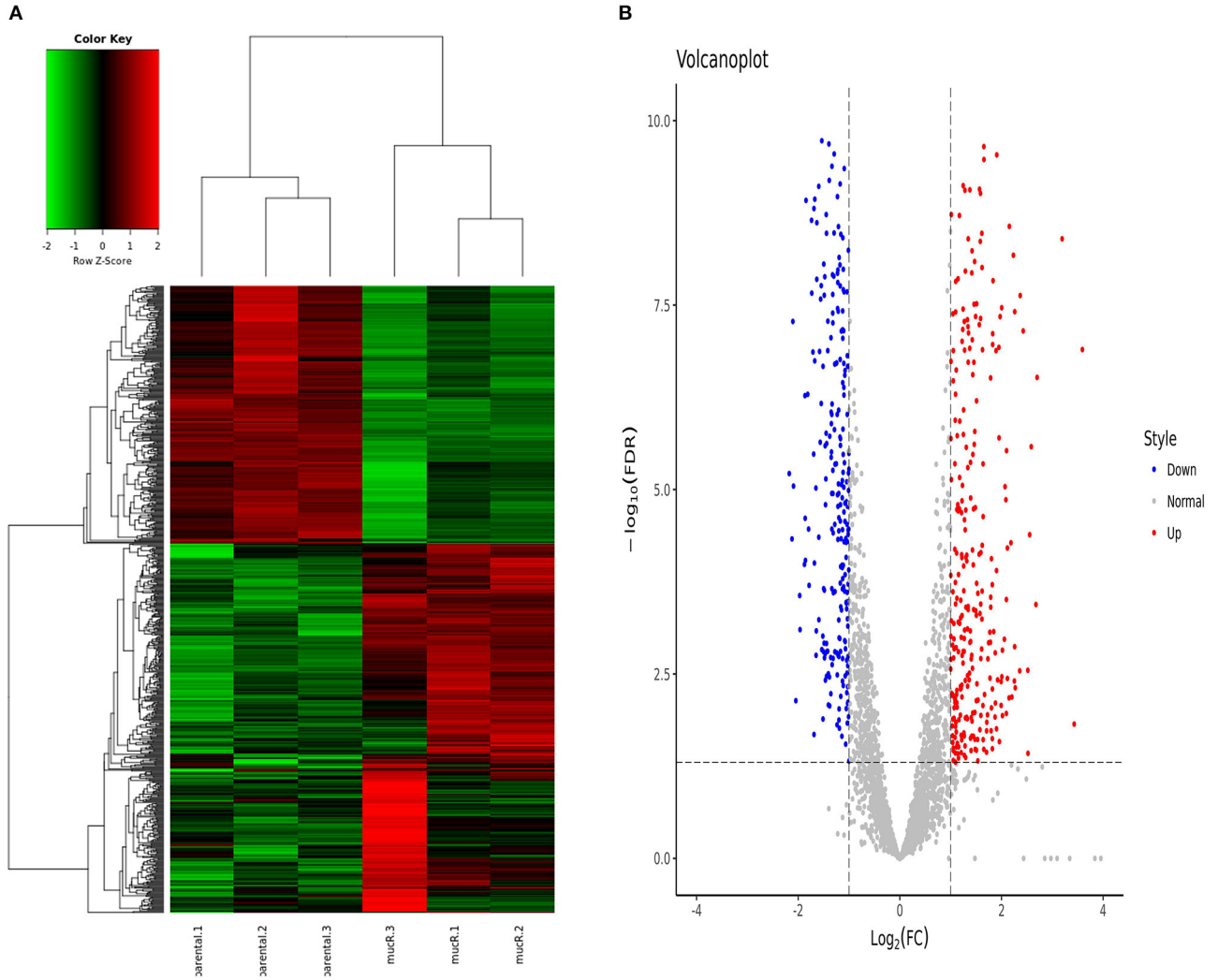

FIGURE 5 | Differentially expressed genes identified by RNA-seq ($n = 3$ per group). **(A)** Heat map of the comparative transcriptome analysis of *B. canis* RM6/66 and Δ*mucR*. **(B)** Volcano plot of relative RNA expression from Δ*mucR* as compared to *B. canis* RM6/66. Genes in the upper left and right quadrants are significantly differentially expressed.

measured. In the concentrations evaluated, the presence of 2,2-dipyridyl restricted the growth of all three strains. As compared with *B. canis* RM6/66, the growth of Δ*mucR* was significantly reduced at 2.5 mM 2,2-dipyridyl ($p < 0.05$) and abolished at a higher concentration (**Figure 4C**).

mucR Mutant Is More Sensitive to Various Antibiotics

The susceptibilities of RM6/66, Δ*mucR*, and C*mucR* to β-lactam and non-β-lactam drugs were examined using standard procedures. The sensitivity of *mucR* mutant to Ciprofloxacin, Gentamicin, and Tetracycline was similar to that of the parental strain RM6/66 or C*mucR*. However, this mutant showed a higher sensitivity to all the three types of β-lactam agents tested. Such enhancement in susceptibility, estimated by MICs, was two-fold compared with its parent strain (**Table 1**).

MucR Affects the Expression of Flagellar Genes in *B. canis*

Previous studies on the role of MucR in *B. melitensis* 16M demonstrated that MucR protein could repress the expression of several flagellar genes (11). Thus, the expression of 15 flagellar genes in the *mucR* mutant strain was analyzed using qRT-PCR. Our results showed that the expression level of eight flagellar genes (*ftcR*, *fliC*, *flgC*, *flhA*, *flgB*, *fliP*, *flgK*, and *fliF*) was significantly increased in *mucR* mutant compared with its parent strain *B. canis* RM6/66 (**Table 2**).

Identification of DEGs in *mucR* Mutant Strain

To uncover the underlying mechanism of virulence attenuation of Δ*mucR* strain, changes of the transcriptional profile of gene expression of Δ*mucR* or RM6/66 were analyzed using

FIGURE 6 | Clusters of orthologous genes (COG) analysis **(A)** and KEGG pathway analysis **(B)** for differentially expressed genes. The red columns indicate that these categories or pathways were significantly enriched ($p < 0.05$), while the blue columns imply that these categories or pathways were not significantly enriched.

transcriptomic analysis. The transcriptional data set was submitted to the Gene Expression Omnibus (GEO) repository (National Center for Biotechnology Information, NCBI) with access number GSE155748. To confirm the RNA-seq data, 12 genes were chosen for qRT-PCR. Transcriptional data of all selected genes gave identical tendencies by both methods RNA-seq and qRT-PCR (**Table 3**).

In total, 694 genes exhibited significant difference ($\log_2$ FC > 1 or <-1 and FDR < 0.05). Among these genes, 409 genes were significantly up-regulated and 285 genes were significantly down-regulated in Δ*mucR* compared to its parent strain RM6/66 (**Figures 5A,B**). Genes, such as DK60_1986, DK60_2665, DK60_1987, K60_1068, DK60_1531, DK60_1985, DK60_2016, DK60_2832, DK60_1984, and *aqpZ2*, were among the top 10 up-regulated genes, while DK60_2150, DK60_1727, DK60_895, *bfr*, DK60_3051, DK60_2926, *ffh*, DK60_1851, *atpC*, and DK60_1852 were among the top 10 down-regulated genes.

According to the result of clusters of orthologous genes (COG) analysis, DEGs were mainly involved in translation, ribosomal structure and biogenesis, signal transduction mechanisms, energy production and conversion, intracellular trafficking, secretion and vesicular transport, and extracellular structures (**Figure 6A**). The Kyoto encyclopedia of genes and genomes (KEGG) pathway analysis demonstrated that the genes which exhibited significant difference were primarily enriched in the ribosome, oxidative phosphorylation, aminoacyl-tRNA biosynthesis, and protein export (**Figure 6B**).

DISCUSSION

In the present study, we report extensive characterization of an in-frame deletion mutant of *B. canis mucR* for the first time. This gene was previously found to regulate virulence in both cellular and murine models of infection in *B. melitensis* and *B. abortus* (11, 13). According to the result of the virulence assay, it was found that the *mucR* gene was also crucial for *B. canis* virulence in both the macrophage infection model and the murine infection model.

In previous studies, deletion of *mucR* gene in *B. abortus* 2308 and *B. melitensis* 16M resulted in a significant growth deficiency and mutant strains produced smaller-size colonies when grown on a solid medium (11, 13). However, we found that the growth curve of RM6/66, Δ*mucR*, and *CmucR* was almost the same when cultured in a TSB medium with the same initial concentration. Moreover, the sizes of the three *B. canis* colonies on blood agar had no significant difference.

In smooth-type *Brucella* strain, MucR protein contributed to the development of resistance to various stress conditions, such as

acidic pH, iron-limitation, oxidative stress, cationic peptide, and detergents (9, 11, 13). Thus, we also comprehensively detected the stress response of *mucR* mutant strain in different conditions in this study. Our results indicated that the *mucR* mutant was more sensitive to heat stress and iron deficiency. In addition, reduced tolerance to these stress conditions, which might be encountered in the host macrophage, could be possible reasons for the attenuation of the *mucR* mutant strain.

In *B. melitensis*, MucR protein was found to be a repressor of flagellar gene expression (11). Based on the RNA-seq data, the expression of four flagellar genes was significantly up-regulated and the result of qRT-PCR also indicated that MucR could repress the transcription of flagellar genes in *B. canis*. Besides, it was reported that the expression of flagellar genes was tightly regulated by the QS regulator VjbR, RpoE1, and RpoH2 in *B. melitensis* (17–19). A recent study from our lab indicated that deletion of the QS regulator VjbR also affected the transcription level of the *ftcR* gene in *B. canis* (14). Whether, flagellar genes of *B. canis* were also regulated by RpoE1 or RpoH2 should be further explored.

To further uncover the mechanisms underlying virulence attenuation in the *mucR* mutant strain, we characterized the transcriptional profile of RM6/66 and Δ*mucR* by transcriptome analysis and up to 694 genes were found to be differentially expressed over two-fold in the mutant strain. The number of up-regulated genes was more than that of the down-regulated genes, which was consistent with the RNA-seq data in *B. melitensis mucR* strain (9). It seemed that MucR protein should be a global negative regulator in *Brucella* strains.

Iron is a necessary element for brucellosis survival (20). Bfr protein played an important role in controlling iron homeostasis, which accounted for about 70% of the intracellular iron content in *B. abortus* (21). Moreover, the heme transporter BhuA was reported to be related to *Brucella* virulence both *in vitro* and *in vivo* (22). In our study, we found that *mucR* mutant was more sensitive to iron-limitation stress and the result of RNA-seq in our study also showed that the expression of *bfr, bhuA*, and DK60_1666 (encoding ferric uptake regulator family protein) was affected. Thus, we speculated that the change in iron-limitation tolerance could also be a result of the abnormal expression of these iron metabolism-related genes.

During bacterial infection pathogen-host interactions expose bacteria to various physiological and biological stresses, including heat stress. To avoid degradation by the host cell defense systems, intracellular pathogens could adapt to changes in their environment by coordinated of gene expression (23). In previous study, the protein synthesis pattern in response to heat stresses were studied by two-dimensional polyacrylamide gel electrophoresis, and the expression of several proteins were increased, such as GroEL, DnaK, AapJ, and Fe and/or Mn SOD (24). In our study, the result of RNA-seq showed that the expression of *aapJ*, *groEL*, and DK60_400 (encoding hsp33 family protein) was affected. It seemed that the change in heat stress tolerance might be a result of the abnormal expression of these genes mentioned above.

Beta-lactam antibiotics can interfere with the final stage of cell wall synthesis by modifying activities of enzymes and penicillin-binding proteins (25). Based on RNA-seq results, up to 38 genes involved in cell wall/membrane/envelope biogenesis (COG: M) were found to be differently expressed in *mucR* deletion strain. Thus, it seemed that the reduced tolerance to β-lactam antibiotics in the *mucR* mutant should be due to changes in bacterial surface integrity.

CONCLUSION

The current study indicated that the transcriptional regulator MucR was essential for bacterial resistance to heat stress, iron limitation and antibiotics, as well as bacterial virulence in *B. canis*. In addition, various genes linked to the phenotype changes of *mucR* mutant were uncovered using RNA-seq assay. Our study not only reveals the pathogenic mechanism of *B. canis* but also provided insight into MucR regulon in different *Brucella* strains.

DATA AVAILABILITY STATEMENT

The datasets presented in this study can be found in online repositories. The names of the repository/repositories and accession number(s) can be found below: https://www.ncbi.nlm.nih.gov/, GSE155748.

ETHICS STATEMENT

The animal study was reviewed and approved by the Animal Ethics Committee of China Institute of Veterinary Drug Control. The affiliation of this ethics committee was NO.33 Qingfeng Road, Daxing District, Beijing.

AUTHOR CONTRIBUTIONS

HD, YQ, and JD designed the experiments. JS, XP, YL, HJ, YF, and QL performed the experiments. JS and HD prepared the manuscript. YL and LZ analyzed the data. All authors have read and approved the final version of this manuscript.

FUNDING

This work was supported by the National Natural Science Foundation of China (No. 31602055) and the National Key Research and Development Program of China (NO. 2016YFD0500903).

ACKNOWLEDGMENTS

We thank Novel Bioinformatics Ltd., Co for the support of bioinformatics analysis with their Novel Bio Cloud Analysis Platform.

SUPPLEMENTARY MATERIAL

The Supplementary Material for this article can be found online at: https://www.frontiersin.org/articles/10.3389/fvets.2021.650942/full#supplementary-material

REFERENCES

1. Moore JA, Bennett M. A previously undescribed organism associated with canine abortion. *Vet Rec.* (1967) 80:604-5. doi: 10.1136/vr.80.20.604
2. Hensel ME, Negron M, Arenas-Gamboa AM. Brucellosis in dogs and public health risk. *Emerg Infect Dis.* (2018) 24:1401-6. doi: 10.3201/eid2408.171171
3. Chacon-Diaz C, Altamirano-Silva P, Gonzalez-Espinoza G, Medina MC, Alfaro-Alarcon A, Bouza-Mora L, et al. *Brucella canis* is an intracellular pathogen that induces a lower proinflammatory response than smooth zoonotic counterparts. *Infect Immun.* (2015) 83:4861-70. doi: 10.1128/IAI.00995-15
4. Stranahan LW, Khalaf OH, Garcia-Gonzalez DG, Arenas-Gamboa AM. Characterization of *Brucella canis* infection in mice. *PLoS ONE.* (2019) 14:e0218809. doi: 10.1371/journal.pone.0218809
5. Glowacka P, Zakowska D, Naylor K, Niemcewicz M, Bielawska-Drozd A. *Brucella*—virulence factors, pathogenesis and treatment. *Pol J Microbiol.* (2018) 67:151-61.doi: 10.21307/pjm-2018-029
6. Kleinman CL, Sycz G, Bonomi HR, Rodriguez RM, Zorreguieta A, Sieira R. ChIP-seq analysis of the LuxR-type regulator VjbR reveals novel insights into the *Brucella* virulence gene expression network. *Nucleic Acids Res.* (2017) 45:5757-69. doi: 10.1093/nar/gkx165
7. Mueller K, Gonzalez JE. Complex regulation of symbiotic functions is coordinated by MucR and quorum sensing in Sinorhizobium meliloti. *J Bacteriol.* (2011) 193:485-96. doi: 10.1128/JB.01129-10
8. Janczarek M, Kutkowska J, Piersiak T, Skorupska A. Rhizobium leguminosarum bv. trifolii rosR is required for interaction with clover, biofilm formation and adaptation to the environment. *BMC Microbiol.* (2010) 10:284. doi: 10.1186/1471-2180-10-284
9. Dong H, Liu W, Peng X, Jing Z, Wu Q. The effects of MucR on expression of type IV secretion system, quorum sensing system and stress responses in *Brucella* melitensis. *Vet Microbiol.* (2013) 166:535-42. doi: 10.1016/j.vetmic.2013.06.023
10. Arenas-Gamboa AM, Rice-Ficht AC, Kahl-McDonagh MM, Ficht TA. Protective efficacy and safety of *Brucella* melitensis 16MDeltamucR against intraperitoneal and aerosol challenge in BALB/c mice. *Infect Immun.* (2011) 79:3653-8. doi: 10.1128/IAI.05330-11
11. Mirabella A, Terwagne M, Zygmunt MS, Cloeckaert A, De Bolle X, Letesson JJ. *Brucella* melitensis MucR, an orthologue of Sinorhizobium meliloti MucR, is involved in resistance to oxidative, detergent, and saline stresses and cell envelope modifications. *J Bacteriol.* (2013) 195:453-65. doi: 10.1128/JB.01336-12
12. Borriello G, Russo V, Paradiso R, RiccardiMG, Criscuolo D, Verde G, et al. Different Impacts of MucR binding to the babR and virB promoters on gene expression in *Brucella* abortus 2308. *Biomolecules.* (2020) 10:788. doi: 10.3390/biom10050788
13. CaswellCC, Elhassanny AE, Planchin EE, Roux CM, Weeks-Gorospe JN, Ficht TA, et al. Diverse genetic regulon of the virulence-associated transcriptional regulator MucR in *Brucella* abortus 2308. *Infect Immun.* (2013) 81:1040-51. doi: 10.1128/IAI.01097-12
14. Liu Y, Sun J, Peng X, Dong H, Qin Y, Shen Q, et al. Deletion of the LuxR-type regulator VjbR in *Brucella canis* affects expression of type IV secretion system and bacterial virulence, and the mutant strain confers protection against *Brucella canis* challenge in mice. *Microb Pathog.* (2020) 139:103865. doi: 10.1016/j.micpath.2019.103865
15. Liu Y, Dong H, Peng X, Gao Q, Jiang H, Xu G, et al. RNA-seq reveals the critical role of Lon protease in stress response and *Brucella* virulence. *Microb Pathog.* (2019) 130:112-9. doi: 10.1016/j.micpath.2019.01.010
16. Liu W, Dong H, Liu W, Gao X, Zhang C, Wu Q. OtpR regulated the growth, cell morphology of *B. melitensis* and tolerance to beta-lactam agents. *Vet Microbiol.* (2012) 159:90-8. doi: 10.1016/j.vetmic.2012.03.022
17. Delory M, Hallez R, Letesson JJ, De Bolle X. An RpoH-like heat shock sigma factor is involved in stress response and virulence in *Brucella melitensis* 16M. *J Bacteriol.* (2006) 188:7707-10. doi: 10.1128/JB.00644-06
18. Ferooz J, Lemaire J, Delory M, De Bolle X, Letesson JJ. RpoE1, an extracytoplasmic function sigma factor, is a repressor of the flagellar system in *Brucella melitensis*. *Microbiology (Reading).* (2011) 157:1263-8. doi: 10.1099/mic.0.044875-0
19. Delrue RM, Deschamps C, Leonard S, Nijskens C, Danese I, Schaus JM, et al. A quorum-sensing regulator controls expression of both the type IV secretion system and the flagellar apparatus of *Brucella melitensis*. *Cell Microbiol.* (2005) 7:1151-61. doi: 10.1111/j.1462-5822.2005.00543.x
20. Roop RN. Metal acquisition and virulence in Brucella. *Anim Health Res Rev.* (2012) 13:10-20. doi: 10.1017/S1466252312000047
21. Almiron MA, Ugalde RA. Iron homeostasis in *Brucella abortus*: the role of bacterioferritin. *J Microbiol.* (2010) 48:668-73. doi: 10.1007/s12275-010-0145-3
22. Paulley JT, Anderson ES, Roop RN. *Brucella abortus* requires the heme transporter BhuA for maintenance of chronic infection in BALB/c mice. *Infect Immun.* (2007) 75:5248-54. doi: 10.1128/IAI.00460-07
23. Murray PJ, Young RA. Stress and immunological recognition in host-pathogen interactions. *J Bacteriol.* (1992) 174:4193-6. doi: 10.1128/jb.174.13.4193-4196.1992
24. Teixeira-Gomes AP, Cloeckaert A, Zygmunt MS. Characterization of heat, oxidative, and acid stress responses in *Brucella melitensis*. *Infect Immun.* (2000) 68:2954. doi: 10.1128/IAI.68.5.2954-2961.2000
25. Bhaskarla C, Das M, Verma T, Kumar A, Mahadevan S, Nandi D. Roles of Lon protease and its substrate MarA during sodium salicylate-mediated growth reduction and antibiotic resistance in *Escherichia coli*. *Microbiology (Reading).* (2016) 162:764-76. doi: 10.1099/mic.0.000271

Conflict of Interest: The authors declare that the research was conducted in the absence of any commercial or financial relationships that could be construed as a potential conflict of interest.

frontiers in Veterinary Science

ORIGINAL RESEARCH
published: 05 August 2021
doi: 10.3389/fvets.2021.723081

African Swine Fever in the Russian Far East (2019–2020): Spatio-Temporal Analysis and Implications for Wild Ungulates

Olga I. Zakharova[1], Ilya A. Titov[2], Andrey E. Gogin[2], Timofey A. Sevskikh[2], Fedor I. Korennoy[1,3], Denis V. Kolbasov[2], Levon Abrahamyan[4]* and Andrey A. Blokhin[1]*

[1] Federal Research Center for Virology and Microbiology, Branch in Nizhny Novgorod, Nizhny Novgorod, Russia, [2] Federal Research Center for Virology and Microbiology, Pokrov, Russia, [3] Federal Center for Animal Health (FGBI ARRIAH), Vladimir, Russia, [4] Swine and Poultry Infectious Diseases Research Center (CRIPA) and Groupe de Recherche sur les Maladies Infectieuses en Production Animale (GREMIP), Faculty of Veterinary Medicine, University of Montreal, Saint-Hyacinthe, QC, Canada

OPEN ACCESS

Edited by:
Shao-Lun Zhai, Guangdong Academy of Agricultural Sciences, China

Reviewed by:
Chang Cai, Zhejiang Agriculture and Forestry University, China
Marie Rene Culhane, University of Minnesota, United States

***Correspondence:**
Olga I. Zakharova
olenka.zakharova.1976@list.ru
Levon Abrahamyan
levon.abrahamyan@umontreal.ca

Specialty section:
This article was submitted to Veterinary Infectious Diseases, a section of the journal Frontiers in Veterinary Science

Received: *11 June 2021*
Accepted: *12 July 2021*
Published: *05 August 2021*

Citation:
Zakharova OI, Titov IA, Gogin AE, Sevskikh TA, Korennoy FI, Kolbasov DV, Abrahamyan L and Blokhin AA (2021) African Swine Fever in the Russian Far East (2019–2020): Spatio-Temporal Analysis and Implications for Wild Ungulates. Front. Vet. Sci. 8:723081. doi: 10.3389/fvets.2021.723081

African swine fever (ASF) is an emerging viral contagious disease affecting domestic pigs (DP) and wild boar (WB). ASF causes significant economic damage to the pig industry worldwide due to nearly 100% mortality and the absence of medical treatments. Since 2019, an intensive spread of ASF has been observed in the Russian Far East region. This spread raises concerns for epidemiologists and ecologists given the potential threat to the WB population, which is an essential member of the region's wild ungulates and provides a notable share of food resources for predatory species. This study aims to determine the genotype of ASF virus circulating in the region, reveal the spatio-temporal patterns of the ASF outbreaks' emergence, and assess the potential reduction of the regional fauna because of expected depopulation of WB. The first historical case of ASF in the study region was caused by an African swine fever virus (ASFV) isolated from DPs and belonging to Genotype 2, CVR1; IGR-2 (TRS +). Sequencing results showed no significant differences among ASFV strains currently circulating in the Russian Federation, Europe, and China. The spatiotemporal analysis with the space-time permutations model demonstrated the presence of six statistically significant clusters of ASF outbreaks with three clusters in DPs and one cluster in WBs. DP outbreaks prevail in the north-west regions of the study area, while northern regions demonstrate a mixture of DP and WB outbreaks. Colocation analysis did not reveal a statistically significant pattern of grouping of one category of outbreaks around the others. The possible damage to the region's fauna was assessed by modeling the total body mass of wild ungulates before and after the wild boars' depopulation, considering a threshold density of WB population of 0.025 head/km^2, according to the currently in force National Plan on the ASF Eradication in Russia. The results suggest the total mass of ungulates of the entire study region will likely decrease by 8.4% (95% CI: 4.1–13.0%), while it may decrease by 33.6% (19.3–46.1%) in the Primorsky Krai, thereby posing an undeniable threat to the predatory species of the region.

Keywords: African swine fever virus, cluster analysis, depopulation, Far East of Russia, genotyping, ungulates, wild boar

INTRODUCTION

African swine fever (ASF) is among the most dangerous diseases of swine and is known to cause considerable damage to pig production in many countries worldwide (1–5).

The ASF virus (ASFV) belongs to the *Asfarviridae* family and affects both domestic pigs (DP) and wild boars (WB). At present, the genetic characteristics of the ASFV are represented by 23 genotypes associated with geographical locations, characterizing the complexity of the virus epidemiology (3, 6–9). ASF epidemics currently occurring in Europe can be treated as two clusters of outbreaks. One of the clusters is located in Sardinia (Italy), where the disease was registered in 1978 and is represented by ASFV strains belonging to genotype 1 (10). The second cluster is widespread in North-Eastern Europe and the Russian Federation caused by strains of the ASFV belonging to genotype 2 (4). The latter is highly virulent, causing acute disease and resulting in mortality rates of 94.5–100.0% in both WB and DP (11–15).

The transcontinental transmission of the ASFV in Georgia in 2007, has resulted in the introduction of the disease into the Russian Federation. The first outbreak of the region was registered in WB in the Chechen Republic (November 2007), with subsequent spread of the virus in the Russian Federation and neighboring European countries (16). The nosoareal of the ASF has recently expanded, reaching the Russian Far East (**Figure 1**) and affecting many countries in South-East Asia (11, 17–21). While insufficient biosecurity on pig farms is considered the main factor in disease spread (22–26), the presence of WB in an ecosystem plays an important role in virus transmission, which is acknowledged by many countries (22, 27, 28).

In some countries with recorded ASF infections, WB populations play the role of an epidemiological reservoir and maintain the virus in the environment. The virus enters WB populations mainly through the animals coming into contact with DP and eating contaminated feed and swill (29, 30).

Wild boars and DP belong to the same species (*Sus scrofa*), as WB are the ancestors of DP. Therefore, the transmission of pathogens is likely bidirectional (31). Wild boars are susceptible to many infections. Although ASF is associated with high mortality, its prevalence in the population does not exceed 3% (32). Nevertheless, every year in the Russian Federation, as in many countries in Europe and Asia, new cases of ASF occur in WB. Proper disposal of infected carcasses (corpses) in compliance with biosafety measures and proper diagnostics for every infected animal are among the essential measures needed to break the ASF transmission cycle (24, 33).

Humans can affect the fluctuations in the numbers of WB, ranging from the maximum possible protection of these animals to their complete eradication. Hunting is the most important risk factor for decline in the WB population, which not only determines their population dynamics, but also has a significant impact on the sex, age, and spatial structure of their populations. Furthermore, WB are the most important hunting trophies and the main prey of large predators (34–37).

One of the measures that has been proposed to control ASF spread is the depopulation of WB, i.e., reducing their numbers to a certain threshold at which the virus' intra-population transmission will stop or significantly slow down owing to the decrease of contact ratio (4, 27, 38). As WB present a significant share of the food resource for many wild predatory species, a decrease in their numbers could disturb the equilibrium of the entire ecosystem and lead to a corresponding decrease in the predator population (39–41). Among the predators of the Russian Far East, the Siberian tiger (*Panthera tigris altaica*) merits mention as a rare protected species, whose population in the region is currently estimated at around 500 individuals (https://wwf.ru/en/regions/amur/amurskiy-tigr/).

Thus, the aims of this study were (1) to conduct an epidemiological and genetic analysis of the ASF situation in the Far Eastern region of Russia, from 2019–2020, and (2) to assess a possible size of WB depopulation and its impact on the whole wild ungulate population of the study region.

MATERIALS AND METHODS

Study Area

In this study, we considered the ASF epidemic situation in the following four administrative divisions located in the Far Eastern Russian Federation: Primorsky Krai, Khabarovsk Krai, the Jewish Autonomous Oblast, and Amur Oblast (**Figure 2**). These regions are part of the Far Eastern Federal District of the Russian Federation and were selected because the ASF virus was first detected in this region in 2019. The total area of the study region exceeds 1,350,400 km^2 with a mean population density of about three people/km^2. The natural conditions in these areas vary significantly due to the vast extent of the territory from North to South. The climate of the coastal strip in the Far East is relatively warm, humid, and monsoonal. The winters in the Far East are cold and dry, and the summers are hot in continental areas and cool in coastal areas. The climatic conditions in these regions have a huge influence on their economic development. The four aforementioned areas have a rich hydrographic network (http://assoc.khv.gov.ru/regions/information/geography-climate). The leading economic sectors are fishing, forestry, and ore mining. This territory in the Far East contains the country's main ecological reservoir; there are 25 natural reserves and three national parks. A unique feature of this region is the population of Siberian tigers, which is an endangered species listed in the Red Book of the International Union for Conservation of Nature (http://www.nparks.ru/fareast_zapovednik.php).

Data and Sources

To analyze the epidemic situation, the data on ASF outbreaks notified by the Russian Federation to the OIE from 2019 to 2020 were retrieved from the FAO EMPRES-i database (http://empres-i.fao.org/eipws3g/). The database contains information on 205 ASF outbreaks in the study region for the period from 30 Jul 2019 to 27 Dec 2020, of which 71 (35%) were in WB and 134 (65%) in DP (**Figure 2**).

Samples of biological material for the phylogenetic study of the ASF virus were obtained from domestic pigs as a result of monitoring studies in an individual private farm in the village of

FIGURE 1 | The ASF-affected regions of the Russian Federation, 2007–2020 (source: OIE), and the study area.

Ust-Ivanovka, Blagoveshchensk District, Amur Oblast and site of the third reported outbreak in the study area (**Figure 2**).

Data on the population size of WB and other ungulates in the study area were obtained from the Ministry of Natural Resources and Environment of the Russian Federation statistical reports for 2019 (https://www.mnr.gov.ru/en/). Data on wild ungulates' body mass were retrieved from Sokolov (42) and Danilkin (43). The current number of Siberian Tigers in the study area is estimated as ∼500 heads, of which 90% live in Primorsky Krai (the World Wildlife Fund (WWF) reports https://wwf.ru/species/amurskiy-tigr/vsye-ob-amurskom-tigre-khozyaine-taygi/). The population density of ungulates was calculated based on the forestry area of the region, which has been retrieved from the Unified Interdepartmental Information and Statistical System UIISS (https://www.fedstat.ru/indicator/38194).

Sequencing and Phylogenetic Analysis of ASFV

ASF virus "Amur Region/08/19/19," identified in 2019 during monitoring studies was used in this research. Phylogenetic studies were conducted by the Laboratory for Diagnostics and Monitoring of the Federal Research Center for Virology and Microbiology (https://ficvim.ru/en/). Confirmation of the presence of viral genome fragments in nucleic acid samples was carried out by real-time PCR (44). DNA was extracted using a commercial DNA sorb kit (Interlabservis, Russia) in accordance with the manufacturer's instructions. Then, the samples that were identified as positive by real-time PCR were subjected to sequencing of following fragments: *B646L, E183L, I73R/I329L, B602L, EP402R*, and *MGF 505-9R*. Of these, the *B646L* and *E183L* fragments were chosen as genotype determining genes. The other gene fragments were recommended by the OIE ASF reference laboratory (Madrid, Spain) for molecular characterization of ASF virus strains and isolates (8, 45–49).

PCR was performed using specific primers and Quick-Load® Taq 2X Master Mix (NEB, USA). The PCR products were purified using a MinElute Gel Extraction Kit (Qiagen, Germany). DNA sequencing was performed using an ABI 3130 Genetic Analyzer (Applied Biosystems, USA). The samples were prepared using BigDye Terminator v.3.1 cycle sequencing kit followed by a purification step with BigDye XTerminator™ Purification Kit (both from Applied Biosystem, Foster City, CA, USA) according to the manufacturer's instructions.

BioEdit v7.0.4.1. was used to obtain a consensus sequence (50). The sequences were aligned using ClustalX (51). The sequence data of an ASF virus isolate were subjected to BLAST analysis using the NCBI BLAST tool (https://blast.ncbi.nlm.nih.gov/Blast.cgi) and were compared with sequences of commonly used reference strains and other strains represented in the GenBank (https://www.ncbi.nlm.nih.gov/genbank). Phylogenetic trees were constructed using the maximum likelihood method in which phylogenetic distances were estimated using Kimura's two-parameter model (K2P) (52) in the MEGA 7 program (53).

Space–Time Data Analysis

A space–time cluster analysis using the space–time permutation model (54) was applied to detect a potential clustering of ASF outbreaks within the study area. This type of analysis allows

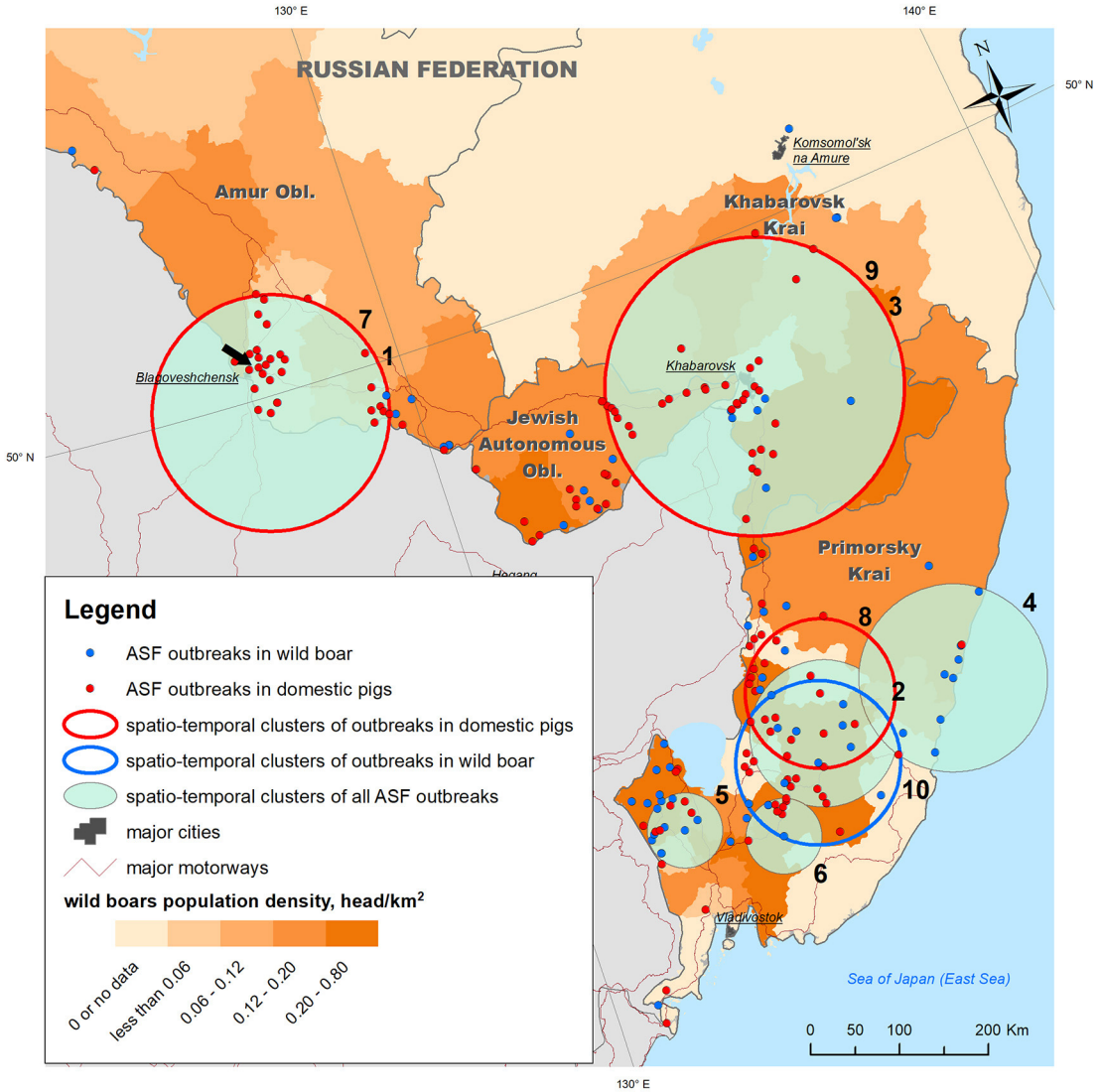

FIGURE 2 | ASF outbreaks (OIE, 2019–2020) and revealed spatio-temporal clusters of outbreaks plotted against wild boar density in the Far East regions of Russia. The black arrow points to the outbreak from which the biological material for ASFV phylogenetic analysis was sampled.

circular areas to be identified where the observed concentrations of outbreaks over a certain time period are significantly higher than would be expected based on the null hypothesis of the random distribution of outbreaks in space and time. The maximum radius and duration of the clusters were taken to be 50% of the whole study area and period, respectively. Clusters where the observed distribution of outbreaks differed from the hypothetical random distribution at levels of significance >95% ($p \leq 0.05$) were considered statistically significant. The ODE value (observed/expected) expresses the ratio of the number of outbreaks observed in a cluster to the expected one. Clusters were detected for: (i) all outbreaks; (ii) DP outbreaks only, and (iii) WB outbreaks only.

To visualize the movement of the ASF epidemic since its first emergence within the study area, we applied mapping of the ASF outbreaks' median centers by month using the Median Center GIS (Geographic Information Systems) procedure (55). For each month of the analyzed period, this tool calculates a median point that provides a minimized overall Euclidean distance to all other ASF outbreaks' locations. This median center can be sought as a conventional measure of central tendency less sensitive to spatial outliers than a mean center.

To explore a potential relationship between the ASF outbreaks in DP and WB, we applied a GIS technique named Colocation Analysis. This technique measures local patterns of spatial association between two categories of point features using the

colocation quotient statistics (56–58). Given two categories of interest in the study area, namely A and B, the colocation quotient (CQ) expresses a local proportion of category B points within a defined neighborhood of category A points. Category B points are then randomly permuted within the whole study area to estimate whether their observed distribution differs from a random one and to obtain a *p*-value. If the above proportion is higher than a global proportion of category B, the CQ will be >1. Otherwise, the CQ will be below 1. The *p*-value obtained determines the statistical significance of the revealed pattern. Given that colocation analysis is not symmetric, we explored relationships between (i) DP and WB, and (ii) WB and DP outbreaks. To provide a neighborhood for the CQ calculation we tested circular bands of the radius equal to the mean neighboring distance for the whole set of ASF outbreaks (i), and of the radius equal to 150 km (ii) based on the previous studies on ASF outbreaks clustering (59, 60). To add an epidemiological meaning to the analysis of relationship between ASF outbreaks, we analyzed colocation using space-time window accounting for a time span of 2 weeks before and after the analyzed outbreaks that reflects our assumption on the average duration of infectious period in acute ASF course (https://www.oie.int/app/uploads/2021/03/african-swine-fever.pdf). This method reflects an assumption that a certain ASF outbreak might be epidemiologically related to a previous outbreak of the other category within the allowed time period (i.e., an outbreak in DP might be resulted by bringing the virus by infected WB from close neighborhood; or WB outbreak might be caused by contaminated waste or improperly utilized pig carcasses from a preceding DP case).

Estimation of the Size of the Expected WB Depopulation

According to some studies, decreases in wild boar (WB) populations have been shown to be a requisite measure to prevent the transmission of ASFV in these populations (3, 6, 24, 37). In the currently in force national guidelines to prevent and eradicate ASF in the Russian Federation (61), a value of 0.25 boars/1,000 ha (0.025 boars/km^2) is recommended as a threshold host density that should be maintained in order to interrupt the circulation of the ASF virus in the WB population within an infected area. Assuming that such a measure may be undertaken in the study region, in this paper we used the above value to estimate the expected size of the WB depopulation.

Estimation of the Possible Decrease in the Total Mass of the Wild Ungulates

To estimate the possible reduction of the food resource for predatory species of the region, a total mass of ungulates living in the study area was assessed: (1) in 2019, before the ASF virus was introduced to this region; and (2) after the decrease of WB number due to expected WB depopulation, considering a threshold density of 0.025 head/km^2. Wild boar, musk deer, roe deer, wild reindeer, moose, and red deer are typical ungulates of the region (39, 40, 62). The body mass of each animal was modeled using a uniform distribution based on maximum and minimum estimates taken from the literature (42). Modeling was performed using a Monte Carlo simulation with 10,000 iterations, which allowed the mean and 95% confidence interval of the ungulates' summary body mass to be estimated. The decrease in the total ungulate mass was assessed: (1) for the whole study area and (2) for only Primorsky Krai, which is home to 90% of the entire Siberian tiger population of the study area and has the highest number of WB.

Software

The cluster analysis was performed using SaTScan software (59). The statistical processing of the data was performed using MS Office Excel application package (Microsoft, Redmond, WA, USA) with @Risk simulation modeling add-on v.6.3 (Palisade Inc., Ithaca, NY, USA). The spatial analysis and results' visualization were carried out using ArcGIS Desktop 10.8.1 and ArcGIS Pro 2.6.3 (Esri, Redlands, CA, USA).

For phylogenetic analysis, BioEdit v7.0.4.1 software (50) was used to obtain a consensus sequence. Nucleotide sequences were aligned with ClustalX (51). To build a phylogenetic tree, the MEGA 7 package (53) was used. To perform a phylogenetic analysis, the analyzed sequences were compared with homological ASFV gene sequences from GenBank database with BLASTN (http://blast.ncbi.nlm.nih.gov/Blast.cgi).

RESULTS

Spatio-Temporal Analysis of ASF in the Far East

The analysis of the ASF spread within the study area from its introduction in July 2019 to December 2020, showed that the disease has become widespread over a large territory in Primorsky Krai, the Jewish Autonomous Oblast, Amur Oblast, and Khabarovsk Krai, and mainly concentrated along the Russian–Chinese border. Distribution of outbreaks shows certain spatial heterogeneity across the study area. Outbreaks in WB were mainly observed in Primorsky Krai and Jewish Autonomous Oblast, both of which have the highest density of WB population, while outbreaks in DP were more evenly distributed across the study region, demonstrating a high concentration in Amur Oblast with no WB outbreaks in the same area.

Space–time cluster analysis revealed six statistically significant clusters of ASF outbreaks; three statistically significant clusters of outbreaks in DP, and just one cluster of outbreaks in WB (**Table 1** and **Figure 2**). Two of all ASF outbreaks' clusters demonstrate full spatio-temporal coincidence with clusters in DP (#1 and 7 in Amur oblast, #3 and 9 in Jewish Autonomous Oblast and Khabarovsk Krai) suggesting that those clusters are formed only by the outbreaks in DP. The clustering pattern is more heterogeneous in Primorsky Krai where four spatio-temporal cluster are formed by a mixture of DP and WB outbreaks, with just single clusters in DP and WB, respectively. The latter clusters do not coincide but demonstrate some spatial and temporal overlap. However, moving north-west along the Russian–Chinese border, DP, and WB outbreaks become more spatially separated with the dominance of DP cases.

Calculation of the outbreaks' median centers by month demonstrates that ASF almost simultaneously emerged in

TABLE 1 | Characteristics of spatiotemporal clusters of ASF outbreaks in domestic pigs and wild boar in the Far East of Russia, 2019–2020.

Cluster #	Territorial coverage	Cluster radius, km	Observed number of outbreaks (in population)	Observed to expected rate ODE	Start date	End date	Cluster duration, days	*P*-value
1 and 7	Amur oblast	138	26* (DP)	4.1 for all outbreaks, 2.8 for DP cluster	16.08.2019	26.09.2019	41	<0.001
2	Primorsky Krai	86	17 (DP+WB)	5.8	28.02.2020	30.07.2020	153	<0.001
3 and 9	Jewish Autonomous Oblast and Khabarovsk Krai	175	29* (DP)	3.0 for all outbreaks, 2.5 for DP cluster	31.07.2020	17.09.2020	48	<0.001
4	Primorsky Krai	110	10 (DP+WB)	8.5	16.10.2020	10.12.2020	55	<0.001
5	Primorsky Krai	44	10 (DP+WB)	6.8	06.12.2019	20.02.2020	76	0.002
6	Primorsky Krai	44	10 (DP+WB)	6.2	21.08.2020	15.10.2020	55	0.007
8	Primorsky Krai	88	12* (DP)	5.9	29.05.2020	30.07.2020	62	<0.001
10	Primorsky Krai	96	10 (WB)	5.0	28.02.2020	15.10.2020	230	<0.001

DP, domestic pigs; WB, wild boars. Cluster numbers correspond to ***Figure 2****.*
**Several WB outbreaks within the cluster do not belong to the cluster time period.*

different regions of the study area adjoining the People's Republic of China: in WB of Primorsky Krai (July 2019) and in DP of Amur Oblast (August 2019). The former region presents a forestry area with the highest density of WB in the region, while the latter is a suburb of Blagoveschensk city that features a direct transport connection with China by a bridge across the Amur River. The direction of median centres' spread suggests consequent epidemic movement from both initial areas north and east with the concentration of most recent outbreaks in Khabarovsk Krai. The direction coincides with the main transportation routes in the region (**Figure 3**).

The mean neighboring distance between all ASF outbreaks within the study area calculated with The Mean Nearest Neighbor GIS tool was found to be 15 km. The colocation analysis of the ASF outbreaks in DP with outbreaks in WB (i.e., testing for an elevated concentration of WB outbreaks in close vicinity to DP outbreaks within 2-weeks time period) showed that:

- Within a neighborhood of 15 km radius, no DP outbreaks were statistically significant collocated with WB outbreaks; only 3 out of 134 (2.2%) DP outbreaks demonstrated statistically non-significant ($p > 0.05$) colocation with WB outbreaks, while 70 (52.2%) DP outbreaks were found to be statistically non-significant isolated;
- Within a neighborhood of 150 km radius, three (2.2%) DP outbreaks were statistically significant ($p < 0.05$) collocated with WB outbreaks (in Primorsky Krai), while 53 DP outbreaks were found to be statistically significant isolated throughout the study area (**Figure 4**).

The colocation analysis of WB outbreaks with DP outbreaks (i.e., testing for an elevated concentration of DP outbreaks in close vicinity to WB outbreaks within 2-weeks time period) demonstrated that:

- Within a neighborhood of 15 km radius, no WB outbreaks were found to be statistically significant collocated with DP outbreaks, while three (4.2%) and 17 (23.9%) of WB outbreaks were statistically non-significant collocated and isolated with DP outbreaks, respectively;
- Within a neighborhood of 150 km radius only one (1.4%) WB outbreak was statistically significant collocated with DP outbreaks (in Jewish Autonomous Oblast), and six (8.5%) WB outbreaks were statistically significant isolated (in Primorsky Krai), while 10 (14.0%) and 43 (60.6%) WB outbreaks were statistically non-significant collocated and isolated, respectively (**Figure 5**).

Sequencing and Phylogenetic Analysis for ASFV

The*B646L*, *E183L*, *I73R/I329L*, *B602L*, *EP402R*, and *MGF 505-9R* gene sequences of the Amur/19.08.19 strain were deposited in GenBank under the accession numbers MT840357, MT840356, MT840354, MT840352, MT840355, and MT840353, respectively.

The phylogenetic analysis of ASFV isolates of the Amur/19.08.19 strain was based on a fragment of the *B646L* gene sequence, which encodes the P72 protein. The analysis revealed that this strain belongs to the second genotype. This genotype was initially widely spread in Eastern Europe, when it was first reported in Georgia, in 2007. Genotypic affiliation of the Amur/19.08.19 strain was also confirmed by calculating the phylogenetic tree using the nucleotide sequencing of the *E183L* gene, encoding the P54 protein (**Figure 6**).

No changes were detected in the central variable region (CVR) of the genome, which includes the *B602L* gene. Thus, studied ASFV isolates belong to the CVR1 variant (according to OIE ASF reference laboratory classification [Madrid, Spain]). Moreover, these isolates belonged to the TRS+ (IGR2) variant by classification, based on *I73R/I329L* sequence (**Figure 7**).

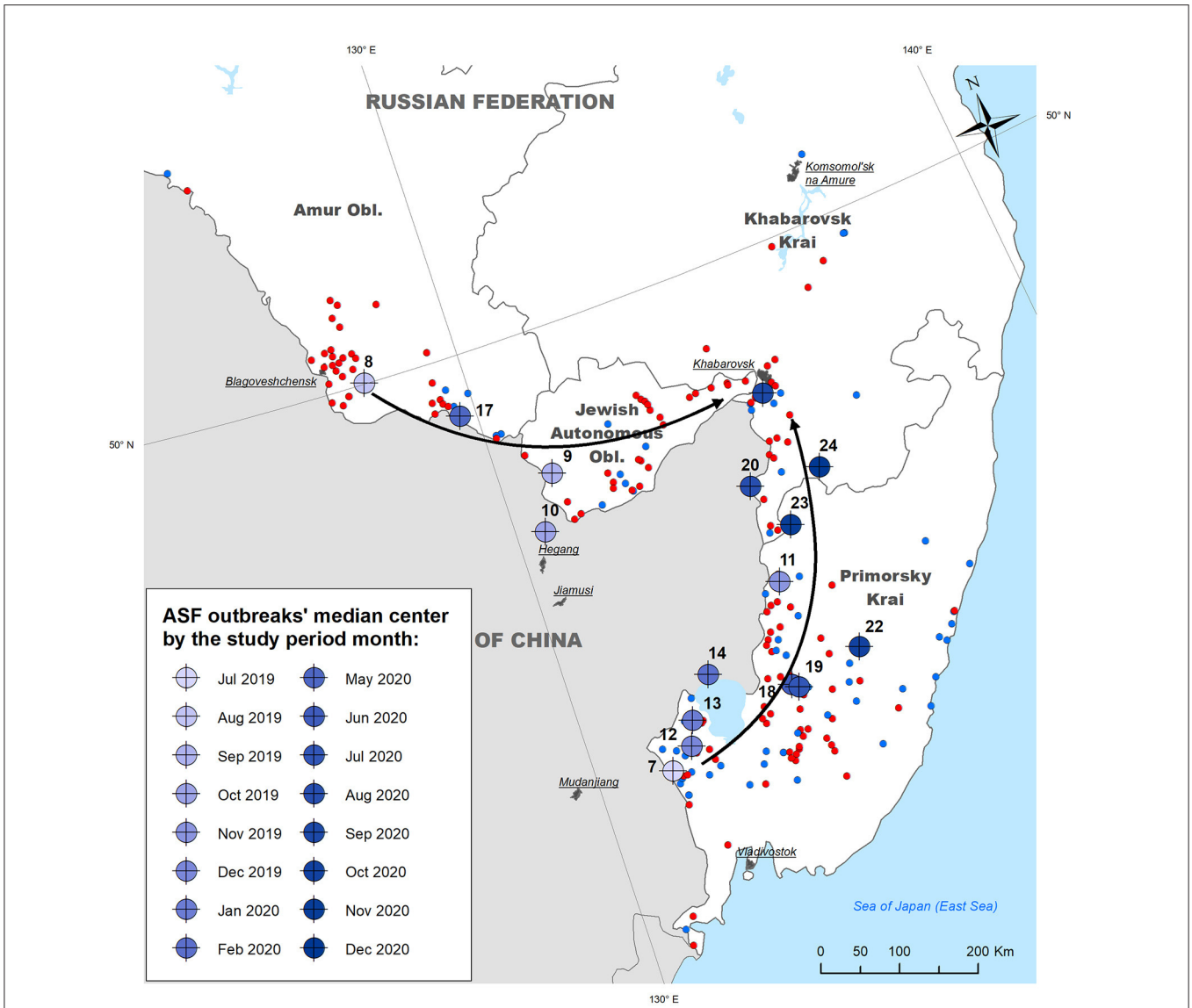

FIGURE 3 | Median centers of ASF outbreaks in the Far East region of Russia by month from July 2019 to December 2020. Arrows indicate the apparent direction of the epidemic movement.

Nucleotide substitutions in the sequences of the *EP402R* and *MGF 505-9R* genes were also not detected.

Assessment of the Decrease in Wild Ungulates' Mass After WB Depopulation

The number of wild ungulates, including the WB, based on the administrative divisions of the study area is shown in **Table 2** (as of 2019). The table also presents the estimates of total mass of all ungulates for 2019 as well as after the expected depopulation of WB until a threshold density of 0.025 head/km^2. The results suggest that the WB population may potentially be reduced by 93% in Primorsky Krai, by 91% in the Jewish Autonomous Oblast, by 46% in Amur Oblast, and by 8% in Khabarovsk Krai. As a result of WB number decline, the total mass of all wild ungulates may decrease by 8.4 % (95% CI: 4.1–13.0%) in the whole study area, while the reduction may be as high as 33.6 % (19.3–46.1%) in Primorsky Krai, which is home to the majority of the Siberian tiger population.

DISCUSSION

The observed pattern of the ASF outbreaks' clustering within the study area likely reflects the multiple ways through which the virus may have entered this region. The initial spread started simultaneously in two distant parts of the study region (Primorsky Krai and Amur Oblast) and resulted

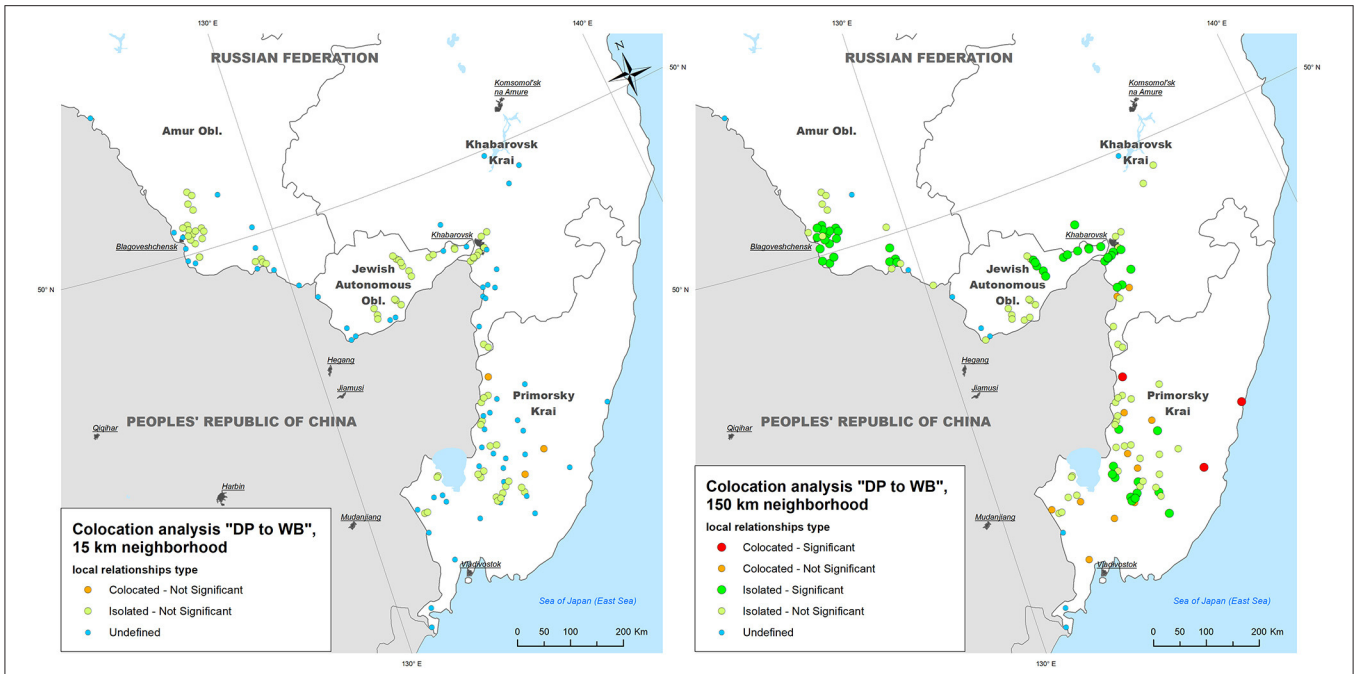

FIGURE 4 | The results of local colocation analysis of ASF outbreaks in domestic pigs (DP) and wild boar (WB). **(Left)** With 15 km as a neighboring distance; **(Right)** with 150 km as neighboring distance.

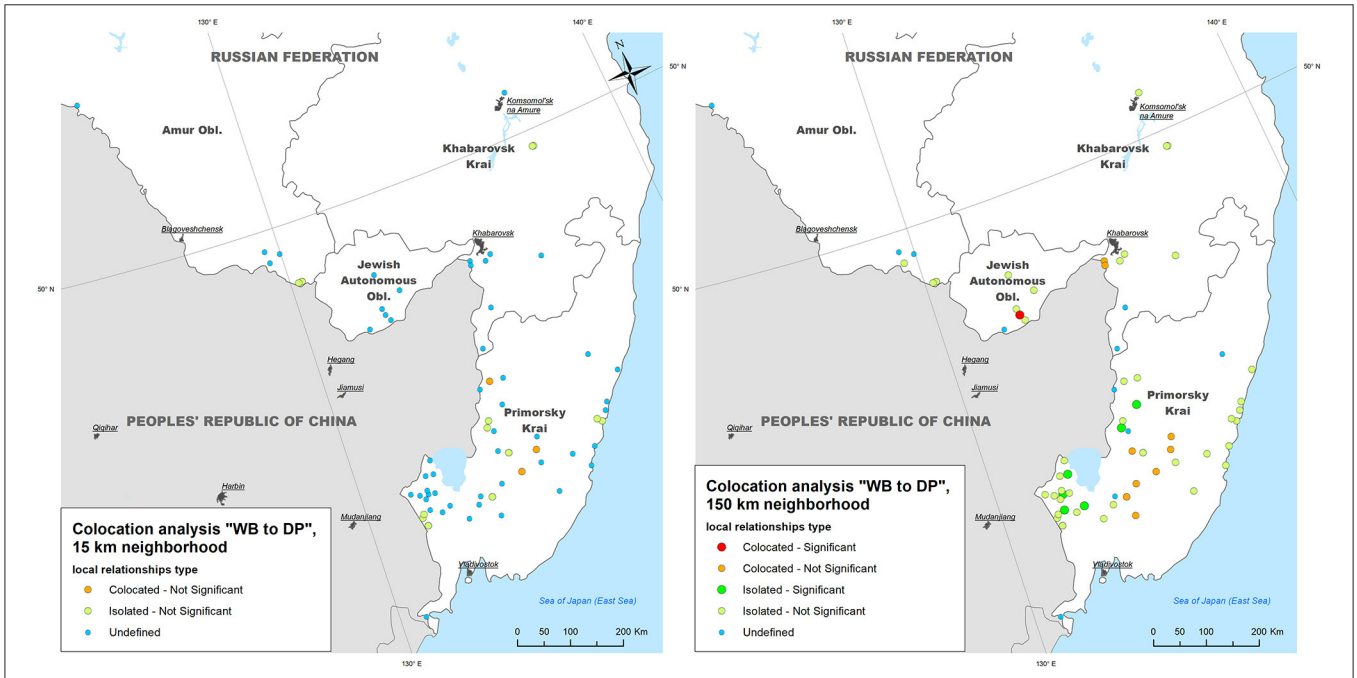

FIGURE 5 | The results of local colocation analysis of ASF outbreaks in wild boar (WB) and domestic pigs (DP). **(Left)** With 15 km as a neighboring distance; **(Right)** with 150 km as neighboring distance.

in a large epidemic involving both DP and WB. The current epidemic situation demonstrates a predominance of DP outbreaks in Amur Oblast, Jewish Autonomous Oblast and Khabarovsk Krai. These outbreaks are mainly concentrated along the Russian—Chinese border and main transportation routes with just several cases of ASF in WB that do not influence the outbreak clustering patterns in these three regions. In contrast, Primorsky Krai shows a mixture of ASF

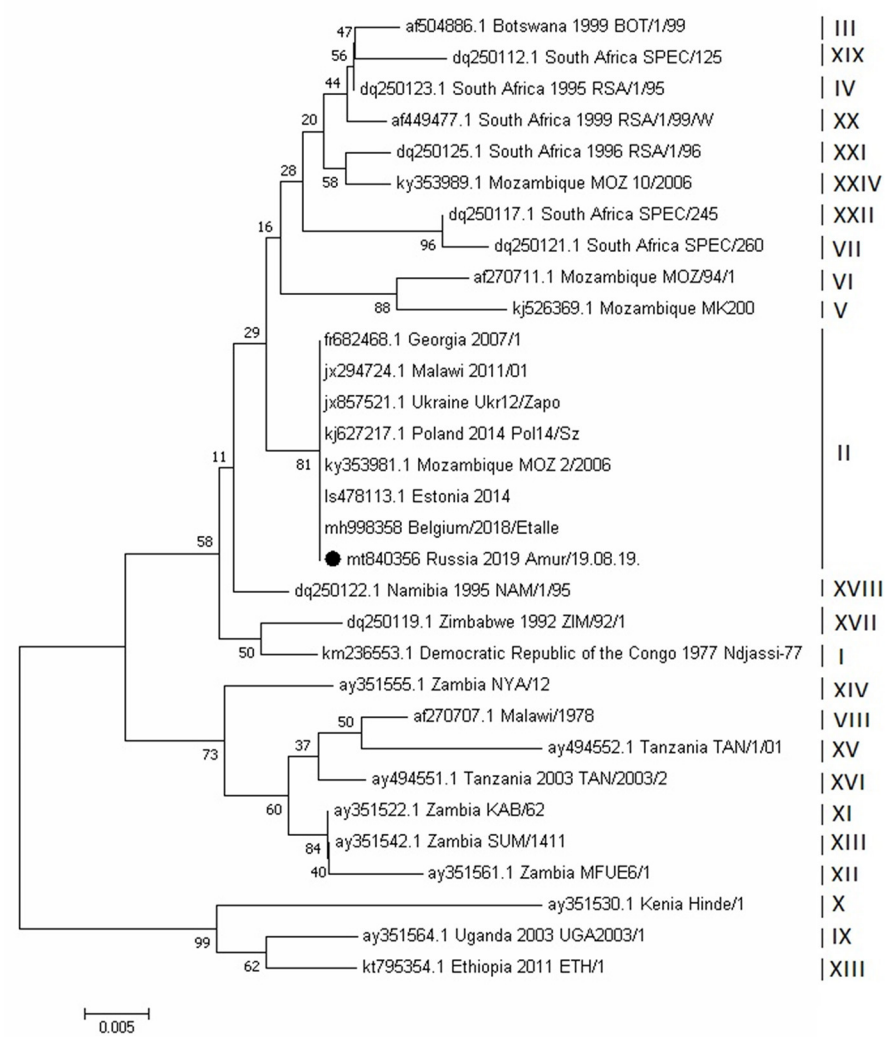

FIGURE 6 | Evolutionary relationships of African swine fever virus strains based on the neighbor-joining phylogeny of the partial p72 gene sequences. The phylogenetic analysis was performed using MEGA7. Bootstrap values (based on 1,000 replicates) for each node are given. GenBank accession numbers, country, and year of collection are indicated for each strain. Corresponding genotypes are labeled I–XXIV. The black circle indicates the African swine fever sequence from Russia, Amur region, 2019. The scale bar indicates nucleotide substitutions per site.

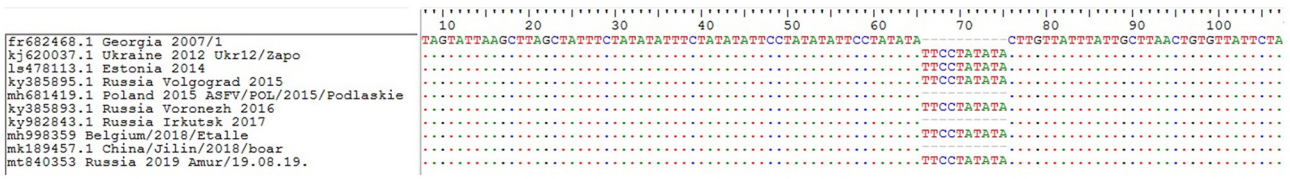

FIGURE 7 | Nucleotide sequence alignment of the partial I73R and I329L intergenic region of the representative African wine fever virus strains. GenBank accession numbers, country, and year of collection are indicated.

outbreaks both in WB and DP, which are widely spread across its area.

Since the first ASF introduction in the Russian Federation, discussions have been conducted in scientific literature as well as in the media on the leading role of either DP or WB population in the spread of the disease (3, 37, 63). To shed some light on this question using the example of the new epidemic in Far East of Russia, we explored the space-time relationships between DP

TABLE 2 | The results of calculating the mass of wild ungulates based on the reduction in the number of WB in the Far East region of Russia.

	Musk deer, head	Reindeer, head	Siberian roe deer, head	Moose, head	Red deer, head	WB (Sus scrofa) by 2019, head	Forestry area, km^2	WB density before depopulation, head/km^2	WB depopulation proportion, %	Decrease of total ungulates body mass, % (mean and 95% CI)
Primorsky Krai	37,588	0	54,046	3,806	33,968	44,517	130,269	0.34	92.7	33.6 (19.3–46.1)
Khabarovsk Krai	38,255	24,268	19,019	61,906	30,730	20,623	755,586	0.03	8.4	0.5 (0.2–0.8)
Jewish Autonomous Oblast	1508	0	14,042	722	3,695	5,973	21,080	0.28	91.2	29.7 (16.2–42.6)
Amur Oblast	24,938	13,794	57,324	22,586	19,201	14,150	305,152	0.05	46.1	3.9 (1.8–6.2)
Body mass minimum, kg	10	80	20	350	93	48				
Body mass maximum, kg	17	180	60	570	148	178				

and WB outbreaks by conducting colocation analysis. This type of analysis looks at the elevated concentration of one category of outbreaks within a close proximity to another and may help to reveal a predominant tendency of DP outbreaks emergence after preceding WB cases, or vice versa. However, our results did not indicate any clear pattern of ASF outbreaks' colocation. The most pronounced results are revealed when taking 150 km as an analysis neighborhood. Most of DP outbreaks, especially in the south-west part of the study area are treated as "isolated" that means an absence or low concentration of WB cases nearby, thus rebutting the hypothesis about the ASF transmission from WB to DP. In Primorsky Krai, the outbreaks' relationships are more heterogeneous, though no obvious pattern is detected as well.

The intensive spread of the ASF virus in the Far Eastern areas of the Russian Federation might have resulted, in part, from insufficient preparedness of the veterinary services and agricultural producers of the region in terms of protection against the virus entry into DP populations. This region has large numbers of poorly protected pig farms, which often practice free range farming techniques, thus with an increased chance for pigs to come into contact with the wild population (64, 65). Therefore, according to the "Cerberus" information system at the Federal Service for Veterinary and Phytosanitary Surveillance, 284 out of 289 registered pig-breeding farms in the Primorsky Krai belong to the first or second biosafety level[1] suggesting low or no biosecurity; in the Khabarovsk Krai, this number is 32 out of 33 farms; in the Jewish Autonomous Oblast, it is 45 out of 45 farms; and in Amur Oblast, it is 2 out of 2 farms. For comparison, in the European part of the Russian Federation, where measures to control the ASF spread have been in place since 2007, the situation is diametrically opposed. In the Belgorod Region (one of the largest agricultural producers in Russia), only 4 out of 371 farms belong to the first or second biosafety level; in the Nizhny Novgorod Region, this number is 22 out of 118 farms; in the Saratov Region, it is 114 out of 183 farms; and in the Volgograd Region, it is 145 out of 235 farms. Although compartmentalization is currently applied to pig producers on a voluntary basis, the above numbers reflect only a part of all pig farms while still being indicative of the ratio between low- and high-biosecurity holdings in the region.

Although some researchers suggest the threshold density of WB that can stop the ASF spread within the population (4, 27, 66, 67), other authors advocate that achieving this level does not guarantee the cessation of the epidemic chain (24, 37, 68). Currently in force national legislation on the ASF prevention and control supposes the WB density reduction in the ASF affected areas till the threshold of 0.025 head/km^2, which may result in an intensive depopulation of WB in the study regions. As a side effect of such a depopulation, a decreased availability of food resources for wild predators of the region can be expected. Particularly, it

[1]According to the agricultural producers' biosafety regulations currently in force, all pig-breeding facilities are categorized into four biosafety levels (or compartments). The first and second compartments are considered low or no biosafety holdings, while the third and fourth compartments are large farms with strict biosecurity measures (https://cerberus.vetrf.ru/cerberus/compartment/pub) (Article in Russian).

may affect the population of a protected species, Siberian tigers, for which WB present a significant and easily available food source (39, 40, 69, 70). In our study, we aimed to estimate a possible decrease in the wild ungulates' biomass in a case of the reduction of WB numbers. Such approach is based on several assumptions, which are potential limitations of the study. Other possible limitations include the following:

First, the numbers of all the animals were considered at a regional level, with no differentiation according to the various municipal districts (because of a lack of district-level data).
Second, the average weight of each animal was estimated using a uniform distribution (i.e., all values from minimum to maximum were considered to be equally possible), while the real distributions may be quite different.
Third, not all of an animal's mass is edible meat. In reality, no more than 70% of its mass can be considered a food resource (62, 69, 71).
Fourth, we did not account for the age structure of the animal populations, which was partly compensated for by a simulated variation in body mass.
Fifth, according to some studies a prey's population may survive a 1-year withdrawal of 15% to 25% of individual animals with no a long-term impact to its numbers (68). This may indicate that a potential impact of depopulation will be most pronounced in the regions with above 25% estimated depopulation proportion (**Table 2**).

To carry out a more detailed assessment of the possible impact of a presumable WB depopulation on the equilibrium of the ecosystem, it would be necessary to first have detailed data on the numbers of all animal species at a finer scale (at least the municipal district level), and second, to apply more complex dynamic population models that allow accounting for interactions between the predators and all potential preys.

CONCLUSIONS

Our results demonstrate the emergence of the ASF virus to the Far Eastern areas of the Russian Federation has led to the rapid spread of the disease over a large territory and support a hypothesis of multiple routes of viral introduction into the region. The ASF virus circulating in the study region demonstrates a close homology with corresponding viruses that have been isolated in Europe, Russia, and China. Due to the very dense WB population in this region, the ASF virus can be expected to persist in this population, which may entail the artificial regulation of this WB population to prevent the spread of the disease. The possible reduction of the WB population in Primorsky Krai may lead to a 33.6% (19.3–46.1%) decrease in the total mass of all ungulates, which may pose a threat to the population of predatory species of the region including the protected population of Siberian tigers.

DATA AVAILABILITY STATEMENT

The genetic datasets presented in this study can be found in online repositories. The names of the repository/repositories and accession number(s) can be found at: NCBI [accession: MT840352-MT840357]. The data on ASF outbreaks were obtained from open sources, which are indicated in the text.

ETHICS STATEMENT

The animal study was reviewed and approved by State Veterinary Service of the Russian Federation. Written informed consent was obtained from the owners for the participation of their animals in this study.

AUTHOR CONTRIBUTIONS

DK: conceptualization and project administration. FK, IT, and AB: methodology. FK and OZ: software and data curation, and visualization. FK, AG, and LA: validation. FK and IT: formal analysis. OZ, AB, and TS: investigation. OZ, LA, and FK: writing—original draft preparation. FK, AG, OZ, and LA: writing—review and editing. AG, LA, and DK: supervision. All authors have read and agree to the published version of the manuscript.

FUNDING

This work was supported by the Federal Research Center for Virology and Microbiology for government assignment.

ACKNOWLEDGMENTS

We thank MSc Mackenzie Waltke for proofreading the manuscript.

REFERENCES

1. Penrith ML, Vosloo W. Review of African swine fever: transmission, spread and control. *J S Afr Vet Assoc.* (2009) 80:58–62. doi: 10.4102/jsava.v80i2.172
2. Costard S, Wieland B, De Glanville W, Jori F, Rowlands R, Vosloo W, et al. African swine fever: how can global spread be prevented? *Philos Trans R Soc B Biol Sci.* (2009) 364:2683–96. doi: 10.1098/rstb.2009.0098
3. Khomenko S, Beltrán-Alcrudo D, Rozstanlnyy A, Gogin A, Kolbasov D, Pinto J, et al. *African Swine Fever in the Russian Federation: Risk Factors for Europe and Beyond.* (2013). Available online at: www.fao.org/ag/empres.html (accessed June 7, 2020).
4. Gervasi V, Marcon A, Bellini S, Guberti V. Evaluation of the efficiency of active and passive surveillance in the detection of African swine fever in wild boar. *Vet Sci.* (2020) 7:5. doi: 10.3390/vetsci7010005
5. Costard S, Mur L, Lubroth J, Sanchez-Vizcaino JM, Pfeiffer DU. Epidemiology of African swine fever virus. *Virus Res.* (2013) 173:191–7. doi: 10.1016/j.virusres.2012.10.030
6. Onzere CK, Bastos AD, Okoth EA, Lichoti JK, Bochere EN, Owido MG, et al. Multi-locus sequence typing of African swine fever viruses from endemic regions of Kenya and Eastern Uganda (2011–2013) reveals

rapid B602L central variable region evolution. *Virus Genes.* (2018) 54:111–23. doi: 10.1007/s11262-017-1521-4
7. Malogolovkin A, Kolbasov D. Genetic and antigenic diversity of African swine fever virus. *Virus Res.* (2019) 271:197673. doi: 10.1016/j.virusres.2019.197673
8. Malogolovkin A, Burmakina G, Titov I, Sereda A, Gogin A, Baryshnikova E, et al. Comparative analysis of African swine fever virus genotypes and serogroups. *Emerg Infect Dis.* (2015) 21:312–315. doi: 10.3201/eid2102.140649
9. Wang L, Luo Y, Zhao Y, Gao GF, Bi Y, Qiu HJ. Comparative genomic analysis reveals an 'open' pan-genome of African swine fever virus. *Transbound Emerg Dis.* (2020) 67:1553–62. doi: 10.1111/tbed.13489
10. Granberg F, Torresi C, Oggiano A, Malmberg M, Iscaro C, De Mia GM, et al. Complete genome sequence of an African swine fever virus isolate from Sardinia, Italy. *Genome Announc.* (2016) 4:1220–36. doi: 10.1128/genomeA.01220-16
11. Gaudreault NN, Madden DW, Wilson WC, Trujillo JD, Richt JA. African swine fever virus: an emerging dna arbovirus. *Front Vet Sci.* (2020) 7:215. doi: 10.3389/fvets.2020.00215
12. Sánchez-Cordón PJ, Nunez A, Neimanis A, Wikström-Lassa E, Montoya M, Crooke H, et al. African swine fever: disease dynamics in wild boar experimentally infected with ASFV isolates belonging to genotype I and II. *Viruses.* (2019) 11:852. doi: 10.3390/v11090852
13. Sánchez-Cordón PJ, Montoya M, Reis AL, Dixon LK. African swine fever: a re-emerging viral disease threatening the global pig industry. *Vet J.* (2018) 233:41–8. doi: 10.1016/j.tvjl.2017.12.025
14. Chenais E, Depner K, Guberti V, Dietze K, Viltrop A, Ståhl K. Epidemiological considerations on African swine fever in Europe 2014-2018. *Porc Heal Manag.* (2019) 5:6. doi: 10.1186/s40813-018-0109-2
15. Galindo I, Alonso C. African swine fever virus: a review. *Viruses.* (2017) 9:103. doi: 10.3390/v9050103
16. Korennoy FI, Gulenkin VM, Malone JB, Mores CN, Dudnikov SA, Stevenson MA. Spatio-temporal modeling of the African swine fever epidemic in the Russian Federation, 2007-2012. *Spat Spatiotemporal Epidemiol.* (2014) 11:135–41. doi: 10.1016/j.sste.2014.04.002
17. Bao J, Wang Q, Lin P, Liu C, Li L, Wu X, et al. Genome comparison of African swine fever virus China/2018/AnhuiXCGQ strain and related European p72 Genotype II strains. *Transbound Emerg Dis.* (2019) 66:1167–76. doi: 10.1111/tbed.13124
18. Karger A, Pérez-Núñez D, Urquiza J, Hinojar P, Alonso C, Freitas FB, et al. An update on African swine fever virology. *Viruses.* (2019) 11:864. doi: 10.3390/v11090864
19. Fekede RJ, van Gils H, Huang LY, Wang XL. High probability areas for ASF infection in China along the Russian and Korean borders. *Transbound Emerg Dis.* (2019) 66:852–64. doi: 10.1111/tbed.13094
20. Liu J, Liu B, Shan B, Wei S, An T, Shen G, et al. Prevalence of African Swine Fever in China, 2018-2019. *J Med Virol.* (2019) 92:1023–34. doi: 10.1002/jmv.25638
21. Vergne T, Korennoy F, Combelles L, Gogin A, Pfeiffer DU. Modelling African swine fever presence and reported abundance in the Russian Federation using national surveillance data from 2007 to 2014. *Spat Spatiotemporal Epidemiol.* (2016) 19:70–7. doi: 10.1016/j.sste.2016.06.002
22. Pepin KM, Golnar AJ, Abdo Z, Podgórski T. Ecological drivers of African swine fever virus persistence in wild boar populations: insight for control. *Ecol Evol.* (2020) 10:2846–59. doi: 10.1002/ece3.6100
23. Halasa T, Boklund A, Bøtner A, Mortensen S, Kjær LJ. Simulation of transmission and persistence of African swine fever in wild boar in Denmark. *Prev Vet Med.* (2019) 167:68–79. doi: 10.1016/j.prevetmed.2019.03.028
24. Guberti V, Khomenko S, Masiulis M, Kerba S. *African Swine Fever in wild Boar Ecology and Biosecurity*. FAO Animal Production and Health Manual No. 22. Rome: FAO, OIE and EC (2019).
25. Taylor RA, Condoleo R, Simons RRL, Gale P, Kelly LA, Snary EL. The risk of infection by African swine fever virus in European swine through boar movement and legal trade of pigs and pig meat. *Front Vet Sci.* (2020) 6:486. doi: 10.3389/fvets.2019.00486
26. Keuling O, Sange M, Acevedo P, Podgorski T, Smith G, Scandura M, et al. Guidance on estimation of wild boar population abundance and density: methods, challenges, possibilities. *EFSA Support Publ.* (2018) 15:1449E. doi: 10.2903/sp.efsa.2018.EN-1449
27. Podgórski T, Apollonio M, Keuling O. Contact rates in wild boar populations: implications for disease transmission. *J Wildl Manage.* (2018) 82:1210–8. doi: 10.1002/jwmg.21480
28. Jori F, Bastos ADS. Role of wild suids in the epidemiology of African swine fever. *Ecohealth.* (2009) 6:296–310. doi: 10.1007/s10393-009-0248-7
29. Probst C, Globig A, Knoll B, Conraths FJ, Depner K. Behaviour of free ranging wild boar towards their dead fellows: potential implications for the transmission of African swine fever. *R Soc Open Sci.* (2017) 4:170054. doi: 10.1098/rsos.170054
30. Podgórski T, Smietanka K. Do wild boar movements drive the spread of African swine fever? *Transbound Emerg Dis.* (2018) 65:1588–96. doi: 10.1111/tbed.12910
31. Bieber C, Ruf T. Population dynamics in wild boar Sus scrofa: ecology, elasticity of growth rate and implications for the management of pulsed resource consumers. *J Appl Ecol.* (2005) 42:1203–13. doi: 10.1111/j.1365-2664.2005.01094.x
32. Zani L, Masiulis M, Bušauskas P, Dietze K, Pridotkas G, Globig A, et al. African swine fever virus survival in buried wild boar carcasses. *Transbound Emerg Dis.* (2020) 67:2086–92. doi: 10.1111/tbed.13554
33. Morelle K, Jezek M, Licoppe A, Podgorski T. Deathbed choice by ASF-infected wild boar can help find carcasses. *Transbound Emerg Dis.* (2019) 66:1821–6. doi: 10.1111/tbed.13267
34. Vajas P, Calenge C, Richard E, Fattebert J, Rousset C, Saïd S, et al. Many, large and early: hunting pressure on wild boar relates to simple metrics of hunting effort. *Sci Total Environ.* (2020) 698:134251. doi: 10.1016/j.scitotenv.2019.134251
35. Urner N, Mõtus K, Nurmoja I, Schulz J, Sauter-Louis C, Staubach C, et al. Hunters' acceptance of measures against African swine fever in wild boar in Estonia. *Prev Vet Med.* (2020) 182:105121. doi: 10.1016/j.prevetmed.2020.105121
36. Pautienius A, Grigas J, Pileviciene S, Zagrabskaite R, Buitkuviene J, Pridotkas G, et al. Prevalence and spatiotemporal distribution of African swine fever in Lithuania, 2014-2017. *Virol J.* (2018) 15:177. doi: 10.1186/s12985-018-1090-8
37. More S, Miranda MA, Bicout D, Bøtner A, Butterworth A, Calistri P, et al. African swine fever in wild boar. *EFSA J.* (2018) 16:e05344. doi: 10.2903/j.efsa.2018.5344
38. Iglesias I, Muñoz MJ, Montes F, Perez A, Gogin A, Kolbasov D, et al. Reproductive ratio for the local spread of African Swine fever in wild boars in the Russian federation. *Transbound Emerg Dis.* (2016) 63:e237–45. doi: 10.1111/tbed.12337
39. Kerley LL, Mukhacheva AS, Matyukhina DS, Salmanova E, Salkina GP, Miquelle DG. A comparison of food habits and prey preference of Amur tiger (*Panthera tigris altaica*) at three sites in the Russian Far East. *Integr Zool.* (2015) 10:354–64. doi: 10.1111/1749-4877.12135
40. Dou H, Yang H, Smith JLD, Feng L, Wang T, Ge J, et al. Prey selection of Amur tigers in relation to the spatiotemporal overlap with prey across the Sino-Russian border. *Wildlife Biol.* (2019) 2019:1–11. doi: 10.2981/wlb.00508
41. Yang H, Dou H, Baniya RK, Han S, Guan Y, Xie B, et al. Seasonal food habits and prey selection of Amur tigers and Amur leopards in Northeast China. *Sci Rep.* (2018) 8:6930. doi: 10.1038/s41598-018-25275-1
42. Sokolov II. *Fauna USSR. Mammals. Ungulate animals. (Detachments Perissodactyla and Artiodactyla).* Vol. 1. Academy of Sciences of the USSR– in Russian. (1959). p. 642. Available online at: http://biblioclub.ru/index.php?page=book&id=114642 (accessed September 23, 2020).
43. Danilkin AA. *Cervidae (Mammals of Russia and Neighboring Regions).* GEOS. (Olenji (Mlekopitayuschie Rossii I sopredelnykh regionov)) – in Russian (1999). p. 552. Available online at: http://geos-books.ru/danilkin-a-a-oleni-cervidae/ (accessed June 27, 2020).
44. King DP, Reid SM, Hutchings GH, Grierson SS, Wilkinson PJ, Dixon LK, et al. Development of a TaqMan® PCR assay with internal amplification control for the detection of African swine fever virus. *J Virol Methods.* (2003) 107:53–61. doi: 10.1016/S0166-0934(02)00189-1
45. Gallardo C, Fernández-Pinero J, Pelayo V, Gazaev I, Markowska-Daniel I, Pridotkas G, et al. Genetic variation among African swine fever genotype II viruses, Eastern and Central Europe. *Emerg Infect Dis.* (2014) 20:1544–7. doi: 10.3201/eid2009.140554
46. Sanna G, Dei Giudici S, Bacciu D, Angioi PP, Giammarioli M, De Mia GM, et al. Improved strategy for molecular characterization of African

swine fever viruses from Sardinia, based on analysis of p30, CD2V and I73R/I329L variable regions. *Transbound Emerg Dis.* (2017) 64:1280–6. doi: 10.1111/tbed.12504
47. Nix RJ, Gallardo C, Hutchings G, Blanco E, Dixon LK. Molecular epidemiology of African swine fever virus studied by analysis of four variable genome regions. *Arch Virol.* (2006) 151:2475–94. doi: 10.1007/s00705-006-0794-z
48. Bastos ADS, Penrith ML, Crucière C, Edrich JL, Hutchings G, Roger F, et al. Genotyping field strains of African swine fever virus by partial p72 gene characterization. *Arch Virol.* (2003) 148:693–706. doi: 10.1007/s00705-002-0946-8
49. Lubisi BA, Bastos ADS, Dwarka RM, Vosloo W. Intra-genotypic resolution of African swine fever viruses from an East African domestic pig cycle: a combined p72-CVR approach. *Virus Genes.* (2007) 35:729–35. doi: 10.1007/s11262-007-0148-2
50. *BioEdit: A User-Friendly Biological Sequence Alignment Editor and Analysis Program for Windows 95/98/NT – ScienceOpen*. Available online at: https://www.scienceopen.com/document?vid=8b59b929-3c37-49f6-936b-f8bf6dd92ace (accessed September 20, 2020).
51. Thompson JD, Gibson TJ, Plewniak F, Jeanmougin F, Higgins DG. The CLUSTAL X windows interface: flexible strategies for multiple sequence alignment aided by quality analysis tools. *Nucleic Acids Res.* (1997) 25:4876–82. doi: 10.1093/nar/25.24.4876
52. Kimura M. A simple method for estimating evolutionary rates of base substitutions through comparative studies of nucleotide sequences. *J Mol Evol.* (1980) 16:111–20. doi: 10.1007/BF01731581
53. Kumar S, Stecher G, Tamura K. MEGA7: molecular evolutionary genetics analysis version 7.0 for bigger datasets. *Mol Biol Evol.* (2016) 33:1870–4. doi: 10.1093/molbev/msw054
54. Space-Time Permutation Model, Kulldorff M, Heffernan R, Hartman J, Assunção RM, Mostashari F. A space-time permutation scan statistic for disease outbreak detection. *PLoS Med.* (2005) 2:216–24. doi: 10.1371/journal.pmed.0020059
55. Burt, JE, Barber GM. *Elementary Statistics for Geographers*. 2nd ed. New York, NY: Guilford Press (1996).
56. How Colocation analysis works. *ArcGIS Pro Online Help*. Esri (2021). Available online at: https://pro.arcgis.com/en/pro-app/latest/tool-reference/spatial-statistics/learnmorecolocationanalysis.htm (accessed January 31, 2021).
57. Leslie TF, Kronenfeld BJ. The colocation quotient: a new measure of spatial association between categorical subsets of points. *Geograph Analy.* (2011) 43:306–26. doi: 10.1111/j.1538-4632.2011.00821.x
58. Wang F, Hu Y, Wang S, Li X. Local indicator of colocation quotient with a statistical significance test: examining spatial association of crime and facilities. *Profess Geograph.* (2017) 69:22–31. doi: 10.1080/00330124.2016.1157498
59. Kulldorff M. *Software for the Spatial and Space-Time Scan Statistics*. Information Management Services, Inc. SaTScan^{TM} v9.6. (2018). Available online at: www.satscan.org (accessed May 9, 2021).
60. Malkhazova S, Korennoy F, Petrova O, Gulenkin V, Karaulov A. Spatio-temporal analysis of the local African swine fever epidemics in the Russian Federation, 2007–2015. *Front Vet Sci.* (2019). doi: 10.3389/conf.fvets.2019.05.00018
61. *On the Acceptance of the Veterinary Rules of Conducting Prophylactic, Diagnostic, Restriction and Other Measures, Quarantine Establishing and Dropping, and Other Restrictions Aimed at the Prevention of the African Swine Fever Spread and Eradication of Its Foci.* The decree of the Ministry of Agriculture of the Russian Federation from 28 January 2021 #37 (in Russian) (2021). Available online at: https://docs.cntd.ru/document/573473462?marker=6500IL#/reg (accessed May 5, 2021).
62. Maksimova DA, Seryodkin I V., Zaitsev VA, Miquelle DG. Research program of musk deer ecology in the sikhote-alin region. *Achiev Life Sci.* (2014) 8:65–71. doi: 10.1016/j.als.2014.11.005
63. Bellini S, Rutili D, Guberti V. Preventive measures aimed at minimizing the risk of African swine fever virus spread in pig farming systems. *Acta Vet Scand.* (2016) 58:82. doi: 10.1186/s13028-016-0264-x
64. Cappai S, Rolesu S, Coccollone A, Laddomada A, Loi F. Evaluation of biological and socio-economic factors related to persistence of African swine fever in Sardinia. *Prev Vet Med.* (2018) 152:1–11. doi: 10.1016/j.prevetmed.2018.01.004
65. Mur L, Sánchez-Vizcaíno JM, Fernández-Carrión E, Jurado C, Rolesu S, Feliziani F, et al. Understanding African Swine Fever infection dynamics in Sardinia using a spatially explicit transmission model in domestic pig farms. *Transbound Emerg Dis.* (2018) 65:123–34. doi: 10.1111/tbed.12636
66. Olševskis E, Schulz K, Staubach C, SerŽants M, Lamberga K, Pule D, et al. African swine fever in Latvian wild boar—a step closer to elimination. *Transbound Emerg Dis.* (2020) 67:2615–29. doi: 10.1111/tbed.13611
67. Pejsak Z, Truszczyński M, Niemczuk K, Kozak E, Markowska-Daniel I. Epidemiology of African Swine Fever in Poland since the detection of the first case. *Pol J Vet Sci.* (2014) 17:665–72. doi: 10.2478/pjvs-2014-0097
68. Danilkin AA. *Management of Wild Boar and Other Animal Resources in African Swine Fever*. (2020). Available online at: https://www.litres.ru/a-a-danilkin/upravlenie-resursami-kabana-i-drugih-zhivotnyh-pri-a-51267507/
69. Biswas S, Sankar K. Prey abundance and food habit of tigers (*Panthera tigris tigris*) in Pench National Park, Madhya Pradesh, India. *J Zool.* (2006) 256:411–20. doi: 10.1017/S0952836902000456
70. Rozhnov VV, Aramileva TS, Gaponov VV, Darman YA, Zhuravlev YN, Kostyrya AV, et al. *A Strategy of the Siberian Tiger Preservation in the Russian Federation*. Moscow: Ministry of natural resources and ecology of the Russian Federation (in Russian). (2010). p. 49. Available online at: http://amur-tiger.ru/assets/docs/strategita-tigr-russ.pdf (last accessed May 9, 2021).
71. Ramesh T, Snehalatha V, Sankar K, Qureshi Q. Food habits and prey selection of tiger and leopard in Mudumalai Tiger Reserve, Tamil Nadu, India. *Sci Trans Enviorn Technov.* (2009) 2:170–81. doi: 10.20894/stet.116.002.003.010

Conflict of Interest: The authors declare that the research was conducted in the absence of any commercial or financial relationships that could be construed as a potential conflict of interest.

frontiers in Veterinary Science

ORIGINAL RESEARCH
published: 06 September 2021
doi: 10.3389/fvets.2021.719859

A High-Throughput Method to Analyze the Interaction Proteins With p22 Protein of African Swine Fever Virus *In Vitro*

Xuejiao Zhu[1,2,3], *Baochao Fan*[1,2,3,4], *Junming Zhou*[1,2,3], *Dandan Wang*[1,2,3], *Huiying Fan*[5] *and Bin Li*[1,2,3,6]*

[1] Institute of Veterinary Medicine, Jiangsu Academy of Agricultural Sciences, Key Laboratory of Veterinary Biological Engineering and Technology, Ministry of Agriculture, Nanjing, China, [2] Jiangsu Co-innovation Center for Prevention and Control of Important Animal Infectious Diseases and Zoonoses, Yangzhou, China, [3] Jiangsu Key Laboratory for Food Quality and Safety—State Key Laboratory Cultivation Base of Ministry of Science and Technology, Nanjing, China, [4] School of Life Sciences, Jiangsu University, Zhenjiang, China, [5] College of Veterinary Medicine, South China Agricultural University, Guangzhou, China, [6] School of Food and Biological Engineering, Jiangsu University, Zhenjiang, China

OPEN ACCESS

Edited by:
Yashpal S. Malik,
Indian Veterinary Research Institute (IVRI), India

Reviewed by:
Yuan Wanzhe,
Agricultural University of Hebei, China
Tongling Shan,
Shanghai Veterinary Research Institute, Chinese Academy of Agricultural Sciences (CAAS), China

***Correspondence:**
Bin Li
libinana@126.com

Specialty section:
This article was submitted to Veterinary Infectious Diseases, a section of the journal Frontiers in Veterinary Science

Received: 03 June 2021
Accepted: 03 August 2021
Published: 06 September 2021

Citation:
Zhu X, Fan B, Zhou J, Wang D, Fan H and Li B (2021) A High-Throughput Method to Analyze the Interaction Proteins With p22 Protein of African Swine Fever Virus In Vitro. Front. Vet. Sci. 8:719859. doi: 10.3389/fvets.2021.719859

African swine fever virus (ASFV) has been identified as the agent of African swine fever, resulting in a mortality rate of nearly 100% in domestic pigs worldwide. Protein p22 encoded by gene KP177R has been reported to be localized at the inner envelope of the virus, while the function of p22 remains unclear. In this study, p22 interacting proteins of the host were identified by a high-throughput method and analyzed by Gene ontology terms and Kyoto Encyclopedia of Gene and Genomes (KEGG) pathways; numerous cellular proteins in 293-T that interacted with p22 protein were identified. These interacting proteins were related to the biological processes of binding, cell structure, signal transduction, cell adhesion, etc. At the same time, the interacted proteins participated in several KEGG pathways like ribosome, spliceosome, etc. The key proteins in the protein–protein interaction network were closely related to actin filament organization and movement, resulting in affecting the process of phagocytosis and endocytosis. A large number of proteins that interacted with p22 were identified, providing a large database, which should be very useful to elucidate the function of p22 in the near future, laying the foundation for elucidating the mechanism of ASFV.

Keywords: African swine fever virus, protein p22, GO KEGG pathways analysis, liquid chromatography, mass spectrometry

INTRODUCTION

African swine fever (ASF) is caused by African swine fever virus (ASFV), a linear, large, double-stranded DNA virus that is the only member of the Asfarviridae family (1). ASFV is an enveloped DNA virus with genome length of 170–193 kbp (1). The genome encoded 151–167 open reading frames. ASFV is an icosahedral symmetric virus that replicates in the cytoplasm of infected cells. Warthogs, Bush pigs, and soft ticks are natural hosts of the virus, which can persist to infect without any signs of disease (2). Once introduced into domestic pigs, ASFV is a highly pathogenic virus and could spread directly among pigs, resulting in nearly 100% mortality (3). Typical clinical symptoms

include high fever, cyanosis, hemorrhagic lesions, anorexia, and ataxia (4). The lesion tissues display severe pathological vascular changes, such as renal ecchymosis, skin erythema, and diffuse hemorrhages in lymph nodes, kidneys, lungs, and urinary bladder; pulmonary edema; disseminated intravascular coagulation; and thrombocytopenia (5).

The disease has caused serious economic losses to the pig industry and has a severe impact on the world. Especially in 2018, the breakout of ASF in China spread quickly over the country, threatening the pig industry severely (6). Recent studies have shown that some viral proteins are involved in the adhesion and entry of ASFV. Some encoded structural proteins are involved in genome replication and virus infection (7). It is reported that 15 of the 26 virus-encoded proteins were detected in the virus proteome with predicted transmembrane domains (8). However, some detected proteins remain uncharacterized. Among the detected proteins on the membrane, protein p22 (pKP177R) has been predicted to be externally located in the virion (9). Some studies have reported that p22 was localized around the virus factories rather than at the cell surface (10, 11). In another study, it was tricky that protein p22 was weakly detected throughout the cytoplasm, including the virus factories, but could be detected at the periphery of assembling and mature icosahedral particles. Protein p22 was localized at the inner envelope (12). Other viral membrane proteins, like p17, pE183L, p12, and pE248R, were also at the cell surface but were localized at precursor viral membranes and intracellular icosahedral particles within the viral factories (13–16). Some structural proteins have been reported to be involved in virus entry, like p12, pE248R, and pE199L; some are required for the assembly process, like protein p17 and pE183L (17). These proteins are localized at the membrane of the virus, helping the entry or assembly process of the virus. However, the receptors of ASFV are still unclear. In recent study, p22 was proven not to be involved in virus replication or virulence in swine by KP177R gene deletion in recombinant virus (18). It might be due to the potential replacement of the KP177R gene by one of the L101L genes; there might be a potential overlapping in the function of these two genes. Therefore, the function of p22 is still unknown.

In this study, we studied the proteins that interacted with p22 of ASFV by proteomics analysis. Although a large number of structural protein studies have been performed, further researches on the function and molecular mechanism are desperately in need and will help prevent and control the spread of the disease.

Abbreviations: ASFV, African Swine Fever Virus; LCMS, Liquid Chromatography Mass Spectrometry; GO, Gene ontology; KEGG, Kyoto Encyclopedia of Gene and Genomes; PPI, Protein-protein interaction; MYH9, Myosin-9; ARPC2, Actin-related protein 2/3 complex subunit 2; ARF6, ADP-ribosylation factor 6; ACTBL2, Beta-actin-like protein 2; ACTN4, Alpha-actinin-4; CLTC, Clathrin heavy chain A; RAB10, Ras-related protein-10; pre-mRNA, precursor messenger RNA; cGMP, Cyclic GMP; PKG, cGMP-dependent protein kinase; NO, nitric oxide; AMPK, AMP-activated protein kinase.

MATERIALS AND METHODS

Sample Preparation

Gene KP177R (p22) of the ASFV and tagged by hemagglutinin (HA) at C terminus was synthesized into the plasmid pcDNA-3.1(+) by the GeneScript Corporation (Shanghai, China) and sequenced correctly. The 293-T cells were grown into 80% confluency in Dulbecco's modified Eagle's medium, supplemented with 10% fetal bovine serum (FBS) and antibiotics (penicillin/streptomycin) (Thermo Fisher, MA, USA) in tissue culture plates. Cells were maintained at 37°C in a humidified atmosphere and supplemented with 5% CO_2. The cells were then separately transfected with pcDNA3.1(+)-p22-HA and pcDNA3.1(+) (1 μg each) by Lipofectamine 3000 according to the instruction of the manufacturer (Thermo scientific, MA, USA) and were proven successfully expressed in 293-T cells. At 24 h post-transfection, p22-expressed or mock cells were washed once in cold phosphate-buffered saline (PBS) and suspended in 1 ml of cold immunoprecipitation (IP) buffer (Beyotime, Shanghai, China) (50 mM Tris-HCl, pH 7.4, 150 mM NaCl, 1 mM EDTA) supplemented with 0.5% Nonidet P-40 Substitute (NP-40, Fluka Analytical) on ice with 1% protease inhibitor cocktail (Roche, Shanghai, China). Cells were lysed for 30 min at 4°C with constant rotation, and the lysates were cleared by centrifugation at 5,000 × g for 5 min; lysate was removed for Western blot analysis (whole-cell lysate fraction). The remaining lysate was incubated with 1 μg of anti-HA antibody (Santa Cruz, Shanghai, China) overnight at 4°C, and then pre-coupled to 40 μl of A/G Plus agarose beads for 4 h at 4°C according to the instruction of the manufacturer. The immune complexes were precipitated, washed, and subjected to SDS-PAGE gels and Western blotting analysis.

Liquid Chromatography Tandem Mass Spectrometry (LC-MS/MS) Analysis and Data Processing

The preparation of peptides for MS of triplicate samples of each group and LC-MS/MS were all performed by the Shanghai Applied Protein Technology Company, and the LC-MS/MS was executed on an Q Exactive HF mass spectrometer (Thermo Scientific, MA, USA). In order to exclude possible contaminants, the databases were deleted in p22-immunoprecipitated proteins, which were obtained in mock immunoprecipitated proteins (the brief procedures are seen in **Figure 1**).

Western Blot

293-T cells were transfected with 1 μg of pcDNA3.1-p22-HA or mock plasmid for 24 h. At 24 h post-transfection, 293-T cells were lysed with lysis buffer containing 1% protein inhibitor. The cell lysates were subjected to SDS-PAGE and transferred onto 0.22-μm nitrocellulose membranes (Pall, Port Washington, NY, USA). Then, the membranes were incubated with 5% defatted milk at room temperature for 2 h, washed with PBS containing 0.05% Tween 20 three times, followed by anti-HA rabbit polyclonal antibody incubation at 4°C overnight, washed with PBST three times, and then incubated with horseradish peroxidase-conjugated goat anti-rabbit IgG secondary antibody

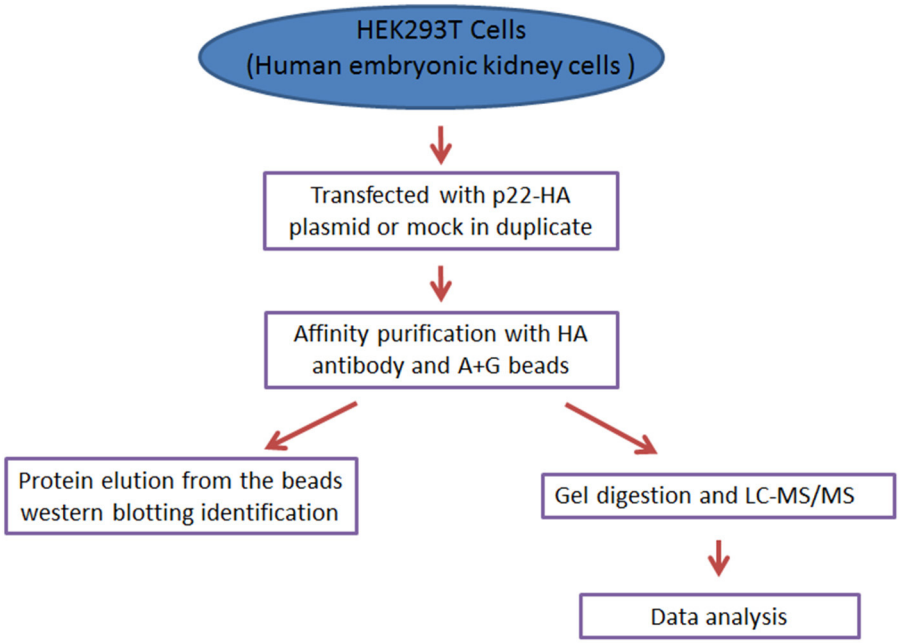

FIGURE 1 | The concise procedure for sample preparation and process.

at room temperature for 1 h. After washing three times with PBST, detection was performed using the ECL Kit (Thermo Fisher Scientific).

Indirect Immunofluorescence Assay (IFA)

293-T cells were transfected with 1 μg of pcDNA3.1(+)-p22-HA or mock plasmid for 24 h. At 24 h post-transfection, cells were fixed in 4% paraformaldehyde at 4°C for 30 min, and then the cell membranes were permeabilized with PBS containing 0.2% Triton X-100 for 5 min. The cells were incubated with 1:200 diluted anti-HA antibody at 37°C for 1 h. Then, the cells were incubated with Alexa Fluor 555-conjugated goat anti-rabbit IgG at 1:400 dilution at 37°C for 1 h and washed with PBS three times before examination.

Gene Ontology (GO) Enrichment and Kyoto Encyclopedia of Gene and Genomes (KEGG) Pathway Analysis of p22 Interacting Proteins

GO is the concept of the combination of gene–gene functions and is designed to detect cell biological functions *via* a systematically dynamic and computational interpretation of genes, RNA, and proteins. It covers three main areas (19) including cellular components, molecular function, and biological processes. The KEGG database aims to systematically analyze genes and their related gene functions with an interacting network of molecules in the cells in a hierarchical order (20). GO enrichment and KEGG pathway analysis of p22 interacting proteins were conducted. DAVID (http://david.abcc.ncifcrf.gov/) used in this study is short for Database for Annotation, Visualization, and Integrated Discovery.

Protein–Protein Interaction (PPI) Network Construction

The PPI plays an extremely important role in understanding cellular or systemic processes of cell growth, reproduction, and metabolism (21) and provides a platform for the annotation of functional, structural, and evolutionary properties of proteins. To further investigate the molecular mechanism of p22 of ASFV, PPI networks of p22 interacting proteins were constructed through the STRING database (http://www.string-db.org/). STRING is an online database that includes experimental as well as predicted interaction information and comprises >1,100 completely sequenced organisms. To select core genes from the PPI network, we analyzed the top biological structure of the network and obtained the proteins that directly interact with the target protein in the network. We selected the PPIs to construct the PPI network for visualization and analysis.

RESULTS

Sample Identification

Protein p22 was expressed in the 293-T cells by Western blotting analysis; the band was shown as the predicted size of 25 kDa (**Figure 2A**). The sample of p22-HA and its mock immunoprecipitated for LC-MS/MS were also identified (**Figure 2B**). IFA analysis also proved the p22 protein expressed in 293-T cells in both the nucleus and plasma (**Figure 2C**).

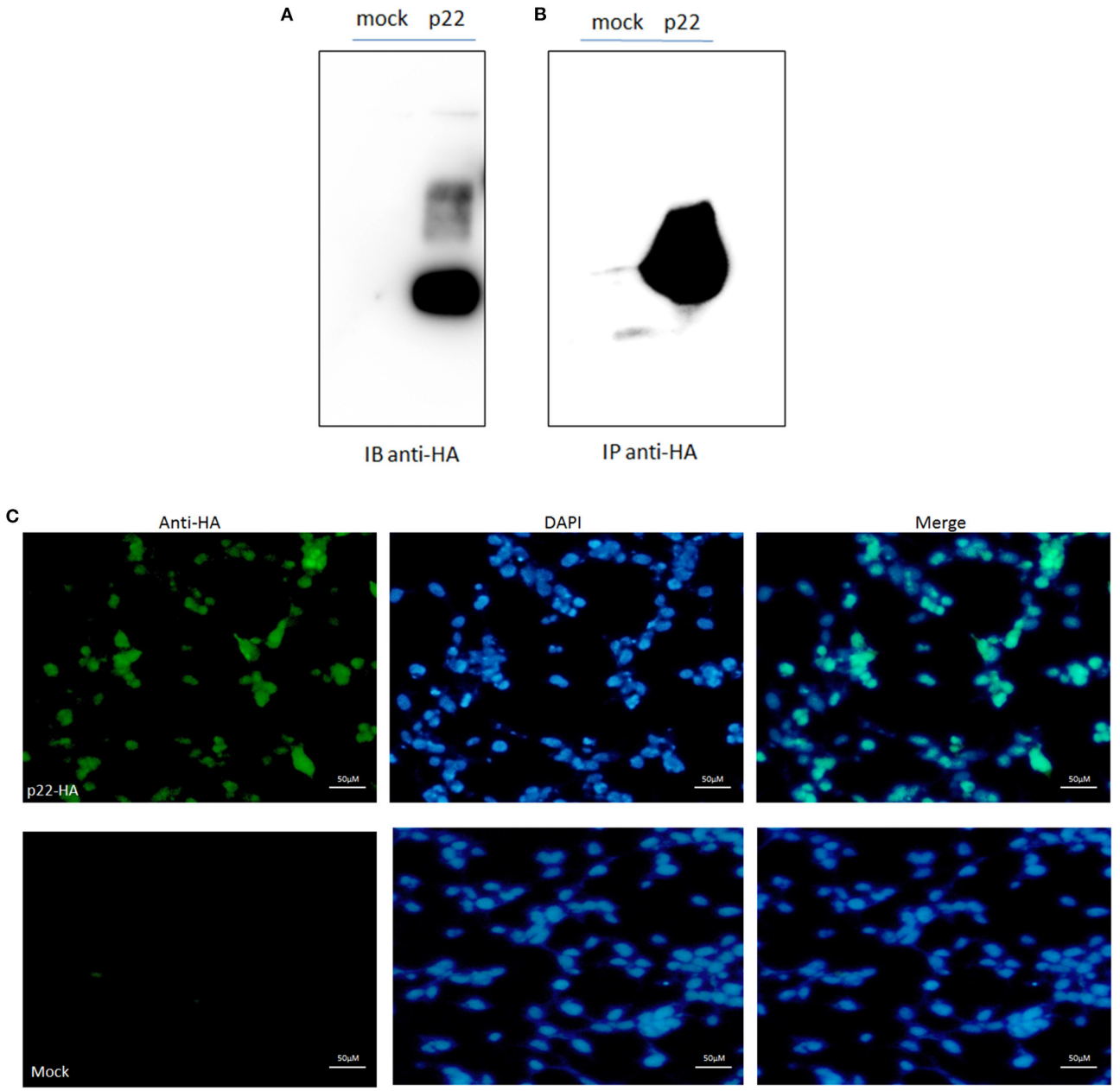

FIGURE 2 | p22 expression identification. **(A)** pcDNA3.1(+)-p22-HA and its mock were transfected into the 293-T cells and at 24 h post-transfection. Cells were lysed and subjected to Western blotting analysis. The band of p22 of ASFV was shown as the predicted size. **(B)** The p22 protein was immunoprecipitated with HA and identified by Western blotting analysis. **(C)** IFA identification. The green fluorescence represented the p22 protein, and the DAPI stain represented the nucleus.

Enriched GO Terms Analysis

In this study, to establish the host cell proteins or pathways that have been enriched in the p22 interacting partners' interaction networks, we performed gene ontology annotation and analysis of the target proteins in the p22 protein expressed 293-T cells to predict the biological function. There were 578 p22-interacted partners screened out compared with control samples in total (the data that repeated with mocked-interacted proteins were deleted to exclude the background contamination). From the GO map, thousands of enriched GO terms were obtained, and their corresponding proteins are shown in **Supplementary Tables 1, 3**. Go terms mainly covered three parts: biological process, molecular function and cellular component. A total of 359 proteins were related to the biological process (**Figure 3**). The top two enriched GO terms of the biological process were cellular process and metabolic process, followed by biological regulation, cellular component organization or biogenesis, etc. A total of 463 proteins were related to molecular function

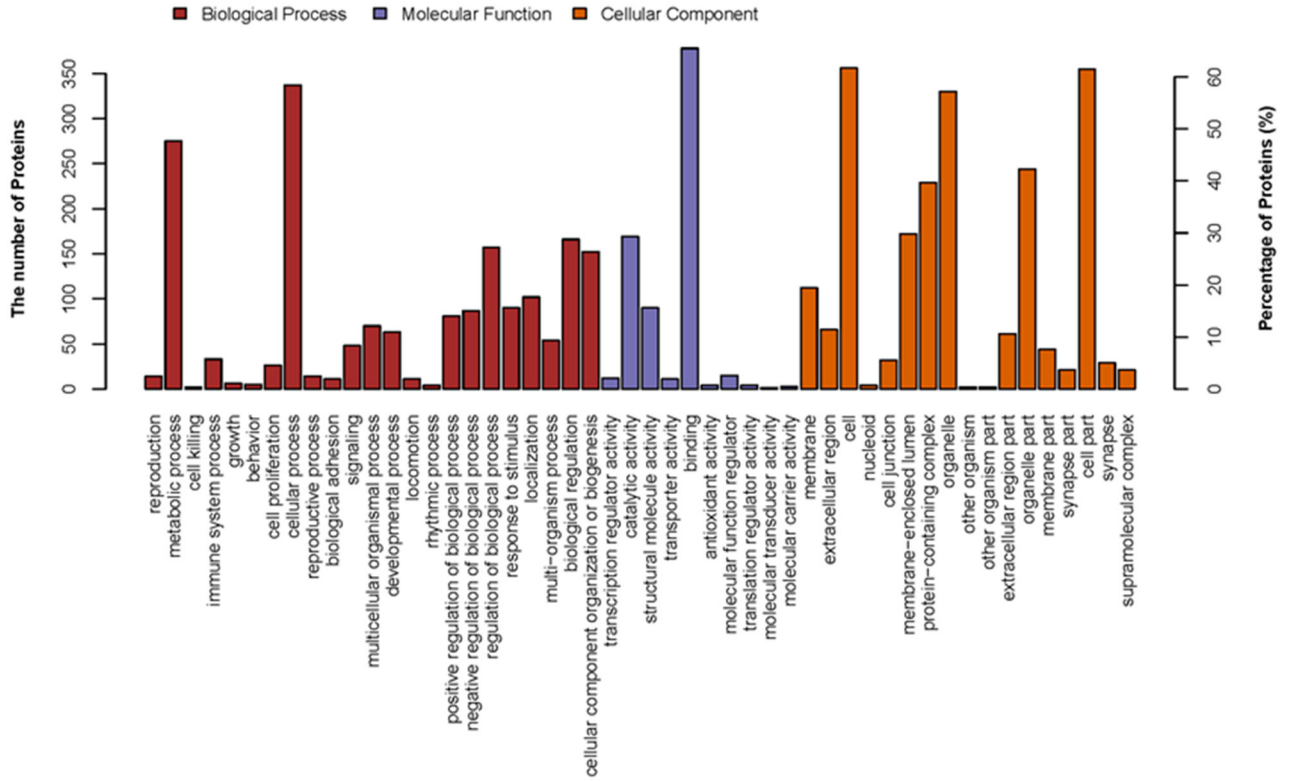

FIGURE 3 | Distribution of GO terms on three groups: biological process, molecular function, and cellular component. Up coordinate represents the number of the proteins; right vertical coordinates represent the percentage of proteins.

(**Figure 3**). Major enriched GO terms of molecular function were binding (as high as 378 proteins were included), catalytic activity, structural molecule activity, etc., indicating that p22 may play an important role in virus entry. For the cellular component, 374 proteins were involved. The GO terms analysis of the interacted proteins mainly included cell part, organelle, protein-containing complex, and membrane-enclose lumen membrane, indicating that p22 interacting partners may participate in cell structure maintenance. Collectively, the GO annotation and analysis of target proteins inferred that the p22 protein may participate in several processes such as protein binding, catalytic activity, and metabolism.

KEGG Pathways Analysis

To further predict the cellular pathways and signal transduction of p22-interacted host protein candidates, the KEGG and the top 20 enriched pathways with the highest representation of each term were enlisted (**Figure 4A**). A total of 165 KEGG pathways were screened out, and their corresponding protein numbers are shown in **Supplementary Tables 2**, **3**. According to the result, the KEGG pathways in which the p22-related proteins were involved were ribosomes (**Figure 4B**) and spliceosome (**Figure 4C**), wherein the involved protein numbers were as high as 31 and 23, respectively. Furthermore, enrichment analysis also indicated that the proteins might participate in pathogenic *Escherichia coli* infection, tight junction, necroptosis, ribosome biogenesis in eukaryotes, RNA transport, regulation of actin cytoskeleton, cardiac muscle contraction, adrenergic signaling in cardiomyocytes, etc. It is noteworthy that KEGG pathway analysis showed that seven related proteins participated in endocytosis (**Figure 4D**), and six proteins were involved in cyclic GMP-dependent protein kinase (cGMP-PKG) signaling pathway and focal adhesion. Minor proteins (four proteins) participated in the cAMP signaling pathway and AMP-activated protein kinase (AMPK) signaling pathway. The KEGG enrichment analysis suggested that pathways involved in immune response, regulation of necroptosis, ribosome biogenesis, and endocytosis were preferentially targeted.

PPI Network

The p22-interacted proteins were placed in the STRING database for PPI analysis and visualization in Cytoscape software. The selected proteins that interacted with p22 protein in the endocytosis process were connected as a network. The proteins included myosin-9 (MYH9), actin-related protein 2/3 complex subunit 2 (ARPC2), actin-related protein 2, actin-related protein 2/3 complex subunit 1B, ADP-ribosylation factor 6 (ARF6), beta-actin-like protein 2 (ACTBL2), alpha-actinin-4 (ACTN4), clathrin heavy chain A (CLTC), and Ras-related protein-10 (RAB10). The PPI network

contained eight nodes and 20 edges. All the hub proteins were at key positions in the interaction network. The nodes represented the interacted proteins, and the edges represented the interactions between these proteins. The selected proteins in the PPI network might relate to p22 more closely in the process of endocytosis. In addition to endocytosis, other PPI networks were also involved, including regulation of actin cytoskeleton, DNA replication, spliceosome, tRNA ligases, and mitochondria, implying that p22-interacted proteins functioned widely (**Figure 5**).

DISCUSSION

As the protein localized at the inner envelope of ASFV, the function of p22 is rarely known. In an attempt to acquire the p22 function, p22-interacted proteins of the host were identified by a high-throughput method and analyzed by GO terms and KEGG pathways; numerous cellular proteins in 293-T that interacted with p22 protein were identified. Although the facility to transfect 293-T cells made us select this cell type as the target cell, the interacted partners with p22 protein in the host cell derived from pig will be further investigated in the future. This study provides a large database and a useful tool to figure out the function of p22.

In this study, GO terms mainly covered three parts: biological process, molecular function, and cellular component. The top two enriched GO terms of the biological process were cellular process and metabolic process, implying that p22 might utilize the host proteins directly or indirectly to affect cell growth, function, and stability. Main enriched GO terms of molecular function were binding, catalytic activity. GO analysis revealed that the most significant ontology categories of molecular function of p22 interacting proteins is binding, suggesting a role of p22 as the protein at the inner envelop in virus binding and entry into the cell. The interesting result would inspire us to dig out the real function of p22 in virus entry.

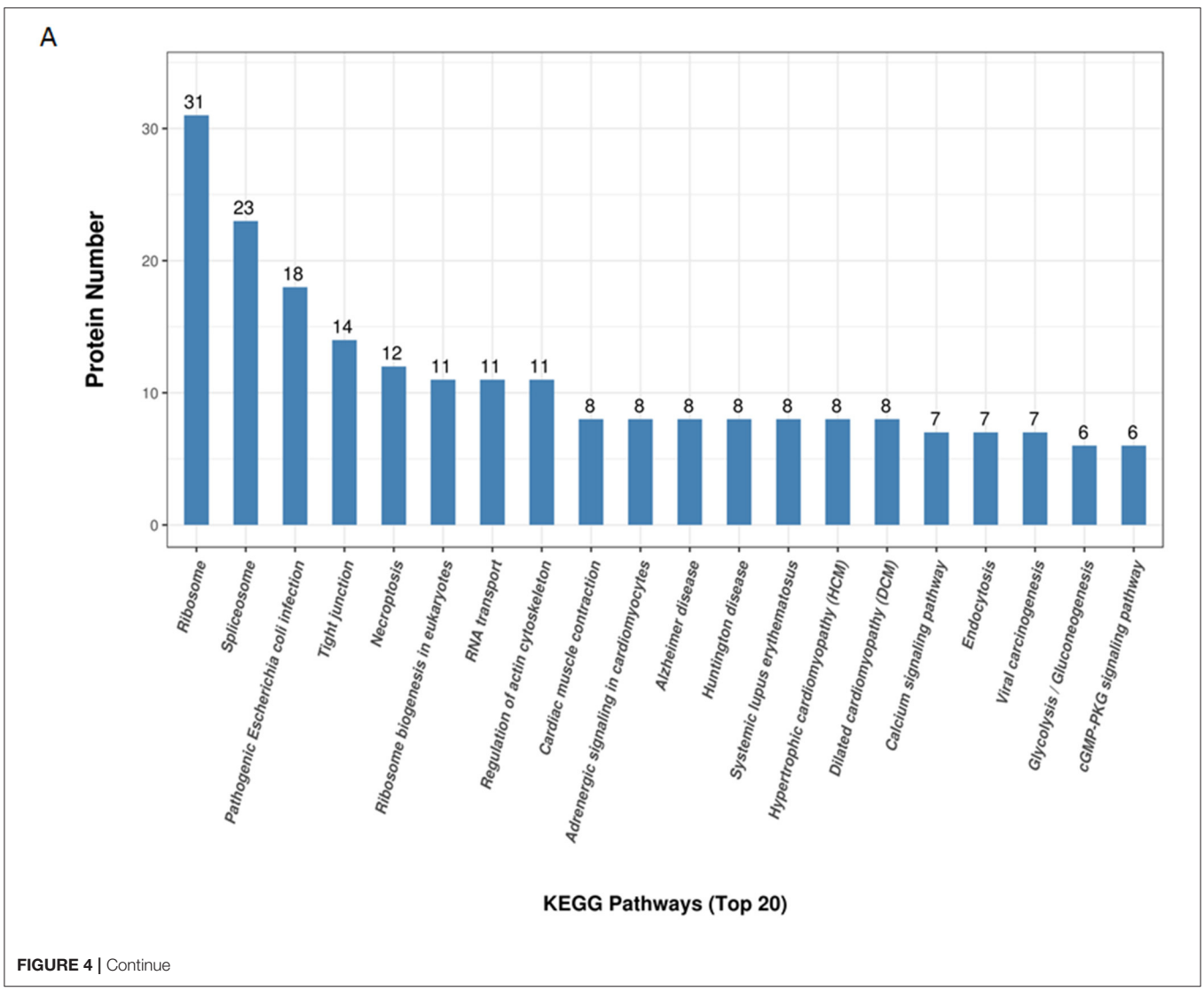

FIGURE 4 | Continue

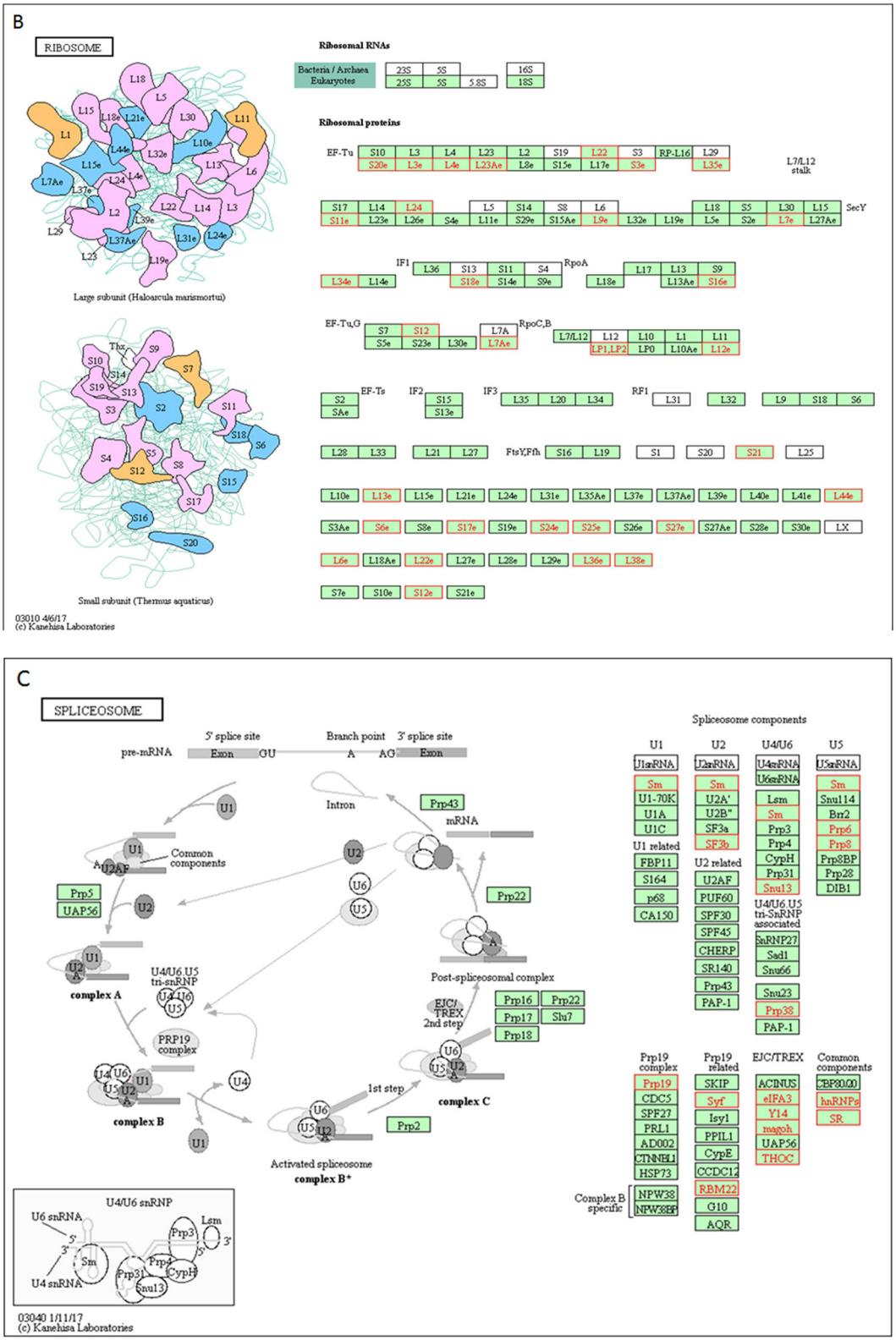

FIGURE 4 | Continue

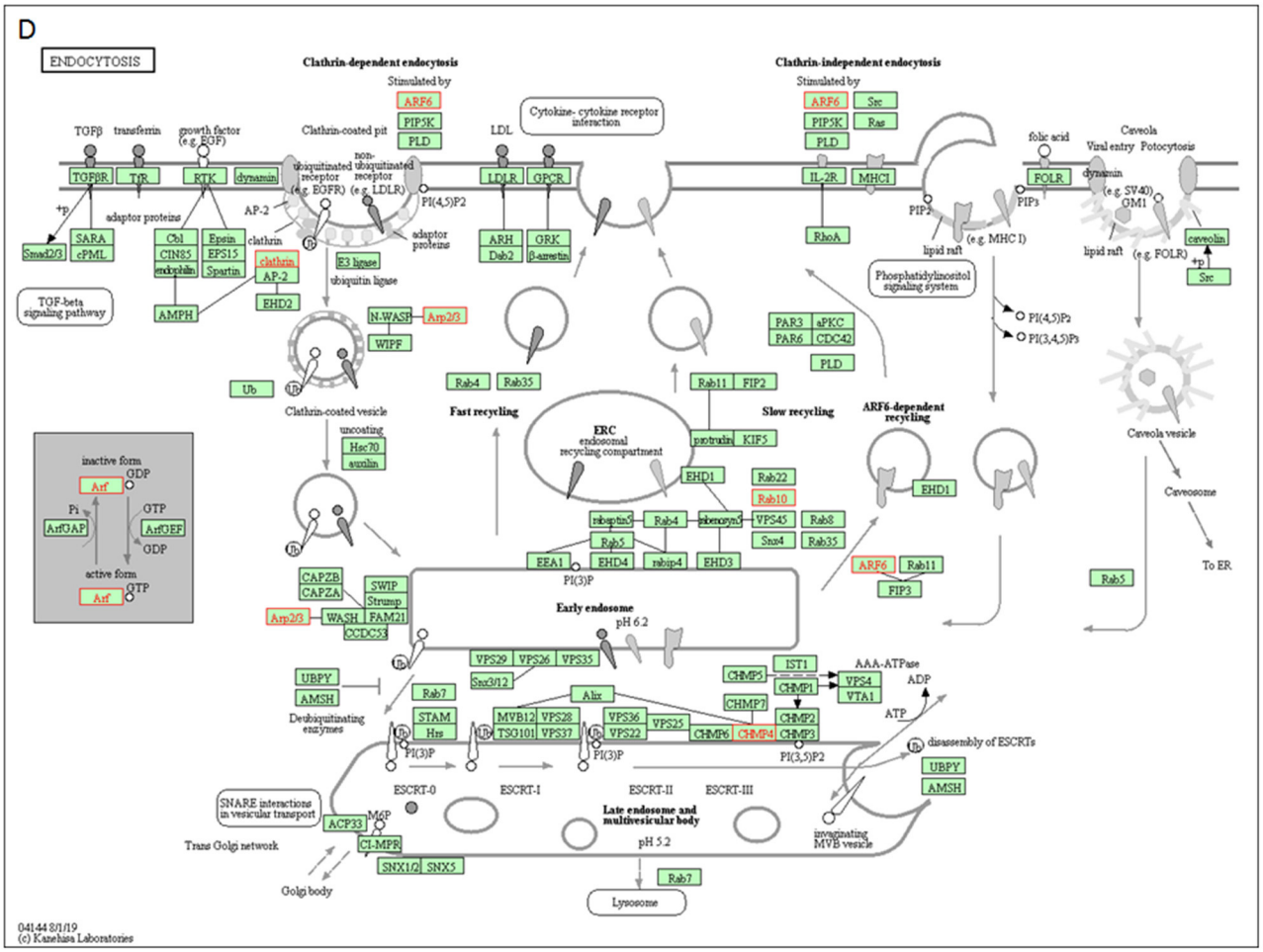

FIGURE 4 | KEGG pathways analysis of p22 interacting proteins. **(A)** Top 20 enriched KEGG pathway distribution. KEGG pathways that p22 interacting proteins were involved in mainly were **(B)** ribosomes, **(C)** splicesome, and **(D)** endocytosis. The p22-interacting proteins in the KEGG pathways were marked in red.

The GO term analysis of the p22 interacting proteins in the cell component mainly included cell part, organelle, protein-containing complex, membrane-enclose lumen, and membrane; the results further verified the conclusion that p22 located at the membrane of the viron might participate in virus structure maintenance and contact with the host membrane *via* the binding and endocytosis process. Of course the suspicion needs further to be proven.

For KEGG pathways analysis, a large number of KEGG pathways were screened out (as high as 165); the KEGG pathways that p22 interacting proteins participated in mainly were ribosomes and spliceosome. Ribosomes are essential nanomachines for protein production and protein synthesis. The initial steps of ribosome biogenesis take place in the cell compartment. Spliceosome executes eukaryotic precursor messenger RNA (pre-mRNA) splicing to remove non-coding introns. It depends on the interactions of RNA–RNA, RNA–protein, and protein–protein. It is composed of several nucleoproteins and has the function of recognizing 5′ splicing site, 3′ splicing site, and branching point of mRNA precursor. It indicated that p22 interacting proteins mainly participated in the process of gene expression in the host cells, gave us a hint that p22 affected the gene and protein expression of cell host, and directly or indirectly affected the function of the biological process.

Furthermore, it is interesting that p22 interacting proteins were involved in pathogenic *E. coli* infection, tight junction, necroptosis, ribosome biogenesis in eukaryotes, RNA transport, regulation of actin cytoskeleton, cardiac muscle contraction, adrenergic signaling in cardiomyocytes, etc. The widely affected pathways reflected the wide range functions of p22 or its related proteins.

It is noteworthy that KEGG pathway analysis showed that seven of p22 interacting proteins participated in endocytosis. The results of the GO analysis indicated that a large number of p22 interacting proteins participated in binding. Above all, p22 was predicted to be involved in the entry process at the envelop of the virus.

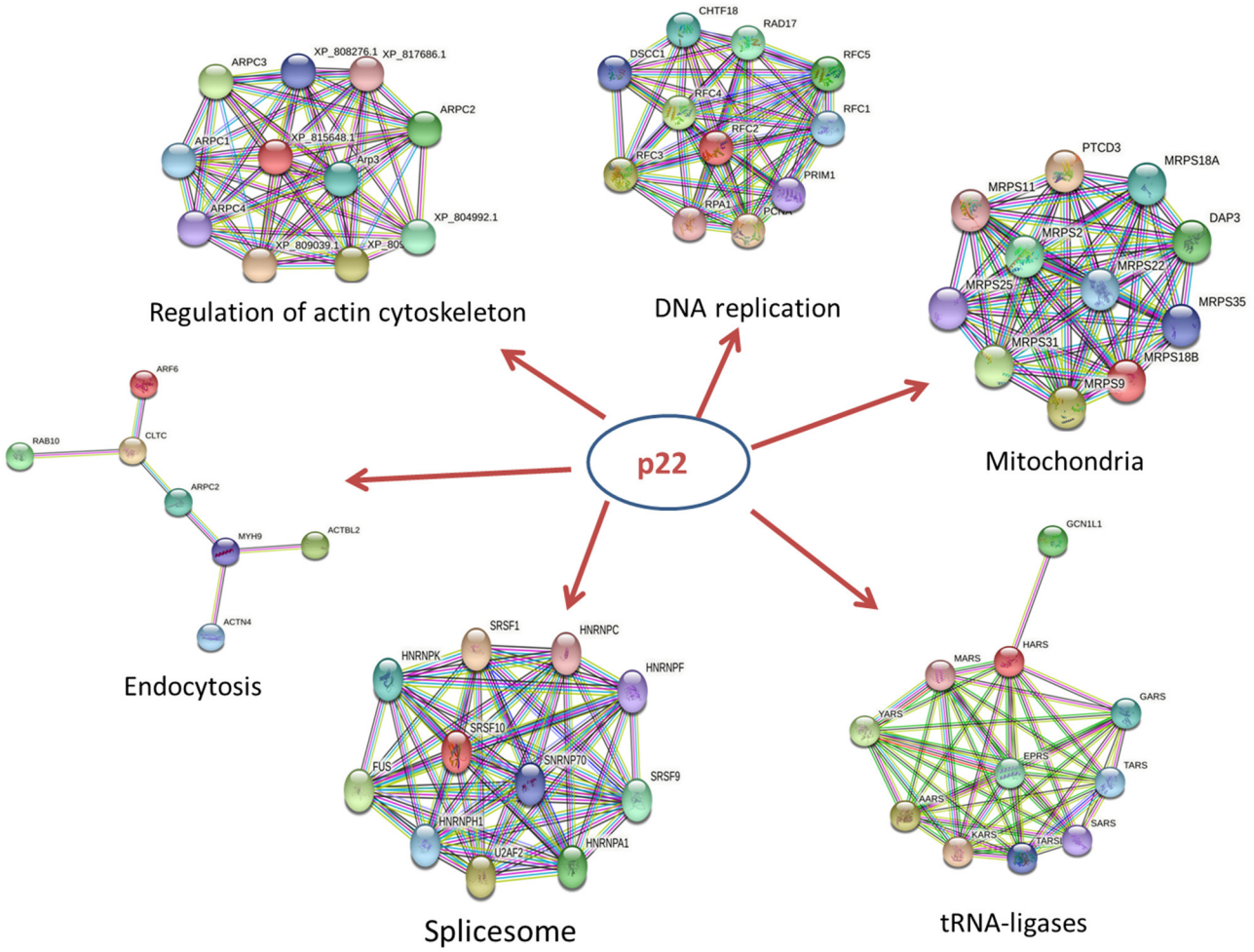

FIGURE 5 | PPI network of key proteins that interacted with p22 in the endocytosis process. The size of each node in the PPI networks presents the connect degree of each gene. Those nodes that were not connected to any node were omitted in the network. The selected proteins that interacted with the p22 protein in the endocytosis process were connected as a network. The network was generated in the STRING database.

At last, it was possible that other pathways had an important influence on the progression of ASFV entry *via* some biological process, such as cGMP-PKG signaling pathway, cAMP signaling pathway, and AMPK signaling pathway, which were screened out by KEGG analysis. cGMP is the intracellular second messenger that mediates the action of nitric oxide (NO) and natriuretic peptides (NPs), affecting a wide range of physiologic processes (22). cGMP/PKG signaling pathway was associated with the replication of some viruses (23, 24). cAMP is also one of the most common and universal second messengers; cAMP regulates pivotal physiologic processes including metabolism, secretion, calcium homeostasis, muscle contraction, cell fate, and gene transcription (25). AMPK is a central regulator of cellular energy homeostasis, regulating growth and reprogramming metabolism, as well as in cellular processes including autophagy and cell polarity (26). cAMP and AMPK are also closely connected with virus replication (27, 28). These involved pathways put forward the possibility that p22 and its interacting proteins might affect the replication of ASFV.

In those hub proteins connected in the PPI network, the ADP-ribosylation factor (Arf) protein family is part of the large Ras superfamily that encompasses small GTPases (29). Among this family, ARF6 stimulates actin polymerization, drives phagocytosis through multiple mechanisms, and assists autophagy as well (30). Other than Arf6, RAB10 also influences the GTPase activity (29), Rab10 is located on both Golgi and early endosomal/recycling compartments and plays an important role in lysosome exocytosis and plasma membrane repair (31). Alpha actinin belongs to the spectrin gene superfamily, which represents a diverse group of cytoskeletal proteins. Alpha actinin is an actin-binding protein. In non-muscle cells, it is involved in actin binding to the membrane. In skeletal, cardiac, and smooth muscle isoforms, it is localized to the Z-disc and analogous dense bodies and participates in anchoring the myofibrillar

actin filaments. ACTN4 encodes a non-muscle, alpha actinin isoform, which is concentrated in the cytoplasm and involved in metastatic processes (32). MYH9 is involved in several important functions, including cytokinesis, cell motility, and maintenance of cell shape (33). ARPC2, actin-related protein 2/3 complex subunit 2, contains seven subunits, of which Arp2 and Arp3 belong to actin-related proteins (34). The activation of Arp2/3 complex could promote the synthesis of F-actin in the suitable condition (35). The Arp2/3 complex is involved in the rearrangement of the macrophage cytoskeleton and affected the phagocytosis of macrophages (36). Knockout of the Arp2/3 complex APC2 gene in mouse macrophages results in a decrease in F-actin polymerization and subsequent reduction in phagocytic capacity (37). In summary, the key proteins mentioned above and other hub proteins in PPI network were closely related to actin filament organization and movement, resulting in affecting the process of phagocytosis and endocytosis. Additional studies on the role of p22 in the process of endocytosis should be conducted. In addition to endocytosis, other PPI networks including regulation of actin cytoskeleton, DNA replication, spliceosome, tRNA ligases, and mitochondria were screened out, indicating that p22 interacting proteins functioned widely and participated in several biological processes.

CONCLUSIONS

Although several studies have been reported to elucidate the pathogenesis of ASFV, the viral protein function remains unclear. In this research, the proteins in the host cells interacted with p22, and the signaling pathways they might participate in were screened out by a high-throughput method, laying the foundation to elucidate the function of p22. For the pig industry, it would also be advantageous to study the pathogenesis of the disease and to monitor and predict the outcome to control the disease in the near future.

DATA AVAILABILITY STATEMENT

The original contributions presented in the study are included in the article/**Supplementary Material**, further inquiries can be directed to the corresponding author/s.

AUTHOR CONTRIBUTIONS

BF: conceptualization. BF and JZ: methodology and resources. DW: investigation. XZ: writing and original draft. XZ and BL: writing. BL and HF: funding acquisition and supervision. All authors contributed to the article and approved the submitted version.

FUNDING

This work was supported by the Natural Science Foundation of China (31941013).

ACKNOWLEDGMENTS

We thank the other members of the Institute of Veterinary Medicine, Jiangsu Academy of Agricultural Sciences, Key Laboratory of Veterinary Biological Engineering and Technology, and College of Veterinary Medicine, South China Agricultural University, without whom this work could not have been conducted.

SUPPLEMENTARY MATERIAL

The Supplementary Material for this article can be found online at: https://www.frontiersin.org/articles/10.3389/fvets.2021.719859/full#supplementary-material

Supplementary Table 1 | GO terms and corresponding proteins.

Supplementary Table 2 | KEGG pathways and corresponding proteins.

Supplementary Table 3 | Proteins accession numbers and description.

REFERENCES

1. Chapman DA, Darby AC, Da Silva M, Upton C, Radford AD, Dixon LK. Genomic analysis of highly virulent Georgia 2007/1 isolate of African swine fever virus. *Emerg Infect Dis*. (2011) 17:599–605. doi: 10.3201/eid1704.101283
2. Costard S, Mur L, Lubroth J, Sanchez-Vizcaino JM, Pfeiffer DU. Epidemiology of African swine fever virus. *Virus Res*. (2013) 173:191–7. doi: 10.1016/j.virusres.2012.10.030
3. Howey EB, O'Donnell V, de Carvalho Ferreira HC, Borca MV, Arzt J. Pathogenesis of highly virulent African swine fever virus in domestic pigs exposed via intraoropharyngeal, intranasopharyngeal, and intramuscular inoculation, and by direct contact with infected pigs. *Virus Res*. (2013) 178:328–39. doi: 10.1016/j.virusres.2013.09.024
4. Blome S, Gabriel C, Beer M. Pathogenesis of African swine fever in domestic pigs and European wild boar. *Virus Res*. (2013) 173:122–30. doi: 10.1016/j.virusres.2012.10.026
5. Galindo-Cardiel I, Ballester M, Solanes D, Nofrarias M, Lopez-Soria S, Argilaguet JM, et al. Standardization of pathological investigations in the framework of experimental ASFV infections. *Virus Res*. (2013) 173:180–90. doi: 10.1016/j.virusres.2012.12.018
6. Zhao D, Liu R, Zhang X, Li F, Wang J, Zhang J, et al. Replication and virulence in pigs of the first African swine fever virus isolated in China. *Emerg Microbes Infect*. (2019) 8:438–47. doi: 10.1080/22221751.2019.1590128
7. Dixon LK, Chapman DA, Netherton CL, Upton C. African swine fever virus replication and genomics. *Virus Res*. (2013) 173:3–14. doi: 10.1016/j.virusres.2012.10.020
8. Yanez RJ, Rodriguez JM, Nogal ML, Yuste L, Enriquez C, Rodriguez JF, et al. Analysis of the complete nucleotide sequence of African swine fever virus. *Virology*. (1995) 208:249–78. doi: 10.1006/viro.1995.1149
9. Camacho A, Vinuela E. Protein p22 of African swine fever virus: an early structural protein that is incorporated into the membrane of infected cells. *Virology*. (1991) 181:251–7. doi: 10.1016/0042-6822(91)90490-3
10. Lithgow P, Takamatsu H, Werling D, Dixon L, Chapman D. Correlation of cell surface marker expression with African swine fever virus infection. *Vet Microbiol*. (2014) 168:413–9. doi: 10.1016/j.vetmic.2013.12.001
11. Goatley LC, Dixon LK. Processing and localization of the african swine fever virus CD2v transmembrane protein. *J Virol*. (2011) 85:3294–305. doi: 10.1128/JVI.01994-10

12. Alejo A, Matamoros T, Guerra M, Andres G. A proteomic atlas of the African swine fever virus particle. *J Virol*. (2018) 92:e01293–18. doi: 10.1128/JVI.01293-18
13. Salas ML, Andres G. African swine fever virus morphogenesis. *Virus Res*. (2013) 173:29–41. doi: 10.1016/j.virusres.2012.09.016
14. Brookes SM, Sun H, Dixon LK, Parkhouse RM. Characterization of African swine fever virion proteins j5R and j13L: immuno-localization in virus particles and assembly sites. *J Gen Virol*. (1998) 79:1179–88. doi: 10.1099/0022-1317-79-5-1179
15. Suarez C, Gutierrez-Berzal J, Andres G, Salas ML, Rodriguez JM. African swine fever virus protein p17 is essential for the progression of viral membrane precursors toward icosahedral intermediates. *J Virol*. (2010) 84:7484–99. doi: 10.1128/JVI.00600-10
16. Rodriguez I, Nogal ML, Redrejo-Rodriguez M, Bustos MJ, Salas ML. The African swine fever virus virion membrane protein pE248R is required for virus infectivity and an early postentry event. *J Virol*. (2009) 83:12290–300. doi: 10.1128/JVI.01333-09
17. Hernaez B, Guerra M, Salas ML, Andres G. African swine fever virus undergoes outer envelope disruption, capsid disassembly and inner envelope fusion before core release from multivesicular endosomes. *PLoS Pathog*. (2016) 12:e1005595. doi: 10.1371/journal.ppat.1005595
18. Vuono EA, Ramirez-Medina E, Pruitt S, Rai A, Espinoza N, Velazquez-Salinas L, et al. Evaluation of the function of the ASFV KP177R gene, encoding for structural protein p22, in the process of virus replication and in swine virulence. *Viruses*. (2021) 13:986. doi: 10.3390/v13060986
19. Gene Ontology Consortium. Gene Ontology Consortium: going forward. *Nucleic Acids Res*. (2015) 43:D1049–1056. doi: 10.1093/nar/gku1179
20. Kanehisa M, Goto S. KEGG: kyoto encyclopedia of genes and genomes. *Nucleic Acids Res*. (2000) 28:27–30. doi: 10.1093/nar/28.1.27
21. Safari-Alighiarloo N, Taghizadeh M, Rezaei-Tavirani M, Goliaei B, Peyvandi AA. Protein-protein interaction networks (PPI) and complex diseases. *Gastroenterol Hepatol Bed Bench*. (2014) 7:17–31.
22. Qin L, Zang M, Xu Y, Zhao R, Wang Y, Mi Y, et al. Chlorogenic acid alleviates hyperglycemia-induced cardiac fibrosis through activation of the NO/cGMP/PKG pathway in cardiac fibroblasts. *Mol Nutr Food Res*. (2020) 65:e2000810. doi: 10.1002/mnfr.202000810
23. Zhang A, Zhao L, Li N, Duan H, Liu H, Pu F, et al. Carbon monoxide inhibits porcine reproductive and respiratory syndrome virus replication by the cyclic GMP/protein kinase G and NF-kappaB signaling pathway. *J Virol*. (2017) 91:e01866–16. doi: 10.1128/JVI.01866-16
24. Li C, Li L, Jin L, Yuan J. Heme Oxygenase-1 inhibits spring viremia of carp virus replication through carbon monoxide mediated cyclic GMP/Protein kinase G signaling pathway. *Fish Shellfish Immunol*. (2018) 79:65–72. doi: 10.1016/j.fsi.2018.05.014
25. Johnstone TB, Agarwal SR, Harvey RD, Ostrom RS. cAMP signaling compartmentation: adenylyl cyclases as anchors of dynamic signaling complexes. *Mol Pharmacol*. (2018) 93:270–6. doi: 10.1124/mol.117.110825
26. Li B, Li P, Weng R, Wu Z, Qin B, Fang J, et al. Trehalose protects motorneuron after brachial plexus root avulsion by activating autophagy and inhibiting apoptosis mediated by the AMPK signaling pathway. *Gene*. (2020) 768:145307. doi: 10.1016/j.gene.2020.145307
27. Evripioti AA, Ortega-Prieto AM, Skelton JK, Bazot Q, Dorner M. Phosphodiesterase-induced cAMP degradation restricts hepatitis B virus infection. philosophical transactions of the royal society of London. *Series B, Biol sci*. (2019) 374:20180292. doi: 10.1098/rstb.2018.0292
28. Meng Z, Liu Q, Sun F, Qiao L. Hepatitis C virus nonstructural protein 5A perturbs lipid metabolism by modulating AMPK/SREBP-1c signaling. *Lipids Health Dis*. (2019) 18:191. doi: 10.1186/s12944-019-1136-y
29. Wennerberg K, Rossman KL, Der CJ. The Ras superfamily at a glance. *J Cell Sci*. (2005) 118:843–6. doi: 10.1242/jcs.01660
30. Van Acker T, Tavernier J, Peelman F. The small GTPase Arf6: an overview of its mechanisms of action and of its role in host(-)pathogen interactions and innate immunity. *Int J Mol Sci*. (2019) 20:2209. doi: 10.3390/ijms20092209
31. Vieira OV. Rab3a and Rab10 are regulators of lysosome exocytosis and plasma membrane repair. *Small GTPases*. (2018) 9:349–351. doi: 10.1080/21541248.2016.1235004
32. Tentler D, Lomert E, Novitskaya K, Barlev NA. Role of ACTN4 in tumorigenesis, metastasis, and EMT. *Cells*. (2019) 8:1427. doi: 10.3390/cells8111427
33. Pecci A, Ma X, Savoia A, Adelstein RS. MYH9: structure, functions and role of non-muscle myosin IIA in human disease. *Gene*. (2018) 664:152–67. doi: 10.1016/j.gene.2018.04.048
34. Rotty JD, Wu C, Bear JE. New insights into the regulation and cellular functions of the ARP2/3 complex. *Nat Rev Mol Cell Biol*. (2013) 14:7–12. doi: 10.1038/nrm3492
35. Goley ED, Rodenbusch SE, Martin AC, Welch MD. Critical conformational changes in the Arp2/3 complex are induced by nucleotide and nucleation promoting factor. *Mol cell*. (2004) 16:269–79. doi: 10.1016/j.molcel.2004.09.018
36. May RC, Caron E, Hall A, Machesky LM. Involvement of the Arp2/3 complex in phagocytosis mediated by FcgammaR or CR3. *Nat Cell Biol*. (2000) 2:246–248. doi: 10.1038/35008673
37. Rotty JD, Brighton HE, Craig SL, Asokan SB, Cheng N, Ting JP, et al. Arp2/3 complex is required for macrophage integrin functions but is dispensable for FcR phagocytosis and *in vivo* motility. *Dev Cell*. (2017) 42:498–513 e496. doi: 10.1016/j.devcel.2017.08.003

Conflict of Interest: The authors declare that the research was conducted in the absence of any commercial or financial relationships that could be construed as a potential conflict of interest.

Publisher's Note: All claims expressed in this article are solely those of the authors and do not necessarily represent those of their affiliated organizations, or those of the publisher, the editors and the reviewers. Any product that may be evaluated in this article, or claim that may be made by its manufacturer, is not guaranteed or endorsed by the publisher.

frontiers in Veterinary Science

ORIGINAL RESEARCH
published: 12 October 2021
doi: 10.3389/fvets.2021.707368

Presence of Antibodies to SARS-CoV-2 in Domestic Cats in Istanbul, Turkey, Before and After COVID-19 Pandemic

*Aysun Yilmaz[1], Abdullah Kayar[2], Nuri Turan[1], Onur Iskefli[2], Alper Bayrakal[2], Gleyder Roman-Sosa[3], Erman Or[2], Hasan Emre Tali[1], Bekir Kocazeybek[4], Ridvan Karaali[5], Dashzeveg Bold[3], Jean-Remy Sadeyen[6], Deimante Lukosaityte[6], Pengxiang Chang[6], Munir Iqbal[6], Juergen A. Richt[3] and Huseyin Yilmaz[1]**

[1] Department of Virology, Veterinary Faculty, Istanbul University-Cerrahpasa, Istanbul, Turkey, [2] Department of Internal Medicine, Veterinary Faculty, Istanbul University-Cerrahpasa, Istanbul, Turkey, [3] Department of Diagnostic Medicine and Pathobiology, College of Veterinary Medicine, Kansas State University, Manhattan, KS, United States, [4] Department of Medical Microbiology, Cerrahpasa Faculty of Medicine, Istanbul University-Cerrahpasa, Istanbul, Turkey, [5] Department of Infectious Diseases and Clinical Microbiology, Cerrahpasa Faculty of Medicine, Istanbul University-Cerrahpasa, Istanbul, Turkey, [6] Avian Influenza Group, The Pirbright Institute, Woking, United Kingdom

OPEN ACCESS

Edited by:
Yashpal S. Malik,
Indian Veterinary Research Institute (IVRI), India

Reviewed by:
Mortola Carlos Mortola,
Universidad Nacional de La Plata, Argentina
Anna Costagliola,
University of Naples Federico II, Italy

***Correspondence:**
Huseyin Yilmaz
hyilmaz@iuc.edu.tr

Specialty section:
This article was submitted to Veterinary Epidemiology and Economics, a section of the journal Frontiers in Veterinary Science

Received: 10 May 2021
Accepted: 02 September 2021
Published: 12 October 2021

Citation:
Yilmaz A, Kayar A, Turan N, Iskefli O, Bayrakal A, Roman-Sosa G, Or E, Tali HE, Kocazeybek B, Karaali R, Bold D, Sadeyen J-R, Lukosaityte D, Chang P, Iqbal M, Richt JA and Yilmaz H (2021) Presence of Antibodies to SARS-CoV-2 in Domestic Cats in Istanbul, Turkey, Before and After COVID-19 Pandemic. Front. Vet. Sci. 8:707368. doi: 10.3389/fvets.2021.707368

Recent studies demonstrated that domestic cats can be naturally and experimentally infected with severe acute respiratory syndrome coronavirus-2 (SARS-CoV-2). This study was performed to investigate the presence of SARS-CoV-2-specific antibodies within the domestic cat population in Istanbul, Turkey, before the coronavirus disease 2019 (COVID-19) and during the COVID-19 pandemic. Overall, from 155 cat sera analyzed, 26.45% (41/155) tested positive in the spike protein-ELISA (S-ELISA), 28.38% (44/155) in the receptor-binding domain-ELISA (RBD-ELISA), and 21.9% (34/155) in both, the S- and RBD-ELISAs. Twenty-seven of those were also positive for the presence of antibodies to feline coronavirus (FCoV). Among the 34 SARS-CoV-2-positive sera, three of those were positive on serum neutralization assay. Six of the 30 cats before COVID-19 and 28 of the 125 cats during COVID-19 were found to be seropositive. About 20% of ELISA-positive cats exhibited mainly respiratory, gastrointestinal, and renal signs and skin lesions. Hematocrit, hemoglobin, white blood cells, lymphocyte, and platelet numbers were low in about 30% of ELISA-positive cats. The number of neutrophils and monocytes were above normal values in about 20% of ELISA-positive cats. The liver enzyme alanine aminotransferase levels were high in 23.5% ELISA-positive cats. In conclusion, this is the first report describing antibodies specific to SARS-CoV-2 antigens (S and RBD) in cats in Istanbul, Turkey, indicating the risk for domestic cats to contract SARS-CoV-2 from owners and/or household members with COVID-19. This study and others show that COVID-19-positive pet owners should limit their contact with companion animals and that pets with respiratory signs should be monitored for SARS-CoV-2 infections.

Keywords: SARS-CoV-2, spike, RBD, ELISA, cat, Turkey

INTRODUCTION

High numbers of severe respiratory infections in humans were first reported in December 2019 in Wuhan, China; the etiological agent was later characterized as severe acute respiratory syndrome coronavirus 2 (SARS-CoV-2) as an enveloped single-stranded RNA virus classified as betacoronavirus in the *Coronaviridae* family, and the disease was designated coronavirus disease 2019 (COVID-19) by the World Health Organization (WHO) (1–3). The virus spread rapidly worldwide and became a pandemic disease that has been causing very serious threats to public health and economies globally (4–6).

SARS-CoV-2 is a zoonotic agent and was most likely transmitted from bats to humans; however, it is not well-understood which animals are susceptible to and can spread COVID-19. Susceptible animals may not only serve as a reservoir for disease posing a risk to humans but also drive further virus changes (1, 7). It has been demonstrated that SARS-CoV-2 uses the angiotensin-converting enzyme 2 (ACE2) as its cellular receptor (1). The ACE2 of a cat shares a high amino acid sequence identity (85.2%) with human ACE2 (7). Feline ACE2 differs at only four out of a total of 20 residues compared with the human ACE2 conforming receptor binding pocket. However, these residues are the key determinants for virus-host range differentiating the susceptibility of a species to SARS-CoV-2 and can affect the efficiency of receptor-binding domain (RBD) binding to ACE2 (8).

Considering the host receptor-virus relationship, the presence of SARS-CoV-2 antigen or antibodies against the virus has been reported in a considerable number of animals including but not limited to cats, dogs, minks, tigers, and lions (8–12). Among these, cats received great attention because of close contact with humans. Recent studies of SARS-CoV-2 infections in cats demonstrated that cats can be naturally and experimentally infected with SARS-CoV-2 (9, 11–14). Cats can be infected by two different coronaviruses including types I and II coronaviruses responsible for feline infectious peritonitis (7, 15, 16) or SARS-CoV-2 (8). SARS-CoV-2 is genetically distinct from the feline coronaviruses which are classified to belong to the alphacoronavirus genus (2). In addition, clinical, virological, pathological, and tomography findings of these infections are different from each other (16).

The first suspected case of a cat with SARS-CoV-2 was reported in Hong Kong by the Hong Kong Agriculture, Fisheries and Conservation Department (AFCD) (17). Another case of SARS-CoV-2 in cats was reported in Belgium in March 2020 (18) and later in other countries like the USA (19), France (20, 21), Germany (13), Italy (22), and Spain (23, 24). Infected animals can become sick, but the clinical disease seems to be mild and self-limited (18, 25). This was confirmed by experimental infections, indicating that SARS-CoV-2 causes mild respiratory signs in some instances (11); however, most cases remain asymptomatic (26). Importantly, infected cats were demonstrated to be capable of transmitting SARS-CoV-2 to other cats in the experimental environment (12).

Cats are very important companion animals living in close proximity to humans, and ∼50% of people keep companion animals in Europe and the USA and in some localities in Turkey (27) (Turkish Veterinary Association, personal communication). Therefore, it is important to determine whether domestic cats pose a potential risk to people. Generally, ELISA, virus neutralization, and Western blot tests are used to investigate the serological response of cats to SARS-CoV-2. We investigated the presence of SARS-CoV-2-specific antibodies within the cat population in Istanbul, Turkey. For this purpose, *in-house* indirect ELISA tests were established using the recombinant spike (S) and RBD proteins of SARS-CoV-2. Then, the sera collected from domestic cats were subjected to the in-house ELISA tests in order to determine the presence of antibodies specific for S and RBD proteins of SARS-CoV-2.

MATERIALS AND METHODS

Study Population, Clinical Examination, and Sampling

This study was performed on cats admitted to the Veterinary Faculty of Istanbul University-Cerrahpasa, Turkey, for clinical examination. All cats were household cats with no access to the street. The study population consisted of two groups of cats, one group named "before COVID-19" and the second group "during COVID-19." Samples from the before COVID-19 group were collected between January 2018 and January 2019. The samples from the during COVID-19 group were collected after December 2019, the first reported SARS-CoV-2 human infection case in China.

The before COVID-19 group consisted of a total of 30 cats, and the during COVID-19 group consisted of 125 cats, between 2 months and 15 years of age. All cats were clinically examined and the gender, breed, and age of the animal were recorded. On clinical examination, presence of fever, depression, and clinical signs related to organ system dysfunction were recorded: respiratory (cough, wheezing, dyspnea, and abnormal lung sounds); gastrointestinal (mouth lesions, anorexia, vomitus, diarrhea, weight loss, abdominal distension, and/or ascites); circulatory (lymphadenopathy, anemia, icterus); urinary (cystitis, renal insufficiency, urinary infections); ocular lesions (conjunctivitis, keratic precipitates, uveitis, hyphema, iridocyclitis, chorioretinitis); skin lesions; and central nervous system (epileptic seizures, ataxia) symptoms. Sera from all cats were collected by venipuncture.

Development of ELISA for Detection of Antibodies to S and RBD Proteins of SARS-CoV-*2*

The SARS-CoV-2 S and RBD proteins were initially produced and characterized in Professor Munir Iqbal's laboratory (The Pirbright Institute, UK) and in Professor Juergen Richt's laboratory (Kansas State University, Manhattan, KS, USA). Adopting methods established by the two labs, we produced both proteins in our laboratory.

Two methods were used to produce SARS-CoV-2 S and RBD proteins as described below:

Method 1: This method was used to produce SARS-CoV-2 S protein, as described previously (28, 29). Briefly, the expression cassettes containing SARS-CoV-2 S nucleotide sequences of BetaCov/Wuhan/WH04/2020 (accession number EPI-ISL-406801) were retrieved from the Global Initiative on Sharing All Influenza Data (GISAID) database. Nucleotide sequences were codon optimized for expression in *Drosophila melanogaster* Schneider 2 (S2) cells. The N-terminus signal sequence of S protein was replaced with Drosophila immunoglobulin heavy chain binding protein (BiP) signal sequence, and the C-terminus were fused with T4 foldon sequence (GSGYIPEAPRDGQAYVRKDGEWVLLSTFL) and a C-tag sequence (EPEA) for affinity purification. The protein expression cassettes were commercially synthesized (GeneArt, ThermoFisher Scientific, Regensburg, Germany) and cloned into pExpres2.1 expression vector (ExpreS2ion Biotechnologies, Hørsholm, Denmark). The recombinant plasmids were transfected into *Drosophila* S2 cells using Calcium Phosphate Transfection Kit (Thermo Fisher Scientific, Paisley, Scotland, UK). Following antibiotic selection with Zeocin (InvivoGen, Toulouse, France), cells were propagated in *Drosophila* EX-CELL® 420 Serum-Free Medium (Merck Life Science) at 25°C. Recombinant S trimeric protein secreted in cell culture supernatants was purified using the CaptureSelect™ C-tag Affinity Matrix (Thermo Fisher Scientific) and eluted protein dialyzed into PBS overnight. The concentration of purified recombinant S protein was determined by Pierce™ BCA Protein Assay Kit (Thermo Fisher Scientific), and the purity was assessed by sodium dodecyl sulphate-polyacrylamide gel electrophoresis (SDS-PAGE).

Method 2: This method was used to produce RBD region of the S protein in mammalian cells (human embryonic kidney 293 cells-HEK 293) in Professor Juergen Richt's laboratory (Kansas State University, Manhattan, KS). Briefly, the nucleotide sequence encoding the RBD spike protein of the SARS-CoV-2 isolate Wuhan-Hu-1 (GenBank accession: MT380725.1) plus two strep tags on the 3′ end was used and cloned into the mammalian expression vector pHL (Addgene, Cambridge, MA, USA). The RBD recombinant protein was produced in HEK 293 cells by transfections of these cells with purified DNA using QIAGEN Plasmid Midi Kit (Qiagen, Germantown, MD, USA). Transfected HEK 293 cells were cultured in DMEM (Fisher Scientific, Chicago, IL, USA). Supernatants from transfected cells were harvested on day 3 posttransfection and supernatant samples were centrifuged at 4,000×*g* for 20 min. Recombinant proteins with strep-tags were purified *via* affinity chromatography using Strep-Tactin® (IBA Lifesciences, Göttingen, Germany) under native conditions using StrepTacting Superflow Agarose (Millipore Sigma, MA, USA) and expression of the recombinant protein was confirmed by Western blotting.

Standardization of ELISA for Estimation of S and RBD Antibody Levels in Serum Samples Collected From Cats

In house, ELISA methods were standardized to analyze the sera of cats for the presence of antibodies to SARS-CoV-2 by using the purified recombinant S and RBD proteins of SARS-CoV-2 as the target antigen. Indirect ELISA protocols were standardized using checkerboard titration protocol, as described previously (30). For this, two-fold dilutions of the S and RBD proteins were prepared at a range of 250–4,000 ng/ml in PBS (Sigma) on 96-well ELISA plates (MaxiSorb flat bottom). The negative control sera were from the cats taken before the COVID-19 epidemic having low OD values and also being negative for the FCoV antibodies and in-house FCoV PCR. *Human sera which tested positive or negative for SARS-CoV-2 antibodies by a commercial ELISA (Roche, Basel, Switzerland) and human swab samples were positive for SARS-CoV-2 RNA by a real-time RT-PCR* (IDEXX, Westbrook, ME, USA) were included in the standardization of ELISA.

The SARS-CoV-2-positive and SARS-CoV-2-negative human sera were diluted two-fold (from 1:50 to 1:1,600), and HRP-conjugated goat anticat antibody (Santa Cruz, Santa Cruz, CA, USA) for cat IgG and HRP-conjugated goat antihuman IgG for human sera (Santa Cruz, sc2428) was diluted 1:3,000 in PBS-Tween plus 1% (w/v) skimmed milk powder (BioShop Canada, Burlington, ON, Canada). The results of the standardization of the ELISA revealed that the optimal amount of the recombinant S and RBD proteins to use in ELISA ranged from 1 μg to 2 μg/ml in 50 μl buffer, whereas the optimal dilution of SARS-CoV-2-positive cat and human serum ranged from 1:200 to 1:800, and the antispecies secondary antibodies were diluted to 1:3,000 (as per supplier instruction).

The cutoff value was calculated by using the (receiver operating characteristic (ROC) curve analysis to determine the OD value range of positive samples. The ELISA cutoff value was determined by the addition of three standard deviations to the mean OD value of the negative control sera in each plate. OD values above the cutoff value were taken as positive. The cutoff value was recalculated with a ROC curve analysis by using a MedCalc program (31). Thus, a cutoff OD value of 0.692 (sensitivity: 78.57%; specificity: 93.81%) was determined for the in-house indirect S-ELISA and an OD value of 0.493 (sensitivity: 100%; specificity: 98.23%) for the RBD-ELISA.

Analysis of Cat Sera for Antibodies to SARS-CoV-2

After standardization of the ELISA, the two groups of cat sera before COVID-19 and during COVID-19 were analyzed for the presence of antibodies to SARS-CoV-2. For this, a 96-well plate (Nunc MaxiSorb, Thermo Fisher Scientific) was coated overnight at 4°C with 100 ng of either S or RBD proteins/per well in 50 μl PBS buffer (Sigma, C-3041). The next morning, plate was washed three times and non-specific interactions blocked for 1 h at room temperature with a blocking buffer (PBS containing 3% (w/v) skim milk powder and 0.1% Tween 20). This was followed by wash steps, a volume of 100 μl of test sera, diluted 1:400 in PBS-Tween plus 1% (w/v) skimmed milk non-fat powder (BioShop Canada), was added and incubated for 2 h at room temperature (20°C). Each serum sample was tested in duplicate, and each test plate included duplicate negative sera as indicated in the standardization of ELISA. Once again, wash step was performed and HRP-conjugated goat anticat antibody

(Santa Cruz Biotechnology, Cat. No. sc2428), diluted 1:3,000, was added to the wells and incubated at RT (20°C) for 1 h. One hundred microliters of TMB substrate (Thermo Scientific-C34021) solution was added to each well and incubated at room temperature for 10 min. The reaction was stopped by adding 50 µl/well of 2 M H_2SO_4, and absorbance (optical density) was measured at 450 nm using a microplate reader (SLT-Spectra, SLT Lab Instruments, Crailsheim, Germany). The ELISA cutoff value was determined as explained in the standardization of ELISA, thus a cutoff OD value of 0.692 for the in-house indirect S-ELISA and an OD value of 0.493 for the RBD-ELISA.

Comparison With Commercial ELISA Tests

To assess the reliability of the performance of our in-house indirect S- and RBD-ELISA tests, along with cat sera, sera from human patients were employed which were positive for SARS-CoV-2-specific antibodies by a commercial ELISA (Roche) antibody assay and positive for SARS-CoV-2 RNA by a real-time RT-PCR. Similarly, prechecked negative human sera by ELISA and real-time RT-PCR were used as negative control.

Surrogate Virus Neutralization Test

In order to detect neutralizing activity against SARS-CoV-2-RBD of the spike protein, a commercial (GenScript Inc., Piscataway, NJ, USA) SARS-CoV-2 Surrogate Virus Neutralization Test Kit was used. This test detects blocking antibodies for binding of SARS-CoV-2-RBD to the ACE2 receptor on a cell surface in an ELISA system. In this study, the cat sera found to be positive in S- and RBD-ELISA were tested by surrogate virus neutralization test, as described by the manufacturer (GenScript Inc., Piscataway, NJ, USA).

Analysis of Serum Samples for Antibodies to FCoV

Cat sera found to be positive for SARS-CoV-2 antibodies were analyzed for the presence of antibodies to FCoV (Bionote, Anigen, FCoV Antibody and Biogal, FCoV Immunocomb ELISA) according to the manufacturer's instructions.

Hematological and Biochemical Analyses

Reference values were taken from IDEXX kit instructions used in the laboratory of the Department of Internal Medicine. The reference values for alanine aminotransferase (ALT) and alkaline phosphatase (ALP) were taken from a previous study published by Natalie and others (32). Blood samples from cats were analyzed in detail by a complete blood hemogram-histogram; specifically, total white blood cell counts (WBC), red blood cell counts (RBC), hemoglobin, hematocrit, lymphocyte, neutrophil, monocyte, and platelet counts by using the IDEXX ProCyte Dx™ instrument as described by the manufacturer (IDEXX Procyte Dx Reagent Kit).

Samples from cats were also analyzed for blood biochemistry; ALT, ALP, total protein, blood urea nitrogen (BUN), creatinine levels were measured by the IDEXX Catalyst One instrument as described by the manufacturer (IDEXX Catalyst Chem 10 and IDEXX Catalyst Chem 17).

Statistical Analysis

Data were analyzed using MedCalc (version 20.010) software. Chi-square test was used to compare the proportion of serological results to age and gender of cats.

RESULTS

Assessment of S- and RBD-Specific ELISAs Used in This Study

SARS-CoV-2-S- and SARS-CoV-2-RBD-specific ELISAs, established in house, were used to detect the presence of antibodies to SARS-CoV-2 in serum collected from cats. The OD cutoff value of the in-house ELISAs were set at an OD of 0.692 for S-ELISA and 0.493 for RBD-ELISA. Of the 155 cat sera analyzed, 26.45% (41/155) tested positive in the in-house S-ELISA, whereas 28.38% (44/155) tested positive in the in-house RBD-ELISA (**Figure 1**). Thirty-four (21.9%; 34/155) cat sera tested positive in both the S- and RBD-ELISA (**Figure 1**), five sera were positive only in S-ELISA, and nine sera were positive only in RBD-ELISA (**Figure 1**). Interestingly, the six sera which were taken before the first reported COVID-19 patient in Istanbul, Turkey, were positive with the RBD-ELISA but negative with the S-ELISA, one was positive by the S-ELISA (**Figure 1**). All control cat sera were negative for SARS-CoV-2-specific antibodies by both ELISAs.

Both ELISAs were analyzed by kappa statistics, and the kappa value was determined as 0.76. This kappa value indicates that both ELISAs have an excellent agreement based on established criteria reported previously (31).

According to results obtained in the assessment study, a cat serum was defined as positive for SARS-CoV-2-specific antibodies when the serum reacted positive in both, the S- and RBD-ELISAs (agreement in both tests).

Antibodies to FCoV and SARS-CoV-2 in Cat Sera Collected Before COVID-19

Thirty cat sera obtained before the first COVID-19 patient was reported in Turkey were analyzed for the presence of FCoV-specific antibodies by ELISA. When these 30 cats were tested for antibodies to SARS-CoV-2, six (20%) cats were found to be positive for SARS-CoV-2 by both the S- and RBD-ELISAs (**Table 1**). OD values of six positive sera ranged between 0.850 and 0.973 in the S-ELISA and 0.710 and 0.987 in the RBD-ELISA (**Figure 1**). Among the six SARS-CoV-2 seropositive cats, five cats had antibodies to FCoV. One cat had no antibodies to FCoV, and the OD values of this cat to SARS-CoV-2 were 0.801 in the S-ELISA and 0.712 in the RBD-ELISA (**Table 1**; **Figure 1**).

Antibodies to FCoV and SARS-CoV-2 in Cat Sera Collected During COVID-19

One hundred twenty-five cat sera collected during the COVID-19 pandemic were analyzed for the presence of FCoV antibodies. When these 125 cat sera were analyzed for antibodies to SARS-CoV-2, 28 (22.4%) cats were found to be positive for SARS-CoV-2 by both ELISAs (**Table 1**). OD values of the 28 positive sera ranged between 0.750 and 0.995 for the S-ELISA and 0.670 and 0.944 for the RBD-ELISA (**Table 1**; **Figure 1**). Among the

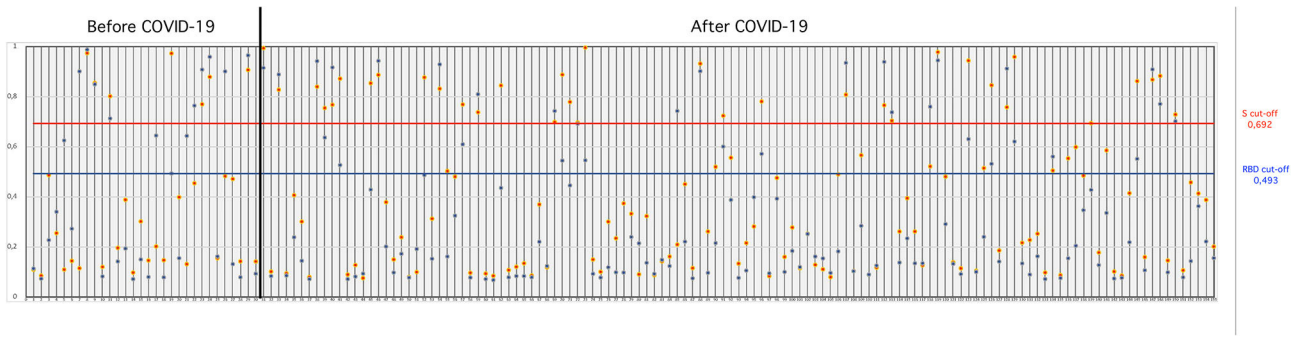

FIGURE 1 | OD values of cat sera collected "before COVID-19" and "during COVID-19" tested in the S- and RBD-ELISAs. The blue horizontal line (bottom line) indicates the "cut-off" value for the RBD-ELISA and the red horizontal line (upper line) indicates the "cut-off" value for the S-ELISA.

TABLE 1 | Cut-off values and number of positive and negative cat sera as determined by the S- and RBD-ELISA.

	Cutoff value (optical density)	Positive	Negative	Positive sera taken "before COVID-19"	Positive sera taken "during COVID-19"
S-ELISA	0.692	41	114	7	34
RBD-ELISA	0.493	44	111	12	32
Positive in both S- and RBD-ELISA		34		6	28
Positive only in S-ELISA		5		1	5
Positive only in RBD-ELISA		9		6	3

A total 155 cat sera comprising 30 sera "before COVID-19" and 125 sera "during COVID-19" were analyzed.

28 SARS-CoV-2 seropositive cats, 22 cats had antibodies to FCoV (**Table 2**).

Surrogate Virus Neutralization Test

Cat sera (6) positive in S and RBD-ELISA collected before COVID-19 were all negative in surrogate virus neutralization test (sVNT) test. When 28 cat sera positive in S- and RBD-ELISAs collected during COVID-19 tested by sVNT test, three cat sera were found to be positive. Two of these sera were also positive for FCoV antibodies and one cat was living with an owner who recovered from the COVID-19 disease.

Signalments and Clinical Signs in SARS-CoV-2 Seropositive Cats ($n = 34$)

The signalments and clinical signs of the SARS-CoV-2 seropositive cat cohort at the time of blood collection are shown in **Table 2**. Most of the seropositive cats ($n = 21$) were below 3 years old. Similarly, 67% (23/34) of the cats were female and the remaining 33% (11/34) were male. Seropositive cats were mainly (85%) cross-breeds ($n = 29$) and only five cats (15%) were pure breeds (**Table 2**). Seropositive cats exhibited mainly respiratory ($n = 8$), gastrointestinal ($n = 10$), renal ($n = 6$), and skin lesions ($n = 6$). A high body temperature was measured only in three seropositive cats (**Table 2**).

Hematological and Biochemical Findings in SARS-CoV-2 Seropositive Cats

Results of the hematology and biochemistry are shown in **Table 2**. HCT ($n = 9$), HGB ($n = 8$), WBC ($n = 7$), and platelets ($n = 8$) were low in several seropositive cats. Lymphopenia was seen in 11 cats (33%), and these lymphopenic cats had high titers of antibodies to the S and RBD proteins. The number of neutrophils and monocytes were above the normal in six and eight cats, respectively (**Table 2**). Creatinine was found to be low in three cats and high in six cats. The liver enzyme ALT level was high in eight cats (**Table 2**), and these cats also had a very high titer of antibodies to the S and RBD proteins.

Statistical Analysis

The seroprevalence of age and gender was not statistically significantly different between seropositive and negative cats ($p > 0.05$).

DISCUSSION

A considerable number of reports indicated that domestic and wild felids have been shown to be highly susceptible to natural and experimental SARS-CoV-2 infections (9, 11, 12, 17), indicating that cats can be infected with both, FCoV and SARS-CoV-2; therefore, serological cross-reaction might complicate serological diagnosis. So far, no comprehensive data are available on the analysis of cat sera for the presence of antibodies to SARS-CoV-2 before the emergence of SARS-CoV-2, December 2019

TABLE 2 | Demographics, clinical, hematological, and biochemical findings in *SARS-CoV-2 seropositive cats*.

Clinical signs and demographics					**Circulatory, liver, and renal functions of SARS-CoV-2–positive cats**					
	SARS-CoV-2 positives (*N* = 34)		**FCoV positives (*N* = 27)**		**Hematological findings and reference values**	**L**	**H**	**Biochemical findings and reference values**	**L**	**H**
	Before COVID-19 (*n* = 6)	**During COVID-19 (*n* = 28)**	**Before COVID-19 (*n* = 5)**	**During COVID-19 (*n* = 22)**						
Age										
0–3	6	15	5	14	HCT:	9 cats:	3 cats:	Creatinin:	3 cats:	6 cats:
4–7	0	8	0	5	30.3–52.3	18–27	53–56	0.8–2.0	0.2–0.7	2.3–6.1
8–11	0	5	0	3						
Gender										
F	5	18	4	16	HGB:	8 cats:	1 cat:	BUN:	2 cats:	2 cats:
M	1	10	1	6	9.8–16.2	5.8–9.2	17.5	16–36	8–9	42–106
Breed										
Cross	5	24	4	21	RBC:	2 cats:	0	Total protein:	0	2 cats:
Pure	1	4	1	1	6.54–12.2	3.5–6.15		5.7–8.9		9.1–9.3
Fever	1	2			WBC: 5.87–17.02	7 cats: 2.8–4.7	2 cats: 19.8–58.5	ALT: 19–71	0	8 cats: 78–253
Depression/dullness	3	2			Neutrophil: 2.3–10.29	1 cat: 0.68	6 cats: 16.1–42.5	ALP: 6–46	0	2 cats: 54–117
Anorexia	2	3			Lymphocytes: 0.92–6.88	11 cats: 0.67–0.69	4 cats: 6.9–12.01			
Weight loss	3	3			Monocytes: 0.05–0.67	0	8 cats: 0.69–0.87			
Respiratory signs (cough, dyspnea, excretion)	2	6			Platelets: 151–600	8 cats: 25–96	2 cats: 660–686			
Gastrointestinal (diarrhea, constipation, vomitus)	2	8								
Urinary (renal insufficiency, cystitis)	1	5								
Neurological	3	2								
Skin lesions	0	6								

M, male; F, female; H, high; L, low. Reference values were taken from IDEXX kit instructions used in the laboratory of the Department of Internal Medicine. The reference values for ALT and ALP were taken from a previous study published by Natalie and others (32).

(33), and there is no report on the seropositivity of cats to SARS-CoV-2 in Turkey. Therefore, in the present study, the presence of SARS-CoV-2-specific antibodies within the cat population in Istanbul, Turkey was investigated.

SARS-CoV-2 seems to have originated from bats (1, 17) although this has not been proven; also, the involvement of an intermediate mammalian host such as the pangolin or raccoon dogs (8, 10, 34) before transmission to humans has been discussed. COVID-19 patients can transmit SARS-CoV-2 to domestic and large cats while cat to human transmission has not been reported yet (12, 14, 17). Seroprevalence studies in cats indicated that cats can be infected with SARS-CoV-2 presumably by their SARS-CoV-2-infected owners, showing mostly mild disease (17). Natural SARS-CoV-2 in cats has been reported in several countries, e.g., in Belgium (25), Hong Kong (35), USA (36), France (20), Spain (23, 24, 26), Germany (13), UK (17), Italy (37), Switzerland (38), China (14), and SARS-CoV-2-positive cats have been reported to the OIE from Russia, Denmark, Sweden, Chile, Japan, Brazil, and Argentina (39).

In Wuhan, China, 102 cats were analyzed for the presence of antibodies to SARS-CoV-2 by ELISA, and 15 of 102 (14.7%) cat sera were found to be SARS-CoV-2 positive (14). Eleven of the 15 ELISA-positive cats had neutralizing antibodies with titers ranging from 1/20 to 1/1,080, which is rather high compared with titers reported in other cat studies. No obvious clinical signs were observed in SARS-CoV-2 seropositive cats. Three of the SARS-CoV-2-positive cats were living in households with COVID-19 patients, indicating that the close contact to the SARS-CoV-2-positive owners could be the most likely source of infection ("reverse zoonosis"). Ten out of 39 serum samples collected before the emergence of SARS-CoV-2 in December 2019 were positive for SARS-CoV-2 antibodies (14). The authors indicated that no serological cross-reactivity was observed in their serological assay between antibodies against SARS-CoV-2 and type I or II feline coronavirus (14). In Germany, a total of 920 cat sera were screened by an indirect multispecies ELISA, indirect immunofluorescence test (iIFT), and neutralization test specific for SARS-CoV-2 antibodies. Overall, six (0.69% or 6/920) serum samples tested positive for antibodies to SARS-CoV-2 by both ELISA and iIFT, and two of these sera were also positive in the virus neutralization assay (13). The prevalence of SARS-CoV-2 antibodies in cats in Germany is low when compared with other countries. This could be due to the fact that the German serum samples were collected during a time period (March–April 2020) when the incidence of SARS-CoV-2 infections in the German population was low. In contrast, in France, a rather high seroprevalence of SARS-CoV-2 antibodies was found in cats, ranging from 21 to 53% (21). In another study performed in France, 22 cats that had contact to SARS-CoV-2-infected owners were tested for the presence of SARS-CoV-2 RNA by RT-PCR, and sera from 16 cats obtained before the emergence of COVID-19 were analyzed for the presence of antibodies by ELISA. SARS-CoV-2 RNA was detected in one cat, and this cat also tested positive for carrying antibodies to SARS-CoV-2 by ELISA. No antibodies to SARS-CoV-2 were detected in cats sampled before the emergence of COVID-19 (20). In Texas, USA, eight of 17 cats living in COVID-19-affected households were found to be positive either for SARS-CoV-2 RNA or SARS-CoV-2-specific neutralizing antibodies (17, 19). In a study performed in Italy, 5.8% of cats had neutralizing antibodies to SARS-CoV-2 (17, 22). The authors indicated that 22 cat sera originated from COVID-19-affected households (17, 22). In a study performed in Spain, 114 stray cats were tested for SARS-CoV-2 and four cats (3.51%) were found to be positive for SARS-CoV-2 antibodies (24). In another study in Spain, a cat living with a family with several members affected by COVID-19 was analyzed and found to be positive for SARS-CoV-2 RNA. The cat and also another cat in the same household seroconverted against SARS-CoV-2 (23). Similarly, a cat in Belgium diagnosed with severe acute respiratory syndrome, and living with a COVID-19-positive owner, tested positive for SARS-CoV-2 RNA and developed a SARS-CoV-2-specific antibody titer of 1:512 (25). In a study performed in Croatia, 131 cats were tested and 10 cats (0.76%, 10/131) were found to be positive for SARS-CoV-2 antibodies (40).

In the present study, evidence of the presence of antibodies to SARS-CoV-2-specific S and RBD proteins was found in cats sampled before COVID-19 and during COVID-19. A total of 155 cat sera were tested, with 34 (21.9%) being positive for both, the S and RBD proteins. The owner of one seropositive cat had recovered from COVID-19 about 1 month before the cat was sampled, and this cat had high antibody titers to both, S and RBD proteins. Results of our study indicate that SARS-CoV-2 is circulating in cat populations in Istanbul, Turkey, and that SARS-CoV-2 infections in cats were most likely acquired from SARS-CoV-2-positive cat owners. Unfortunately, only limited data on the health status of the cat owners is available since they were not willing to provide detailed information about their SARS-CoV-2 infection status. Importantly, all cats analyzed in this study were household cats and had no access to the outside A similar transmission of SARS-CoV-2 from COVID-19 patients to cats has been shown in numerous cases previously (17, 22, 23). Interestingly, six of the 34 SARS-CoV-2 seropositive cats were sampled before the emergence of COVID-19 in humans, i.e., before December 2019. This could be due to: (i) a cross-reactivity of immune responses between FCoV and SARS-CoV-2, most likely to the nucleocapsid protein; or (ii) a SARS-CoV-2-like virus circulating in cats in Istanbul. Since we do not have any virus/RNA isolates from these cats, the latter possibility is rather speculative. It is most likely that SARS-CoV-2 seropositivity in cats sampled before the COVID-19 is due to cross-reacting antigens between SARS-CoV-2 and FCoV, since five of these six SARS-CoV-2 seropositive cats also had antibodies to FCoV. Only one cat was negative for FCoV antibodies. This observation warrants further investigations.

In the present study, two ELISA tests, one for the SARS-CoV-2 spike protein and one for the RBD region of the spike protein were used to determine the antibody status of cats. The kappa value (0.76) obtained indicates that both the S- and RBD-specific ELISAs had an excellent agreement based on established criteria reported previously (31). This shows that either one of these tests can be used for prescreening cats for antibodies against SARS-CoV-2 in cats. Since we do not have BSL-3 facilities at our institution, the ELISA-positive sera

could not be tested by a classical virus neutralization assay. Therefore, we tested the ELISA-positive cat sera for the presence of neutralizing antibodies using the GenScript ACE2-based SARS-CoV-2 surrogate virus neutralization test (sVNT); three of our ELISA-positive cat sera were found to be sVNT positive, indicating that these cats were exposed to SARS-CoV-2. It is important to note that previous cat studies revealed that some ELISA-positive sera were negative in classical virus neutralization assays (13, 14, 21). The respective authors attributed the negative virus neutralization results in the delayed production of neutralizing antibodies (13). In addition, results of experimental SARS-CoV-2 infection of ferrets indicated that SARS-CoV-2 neutralizing antibodies in the ferret COVID-19 model can only be detected about 2 weeks after the initial detection of SARS-CoV-2-specific antibodies using an iIFT (13, 40). A similar situation as mentioned above could be the reason that only three out of 34 SARS-CoV-2-positive sera tested also positive in the surrogate sVNT assay. Therefore, based on the results obtained by others, the SARS-CoV-2 ELISA-positive but sVNT-negative cats identified in this study were either in early stages of SARS-CoV-2 infection or exposed to a feline coronavirus inducing cross-reactive antibodies to the SARS-CoV-2-S and SARS-CoV-2-RBD proteins. The latter one most likely applies to the six ELISA-positive cats sampled before the emergence of COVID-19, since five of these cats also had antibodies to FCoV. Future studies are needed to investigate if there is cross-reactivity between SARS-CoV-2 and FCoV, although several reports indicate no cross-reactivity (10, 13, 21, 41).

Mild clinical signs or no signs were reported in cats infected with SARS-CoV-2 (10, 20, 35). In the present study, the majority of the seropositive cats ($N = 21$) were between 0 and 3 years old, and respiratory (8/34) and gastrointestinal (10/34) signs were prominent with low hematocrit (9/34), hemoglobin (8/34), lymphocyte (11/34), and platelet (8/34) levels. Alanine aminotransferase levels were increased in eight seropositive cats. These findings are similar to those seen in another cat study (32) and people infected with SARS-CoV-2 (42).

In conclusion, this is the first report describing antibodies to SARS-CoV-2 in cats in Istanbul indicating the risk of cats getting infected with SARS-CoV-2. It is important that cat owners are aware that when they acquire COVID-19, they should apply preventive measures to avoid transmission of the virus to their cats (or other susceptible pets). For this reason, suspected companion animals should be monitored for SARS-CoV-2 infection and separated from naive people and susceptible animals until recovery. Currently, the CDC (43) and OIE (44) recommend the separation of people infected with COVID-19 from their companion animals. Also, the European Advisory Board on Cat Diseases (ABCD) (45) advises isolating positive animals from unexposed ones. For preventive measurements, a "*One Health*" approach should be implemented, with the inclusion of Public Health and Veterinary Services.

DATA AVAILABILITY STATEMENT

The raw data supporting the conclusions of this article will be made available by the authors, without undue reservation.

ETHICS STATEMENT

Ethical review and approval was not required for the animal study because as indicated in the study, only the sera taken from the sick animals that submitted to the Veterinary Faculty of Istanbul University for the diagnosis were investigated. Informed consent was taken from the cat owners. National and international guidelines were followed for the care of animals during the study. Written informed consent was obtained from the owners for the participation of their animals in this study.

AUTHOR CONTRIBUTIONS

AY, HY, BK, NT, JAR, and MI: conceptualization. HY, GR-S, J-RS, PC, JAR, and MI: supervision. AY, HT, AK, OI, AB, and EO: data collection. AK, OI, AB, EO, HT, and RK: sample collection. AY, HY, AK, NT, EO, BK, RK, J-RS, DB, GR-S, DL, PC, MI, and JAR: methodology. AY, HY, DB, GR-S, J-RS, DL, PC, MI, and JAR: recombinant protein production. AY, OI, AB, HT, DB, GR-S, J-RS, DL, and PC: laboratory analyses and validation. AY, HY, MI, and JAR: writing the original draft. AY, HY, NT, AK, BK, RK, DL, PC, MI, and JAR: review and editing. All authors have read, discussed the results, and agreed to the final version of the manuscript for publication.

FUNDING

This study was funded by the Istanbul University-Cerrahpasa (BAP Project No: TSG-2020-34882). The study was partially supported by the NIAID Centers of Excellence for Influenza Research and Surveillance under contract number HHSN 272201400006C, the MCB Core of the National Institute of General Medical Sciences (NIGMS) of the National Institutes of Health under award number P20GM130448, and the Department of Homeland Security Center of Excellence for Emerging and Zoonotic Animal Diseases under Grant Number HSHQDC 16-A-B0006 to JAR. The funding from UK Research and Innovation (UKRI) Biotechnology and Biological Sciences Research Council (BBSRC) Grants (BBS/E/I/00007031 and BB/S013792/1) also contributed to this study.

REFERENCES

1. Zhou P, Yang XL, Wang XG, Hu B, Zhang L, Zhang W, et al. A pneumonia outbreak associated with a new coronavirus of probable bat origin. *Nature.* (2020) 579:270–3. doi: 10.1038/s41586-020-2012-7
2. Wu F, Zhao S, Yu B, Chen YM, Wang W, Song ZG, et al. A new coronavirus associated with human respiratory disease in China. *Nature.* (2020) 579:265–9. doi: 10.1038/s41586-020-2008-3
3. Chen N, Zhou M, Dong X, Qu J, Gong F, Han Y, et al. Epidemiological and clinical characteristics of 99 cases of 2019 novel coronavirus

pneumonia in Wuhan, China: a descriptive study. *Lancet*. (2020) 395:507–13. doi: 10.1016/S0140-6736(20)30211-7
4. Bernard Stoecklin S, Rolland P, Silue Y, Mailles A, Campese C, Simondon A, et al. First cases of coronavirus disease 2019 (COVID-19) in France: surveillance, investigations and control measures, January 2020. *Euro Surveill*. (2020). 25:2000094. doi: 10.2807/1560-7917.ES.2020.25.6.2000094
5. Ghinai I, McPherson TD, Hunter JC, Kirking HL, Christiansen D, Joshi K, et al. First known person-to-person transmission of severe acute respiratory syndrome coronavirus 2 (SARS-CoV-2) in the USA. *Lancet*. (2020) 395:1137–44. doi: 10.1016/S0140-6736(20)30607-3
6. Tuite AR, Fisman DN, Greer AL. Mathematical modelling of COVID-19 transmission and mitigation strategies in the population of Ontario, Canada. *CMAJ*. (2020) 192:497–505. doi: 10.1503/cmaj.200476
7. Stout AE, André NM, Jaimes JA, Millet JK, Whittaker GR. Coronaviruses in cats and other companion animals: where does SARS-CoV-2/COVID-19 fit? *Vet Microbiol*. (2020) 247:108777. doi: 10.1016/j.vetmic.2020.108777
8. Gryseels S, De Bruyn L, Gyselings R, Calvignac-Spencer S, Leendertz FH, Leirs, et al. Risk of human-to-wildlife transmission of SARS-CoV-2. *Mam Rev*. (2021) 51:272–92. doi: 10.1111/mam.12225
9. McNamara T, Richt JA, Glickman LA. Critical needs assessment for research in companion animals and livestock following the pandemic of COVID-19 in humans. *Vector Borne Zoonotic Dis*. (2020) 20:393–405. doi: 10.1089/vbz.2020.2650
10. Zhang T, Wu Q, Zhang Z. Probable pangolin origin of SARS-CoV-2 associated with the COVID-19 outbreak. *Curr Biol*. (2020) 30:1578. doi: 10.1016/j.cub.2020.03.063
11. Costagliola A, Liguori G, d'Angelo D, Costa C, Ciani F, Giordano, et al. Do animals play a role in the transmission of severe acute respiratory syndrome coronavirus-2 (SARS-CoV-2)? A commentary. *Animals*. (2020) 11:16. doi: 10.3390/ani11010016
12. Gaudreault NN, Trujillo JD, Carossino M, Meekins DA, Morozov I, Madden DW, et al. SARS-CoV-2 infection, disease and transmission in domestic cats. *Emerg Microbes Infect*. (2020) 9:2322–32. doi: 10.1080/22221751.2020.1833687
13. Michelitsch A, Hoffmann D, Wernike K, Beer, M. Occurrence of antibodies against SARS-CoV-2 in the domestic cat population of Germany. *Vaccines*. (2020) 8:772. doi: 10.3390/vaccines8040772
14. Zhang Q, Zhang H, Gao J, Huang K, Yang Y, Hui X, et al. A serological survey of SARS-CoV-2 in cat in Wuhan. *Emerg Microbes Infect*. (2020) 9:2013–9. doi: 10.1080/22221751.2020.1817796
15. Tekelioglu BK, Berriatua E, Turan N, Helps CR, Kocak M, Yilmaz, et al. A retrospective clinical and epidemiological study on feline coronavirus (FCoV) in cats in Istanbul, Turkey. *Prev Vet Med*. (2015) 119:41–7. doi: 10.1016/j.prevetmed.2015.01.017
16. Paltrinieri S, Giordano A, Stranieri A, Lauzi, S. Feline infectious peritonitis (FIP) and coronavirus disease 19 (COVID-19): are they similar?. *Transbound Emerg Dis*. (2020) 68:1786–99. doi: 10.1111/tbed.13856
17. Hosie MJ, Hofmann-Lehmann R, Hartmann K, Egberink H, Truyen U, Addie DD, et al. Anthropogenic infection of cats during the 2020 COVID-19 pandemic. *Viruses*. (2021) 13:185. doi: 10.3390/v13020185
18. *OIE Infection With SARS CoV-2 in Animals*. Available online at: https://www.oie.int/fileadmin/Home/MM/EN_Factsheet_SARS-CoV-2.pdf (accessed June 2020).
19. Hamer SA, Pauvolid-Corrêa A, Zecca IB, Davila E, Auckland LD, Roundy CM, et al. Natural SARS-CoV-2 infections, including virus isolation, among serially tested cats and dogs in households with confirmed human COVID-19 cases in Texas, USA. *bioRxiv [Preprint]*. (2020). doi: 10.1101/2020.12.08.416339
20. Sailleau C, Dumarest M, Vanhomwegen J, Delaplace M, Caro V, Kwasiborski A, et al. First detection and genome sequencing of SARS-CoV-2 in an infected cat in France. *Transbound Emerg Dis*. (2020) 67:2324–8. doi: 10.1111/tbed.13659
21. Fritz M, Rosolen B, Krafft E, Becquart P, Elguero E, Vratskikh O, et al. High prevalence of SARS-CoV-2 antibodies in pets from COVID-19+ households. *One Health*. (2021) 11:100192. doi: 10.1016/j.onehlt.2020.100192
22. Patterson EI, Elia G, Grassi A, Giordano A, Desario C, Medardo M, et al. Evidence of exposure to SARS-CoV-2 in cats and dogs from households in Italy. *Nat Commun*. (2020) 11:6231. doi: 10.1038/s41467-020-20097-0
23. Segalés J, Puig M, Rodon J, Avila-Nieto C, Carrillo J, Cantero G, et al. Detection of SARS-CoV-2 in a cat owned by a COVID-19-affected patient in Spain. *Proc Natl Acad Sci USA*. (2020) 117:24790–24793. doi: 10.1073/pnas.2010817117
24. Villanueva-Saz S, Giner J, Tobajas AP, Pérez MD, González-Ramírez AM, Macías-León J, et al. Serological evidence of SARS-CoV-2 and co-infections in stray cats in Spain. *Transbound Emerg Dis*. (2021) 1–9. doi: 10.1111/tbed.14062
25. Garigliany M, Van Laere AS, Clercx C, Giet D, Escriou N, Huon C, et al. SARS-CoV-2 natural transmission from human to cat, Belgium, March 2020. *Emerg Infect Dis*. (2020) 26:3069–71. doi: 10.3201/eid2612.202223
26. Ruiz-Arrondo I, Portillo A, Palomar AM, Santibanez S, Santibanez P, Cervera C, et al. Detection of SARS-CoV-2 in pets living with COVID-19 owners diagnosed during the COVID-19 lockdown in Spain: a case of an asymptomatic cat with SARS-CoV-2 in Europe. *Transbound Emerg Dis*. (2020) 68:973–76. doi: 10.1101/2020.05.14.20101444
27. Leroy EM, Ar Gouilh M, Brugère-Picoux J. The risk of SARS-CoV-2 transmission to pets and other wild and domestic animals strongly mandates a one-health strategy to control the COVID-19 pandemic. *One Health*. (2020) 10:100–33. doi: 10.1016/j.onehlt.2020.100133
28. Lukosaityte D, Sadeyen JR, Shrestha A, Sealy JE, Bhat S, Chang P, et al. Engineered recombinant single chain variable fragment of monoclonal antibody provides protection to chickens infected with H9N2 avian influenza. *Vaccines*. (2020) 8:118. doi: 10.3390/vaccines8010118
29. Park JG, Oladunni FS, Rohaim MA, Whittingham-Dowd J, Tollitt J, Assas BM, et al. Immunogenicity and protective efficacy of an intranasal live-attenuated vaccine against SARS-CoV-2 in preclinical animal models. *bioRxiv [Preprint]*. (2021). doi: 10.1101/2021.01.08.425974
30. Yilmaz H, Faburay B, Turan N, Cotton-Caballero M, Cetinkaya B, Gurel A, et al. Production of recombinant n protein of infectious bronchitis virus using the baculovirus expression system and its assessment as a diagnostic antigen. *Appl Biochem Biotechnol*. (2019) 187:506–17. doi: 10.1007/s12010-018-2815-2
31. Kirkwood BR, Sterne JAC. *Essential Medical Statistics*. 2nd ed. Malden, MA: Blackwell Science (2003).
32. Natale A, Mazzotta E, Mason N, Ceglie L, Mion M, Stefani A, et al. SARS-Cov-2 natural infection in a symptomatic **cat**: diagnostic, clinical and medical management in a one health vision. *Animals*. (2021) 11:1640. doi: 10.3390/ani11061640
33. *WHO Director-General's Opening Remarks at the Media Briefing on COVID-19 - 11 March 2020*. Available online at: https://www.who.int/dg/speeches/detail/who-director-general-s-opening-remarks-at-the-media-briefing-on-covid-19-$-$11-march-2020 (accessed 13 March 2020).
34. Lam TT, Jia N, Zhang YW, Shum MH, Jiang JF, Zhu HC, et al. Identifying SARS-CoV-2-related coronaviruses in Malayan pangolins. *Nature*. (2020) 583:282–5. doi: 10.1038/s41586-020-2169-0
35. Barrs VR, Peiris M, Tam KWS, Law PYT, Brackman CJ, To EMW, et al. SARS-CoV-2 in quarantined domestic cats from COVID-19 households or close contacts, Hong Kong, China. *Emerg Infect Dis*. (2020) 26:3071–4. doi: 10.3201/eid2612.202786
36. Newman A, Smith D, Ghai RR, Wallace RM, Torchetti MK, Loiacono C, et al. First reported cases of SARS-CoV-2 infection in companion animals - New York, March-April 2020. *MMWR Morb Mortal Wkly Rep*. (2020) 69:710–3. doi: 10.15585/mmwr.mm6923e3
37. Musso N, Costantino A, La Spina S, Finocchiaro A, Andronico F, Stracquadanio S, et al. New SARS-CoV-2 infection detected in an Italian pet cat by RT-qPCR from deep pharyngeal swab. *Pathogens*. (2020) 9:746. doi: 10.3390/pathogens9090746
38. Klaus J, Meli ML, Willi B, Nadeau S, Beisel C, Stadler T, et al. Detection and genome sequencing of SARS-CoV-2 in a domestic cat with respiratory signs in Switzerland. *Viruses*. (2021) 13:496. doi: 10.3390/v13030496
39. *COVID-19 Portal Questions and Answers on COVID-19*. Available online at: https://www.oie.int/en/scientific-expertise/specific-information-and-recommendations/questions-and-answers-on-2019novel-coronavirus (accessed 22 January 2021).
40. Stevanovic V, Vilibic-Cavlek T, Tabain I, Benvin I, Kovac S, Hruskar Z, et al. Seroprevalence of SARS-CoV-2 infection among pet animals in Croatia and

potential public health impact. *Transbound Emerg Dis.* (2020) 68:1767–73. doi: 10.1111/tbed.13924

41. Perera RA, Mok CK, Tsang OT, Lv H, Ko RL, Wu NC, et al. Serological assays for severe acute respiratory syndrome coronavirus 2 (SARS-CoV-2), March 2020. *Euro Surveill.* (2020) 25:2000421. doi: 10.2807/1560-7917.ES.2020.25.16.2000421
42. Ponti G, Maccaferri M, Ruini C, Tomasi A, Ozben, T. Biomarkers associated with COVID-19 disease progression. *Crit Rev Clin Lab Sci.* (2020) 57:389–99. doi: 10.1080/10408363.2020.1770685
43. *COVID-19 and Animals*. Available online at: https://www.cdc.gov/coronavirus/2019-ncov/daily-life-coping/animals.html (accessed 25 March 2021).
44. OIE. *COVID-19 Portal: Events in Animals*. Available online at: https://www.oie.int/scientific-expertise/specific-information-and-recommendations/questions-and-answers-on-2019novel-coronavirus/events-in-animals/ (accessed 29 December 2020).
45. *European Advisory Board on Cat Diseases SARS-Coronavirus (CoV)-2 and Cats*. Available online at: http://www.abcdcatsvets.org/sars-coronavirus-2-and-cats-/ (accessed 31 January 2021).

Conflict of Interest: The authors declare that the research was conducted in the absence of any commercial or financial relationships that could be construed as a potential conflict of interest.

frontiers in Veterinary Science

REVIEW
published: 18 October 2021
doi: 10.3389/fvets.2021.719834

Evolution, Interspecies Transmission, and Zoonotic Significance of Animal Coronaviruses

*Prapti Parkhe and Subhash Verma**

Department of Veterinary Microbiology, DGCN College of Veterinary and Animal Sciences, Chaudhary Sarwan Kumar Himachal Pradesh Krishi Vishvavidyalaya, Palampur, India

Coronaviruses are single-stranded RNA viruses that affect humans and a wide variety of animal species, including livestock, wild animals, birds, and pets. These viruses have an affinity for different tissues, such as those of the respiratory and gastrointestinal tract of most mammals and birds and the hepatic and nervous tissues of rodents and porcine. As coronaviruses target different host cell receptors and show divergence in the sequences and motifs of their structural and accessory proteins, they are classified into groups, which may explain the evolutionary relationship between them. The interspecies transmission, zoonotic potential, and ability to mutate at a higher rate and emerge into variants of concern highlight their importance in the medical and veterinary fields. The contribution of various factors that result in their evolution will provide better insight and may help to understand the complexity of coronaviruses in the face of pandemics. In this review, important aspects of coronaviruses infecting livestock, birds, and pets, in particular, their structure and genome organization having a bearing on evolutionary and zoonotic outcomes, have been discussed.

Keywords: coronavirus, evolution, interspecies transmission, host cell receptor, protein binding motif, zoonotic animal origin, classification, animal coronaviruses

OPEN ACCESS

Edited by:
Yashpal S. Malik, Indian Veterinary Research Institute (IVRI), India

Reviewed by:
Hicham Sid, Technical University of Munich, Germany
Pankaj Dhaka, Guru Angad Dev Veterinary and Animal Sciences University, India

***Correspondence:**
Subhash Verma
sverma8@gmail.com

Specialty section:
This article was submitted to Veterinary Infectious Diseases, a section of the journal Frontiers in Veterinary Science

Received: *03 June 2021*
Accepted: *07 September 2021*
Published: *18 October 2021*

Citation:
Parkhe P and Verma S (2021) Evolution, Interspecies Transmission, and Zoonotic Significance of Animal Coronaviruses. Front. Vet. Sci. 8:719834. doi: 10.3389/fvets.2021.719834

INTRODUCTION

Coronaviruses (CoVs) form the subfamily *Orthocoronavirinae* of family *Coronaviridae* under order *Nidovirales* and realm *Riboviria*. These are pleomorphic, enveloped, single molecule of linear, positive-sense, single-stranded RNA viruses containing genome sizes of around 30 kb among known RNA viruses (1). The club-shaped peplomers composed of large viral glycoprotein (spike or S protein responsible for attachment to cells) projecting from the envelope give a crown-like appearance of the virus under a transmission electron microscope, thus named corona meaning crown. CoV was considered a minor pathogen of the respiratory tract until 2002 in humans (2). The increased interest in its replication, transmission, pathogenesis, and distribution was pursued after an outbreak linked to the emergence of a new CoV [severe acute respiratory syndrome (SARS)-CoV] causing SARS after 2002 (2–5). Another virus called Middle East respiratory syndrome CoV (MERS-CoV) in 2014, distinct from SARS-CoV, was isolated from an outbreak of severe respiratory infection in the Middle East (6). On the other hand, an acute respiratory infection caused by an avian CoV, later named as infectious bronchitis virus with high mortality (40–90%), had shown up in the late 1920s and was the earliest report of a CoV infection in animals (7, 8). Currently, the SARS-CoV-2 and its mutated strains predominantly infecting humans with contentious animal origin have created a platform for researchers to study its genomics in-depth. Animal species play an important role as a host or reservoir in the transmission cycle of CoV, and

specific receptors on their cell provide essential factors for replication and mutations within the genome of CoVs. CoVs infect various animal species ranging from livestock, poultry, cats, dogs, mice, bats, pangolins, wild felids, and other species of animals such as minks, rabbits, ducks, guinea fowls, gooses, beluga whales, etc., (9–12). These mammals are frequently studied for understanding their coevolution with human CoVs, interspecies transmission, and the emergence of new mutant strains. CoV infection in animals is mainly associated with respiratory and gastrointestinal systems resulting in mild to fatal diseases. The bovine, avian, and porcine animal groups form a major part of production industries, and in like manner, the canine and feline species have paramount importance as pets commercially due to their high demand in society. The incidence of diseases in these animal species represents a threat to the animal welfare, environment, public health, and economy, reflecting as losses in productivity, trade, market value, control costs, and food security. In this review, CoVs infecting important livestock, poultry, and pets have been discussed in relation to their structure and genome organization having a bearing on evolutionary and zoonotic outcomes.

CORONAVIRUS STRUCTURE, MAJOR PROTEINS, AND THEIR FUNCTIONS

Virions are roughly spherical and enveloped with marked spike (S) proteins that identify various specific host cell receptors and co-receptors for attachment, fusion, and entry of the virus into the cell. In addition to S proteins, other structural proteins are nucleocapsid (N) proteins, the most abundant membrane (M) proteins, envelope (E) proteins, and other non-glycosylated envelope proteins present in lower quantities, which help in the formation of an envelope. The flexible nucleocapsid within the envelope consists of genomic RNA linked to the nucleoprotein (**Figure 1**).

The functions of these major structural proteins of CoV are stated in **Table 1**.

TABLE 1 | Major proteins of coronavirus and their functions.

Major protein	Function
Nucleocapsid protein (N)	Multifunctional protein
	Forms complexes with genome RNA to make up nucleocapsid
	Interacts with the membrane proteins during virus life cycle, especially for virion assembly and viral budding
	Enhances the efficiency of virus transcription
	Principle target for vaccine development as a major immunogen (13)
	An important diagnostic marker for coronavirus disease (13, 14)
Spike or peplomer protein (S)	Critical for binding to host cell receptors to facilitate entry into host cell (15)
Envelope protein (E)	Smallest of the major proteins
	Interacts with M protein to form viral envelop
	Expressed abundantly inside the infected cell but only a small portion incorporated into virion envelope (16)
	A majority is localized at the site of intracellular trafficking, i.e., the ER, Golgi, and ER–Golgi intermediate compartment where it participates in virus assembly and budding (17)
Membrane protein (M)	Most abundant structural protein
	Central organizer of CoV assembly (18, 19)
	Defines shape of viral envelope
	Responsible for transmembrane transport of nutrients and bud release
Hemagglutinin-esterase glycoprotein	Mediate reversible attachment to sialic acids
	Act both as carbohydrate-binding lectin and as a receptor-destroying enzyme (RDE) (20)
	Responsible for enzymatic activity
	Lack membrane fusion activity
	Accessory to spike glycoprotein in virion (21)

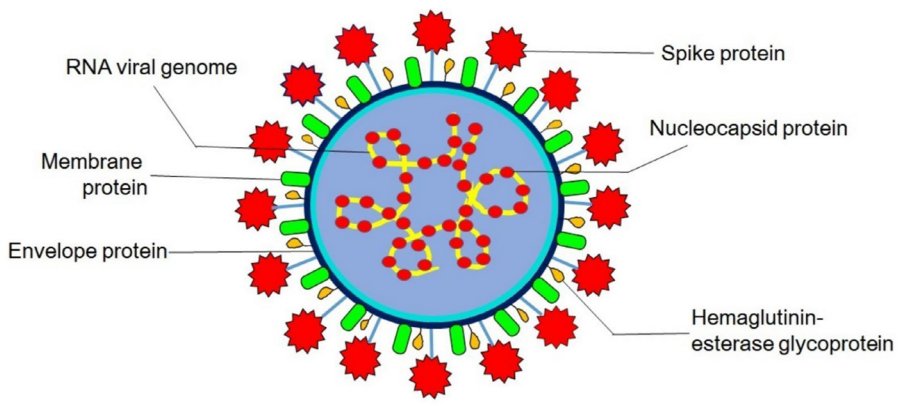

FIGURE 1 | Structure of coronavirus. Hemagglutinin-esterase glycoprotein is exclusively present in members of Betacoronavirus (human and bovine coronavirus).

CLASSIFICATION OF CORONAVIRUS

Initially, the classification was based on their serological and antigenic properties—groups 1, 2, and 3 as opposed to newly revised taxonomy based on the level of viral genetic phylogeny. The phylogenetic analysis for classification of CoV is usually acquired by using short fragments of several conserved genes that are present in all CoV genomes and are of a significant length, such as Pol (RNA-dependent RNA polymerase), N (nucleoprotein), S (spike protein), and chymotrypsin-like protease and helicase. The envelope and membrane genes are not used in phylogenetic studies due to their short lengths (1, 22). Furthermore, complete genome sequence and proteomic approaches are also carried out to construct the phylogenetic tree of CoVs. Now, the subfamily *Orthocoronavirinae* is classified into four genera: alpha, beta, gamma, and delta CoVs infecting a wide variety of animal and avian species (23, 24). *Betacoronavirus* genus is further classified into lineages A, B, C, and D (1) and other subgenus *Hibecovirus* (25). The list of important CoV species classified under individual genera is given later (**Table 2**). Apart from this, several other animal species that harbor the CoVs are rodents, rabbits, bats, pangolin, ferrets, mink, snake, frogs, marmots, hedgehogs, and many other wild animals, as carriers or reservoirs that may need attention regarding zoonotic interventions (26–33).

TABLE 2 | Important coronavirus species within individual genera.

Genus	Species
ALPHACORONAVIRUS	
	Human coronavirus 229E
	Human coronavirus NL63
	Porcine epidemic diarrhea virus (PEDV)
	Transmissible gastroenteritis virus (TGEV)
	Porcine respiratory coronavirus (PRCV)
	Feline infectious peritonitis virus (FIPV)
	Canine enteric coronavirus (CCoV)
	Rhinolophus bat coronavirus HKU2
BETACORONAVIRUS SUBGENUS	
Embecovirus (Lineage A)	Human coronavirus HKU1
	Human coronavirus OC43
	Bovine coronavirus (BCoV)
	Porcine hemagglutinating encephalomyelitis virus (PHEV)
	Canine respiratory coronavirus (CRCoV)
	Feline enteric coronavirus (FCoV)
	Murine hepatitis virus (MHV)
Sarbecovirus (Lineage B)	Severe acute respiratory syndrome (SARS) related coronavirus (SARS-CoV-1, SARS-CoV-2)
Merbecovirus (Lineage C)	Middle east respiratory syndrome (MERS) related coronavirus
Nobecovirus (Lineage D)	Bat coronaviruses
Hibecovirus	Bat Hp-betacoronavirus Zhejiang 2013
GAMMACORONAVIRUS	
	Infectious bronchitis virus (IBV)
	Bluecomb virus of turkey
DELTACORONAVIRUS	
	Porcine deltacoronavirus (PdCV)
	Avian coronaviruses

LIFE CYCLE

The viral replication cycle of all the CoVs is confined to the cytoplasm (**Figure 2**); additionally, murine CoVs can also replicate in enucleated cells (34–36).

The first essential step of the viral replication cycle is host cell receptor recognition by S protein and its attachment to the cell. The membrane fusion event results in penetration of virion aided by "fusion peptide," which is exposed after variable rearrangement of S protein initiated by proteolytic cleavage of spike protein and acidic pH. This is followed by synthetic events such as translation of replicase gene from viral genome and formation of polyproteins, transcription, and RNA synthesis. After replication and RNA synthesis, the S, E, and M viral structural proteins are translated and inserted into the endoplasmic reticulum. Both M and E proteins function together to form envelope and virus-like proteins. The N protein binds to viral RNA and is later accompanied by M protein, which keeps the N protein and RNA complex stable. This interaction facilitates the assembly of virus particles on the membrane of the endoplasmic reticulum–Golgi intermediate compartment and initiates the budding process. Mature virions formed within the membrane-bound vesicles are released by exocytosis. The *viroporin* of E protein with ion channel activity promotes virus release by altering cell secretory pathways.

GENOME ORGANIZATION AND ROLE OF SPIKE PROTEIN IN EVOLUTION OF CORONAVIRUSES

The organization of large 20–32-kb size, capped and polyadenylated genome of CoV contains seven common genes in the following order, 5′-leader-untranslated region (UTR)-replicase-Spike (S)-Envelope (E)-Membrane (M)-Nucleocapsid (N)-3′ UTR-poly (A) tail.

The receptor-binding S1 subunit of spike proteins contains two distinct domains, the N-terminal domain (S1-NTD) and the C-terminal domain (S1-CTD). These domains recognize at least four protein receptors and three sugar receptors of the host cell (**Figure 3**) and, thus, can form the basis for classification according to the host cell recognition pattern (35, 37). The open reading frame (ORF) 1a/b encompasses a much larger section, i.e., the initial two-thirds of the genome encoding two viral replicase polyproteins—pp1a and pp1ab. These polyproteins are then further processed into 16 non-structural proteins (nsp1–16) by viral proteases and assemble to form a membrane-associated viral replicase–transcriptase complex (38–40). These are conserved among the subgroups of CoVs and thus share their relative position in the genome (41–44). Structural and some accessory proteins occupy only the last third of the coding

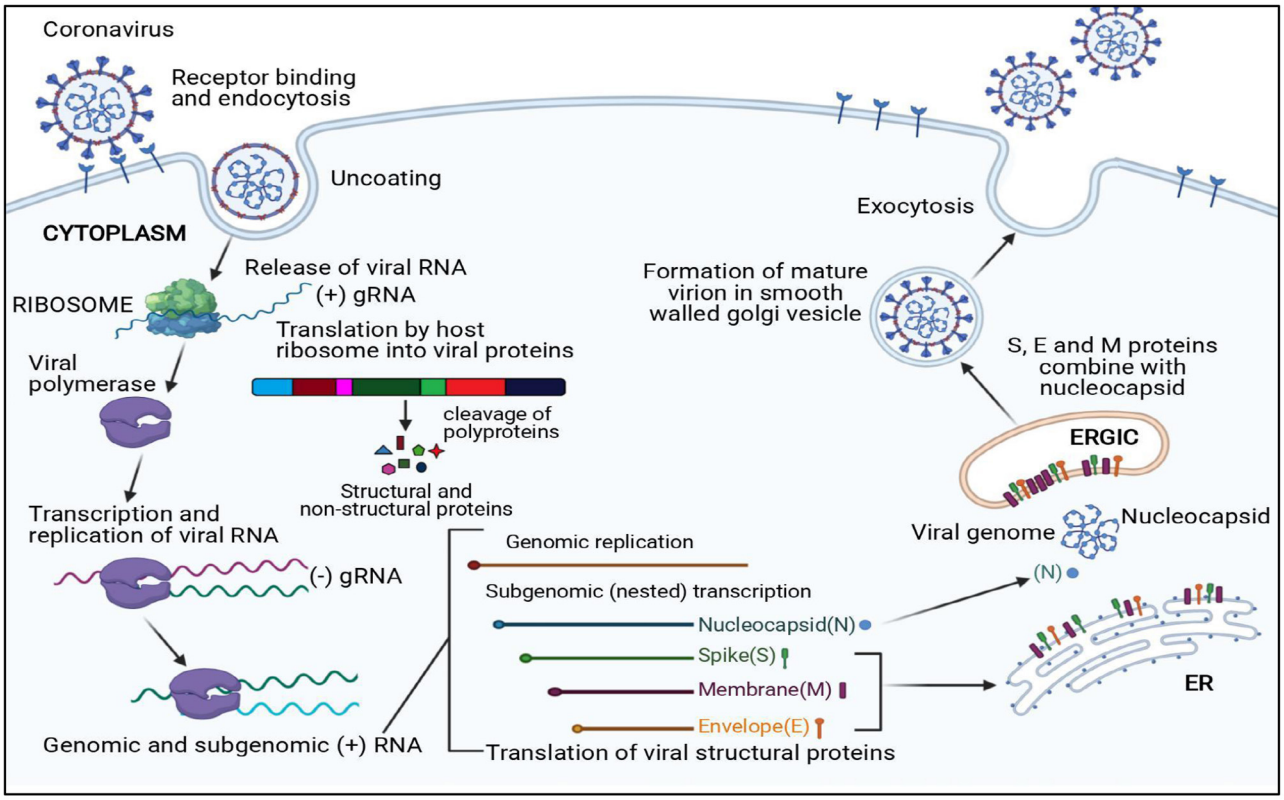

FIGURE 2 | Replication cycle of coronavirus. N, Nucleocapsid; S, Spike protein; M, Membrane protein; E, Envelope protein; ER, Endoplasmic reticulum; ERGIC, Endoplasmic reticulum–Golgi intermediate compartment.

capacity of the genome (45, 46) despite their range of complexity and function (40, 47).

Divergence in the sequence and motifs or residues of these proteins among CoVs may corroborate in classifying them in groups. Many researchers have demonstrated the phylogenetic relationships among their genomes based on the analysis of ORF1b replicase protein, 3C-like proteinase, polymerase, and structural proteins, which confirm the presence of different CoV group clusters (48–51). For instance, pairwise alignments of the corresponding ORFs and proteins of HCoV-OC43, bovine CoV (BCoV), PHEV, ECoV, and MHV suggest sequence similarity among them under the β-CoV group (50, 51). ORF8, a highly variable accessory gene and showing structural changes, plays a significant role in the evolution of SARS-related CoVs (52). The absence of a 29-nucleotide (nt) sequence in ORF8 and the presence of characteristic motif of single-nucleotide variations located in the S gene were observed in later phases of the SARS-CoV outbreak in 2002–2003 (53, 54).

The interaction between receptor-binding domain (RBD) and its host cell receptor helps in determining the CoV host range and cross-species infection (55, 56). This is dependent on the topology of RBD, its receptor-binding motif (RBM), and virus-binding motifs on specific proteins or sugars that complement each other in shape and chemical details. Both the distinctive domains, S1-NTD and S1-CTD of receptor-binding S1 subunit of CoV spike protein, can function as RBDs (57).

CoVs have been shown to mutate with high rate and recombination frequencies in their RNA genome ($\sim 10^{-4}$ nucleotide substitution/site/year). The mutations in the RBD of the spike gene are of significance, along with errors in the O-linked glycans and furin cleavage site, enzymes such as replicase and RNA-dependent RNA polymerase (58–60). The Indian SARS-CoV-2 Consortium on Genomics working on genome sequencing of new variants of SARS-CoV-2 has been reporting mutations and deletions in the amino acid sequence of spike protein since the SARS-CoV-2 pandemic. These mutational changes have led to the emergence of new double and triple mutants, alpha, beta, gamma, and delta variants with the capability of immune escape, increased virulence, transmissibility, and changes in clinical disease presentation (61).

The S1 subunits from the same genus share significant sequence similarity, whereas those from different genera have little sequence similarity (57). However, the speculation on members placed in different genera identifying the same receptor protein or those in the same genera identifying different receptor proteins still holds, despite evidence of a common evolutionary origin for the S1 subunit. The studies reveal that viral RBDs of CoVs of the same genus have a conserved CTD core structure

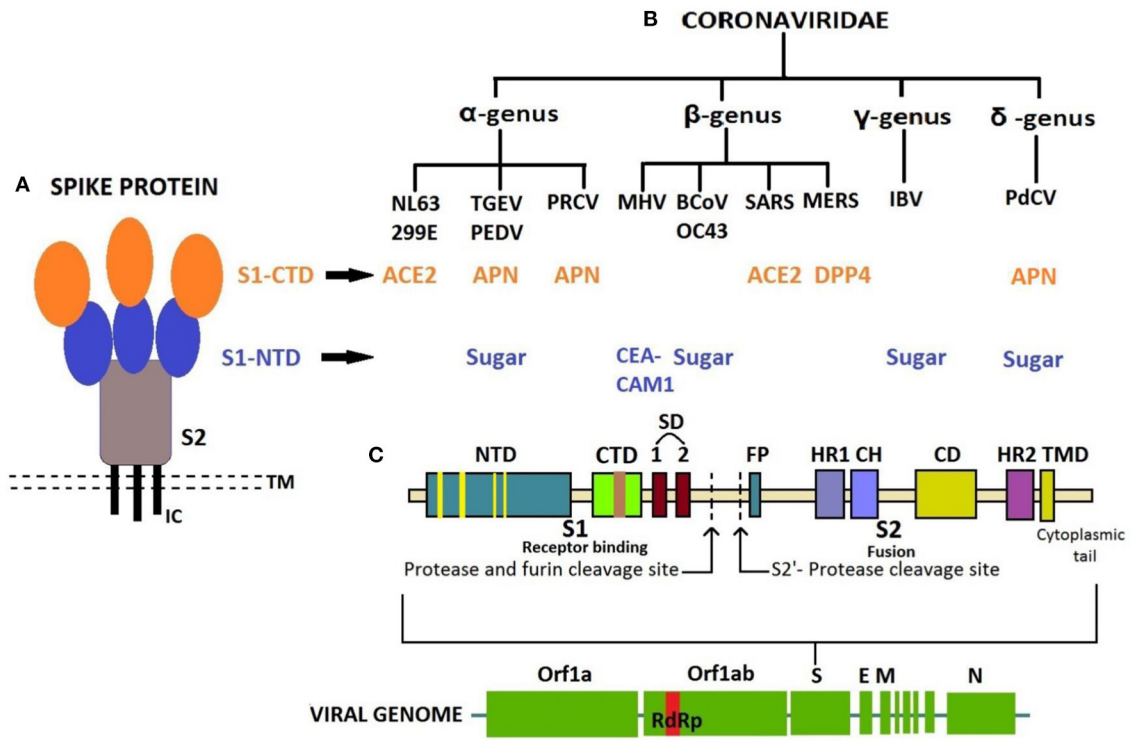

FIGURE 3 | (A) Structure of Spike protein. **(B)** Classification of coronaviruses based on host cell recognition pattern by spike protein. **(C)** Genome organization of coronavirus and single S protein, from N- to C-terminus in left-to-right orientation. N-terminal domain in blue with receptor-binding motif (RBM) in yellow; C-terminal domain in green with RBM in brown. CTD, C-terminal domain; NTD, N-terminal domain; TMD, Transmembrane domain; IC, Intracellular tail; ACE2, Angiotensin-converting enzyme 2; APN, Aminopeptidase N; CEACAM1, Carcinoembryonic antigen-related cell adhesion molecule 1; DPP4, Dipeptidyl peptidase 4; SD, Subdomain; FP, Fusion peptide; HR1, Heptad repeat 1; HR2, Heptad repeat 2; CH, Central helix; CD, Connector domain.

but marked structural variations in their RBMs that enforce recognition of different receptors (62–65). Also, several other studies demonstrate that the viral RBDs of CoVs from different genus can bind to the same protein receptor due to the presence of a common virus-binding hot spot on the protein (62, 66). Thus, the data mentioned earlier provide an insight into an extensive divergent evolution of CoV S1-CTDs (67).

The crystal structure of β-genus MHV S1-NTD complexed with mouse CEACAM1 protein and BCoV S1-NTD with a sialic acid (SA) named Neu5, 9Ac2 (5-N-acetyl-9-O-acetylneuraminic acid) have the same structural fold in its core structure as for human galectins (galactose-binding lectins). Nevertheless, the BCoV S1-NTD is determined by its sugar-binding site instead of protein due to subtle changes in the conformations of their RBM loops and mutagenesis (68). This suggests that the ancestral CoVs inserted the host galectin gene into 5′ end of their spike gene, which resulted in CoV S1-NTD. After that, CoV S1-NTDs underwent divergent evolution in α, β, and γ genera, out of which S1-NTDs of β-genus BCoV, α-genus transmissible gastroenteritis virus (TGEV), and γ-genus infectious bronchitis virus (IBV) evolved their lectin activity and specificity for a different sugar receptor other than galactose. On the other hand, β-genus MHV S1-NTD subsequently lost its lectin activity and evolved specificity for a novel protein receptor, CEACAM1 (62). The S1-NTD of newly identified porcine delta coronavirus (PdCoV) (1, 69) shares a similar structure as α-CoV, β-CoV, and host galectins; thus, it recognizes sugar as its potential receptor and binds to sugar moiety of mucin to facilitate initial viral attachment, whereas the S1-CTD has the same structural fold as α-CoV S1-CTDs, but it differs from that of S1-CTDs of β-CoV (70). The PdCoV S1-CTD has a significant affinity for pig cells known to express aminopeptidase N (APN) as efficiently as TGEV-S1. Therefore, the porcine APN acts as a functional cross-genus receptor for both enteropathogenic PdCoV and TGEV for cellular entry (71). Such similarities suggest a close relationship between PdCoV, α-CoV, and β-CoV evolutionarily; however, PdCoV belongs to Deltacoronavirus owing to its genomic similarities with the avian species suggesting an ancestral avian origin (24).

The evolution of the spike protein of CoVs has also been proposed to help the virus in surviving against host immune response similar to the influenza virus (72, 73). The S1-NTDs of CoVs have also evolved the ceiling-like structure on top of its core to protect these sites and to evade the immune surveillance by the host immune system (74). As per the location of S1-NTDs and S1-CTDs on spike protein, the tips with S1-CTD

are the protruding region and most exposed directly to the host immune system and therefore evolves at an increased pace to combat the host immune surveillance. Based on the immune pressure and different receptors (some of which are still unidentified) recognized by different animal CoV groups, it is clear that the S1-CTD exhibits a common evolutionary origin and has undergone divergent evolution. Moreover, the monoclonal antibodies directed against spike protein demonstrate common antigenic determinants for β-CoVs, especially the members of subgroup embecovirus, i.e., BCoV, PHEV, and HCoV-OC43, which corresponds to a close antigenic relationship (75, 76). This can put forward some hypotheses concerning the origin of β-CoV members, adaptation to a human host, and recombination events leading to novel CoVs with different species specificity responsible for emergence.

TOPOLOGY AND PROPERTIES OF OTHER IMPORTANT STRUCTURAL PROTEINS

The crystal structure of the N-terminal domain of nucleocapsid protein of MHV shares a similar topology structure with that of SARS-CoV and IBV containing five short β-strands (arranged as β4-β2-β3-β1-β5) across a U-shaped β-platform (**Figure 4**) but differs in its potential surface, indicating a possible varied RNA-binding module (77). The three residues, Arg-125 and Tyr-127 on the β3 strand and Tyr-190 on the β5 strand, provide a key role in transcriptional regulatory sequence RNA binding and helix destabilization essential for replication. These residues are totally invariant in betacoronavirus N proteins and incisively occupy analogous positions on the fold of each NTD, therefore likely to define similar RNA binding grooves between them (78). On the other hand, the sequence comparison of the C-terminal domain of N protein, also referred to as the dimerization domain as its residues form homodimers and homo-oligomers (oligomerization) (79, 80), shows that the domain is conserved at least among the alpha, beta, and gamma groups of CoVs, suggesting a common role for this domain.

The positively charged groove formed by the presence of the eight positively charged lysine and arginine residues of CTD is similar in SARS-related viruses and IBV-N CTD, except that the positively charged surface area in the SARS-CoV is larger than IBV (81) due to the absence of two lysine residues and the presence of additional negatively charged residues in the IBV N protein (82). Oligomerization and interaction of proteins with the viral genome is required for packaging of the genome by CoV N proteins to form ribonucleoprotein complexes for viral assembly (83). These functions of N proteins are performed similarly by SARS-CoV, IBV, and MHV. Thus, the overall similarity in the topology of the NTD and CTD domains of the N protein from SARS-CoV, IBV, and MHV fortifies a conserved mechanism of nucleocapsid formation for CoVs (74).

The primary sequence of the E proteins shows large variations in sequence and size among the groups with <30% identity and conserved membrane amino acid residues (84). Multiple membrane topologies of E proteins have been determined between different CoVs depending on the level of protein expression and oligomerization (84). The experimental studies have shown that the IBV E protein exhibits topology of cytoplasmic C-terminus while N-terminus in the lumen of the

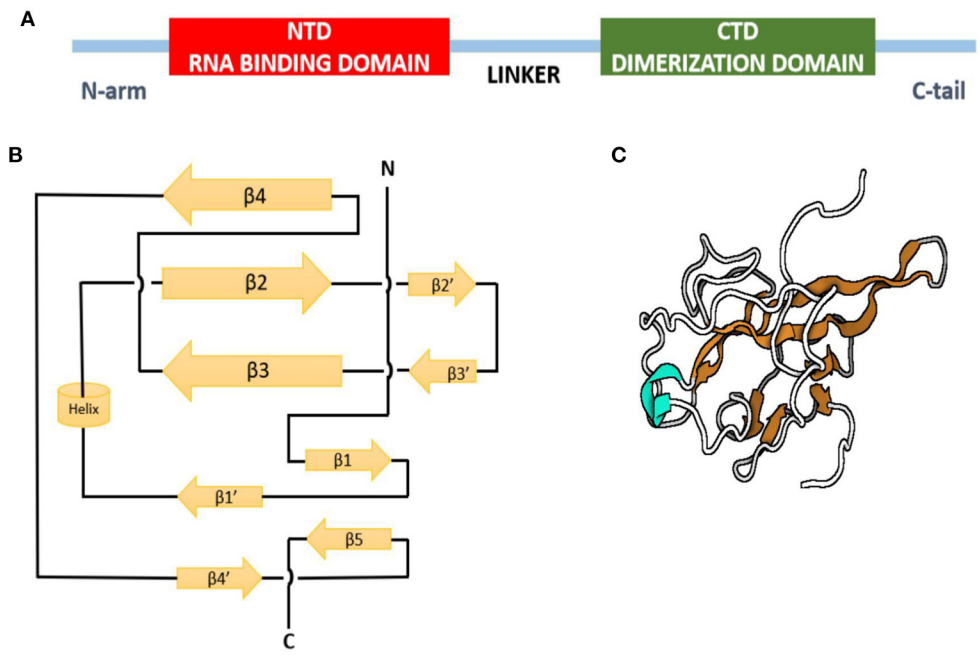

FIGURE 4 | Nucleocapsid protein of infectious bronchitis virus. **(A)** Domain structure of N protein. **(B)** Topology diagram of N protein. **(C)** Three-dimensional structure of N protein. Beta strands in orange, and helix is shown in cyan.

Golgi complex (85). Conversely, the TGEV E protein has a luminal C-terminus and N-terminus located cytoplasmically (86, 87). The CoV E proteins of only IBV, SARS-CoV, and MHV function for palmitoylation, i.e., modulation of protein–protein interactions, subcellular trafficking of proteins across the membrane, and membrane anchoring (88–91). A protein-binding motif located at the end of the C-terminus is highly conserved in α- and β-CoVs and is not found in the γ-CoVs (92).

The primary M protein sequence varies, although the secondary structures and an amphipathic region of the transmembrane domain are also conserved in almost all the members of the family (93). The type of glycosylation in the M protein of α- and δ-CoVs is N-linked, whereas O-linked glycosylation is found in the β-CoVs, but it is not critical for the viral assembly (19, 94–96).

HEMAGGLUTININ-ESTERASE GLYCOPROTEIN IN β-CORONAVIRUSES

The hemagglutinin-esterase (HE) gene is exclusively present in members of β-CoVs. CoV HE proteins were firstly identified from the PHEV, BCoV, and HCoV-OC43 bearing SA-9-O-acetylesterases similar to a hemagglutinin-esterase fusion protein of influenza C virus (97). The HE gene of CoV shares 30% sequence identity with the subunit of a HE fusion protein and has been found to be acquired by independent, non-homologous recombination events or evolutionary trajectories between influenza virus, torovirus, and CoV (98–100). All the CoV HEs are O-acetyesterases, whereas BCoV and HCoV-OC43 have dual activity of both hemagglutination and acetylesterase (101). Both these CoVs can agglutinate chicken erythrocytes, whereas purified HE protein of BCoV only agglutinates Neu5, 9Ac2-enriched erythrocytes of rodents. On the contrary, purified S glycoprotein can agglutinate chicken erythrocytes (102). This indicates that the major hemagglutinin is the S protein that also acts as the major SA-binding protein. The function of the hemagglutinin-esterase enzyme relies on the distinctive carbohydrate-binding domain as lectin and receptor-destroying enzyme domain (**Figure 5**).

HE protein with these domains and SA-O-acetylesterase activity mediates viral entry with S glycoprotein and attachment to the O-acetylated SA receptors on the host cell. The acetylesterase of murine CoVs prefers to esterize 4-O-acetyl-NeuAc and thus has different substrate-binding specificity than BCoV and HCoV-OC43, which targets 9-O-acetyl-SA (103). The combined activity of S glycoprotein and HE is specific for human CoV attachment to SA-associated receptors on the host cell (104), but the role of HE protein in HCoV other than HCoV-OC43 is not known much. However, the HE protein of SARS-CoV-2 also acts as the classical glycan-binding lectin and receptor-destroying enzyme and may show evolutionary adaption toward recognition of O-acetylated SA and virus entry for viral–host interaction (105).

BOVINE CORONAVIRUS (BCOV)

BCoV belonging to genera Betacoronaviruses subgroup A along with swine HEV, canine respiratory CoV, feline enteric CoV,

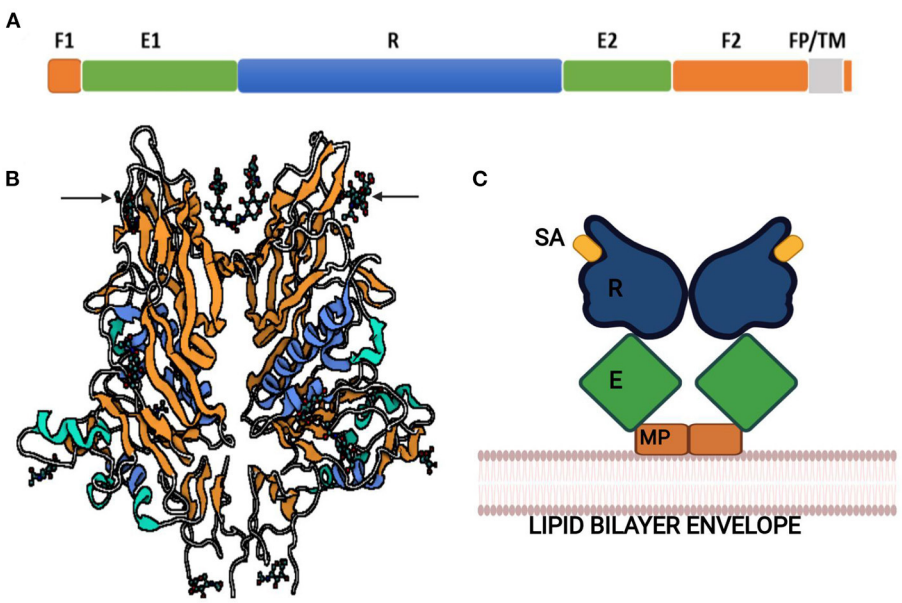

FIGURE 5 | Hemagglutinin-esterase protein of bovine coronavirus. **(A)** Linear order of sequence segments HE protein. F1 and F2, Fusion domains; E1 and E2, Enzyme domains; R, Receptor domain; FP, Fusion peptide; TM, Transmembrane domain. **(B)** Ribbon representation of HE protein. Lectin domain in orange, esterase domain in blue, and structures shown by arrows are sialic acids (sialic acid-9-O-acetylesterase) bound to lectin domain. **(C)** Schematic illustration of HE dimer. SA, Sialic acid; R, Receptor domain; E, Enzyme domain; MP, Membrane-proximal domain.

human CoV-OC43, and HKU1 is associated with three major clinical syndromes: neonatal calf diarrhea, hemorrhagic winter dysentery in adult cattle, and respiratory infections in cattle of different ages (106–118). It is an important livestock pathogen having an economic impact on the cattle industry worldwide (119). It is a leading cause of enteritis in combination with other enteric bacterial, viral, parasitic, and protozoal pathogens and is also found to be involved in the bovine respiratory disease complex in feedlot cattle since its discovery in 1993 (106). The host range includes all breeds of cattle and wildlife ruminants. The SA receptor for BCoV reflects wide tissue tropism due to the presence of sugars in abundance for interaction between viral spike glycoprotein and a specific carbohydrate receptor (102).

The BCoV variants, which are genetically and/or antigenically related, have also been isolated from other animal species along with humans representing a similar respiratory and enteric form of the disease (9, 120–123). Despite antigenic variations between different strains and interspecies transmission, only a single serotype is evident (124).

Epidemiology

Infection is probably distributed worldwide—Africa, Asia, Europe, Oceania, and North and South America (125). The virus is shed in feces and nasal secretions predominantly. A study on naturally and experimentally infected animals revealed an excess of virus load isolated from nasal swabs and massive replication in airways, whereas the fecal shedding started later (126). It is readily transmitted by the feco-oral or respiratory route indirectly and directly by direct contact or aerosols on farms, maintained by a clinically normal cow and calves where adult animals can act as carriers. Calves of 1 week to 3 months of age are highly susceptible due to inadequate maternal antibodies. The adults are usually subclinically affected, and the virus may be excreted intermittently at low titer (127).

Pathogenesis

The virus replicates in the epithelial cells of the upper (nasal turbinate, trachea) and lower (terminal bronchioles, lungs) respiratory tract: intestinal tract mainly along the lining of villi and crypts of epithelial cells. These cells are capable of resisting viruses and have the ability to replace the damaged cells (106), and thus, calves may recover from infection. The replication results in the destruction of mature absorptive cells lining the villi and mucosal surface in the large intestine, necrosis of cells in mesenteric lymph nodes and payer's patches, and subsequently viremia (125). This diminishes the absorption in the gut, failure to secrete digestive enzymes impairing the glucose and lactose metabolism and causing malabsorptive diarrhea. Pathological lesions such as marked intestinal hemorrhages and extensive cell necrosis within crypts are observed, whereas lesions of the respiratory system include hemorrhages, atelectasis, intestinal pneumonia, and emphysema (128).

Clinical Features

Infection in calves depends on age and their immune status. Coinfection with *Campylobacter jejuni*, enterotoxigenic or enteropathogenic *Escherichia coli*, and Rotavirus may expedite the severity of the disease. The morbidity rate is 20–100% in affected animals, but mortality is 1–2% depending on the level of maternally or actively derived antibodies and severity of dehydration (119). The incubation period in calves is 24–48 h, and the clinical signs include profuse diarrhea, which subsequently results in dehydration, acidosis, and death in uncontrolled cases (123). In adult animals, the incubation period is 2–7 days and is the cause of acute sporadic enteritis prevalent during winter months, thus named winter dysentery. The disease is characterized by explosive, often hemorrhagic diarrhea, anorexia, emaciation, and unthriftiness along with decreased milk production along and frequent respiratory signs including fever, rhinitis, dyspnea, rales, pneumonia in 2–6 months old calves, and serious respiratory distress followed by death (125). The pneumotropic strains of the virus in adults are the precipitating cause of the bovine respiratory disease complex that exacerbate the fatality when manifested by superimposed environmental or managemental stress.

INFECTIOUS BRONCHITIS VIRUS (IBV) IN POULTRY

Infectious bronchitis is an acute, highly contagious disease responsible for the economic impact on the poultry industry. The majority of CoV of avian species are classified into genera gamma- and delta-CoVs, within which IBV is of significance belonging to the gamma genus. Chickens and pheasants are the natural hosts but have also been detected in turkey, duck, guinea fowl, pigeon, peafowl, goose, teal, and partridge (129). IBV has a primary affinity for the respiratory system, accompanied by infection in the reproductive, renal, and alimentary systems. IBV occurs in various antigenic variants with a difference in virulence and tissue tropism as a result of mutations and recombination in its genome. The multiple serotypes of IBV based on S1 spike protein difference present a challenge in establishing an effective vaccination program, as cross-protection is found to be poor (130–132).

Epidemiology

The distribution is worldwide, but some may have restricted geographical spread where different antigenic variants can co-circulate in a given region (133). It is of significant concern in poultry industries due to poor weight gains in broilers and suboptimal downgrading of egg production in layers (134). Birds of all ages are susceptible to the infection, but the severity and clinical signs may vary (135). In the acute phase of infection, IBV is copiously shed in respiratory secretions, tracheobronchial exudate, and feces and is spread by aerosols, ingestion of contaminated feed, drinking water with feces, and indirect transmission between birds at the farm over long distances through fomites (136). The vertical transmission is not clearly understood; however, the virus was isolated from day-old chicks and recovered from the semen of cockerels after inoculation (137, 138). The excretion and persistence of some strains of virus for a considerable time in target sites such as kidney

or alimentary tract, particularly cecal tonsils followed by re-excretion, is suspected to be influenced by adverse environmental or changed physiological conditions, which suggests carrier state or latency (134). The strain of virus, route of exposure, age, diet, nutrition (level of calcium), and external factors such as cold stress in winter, poor ventilation, and coinfection with enteric bacteria provoke the disease; also, breed factor, such as some heavier birds become more susceptible, may be related to immune response (129). Although the morbidity rate is high as 100%, the mortality rate can vary from 20 to 30% and more depending on vast tissue tropism, secondary bacterial infection, and standards of management in an infected flock (139).

Pathogenesis

The initial replication occurs in ciliated epithelial cells of the respiratory tract, which cause histopathological lesions mainly in the trachea, such as ciliary loss, desquamation, epithelial hyperplasia, edema, marked lymphoplasmocytic inflammation, and mononuclear and heterophilic cell infiltration of the submucosa, which resumes in 14–21 days after infection (140, 141). A succinct viremia within 1–2 days eventually leads to extensive spread to the reproductive system, kidneys, and intestinal tract, but the damage is minimal, and bursa of fabricius may be the cause of immunosuppression. The main attachment factor for IBV is the receptor-binding domain in S1 spike glycoprotein and SA glycans (142, 143) widely distributed in host tissues; thus, variation in the glycoprotein and glycans partly determine the virulence, tissue binding, and tropism. The gross pathological findings include congested respiratory tract with serous or catarrhal exudate in nasal passages, trachea, extrapulmonary bronchi, and air sacs. The main bronchi get blocked with caseous casts in young chicks, the probable cause of death. The epithelial cells of the oviduct, mainly the goblet cells, become cuboidal, hypoglandular oviduct, ovarian regression, and congestion; sometimes, the ova may rupture, resulting in free yolk in the abdominal cavity (144, 145). Extensive tubular degeneration, interstitial inflammatory response characterized by the pale, enlarged, or marbled kidney, ureters distended with deposits of urates, and large uroliths are seen in the chronic stage of nephritis (141, 146, 147). Certain IBV strains also induce pathological lesions in deep and superficial pectoral muscles, i.e., bilateral myopathy in broilers and breeders (148).

Clinical Features

The incubation period is 18–48 h; the course of the disease lasts for 5–7 days and, in outbreaks, up to 14 days (146, 149). Chicks with an age of 2–6 weeks are severely affected, although birds of all age groups are susceptible. The main three clinical manifestations are respiratory, reproductive disorder, and nephritis (134). The most conspicuous clinical findings are the initial respiratory signs—gasping, tracheal rales, dyspnea, swollen sinus, conjunctivitis, profuse lacrimation, cellulitis of periorbital tissues, and coughing with or without nasal discharge. This is followed by lethargy, ruffled feathers, anorexia, rapid weight loss, stooped stance, scouring, excessive water intake, and characteristic wet litter implying nephritis. The reproductive disorder shows signs of rales followed by a marked decline in egg production up to 50–70%, usually within 8–12 days, which differs depending on the stage of lay at infection, hampering the hatchability rate (150). The external and internal quality of the egg is highly affected, exhibiting misshapen eggs, thin, soft, or no shell, ridging and distortions, watery albumen, which may resume within 8 weeks or more. It may also lead to permanent damage to immature oviduct resulting in so-called false layer syndrome, as the layers or breeders never resume the loss of egg production. The concurrent secondary infection with *E. coli*, avian mycoplasma species, etc., or nephropathogenic strain of IBV may expedite the infection causing air-sacculitis and interstitial nephritis (151). Chicks may die suddenly by occlusion in bronchi as a probable cause of death.

PORCINE CORONAVIRUSES

Transmissible Gastroenteritis Virus (TGEV)

Among few porcine CoVs known, the clinical disease is mainly associated with the TGEV. It is highly contagious among young pigs and is found to be a significant cause of economic loss more in breeding herds than the rearing and finishing herds, primarily due to piglet mortality (152). The porcine epidemic diarrhea virus (PEDV) is clinically similar but serologically unrelated to TGEV and comparatively spreads slowly in the herd (11). The porcine respiratory coronavirus (PRCV) is a non-pathogenic respiratory variant of TGEV (153, 154). It can cause subclinical mild respiratory disease and serologically cross-reacts with TGEV, but tests are available to distinguish them. These porcine CoVs are grouped in genus Alphacoronavirus; however, a new porcine delta-CoV genetically distinct from TGEV and PEDV associated with enteric disease in pigs has recently been found (155).

Epidemiology

TGEV is reported all over the world, affecting the global pork industry (156). It spreads between and within farms by shedding infected feces for up to 2–3 weeks. The virus may also spread through fomites, aerosols at least for short distances, or mechanical spread by animals, insects, or birds, particularly starlings and in milk or feces to the piglets (157). The infection occurs throughout the year but mainly follows a seasonal pattern with a higher incidence in colder months (158). Infection results in two different clinical presentations: epidemic and endemic (159). In epidemics, when a virus enters a naive herd, pigs of all ages are affected, particularly the newborn piglets, whereas the infection is self-limiting in farrowing and finishing herds. The endemic disease is observed in farms after the epidemic phase due to incomplete all-in-all-out management or continuous movement of naive gilts in breeding farms. TGEV can end up showing mild disease, thus presenting high morbidity up to 100% in neonatal piglets but low mortality (11).

Pathogenesis

The virus enters through the oro-nasal route and replicates in enterocytes of the small and large intestines. The replication causes shortening and blunting of villi, mainly in jejunum and ileum, due to the segmental nature of lesions followed by

malabsorption, disruption of cellular transport of nutrients and electrolytes, and increased osmolarity, thinning of the gut wall, and diarrhea (160, 161). The crypts of epithelial cells usually remain uninfected; thus, recovery of function of villi is rather rapid. In neonates and piglets, a combination of these factors coupled with the slow regeneration time of epithelial cells results in death. TGEV has also been found to replicate in extra-intestinal tissues, including lungs and mammary gland, causing imprecise pneumonia and agalactia, respectively (162, 163).

Clinical Features

The incubation period is short 12 to 72 h, i.e., up to 3 days (164). TGEV presents a mild disease except in piglets ≤3 weeks of age that may succumb to death and in sows infected at or near farrowing. Vomition is the initial sign in a non-immune herd followed by profuse watery diarrhea, rapid dehydration, weight loss, marked thirst, and agalactia with recovery within 5–10 days (11, 165). As the disease progress in unweaned piglets, feces often contain curds of undigested milk and may approach 100% mortality due to the slow replacement rate of villous cells. The course of disease in porcine CoV infections does not exceed 3–4 weeks normally due to rapid herd immunity; thus, the mortality is low, but morbidity is high (159). In some herds, the TGEV remains subclinical, although there may be short episodes of clinical reemerging infection particularly due to the purchase and replacement of breeding pigs and their litters.

FELINE CORONAVIRUSES

Feline CoVs are classified into two biotypes based on the pathogenicity referred to as feline enteric coronavirus (FECV) and feline infectious peritonitis virus (FIPV) belonging to genus betacoronavirus and alphacoronavirus, respectively. Higher sequence similarity in both the biotypes indicates a close relationship but with distinct virulence properties (166–169). The FIPV is primarily observed in a cat population that is tenaciously infected with FECV (170, 171). These recurrent observations and animal experiments have led to the widely accepted theory of "internal mutation" that suggests an evolution of FIPV from non-pathogenic FECV by specific mutation(s) occurring in the viral genomes (172–179). The sequence differences in spike and membrane protein, mutations in theS1/S2 locus, furin recognition site, and disrupted NSP3c genes may further contribute to the risk of FIP in the individual (180). However, very less is known about the stage at which mutation(s) occur during the development of FIP. The FCoVs are further separated into two serotypes based on the serological properties of the virus (181). Some independent studies provide constant evidence that the emergence of serotype II viruses is *via* double homologous recombination between serotype I FCoV and canine enteric coronavirus (CCoV) (170, 182–186). Both serotypes I and II can cause FIP and clinically inapparent FECV infections.

Epidemiology

FCoV infection is widely disseminated in the domestic and wild feline population. The seropositivity varies from 20 to 60% and approaching up to 90% in domiciled cats, multi-cat households, catteries, and animal shelters, according to the global data (171, 187–189). The serotype I FCoVs are mostly responsible for natural infections (187, 190–192). Serotype I FCoV strains are vastly isolated from the United States and Europe (80–95%), whereas serotype II predominates in Asia in up to 25% (192–196) analysis. The seroprevalence studies had demonstrated high incidences and seropositivity in cats from 3 months to 3 years old and in adult individuals (190, 197, 198). There is no significant difference in seropositivity related to sex and breed of cats; however, genetic predisposition can affect the reproductive condition, hereditary factors and systemically manifest the disease (171, 199). FIPVs in animals are less likely to be transmitted horizontally, and infection due to contact with feces from diseased cats (172, 178, 200–202) is thought to be limited. However, immunosuppression favored by stress or coinfections with feline immunodeficiency virus and feline leukemia virus may trigger the progression of FIP in some cases (171). In contrast, FECV is highly contagious and transmitted horizontally through the fecal–oral route (167, 171, 188). The infected cats can continually shed FECVs in their feces for a longer period and even in postinfection, which may last for several months but with low virus load (167, 203).

Pathogenesis

The main site of FECV replication is the apical epithelium of the villi from the lower portion of the small intestines extending to the cecum (167, 203). In addition, the viral RNA can be recovered from blood and different tissues as well, suggesting the capability of FECV to infect peripheral monocytes, albeit less efficiently (179, 203–207). FIPV presents an altered cell tropism and infects both monocytes and macrophages (170, 206, 208, 209). The distribution of macrophages in the body results in viral dissemination from the intestine to the spleen, liver, and central nervous system. Thus, it is considered as an immune complex disease involving activation of these cells (210) and expression of tumor necrosis factor-α, interleukin-1β, adhesion molecules, matrix metalloproteinase-9, vascular endothelial growth factor, vasoactive amines, and inflammatory mediators (210–217). These factors, along with less susceptible leukocytes activated by an unknown mechanism during FIPV infection, induce capillary endothelial cell retraction, increased vascular permeability, and hence protein-rich effusion in body cavities (218, 219). Therefore, the FIPV infection is characterized by fibrinous and granulomatous serositis, protein-rich serous exudates in body cavities, and/or pyogranulomas (213, 220–223).

Clinical Signs

The infection caused by FECV remains persistent and asymptomatic and/or induces mild and transient diarrhea and occasionally causes severe enteritis (224). Feline infectious peritonitis is an immune-mediated, systemic, and fatal disease (190). The infection can be clinically distinguished into three forms based on the presence or absence of protein-rich effusions in the pleural and abdominal cavities—wet (effusive), dry (non-effusive), and a combination referred to as mixed form (171, 188, 213, 225, 226). The clinical progression of the disease

is believed to be dependent on the host cellular and humoral immune responses. The wet form is associated with weak cellular but robust B cell responses, whereas the dry form is caused by strong T cell immune responses (171, 188). It has been observed that wet form is more prevalent in natural infections than other forms and frequently develops in the terminal stage of dry form resulting in subsidence of the immune system (171, 188). The wet form is characterized by abdominal, thoracic, or pericardial effusions leading to fluidic waves in the abdomen, visceral and omental adhesions or enlarged mesenteric lymph nodes, dyspnea, or tachypnea, cyanotic mucous membranes, and muffled sounds in the lungs and heart. The dry form is characterized by granulomatous changes in several organs, including the central nervous system and the eye. The ocular lesions include white sheathing of retinal vasculature, mild uveitis, keratin deposition in the cornea, and hemorrhages in the anterior chamber and retina. In cats with FIP, the neurological signs are variable and can induce multifocal lesions. Ataxia with subsequent seizures, tremors, nystagmus, incoordination, and hyperesthesia is the most common clinical sign. When FIP lesions are associated with cranial nerve, visual impairment and loss of menace response are observed, whereas lameness or paresis can be seen in peripheral nerve involvement.

CANINE CORONAVIRUSES

CoVs of Canidae family fall in two groups— CCoV in group 1 alphacoronavirus and canine respiratory coronavirus (CRCoV) in group 2 betacoronavirus. CCoV has been described since 1971 (227) and exists in two closely related serotypes—CCoV-I and CCoV-II based on random point mutations and recombination associated with the spike protein and distinct serological properties (182). Type I and II CCoVs and FCoVs have been proposed to be closely related based on their evolution through recombination events from a common but unknown genetic source (186, 228). CCoV-II can be further classified into CCoV-IIa and CCoV-IIb as a result of the recombinant origin of CCoV with NTD of spike protein homologous to TGEV (229, 230). A novel CCoV with CCoV-I- or FCoV-I-like NTD was discovered in 2014 and was referred to as CCoV-IIc but has not been classified into any clade yet (231–233). CCoV generally causes mild and self-limiting diarrhea with low mortality and high morbidity (234, 235). Virulent and pantropic strains of CCoV causing severe enteric and fatal systemic diseases in the absence of coinfection with canine adenovirus type I and canine parvovirus type 2 have also been reported (236–244). Therefore, CCoV is now considered a significant pathogen in the dog population due to its ability to evolve into variants with altered tissue tropism and pathogenicity.

CRCoV was newly recognized in 2003 from the tracheal and lung samples of dogs facing enzootic respiratory disease (9). It is one of the members of multiple etiologies causing canine infectious respiratory disease along with canine parainfluenza virus, canine *adenovirus (CAV) type 2*, *canine herpesvirus and canine influenza virus*, *Bordetella bronchiseptica, Streptococcus equi* subsp. *zooepidemicus*, and *Mycoplasma* spp (245, 246). CRCoV was found to carry an additional gene encoding for HE protein; thus, it shows high sequence identity up to 98% with BCoV and human CoV OC43 along with similarities in spike protein and polymerase gene sequences (9, 247).

Epidemiology

Both CCoV and CRCoV are common infections of the canine population with worldwide distribution (121, 248–258). Single, as well as multiple infections, have been reported with more than one genotype of CCoV that indicates co-circulating of CCoV–I, CCoV-IIa, and CCoV-IIb strains in prevalent regions (259). Canine CoVs are highly prevalent in dogs living in dense populations such as shelters, kennels, or grouped environments and thus exhibit rapid transmission through feco-oral and naso-oral routes (260). Dogs are likely to act as clinically normal carriers maintaining the infection in the canine population due to long time shedding of CCoV after postinfection and clinical resolution (261, 262). Apart from the domestic dogs, canine CoV infection has also been reported in foxes, wolves, and raccoon dogs (263, 264). The infection occurs throughout the year in dogs, whereas CRCoV is frequently detected during the fall to winter months (265). Canine CoV infections can occur in all age groups, significantly more in young puppies for CCoV in contrast to CRCoV, which is most prevalent in dogs more than 1 year age (254, 255).

Pathogenesis

The pathogenesis of CCoV is similar to that of other enteric pathogens. It replicates in the apical and lateral mature epithelial cells of intestinal villi resulting in villous atrophy and consequently malabsorption and diarrhea (233). The severe form of enteritis represents gross pathology as moderate, diffuse, segmental hemorrhagic and necrotic enteritis, ileo-cecal intussusception, along with infiltration of lymphocytes and plasmacytes (244). Systemic infection caused by pantropic CCoV produces lesions in several organs, including infarction in the renal cortex, fibrinopurulent bronchopneumonia, fatty change in the centrilobular zone of the liver, multifocal hemorrhages in the spleen, and depletion of gut-associated lymphoid tissue (266).

The pathogenesis of CRCoV is mainly associated with the trachea, nasal cavity, and nasal tonsil with less severity in the lower respiratory tract. It causes distortion of the ciliated respiratory epithelium and infiltration of inflammatory cells resulting in failure to clear the particulate matter in the lungs, bronchi, etc., (267). The virus has also been isolated from the colon, mesenteric lymph nodes, and spleen (121, 257). This suggests dual tissue tropism similar to BCoV, although the ability to replicate in tissues other than the respiratory tract needs further investigation. Furthermore, the possible interaction of multiple pathogens during the canine infectious respiratory disease complex needs to be considered as contributing factor in the pathogenesis of CRCoV.

Clinical Signs

CCoV generally causes mild and self-limiting diarrhea in dogs. The severity of enteric disease increases when infected with

multiple pathogens or pantropic strains (CCoV-IIa biotype) of CCoV. The clinical signs thus include gastrointestinal distress, hemorrhagic diarrhea, along with neurological signs (268, 269). The infection with CRCoV exhibits common and mild clinical signs associated with the upper respiratory tract, including sneezing, coughing, and nasal and ocular discharge (267), which may progress to bronchopneumonia and multisystemic illness depending on the involvement of other organs.

DIAGNOSIS OF ANIMAL CORONAVIRUSES

Enteric and respiratory infections of CoVs are mainly associated with the shedding of the virus through feces and nasal secretions, respectively. The clinical samples for diagnosis include feces, intestinal contents, nasal secretions, tracheobronchial lavage fluids, and postmortem specimens comprising of nasal, pharyngeal, tracheal, lungs, and tissues from different regions of the gut focusing primarily on the distal small intestine. In addition, trachea, kidney, proventriculus, tonsil, and oviduct specimens for IBV and aqueous humor, whole blood and fine-needle aspiration, a biopsy of the liver, spleen, and mesenteric lymph nodes for FIP are obtained for diagnosis depending on the clinical presentation of the animal. Direct detection of virus in clinical samples by transmission electron microscopy, immunofluorescence, immunoperoxidase, or immunohistochemical staining of tissues using hyperimmune antiserum or monoclonal antibodies provides definitive diagnosis (171, 213, 221, 270–284). Immunohistochemistry using an antibody directed against BCoV can also help in detecting CRCoV (285). The laboratory tests using effusions have more diagnostic value than blood tests for FIP (286, 287). Cytological and macroscopic examination, along with cell count and biochemical properties of effusions, can be carried out for differential diagnosis (283, 286, 288–290). A simple, quick, and inexpensive "Rivalta's test" with more than 90% sensitivity and 66–81% specificity for differentiating transudate from an exudate can be useful to exclude FIP and rule out other causes for the effusions (287, 291).

Tracheal organ culture, McClurkin swine testicle (ST) cell line, human rectal tumor HRT-18 cells, Vero, and other cell lines derived from specific host species can be used for primary and secondary virus isolation and propagation favoring syncytia, plaque, or cytolysis induction (111, 112, 116, 118, 231, 291–297). To improve the detection of the typical cytopathic effect, it may require the addition of pancreatin or trypsin to the cell culture along with additional blind passages. The allantoic cavity of 9–10-day-old chicken embryo inoculated with IBV-infected material exhibits curling and dwarfism as characteristic IBV lesions observed in the embryo (298, 299). On the other hand, virus isolation of CCoV-I and CRCoV is often unsuccessful and, even if achieved, does not produce cytopathic effects (121, 183, 184).

Serological assays such as enzyme-linked immunosorbent assay (ELISA), virus neutralization test, immunofluorescence antibody test, rapid immunochromatographic tests, and blocking ELISA using monoclonal antibodies to differentiate between strains and serotypes of particular CoV are used (300–309). Serological tests are of limited value in IBV, CCoV, and FCoV, as they fail to discriminate between several serotypes. The BCoV antigens can also be used against canine sera instead of CRCoV in ELISA, serum neutralization, or hemagglutination inhibition test (9, 238, 256). The supernatant from CRCoV-infected cell culture was able to agglutinate chicken erythrocytes at 4°C, which means that hemagglutination assays can be optimized to detect CRCoV (310).

The highly sensitive molecular assays including serotype-specific reverse transcription-polymerase chain reaction (RT-PCR), nested PCR, real-time quantitative RT-PCR using conserved gene regions—UTR, N-gene, S1 gene, or HE gene (257), reverse transcription loop-mediated isothermal amplification assay, reverse transcription recombinase polymerase amplification assay, pan CoV RT-PCR are used providing high detection rates than other assays (176, 261, 286, 302, 311–339). The next-generation sequencing to decipher the whole genome within a short period is currently being used in advanced laboratories (340, 341).

NOVEL DIAGNOSTIC TOOLS

With an increasing rate at which serious infections with new variant strains of human CoVs, especially SARS-CoV-2 spread, the need was felt to deploy rapid, accurate, and precise diagnostic tools for laboratory and point-of-care (POC)-based settings. This includes nucleic acid amplification testing such as the centralized laboratory-based real-time RT-PCR (the current gold standard for etiological diagnosis), rapid POC based tests such as lateral flow assays, rapid serological (antibody or antigen) tests, LAMP test, and serological assays such as ELISA and automated EIA (342–345). Some novel strategies for SARS-CoV-2 detection include CRISPR/Cas (reliable on-site diagnostic method)-based paper strip test, matrix-assisted laser desorption/ionization time-of-flight mass spectrometry combined with artificial intelligence, surface-enhanced Raman scattering spectroscopy, metabolomic approaches, aptamer (third-generation molecular probe)-based diagnostic tests, proteome microarray, optical biosensor, antigen-Au/Ag nanoparticle-based electrochemical biosensor, and surface plasmon resonance (346–350). Despite rapid refinement in existing tools and deployment of novel strategies, the advancement in diagnostics of animal CoVs comparatively fall behind and mostly rely on clinical diagnosis, detection, and titration of CoV particles (plaque assay, electron microscopy, and transmission electron microscopy), detection of CoV antibodies (ELISA and EIA), detection of CoV antigen (monoclonal- and polyclonal-based ELISA, rapid Ag detection tests, immunofluorescence, and immunochromatographic assays), and nucleic acid-based assays (RT-PCR, real-time PCR, and loop-mediated isothermal amplification-PCR). Although these molecular and serology-based methods provide accurate results, they require well-trained technicians, specific types of equipment, and ample time and effort and are not convenient for use on farms or by breeders. For this purpose, various studies have been undertaken to develop efficient and

appropriate diagnostic tools for animal CoVs as has been seen with SARS-CoV-2. The diagnosis for a newly identified pathogen, porcine delta CoV, was made possible by developing a cost-effective fluorescent microsphere immunoassay as used for PEDV (351) that could detect antibodies against multiple target antigens of porcine delta CoV for better efficiency and sero-surveillance on a herd level (352). Recently, a europium (III) chelate microparticle-based lateral flow test strip was developed for identification and epidemiological surveillance of PEDV with high reliability and sensitivity (353). A novel multiplex PCR-electronic microarray assay for rapid and comprehensive detection of bovine respiratory and enteric pathogens, including BCoV, was also developed (354). A highly specific plaque reduction neutralization test was combined with two sensitive molecular methods: real-time RT-PCR and Sanger sequencing, to investigate SARS-CoV-2 infection in cats and dogs in Brazil (355). Similarly, a Luciferase Immunoprecipitation System assay using the fragments of spike protein and nucleoprotein as antigens was used to detect antibodies against SARS-CoV-2 in dogs and cats and MERS-CoV in dromedary camels and monkeys (356–358). For Luciferase Immunoprecipitation System assay, there is no need for a BSL-3 laboratory set up and species-specific labeled secondary antibodies for detection as required for other tests such as microneutralization, immunofluorescence assay, and the plaque reduction neutralization test. Moreover, many researchers have envisaged the use of lateral flow assays for diagnosis and pseudovirus-based neutralization assay for evaluation of antiviral mechanism for SARS-CoV-2 in animals as well (359, 360). As far as the specific and sensitive diagnosis of animal CoVs is concerned, currently available methods might not resolve the unprecedented challenges associated with CoVs due to rapid mutations, interspecies jumps, and the emergence of new variants. This warrants continual efforts to develop robust, sensitive, and rapid tests, POC devices, and multiple diagnostic techniques to achieve a cost-effective and multidimensional diagnostic efficiency for clinical and epidemiological investigations.

NOVEL VACCINATION STRATEGIES

The CoV infection in animals is routinely managed by the whole cell-based inactivated or modified live vaccines (361–370). The inactivated vaccines give rise to a high titer of circulating antibodies, whereas modified or attenuated live vaccines provide stimulation of cell-mediated immunity and accelerate IgA response against local mucosal infection and thus are of more value to commercial farms. The protection against animal CoVs is mainly dependent on IgA production; thus, parental vaccination is not favored generally in many of these infections (362, 371–373). The intranasal vaccination in adult cattle entering the feedlots using live attenuated enteric CoV against diverse field strains causing BCoV infections has been suggested as an ideal strategy to develop a protective immune response at the site of entry (oro-nasal) of the virus (123). Currently, the attenuated live vaccines used in broilers, layers, and brooders provide relatively inferior protection due to the presence of several serotypes of IBV and poor cross-protection. Therefore, a protectotype vaccine strategy based on shared antigens among variants has been proposed based on knowledge about serotypes, immunity, and the prevalence of variant strains of IBV (374). These protectotypes are quite effective in inducing cross-protection against heterologous serotypes (375). The feline CoV vaccination may enhance the risk of immune-mediated FIP; therefore, activation of IgA response is more relevant than IgG production. The administration of a modified live intranasal vaccine (temperature-sensitive), which activates IgA in the oropharynx as a consequence of replication of a temperature-sensitive mutant of the FCoV strain, is found to be more effective in FCoV (362). Canine CoV infection is mild and self-limiting and thus discourages the wide application of vaccines even if inactivated and live attenuated vaccines have been successfully developed for CCoV (369). In an experimental trial, a beta-propiolactone-inactivated MF59-adjuvanted vaccine was developed against the CCoV/TGEV recombinant, which failed to prevent the shedding of the virus totally but was considered to be safe (376). Novel experimental vaccines for TGEV and PEDV such as plasmid-vectored DNA vaccines encoding S, N, or M (377, 378) and recombinant vaccines or vectored vaccines using engineered swinepox virus or porcine adenoviruses to deliver the TGEV spike protein (379) were also developed. These vaccines were efficient in inducing both a systemic and a local humoral immune response with sufficient neutralizing antibodies. An RNA vaccine derived from Venezuelan equine encephalitis replicon expressing the PEDV spike gene was also developed against PEDV infections (379). Subunit vaccines have also been developed in an effort to express the S1 domain of spike protein in Baculovirus, yeast, or plant-based delivery system and have been found to work well in pigs (380–382). The oil adjuvanted vaccine comprising of a solubilized cell extract of BCoV-infected cells overexpressing viral hemagglutinin of BCoV was developed by Takamura et al. (383). This induced high hemagglutinating antibody titers without any adverse effects and was suggested to prevent winter dysentery in dairy cows (383). It is possible to combine two or more immunogenic strains of protectotype candidate against animal CoVs in a single vaccine with combined benefits such as the stimulation of cell-mediated immunity and higher IgA production for local mucosal immunity. Animal CoVs such as PEDV and IBV undergo frequent genetic shifts, and as a result, the protection level remains low despite using innovative vaccine strategies. Also, the vaccination in animals provides relatively a short duration of protective immunity with low efficacy due to focus mainly on whole-cell preparations rather than specific proteins or antigens for developing vaccines. Hence, effective and safe vaccines providing long immunity in animals still remain elusive. The scientists working on developing veterinary vaccines must take a cue from innovative and successful emerging technologies being used in developing SARS-CoV-2 vaccines so that suitable prophylaxis also becomes available for animals.

INTERSPECIES TRANSMISSION AND ZOONOTIC POTENTIAL OF ANIMAL CORONAVIRUSES

Interspecies Transmission

CoVs are capable of producing a broad spectrum of disease outcomes in mammals and avian species. These viruses are well-recognized to alter their tissue tropism and cross interspecies barriers to adapt to various ecological niches for abundance and persistence. The RBD of CoVs can recognize the same receptor present in multiple animal species. These virus–receptor interactions, evolutionary selection, and viral genetic diversity by frequent homologous recombination, inherent point mutations enable the virus to jump the species barrier and rapidly adapt to a new host species. It has been observed that CoVs, apart from infecting their primary host, do cause occasional infections in other animal species, *per se* dog and cat CoV, pig CoV, and TGEV can cross-infect, resulting in different disease outcomes suggesting host range mutants of an ancestral CoV. The BCoV is an excellent example that crosses interspecies barriers. Variants having genetic and antigenic relatedness with BCoV have been identified in the respiratory secretions of dogs infected subclinically (121–123), humans (120), and diverse groups of other domestic (124) and wild ruminant species such as camelids, waterbuck, sambar deer, white-tailed deer, and giraffe. Moreover, it can experimentally infect and cause enteric diseases in avian hosts, including turkey poults (384) that were found to transmit viruses to the control birds. These variant strains with established cross-species transmission are termed as Bovine-like CoVs (385) and classified as host range variants rather than a distinct virus. Furthermore, the BCoV has also been shown to procure new genes *via* recombination, i.e., acquisition of an influenza C-like hemagglutinin that may have a possible role in binding to different cell types (386).

An amino acid composition of APN receptor of human, feline, and porcine CoVs shows strong 78% identity. However, the APN receptor used by α-CoVs is species-specific, and the feline APN is a functional receptor for other members of α-CoVs, including FIPV and FECV, TGEV, canine CoV, and HCoV-229E. Due to this property of feline APN, cats can get infected by TGEV, CCoV, or HCoV-229E with or without developing symptoms. Similarly, the sequence comparisons reveal that TGEV has resulted from the host species jump of CCoV-II from dogs to pigs (40). The generation of less virulent porcine respiratory CoV from TGEV by spike gene deletion (153, 154) accounted for altered tissue tropism from the enteric to the respiratory system (387). The FIPV type II and CCoV-IIb strains from double recombination events between FIPV type I-CCoV and CCoV-II-TGEV, respectively, are also the results of genomic characteristics within CoVs for rapid adaption to novel CoV species suggesting coinfection in at least one host species.

A chimeric virus with spike protein of PEDV and backbone of TGEV was identified as a variant genotype of TGEV strain with unique deletions and distinct amino acid changes similar to PRCV, suggesting a recombination event between the variant TGEV, PEDV, and PRCV (388–391).

Zoonotic Link Between Human and Animal Coronaviruses

In humans, CoVs can cause infections ranging from the common cold to highly pathogenic diseases such as SARS and MERS. The seven human CoVs known to date are HCoV-229E, HCoV-NL63, HCoV-OC43, HCoV-HKU1 causing mild symptoms, and the highly pathogenic MERS-CoV, SARS-CoV, and SARS-CoV-2 causing adverse lower respiratory tract infection. The phylogenetic analysis has shown that bats, mice, or domestic animals serve as gene sources for all the seven HCoV (392). The HCoVs triggering common cold circulate in the human population without any need of an animal reservoir, whereas SARS-CoV and MERS-CoV need to maintain and propagate in their zoonotic intermediate host for possible transmission to human targets. Also, the frequent crossing of species by CoV has led to the emergence of important human pathogens. The key determinants for CoV–host specificity, such as variability in spike glycoprotein, its RBD in different species, and identical nucleotide sequence, provide a framework to understand the switch of hosts and positive selection during inter- and intraspecies transmission events.

The complete genome sequence analysis suggests that BCoV is possibly related to HCoV OC43 (50). It is believed that an interspecies jump was responsible for this genetic similarity, albeit there are no case reports suggesting infection resulting in disease by BCoV in humans. The findings of various studies suggest cross-protection among HCoV and BCoV and evidence of viral RNA in the human nasal mucosa for a short duration after exposure to BCoV (393). A human enteric CoV strain HECV-4408 isolated from a child suffering from acute diarrhea was passaged four times in HRT-18 cells and was inoculated orally in four gnotobiotic calves followed by challenging with BCoV-DB2 strain. The calves inoculated with HECV-4408 developed diarrhea and mild clinical signs along with detection of virus in the feces and nasal shedding by RT-PCR, whereas after BCoV inoculation, no diarrhea or virus shedding was observed in the calves. This experiment fairly suggests that (i) the less severe clinical signs in calves inoculated with HECV-4408 may be due to naturally lower virulence of HECV in calves or that the virulence was altered by a passage in cell culture, as it affects the efficiency of agglutination of RBCs (120, 127), its intestinal replication (128), antigenic composition (394), and associated mutations in the genome (395). (ii) Fecal and serum IgG titers were detected, which either remained the same or increased 2-fold after the challenge. This indicated that the HECV-4408 inoculation developed a protective immune response such that no replication of the virus was observed after challenging with the BCoV-DB2 strain.

There is no risk suspected yet to the public health from IBV. Humans are not considered as a reservoir for replication of IBV. There is no evidence of transmission of virus between humans and from humans to animals. Various mechanical means leading to infections in chicks have been reported. The persons working in commercial poultry farms may be at risk of getting an infection, but the significance is not known (396). IBV has also been detected in wild birds, which may serve as a

vector for transmission between free-living and domestic birds (397). Therefore, the wild birds could feature as essential for recombination events that may further lead to the emergence of variants of concerns for humans. The isolation of avian IBV such as viruses from a man with a morphological resemblance with 229E strain of human CoV was reported, which was later confirmed to be an isolate of HCoV and not otherwise (398). This illustrates a likely possibility of the origin of avian and human CoVs from a common gene source resulting in divergent evolution.

The PEDV is genetically closely related to HCoV-229E than to other α-CoVs, and it can also be cultured in Vero cells such as SARS-CoV (399). It is relevant to mention that the swine had always been a predominant species for the evolution of outbreak-causing viruses such as new strains of influenza A virus and are also found to be infected by bat CoVs. The role of pigs and the possibility of the emergence of new strains of viruses, including human CoVs, should not be overlooked and need explorative studies (32, 400, 401). However, Shi et al. (402) had reported that there is no significant susceptibility of pigs to SARS-CoV-2.

The wild mammals and birds harbor CoV resulting in undetected transmission. Genetically similar human CoVs were identified in civets, raccoons, and horseshoe bats (403), and an experimental infection caused disease in macaques, ferrets, and subclinical infection in cats (404, 405). The CoVs in these animals show nucleotide sequence homology (88–90%) with other HCoVs and use ACE2 receptors to bind to spike glycoprotein for entry as seen with SARS-CoV and SARS-CoV-2 (406, 407). These findings suggest their role as intermediate or reservoir hosts. Bats are found to be reservoir hosts for pathogenic HCoV but not as immediate hosts due to few sequence divergence (408). Similarly, the highest genome sequence homology has been found in RBDs of SARS-CoV-2, pangolins, and bats, but still, there is no direct supportive evidence for their origin from a common ancestor, and thus, the evolutionary pathway remains obscure (392). However, a study on analysis of the evolutionary origin of SARS using phylogenetic analysis suggested an avian-like origin for nucleocapsid and matrix protein, mammalian-like origin for replicase proteins, and a mosaic of mammalian–avian-like origin for spike protein. The spike gene was also subjected to a bootscan recombination analysis that revealed high nucleotide sequence similarity between the SARS virus and FIPV (409).

MERS also serves as another example where interspecies transmission is important. The dromedary camels of Middle East countries in Asia and Africa, such as Egypt and Qatar, were detected with MERS-CoV isolated from their nasal swabs and were found seropositive with neutralizing antibodies for MERS-CoV species (410–416). Also, the study on experimental MERS infection in camels revealed massive shedding of a large amount of virus through not only respiratory route but also feco-oral route and milk, suggesting the risk of foodborne transmission to humans and occupational exposure (417–419). This indicates that the camels serve as the *bona fide* reservoir host of MERS-CoV. In a case report, the full genome sequences of two isolates obtained from a dromedary camel with rhinorrhea and a human in close contact with the camel were identical and positive for MERS-CoV RNA (420). The rate of secondary transmission within humans is also observed to be low, only up to 5% (421). A case of a 39-year-old male who developed fever and cough with a history of close contact with dromedary camels at his farm tested positive for MERS-CoV by RT-PCR (422). However, other study reports suggest there is no contact history with camels before the onset of symptoms in many confirmed cases of MERS in humans (423), which attributed to either human-to-human transmission or other transmission routes involving unknown animal species paving the way for further investigations.

The phylogenetic analyses on the molecular level reveal that SARS-CoV-2 is close to SARS-CoV with bat origin and shares 50–51.8% and 79% identity with MERS-CoV and SARS-CoV, respectively (32, 424–426). The recent reports on the detection of SARS-CoV-2 with mild respiratory illness in animals such as cats, dogs, and tigers in contact with humans suggest true infection caused by human-to-animal transmission (427). The two dogs reported from Hong Kong and a dog in New York living in close contact with their SARS-CoV-2 positive owners tested positive through RT-PCR in both nasal and oral samples (428–430). Seroconversion in dogs was observed when the blood samples were tested in the later stages, with weak positive results indicating low viral infection that resulted in the production of antibodies against SARS-CoV-2. Similarly, cats can be found susceptible to SARS-CoV-2 through experimental inoculation and can spread infection through droplets (402, 431). A serological study on the immune response of cats against SARS-CoV-2 revealed high titers of neutralizing antibodies (432). The big feline such as tigers in proximity to asymptomatic positive zookeepers of Bronx Zoo in New York City tested positive for SARS-CoV-2 after showing mild respiratory symptoms (433). Recently, two cases of human-to-cat transmission of SARS-CoV-2 were identified during a screening program of a feline population of households in the United Kingdom (434). The first case of transmission of SARS-CoV-2 from an asymptomatic human carrier, probably caretakers, to eight Asiatic lions at Hyderabad's Nehru Zoological Park was reported in India (435).

The high percent identity between feline and human ACE2 protein sequences, particularly within the receptor-binding interface region, may explain the incidence of cross-species transmission between them. The ferrets were also found to harbor SARS-CoV-2 infection with isolation of virus from the upper respiratory tract and development of mild clinical signs during experimental investigations (402). Therefore, SARS-CoV-2 infection in these companion animals demonstrates their susceptibility under natural and experimental settings. Other farmed animals such as minks, when infected with SARS-CoV-2, may show respiratory and gastrointestinal signs with increased mortality (436, 437). There is evidence that SARS-CoV-2 has evolved at the genetic level into a variant strain in minks in Denmark, and mink-to-mink and mink-to-human transmissions have been observed on farms of Denmark and the Netherlands, whereas ferrets have been reported to transmit the virus to other ferrets in an experimental study (432, 437). Natural SARS-CoV-2 infection in gorillas of San Diego Zoo in California (438) and Asian small-clawed otters (439) have also been reported with high susceptibility to the infection and clinical signs. Experimental investigations on SARS-CoV-2 infection in

raccoon dogs, rabbits, pigs, cattle, poultry, hamsters, fruit bats, white-tailed deer, macaques, voles, and mice suggested low to high susceptibility, none to mild clinical signs, and pieces of evidence of low transmissibility between respective animals (440–447). These findings, however, do not hold any substantial evidence for zoonoses, as the transmissibility is low due to insufficient viral load and its replication (427, 431). The viruses in these animals do not satisfy Koch's postulates, and thus, it is inconclusive to declare these species as reservoir hosts for SARS-CoV-2 (448).

Approaches to Study Interspecies Spillover, Evolution and Zoonoses

The novel animal and human CoVs are the outcomes of recombination, divergence, and subsequent evolution. An efficient genomic, phylogenetic, evolutionary rate, and divergence time analyses are now possible with improved bioinformatics tools and the availability of a large pool of CoVs discovered over time. This is done using different approaches incorporating molecular clock analysis or similar techniques that evaluate mutation rates of biomolecules such as DNA, RNA, or amino acid sequences for proteins. The ecological approaches focus on the spatial distribution of pathogen and host populations and their interactions with each other and their environment. Molecular approaches rely on genetic and cellular aspects of the host–pathogen relationship at the individual and population levels. A combination of these approaches, epidemiological data, and whole-genome sequencing along with some anticipative strategies are essential to clarify the mechanisms by which the virus jumps from one species to another. Interspecies transmission and emergence of novel CoVs are studied through molecular epidemiology, which describes the distribution of genes or their variants by considering parameters such as place, time, and population. Moreover, phylogenomic analysis intersects genomics, origin, and evolution of CoVs carried out exclusively after outbreaks of SARS in humans. This analysis provided evidence for interspecies transmission events such as the emergence of HCoV-OC43 from bovines to humans, TGEV from CCoV-II, FCoV-II, and CCoV-II from recombination between early CCoV-I and FCoV-I and porcine CoV HKU15 likely from a sparrow. Many researchers use the Rob Lanfear's method (449) and the maximum likelihood method with FastTree software (MicrobesOnline, Berkeley, CA, USA) to construct a phylogenetic tree and sequence alignment with the best setting determined by Global Initiative for Sharing All Influenza Data database (https://www.gisaid.org/) and Nextstrain (https://nextstrain.org) (450). Although Bayesian Evolutionary Analysis Sampling Trees is the most widely used approach, it uses different genes (RdRp, ORF1ab, S, N, and helicase genes) and molecular datasets for the purpose to estimate the considerable difference in the life history and evolution of CoVs (1, 22, 451). Klompus et al. demonstrated interspecies cross-reactivity mediated by reactive monoclonal antibodies that bind to antigens from human CoVs (hCoV-OC43 and hCoV-HKU1) and several animal CoVs with shared motifs to SARS-CoV-2. This serological strategy based on cross-reactive antibody responses along with DNA sequencing and RT-qPCR testing has been a dominant methodology and potential diagnostic strategy for infections of novel CoV spillovers (452).

CONCLUSION

CoV has a wide host range affecting domestic livestock, wild animals, and birds, often resulting in serious disease outcomes and economic losses. Furthermore, pets and various livestock species share a common environment with humans and continue to pose a threat to the public at risk. The presence of antibodies against animal CoVs in humans could merely be a normal immune response to an occasional or occupational exposure without any apparent disease. However, frequent and prolonged exposure to animal CoVs and the need for the virus to mutate to bypass the protective host-immune responses would likely result in newer CoV strains with a better ability to infect immunocompromised human hosts. Interestingly, it has been observed that companion animals are susceptible hosts for human CoVs such as SARS-CoV-2. The similarities in the CoV key proteins having a role in initiating infections, together with genetic and evolutionary relatedness and habitat sharing by diverse hosts, will drive future disease outcomes and virus evolution. At present, there is no strong evidence suggesting the role of livestock, poultry, and pets' CoVs to cause serious disease in humans; however, ample scope to undergo mutations and cross-jump species barrier to cause life-threatening illnesses exists. The enigmatic nature of CoVs to cause alteration in tissue tropism, jump species barriers, and form variants is remarkable and needs elucidation. CoVs tend to rapidly adapt to changing ecological niches and enhance the possibility of the emergence of novel CoVs due to high mutational errors particularly in the RBD of spike protein, along with inconstancy of replication enzymes and cleavage sites. These errors in S protein, important for host receptor usage, are essential for the emergence of mutants and the establishment of an effective and productive human infection. Consequently, the occurrence of double and triple mutants has made researchers focus on establishing epidemiological linkage to correlate these variants of concerns with the existing public health scenario. Furthermore, the proven propensity of CoVs for interspecies transmission, to emerge potentially from unknown reservoirs and to genetically relate with CoVs from different hosts, indicates the continued introduction of animal CoVs into the human population. The outbreaks of SARS-CoV in the year 2002 and MERS-CoV in 2012 in the form of severe acute respiratory distress had less impact than the current pandemic caused by SARS-CoV-2 that accounted for nearly 216.30 million confirmed cases with a death toll nearing four million by August 30, 2021, globally (453). Although these numbers are way higher, the case fatality rate of SARS-CoV-2 is around 4%, which is still lower than SARS-CoV and MERS-CoV outbreaks, which ranged between 0 and 50% (454–456). The genome of novel SARS-COV-2 is chimeric in the sense that the majority of it shares homology with the bat CoV genome, whereas the RBD portion bears a sequence similar to pangolin CoV. It is this specific RBD sequence that enables SARS-COV-2 to bind with

high affinity to hACE2, resulting in productive infection and deaths. This is an unambiguous example of how recombination and mutation events result in highly virulent strains claiming lives and damaging economies.

The definitive understanding of the origin of SARS-CoV-2 will have marked repercussions on how humans interact with the ecosystem and on laboratory practice policies and biosafety regulations. Therefore, the emergence and evolution of novel CoVs because of their widespread association and frequent infections in animal hosts, both livestock and wild, combined with a high mutation rate, need to be contemplated to meet future challenges. There is an impending need to implement an effective strategy and monitor animal coronavirome as a potential reservoir of CoV reintroduction to humans. Large-scale sampling, metagenomic sequencing, and comparative genome analysis from animals of different geographical locations, especially those in frequent contact with human and wildlife habitats, should be considered. Baseline samples of unexposed individuals, preferably from a pre-pandemic population, need to be collected to compare with the individuals infected with new spillovers. The establishment of phage antibody libraries for profiling antibody responses against novel CoVs and enhancing the immediate availability of animal CoV serological assays will assist in the screening of numerous antigens in a critically early phase of future outbreaks (452). Despite the availability of established and novel diagnostic technologies, the detection of animal CoVs is still based on conventional, time-consuming, and less-sensitive molecular techniques. Therefore, there is a need to drive efforts for the development of rapid, cost-effective, and sensitive laboratory or POC diagnostic tools with a multi-prong approach to potentially increase the efficiency and specificity of diagnosis. These upgraded testing efforts will help in limiting the spread of animal CoV infections in farms, multi-pet households, and wildlife niches. The commonly used whole cell-based vaccine strategies to combat animal CoV infections on the field deliver poor protection in farm and pet animals. This calls for the exploitation of viral-vectored and nucleic acid-based vaccines as promising candidates. The knowledge about factors responsible for the success or failure of animal CoV vaccines can also provide better insight into the design of vaccines for humans against pandemic-causing CoVs. The standard measures used for the prevention of infectious diseases at farms and elsewhere should be followed besides maintaining personal hygiene and avoiding contact with wildlife to restrict exposure to animal CoVs. Needless to mention that the development of novel diagnostics, vaccines, detailed epidemiological studies, and sequencing of variants of interest and concern will, of course, need budgetary provisions.

AUTHOR CONTRIBUTIONS

PP: reviewed the literature and wrote the manuscript. SV: finalized the manuscript. All authors contributed to the article and approved the submitted version.

REFERENCES

1. Woo PC, Lau SK, Huang Y, Yuen KY. Coronavirus diversity, phylogeny and interspecies jumping. *Exp Biol Med.* (2009) 234:1117–27. doi: 10.3181/0903-MR-94
2. Ksiazek TG, Erdman D, Goldsmith CS, Zaki SR, Peret T, Emery S, et al. A novel coronavirus associated with severe acute respiratory syndrome. *N Engl J Med.* (2003) 348:1953–66. doi: 10.1056/NEJMoa030781
3. Drosten C, Günther S, Preiser W, van der Werf S, Brodt HR, Becker S, et al. Identification of a novel coronavirus in patients with severe acute respiratory syndrome. *N Engl J Med.* (2003) 348:1967–76. doi: 10.1056/NEJMoa030747
4. Zhong NS, Zheng BJ, Li YM, Poon LL, Xie ZH, Chan KH, et al. Epidemiology and cause of severe acute respiratory syndrome (SARS) in Guangdong, People's Republic of China, in February, 2003. *Lancet.* (2003) 362:1353–8. doi: 10.1016/S0140-6736(03)14630-2
5. Fouchier RA, Kuiken T, Schutten M, van Amerongen G, van Doornum GJ, van den Hoogen BG, et al. Aetiology: Koch's postulates fulfilled for SARS virus. *Nature.* (2003) 423:240. doi: 10.1038/423240a
6. Zaki AM, van Boheemen S, Bestebroer TM, Osterhaus AD, Fouchier RA. Isolation of a novel coronavirus from a man with pneumonia in Saudi Arabia. *N Engl J Med.* (2012) 367:1814–20. doi: 10.1056/NEJMoa1211721
7. Estola T. Coronaviruses, a new group of animal RNA viruses. *Avian Dis.* (1970) 14:330–6. doi: 10.2307/1588476
8. Fabricant J. The early history of infectious bronchitis. *Avian Dis.* (1998) 42:648–50. doi: 10.2307/1592697
9. Erles K, Toomey C, Brooks H, Brownlie J. Detection of a group 2 coronavirus in dogs with canine infectious respiratory disease. *Virology.* (2003) 310:216–23. doi: 10.1016/S0042-6822(03)00160-0
10. Li W, Hulswit RJG, Kenney SP, Widjaja I, Jung K, Alhamo MA, et al. Broad receptor engagement of an emerging global coronavirus may potentiate its diverse cross-species transmissibility. *Proc Natl Acad Sci USA.* (2018) 115:E5135–43. doi: 10.1073/pnas.1802879115
11. Wang Q, Vlasova AN, Kenney SP, Saif LJ. Emerging and re-emerging coronaviruses in pigs. *Curr Opin Virol.* (2019) 34:39–49. doi: 10.1016/j.coviro.2018.12.001
12. Tang X, Wu C, Li X, Song Y, Yao X, Wu X, et al. On the origin and continuing evolution of SARS-CoV-2. *Natl Sci Rev.* (2020) 7:1012–23. doi: 10.1093/nsr/nwaa036
13. McBride R, van Zyl M, Fielding BC. The coronavirus nucleocapsid is a multifunctional protein. *Viruses.* (2014) 6:2991–3018. doi: 10.3390/v6082991
14. Liang FY, Lin LC, Ying TH, Yao CW, Tang TK, Chen YW, et al. Immunoreactivity characterisation of the three structural regions of the human coronavirus OC43 nucleocapsid protein by Western blot: implications for the diagnosis of coronavirus infection. *J Virol Methods.* (2013) 187:413–20. doi: 10.1016/j.jviromet.2012.11.009
15. Bosch BJ, van der Zee R, de Haan CA, Rottier PJ. The coronavirus spike protein is a class I virus fusion protein: structural and functional characterization of the fusion core complex. *J Virol.* (2003) 77:8801–11. doi: 10.1128/JVI.77.16.8801-8811.2003
16. Woo PCY, Huang Y, Lau SKP, Yuen KY. Coronavirus genomics and bioinformatics analysis. *Viruses.* (2010) 2:1804–20. doi: 10.3390/v2081803
17. Venkatagopalan P, Daskalova SM, Lopez LA, Dolezal KA, Hogue BG. Coronavirus envelope (E) protein remains at the site of assembly. *Virology.* (2015) 478:75–85. doi: 10.1016/j.virol.2015.02.005
18. Kuo L, Hurst-Hess KR, Koetzner CA, Masters PS. Analyses of coronavirus assembly interactions with interspecies membrane and nucleocapsid protein chimeras. *J Virol.* (2016) 90:4357–68. doi: 10.1128/JVI.03212-15
19. Arndt AL, Larson BJ, Hogue BG. A conserved domain in the coronavirus membrane protein tail is important for virus assembly. *J Virol.* (2010) 84:11418–28. doi: 10.1128/JVI.01131-10
20. Zeng Q, Langereis MA, van Vliet ALW, Huizinga EG, de Groot RJ. Structure of coronavirus hemagglutinin-esterase offers insight into corona and influenza virus evolution. *Proc Natl Acad Sci USA.* (2008) 105:9065–9. doi: 10.1073/pnas.0800502105

21. Lang Y, Li W, Li Z, Koerhuis D, van den Burg ACS, Rozemuller E, et al. Coronavirus hemagglutinin-esterase and spike proteins coevolve for functional balance and optimal virion avidity. *Proc Natl Acad Sci USA*. (2020) 117:25759–70. doi: 10.1073/pnas.2006299117
22. Nieto-Torres JL, DeDiego ML, Álvarez E, Jiménez-Guardeño JM, Regla-Nava JA, Llorente M, et al. Subcellular location and topology of severe acute respiratory syndrome coronavirus envelope protein. *Virology*. (2011) 415:69–82. doi: 10.1016/j.virol.2011.03.029
23. *ICTV Virus Taxonomy*. (2009). Available online at: http://ictvonline.org/virusTaxonomy.asp?version=2009 (accessed August 1, 2010).
24. Woo PCY. Discovery of seven novel mammalian and avian coronaviruses in the genus deltacoronavirus supports bat coronaviruses as the gene source of alphacoronavirus and betacoronavirus and avian coronaviruses as the gene source of gammacoronavirus and deltacoronavirus. *J Virol.* (2012) 86:3995–4008. doi: 10.1128/JVI.06540-11
25. Wong ACP, Li X, Lau SKP, Woo PCY. Global epidemiology of bat coronaviruses. *Viruses.* (2019) 11:174. doi: 10.3390/v11020174
26. World Health Organization. *Consensus Document on the Epidemiology of Severe Acute Respiratory Syndrome (SARS)*. (2003). Available online at: https://apps.who.int/iris/handle/10665/70863
27. Dhama K, Pawaiya RVS, Chakraborty S, Tiwari R, Saminathan M, Verma AK. Coronavirus infection in equines: a review. *Asian J Anim Vet Adv*. (2014) 9:164–76. doi: 10.3923/ajava.2014.164.176
28. Dhama K, Singh SD, Rajamani B, Desingu P, Sandip C, Ruchi T, et al. Emergence of avian infectious bronchitis virus and its variants need better diagnosis, prevention and control strategies: a global perspective. *Pak J Biol Sci.* (2014) 17:751–67. doi: 10.3923/pjbs.2014.751.767
29. Monchatre-Leroy E, Boué F, Boucher J-M, Renault C, Moutou F, Ar Gouilh M, et al. Identification of alpha and beta coronavirus in wildlife species in France: bats, rodents, rabbits, and hedgehogs. *Viruses.* (2017) 9:364. doi: 10.3390/v9120364
30. Dhama K, Khan S, Tiwari R, Dadar M, Malik Y, Singh K, et al. COVID-19, an emerging coronavirus infection: advances and prospects in designing and developing vaccines, immunotherapeutics and therapeutics—a mini-review. *Hum Vaccin Immunother.* (2020) 16:1232–8. doi: 10.1080/21645515.2020.1735227
31. Ji W, Wang W, Zhao X, Zai J, Li X. Cross species transmission of the newly identified coronavirus 2019 nCoV. *J Med Virol.* (2020) 92:433–40. doi: 10.1002/jmv.25682
32. Malik YS, Sircar S, Bhat S, Sharun K, Dhama K, Dadar M, et al. Emerging novel coronavirus (2019-nCoV)-current scenario, evolutionary perspective based on genome analysis and recent developments. *Vet Q.* (2020) 40:68–76. doi: 10.1080/01652176.2020.1727993
33. Xu Y. Genetic diversity and potential recombination between Ferret coronaviruses from European and American lineages. *J Infect.* (2020) 80:350–71. doi: 10.1016/j.jinf.2020.01.016
34. Wilhelmsen KC, Leibowitz JL, Bond CW, Robb JA. The replication of murine coronaviruses in enucleated cells. *Virology*. (1981) 110:225–30. doi: 10.1016/0042-6822(81)90027-1
35. Fehr A, Perlman S. Coronaviruses: an overview of their replication and pathogenesis. *Methods Mol Biol.* (2015) 1282:1–23. doi: 10.1007/978-1-4939-2438-7_1
36. Xian Y, Zhang J, Bian Z, Zhou H, Zhang Z, Lin Z, et al. Bioactive natural compounds against human coronaviruses: a review and perspective. *Acta Pharm Sin B.* (2020) 10:1163–74. doi: 10.1016/j.apsb.2020.06.002
37. Pyrc K, Berkhout B, van der Hoek L. The novel human coronaviruses NL63 and HKU1. *J Virol.* (2007) 81:3051–7. doi: 10.1128/JVI.01466-06
38. Snijder EJ, van der Meer Y, Zevenhoven-Dobbe J, Onderwater JJ, van der Meulen J, Koerten HK, et al. Ultrastructure and origin of membrane vesicles associated with the severe acute respiratory syndrome coronavirus replication complex. *J Virol.* (2006) 80:5927–40. doi: 10.1128/JVI.02501-05
39. Fang SG, Shen H, Wang J, Tay FP, Liu DX. Proteolytic processing of polyproteins 1a and 1ab between non-structural proteins 10 and 11/12 of Coronavirus infectious bronchitis virus is dispensable for viral replication in cultured cells. *Virology*. (2008) 379:175–80. doi: 10.1016/j.virol.2008.06.038
40. Perlman S, Netland J. Coronaviruses post-SARS: update on replication and pathogenesis. *Nat Rev Microbiol.* (2009) 7:439–50. doi: 10.1038/nrmicro2147
41. Brown TDK, Brierley I. The coronavirus nonstructural proteins. In Siddell SG, editor *The Coronaviridae. The Viruses*. Boston, MA: Springer (1995). p. 191–217. doi: 10.1007/978-1-4899-1531-3_10
42. de Vries AF, Horzinek MC, Rottier PJM, de Groot RJ. The genome organization of the nidovirales: similarities and differences between arteri-, toro-, and coronaviruses. *Semin Virol.* (1997) 8:33–47. doi: 10.1006/smvy.1997.0104
43. Lai MM, Cavanagh D. The molecular biology of coronaviruses. *Adv Virus Res.* (1997) 48:1–100. doi: 10.1016/S0065-3527(08)60286-9
44. Lai MMC, Holmes KV. Coronaviridae their replication. In: Knipe D, et al., editors. *Fields' Virology*. Philadelphia, PA: Lippincott Williams & Wilkins (2001). p. 1163–85.
45. Snijder EJ, Bredenbeek PJ, Dobbe JC, Thiel V, Ziebuhr J, Poon LL, et al. Unique and conserved features of genome and proteome of SARS-coronavirus, an early split-off from the coronavirus group 2 lineage. *J Mol Biol.* (2003) 331:991–1004. doi: 10.1016/S0022-2836(03)00865-9
46. Thiel V, Ivanov KA, Putics Á, Hertzig T, Schelle B, Bayer S, et al. Mechanisms and enzymes involved in SARS coronavirus genome expression. *J Gen Virol.* (2003) 84:2305–15. doi: 10.1099/vir.0.19424-0
47. Reguera J, Mudgal G, Santiago C, Casasnovas JM. A structural view of coronavirus-receptor interactions. *Virus Res.* (2014) 194:3–15. doi: 10.1016/j.virusres.2014.10.005
48. Marra MA, Jones SJ, Astell CR, Holt RA, Brooks-Wilson A, Butterfield YS, et al. The Genome sequence of the SARS-associated coronavirus. *Science.* (2003) 300:1399–404. doi: 10.1126/science.1085953
49. Rota PA, Oberste MS, Monroe SS, Nix WA, Campagnoli R, Icenogle JP, et al. Characterization of a novel coronavirus associated with severe acute respiratory syndrome. *Science.* (2003) 300:1394–9. doi: 10.1126/science.1085952
50. Vijgen L, Keyaerts E, Moës E, Thoelen I, Wollants E, Lemey P, et al. Complete genomic sequence of human coronavirus OC43: molecular clock analysis suggests a relatively recent zoonotic coronavirus transmission event. *J Virol.* (2005) 79:1595–604. doi: 10.1128/JVI.79.3.1595-1604.2005
51. Vijgen L, Keyaerts E, Lemey P, Moës E, Li S. Circulation of genetically distinct contemporary human coronavirus OC43 strains. *Virology.* (2005) 337:85–92. doi: 10.1016/j.virol.2005.04.010
52. Alkhansa A, Lakkis G, El Zein L. Mutational analysis of SARS-CoV-2 *ORF8* during six months of COVID-19 pandemic. *Gene Rep.* (2021) 23:101024. doi: 10.1016/j.genrep.2021.101024
53. Lan YC, Liu TT, Yang JY, Lee CM, Chen YJ, Chan YJ, et al. Molecular epidemiology of severe acute respiratory syndrome-associated coronavirus infections in Taiwan. *J Infect Dis*. (2005) 191:1478–89. doi: 10.1086/428591
54. Lan YC, Liu TT, Yang JY, Lee CM, Chen YJ, Chan YJ. Characterizing 56 complete SARS-CoV S-gene sequences from Hong Kong. *J Clin Virol.* (2007) 38:19–26. doi: 10.1016/j.jcv.2006.10.001
55. Li WH, Wong SK, Li F, Kuhn JH, Huang IC, Choe H, et al. Animal origins of the severe acute respiratory syndrome coronavirus: insight from ACE2-S-protein interactions. *J Virol.* (2006) 80:4211–9. doi: 10.1128/JVI.80.9.4211-4219.2006
56. Li F. Receptor recognition and cross-species infections of SARS coronavirus. *Antiviral Res.* (2013) 100:246–54. doi: 10.1016/j.antiviral.2013.08.014
57. Li F. Evidence for a common evolutionary origin of coronavirus spike protein receptor-binding subunits. *J Virol.* (2012) 86:2856–8. doi: 10.1128/JVI.06882-11
58. Su S, Wong G, Shi W, Liu J, Lai ACK, Zhou J, et al. Epidemiology, genetic recombination, and pathogenesis of coronaviruses. *Trends Microbiol.* (2016) 24:490–502. doi: 10.1016/j.tim.2016.03.003
59. Chen J. Pathogenicity and transmissibility of 2019-nCoV—a quick overview and comparison with other emerging viruses. *Microbes Infect.* (2020) 22:69–71. doi: 10.1016/j.micinf.2020.01.004
60. Patel A, Jernigan DB, 2019-nCoV CDC Response Team. Initial public health response and interim clinical guidance for the 2019 novel coronavirus outbreak - United States, December 31, 2019-February 4, 2020. *MMWR Morb Mortal Wkly Rep*. (2020) 69:140–6. doi: 10.15585/mmwr.mm6905e1
61. *INSACOG Power Point Presentation*. INSACOG: Indian SARS-CoV-2 Genomics Consortium (2021). Available online at: https://dbtindia.gov.in/sites/default/files/INSACOG%20ppt%2023-06-2021.pdf (accessed June 23, 2021).

62. Li F. Receptor recognition mechanisms of coronaviruses: a decade of structural studies. *J Virol.* (2015) 89:1954–64; doi: 10.1128/JVI.02615-14
63. Tusell SM, Schittone SA, Holmes KV. Mutational analysis of aminopeptidase N, a receptor for several group 1 coronaviruses, identifies key determinants of viral host range. *J Virol.* (2007) 81:1261–73. doi: 10.1128/JVI.01510-06
64. Wu K, Li W, Peng G, Li F. Crystal structure of NL63 respiratory coronavirus receptor-binding domain complexed with its human receptor. *Proc Natl Acad Sci USA.* (2009) 106:19970–4. doi: 10.1073/pnas.0908837106
65. Reguera J, Santiago C, Mudgal G, Ordoño D, Enjuanes L, Casasnovas JM. Structural bases of coronavirus attachment to host aminopeptidase N and its inhibition by neutralizing antibodies. *PLoS Pathog.* (2012) 8:e1002859. doi: 10.1371/journal.ppat.1002859
66. Wu K, Chen L, Peng G, Zhou W, Pennell CA, Mansky LM, et al. A virus-binding hot spot on human angiotensin-converting enzyme 2 is critical for binding of two different coronaviruses. *J Virol.* (2011) 85:5331–7. doi: 10.1128/JVI.02274-10
67. Li F. Structure, function, and evolution of coronavirus spike proteins. *Annu Rev Virol.* (2016) 3:237–61. doi: 10.1146/annurev-virology-110615-042301
68. Peng G, Xu L, Lin YL, Chen L, Pasquarella JR, Holmes KV, et al. Crystal structure of bovine coronavirus spike protein lectin domain. *J Biol Chem.* (2012) 287:41931–8. doi: 10.1074/jbc.M112.418210
69. Hu H, Jung K, Vlasova AN, Chepngeno J, Lu Z, Wang Q, et al. Isolation and characterization of porcine deltacoronavirus from pigs with diarrhea in the United States. *J Clin Microbiol.* (2015) 53:1537–48. doi: 10.1128/JCM.00031-15
70. Shang J, Zheng Y, Yang Y, Liu C, Geng Q, Tai W, et al. Cryo-electron microscopy structure of porcine deltacoronavirus spike protein in the prefusion state. *J Virol.* (2018) 92:e01556–17. doi: 10.1128/JVI.01556-17
71. Wang B, Liu Y, Ji C, Yang Y, Liang Q, Zhao P, et al. Porcine deltacoronavirus engages the transmissible gastroenteritis virus functional receptor porcine aminopeptidase N for infectious cellular entry. *J Virol.* (2018) 92:e00318–18. doi: 10.1128/JVI.00318-18
72. Wilson IA, Skehel JJ, Wiley DC. Structure of the haemagglutinin membrane glycoprotein of influenza virus at 3 A resolution. *Nature.* (1981) 289:366–73. doi: 10.1038/289366a0
73. Wang J. Protein recognition by cell surface receptors: physiological receptors versus virus interactions. *Trends Biochem Sci.* (2002) 27:122–6. doi: 10.1016/S0968-0004(01)02038-2
74. Rossmann MG. The canyon hypothesis. Hiding the host-cell receptor attachment site on a viral surface from immune surveillance. *J Biol Chem.* (1989) 264:14587–90. doi: 10.1016/S0021-9258(18)63732-9
75. Vautherot JF, Laporte J. Utilization of monoclonal antibodies for antigenic characterization of coronaviruses. *Ann Rech Vet.* (1983) 14:437–44.
76. Vieler E, Schlapp T, Anders C, Herbst W. Genomic relationship of porcine hemagglutinating encephalomyelitis virus to bovine coronavirus and human coronavirus OC43 as studied by the use of bovine coronavirus S gene-specific probes. *Arch Virol.* (1995) 140:1215–23. doi: 10.1007/BF01322747
77. Ma Y, Tong X, Xu X, Li X, Lou Z, Rao Z. Structures of the N- and C-terminal domains of MHV-A59 nucleocapsid protein corroborate a conserved RNA-protein binding mechanism in coronavirus. *Protein Cell.* (2010) 1:688–97. doi: 10.1007/s13238-010-0079-x
78. Keane SC, Liu P, Leibowitz JL, Giedroc DP. Functional transcriptional regulatory sequence (TRS) RNA binding and helix destabilizing determinants of murine hepatitis virus (MHV) nucleocapsid (N) protein. *J Biol Chem.* (2012) 287:7063–73. doi: 10.1074/jbc.M111.287763
79. Chang CK, Sue SC Yu TH, Hsieh CM, Tsai CK, Chiang YC, et al. Modular organization of SARS coronavirus nucleocapsid protein. *J Biomed Sci.* (2006) 13:59–72. doi: 10.1007/s11373-005-9035-9
80. Lo YS, Lin SY, Wang SM, Wang CT, Chiu YL, Huang TH, et al. Oligomerization of the carboxyl terminal domain of the human coronavirus 229E nucleocapsid protein. *FEBS Lett.* (2013) 587:120–7. doi: 10.1016/j.febslet.2012.11.016
81. Jayaram H, Fan H, Bowman BR, Ooi A, Jayaram J, Collisson EW, et al. X-ray structures of the N- and C-terminal domains of a coronavirus nucleocapsid protein: implications for nucleocapsid formation. *J Virol.* (2006) 80:6612–20. doi: 10.1128/JVI.00157-06
82. Chen CY, Chang CK, Chang YW, Sue SC, Bai HI, Riang L, et al. Structure of the SARS coronavirus nucleocapsid protein RNA-binding dimerization domain suggests a mechanism for helical packaging of viral RNA. *J Mol Biol.* (2007) 368:1075–86. doi: 10.1016/j.jmb.2007.02.069
83. Zlotnick A. Theoretical aspects of virus capsid assembly. *J Mol Recogn.* (2005) 18:479–90. doi: 10.1002/jmr.754
84. Ruch TR, Machamer CE. The coronavirus E protein: assembly and beyond. *Viruses.* (2012) 4:363–82. doi: 10.3390/v4030363
85. Kuo L, Hurst KR, Masters PS. Exceptional flexibility in the sequence requirements for coronavirus small envelope protein function. *J Virol.* (2007) 81:2249–62. doi: 10.1128/JVI.01577-06
86. Corse E, Machamer CE. Infectious bronchitis virus E protein is targeted to the Golgi complex and directs release of virus-like particles. *J Virol.* (2000) 74:4319–26. doi: 10.1128/JVI.74.9.4319-4326.2000
87. Godet M, L'Haridon R, Vautherot JF, Laude H. TGEV corona virus ORF4 encodes a membrane protein that is incorporated into virions. *Virology.* (1992) 188:666–75. doi: 10.1016/0042-6822(92)90521-P
88. Schoeman D, Fielding BC. Coronavirus envelope protein: current knowledge. *Virol J.* (2019) 16:69. doi: 10.1186/s12985-019-1182-0
89. Corse E, Machamer CE. The cytoplasmic tail of infectious bronchitis virus E protein directs Golgi targeting. *J Virol.* (2002) 76:1273–84. doi: 10.1128/JVI.76.3.1273-1284.2002
90. Liao Y, Yuan Q, Torres J, Tam JP, Liu DX. Biochemical and functional characterization of the membrane association and membrane permeabilizing activity of the severe acute respiratory syndrome coronavirus envelope protein. *Virology.* (2006) 349:264–75. doi: 10.1016/j.virol.2006.01.028
91. Lopez LA, Riffle AJ, Pike SL, Gardner D, Hogue BG. Importance of conserved cysteine residues in the coronavirus envelope protein. *J Virol.* (2008) 82:3000–10. doi: 10.1128/JVI.01914-07
92. Salaun C, Greaves J, Chamberlain LH. The intracellular dynamic of protein palmitoylation. *J Cell Biol.* (2010) 191:1229–38. doi: 10.1083/jcb.201008160
93. Jimenez-Guardeño JM, Nieto-Torres JL, DeDiego ML, et al. The PDZ-binding motif of severe acute respiratory syndrome coronavirus envelope protein is a determinant of viral pathogenesis. *PLoS Pathog.* (2014) 10:e1004320. doi: 10.1371/journal.ppat.1004320
94. de Haan CA, Kuo L, Masters PS, Vennema H, Rottier PJ. Coronavirus particle assembly: primary structure requirements of the membrane protein. *J Virol.* (1998) 72:6838–50. doi: 10.1128/JVI.72.8.6838-6850.1998
95. Oostra M, de Haan CA, de Groot RJ, Rottier PJ. Glycosylation of the severe acute respiratory syndrome coronavirus triple-spanning membrane proteins 3a and M. *J Virol.* (2006) 80:2326–36. doi: 10.1128/JVI.80.5.2326-2336.2006
96. Rohrbach BW, Legendre AM, Baldwin CA, Lein DH, Reed WM, Wilson RB. Epidemiology of feline infectious peritonitis among cats examined at veterinary medical teaching hospitals. *J Am Vet Med Assoc.* (2001) 218:1111–5. doi: 10.2460/javma.2001.218.1111
97. Vlasak R, Luytjes W, Spaan W, Palese P. Human and bovine coronaviruses recognize sialic acid-containing receptors similar to those of influenza C viruses. *Proc Natl Acad Sci USA.* (1988) 85:4526–9. doi: 10.1073/pnas.85.12.4526
98. Luytjes W, Bredenbeek PJ, Noten AFH, Horzinek MC, Spaan WJM. Sequence of mouse hepatitis virus A59 mRNA 2: indications for RNA recombination between coronaviruses and influenza C virus. *Virology.* (1988) 166:415–22. doi: 10.1016/0042-6822(88)90512-0
99. Snijder EJ, den Boon JA, Horzinek MC, Spaan WJ. Comparison of the genome organization of toro- and coronaviruses: evidence for two nonhomologous RNA recombination events during Berne virus evolution. *Virology.* (1991) 180:448–52. doi: 10.1016/0042-6822(91)90056-H
100. de Groot RJ. Structure, function and evolution of the hemagglutinin-esterase proteins of corona- and toroviruses. *Glycoconj J.* (2006) 23:59–72. doi: 10.1007/s10719-006-5438-8
101. Schultze B, Wahn K, Klenk HD, Herrler G. Isolated HE-protein from hemagglutinating encephalomyelitis virus and bovine coronavirus has receptor-destroying and receptor-binding activity. *Virology.* (1991) 180:221–8. doi: 10.1016/0042-6822(91)90026-8
102. Schultze B, Gross HJ, Brossmer R, Herrler G. The S protein of bovine coronavirus is a hemagglutinin recognizing 9-O-acetylated sialic acid as a receptor determinant. *J Virol.* (1991) 65:6232–7. doi: 10.1128/jvi.65.11.6232-6237.1991
103. Smits SL, Gerwig GJ, van Vliet AL, Lissenberg A, Briza P, Kamerling JP, et al. Nidovirus sialate-O-acetylesterases: evolution and substrate specificity of

coronaviral and toroviral receptor-destroying enzymes. *J Biol Chem.* (2005) 280:6933–41. doi: 10.1074/jbc.M409683200
104. Tortorici MA, Walls AC, Lang Y, Wang C, Li Z, Koerhuis D, et al. Structural basis for human coronavirus attachment to sialic acid receptors. *Nat Struct Mol Biol.* (2019) 26:481–9. doi: 10.1038/s41594-019-0233-y
105. Kim CH. SARS-CoV-2 Evolutionary adaptation toward host entry and recognition of receptor o-acetyl sialylation in virus-host interaction. *Int J Mol Sci.* (2020) 21:4549. doi: 10.3390/ijms21124549
106. Clark MA. Bovine coronavirus. *Br Vet J.* (1993) 149:51–70. doi: 10.1016/S0007-1935(05)80210-6
107. Van Kruiningen HJ, Khairallah LH, Sasseville VG, Wyand MS, Post JE. Calfhood coronavirus enterocolitis: a clue to the etiology of winter dysentery. *Vet Pathol.* (1987) 24:564–7. doi: 10.1177/030098588702400616
108. Heckert RA, Saif LJ, Hoblet KH, Agnes AG, A. longitudinal study of bovine coronavirus enteric and respiratory infections in dairy calves in two herds in Ohio. *Vet Microbiol.* (1990) 22:187–201. doi: 10.1016/0378-1135(90)90106-6
109. Saif LJ. A review of evidence implicating bovine coronavirus in the etiology of winter dysentery in cows: an enigma resolved? *Cornell Vet.* (1990) 80:303–11.
110. Tsunemitsu H, Saif LJ. Antigenic and biological comparisons of bovine coronaviruses derived from neonatal calf diarrhea and winter dysentery of adult cattle. *Arch Virol.* (1995) 140:1303–11. doi: 10.1007/BF01322757
111. Storz J, Stine L, Liem A, Anderson GA. Coronavirus isolation from nasal swab samples in cattle with signs of respiratory tract disease after shipping. *J Am Vet Med Assoc.* (1996) 208:1452–5.
112. Hasoksuz M, Lathrop SL, Gadfield KL, Saif LJ. Isolation of bovine respiratory coronaviruses from feedlot cattle and comparison of their biological and antigenic properties with bovine enteric coronaviruses. *Am J Vet Res.* (1999) 60:1227–33.
113. Tsunemitsu H, Smith DR, Saif LJ. Experimental inoculation of adult dairy cows with bovine coronavirus and detection of coronavirus in feces by RT-PCR. *Arch Virol.* (1999) 144:167–75. doi: 10.1007/s007050050493
114. Cho KO, Halbur PG, Bruna JD, Sorden SD, Yoon KJ, Janke BH, et al. Detection and isolation of coronavirus from feces of three herds of feedlot cattle during outbreaks of winter dysentery-like disease. *J Am Vet Med Assoc.* (2000) 217:1191–4. doi: 10.2460/javma.2000.217.1191
115. Lathrop SL, Wittum TE, Loerch SC, Perino LJ, Saif LJ. Antibody titers against bovine coronavirus and shedding of the virus via the respiratory tract in feedlot cattle. *Am J Vet Res.* (2000) 61:1057–61. doi: 10.2460/ajvr.2000.61.1057
116. Storz J, Purdy CW, Lin X, Burrell M, Truax RE, Briggs RE, et al. Isolation of respiratory bovine coronavirus, other cytocidal viruses, and *Pasteurella* spp from cattle involved in two natural outbreaks of shipping fever. *J Am Vet Med Assoc.* (2000) 216:1599–604. doi: 10.2460/javma.2000.216.1599
117. Tråvén M, Näslund K, Linde N, Linde B, Silván A, Fossum C, et al. Experimental reproduction of winter dysentery in lactating cows using BCV – comparison with BCV infection in milk-fed calves. *Vet Microbiol.* (2001) 81:127–51. doi: 10.1016/S0378-1135(01)00337-6
118. Hasoksuz M, Hoet AE, Loerch SC, Wittum TE, Nielsen PR, Saif LJ. Detection of respiratory and enteric shedding of bovine coronaviruses in cattle in an Ohio feedlot. *J Vet Diagn Invest.* (2002) 14:308–13. doi: 10.1177/104063870201400406
119. Boileau MJ, Kapil S. Bovine coronavirus associated syndromes. *Vet Clin North Am Food Anim Pract.* (2010) 26:123–46. doi: 10.1016/j.cvfa.2009.10.003
120. Zhang XM, Herbst W, Kousoulas KG, Storz J. Biological and genetic characterization of a hemagglutinating coronavirus isolated from a diarrhoeic child. *J Med Virol.* (1994) 44:152–61. doi: 10.1002/jmv.1890440207
121. Decaro N, Desario C, Elia G, Mari V, Lucente MS, Cordioli P, et al. Serological and molecular evidence that canine respiratory coronavirus is circulating in Italy. *Vet Microbiol.* (2007) 121:225–30. doi: 10.1016/j.vetmic.2006.12.001
122. Lorusso A, Desario C, Mari V, Campolo M, Lorusso E, Elia G, et al. Molecular characterization of a canine respiratory coronavirus strain detected in Italy. *Virus Res.* (2009) 141:96–100. doi: 10.1016/j.virusres.2008.12.011
123. Saif LJ. Bovine respiratory coronavirus. *Vet Clin North Am Food Anim Pract.* (2010) 26:349–64. doi: 10.1016/j.cvfa.2010.04.005
124. Hasoksuz M, Lathrop S, Al-dubaib MA, Lewis P, Saif LJ. Antigenic variation among bovine enteric coronaviruses (BECV) and bovine respiratory coronaviruses (BRCV) detected using monoclonal antibodies. *Arch Virol.* (1999) 144:2441–7. doi: 10.1007/s007050050656
125. *Bovine Coronavirus Infection. Invasive Species Compendium*. Centre for Agriculture and Biosciences International (2019). Available online at: https://www.cabi.org/isc/datasheet/91704 (accessed November 21, 2019).
126. Saif LJ, Redman DR, Moorhead PD, Theil KW. Experimentally induced coronavirus infections in calves: viral replication in the respiratory and intestinal tracts. *Am J Vet Res.* (1986) 47:1426–32.
127. Kapil S, Richardson KL, Maag TR, Goyal SM. Characterization of bovine coronavirus isolates/from eight different states in the USA. *Vet Microbiol.* (1999) 67:221–30. doi: 10.1016/S0378-1135(99)00042-5
128. Kapil S, Trent AM, Goyal SM. Excretion and persistence of bovine coronavirus in neonatal calves. *Arch Virol.* (1990) 115:127–32. doi: 10.1007/BF01310629
129. Cavanagh D. Coronavirus avian infectious bronchitis virus. *Vet Res.* (2007) 38:281–97. doi: 10.1051/vetres:2006055
130. Cavanagh D, Davis PJ, Mockett AP. Amino acids within hypervariable region 1 of avian coronavirus IBV (Massachusetts serotype) spike glycoprotein are associated with neutralization epitopes. *Virus Res.* (1988) 11:141–50. doi: 10.1016/0168-1702(88)90039-1
131. Cavanagh D, Davis PJ, Darbyshire JH, Peters RW. Coronavirus IBV: virus retaining spike glycopolypeptide S2 but not S1 is unable to induce virus-neutralizing or haemagglutination-inhibiting antibody, or induce chicken tracheal protection. *J Gen Virol.* (1986) 67:1435–42. doi: 10.1099/0022-1317-67-7-1435
132. Casais R, Dove B, Cavanagh D, Britton P. Recombinant avian infectious bronchitis virus expressing a heterologous spike gene demonstrates that the spike protein is a determinant of cell tropism. *J Virol.* (2003) 77:9084–9. doi: 10.1128/JVI.77.16.9084-9089.2003
133. Ramakrishnan S, Kappala D. Avian infectious bronchitis virus. *Recent Adv Anim. Virol.* (2019) 301—19. doi: 10.1007/978-981-13-9073-9_16
134. Ignjatović J, Sapats S. Avian infectious bronchitis virus. *Rev Sci Tech.* (2000) 19:493–508. doi: 10.20506/rst.19.2.1228
135. Bande B, Arshad SS, Omar AR, Bejo MH, Abubakar MS, Abba Y. Pathogenesis and diagnostic approaches of avian infectious bronchitis. *Adv Virol.* (2016) 11:4621659. doi: 10.1155/2016/4621659
136. Jackwood MW. Review of infectious bronchitis virus around the world. *Avian Dis.* (2012) 56:634–41. doi: 10.1637/10227-043012-Review.1
137. McFerran JB, Clarke JK, Curran WL. The application of negative contrast electron microscopy to routine veterinary virus diagnosis. *Res Vet Sci.* (1971) 12:253–7. doi: 10.1016/S0034-5288(18)34187-0
138. Gallardo RA, Hoerr FJ, Berry WD, van Santen VL, Toro H. Infectious bronchitis virus in testicles and venereal transmission. *Avian Dis.* (2011) 55:255–8. doi: 10.1637/9592-102910-Reg.1
139. Bisgaard M. Infektiøs bronchitis virus indflydelse på aeglaegning, befrugtnings og klaekningsprocent og afgang af høner [The influence of infectious bronchitis virus on egg production, fertility, hatchability and mortality rate in chickens (author's transl)]. *Nord Vet Med.* (1976) 28:368–76.
140. Purcell, DA, McFerran JB. The histopathology of infectious bronchitis in the domestic fowl. *Res Vet Sci.* (1972) 13:116–22. doi: 10.1016/S0034-5288(18)34055-4
141. Boroomand Z, Asasi K, Mohammadi A. Pathogenesis and tissue distribution of avian infectious bronchitis virus isolate IRFIBV32 (793/B serotype) in experimentally infected broiler chickens. *Sci World J.* (2012) 2012:402537. doi: 10.1100/2012/402537
142. Babcock GJ, Esshaki DJ, Thomas WD, Ambrosino DM. Amino acids 270 to 510 of the severe acute respiratory syndrome coronavirus spike protein are required for interaction with receptor. *J Virol.* (2004) 78:4552–60. doi: 10.1128/JVI.78.9.4552-4560.2004
143. Promkuntod N, van Eijndhoven RE, de Vrieze G, Gröne A, Verheije MH. Mapping of the receptor-binding domain and amino acids critical for attachment in the spike protein of avian coronavirus infectious bronchitis virus. *Virology.* (2014) 448:26–32. doi: 10.1016/j.virol.2013.09.018
144. Chousalkar KK, Roberts JR. Ultrastructural study of infectious bronchitis virus infection in infundibulum and magnum of commercial laying hens. *Vet Microbiol.* (2007) 22:223–6. doi: 10.1016/j.vetmic.2007.01.021
145. Chousalkar KK, Roberts JR, Reece R. Comparative histopathology of two serotypes of infectious bronchitis virus (T and N1/88) in laying

hens and cockerels. *Poult Sci.* (2007) 86:50–8. doi: 10.1093/ps/86.1.50
146. Cavanagh D, Gelb J. Infectious bronchitis. In: Saif YM, Fadly AM, Glisson JR, McDougald LR, Nolan LK, Swayne DE, editors. *Diseases of Poultry*. Ames, IA: Blackwell (2008). p. 117–35.
147. Cong F, Liu X, Han Z, Shao Y, Kong X, Liu S, et al. Transcriptome analysis of chicken kidney tissues following coronavirus avian infectious bronchitis virus infection. *BMC Genomics.* (2013) 14:743. doi: 10.1186/1471-2164-14-743
148. Gough RE, Randall CJ, Dagless M, Alexander DJ, Cox WJ, Pearson D, et al. 'New' strain of infectious bronchitis virus infecting domestic fowl in Great Britain. *Vet Rec.* (1992) 130:493–4. doi: 10.1136/vr.130.22.493
149. Alexander DJ, Gough RE. Isolation of avian infectious bronchitis virus from experimentally infected chickens. *Res Vet Sci.* (1977) 23:344–7. doi: 10.1016/S0034-5288(18)33129-1
150. Boltz DA, Nakai M, Bahra JM. Avian infectious bronchitis virus: a possible cause of reduced fertility in the rooster. *Avian Dis.* (2004) 48:909–15. doi: 10.1637/7192-040808R1
151. Liu H, Yang X, Zhang Z, Li J, Zou W, Zeng F, et al. Comparative transcriptome analysis reveals induction of apoptosis in chicken kidney cells associated with the virulence of nephropathogenic infectious bronchitis virus. *Microb Pathog.* (2017) 113:451–9. doi: 10.1016/j.micpath.2017.11.031
152. Zuñiga S, Pascual-Iglesias A, Sanchez CM, Sola I, Enjuanes L. Virulence factors in porcine coronaviruses and vaccine design. *Virus Res.* (2016) 226:142–51. doi: 10.1016/j.virusres.2016.07.003
153. Laude H, Van Reeth K, Pensaert M. Porcine respiratory coronavirus: molecular features and virus-host interactions. *Vet Res.* (1993) 24:125–50.
154. Schultze B, Krempl C, Ballesteros ML, Shaw L, Schauer R, Enjuanes L, et al. Transmissible gastroenteritis coronavirus, but not the related porcine respiratory coronavirus, has a sialic acid (N-glycolylneuraminic acid) binding activity. *J Virol.* (1996) 70:5634–7. doi: 10.1128/jvi.70.8.5634-5637.1996
155. Chen Q, Gauger P, Stafne M, Thomas J, Arruda P, Burrough E, et al. Pathogenicity and pathogenesis of a United States porcine deltacoronavirus cell culture isolate in 5-day-old neonatal piglets. *Virology.* (2015) 482:51–9. doi: 10.1016/j.virol.2015.03.024
156. Chen F, Knutson TP, Rossow S, Saif LJ, Marthaler DG. Decline of transmissible gastroenteritis virus and its complex evolutionary relationship with porcine respiratory coronavirus in the United States. *Sci Rep.* (2019) 9:3953. doi: 10.1038/s41598-019-40564-z
157. Niederwerder MC, Hesse RA. Swine enteric coronavirus disease: a review of 4 years with porcine epidemic diarrhoea virus and porcine deltacoronavirus in the United States and Canada. *Transb Emerg Dis.* (2018) 65:660–75. doi: 10.1111/tbed.12823
158. Piñeyro PE, Lozada MI, Alarcón LV, Sanguinetti R, Cappuccio JA, Pérez EM, et al. First retrospective studies with etiological confirmation of porcine transmissible gastroenteritis virus infection in Argentina. *BMC Vet Res.* (2018) 14:292. doi: 10.1186/s12917-018-1615-9
159. Laber KE, Whary MT, Bingel SA, Goodrich JA, Smith AC, Swindle MM. Biology and diseases of swine. *Lab Anim Med.* (2002) 615–73. doi: 10.1016/B978-012263951-7/50018-1
160. Moon HW. Mechanisms in the pathogenesis of diarrhea: a review. *J Am Vet Med Assoc.* (1978) 172:443–8.
161. Bohl EH, Kohler EM, Saif LJ, Cross RF, Agnes AG, Theil KW. Rotavirus as a cause of diarrhea in pigs. *J Am Vet Med Assoc.* (1978) 172:458–63.
162. Kemeny LJ, Wiltsey VL, Riley JL. Upper respiratory infection of lactating sows with transmissible gastroenteritis virus following contact exposure to infected piglets. *Cornell Vet.* (1975) 65:352–62.
163. Vlasova AN, Wang Q, Jung K, Langel SN, Malik YS, Saif LJ. Porcine coronaviruses. *Emerg Transbound Anim Viruses.* (2020) 79—110. doi: 10.1007/978-981-15-0402-0_4
164. MacLachlan JN, Dubovi EJ. *Coronaviridae.* In MacLachlan JN, Dubovi EJ, editor *The Fenner's Veterinary Virology.* 5th ed. Academic Press (2017). p. 435–61.
165. Underdahl NR, Mebus CA, Torres-Medina A. Recovery of transmissible gastroenteritis virus from chronically infected experimental pigs. *Am J Vet Res.* (1975) 36:1473–6.
166. Herrewegh AA, Vennema H, Horzinek MC, Rottier PJ, de Groot RJ. The molecular genetics of feline coronaviruses: comparative sequence analysis of the ORF7a/7b transcription unit of different biotypes. *Virology.* (1995) 212:622–31. doi: 10.1006/viro.1995.1520
167. Pedersen NC, Boyle JF, Floyd K, Fudge A, Barker J. An enteric coronavirus infection of cats and its relationship to feline infectious peritonitis. *Am J Vet Res.* (1981) 42:368–77.
168. Poland AM, Vennema H, Foley JE, Pedersen NC. Two related strains of feline infectious peritonitis virus isolated from immunocompromised cats infected with a feline enteric coronavirus. *J ClinMicrobiol.* (1996) 34:3180–4. doi: 10.1128/jcm.34.12.3180-3184.1996
169. Vennema H, Poland A, Foley J, Pedersen NC. Feline infectious peritonitis viruses arise by mutation from endemic feline enteric coronaviruses. *Virology.* (1998) 243:150–7. doi: 10.1006/viro.1998.9045
170. Haijema BJ, Rottier PJM, de Groot RJ. Feline Coronaviruses: a tale of two-faced types. In: Thiel V, editor. *Coronaviruses: Molecular and Cellular Biology*. Caister: Academic Press (2007). p. 182–203.
171. Pedersen NC. A review of feline infectious peritonitis virus infection: 1963–2008. *J Feline Med Surg.* (2009) 11:225–58. doi: 10.1016/j.jfms.2008.09.008
172. Bank-Wolf BR, Stallkamp I, Wiese S, Moritz A, Tekes G, Thiel HJ. Mutations of 3c and spike protein genes correlate with the occurrence of feline infectious peritonitis. *Vet Microbiol.* (2014) 173:177–88. doi: 10.1016/j.vetmic.2014.07.020
173. Barker EN, Tasker S, Gruffydd-Jones TJ, Tuplin CK, Burton K, Porter E, et al. Phylogenetic analysis of feline coronavirus strains in an epizootic outbreak of feline infectious peritonitis. *J Vet Intern Med.* (2013) 27:445–50. doi: 10.1111/jvim.12058
174. Chang HW, de Groot RJ, Egberink HF, Rottier PJ. Feline infectious peritonitis: insights into feline coronavirus pathobiogenesis and epidemiology based on genetic analysis of the viral 3c gene. *J Gen Virol.* (2010) 91:415–20. doi: 10.1099/vir.0.016485-0
175. Chang HW, Egberink HF, Halpin R, Spiro DJ, Rottier PJ. Spike protein fusion peptide and feline coronavirus virulence. *Emerg Infect Dis.* (2012) 18:1089–95. doi: 10.3201/eid1807.120143
176. Lewis CS, Porter E, Matthews D, Kipar A, Tasker S, Helps CR, et al. Genotyping coronaviruses associated with feline infectious peritonitis. *J Gen Virol.* (2015) 96:1358–68. doi: 10.1099/vir.0.000084
177. Licitra BN, Millet JK, Regan AD, Hamilton BS, Rinaldi VD, Duhamel GE, et al. Mutation in spike protein cleavage site and pathogenesis of feline coronavirus. *Emerg Infect Dis.* (2013) 19:1066–73. doi: 10.3201/eid1907.121094
178. Pedersen NC, Liu H, Scarlett J, Leutenegger CM, Golovko L, Kennedy H, et al. Feline infectious peritonitis: role of the feline coronavirus 3c gene in intestinal tropism and pathogenicity based upon isolates from resident and adopted shelter cats. *Virus Res.* (2012) 165:17–28. doi: 10.1016/j.virusres.2011.12.020
179. Porter E, Tasker S, Day MJ, Harley R, Kipar A, Siddell SG, et al. Amino acid changes in the spike protein of feline coronavirus correlate with systemic spread of virus from the intestine and not with feline infectious peritonitis. *Vet Res.* (2014) 45:49. doi: 10.1186/1297-9716-45-49
180. Tekes G, Thiel HJ. Feline coronaviruses: pathogenesis of feline infectious peritonitis. *Adv Virus Res.* (2016) 96:193–218. doi: 10.1016/bs.aivir.2016.08.002
181. Fiscus SA, Teramoto YA. Antigenic comparison of feline coronavirus isolates: evidence for markedly different peplomer glycoproteins. *J Virol.* (1987) 61:2607–13. doi: 10.1128/jvi.61.8.2607-2613.1987
182. Decaro N, Buonavoglia C. An update on canine coronaviruses: viral evolution and pathobiology. *Vet Microbiol.* (2008) 132:221–34. doi: 10.1016/j.vetmic.2008.06.007
183. Herrewegh AA, Smeenk I, Horzinek MC, Rottier PJ, de Groot RJ. Feline coronavirus type II strains 79-1683 and 79-1146 originate from a double recombination between feline coronavirus type I and canine coronavirus. *J Virol.* (1998) 72:4508–14. doi: 10.1128/JVI.72.5.4508-4514.1998
184. Lin CN, Chang RY, Su BL, Chueh LL. Full genome analysis of a novel type II feline coronavirus NTU156. *Virus Genes.* (2013) 46:316–22. doi: 10.1007/s11262-012-0864-0
185. Terada Y, Matsui N, Noguchi K, Kuwata R, Shimoda H, Soma T, et al. Emergence of pathogenic coronaviruses in cats by homologous

recombination between feline and canine coronaviruses. *PLoS ONE.* (2014) 9:e106534. doi: 10.1371/journal.pone.0106534
186. Lorusso A, Decaro N, Schellen P, Rottier PJ, Buonavoglia C, Haijema BJ, et al. Gain, preservation, and loss of a group 1a coronavirus accessory glycoprotein. *J Virol.* (2008) 82:10312–7. doi: 10.1128/JVI.01031-08
187. Hohdatsu T, Okada S, Ishizuka Y, Yamada H, Koyama H. The prevalence of types I and II feline coronavirus infections in cats. *J Vet Med Sci.* (1992) 54:557–62. doi: 10.1292/jvms.54.557
188. Pedersen NC. An update on feline infectious peritonitis: virology and immunopathogenesis. *Vet J.* (2014) 201:123–32. doi: 10.1016/j.tvjl.2014.04.017
189. Brown MA, Troyer JL, Pecon-Slattery J, Roelke ME, O'Brien SJ. Genetics and pathogenesis of feline infectious peritonitis virus. *Emerg Infect Dis.* (2009) 15:1445–52. doi: 10.3201/eid1509.081573
190. Addie DD, Schaap IAT, Nicolson L, Jarrett O. Persistence and transmission of natural type I feline coronavirus infection. *J Gen Virol.* (2003) 84:2735–44. doi: 10.1099/vir.0.19129-0
191. Kennedy M, Citino S, McNabb AH, Moffatt AS, Gertz K, Kania S. Detection of feline coronavirus in captive Felidae in the USA. *J Vet Diagn Invest.* (2002) 14:520–2. doi: 10.1177/104063870201400615
192. Kummrow M, Meli ML, Haessig M, Goenczi E, Poland A, Pedersen NC, et al. Feline coronavirus serotypes 1 and 2: seroprevalence and association with disease in Switzerland. *Clin Diagn Lab Immunol.* (2005) 12:1209–15. doi: 10.1128/CDLI.12.10.1209-1215.2005
193. Benetka V, Kübber-Heiss A, Kolodziejek J, Nowotny N, Hofmann-Parisot M, Möstl K. Prevalence of feline coronavirus types I and II in cats with histopathologically verified feline infectious peritonitis. *Vet Microbiol.* (2004) 99:31–42. doi: 10.1016/j.vetmic.2003.07.010
194. Amer A, Siti Suri A, Abdul Rahman O, Mohd HB, Faruku B, Saeed S, et al. Isolation and molecular characterization of type I and type II feline coronavirus in Malaysia. *Virol J.* (2012) 9:278. doi: 10.1186/1743-422X-9-278
195. An DJ, Jeoung HY, Jeong W, Park JY, Lee MH, Park BK. Prevalence of Korean cats with natural feline coronavirus infections. *Virol J.* (2011) 8:455. doi: 10.1186/1743-422X-8-455
196. Sharif S, Arshad SS, Hair-Bejo M, Omar AR, Zeenathul NA, Fong LS, et al. Descriptive distribution and phylogenetic analysis of feline infectious peritonitis virus isolates of Malaysia. *Acta Vet Scand.* (2010) 52:1. doi: 10.1186/1751-0147-52-1
197. Akkan HA, Karaca M. Studies on the seroprevalence, age, and gender on the distribution of feline coronavirus in van cat kept in a multiple-cat environment. *Bull Vet Inst Pulawy.* (2009) 53:183–6.
198. Addie DD, McLachlan SA, Golder M, Ramsey I, Jarrett O. Evaluation of an in-practice test for feline coronavirus antibodies. *J Feline Med Surg.* (2004) 6:63–7. doi: 10.1016/j.jfms.2004.01.001
199. Almeida A, Galdino MV, Araújo JP. Seroepidemiological study of feline coronavirus (FCoV) infection in domiciled cats from small animal diseases. *Pesq Vet Bras.* (2019) 39:129–33. doi: 10.1590/1678-5150-pvb-5706
200. Bell ET, Malik R, Norris JM. The relationship between the feline coronavirus antibody titre and the age, breed, gender and health status of Australian cats. *Aust Vet J.* (2006) 84:2–7. doi: 10.1111/j.1751-0813.2006.tb13114.x
201. Tekes G, Spies D, Bank-Wolf B, Thiel V, Thiel HJ. A reverse genetics approach to study feline infectious peritonitis. *J Virol.* (2012) 86:6994–8. doi: 10.1128/JVI.00023-12
202. Thiel V, Thiel HJ, Tekes G. Tackling feline infectious peritonitis via reverse genetics. *Bioengineered.* (2014) 5:396–400. doi: 10.4161/bioe.32133
203. Vogel L, Van der Lubben M, Te Lintelo EG, Bekker CP, Geerts T, Schuijff LS, et al. Pathogenic characteristics of persistent feline enteric coronavirus infection in cats. *Vet Res.* (2010) 41:71. doi: 10.1051/vetres/2010043
204. Herrewegh AA, Mähler M, Hedrich HJ, Haagmans BL, Egberink HF, Horzinek MC, et al. Persistence and evolution of feline coronavirus in a closed cat-breeding colony. *Virology.* (1997) 234:349–63. doi: 10.1006/viro.1997.8663
205. Kipar A, Meli ML, Baptiste KE, Bowker LJ, Lutz H. Sites of feline coronavirus persistence in healthy cats. *J Gen Virol.* (2010) 91:1698–707. doi: 10.1099/vir.0.020214-0
206. Dewerchin HL, Cornelissen E, Nauwynck HJ. Replication of feline coronaviruses in peripheral blood monocytes. *Arch Virol.* (2005) 150:2483–500. doi: 10.1007/s00705-005-0598-6
207. Meli M, Kipar A, Müller C, Jenal K, Gönczi E, Borel N, et al. High viral loads despite absence of clinical and pathological findings in cats experimentally infected with feline coronavirus (FCoV) type I and in naturally FCoV-infected cats. *J Feline Med Surg.* (2004) 6:69–81. doi: 10.1016/j.jfms.2003.08.007
208. Rottier PJ, Nakamura K, Schellen P, Volders H, Haijema BJ. Acquisition of macrophage tropism during the pathogenesis of feline infectious peritonitis is determined by mutations in the feline coronavirus spike protein. *J Virol.* (2005) 79:14122–30. doi: 10.1128/JVI.79.22.14122-14130.2005
209. Stoddart CA, Scott FW. Intrinsic resistance of feline peritoneal macrophages to coronavirus infection correlates with *in vivo* virulence. *J Virol.* (1989) 63:436–40. doi: 10.1128/jvi.63.1.436-440.1989
210. Regan AD, Cohen RD, Whittaker GR. Activation of p38 MAPK by feline infectious peritonitis virus regulates pro-inflammatory cytokine production in primary blood-derived feline mononuclear cells. *Virology.* (2009) 384:135–43. doi: 10.1016/j.virol.2008.11.006
211. Kipar A, Baptiste K, Barth A, Reinacher M. Natural FCoV infection: cats with FIP exhibit significantly higher viral loads than healthy infected cats. *J Feline Med Surg.* (2006) 8:69–72. doi: 10.1016/j.jfms.2005.07.002
212. Kipar A, Meli ML, Failing K, Euler T, Gomes-Keller MA, Schwartz D, et al. Natural feline coronavirus infection: differences in cytokine patterns in association with the outcome of infection. *Vet Immunol Immunopathol.* (2006) 112:141–55. doi: 10.1016/j.vetimm.2006.02.004
213. Kipar A, Meli ML. Feline infectious peritonitis: still an enigma? *Vet Pathol.* (2014) 51:505–26. doi: 10.1177/0300985814522077
214. Kiss I, Poland AM, Pedersen NC. Disease outcome and cytokine responses in cats immunized with an avirulent feline infectious peritonitis virus (FIPV)-UCD1 and challenge-exposed with virulent FIPV-UCD8. *J Feline Med Surg.* (2004) 6:89–97. doi: 10.1016/j.jfms.2003.08.009
215. Takano T, Azuma N, Satoh M, Toda A, Hashida Y, Satoh R, et al. Neutrophil survival factors (TNF-alpha, GM-CSF, and G-CSF) produced by macrophages in cats infected with feline infectious peritonitis virus contribute to the pathogenesis of granulomatous lesions. *Arch Virol.* (2009) 154:775–81. doi: 10.1007/s00705-009-0371-3
216. Takano T, Hohdatsu T, Hashida Y, Kaneko Y, Tanabe M, Koyama H, et al. "Possible" involvement of TNF-alpha in apoptosis induction in peripheral blood lymphocytes of cats with feline infectious peritonitis. *Vet Microbiol.* (2007) 119:121–31. doi: 10.1016/j.vetmic.2006.08.033
217. Takano T, Hohdatsu T, Toda A, Tanabe M, Koyama H. TNF-alpha, produced by feline infectious peritonitis virus (FIPV)-infected macrophages, upregulates expression of type II FIPV receptor feline aminopeptidase N in feline macrophages. *Virology.* (2007) 364:64–72. doi: 10.1016/j.virol.2007.02.006
218. Takano T, Ohyama T, Kokumoto A, Satoh R, Hohdatsu T. Vascular endothelial growth factor (VEGF), produced by feline infectious peritonitis (FIP) virus-infected monocytes and macrophages, induces vascular permeability and effusion in cats with FIP. *Virus Res.* (2011) 158:161–8. doi: 10.1016/j.virusres.2011.03.027
219. Olyslaegers DA, Dedeurwaerder A, Desmarets LM, Vermeulen BL, Dewerchin HL, Nauwynck HJ. Altered expression of adhesion molecules on peripheral blood leukocytes in feline infectious peritonitis. *Vet Microbiol.* (2013) 166:438–49. doi: 10.1016/j.vetmic.2013.06.027
220. Hayashi T, Goto N, Takahashi R, Fujiwara K. Systemic vascular lesions in feline infectious peritonitis. *Nihon JuigakuZasshi.* (1977) 39:365–77. doi: 10.1292/jvms1939.39.365
221. Kipar A, Bellmann S, Kremendahl J, Köhler K, Reinacher M. Cellular composition, coronavirus antigen expression and production of specific antibodies in lesions in feline infectious peritonitis. *Vet Immunol Immunopathol.* (1998) 65:243–57. doi: 10.1016/S0165-2427(98)00158-5
222. Kipar A, May H, Menger S, Weber M, Leukert W, Reinacher M. Morphologic features and development of granulomatous vasculitis in feline infectious peritonitis. *Vet Pathol.* (2005) 42:321–30. doi: 10.1354/vp.42-3-321
223. Weiss RC, Scott FW. Pathogenesis of feline infetious peritonitis: pathologic changes and immunofluorescence. *Am J Vet Res.* (1981) 42:2036–48.
224. Kipar A, Kremendahl J, Addie DD, Leukert W, Grant CK, Reinacher M. Fatal enteritis associated with coronavirus infection in cats. *J Comp Pathol.* (1998) 119:1–14. doi: 10.1016/S0021-9975(98)80067-4

225. Drechsler Y, Alcaraz A, Bossong FJ, Collisson EW, Diniz PP. Feline coronavirus in multicat environments. *Vet Clin North Am Small Anim Pract.* (2011) 41:1133–69. doi: 10.1016/j.cvsm.2011.08.004
226. Hartmann K. Feline infectious peritonitis. *Vet Clin North Am Small Anim Pract.* (2005) 35:39–79, vi. doi: 10.1016/j.cvsm.2004.10.011
227. Binn LN, Lazar EC, Keenan KP, Huxsoll DL, Strano AJ. Recovery and characterization of a coronavirus from military dogs with diarrhea. *Proc Annu Meet US Anim Health Assoc.* (1974) 78:359–66.
228. Pratelli A, Martella V, Decaro N, Tinelli A, Camero M, Cirone F, et al. Genetic diversity of a canine coronavirus detected in pups with diarrhoea in Italy. *J Virol Methods.* (2003) 110:9–17. doi: 10.1016/S0166-0934(03)00081-8
229. Decaro N, Mari V, Campolo M, Lorusso A, Camero M, Elia G, et al. Recombinant canine coronaviruses related to transmissible gastroenteritis virus of Swine are circulating in dogs. *J Virol.* (2009) 83:1532–7. doi: 10.1128/JVI.01937-08
230. Decaro N, Mari V, Elia G, Addie DD, Camero M, Lucente MS, et al. Recombinant canine coronaviruses in dogs, Europe. *Emerg Infect Dis.* (2010) 16:41–7. doi: 10.3201/eid1601.090726
231. Regan AD, Millet JK, Tse LP, Chillag Z, Rinaldi VD, Licitra BN, et al. Characterization of a recombinant canine coronavirus with a distinct receptor-binding (S1) domain. *Virology.* (2012) 430:90–9. doi: 10.1016/j.virol.2012.04.013
232. Escutenaire S, Isaksson M, Renström LH, Klingeborn B, Buonavoglia C, Berg M, et al. Characterization of divergent and atypical canine coronaviruses from Sweden. *Arch Virol.* (2007) 152:1507–14. doi: 10.1007/s00705-007-0986-1
233. Licitra BN, Duhamel GE, Whittaker GR. Canine enteric coronaviruses: emerging viral pathogens with distinct recombinant spike proteins. *Viruses.* (2014) 6:3363–76. doi: 10.3390/v6083363
234. Keenan KP, Jervis HR, Marchwicki RH, Binn LN. Intestinal infection of neonatal dogs with canine coronavirus 1-71: studies by virologic, histologic, histochemical, and immunofluorescent techniques. *Am J Vet Res.* (1976) 37:247–56.
235. Tennant BJ, Gaskell RM, Kelly DF, Carter SD, Gaskell CJ. Canine coronavirus infection in the dog following oronasal inoculation. *Res Vet Sci.* (1991) 51:11–8. doi: 10.1016/0034-5288(91)90023-H
236. Pratelli A, Tempesta M, Roperto FP, Sagazio P, Carmichael L, Buonavoglia C. Fatal coronavirus infection in puppies following canine parvovirus 2b infection. *J Vet Diagn Invest.* (1999) 11:550–3. doi: 10.1177/104063879901100615
237. Pratelli A, Martella V, Elia G, Tempesta M, Guarda F, Capucchio MT, et al. Severe enteric disease in an animal shelter associated with dual infections by canine adenovirus type 1 and canine coronavirus. *J Vet Med B Infect Dis Vet Public Health.* (2001) 48:385–92. doi: 10.1046/j.1439-0450.2001.00466.x
238. Decaro N, Martella V, Elia G, Campolo M, Desario C, Cirone F, et al. Molecular characterisation of the virulent canine coronavirus CB/05 strain. *Virus Res.* (2007) 125:54–60. doi: 10.1016/j.virusres.2006.12.006
239. Ntafis V, Xylouri E, Mari V, Papanastassopoulou M, Papaioannou N, Thomas A, et al. Molecular characterization of a canine coronavirus NA/09 strain detected in a dog's organs. *Arch Virol.* (2012) 157:171–5. doi: 10.1007/s00705-011-1141-6
240. Zicola A, Jolly S, Mathijs E, Ziant D, Decaro N, Mari V, et al. Fatal outbreaks in dogs associated with pantropic canine coronavirus in France and Belgium. *J Small Anim Pract.* (2012) 53:297–300. doi: 10.1111/j.1748-5827.2011.01178.x
241. Buonavoglia C, Decaro N, Martella V, Elia G, Campolo M, Desario C, et al. Canine coronavirus highly pathogenic for dogs. *Emerg Infect Dis.* (2006) 12:492–4. doi: 10.3201/eid1203.050839
242. Alfano F, Fusco G, Mari V, Occhiogrosso L, Miletti G, Brunetti R, et al. Circulation of pantropic canine coronavirus in autochthonous and imported dogs, Italy. *Transbound Emerg Dis.* (2020) 67:1991–9. doi: 10.1111/tbed.13542
243. Alfano F, Dowgier G, Valentino MP, Galiero G, Tinelli A, Nicola D, et al. Identification of pantropic canine coronavirus in a wolf (Canis lupus italicus) in Italy. *J Wildl Dis.* (2019) 55:504–8. doi: 10.7589/2018-07-182
244. Evermann JF, Abbott JR, Han S. Canine coronavirus-associated puppy mortality without evidence of concurrent canine parvovirus infection. *J Vet Diagn Invest.* (2005) 17:610–4. doi: 10.1177/104063870501700618
245. Decaro N, Mari V, Larocca V, Losurdo M, Lanave G, Lucente MS, et al. Molecular surveillance of traditional and emerging pathogens associated with canine infectious respiratory disease. *Vet Microbiol.* (2016) 192:21–5. doi: 10.1016/j.vetmic.2016.06.009
246. Lavan R, Knesl O. Prevalence of canine infectious respiratory pathogens in asymptomatic dogs presented at US animal shelters. *J Small Anim Pract.* (2015) 56:572–6. doi: 10.1111/jsap.12389
247. Erles K, Brownlie J. Canine respiratory coronavirus: an emerging pathogen in the canine infectious respiratory disease complex. *Vet Clin North Am Small Anim Pract.* (2008) 38:815–25. doi: 10.1016/j.cvsm.2008.02.008
248. Soma T, Ohinata T, Ishii H, Takahashi T, Taharaguchi S, Hara M. Detection and genotyping of canine coronavirus RNA in diarrheic dogs in Japan. *Res Vet Sci.* (2011) 90:205–7. doi: 10.1016/j.rvsc.2010.05.027
249. Costa EM, de Castro TX, Bottino Fde O, Garcia Rde C. Molecular characterization of canine coronavirus strains circulating in Brazil. *Vet Microbiol.* (2014) 168:8–15. doi: 10.1016/j.vetmic.2013.10.002
250. Ntafis V, Mari V, Decaro N, Papanastassopoulou M, Pardali D, Rallis TS, et al. Canine coronavirus, Greece. Molecular analysis and genetic diversity characterization infect. *Genet Evol.* (2013) 16:129–36. doi: 10.1016/j.meegid.2013.01.014
251. Wang X, Li C, Guo D, Wang X, Wei S, Geng Y, et al. Co-circulation of canine coronavirus I and IIa/b with high prevalence and genetic diversity in Heilongjiang Province, Northeast China. *PLoS ONE.* (2016) 11:e0146975. doi: 10.1371/journal.pone.0146975
252. van Nguyen D, Terada Y, Minami S, Yonemitsu K, Nagata N, Le TD, et al. Characterization of canine coronavirus spread among domestic dogs in Vietnam. *J Vet Med Sci.* (2017) 79:343–9. doi: 10.1292/jvms.16-0538
253. Naylor MJ, Walia CS, McOrist S, Lehrbach PR, Deane EM, Harrison GA. Molecular characterization confirms the presence of a divergent strain of canine coronavirus (UWSMN-1) in Australia. *J Clin Microbiol.* (2002) 40:3518–22. doi: 10.1128/JCM.40.9.3518-3522.2002
254. Priestnall SL, Brownlie J, Dubovi EJ, Erles K. Serological prevalence of canine respiratory coronavirus. *Vet Microbiol.* (2006) 115:43–53. doi: 10.1016/j.vetmic.2006.02.008
255. Priestnall SL, Pratelli A, Brownlie J, Erles K. Serological prevalence of canine respiratory coronavirus in southern Italy and epidemiological relationship with canine enteric coronavirus. *J Vet Diagn Invest.* (2007) 19:176–80. doi: 10.1177/104063870701900206
256. Kaneshima T, Hohdatsu T, Satoh K, Takano T, Motokawa K, Koyama H. The prevalence of a group 2 coronavirus in dogs in Japan. *J Vet Med Sci.* (2006) 68:21–5. doi: 10.1292/jvms.68.21
257. Yachi A, Mochizuki M. Survey of dogs in Japan for group 2 canine coronavirus infection. *J Clin Microbiol.* (2006) 44:2615–8. doi: 10.1128/JCM.02397-05
258. Knesl O, Allan FJ, Shields S. The seroprevalence of canine respiratory coronavirus and canine influenza virus in dogs in New Zealand. *N Z Vet J.* (2009) 57:295–8. doi: 10.1080/00480169.2009.58624
259. He HJ, Zhang W, Liang J, Lu M, Wang R, Li G, et al. Etiology and genetic evolution of canine coronavirus circulating in five provinces of China, during 2018-2019. *Microb Pathog.* (2020) 145:104209. doi: 10.1016/j.micpath.2020.104209
260. Stavisky J, Pinchbeck GL, German AJ, Dawson S, Gaskell RM, Ryvar R, et al. Prevalence of canine enteric coronavirus in a cross-sectional survey of dogs presenting at veterinary practices. *Vet Microbiol.* (2010) 140:18–24. doi: 10.1016/j.vetmic.2009.07.012
261. Decaro N, Martella V, Ricci D, Elia G, Desario C, Campolo M, et al. Genotype-specific fluorogenic RT-PCR assays for the detection and quantitation of canine coronavirus type I and type II RNA in faecal samples of dogs. *J Virol Methods.* (2005) 130:72–8. doi: 10.1016/j.jviromet.2005.06.005
262. Pratelli A, Elia G, Martella V, Tinelli A, Decaro N, Marsilio F, et al. M Gene evolution of canine coronavirus in naturally infected dogs. *Vet Rec.* (2002) 151:758–61. doi: 10.1136/vr.151.25.758
263. Ma GG, Lu CP. [Two genotypes of Canine coronavirus simultaneously detected in the fecal samples of healthy foxes and raccoon dogs]. *Wei Sheng Wu Xue Bao.* (2005) 45:305–8.
264. Zarnke RL, Evermann J, Ver Hoef JM, McNay ME, Boertje RD, Gardner CL, et al. Serologic survey for canine coronavirus in wolves

from Alaska. *J Wildl Dis.* (2001) 37:740–5. doi: 10.7589/0090-3558-37.4.740
265. Arsevska E, Priestnall SL, Singleton DA, Jones PH, Smyth S, Brant B, et al. Small animal disease surveillance: respiratory disease 2017. *Vet Rec.* (2018) 182:369–73. doi: 10.1136/vr.k1426
266. Zappulli V, Caliari D, Cavicchioli L, Tinelli A, Castagnaro M. Systemic fatal type II coronavirus infection in a dog: pathological findings and immunohistochemistry. *Res Vet Sci.* (2008) 84:278–82. doi: 10.1016/j.rvsc.2007.05.004
267. Mitchell JA, Brooks HW, Szladovits B, Erles K, Gibbons R, Shields S, et al. Tropism and pathological findings associated with canine respiratory coronavirus (CRCoV). *Vet Microbiol.* (2013) 162:582–94. doi: 10.1016/j.vetmic.2012.11.025
268. Decaro N, Campolo M, Lorusso A, Desario C, Mari V, Colaianni ML, et al. Experimental infection of dogs with a novel strain of canine coronavirus causing systemic disease and lymphopenia. *Vet Microbiol.* (2008) 128:253–60. doi: 10.1016/j.vetmic.2007.10.008
269. Decaro N, Cordonnier N, Demeter Z, Egberink H, Elia G, Grellet A, et al. European surveillance for pantropic canine coronavirus. *J Clin Microbiol.* (2013) 51:83–8. doi: 10.1128/JCM.02466-12
270. Saif LJ, Brock KV, Redman DR, Kohler EM. Winter dysentery in dairy herds: electron microscopic and serological evidence for an association with coronavirus infection. *Vet Rec.* (1991) 128:447–9. doi: 10.1136/vr.128.19.447
271. Patterson S, Bingham RW. Electron microscope observations on the entry of avian infectious bronchitis virus into susceptible cells. *Arch Virol.* (1976) 52:191–200. doi: 10.1007/BF01348016
272. Bezuidenhout A, Mondal SP, Buckles EL. Histopathological and immunohistochemical study of air sac lesions induced by two strains of infectious bronchitis virus. *J Comp Pathol.* (2011) 145:319–26. doi: 10.1016/j.jcpa.2011.01.011
273. Arshad SS, Al-Salihi KA. Immunohistochemical detection of infectious bronchitis virus antigen in chicken respiratory and kidney tissues. In: *Proceedings of the 12th Federation of Asian Veterinary Associations Congress/14th Veterinary Association Malaysia Scientific Congress* (2002).
274. Abdel-Moneim AS, Zlotowski P, Veits J, Keil GM, Teifke JP. Immunohistochemistry for detection of avian infectious bronchitis virus strain M41 in the proventriculus and nervous system of experimentally infected chicken embryos. *Virol J.* (2009) 6:15. doi: 10.1186/1743-422X-6-15
275. Yagyu K, Ohta S. Detection of infectious bronchitis virus antigen from experimentally infected chickens by indirect immunofluorescent assay with monoclonal antibody. *Avian Dis.* (1990) 34:246–52. doi: 10.2307/1591405
276. Saif LJ, Bohl EH, Kohler EM, Hughes JH. Immune electron microscopy of transmissible gastroenteritis virus and rotavirus (reovirus-like agent) of swine. *Am J Vet Res.* (1977) 38:13–20.
277. Pensaert M, Haelterman EO, Burnstein T. Transmissible gastroenteritis of swine: virus-intestinal cell interactions. I Immunofluorescence, histopathology and virus production in the small intestine through the course of infection. *Arch Gesamte Virusforsch.* (1970) 31:321–34. doi: 10.1007/BF01253767
278. Shoup DI, Swayne DE, Jackwood DJ, Saif LJ. Immunohistochemistry of transmissible gastroenteritis virus antigens in fixed paraffin-embedded tissues. *J Vet Diagn Invest.* (1996) 8:161–7. doi: 10.1177/104063879600800204
279. Lanza I, Shoup DI, Saif LJ. Lactogenic immunity and milk antibody isotypes to transmissible gastroenteritis virus in sows exposed to porcine respiratory coronavirus during pregnancy. *Am J Vet Res.* (1995) 56:739–48.
280. Sestak K, Lanza I, Park SK, Weilnau PA, Saif LJ. Contribution of passive immunity to porcine respiratory coronavirus to protection against transmissible gastroenteritis virus challenge exposure in suckling pigs. *Am J Vet Res.* (1996) 57:664–71.
281. Sestak K, Lanza I, Park SK, Weilnau PA, Saif LJ. Contribution of passive immunity to porcine respiratory coronavirus to protection against transmissible gastroenteritis virus challenge exposure in suckling pigs. *Am J Vet Res.* (1996) 57:664–71.
282. van Nieuwstadt AP, Cornelissen JB, Zetstra T. Comparison of two methods for detection of transmissible gastroenteritis virus in feces of pigs with experimentally induced infection. *Am J Vet Res.* (1988) 49:1836–43.
283. Giori L, Giordano A, Giudice C, Grieco V, Paltrinieri S. Performances of different diagnostic tests for feline infectious peritonitis in challenging clinical cases. *J Small Anim Pract.* (2011) 52:152–7. doi: 10.1111/j.1748-5827.2011.01042.x
284. Addie DD, Paltrinieri S, Pedersen NC. Recommendations from workshops of the second international feline coronavirus/feline infectious peritonitis symposium. *J Feline Med Surg.* (2004) 6:125–30. doi: 10.1016/j.jfms.2003.12.009
285. Ellis JA, McLean N, Hupaelo R, Haines DM. Detection of coronavirus in cases of tracheobronchitis in dogs: a retrospective study from 1971 to 2003. *Can Vet J.* (2005) 46:447–8.
286. Stranieri A, Giordano A, Paltrinieri S, Giudice C, Cannito V, Lauzi S. Comparison of the performance of laboratory tests in the diagnosis of feline infectious peritonitis. *J Vet Diagn Investig.* (2018) 30:459–63. doi: 10.1177/1040638718756460
287. Hartmann K, Binder C, Hirschberger J, Cole D, Reinacher M, Schroo S, et al. Comparison of different tests to diagnose feline infectious peritonitis. *J Vet Intern Med.* (2003) 17:781–90. doi: 10.1111/j.1939-1676.2003.tb02515.x
288. Hirschberger J. Zytologievon Körperhöhlenergüssen [Cytology of body cavity effusions]. *TierarztlPrax.* (1995) 23:192–9.
289. Hirschberger J, Koch S. Validation of the determination of the activity of adenosine deaminase in the body effusions of cats. *Res Vet Sci.* (1995) 59:226–9. doi: 10.1016/0034-5288(95)90007-1
290. Hirschberger J, Sauer G. Clinical and chemical investigations of body cavity effusions. *TieraerztlichePrax.* (1991) 19:431–4.
291. Bohl EH, Kumagai T. The use of cell cultures for the study of swine transmissible gastroenteritis virus. In: *United States Livestock Sanitary Association Meeting.* (1965). p. 343–50.
292. Laude H, Gelfi J, Aynaud JM. *In vitro* properties of low- and high-passaged strains of transmissible gastroenteritis coronavirus of swine. *Am J Vet Res.* (1981) 42:447–9.
293. Witte KH. Isolation of the virus of transmissible gastroenteritis (TGE) from naturally infected piglets in cell culture. *Zentralbl Veterinarmed B.* (1971) 18:770–8. doi: 10.1111/j.1439-0450.1971.tb01654.x
294. McClurkin AW, Norman JO. Studies on transmissible gastroenteritis of swine. *II* Selected characteristics of a cytopathogenic virus common to five isolates from transmissible gastroenteritis. *Can J Comp Med Vet Sci.* (1966) 30:190–8.
295. Otsuki K, Yamamoto H, Tsubokura M. Studies on avian infectious bronchitis virus (IBV). I. Resistance of IBV to chemical and physical treatments. *Arch Virol.* (1979) 60:25–32. doi: 10.1007/BF01318094
296. Jones BV, Hennion RM. The preparation of chicken tracheal organ cultures for virus isolation, propagation, and titration. *Methods Mol Biol.* (2008) 454:103–7. doi: 10.1007/978-1-59745-181-9_9
297. Bhattacharjee PS, Naylor CJ, Jones RC. A simple method for immunofluorescence staining of tracheal organ cultures for the rapid identification of infectious bronchitis virus. *Avian Pathol.* (1994) 23:471–80. doi: 10.1080/03079459408419017
298. Beaudette F, Hudson C. Cultivation of the virus of infectious bronchitis. *J Am Vet Med Assoc.* (1937) 90:51–60.
299. Loomis LN, Cunningham CH, Gray ML, Thorp F. Pathology of the chicken embryo infected with infectious bronchitis virus. *Am J Vet Res.* (1950) 11:245–51.
300. Bernard S, Bottreau E, Aynaud JM, Have P, Szymansky J. Natural infection with the porcine respiratory coronavirus induces protective lactogenic immunity against transmissible gastroenteritis. *Vet Microbiol.* (1989) 21:1–8. doi: 10.1016/0378-1135(89)90013-8
301. Garwes DJ, Stewart F, Cartwright SF, Brown I. Differentiation of porcine coronavirus from transmissible gastroenteritis virus. *Vet Rec.* (1988) 122:86–7. doi: 10.1136/vr.122.4.86
302. Callebaut P, Pensaert MB, Hooyberghs J. A competitive inhibition ELISA for the differentiation of serum antibodies from pigs infected with transmissible gastroenteritis virus (TGEV) or with the TGEV-related porcine respiratory coronavirus. *Vet Microbiol.* (1989) 20:9–19. doi: 10.1016/0378-1135(89)90003-5
303. Pedersen NC. Serologic studies of naturally occurring feline infectious peritonitis. *Am J Vet Res.* (1976) 37:1449–53.

304. Addie DD, Jarrett O. Feline coronavirus antibodies in cats. *Vet Rec.* (1992) 131:202–3. doi: 10.1136/vr.131.9.202-a
305. Addie DD, le Poder S, Burr P, Decaro N, Graham E, Hofmann-Lehmann R, et al. Utility of feline coronavirus antibody tests. *J Feline Med Surg.* (2015) 17:152–62. doi: 10.1177/1098612X14538873
306. Osterhaus AD, Horzinek MC, Reynolds DJ. Seroepidemiology of feline infectious peritonitis virus infections using transmissible gastroenteritis virus as antigen. *Zentralbla Veterinärmed B.* (1977) 24:835–41. doi: 10.1111/j.1439-0450.1977.tb00976.x
307. Horzinek MC, Osterhaus AD. Feline infectious peritonitis: a worldwide serosurvey. *Am J. Vet. Res.* (1979) 40:1487–92.
308. Pratelli A. Comparison of serologic techniques for the detection of antibodies against feline coronaviruses. *J Vet Diagn Investig.* (2008) 20:45–50. doi: 10.1177/104063870802000108
309. Chen L, Li F. Structural analysis of the evolutionary origins of influenza virus hemagglutinin and other viral lectins. *J Virol.* (2013) 87:4118–20. doi: 10.1128/JVI.03476-12
310. Erles K, Shiu KB, Brownlie J. Isolation and sequence analysis of canine respiratory coronavirus. *Virus Res.* (2007) 124:78–87. doi: 10.1016/j.virusres.2006.10.004
311. Qiao J, Meng Q, Cai X, Chen C, Zhang Z, Tian Z. Rapid detection of Betacoronavirus 1 from clinical fecal specimens by a novel reverse transcription loop-mediated isothermal amplification assay. *J Vet Diagn Invest.* (2012) 24:174–7. doi: 10.1177/1040638711425937
312. Amer HM, Abd El Wahed A, Shalaby MA, Almajhdi FN, Hufert FT, Weidmann M, et al. new approach for diagnosis of bovine coronavirus using a reverse transcription recombinase polymerase amplification assay. *J Virol Methods.* (2013) 193:337–40. doi: 10.1016/j.jviromet.2013.06.027
313. Stephensen CB, Casebolt DB, Gangopadhyay NN. Phylogenetic analysis of a highly conserved region of the polymerase gene from 11 coronaviruses and development of a consensus polymerase chain reaction assay. *Virus Res.* (1999) 60:181–9. doi: 10.1016/S0168-1702(99)00017-9
314. Lin Z, Kato A, Kudou Y, Umeda K, Ueda S. Typing of recent infectious bronchitis virus isolates causing nephritis in chicken. *Arch Virol.* (1991) 120:145–9. doi: 10.1007/BF01310957
315. Zwaagstra KA, van der Zeijst BA, Kusters JG. Rapid detection and identification of avian infectious bronchitis virus. *J Clin Microbiol.* (1992) 30:79–84. doi: 10.1128/jcm.30.1.79-84.1992
316. Kwon HM, Jackwood MW, Gelb J. Differentiation of infectious bronchitis virus serotypes using polymerase chain reaction and restriction fragment length polymorphism analysis. *Avian Dis.* (1993) 37:194–202. doi: 10.2307/1591474
317. Keeler CL, Reed KL, Nix WA, Gelb J. Serotype identification of avian infectious bronchitis virus by RT-PCR of the peplomer (S-1) gene. *Avian Dis.* (1998) 42:275–84. doi: 10.2307/1592477
318. Lin Z, Kato A, Kudou Y, Ueda S. A new typing method for the avian infectious bronchitis virus using polymerase chain reaction and restriction enzyme fragment length polymorphism. *Arch Virol.* (1991) 116:19–31. doi: 10.1007/BF01319228
319. Mardani K, Noormohammadi AH, Ignatovic J, Browning GF. Typing infectious bronchitis virus strains using reverse transcription-polymerase chain reaction and restriction fragment length polymorphism analysis to compare the 3' 75 kb of their genomes. *Avian Pathol.* (2006) 35:63–9. doi: 10.1080/03079450500465817
320. Montassier MDFS, Brentano L, Montassier HJ, Richtzenhain LG. Genetic grouping of avian infectious bronchitis virus isolated in Brazil based on RT-PCR/RFLP analysis of the S1 gene. *Pesqui Vet Bras.* (2008) 28:190–4 doi: 10.1590/S0100-736X2008000300011
321. Chousalkar KK, Cheetham BF, Roberts JR. LNA probe-based real-time RT-PCR for the detection of infectious bronchitis virus from the oviduct of unvaccinated and vaccinated laying hens. *J Virol Methods.* (2009) 155:67–71. doi: 10.1016/j.jviromet.2008.09.028
322. Acevedo AM, Perera CL, Vega A, Ríos L, Coronado L, Relova D, et al. A duplex SYBR green I-based real-time RT-PCR assay for the simultaneous detection and differentiation of massachusetts and non-massachusetts serotypes of infectious bronchitis virus. *Mol Cell Probes.* (2013) 27:184–92. doi: 10.1016/j.mcp.2013.06.001
323. Meir R, Maharat O, Farnushi Y, Simanov L. Development of a real-time TaqMan RT-PCR assay for the detection of infectious bronchitis virus in chickens, and comparison of RT-PCR and virus isolation. *J Virol Methods.* (2010) 163:190–4. doi: 10.1016/j.jviromet.2009.09.014
324. Chen HW, Wang CH. A multiplex reverse transcriptase-PCR assay for the genotyping of avian infectious bronchitis viruses. *Avian Dis.* (2010) 54:104–8. doi: 10.1637/8954-060609-Reg.1
325. Chen HT, Zhang J, Ma YP, Ma LN, Ding YZ, Liu XT, et al. Reverse transcription loop-mediated isothermal amplification for the rapid detection of infectious bronchitis virus in infected chicken tissues. *Mol Cell Probes.* (2010) 24:104–6. doi: 10.1016/j.mcp.2009.10.001
326. Kim SY, Song DS, Park BK. Differential detection of transmissible gastroenteritis virus and porcine epidemic diarrhea virus by duplex RT-PCR. *J Vet Diagn Invest.* (2001) 13:516–20. doi: 10.1177/104063870101300611
327. Masuda T, Tsuchiaka S, Ashiba T, Yamasato H, Fukunari K, Omatsu T, et al. Development of one-step real-time reverse transcriptase-PCR-based assays for the rapid and simultaneous detection of four viruses causing porcine diarrhea. *Jpn J Vet Res.* (2016) 64:5–14.
328. Ogawa H, Taira O, Hirai T, Takeuchi H, Nagao A, Ishikawa Y, et al. Multiplex PCR and multiplex RT-PCR for inclusive detection of major swine DNA and RNA viruses in pigs with multiple infections. *J Virol Methods.* (2009) 160:210–4. doi: 10.1016/j.jviromet.2009.05.010
329. Longstaff L, Porter E, Crossley VJ, Hayhow SE, Helps CR, Tasker S. Feline coronavirus quantitative reverse transcriptase polymerase chain reaction on effusion samples in cats with and without feline infectious peritonitis. *J Feline Med Surg.* (2017) 19:240–5. doi: 10.1177/1098612X15606957
330. Felten S, Leutenegger CM, Balzer HJ, Pantchev N, Matiasek K, Sangl L, et al. Evaluation of a discriminative realtimert-PCR in cerebrospinal fluid for the diagnosis of feline infectious peritonitis. In: *Proceedings of the 27th ECVIM-CA Congress*. St. Julian's (2017). p. 14–6.
331. Felten S, Emmler L, Matiasek K, Balzer H-J, Pantchev N, Leutenegger CM, et al. Detection of mutated and non-mutated feline coronavirus in tissues and body fluids of cats with feline infectious peritonitis. In: *Proceedings of the 2018 ISCAID Symposium*. Portland, OR (2018).
332. Felten S, Sangl L, Matiasek K, Leutenegger CM, Pantchev N., Balzer H-J. Comparison of different diagnostic methods in aqueous humor to diagnose feline infectious peritonitis. In: *Proceedings of the 2016 ISCAID Symposium*. Bristol (2016).
333. Li X, Scott FW. Detection of feline coronaviruses in cell cultures and in fresh and fixed feline tissues using polymerase chain reaction. *Vet Microbiol.* (1994) 42:65–77. doi: 10.1016/0378-1135(94)90078-7
334. Barker EN, Stranieri A, Helps CR, Porter EL, Davidson AD, Day MJ, et al. Limitations of using feline coronavirus spike protein gene mutations to diagnose feline infectious peritonitis. *Vet Res.* (2017) 48:60. doi: 10.1186/s13567-017-0467-9
335. Freiche GM, Guidez CL, Duarte M, Le Poder YB. Sequencing of 3c and spike genes in feline infectious peritonitis: which samples are the most relevant for analysis? A retrospective study of 33 cases from 2008 to 2014. *J Vet Intern Med.* (2016) 30:436.
336. Felten S, Weider K, Doenges S, Gruendl S, Matiasek K, Hermanns W, et al. Detection of feline coronavirus spike gene mutations as a tool to diagnose feline infectious peritonitis. *J Feline Med Surg.* (2017) 19:321–35. doi: 10.1177/1098612X15623824
337. Felten S, Leutenegger CM, Balzer HJ, Pantchev N, Matiasek K, Wess G, et al. Sensitivity and specificity of a real-time reverse transcriptase polymerase chain reaction detecting feline coronavirus mutations in effusion and serum/plasma of cats to diagnose feline infectious peritonitis. *BMC Vet Res.* (2017) 13:228. doi: 10.1186/s12917-017-1147-8
338. Decaro N, Pratelli A, Campolo M, Elia G, Martella V, Tempesta M, et al. Quantitation of canine coronavirus RNA in the faeces of dogs by TaqMan RT-PCR. *J Virol Methods.* (2004) 119:145–50. doi: 10.1016/j.jviromet.2004.03.012
339. Gizzi AB, Oliveira ST, Leutenegger CM, Estrada M, Kozemjakin DA, Stedile R, et al. Presence of infectious agents and co-infections in diarrheic dogs determined with a real-time polymerase chain reaction-based panel. *BMC Vet Res.* (2014) 10:23. doi: 10.1186/1746-6148-10-23

340. Zulperi ZM, Omar AR, Arshad SS. Sequence and phylogenetic analysis of S1, S2, M, and N genes of infectious bronchitis virus isolates from Malaysia. *Virus Genes.* (2009) 38:383–91. doi: 10.1007/s11262-009-0337-2
341. Abro SH, Renström LH, Ullman K, Isaksson M, Zohari S, Jansson DS, et al. Emergence of novel strains of avian infectious bronchitis virus in Sweden. *Vet Microbiol.* (2012) 155:237–46. doi: 10.1016/j.vetmic.2011.09.022
342. Wang W, Xu Y, Gao R, Lu R, Han K, Wu G, et al. Detection of SARS-CoV-2 in different types of clinical specimens. *JAMA*. (2020) 323:1843–4. doi: 10.1001/jama.2020.3786
343. Yu L, Wu S, Hao X, Dong X, Mao L, Pelechano V, et al. Rapid detection of COVID-19 coronavirus using a reverse transcriptional loop-mediated isothermal amplification (RT-LAMP) diagnostic platform. *Clin Chem.* (2020) 66:975–7. doi: 10.1093/clinchem/hvaa102
344. Vashist SK. *In vitro* diagnostic assays for COVID-19: recent advances and emerging trends. *Diagnostics.* (2020) 10:202. doi: 10.3390/diagnostics10040202
345. Younes N, Al-Sadeq DW, Al-Jighefee H, et al. Challenges in laboratory diagnosis of the novel coronavirus SARS-CoV-2. *Viruses.* (2020) 12:582. doi: 10.3390/v12060582
346. Rao VK. Point of care diagnostic devices for rapid detection of novel coronavirus (SARS-nCoV19) pandemic: a review. *Front. Nanotechnol.* (2021) 2:2673–3013 doi: 10.3389/fnano.2020.593619
347. Samson R, Navale GR, Dharne MS. Biosensors: frontiers in rapid detection of COVID-19. *Biotech.* (2020) 10:385. doi: 10.1007/s13205-020-02369-0
348. Wang X, Zhong M, Liu Y, Ma P, Dang L, Meng Q, et al. Rapid and sensitive detection of COVID-19 using CRISPR/Cas12a-based detection with naked eye readout, CRISPR/Cas12a-NER. *Sci Bull.* (2020) 65:1436–9. doi: 10.1016/j.scib.2020.04.041
349. Chen Z, Wu Q, Chen J, Ni X, Dai J, A DNA. Aptamer based method for detection of SARS-CoV-2 nucleocapsid protein. *Virol Sin.* (2020) 35:351–4. doi: 10.1007/s12250-020-00236-z
350. Fraser DD, Slessarev M, Martin CM, Daley M, Patel MA, Miller MR, et al. Metabolomics profiling of critically ill coronavirus disease 2019 patients: identification of diagnostic and prognostic biomarkers. *Crit Care Explor.* (2020) 2:e0272. doi: 10.1097/CCE.0000000000000272
351. Okda F, Liu X, Singrey A, Clement T, Nelson J, Christopher-Hennings J, et al. Development of an indirect ELISA, blocking ELISA, fluorescent microsphere immunoassay and fluorescent focus neutralization assay for serologic evaluation of exposure to North American strains of porcine epidemic diarrhea virus. *BMC Vet Res.* (2015) 11:180. doi: 10.1186/s12917-015-0500-z
352. Okda F, Lawson S, Liu X, Singrey A, Clement T, Hain K, et al. Development of monoclonal antibodies and serological assays including indirect ELISA and fluorescent microsphere immunoassays for diagnosis of porcine deltacoronavirus. *BMC Vet Res.* (2016) 12:95. doi: 10.1186/s12917-016-0716-6
353. Liu J, Shi H, Cong G, Chen J, Zhang X, Shi D, et al. Development of a rapid and sensitive europium (III) chelate microparticle-based lateral flow test strip for the detection and epidemiological surveillance of porcine epidemic diarrhea virus. *Arch Virol.* (2020) 165:1049–56. doi: 10.1007/s00705-020-04566-x
354. Thanthrige-Don N, Lung O, Furukawa-Stoffer T, Buchanan C, Joseph T, Godson DL, et al. A novel multiplex PCR-electronic microarray assay for rapid and simultaneous detection of bovine respiratory and enteric pathogens. *J Virol Methods.* (2018) 261:51–62. doi: 10.1016/j.jviromet.2018.08.010
355. Calvet GA, Pereira SA, Ogrzewalska M, Pauvolid-Corrêa A, Resende PC, Tassinari W, et al. Investigation of SARS-CoV-2 infection in dogs and cats of humans diagnosed with COVID-19 in Rio de Janeiro, Brazil. *PLoS ONE.* (2021) 16:e0250853. doi: 10.1371/journal.pone.0250853
356. Haljasmägi L, Remm A, Rumm AP, Krassohhina E, Sein H, Tamm A, et al. LIPS method for the detection of SARS-CoV-2 antibodies to spike and nucleocapsid proteins. *Eur J Immunol.* (2020) 50:1234–6. doi: 10.1002/eji.202048715
357. Temmam S, Barbarino A, Maso D, Behillil S, Enouf V, Huon C, et al. Absence of SARS-CoV-2 infection in cats and dogs in close contact with a cluster of COVID-19 patients in a veterinary campus. One *Health.* (2020) 10:100164. doi: 10.1016/j.onehlt.2020.100164
358. Wang W, Wang T, Deng Y, Niu P. Ruhan A, Zhao J, et al. A novel luciferase immunosorbent assay performs better than a commercial enzyme-linked immunosorbent assay to detect MERS-CoV specific IgG in humans and animals. *Biosaf Health.* (2019) 1:134–43. doi: 10.1016/j.bsheal.2019.12.006
359. Csiszar A, Jakab F, Valencak TG, Lanszki Z, Tóth GE, Kemenesi G, et al. Companion animals likely do not spread COVID-19 but may get infected themselves. *Geroscience.* (2020) 42:1229–36. doi: 10.1007/s11357-020-00248-3
360. Nie J, Li Q, Wu J, Zhao C, Hao H, Liu H, et al. Establishment and validation of a pseudovirus neutralization assay for SARS-CoV-2. *Emerg Microbes Infect.* (2020) 9:680–6. doi: 10.1080/22221751.2020.1743767
361. Decaro N, Campolo M, Mari V, Desario C, Colaianni ML, Di Trani L, et al. A candidate modified-live bovine coronavirus vaccine: safety and immunogenicity evaluation. *New Microbiol.* (2009) 32:109–13.
362. Tizard IR. *Vaccines for Veterinarians.* 1st ed. St Louis, MI: Elsevier (2020).
363. Zhang Y, Huang S, Zeng Y, Xue C, Cao Y. Rapid development and evaluation of a live-attenuated QX-like infectious bronchitis virus vaccine. *Vaccine.* (2018) 36:4245–54. doi: 10.1016/j.vaccine.2018.05.123
364. Bohl EH, Gupta RP, Olquin MF, Saif LJ. Antibody responses in serum, colostrum, and milk of swine after infection or vaccination with transmissible gastroenteritis virus. *Infect Immun.* (1972) 6:289–301. doi: 10.1128/iai.6.3.289-301.1972
365. Saif LJ, Bohl E. Passive immunity to transmissible gastroenteritis virus: intramammary viral inoculation of sows. *Ann N Y Acad Sci.* (1983) 409:708. doi: 10.1111/j.1749-6632.1983.tb26910.x
366. Baek PS, Choi HW, Lee S, Yoon IJ, Lee YJ, Lee du S, et al. Efficacy of an inactivated genotype 2b porcine epidemic diarrhea virus vaccine in neonatal piglets. *Vet Immunol Immunopathol.* (2016) 174:45–9. doi: 10.1016/j.vetimm.2016.04.009
367. Sato T, Takeyama N, Katsumata A, Tuchiya K, Kodama T, Kusanagi K. Mutations in the spike gene of porcine epidemic diarrhea virus associated with growth adaptation *in vitro* and attenuation of virulence *in vivo*. *Virus Genes.* (2011) 43:72–8. doi: 10.1007/s11262-011-0617-5
368. Gerdts V, Zakhartchouk A. Vaccines for porcine epidemic diarrhea virus and other swine coronaviruses. *Vet Microbiol.* (2017) 206:45–51. doi: 10.1016/j.vetmic.2016.11.029
369. Pratelli A, Tinelli A, Decaro N, Martella V, Camero M, Tempesta M, et al. Safety and efficacy of a modified-live canine coronavirus vaccine in dogs. *Vet Microbiol.* (2004) 99:43–9. doi: 10.1016/j.vetmic.2003.07.009
370. Pratelli A. Genetic evolution of canine coronavirus and recent advances in prophylaxis. *Vet Res.* (2006) 37:191–200. doi: 10.1051/vetres:2005053
371. Zhang D, Huang X, Zhang X, Cao S, Wen X, Wen Y, et al. Construction of an oral vaccine for transmissible gastroenteritis virus based on the TGEV N gene expressed in an attenuated Salmonella typhimurium vector. *J Virol Methods.* (2016) 227:6–13. doi: 10.1016/j.jviromet.2015.08.011
372. Yuan X, Lin H, Fan H. Efficacy and immunogenicity of recombinant swinepox virus expressing the A epitope of the TGEV S protein. *Vaccine.* (2015) 33:3900–6. doi: 10.1016/j.vaccine.2015.06.057
373. Orr-Burks N, Gulley SL, Toro H, van Ginkel FW. Immunoglobulin A as an early humoral responder after mucosal avian coronavirus vaccination. *Avian Dis.* (2014) 58:279–86. doi: 10.1637/10740-120313-Reg.1
374. Jordan B. Vaccination against infectious bronchitis virus: a continuous challenge. *Vet Microbiol.* (2017) 206:137–43. doi: 10.1016/j.vetmic.2017.01.002
375. Smialek M, Tykalowski B, Dziewulska D, Stenzel T, Koncicki A. Immunological aspects of the efficiency of protectotype vaccination strategy against chicken infectious bronchitis. *BMC Vet Res.* (2017) 13:44. doi: 10.1186/s12917-017-0963-1
376. Decaro N, Mari V, Sciarretta R, Colao V, Losurdo M, Catella C, et al. Immunogenicity and protective efficacy in dogs of an MF59^{TM}-adjuvanted vaccine against recombinant canine/porcine coronavirus. *Vaccine.* (2011) 29:2018–23. doi: 10.1016/j.vaccine.2011.01.028
377. Zhang Y, Zhang X, Liao X, Huang X, Cao S, Wen X, et al. Construction of a bivalent DNA vaccine co-expressing S genes of transmissible gastroenteritis virus and porcine epidemic diarrhea virus delivered by attenuated Salmonella typhimurium. *Virus Genes.* (2016) 52:354–64. doi: 10.1007/s11262-016-1316-z

378. Meng F, Ren Y, Suo S, Sun X, Li X, Li P, et al. Evaluation on the efficacy and immunogenicity of recombinant DNA plasmids expressing spike genes from porcine transmissible gastroenteritis virus and porcine epidemic diarrhea virus. *PLoS ONE.* (2013) 8:e57468. doi: 10.1371/journal.pone.0057468
379. Tuboly T, Nagy É. Construction and characterization of recombinant porcine adenovirus serotype 5 expressing the transmissible gastroenteritis virus spike gene. *J Gen Virol.* (2001) 82:183–90. doi: 10.1099/0022-1317-82-1-183
380. Oh J, Lee KW, Choi HW, Lee C. Immunogenicity and protective efficacy of recombinant S1 domain of the porcine epidemic diarrhea virus spike protein. *Arch Virol.* (2014) 159:2977–87. doi: 10.1007/s00705-014-2163-7
381. Makadiya N, Brownlie R, van den Hurk J, Berube N, Allan B, Gerdts V, et al. S1 domain of the porcine epidemic diarrhea virus spike protein as a vaccine antigen. *Virol J.* (2016) 13:57. doi: 10.1186/s12985-016-0512-8
382. Lamphear BJ, Jilka JM, Kesl L, Welter M, Howard JA, Streatfield SJ, et al. corn-based delivery system for animal vaccines: an oral transmissible gastroenteritis virus vaccine boosts lactogenic immunity in swine. *Vaccine.* (2004) 22:2420–4. doi: 10.1016/j.vaccine.2003.11.066
383. Takamura K, Matsumoto Y, Shimizu Y. Field study of bovine coronavirus vaccine enriched with hemagglutinating antigen for winter dysentery in dairy cows. *Can J Vet Res.* (2002) 66:278–81.
384. Ismail MM, Cho KO, Ward LA, Saif LJ, Saif YM. Experimental bovine coronavirus in turkey poults and young chickens. *Avian Dis.* (2001) 45:157–63. doi: 10.2307/1593023
385. Tsunemitsu H, el-Kanawati ZR, Smith DR, Reed HH, Saif LJ. Isolation of coronaviruses antigenically indistinguishable from bovine coronavirus from wild ruminants with diarrhea. *J Clin Microbiol.* (1995) 33:3264–9. doi: 10.1128/jcm.33.12.3264-3269.1995
386. Brian DA, Hogue BG, Kienzle TE. The coronavirus hemagglutinin esterase glycoprotein. In: Siddell S, editor. *The Coronaviridae*. New York, NY: Plenum Press (1995). p. 165–79.
387. Ballesteros ML, Sánchez CM, Enjuanes L. Two amino acid changes at the N-terminus of transmissible gastroenteritis coronavirus spike protein result in the loss of enteric tropism. *Virology.* (1997) 227:378–88. doi: 10.1006/viro.1996.8344
388. Saif L, Wesley R. Transmissible gastroenteritis virus. In: Straw BE, D'Allaire S, Mengeling WL, Taylor D, editors. *Diseases of Swine*. Ames, IA: Iowa State University Press (1998).
389. Akimkin V, Beer M, Blome S, Hanke D, Höper D, Jenckel M, et al. New chimeric porcine coronavirus in swine feces, Germany, 2012. *Emerg Infect Dis.* (2016) 22:1314–5. doi: 10.3201/eid2207.160179
390. Belsham GJ, Rasmussen TB, Normann P, Vaclavek P, Strandbygaard B, Bøtner A. Characterization of a novel chimeric swine enteric coronavirus from diseased pigs in Central Eastern Europe in 2016. *Transbound Emerg Dis.* (2016) 63:595–601. doi: 10.1111/tbed.12579
391. Boniotti MB, Papetti A, Lavazza A, Alborali G, Sozzi E, Chiapponi C, et al. Porcine epidemic diarrhea virus and discovery of a recombinant swine enteric coronavirus, Italy. *Emerg Infect Dis.* (2016) 22:83–7. doi: 10.3201/eid2201.150544
392. Ye ZW, Yuan S, Yuen KS, Fung SY, Chan CP, Jin DY. Zoonotic origins of human coronaviruses. *Int J Biol Sci.* (2020) 16:1686–97. doi: 10.7150/ijbs.45472
393. Oma VS, Klem T, Tråvén M, Alenius S, Gjerset B, Myrmel M, et al. Temporary carriage of bovine coronavirus and bovine respiratory syncytial virus by fomites and human nasal mucosa after exposure to infected calves. *BMC Vet Res.* (2018) 14:22. doi: 10.1186/s12917-018-1335-1
394. Hussain KA, Storz J, Kousoulas KG. Comparison of bovine coronavirus (BCV) antigens: monoclonal antibodies to the spike glycoprotein distinguish between vaccine and wild-type strains. *Virology.* (1991) 183:442–5. doi: 10.1016/0042-6822(91)90163-6
395. Poon LLM, Chu DKW, Chan KH, Wong OK, Ellis TM, Leung YHC, et al. Identification of a novel coronavirus in bats. *J Virol.* (2005) 79:2001–9. doi: 10.1128/JVI.79.4.2001-2009.2005
396. Promkuntod N. Dynamics of avian coronavirus circulation in commercial and non-commercial birds in Asia—a review. *Vet Q.* (2016) 36:30–−44, doi: 10.1080/01652176.2015.1126868
397. Miłek J, Blicharz-Domańska K. Coronaviruses in avian species—review with focus on epidemiology and diagnosis in wild birds. *J Vet Res.* (2018) 62:249–55. doi: 10.2478/jvetres-2018-0035
398. McIntosh K, Kapikian AZ, Hardison KA, Hartley JW, Chanock RM. Antigenic relationships among the coronaviruses of man and between human and animal coronaviruses. *J Immunol.* (1969) 102:1109–18.
399. Hofmann M, Wyler R. Propagation of the virus of porcine epidemic diarrhea in cell culture. *J Clin Microbiol.* (1988) 26:2235–9. doi: 10.1128/jcm.26.11.2235-2239.1988
400. Brown IH. The pig as an intermediate host for influenza a viruses between birds and humans. *Int Congr Ser.* (2001) 1219:173–8. doi: 10.1016/S0531-5131(01)00666-5
401. Dhama K, Verma AK, Rajagunalan S, Deb R, Karthik K, Kapoor S, et al. Swine flu is back again: a review. *Pak J Biol Sci.* (2012) 15:1001–9. doi: 10.3923/pjbs.2012.1001.1009
402. Shi J, Wen Z, Zhong G, Yang H, Wang C, Huang B, et al. Susceptibility of ferrets, cats, dogs, and other domesticated animals to SARS-coronavirus 2. *Science.* (2020) 368:1016–20. doi: 10.1126/science.abb7015
403. Decaro N, Lorusso A. Novel human coronavirus (SARS-CoV-2): a lesson from animal coronaviruses. *Vet Microbiol.* (2020) 244. doi: 10.1016/j.vetmic.2020.108693
404. Martina BE, Haagmans BL, Kuiken T, Fouchier RA, Rimmelzwaan GF, Van Amerongen G, et al. Virology: SARS virus infection of cats and ferrets. *Nature.* (2003) 425:915. doi: 10.1038/425915a
405. Bosco-Lauth AM, Hartwig AE, Porter SM, Gordy PW, Nehring M, Byas AD, et al. Experimental infection of domestic dogs and cats with SARS-CoV-2: pathogenesis, transmission, and response to reexposure in cats. *Proc Natl Acad Sci USA.* (2020) 117:26382–8. doi: 10.1073/pnas.2013102117
406. Ge XY Li JL, Yang XL, Chmura AA, Zhu G, Epstein JH, et al. Isolation and characterization of a bat SARS-like coronavirus that uses the ACE2 receptor. *Nature.* (2013) 503:535–8. doi: 10.1038/nature12711
407. Benton DJ, Wrobel AG, Xu P, et al. Receptor binding and priming of the spike protein of SARS-CoV-2 for membrane fusion. *Nature.* (2020) 588:327–30. doi: 10.1038/s41586-020-2772-0
408. Zhou H, Chen X, Hu T, Song H, Liu Y, Wang P, et al. A novel bat coronavirus closely related to SARS- CoV-2 contains natural insertions at the S1/S2 cleavage site of the spike proteins. *Curr Biol.* (2020) 30:2196–203.e3 doi: 10.1016/j.cub.2020.05.023
409. Stavrinides J, Guttman D. Mosaic evolution of the severe acute respiratory syndrome coronavirus. *J Virol.* (2004) 78:76–82. doi: 10.1128/JVI.78.1.76-82.2004
410. Hemida MG, Perera RA, Wang P, Alhammadi MA, Siu LY Li M, et al. Middle East Respiratory Syndrome (MERS) coronavirus seroprevalence in domestic livestock in Saudi Arabia, 2010 to 2013. *Euro Surveill.* (2013) 18:20659. doi: 10.2807/1560-7917.ES2013.18.50.20659
411. Reusken CB, Haagmans BL, Müller MA, Gutierrez C, Godeke GJ, Meyer B, et al. Middle East respiratory syndrome coronavirus neutralising serum antibodies in dromedary camels: a comparative serological study. *Lancet Infect Dis.* (2013) 13:859–66. doi: 10.1016/S1473-3099(13)70164-6
412. Briese T, Mishra N, Jain K, Zalmout IS, Jabado OM, Karesh WB, et al. Middle East respiratory syndrome coronavirus quasispecies that include homologues of human isolates revealed through whole-genome analysis and virus cultured from dromedary camels in Saudi Arabia. *MBio.* (2014) 5:e01146-14. doi: 10.1128/mBio.01146-14
413. Haagmans BL, Al Dhahiry SH, Reusken CB, Raj VS, Galiano M, Myers R, et al. Middle East respiratory syndrome coronavirus in dromedary camels: an outbreak investigation. *Lancet Infect Dis.* (2014) 14:140–5. doi: 10.1016/S1473-3099(13)70690-X
414. Meyer B, Müller MA, Corman VM, Reusken CB, Ritz D, Godeke GJ, et al. Antibodies against MERS coronavirus in dromedary camels, United Arab Emirates, 2003 and 2013. *Emerg Infect Dis.* (2014) 20:552–9. doi: 10.3201/eid2004.131746
415. Raj VS, Farag EA, Reusken CB, Lamers MM, Pas SD, Voermans J, et al. Isolation of MERS coronavirus from a dromedary camel, Qatar, 2014. *Emerg Infect Dis.* (2014) 20:1339–42. doi: 10.3201/eid2008.140663
416. Reusken CB, Messadi L, Feyisa A, Ularamu H, Godeke GJ, Danmarwa A, et al. Geographic distribution of MERS coronavirus

among dromedary camels, Africa. *Emerg Infect Dis.* (2014) 20:1370–4. doi: 10.3201/eid2008.140590
417. Reusken CB, Farag EA, Jonges M, Godeke GJ, El-Sayed AM, Pas SD, et al. Middle East respiratory syndrome coronavirus (MERS-CoV) RNA and neutralising antibodies in milk collected according to local customs from dromedary camels, Qatar, April 2014. *Euro Surveill.* (2014) 19:20829. doi: 10.2807/1560-7917.ES2014.19.23.20829
418. Farag EA, Reusken CB, Haagmans BL, Mohran KA, Raj VS, Pas SD, et al. High proportion of MERS-CoV shedding dromedaries at slaughterhouse with a potential epidemiological link to human cases, Qatar 2014. *Infect Ecol Epidemiol.* (2015) 5:28305. doi: 10.3402/iee.v5.28305
419. Reusken CB, Farag EA, Haagmans BL, Mohran KA, Godeke GJ, Raj VS, et al. Occupational Exposure to Dromedaries and Risk for MERS-CoV Infection, Qatar, 2013-2014. *Emerg Infect Dis.* (2015) 21:1422–5. doi: 10.3201/eid2108.150481
420. Azhar EI, El-Kafrawy SA, Farraj SA, Hassan AM, Al-Saeed MS, Hashem AM. Evidence for camel-to-human transmission of MERS coronavirus. *N Engl J Med.* (2014) 370:2499–505. doi: 10.1056/NEJMoa1401505
421. Drosten C, Meyer B, Müller MA, Corman VM, Al-Masri M, Hossain R, et al. Transmission of MERS-coronavirus in household contacts. *Engl J Med.* (2014) 371:828–35. doi: 10.1056/NEJMoa1405858
422. World Health Organization. *Middle East Respiratory Syndrome Coronavirus (MERS-CoV)—United Arab Emirates*. (2021). Available online at: https://www.who.int/emergencies/disease-outbreak-news/item/2021-DON314 (accessed March 17, 2021).
423. Samara EM, Abdoun KA. Concerns about misinterpretation of recent scientific data implicating dromedary camels in epidemiology of Middle East respiratory syndrome (MERS). *MBio.* (2014) 5:e01430-14. doi: 10.1128/mBio.01430-14
424. Mohd HA, Al-Tawfiq JA, Memish ZA. Middle East Respiratory Syndrome Coronavirus (MERS-CoV) origin and animal reservoir. *Virol J.* (2016) 13:87. doi: 10.1186/s12985-016-0544-0
425. Ramadan N, Shaib H. Middle East respiratory syndrome coronavirus (MERS-CoV): a review. *Germs.* (2019) 9:35–42. doi: 10.18683/germs.2019.1155
426. Ren LL, Wang YM, Wu ZQ, Xiang ZC, Guo L, Xu T, et al. Identification of a novel coronavirus causing severe pneumonia in human: a descriptive study. *Chin Med J.* (2020) 133:1015–24. doi: 10.1097/CM9.0000000000000722
427. Almendros A, Gascoigne E. Can companion animals become infected with Covid-19? *Vet Rec.* (2020) 186:419–20. doi: 10.1136/vr.m1322
428. Almendros A. Can companion animals become infected with Covid-19? *Vet Rec.* (2020) 186:388–9. doi: 10.1136/vr.m1194
429. American Veterinary Medical Association. *SARS-CoV-2 in Animals, Including Pets*. (2020). Available online at: https://www.avma.org/resources-tools/animal-health-and-welfare/covid-19/sars-cov-2-animals-including-pets (accessed April 11, 2020).
430. USDA APHIS. *Confirmation of COVID-19 in Pet Dog in New York*. (2020). Available online at: https://www.aphis.usda.gov/aphis/newsroom/stakeholder-info/sa_by_date/sa-2020/sa-06/sars-cov-2-dog (accessed Jun 2, 2020).
431. Mallapaty S. Coronavirus can infect cats - dogs, not so much. *Nature*. (2020) doi: 10.1038/d41586-020-00984-8
432. Zhang Q, Zhang H, Gao J, Huang K, Yang Y, Hui X, et al. A serological survey of SARS-CoV-2 in cat in Wuhan. *Emerg Microbes Infect.* (2020) 9:2013–9. doi: 10.1080/22221751.2020.1817796
433. Daly N. Seven *More Big Cats Test Positive for Coronavirus at Bronx Zoo Animals*, *Coronavirus Coverage*. (2020). Available online at: https://www.nationalgeographic.com/animals/2020/04/tiger-coronavirus-covid19-positive-test-bronx-zoo (accessed April 23, 2020).
434. UK scientists find evidence of human-to-cat Covid transmission. *The Guardian*. (2021). Available online at: https://www.theguardian.com/lifeandstyle/2021/apr/23/uk-scientists-find-evidence-of-human-to-cat-covid-transmission
435. Deshpande A. Eight Asiatic lions test positive in COVID-19, first in India. *The Hindu* (2021).
436. Middlemiss C, Voas S, Glossop C, Huey R. SARS-CoV-2 in ferrets. *Vet Rec.* (2021) 188:133. doi: 10.1002/vetr.104
437. World Health Organization. *SARS-CoV-2 Mink-Associated Variant Strain – Denmark*. (2020). Available online at: https://www.who.int/csr/sars/en/WHOconsensus.pdf (accessed November 6, 2020).
438. USDA APHIS. *USDA Animal and Plant Health Inspection Service. Confirmation of COVID-19 in Gorillas at a California Zoo*. (2021). Available online at: https://www.aphis.usda.gov/aphis/newsroom/stakeholder-info/sa_by_date/sa-2021/sa-01/ca-gorillas-sars-cov-2 (accessed January 11, 2021).
439. Georgia Aquarium. *Asian Small-Clawed Otters at Georgia Aquarium Test Positive for COVID-19*. (2021). Available online at: https://news.georgiaaquarium.org/stories/releases-20210418#:~:text=April%2018%2C%202021-,Asian%20Small%2DClawed%20Otters%20at%20Georgia,Test%20Positive%20for%20COVID%2D19&text=The%20Asian%20small%2Dclawed%20otters,%2C%20mild%20lethargy%2C%20and%20coughing
440. Cohen J. From mice to monkeys, animals studied for coronavirus answers. *Science.* (2020) 368:221–2. doi: 10.1126/science.368.6488.221
441. CDC. *Coronavirus Disease (COVID-19)—Pets & Other Animals*. (2019). Available online at: https://www.cdc.gov/coronavirus/2019-ncov/daily-life-coping/positive-pet.html (accessed May 29, 2020).
442. Schlottau K, Rissmann M, Graaf A, Schön J, Sehl J, Wylezich C, et al. SARS-CoV-2 in fruit bats, ferrets, pigs, and chickens: an experimental transmission study. *Lancet Microbe.* (2020) 1:e218–25. doi: 10.1016/S2666-5247(20)30089-6
443. Pickering, BS, Smith G, Pinette MM, Embury-Hyatt C, Moffat E, et al. Susceptibility of domestic swine to experimental infection with severe acute respiratory syndrome coronavirus 2. *Emerg Infect Dis.* (2021) 27:104–12. doi: 10.3201/eid2701.203399
444. Mykytyn AZ, Lamers MM, Okba NMA, Breugem TI, Schipper D, van den Doel PB, et al. Susceptibility of rabbits to SARS-CoV-2. *Emerg Microbes Infect.* (2021) 10:1–7. doi: 10.1080/22221751.2020.1868951
445. Ulrich L, Wernike K, Hoffmann D, Mettenleiter TC, Beer M. Experimental infection of cattle with SARS-CoV-2. *Emerg Infect Dis.* (2020) 26:2979–81. doi: 10.3201/eid2612.203799
446. Freuling CM, Breithaupt A, Müller T, Sehl J, Balkema-Buschmann A, Rissmann M, et al. Susceptibility of raccoon dogs for experimental SARS-CoV-2 Infection. *Emerg Infect Dis.* (2020) 26:2982–5. doi: 10.3201/eid2612.203733
447. Michelitsch A, Wernike K, Ulrich L, Mettenleiter TC, Beer M. SARS-CoV-2 in animals: from potential hosts to animal models. *Adv Virus Res.* (2021) 110:59–102. doi: 10.1016/bs.aivir.2021.03.004
448. Brownlie J. Conclusive proof needed for animal virus reservoirs. *Vet Rec.* (2020) 186:354. doi: 10.1136/vr.m1076
449. Lanfear R. A global phylogeny of SARS-CoV-2 sequences from GISAID. *Zenodo*. (2020). doi: 10.5281/zenodo.3958883
450. Swaminathan S. The WHO's chief scientist on a year of loss and learning. *Nature*. (2020) 588:583–5. doi: 10.1038/d41586-020-03556-y
451. Chan JF, To KK, Tse H, Jin DY, Yuen KY. Interspecies transmission and emergence of novel viruses: lessons from bats and birds. *Trends Microbiol.* (2013) 21:544–55. doi: 10.1016/j.tim.2013.05.005
452. Klompus S, Leviatan S, Vogl T, Mazor RD, Kalka IN, Stoler-Barak L, et al. Cross-reactive antibodies against human coronaviruses and the animal coronavirome suggest diagnostics for future zoonotic spillovers. *Sci Immunol.* (2021) 6:eabe9950. doi: 10.1126/sciimmunol.abe9950
453. World Health Organization. *WHO Coronavirus Disease (COVID-19) Dashboard*. (2021). Available online at: https://covid19.who.int
454. Sorci G, Faivre B, Morand S. Explaining among-country variation in COVID-19 case fatality rate. *Sci Rep.* (2020) 10:18909. doi: 10.1038/s41598-020-75848-2
455. World Health Organization. *Update 49 - SARS Case-Fatality Ratio, Incubation Period*. Available online at: https://www.who.int/emergencies/disease-outbreak-news/item/2020-DON301#:~:text¯On%205%20November%2C%20the%20Danish,from%20August%20to%20September%202020 (accessed May 7, 2003).

456. WHO EMRO. *Situation Region Update. Middle East Respiratory Syndrome*. Available online at: http://www.emro.who.int/fr/health-topics/mers-cov/situation-update.html

Conflict of Interest: The authors declare that the research was conducted in the absence of any commercial or financial relationships that could be construed as a potential conflict of interest.

Publisher's Note: All claims expressed in this article are solely those of the authors and do not necessarily represent those of their affiliated organizations, or those of the publisher, the editors and the reviewers. Any product that may be evaluated in this article, or claim that may be made by its manufacturer, is not guaranteed or endorsed by the publisher.

frontiers in Veterinary Science

BRIEF RESEARCH REPORT
published: 03 November 2021
doi: 10.3389/fvets.2021.728238

Insight Into an Outbreak of Canine Distemper Virus Infection in Masked Palm Civets in China

Ning Shi[1,2†], Le Zhang[1†], Xiuhua Yu[3†], Xiangyu Zhu[2†], Shu Zhang[1], Daining Zhang[1] and Ming Duan[1]*

[1] Key Laboratory of Zoonosis Research, Ministry of Education, Institute of Zoonosis, College of Veterinary Medicine, Jilin University, Changchun, China, [2] Changchun Veterinary Research Institute, Chinese Academy of Agricultural Sciences, Changchun, China, [3] Department of Pediatrics, The First Hospital of Jilin University, Changchun, China

In August 2019, a suspected outbreak of canine distemper was observed in a masked palm civet farm that also received stray civets and rescued wild civets in Henan Province of China. A virulent canine distemper virus (CDV) strain, named HN19, from vaccinated masked palm civets was the etiologic agent identified in this outbreak using RT-PCR and sequencing of the complete genome. Serological analysis indicated a lower positive rate of CDV-neutralizing antibody in wild civets than in captive civets. Phylogenetic analysis of viral hemagglutinin (H) and the complete genome showed high identities with Rockborn-like strains at the nucleotide (98.7∼99.72%) and the closest nucleotide similarity with a strain that killed lesser pandas in China in 1997, but low identities with America-1 strains (vaccine strains). Most importantly, one distinct amino acid exchange in the H protein at position 540 Asp→Gly (D540G), which confers CDV with an improved ability to adapt and utilize the human receptor, was observed in HN19. This study represents the first reported outbreak of a Rockborn-like CDV strain infection in masked palm civets in China. Based on this report, the existence of Rockborn-like strains in Chinese wild animals may not only cause immune failure in captive animals, but may also confer increased zoonotic potential.

Keywords: canine distemper virus (CDV), civet (*Viverridae*), China, phylogenetic analysis, zoonotic potential

OPEN ACCESS

Edited by:
Lester J. Perez, University of Illinois at Urbana–Champaign, United States

Reviewed by:
Roselene Ecco, Federal University of Minas Gerais, Brazil
Makoto Takeda, National Institute of Infectious Diseases (NIID), Japan

***Correspondence:**
Ming Duan
duan_ming@jlu.edu.cn

† These authors have contributed equally to this work

Specialty section:
This article was submitted to Veterinary Infectious Diseases, a section of the journal Frontiers in Veterinary Science

Received: *21 June 2021*
Accepted: *27 September 2021*
Published: *03 November 2021*

Citation:
Shi N, Zhang L, Yu X, Zhu X, Zhang S, Zhang D and Duan M (2021) Insight Into an Outbreak of Canine Distemper Virus Infection in Masked Palm Civets in China. Front. Vet. Sci. 8:728238. doi: 10.3389/fvets.2021.728238

INTRODUCTION

Morbilliviruses belong to the order *Mononegavirales*, the family *Paramyxoviridae* and include a group of highly pathogenic viruses, such as measles virus (MeV), rinderpest virus (RPV) and canine distemper virus (CDV). In contrast to host-specific Mev and RPV, CDV has higher genetic diversity and causes a highly contagious disease in a wide broad of animals, including dog, civet, phocine, ferret, lion, raccoon, fox, etc. (1–6). Thus, spillover and spillback transmission of CDV between domesticated animals and wildlife reservoir hosts has been documented (6). Even more alarmingly, the host range of CDV has been expanded to other species that are evolutionarily more distant to canids, such as Asian marmots (*Marmota caudata*) and Japanese monkeys (*Macaca fuscat*) (7, 8).

The hemagglutinin (H) gene of CDV encodes the receptor-binding protein. Currently, the signaling lymphocyte activation molecule (SLAM) (also known as CD150) and the cell adhesion molecule Nectin-4 (also known as poliovirus receptor-like protein 4, PVRL4) are known to engage with H protein (9, 10). Of these, SLAM, as the principal cellular receptor for morbilliviruses, has

been shown to be critical for host susceptibility and virus entry, whereas nectin-4 is required for clinical disease and efficient virus shedding (11, 12). A recent study revealed that a substitution in CDV H protein at residue 540, Asp to Gly (D540G), is sufficient to allow CDV to bind to human SLAM *in vitro*, which could cause CDV to potentially adapt human target cells (13).

The masked palm civet *Paguma larvata* (order Carnivora, family *Viverridae*) is distributed in tropical and subtropical Asia (14). In China, masked palm civets are raised as new farm animals mainly in the southern provinces for meat production. Civets have been thought to be potential intermediate hosts that can provide an effective way for the virus, such as severe acute respiratory syndrome (SARS) which appeared in southern China in 2003, to spread from animals to humans (15). In addition, several studies have shown that the masked palm civet may potentially be involved in transmission of some zoonotic pathogens such as *Salmonella enterica*, *Bartonella henselae,* and *Toxoplasma gondii* (16–18).

Up to now, in China, there are none reports of Rockborn-like strain detected from a civet. The present study aimed to investigate the CDV infection in civets, analyze the genotypes of epidemic strains, and report the cross-species transmission of CDV.

MATERIALS AND METHODS

Sample Collection

In August 2019, sudden and unexplained fever, severe lethargy and weakness, loss of appetite, mild-to-marked upper respiratory disease and neurological dysfunction (severe lethargy, loss of appetite, epilepsy and twitching) were observed in a masked palm civet farm that also received stray civets and rescued wild civets in Luoyang city, Henan Province. Seventy percent of the sick civets died on days 7∼10 of the illness after accepting new wild animals. Although the immune status of the wild and stray animals was unclear, all the cultured animals had been vaccinated with the American-1 strain. We randomly collected ocular, nasal and rectal swab specimens, and serum samples from 44 healthy and 57 sick civets. Fresh tissues harvested from 9 dead animals were used for histopathological analysis, immunohistochemical analysis and viral isolation. After collection, the samples were immediately transported to our laboratory in an icebox for further use.

Viral Detection and Isolation

All samples were stored at −80°C and tested, initially by Anigen Rapid CDV Ag Test Kit (BioNote, Inc.Gyeonggi-do, South Korea) according to the manufacturer's instructions. Total RNA was extracted from the tissues with a QIAamp Viral RNA Mini Kit (Qiagen, USA). The RNA was converted into cDNA using a Vazyme HiScript II 1st Strand cDNA Synthesis Kit (Vazyme Biotech Co., Ltd., China) in accordance with the manufacturer's instructions. To validate the presence of CDV, reverse transcription polymerase chain reaction (RT-PCR)/PCR was performed to detect a 681 bp RT-PCR amplicon encompassing the fusion protein signal-peptide (Fsp)-coding region (405 bp) using a previously described primer (19). For virus isolation, the tissues were homogenized in 20 % (w/v) sterile phosphate-buffered saline (PBS, pH 7.4) and filtered through 0.22 um membrane filters. Supernatants of homogenized lung filtered through 0.22 um membrane filters were used to inoculate Vero-raccoon dog-SLAM cells as described previously (20), and the cytopathogenic effect was observed within 120 hours. Vero-raccoon dog-SLAM cells were constructed by the authors and were maintained in DMEM containing 5% FBS (data not published).

Electron Microscopic Analysis

The Vero-SLAM cells at 4 days post-infection were used for electron microscopic analysis. Cell supernatants were centrifuged at 12,000 × g for 5 min at 4°C. Virus-containing supernatants were negatively stained and examined using transmission electron microscopy (TEM) (21).

Whole Genome Sequencing and Phylogenetic Analysis

The complete H gene of the CDV isolate and virus contained in brain and lung samples from deceased civets was amplified for sequencing by RT-PCR using H gene specific primers (20). The entire genome of civets CDV isolated with Vero-raccoon dog-SLAM cells was amplified and sequenced using a set of 15 primer pairs to generate overlapping PCR amplicons (20). Multiple sequence alignments were performed and sequence similarities determined using DNASTAR software. The neighbor-joining (NJ) method with 1,000 bootstrap replicates was used to construct a phylogenetic tree in MEGA version 7.0 (22).

TABLE 1 | Detection of civet CDV in sick and healthy animals using PCR and SN test.

Species	Total No.	Vaccination status	Health status(dead/total)	Rate	
				PCR^+ (swabs)	SN^+ (blood)
Wild and stray	30	Unknown	Healthy (0/4)	1/4	2/4
			Sick (26/26)	25/26	3/26
Captive	291	Vaccinated	Healthy (0/260)	2/40	38/40
			Sick (14/31)	29/31	28/31
Total	321			57/101	71/101

$^+$*Positive.*

Histopathological Examination and Immunohistochemical Analysis

For histological studies, samples intended for histopathological examination (brain, lung, heart, liver, kidney and testicle) were fixed in 4% buffered formaldehyde solution and 4 μm thick paraffin sections were mounted on silane-coated slides. Slides were stained with hematoxylin and eosin (HE) according to the standard histopathological procedure.

Immunohistochemical analysis was performed in the same tissues using the chain polymer-conjugated method (2). Briefly, slides were deparaffinised and rehydrated. After antigen retrieval and endogenous peroxidase blocking, slides were incubated with an anti-CDV nucleoprotein monoclonal antibody at a 1:100 dilution (VMRD Inc., Pullman, WA. Cat. P180221). Then, the slides were incubated using the Dako REAL EnVision Detection System (Dako, Glostrup, Denmark), at 37°C as a secondary antibody, and the positive antigen-antibody complex was then visualized by labeling with 3, 3′-diaminobenzidine tetrahydrochloride (DAB) and counterstaining with Mayer's hematoxylin. Positive control slide was performed on lung tissue from a CDV-infected dog that was positive in the RT-PCR assay, while the Tris-HCl buffer instead of the primary antibody was used as a negative control.

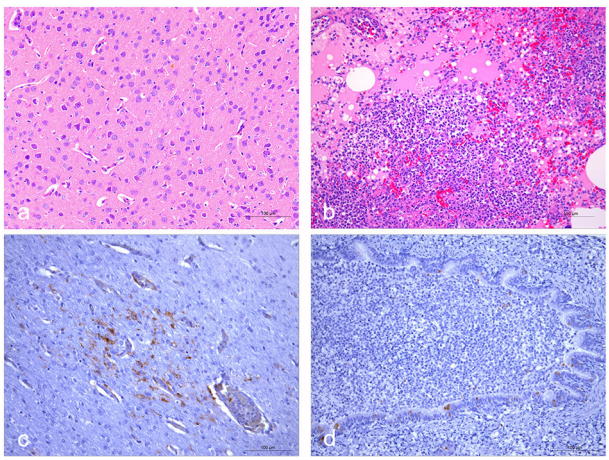

FIGURE 1 | Histopathological and immunohistochemical staining of lungs and brains of fresh dead civets. **(a)** Microscopic examination of brain samples showed neuronal degeneration and necrosis, perivascular edema. **(b)** The alveolar wall capillaries were dilated and congested, and part of the alveolar cavity was filled with abundant inflammatory exudates containing edematous fluid and lymphocytes. Moreover, lymphocytes and macrophages can be seen in the bronchus. **(c)** Immunohistochemical staining showed that some nerve cells in the brain tissue were positive for CDV. **(d)** CDV was positively detected in some bronchial epithelial cells. The scale bar indicates 100 μm.

Virus Neutralizing Antibody Titers (VNT)

CDV virus neutralizing (VN) antibody titers were determined in Vero-SLAM cells using a TCID50 microtiter assay as previously described (23) with minor modifications. Briefly, serial 2-fold dilutions of heat-inactivated serum starting at 1:8 were added to ∼100 $TCID_{50}$ of vaccine strain CDV3 (EU726268) and tested in quadruplicate. The titers were calculated using the method of Reed and Muench.

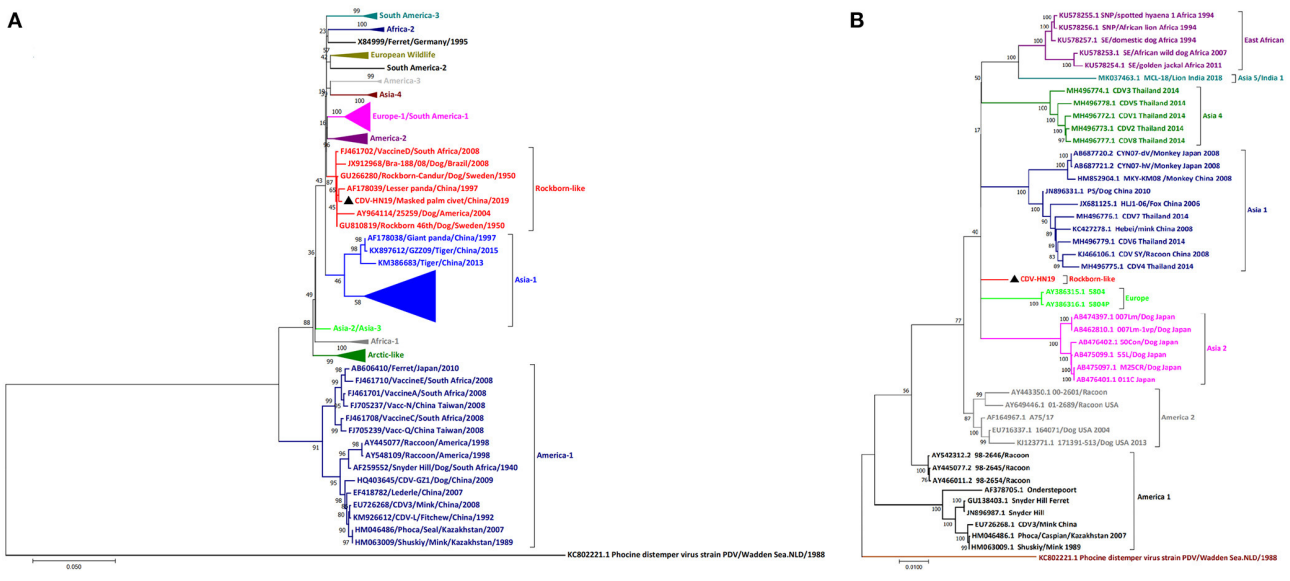

FIGURE 2 | Phylogenetic analyses of CDV HN19 strain. **(A)** Phylogenetic analyses of the nucleotide sequences of the complete genome of CDV HN19 strain. **(B)** Phylogenetic analyses of H gene nucleotide sequences of CDV HN19. Evolutionary history was inferred using the maximum likelihood method with the Tamura-Nei model and gamma-distributed rate heterogeneity in MEGA 7. The percentage of replicates in which the associated virus clustered together in the bootstrap test (1,000 replicates) is shown next to the branch in each tree. The strain isolated in this study is identified by ▲. The percentage bootstrap support is indicated by the value at each node. Scale bar denotes nucleotide substitutions per site.

RESULTS

Fatal CDV Infection in Masked Palm Civets

RT-PCR analysis was used to detect viral nucleic acid. Tissue samples from all of the dead civets were all CDV infection-positive. The swab samples ($n = 101$) showed a detection rate of 56.44%. Serological analysis indicated a lower positive rate of CDV-neutralizing antibody in wild civets than in captive civets, regardless of the health condition. The results of all samples tested by PCR and neutralizing antibodies are summarized in **Table 1**. The cytopathogenic effect (CPE) was observed in Vero-SLAM cells within 96∼120 h after infection from positive lung tissue. Numerous spherical, enveloped virus particles of ∼200 nm in diameter were observed by negative-staining electron microscopy in isolated strain (named HN19) (data not shown).

Histopathological Analysis

Briefly, histopathologic findings in the brain included neuronal degeneration and necrosis, perivascular edema (**Figure 1a**). Interstitial pneumonia with infiltrates of inflammatory cells comprising lymphocytes and macrophages can be seen in the bronchus (**Figure 1b**). Immunohistochemical analysis revealed the CDV antigen in some areas of the lung and brain (**Figures 1c,d**). Additionally, generalized more severe lymphocyte depletion was found in the spleen, liver, intestine, while no obvious pathological changes were found in kidney (data not shown).

Phylogenetic Analysis

The complete viral genome of the HN19 strain was sequenced. This sequence has been deposited in GenBank under the accession number MT448054. Phylogenetic analysis and multiple sequence alignments based on the H gene sequence showed that HN19 strain belongs to the Rockborn-like strain cluster (**Figure 2A**). Sequence comparisons of the H gene of HN19 strain showed high identities with Rockborn-like strains at the nucleotide (98.7∼99.72%) and the deduced amino acid (97.78∼99.15%) levels (**Table 2**). Additionally, HN19 clustered with a strain that killed lesser pandas in China in 1997 (24) (**Figure 2A**). Sequence comparisons of the complete genome showed that HN19 had low sequence identities with America-1 strains (**Figure 2B**). The H gene sequence of the HN19 stain demonstrated a low nucleotide similarity (92.16∼92.68%) with America-1 CDVs. Similarly, at the amino acid level of H gene, HN19 had slightly lower identity (89.48∼90.60%) to America-1 CDVs (**Table 2**).

The complete H gene sequence detected from brain and lung was as same as that detected from the isolate. Sequence analyses of H gene revealed that the same unique amino acid residues 105S and 265S existed in HN19, lesser panda isolates, giant panda isolates and two other tiger derivatives from China. Most importantly, the adaptive mutation D540G in the H protein was unique, which has been supposed to be required for adaptation of CDV to the human entry receptors (13). In addition, there were another two unique amino acid residues, 376T and 548M,

TABLE 2 | Nucleotide and amino acid changes in the H gene of CDV isolated from the civet compared to published sequences.

Lineages	Information	Strain	Position									
			Nucleotide	314	475	592–3	794	1,126–7	1,619	1,642–3	Nucleotide	Amino Acid
			Amino Acid	105	159	198	265	376	540	548		
Rockborn	**Civet/China/2019**	**CDV-HN19**		**C(S)**	**C(L)**	**TT(F)**	**C(S)**	**AC(T)**	**G(G)**	**AT(M)**	**100%**	**100%**
	Dog/Sweden/1950	GU810819		T(L)			T(L)	AA(N)	**A(D)**	AC(T)	99.72%	99.15%
	VaccineD/South Africa/2008	FJ461702		T(L)			T(L)	AA(N)	**A(D)**	AC(T)	99.55%	98.64%
	Lesser panda/China/1997	AF178039						AA(N)	**A(D)**	AC(T)	99.49%	98.98%
	Dog/Brazil/2008	JX912968		T(L)			T(L)	AA(N)	**A(D)**	AC(T)	99.10%	98.47%
	Dog/America/2004	AY964114		T(L)			T(L)	AA(N)	**A(D)**	AC(T)	98.70%	97.78%
	Dog/Sweden/1950	GU266280		T(L)			T(L)	AA(N)	**A(D)**	AC(T)	99.66%	98.98%
Asia-1	Giant panda/China/1997	AF178038						AA(N)	**A(D)**	AC(T)	97.78%	97.60%
	Tiger/China/2015	KX897612						AA(N)	**A(D)**	AC(T)	97.67%	97.26%
	Tiger/China/2013	KM386683						AA(N)	**A(D)**	AC(T)	96.79%	96.03%
American-1				T(L)	A(I)	GT(V)	T(L)	GG(G)	**A(D)**	AC(T)	92.16%∼92.68%	89.48%∼90.60%
Others*				T(L)	&	+	T(L)	*	#	†	89.88%∼97.83%	84.08%∼96.38%

*All remaining strains except Rockborn, Asia-1 and American-1.
&A(I), G(V).
+GT(V), AT(I), TC(S).
*AT(I), AA(N), AG(S), AC(T), GG(G).
#C(A), A(D).
†AT(M), AC(T), CC(P).

which could be associated with vaccination failure and unusual clinical signs.

DISCUSSION

Previous reports have demonstrated that CDV is a lethal infectious agent to susceptible free-living and captive *Viverridae*, including civets (2, 25, 26). Here, we have documented a Rockborn-like CDV strain infection in masked palm civets in China. Because CDV had never appeared at this farm before, and this strain belonged to the Rockborn-like group along with another strain from wild animals, this outbreak might be attributed to stray animal contact or wild animal adoption. The Rockborn vaccine strain, as a canine isolate, was made on primary canine kidney cells in the 1950s (27). Compared with other CDV vaccines, Rockborn strain was considered to be less attenuated and less safe, and withdrawn from several markets after the mid-1990s (28). However, the isolation of Rockborn-like CDVs, respectively, from masked palm civets and lesser pandas in China suggests that Rockborn-like viruses are still circulating in the field or that vaccine-derived viruses were introduced in different carnivores on several occasions in China.

In this farm, vaccination failure was observed in 31/291 captive animals (10.65%) with an America-1 strain vaccination record. The efficacy of vaccines relies on the antigenic relatedness between the vaccine and the circulating field strains. The CDV H gene is the most heterogenic and antigenic variable among all different strains of CDV, which could result in the generation of antibodies with widely different neutralization capacity or vaccine breakdown. Phylogenetic analysis of the complete genome and viral H gene showed that HN19 shared low identities with America-1 strains, which could be a reason for this immune failure.

Morbilliviruses such as MeV and CDV use the species orthologs of CD150 and nectin-4 expressed on immune and epithelial cells, respectively, as receptors. Several studies have demonstrated that amino acid substitutions in the H protein may contribute to the expanded host range (13, 29). Among substitutions, 540 Asp→Gly (D540G) confers good fusion capacity to viral envelope proteins binding with human CD150, which may facilitate CDV adaptation to human target cells (13). The amino acid exchange D540G has been also observed in HN19 strain, a natural isolate from civets, implying that the zoonotic potential of CDV might be a matter of concern.

Through the investigation of CDV infection in civets in China, we formulated three hypotheses. The first was that a kind of Rockborn-like strain was circulating in wild animals in China. The second hypothesis was that the America-1 vaccine could not provide adequate protection for civets. Finally, the third hypothesis was Rockborn-like strain with the D540G mutation in Chinese wild animals might have zoonotic potential. Therefore, the information provided with this study emphasizes the need for the regular surveillance of wild animals, mandatory effective vaccination in wild animals and reduction of the increasing threat of CDV to animals and public health in China.

DATA AVAILABILITY STATEMENT

The datasets presented in this study can be found in online repositories. The names of the repository/repositories and accession number(s) can be found at: https://www.ncbi.nlm.nih.gov/genbank/, MT448054.

ETHICS STATEMENT

The animal study was reviewed and approved by the farm owner and our research team made an agreement in a written way. The Ethical Review Committee approved this agreement. Furthermore, the study was approved by the farm owner and all experimental animals were conducted according to the International Guiding Principles for Biomedical Research. The protocol was approved by the Committee on the Ethics of Animal Experiments of the Jilin University. Written informed consent was obtained from the owners for the participation of their animals in this study.

AUTHOR CONTRIBUTIONS

NS, LZ, XY, XZ, SZ, DZ, and MD performed experimental study and analysis. NS and MD wrote the manuscript. All authors contributed to data collection, data analysis, manuscript revision, read, and approved the submitted version.

FUNDING

This work was supported by the National Natural Sciences Foundation of China (No. 31970154).

REFERENCES

1. Mourya DT, Yadav PD, Mohandas S, Kadiwar RF, Vala MK, Saxena AK, et al. Canine distemper virus in Asiatic lions of Gujarat State, India. *Emerg Infect Dis.* (2019) 25:2128–30. doi: 10.3201/eid2511.190120
2. Techangamsuwan S, Banlunara W, Radtanakatikanon A, Sommanustweechai A, Siriaroonrat B, Lombardini ED, et al. Pathologic and molecular virologic characterization of a canine distemper outbreak in farmed civets. *Vet Pathol.* (2015) 52:724–31. doi: 10.1177/0300985814551580
3. Bhatt M, Rajak KK, Chakravarti S, Yadav AK, Kumar A, Gupta V, et al. Phylogenetic analysis of haemagglutinin gene deciphering a new genetically distinct lineage of canine distemper virus circulating among domestic dogs in India. *Transbound Emerg Dis.* (2019) 66:1252–67. doi: 10.1111/tbed.13142
4. Kennedy S, Kuiken T, Jepson PD, Deaville R, Forsyth M, Barrett T, et al. Mass die-off of Caspian seals caused by canine distemper virus. *Emerg Infect Dis.* (2000) 6:637–9. doi: 10.3201/eid0606.000613
5. Sawatsky B, Cattaneo R, von Messling V. Canine distemper virus spread and transmission to naive ferrets: selective pressure on signaling

lymphocyte activation molecule-dependent entry. *J Virol.* (2018) 92:e00669-18. doi: 10.1128/JVI.00669-18
6. Beineke A, Baumgartner W, Wohlsein P. Cross-species transmission of canine distemper virus-an update. *One Health.* (2015) 1:49–59. doi: 10.1016/j.onehlt.2015.09.002
7. Sakai K, Nagata N, Ami Y, Seki F, Suzaki Y, Iwata-Yoshikawa N, et al. Lethal canine distemper virus outbreak in cynomolgus monkeys in Japan in 2008. *J Virol.* (2013) 87:1105–14. doi: 10.1128/JVI.02419-12
8. Origgi FC, Sattler U, Pilo P, Waldvogel AS. Fatal combined infection with canine distemper virus and orthopoxvirus in a group of Asian Marmots (*Marmota caudata*). *Vet Pathol.* (2013) 50:914–20. doi: 10.1177/0300985813476060
9. Noyce RS, Delpeut S, Richardson CD. Dog nectin-4 is an epithelial cell receptor for canine distemper virus that facilitates virus entry and syncytia formation. *Virology.* (2013) 436:210–20. doi: 10.1016/j.virol.2012.11.011
10. Tatsuo H, Ono N, Yanagi Y. Morbilliviruses use signaling lymphocyte activation molecules (CD150) as cellular receptors. *J Virol.* (2001) 75:5842–50. doi: 10.1128/JVI.75.13.5842-5850.2001
11. Sawatsky B, Wong XX, Hinkelmann S, Cattaneo R, von Messling V. Canine distemper virus epithelial cell infection is required for clinical disease but not for immunosuppression. *J Virol.* (2012) 86:3658–66. doi: 10.1128/JVI.06414-11
12. Sattler U, Khosravi M, Avila M, Pilo P, Langedijk JP, Ader-Ebert N, et al. Identification of amino acid substitutions with compensational effects in the attachment protein of canine distemper virus. *J Virol.* (2014) 88:8057–64. doi: 10.1128/JVI.00454-14
13. Bieringer M, Han JW, Kendl S, Khosravi M, Plattet P, Schneider-Schaulies J. Experimental adaptation of wild-type Canine Distemper Virus (CDV) to the human entry receptor CD150. *PLoS ONE.* (2013) 8:e57488. doi: 10.1371/journal.pone.0057488
14. Masuda R, Lin LK, Pei KJC, Chen YJ, Chang SW, Kaneko Y, et al. Origins and founder effects on the japanese masked palm civet *Paguma larvata* (Viverridae, Carnivora), revealed from a comparison with its molecular phylogeography in Taiwan. *Zool Sci.* (2010) 27:499–505. doi: 10.2108/zsj.27.499
15. Guan Y, Zheng BJ, He YQ, Liu XL, Zhuang ZX, Cheung CL, et al. Isolation and characterization of viruses related to the SARS coronavirus from animals in Southern China. *Science.* (2003) 302:276–8. doi: 10.1126/science.1087139
16. Hou GY, Zhao JM, Zhou HL, Rong G. Seroprevalence and genetic characterization of *Toxoplasma gondii* in masked palm civet (Paguma larvata) in Hainan province, tropical China. *Acta Trop.* (2016) 162:103–6. doi: 10.1016/j.actatropica.2016.06.011
17. Sato S, Kabeya H, Shigematsu Y, Sentsui H, Une Y, Minami M, et al. Small Indian mongooses and masked palm civets serve as new reservoirs of *Bartonella henselae* and potential sources of infection for humans. *Clin Microbiol Infec.* (2013) 19:1181–7. doi: 10.1111/1469-0691.12164
18. Lee K, Iwata T, Nakadai A, Kato T, Hayama S, Taniguchi T, et al. Prevalence of Salmonella, *Yersinia* and *Campylobacter* spp. in feral raccoons (*Procyon lotor*) and masked palm civets (*Paguma larvata*) in Japan. *Zoonoses Public Health.* (2011) 58:424–31. doi: 10.1111/j.1863-2378.2010.01384.x
19. Sarute N, Calderon MG, Perez R, La Torre J, Hernandez M, Francia L, et al. The fusion protein signal-peptide-coding region of canine distemper virus: a useful tool for phylogenetic reconstruction and lineage identification. *PLoS ONE.* (2013) 8:e63595. doi: 10.1371/journal.pone.0063595
20. Feng N, Yu Y, Wang T, Wilker P, Wang J, Li Y, et al. Fatal canine distemper virus infection of giant pandas in China. *Sci Rep.* (2016) 6:27518. doi: 10.1038/srep27518
21. Zhang L, Li S, Huang S, Wang Z, Wei F, Feng X, et al. Isolation and genomic characterization of lymphocytic choriomeningitis virus in ticks from northeastern China. *Transbound Emerg Dis.* (2018) 65:1733–9. doi: 10.1111/tbed.12946
22. Kumar S, Stecher G, Tamura K. MEGA7: molecular evolutionary genetics analysis version 7.0 for bigger datasets. *Mol Biol Evol.* (2016) 33:1870–4. doi: 10.1093/molbev/msw054
23. Stephensen CB, Welter J, Thaker SR, Taylor J, Tartaglia J, Paoletti E. Canine distemper virus (CDV) infection of ferrets as a model for testing Morbillivirus vaccine strategies: NYVAC- and ALVAC-based CDV recombinants protect against symptomatic infection. *J Virol.* (1997) 71:1506–13. doi: 10.1128/jvi.71.2.1506-1513.1997
24. Zhang H, Shan F, Zhou X, Li B, Zhai JQ, Zou SZ, et al. Outbreak and genotyping of canine distemper virus in captive Siberian tigers and red pandas. *Sci Rep.* (2017) 7:8132. doi: 10.1038/s41598-017-08462-4
25. Hirama K, Goto Y, Uema M, Endo Y, Miura R, Kai C. Phylogenetic analysis of the hemagglutinin (H) gene of canine distemper viruses isolated from wild masked palm civets (*Paguma larvata*). *J Vet Med Sci.* (2004) 66:1575–8. doi: 10.1292/jvms.66.1575
26. Takayama I, Kubo M, Takenaka A, Fujita K, Sugiyama T, Arai T, et al. Pathological and phylogenetic features of prevalent canine distemper viruses in wild masked palm civets in Japan. *Comp Immunol Microbiol Infect Dis.* (2009) 32:539–49. doi: 10.1016/j.cimid.2008.07.003
27. Rockborn G. Canine distemper virus in tissue culture. *Archiv Gesamte Virusforschung.* (1958) 8:485–92. doi: 10.1007/BF01243067
28. Martella V, Blixenkrone-Moller M, Elia G, Lucente MS, Cirone F, Decaro N, et al. Lights and shades on an historical vaccine canine distemper virus, the Rockborn strain. *Vaccine.* (2011) 29:1222–7. doi: 10.1016/j.vaccine.2010.12.001
29. Feng N, Liu Y, Wang J, Xu W, Li T, Wang T, et al. Canine distemper virus isolated from a monkey efficiently replicates on Vero cells expressing non-human primate SLAM receptors but not human SLAM receptor. *BMC Vet Res.* (2016) 12:160. doi: 10.1186/s12917-016-0757-x

Conflict of Interest: The authors declare that the research was conducted in the absence of any commercial or financial relationships that could be construed as a potential conflict of interest.

Publisher's Note: All claims expressed in this article are solely those of the authors and do not necessarily represent those of their affiliated organizations, or those of the publisher, the editors and the reviewers. Any product that may be evaluated in this article, or claim that may be made by its manufacturer, is not guaranteed or endorsed by the publisher.

frontiers in Veterinary Science

BRIEF RESEARCH REPORT
published: 16 November 2021
doi: 10.3389/fvets.2021.764982

Isolation and Phylogenetic Analysis of Reemerging Pseudorabies Virus Within Pig Populations in Central China During 2012 to 2019

Hui-Hua Zheng[1†], *Yi-Lin Bai*[2†], *Tong Xu*[1†], *Lan-Lan Zheng*[1], *Xin-Sheng Li*[1], *Hong-Ying Chen*[1*] and *Zhen-Ya Wang*[3*]

[1] Zhengzhou Major Pig Disease Prevention and Control Laboratory, College of Veterinary Medicine, Henan Agricultural University, Zhengzhou, China, [2] College of Veterinary Medicine, Northwest A&F University, Xianyang, China, [3] Key Laboratory of "Runliang" Antiviral Medicines Research and Development, Institute of Drug Discovery & Development, Zhengzhou University, Zhengzhou, China

OPEN ACCESS

Edited by:
Yashpal S. Malik,
Indian Veterinary Research Institute (IVRI), India

Reviewed by:
Bin Li,
Jiangsu Academy of Agricultural Sciences (JAAS), China
Abdelaziz Ed-Dra,
Zhejiang University, China

***Correspondence:**
Hong-Ying Chen
chhy927@163.com
Zhen-Ya Wang
zhenyawang@zzu.edu.cn

[†] These authors have contributed equally to this work

Specialty section:
This article was submitted to Veterinary Infectious Diseases, a section of the journal Frontiers in Veterinary Science

Received: 26 August 2021
Accepted: 15 October 2021
Published: 16 November 2021

Citation:
Zheng H-H, Bai Y-L, Xu T, Zheng L-L, Li X-S, Chen H-Y and Wang Z-Y (2021) Isolation and Phylogenetic Analysis of Reemerging Pseudorabies Virus Within Pig Populations in Central China During 2012 to 2019. Front. Vet. Sci. 8:764982. doi: 10.3389/fvets.2021.764982

To understand the biological characteristics of the reemerging pseudorabies virus (PRV) strains, a total of 392 tissue samples were collected from diseased pigs during reemerging PR outbreaks between 2012 and 2019 on farms in central China where swine had been immunized with Bartha-K61 and 51 (13. 01%) were positive for the gE gene by PCR. Sixteen PRV strains were isolated and caused clinical symptoms and death in mice. Subsequently, gE, gC, gB, and gD complete genes were amplified from the 16 PRV isolates and sequenced. Phylogenetic analysis based on these four gene sequences shows that the 16 PRV isolates were more closely related to the Chinese PRV variants (after 2012) but genetically differed from early Chinese PRV isolates (before 2012). Sequence analysis reveals that PRV isolates exhibited amino acid insertions, substitutions, or deletions compared with early Chinese PRV isolates and European–American PRV strains. In addition, this is the first report that eight isolates (8/16) in this study harbor a unique amino acid substitution at position 280 (F to L) of the gC protein, and six isolates have an amino acid substitution at position 338 (A to V) of the gD protein compared with the Chinese PRV variants. The emulsion containing inactivated PRV NY isolate could provide complete protection against the NY isolate. This study might enrich our understanding of the evolution of reemerging PRV strains as well as pave the way for finding a model virus to develop a novel vaccine based on reemerging PRV strains.

Keywords: pseudorabies virus, sequencing, phylogenetic analysis, reemerging virus, pig disease

INTRODUCTION

Pseudorabies (PR), or Aujeszky's disease, is an economically important viral disease of swine worldwide and poses a great threat to the pork industry (1, 2). Infected pigs display a range of symptoms, including reproductive failure in sows, severe respiratory disease in adult pigs, fatal neurological disorders, and high mortality in newborn piglets (3). The first description of PR was made in America as early as 1813, and the first recorded case in China was in 1948 with a following epidemic in pigs in the late 1980s (4). Due to the use of the gE-negative vaccine strain Bartha-K61

imported from Hungary, PR was well-controlled from the 1990s to 2010 in China (5, 6). Since late 2011, however, reemerging PR outbreaks have occurred among Bartha-K61-immunized swine herds on many Chinese farms and led to tremendous economic losses (6).

The causative agent responsible for PR is the pseudorabies virus (PRV), which is a member of the family *Herpesviridae*, subfamily *Alphaherpesvirinae*, and genus *Varicellovirus*. The genome of PRV is a linear double-stranded DNA that encodes more than 70 proteins (7). Among these proteins, glycoproteins B (gB), C (gC), and D (gD) induce cellular and humoral immune responses and are related to the process of virus fusion (8–11). Furthermore, the gC gene is frequently used to analyze the evolutionary relationships of PRV, and the attachment of the virus to cells is initiated by the binding of the gC protein to heparan sulfate proteoglycans (12–14). The glycoprotein E (gE) is a major virulence determinant of PRV but is not essential for virus replication (15). In light of this fact, gE-deleted vaccines (Bartha-K61 vaccine) were developed, and the vaccines, together with a corresponding serological test to detect antibodies against the gE protein, have played a key role in the program of the elimination of PR.

Some research indicates that the causative agent of currently circulating PRV is confirmed to be novel PRV strains (PRV variants), which are genetically different from the early Chinese PRV strains, and the Bartha-K61 vaccine did not provide full protection against the PRV variants due to enhanced pathogenicity and genetic differentiation of PRV variants (16, 17). Furthermore, Sun's study shows that reemerging PRV strains spread widely to many provinces of China between 2012 and 2017, and other research also reveals that the gE, gC, gB, and gD amino acid (aa) sequences of reemerging PRV strains include alterations (3, 13, 18–20). For further investigating the molecular epidemiology of reemerging PRV strains, this study reports the detection and genetic analysis of PRV from pigs in central China between 2012 and 2019 and is also evaluated to find a candidate virus for the development of novel and efficient PR vaccines.

MATERIALS AND METHODS

Cells, Virus, and Sample Collection

Swine testicle (ST) cells and PRV strain Min-A were purchased from the China Institute of Veterinary Drug Control, Beijing, China, and the ST cells were passaged in Dulbecco's modified Eagle's medium (DMEM) (Gibco, Carlsbad, CA, USA) supplemented with 10% heat-inactivated fetal bovine serum (Gibco).

From 2012 to 2019, a total of 392 tissue samples (including lungs, brains, kidneys, lymph nodes, and spleens) were collected from 392 diseased pigs during reemerging PR outbreaks on 39 farms in central China (including in Kaifeng, Shangqiu, Zhoukou, Luoyang, Sanmenxia, Nanyang, Zhumadian, Xinyang, Anyang, Xinxiang, Jiaozuo, Puyang, Hebi, Zhengzhou, Pingdingshan, Xuchang, and Luohe cities) where swine had been immunized with Bartha-K61, and the sample numbers per year are 80, 50, 60, 56, 32, 36, 38, and 40, respectively.

PCR Detection

Viral DNA was extracted from 200 μL supernatants of the suspension of tissue using the DNA Miniprep Kit (Omega, Norcross, Georgia, USA) according to the manufacturer's instructions and subsequently screened for the presence of the PRV genome by PCR. A pair of primers gEp-F/R (gEp-F: 5′-TGGGACACGTTCGACCTGATG-3′, gEp-R: 5′-CCTTGATGACCGTGACGTA CT-3′) were designed from the reference strain PRV Ea (accession number AF171937) to amplify the partial gE gene with the length of 429 bp. PCR was performed in a 25-μL volume mixture consisting of 12.5 μL Premix *Taq* (Takara, Dalian, China), 3 μL extracted DNA template, 7.5 μL of ddH_2O, 1 μL DMSO, and 0.5 μL each of primer (50 μM), and the cycling protocol was an initial denaturation at 95°C for 5 min, followed by 35 cycles at 95°C for 30 s, 53°C for 30 s, and 72°C for 1 min with a final step of 72°C for 10 min. The PCR amplification using the DNA of PRV strain Min-A was considered as a positive control, and the product with ddH_2O instead of the DNA template was used as the negative control. The PCR product was visualized by electrophoresis in a 1.5% agarose gel containing ethidium bromide under ultraviolet light.

Virus Isolation and Identification

For virus isolation, homogenate supernatants of positive tissue samples confirmed by PCR were filtered using a 0.22-μm filter (EMD Millipore, Billerica, MA, USA) and inoculated into ST cells. The inoculated cells were observed daily. When 80% of cells showed the cytopathic effects (CPEs), viruses were harvested by three freeze–thaw cycles and were further plaque purified. Subsequently, the virus was corroborated by PCR with primers gEp-F/R.

Pathogenic Test in Mice

One hundred seventy six-week-old healthy BALB/c female mice were randomly divided into 17 groups of 10. Mice in PRV-injected groups were inoculated subcutaneously (s.c.) with the different isolates of a virus titer of $10^{5.0}$ 50% tissue culture infectious doses ($TCID_{50}$)/dose as previously described, respectively (21). Mice in the DMEM-injected group were inoculated with the same dose of DMEM as control. After the inoculation, the mice were monitored daily for clinical signs for 7 days.

Physicochemical Properties of Virus

Physicochemical properties of NY isolate as a representative PRV were assayed as described previously (22). Briefly, the 500 μL cell culture medium–infected NY isolate was added into eight 1.5-mL Eppendorf tubes. Tubes 1 and 2 were treated by a water bath at 56°C for 1 h and chloroform at 4°C for 30 min, respectively. Tubes 3 and 4 were treated by adjusting the culture medium pH to 3.0 and 11.0 with 0.1 M HCl/NaOH solutions. After incubation at 37°C for 1 h, the pH values were then adjusted back to 7.0 by 0.1 M NaOH solutions. Tube 5 was digested with trypsin in a 37°C water bath for 1.5 h and then added 4 mL of the inactivated fetal bovine serum to terminate the reaction. Tube 6 was incubated with formaldehyde at 37°C for 2 d. Tube 7 was treated under ultraviolet rays for 30 min. Tube 8 was used as

a negative control. Viruses of the eight tubes were inoculated on ST monolayers, respectively, and $TCID_{50}$ was determined by the Reed–Muench method, respectively (23). In addition, the seventh passage of the NY strain with propagating in ST cells was stained with uranyl acetate and examined using a Hitachi TEM transmission electron microscope (Hitachi, Japan).

Sequencing and Phylogenetic Analysis

The complete gE, gC, and gB genes of PRV were amplified from viral DNA extracted from PRV isolates using specific primers gE-F/R, gC-F/R, and gB-F/R designed in our laboratory (21). The complete gD gene was amplified by PCR from viral DNA using a pair of primers gD-F/R (gD-F: 5′-ATCCACTCCCAGCGGTCCACAAAAT−3′, gD-R: 5′-AAAAACAGCAGCGTCCCGTCTATCG−3′) with the same PCR volume mixture as that of the partial gE gene, and the cycling protocol was as follows: an initial denaturation at 95°C for 5 min, 35 cycles of denaturation at 95°C for 55 s, annealing at 57°C for 1 min, extension at 72°C for 100 s, and a final extension at 72°C for 10 min. Then, the genes were ligated with the vector pMD18-T (Takara) and separately introduced to *Escherichia coli* DH-5α cells (Takara) by transformation according to the manufacturer's instructions. The positive recombinant plasmids carrying gE, gC, gB, and gD genes were sent to Sangon Biotech Shanghai Co., Ltd., for DNA sequencing, and all sequencing reactions were performed in duplicate.

Phylogenetic trees were constructed based on the complete gE, gC, gB, and gD genes of PRV isolates and reference strains available in GenBank using MEGA software, version 7.0 (www.megasoftware.net) by the neighbor-joining (NJ) method with 1,000 bootstrap replicates (24). Evolutionary distances were computed by the pairwise distance method with the maximum composite likelihood model. Sequences of PRV strains listed in **Table 1** retrieved from NCBI were used as references.

Immunogenicity Test

The representative PRV NY isolate was inoculated into ST cells. The cell culture suspension of virus titer of $10^{5.0}$ $TCID_{50}$ was inactivated by incubating with moderate formalin (Sigma-Aldrich) at 37°C for 24 h and then emulsified with Freund's complete adjuvant and Freund's incomplete adjuvant, respectively. Sixty six-week-old healthy BALB/c female mice were randomly divided into four groups of 15 mice each. Mice in Group 1 were injected with 500 μL inactivated NY isolate containing Freund's complete adjuvant in the first week, followed by injecting with an equal volume of emulsifier with Freund's incomplete adjuvant in the third week, and finally with the inactivated virus in the fifth week. Groups 2–4 were injected with the same dose of Bartha-K61, Hubei 98 (the PRV vaccine strain with deleting three important virulence factors) or DMEM in the first, third, and fifth weeks, respectively. On the 32nd day after the final injection, blood samples were collected from five mice of each group for the serum neutralization assay, and the remaining mice of each group were challenged with $10^{5.0}$ $TCID_{50}$ PRV NY isolate. Serum-neutralizing antibodies against PRV were detected as described previously (25).

RESULTS AND DISCUSSION

Of the 392 samples, 51 were positive for the PRV gene, yielding an average positive rate of 13.01% (51/392), which was coincident with the reports of the prevalence of novel PR in China (6, 19, 26, 27). Besides this, the positive rates of PRV detection from 2012 to 2019 were 17.5% (14/80), 20.0% (10/50), 25.0% (15/60), 14.29% (8/56), 12.5% (4/32), 11.11% (4/36), 7.89% (3/38), and 6.61% (8/40), respectively.

PRV gE gene–positive tissue samples were inoculated into ST cells, and distinct CPEs characterized by cell rounding, pyknosis, and degeneration were observed after three blind passages on ST cells. The expected products of 429 bp (**Figure 1A**) were amplified from infected cells with the specific primers of the gE gene. Sixteen PRV isolates were obtained and formally named NY, GY, LGX, MZ1, MZ2, ZM, ZK, JY, M5, YY, WY, BP, YZ, SMX, WZ, and XC (**Table 1**). $TCID_{50}$ of these PRV isolates were during $10^{5.375}$ to $10^{9.0}$/0.1 mL with the highest $TCID_{50}$ of NY and the lowest of XC. The 16 isolates were highly pathogenic in mice and caused skin inflammation, neural symptoms, and death in all experimentally infected mice 48–72 h after challenge. In contrast, all mice of the negative control group survived, which is in agreement with previous studies (21, 28).

The physicochemical property results of the representative PRV NY isolate are shown in **Table 2**. The NY isolate was sensitive to chloroform, trypsin, formaldehyde, and ultraviolet ray, demonstrating that it belonged to the enveloped virus (2). The virus was not inactivated until the heating time was above an hour at 56°C, showing that the NY isolate had high heat resistance. When the culture medium pH was adjusted to 3.0 or 11.0, no detectable titers were observed. In the ST cells infected with NY isolate, a circular viral particle of about 110∼150 nm was observed, and virus particles exhibited envelope protein with a radially arranged spike (**Figure 1B**), which is basically consistent with the morphological features of PRV. These results are identical to the physicochemical properties of PRV (29).

We successfully obtained the gE, gC, gB, and gD genes of 16 PRV isolates with 1,867, 1,587, 2,867, and 1,494 bp and submitted the sequences to GenBank under the accession numbers listed in **Table 1**. Sequencing analysis of the PRV gE, gC, gB, and gD genes reveals maximal aa (nucleotide) sequence divergences of 0.3% (0.2%), 1.7% (0.7%), 2.3% (0.9%), and 1.3% (0.8%) within the 16 isolates and 4.3% (2.3%), 7.9% (4.5%), 4.4% (2.1%), and 3.3% (1.5%) compared with European–American PRV strains, respectively. The maximal aa (nucleotide) sequence divergence of the four genes of the 16 isolates were 2.3% (0.9%), 6.1% (3.5%), 2.0% (0.8%), and 1.0% (0.7%) compared with those strains prevalent in China before 2012 and were 0.9% (0.3%), 1.9% (0.5%), 1.5% (0.7%), and 1.3% (0.8%) after 2012. On the basis of NJ trees of the gE, gC, gB, and gD genes derived from the 16 isolates and PRV reference strains, four trees (**Figure 2**) could be divided into two main clades, Clades 1 and 2. All 16 isolates in this study belong to Clade 2, together with the Chinese PRV strains, and most of them based on the gE and gC genes are clustered in Clade 2-1 along with the six Chinese PRV variants (after 2012), which

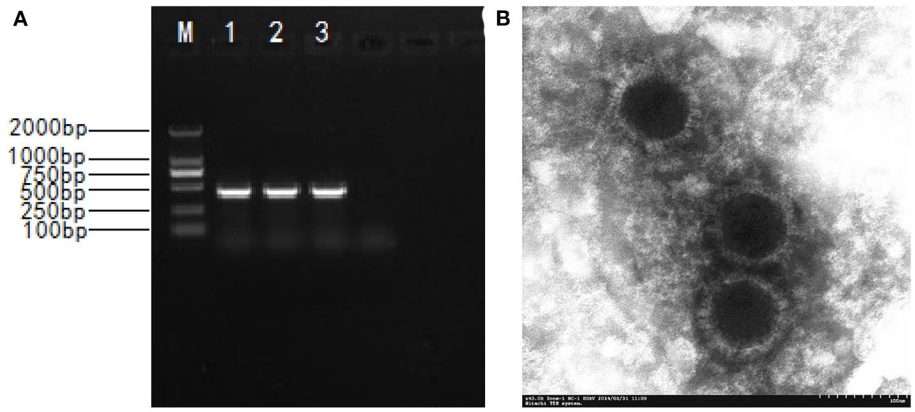

FIGURE 1 | The isolation and identification of the PRV. **(A)** Amplified PCR product of 429 bp; M. DNA marker DL2000; 1-3. PCR products; 4. Negative control; **(B)** Electronograph of PRV NY strain.

TABLE 1 | The information of PRV strains for sequence alignment and phylogenetic analysis.

Study virus	Accession number	Origin	Reference virus	Accession number	Origin
JY	KF017615[E]/KF997104[C]/KX880453[B]/KX880468[D]	Henan, China, 2012	HN2012	KP722022[G]	China, 2012
MZ1	KF130881/KF997097/KX880456/KX880471	Henan, China, 2012	HNX	KM189912	China, 2012
MZ2	KF130882/KF997099/KX880457/KX880472	Henan, China, 2012	HNB	KM189914	China, 2012
LGX	KF042384/KF997098/KX880454/KX880469	Henan, China, 2012	TJ	KJ789182	China, 2012
NY	KF130883/KF997096/KX880458/KX880473	Henan, China, 2012	JS-2012	KP257591	China, 2012
ZK	KF130886/KF997100/KX880464/KX880479	Henan, China, 2012	ZJ01	KM061380	China, 2012
ZM	KF130887/KF997102/KX880465/KX880480	Henan, China, 2012	SC	KT809429	China, 1986
M5	KF130880/KF997095/KX880455/–	Henan, China, 2012	Ea	KU315430	China, 1990
GY	KF042383/KF997103/KX880452/–	Henan, China, 2012	LA	KU552118	China, 1997
SMX	KP192494/KR025920/KX880459/KX880474	Henan, China, 2014	Fa	AF403049 [E]/AF403051 [C]/–[B]/AY196984[D]	China, 1993
WZ	KR119070/KR119071/KX880461/KX880476	Henan, China, 2014	Hercules	KT983810	Greece, 2010
YZ	KP192495/KR153193/KX880463/KX880478	Henan, China, 2014	Kaplan	JF797218	Hungary, 1959
BP	KP318116**/**KP318117**/**KX880451**/**KX880466	Henan, China, 2014	Becker	JF797219	America, 1967
WY	KF130884/KF997094/KX880460/KX880475	Henan, China, 2013	Kolchis	KT983811	Greece, 2010
YY	KF130885/KF997101/KX880462/KP259814	Henan, China, 2013	Bartha	JF797217	Hungary, 1960
XC	MW2388925/MW073286/MW654204/–	Henan, China, 2018			

[E]Represents gE genes of PRV strains. [C]Represents gC genes of PRV strains. [B]Represents gB genes of PRV strains. [D]Represents gD genes of PRV strains. [G]Represents whole genomes of PRV reference strains. The 16 strains sequenced in this study are shown in bold.

TABLE 2 | Detection results of physicochemical property tests for PRV NY isolate.

Treatment	Test group ($TCID_{50}$/0.1 mL)	Control group ($TCID_{50}$/0.1 mL)	Difference
Heat resistance	10^{1}	$10^{9.0}$	8.0
Chloroform resistance	$10^{0.75}$	$10^{9.0}$	8.25
Acid resistance	10^{0}	$10^{9.0}$	9.0
Alkali resistance	10^{0}	$10^{9.0}$	9.0
Trypsin resistance	10^{0}	$10^{9.0}$	9.0
Formaldehyde resistance	$10^{1.1}$	$10^{9.0}$	7.9
Uv resistance	$10^{8.0}$	$10^{9.0}$	1.0

are similar to the PRV variants (19). Clade 1 is composed of the remaining strains (European–American PRV strains). These findings reveal that the 16 isolates are genetically closer to the PRV variants but differ from early Chinese PRV isolates. Interestingly, the 16 isolates are located in different clades for four genes. For gC, gB, and gD genes, isolate BP is in the same small branch as one early Chinese PRV Ea strain (**Figures 2B–D**), whereas the BP isolate belongs to Clade 2-1, including the six Chinese variant PRV strains (**Figure 2A**), suggesting that interclade recombination events might happen among the PRV strains.

In the deduced gE aa sequences, compared with all strains of Clade 1 (**Figure 2A**), two aa insertions at positions 48 (D) and 497 (D) were found in the strains of Clade 2-1, and these were not observed for all other strains. Furthermore, all the 16 isolates of Clade 2-1 had 20 aa interspersed substitutions (at positions 54, 59, 63, 106, 121, 149, 179, 181, 215, 216, 449, 472, 474, 504, 509, 512, 522, 526, 577, and 578) except for the YY isolate at position 512 and BP isolate at position 577 (**Supplementary Table 1**). In comparison with the early Chinese PRV strains, all isolates except for the YY isolate had two aa substitutions at positions 449 (V to I) and 512 (G to S). Compared with the variants, there was an aa substitution at position 386 (T to M) for both isolates NY and BP, and two aa substitutions at positions 329 (W to R) and 532 (S to G) were shared for both WZ and ZK isolates. The gE protein is the major virulent protein of PRV, and only a few aa changes could transform the virulence of the virus in a previous study (30). Hence, these aa changes might also influence the virulence of reemerging PRV strains in China.

Compared with gC proteins of all strains of Clade 1 (**Figure 2B**), seven aa insertions at positions 63–69 (AAASTPA) of the gC protein were found in the strains of Clade 2, and the strains of Clade 2-1 (except for strain Ea) had 24 aa interspersed substitutions at positions 16, 25, 52, 55, 57, 59, 60, 61, 87, 90, 102, 130, 142, 187, 240, 431, 437, 449, 457, 461, 467, 485, 486, and 487 (**Supplementary Table 2**). As the important neutralizing antigen of PRV, gC protein is the main virulent protein, which conducts the adsorption process between virus and target cells (30). Therefore, these changes might alter the structure of gC glycoprotein and then affect the adhesion of the virus to host cells. Interestingly, eight strains, MZ1, NY, LGX, MZ1, XY, ZK, ZM, and GY, in this study harbor an additional aa substitution at position 280 (F to L) compared with reference strains, which is the first report that the characteristic aa substitution (at position 280) exists in the Chinese variant PRV strains' gC.

For the gB protein of the principle immunogen of the virus, alignments of the gB protein show that 16 PRV isolates in this study exist in the insertions, deletions, and substitutions of aa compared with the Bartha strain (**Supplementary Table 3**) and deletion of three aas (S, P, and G) at positions 75, 76, and 77 by comparison with the strains of Clade 1 (**Figure 2C**). These deletions of three aas and some aa changes are in agreement with previous studies (14, 19). The BP, SMX, WY, WZ, YY, and YZ have four aa changes at positions 85 (A to T), 454 (R to K), 563 (H to Q), and 740 (T to A) compared with the Chinese variants, and the remaining isolates have an aa change at position 454 (R to K) in comparison with the early Chinese strains. In addition, there were unique aa substitutions of PRV isolates, such as seven aa interspersed substitutions for JY; five aa changes for YY and LGX; four aa changes for MZ2, WZ, and GY; three aa changes for MZ1 and SMX; two aa changes for ZK, ZM, and M5; and one aa change for NY, WY, and YZ. These aa changes might result in the alteration of the neutralizing epitope of the gB protein and consequently loss of the protective efficacy of the previous vaccine Bartha-K61 in China.

Compared with the gD proteins of all strains of Clade 1 (except for the Becker) (**Figure 2D**), the isolates from this study had 10 aa interspersed substitutions at positions 207, 209, 212, 280, 281, 288, 309, 342, 346, and 395 (**Supplementary Table 4**). Compared with the variants, the NY isolate has three aa changes at positions 384 (K to E), 395 (A to T), and 401 (Q to L), and the YZ isolate has two aa insertions (R and P) at positions 278 and 279 and one aa substitution at position 323 (P to L), respectively. In addition, the ZK isolate harbors two aa substitutions at positions 143 (F to L) and 170 (V to F), and SMX, MZ2, LGX, and ZM have an aa substitution at positions 117 (C to S), 242 (G to D), 331 (P to L), and 353 (R to C), respectively. Remarkably, in six strains, BP, NY, SMX, WY, YZ, and ZK, an additional aa substitution was identified at position 338 (A to V) compared with the Chinese variants, which first reported that the characteristic aa substitution (at position 338) existed in the Chinese variant PRV strains' gD. For PRV, the gD protein is reported to play a role in attachment and affect the infectivity of the virus (30). These aa changes of the gD protein, therefore, might be the reason for the alteration of the virulence of reemerging PRV strains in China.

All mice in the four groups did not display adverse reactions after vaccination (data not shown). After the challenge with the PRV NY isolate, mice in group 1 survived without typical PR symptoms, and the mortality was 0% (0/10). The mortalities of groups 2–4 were 50% (5/10), 30% (3/10), and 100% (10/10), and typical PR symptoms appeared, such as depression, itching, and scratching. As for neutralizing antibodies against PRV, mice in groups 1–3 induced neutralizing antibodies with titers of 1:82, 1:24, and 1:22, respectively. No neutralizing antibodies were detected in group 4 as control. The neutralization titer between the PRV NY isolate and its serum was the highest, followed by the Bartha-K61 and Hubei 98 strains, which indicate that the PRV NY strain might have cross-antigenicity with both the Bartha-K61 and Hubei 98 strains with the different antigenicity. These results agree with previous findings (6), further indicating that the Bartha-K61 vaccine cannot provide full protection against the reemerging PRV strains. Therefore, the development of novel vaccines based on the reemerging PRV strains is urgent.

Live vaccines are currently employed to control PR on many swine farms in China, mainly based on strain Bartha-K61, which is an attenuated strain of PRV produced by extensive *in vitro* passages and has a well-characterized deletion of the complete gE and partial gI genes encoding proteins that attenuate virulence, and Bartha-K61 has played a key role in the eradication of PR (31). From 2005 to 2010, the

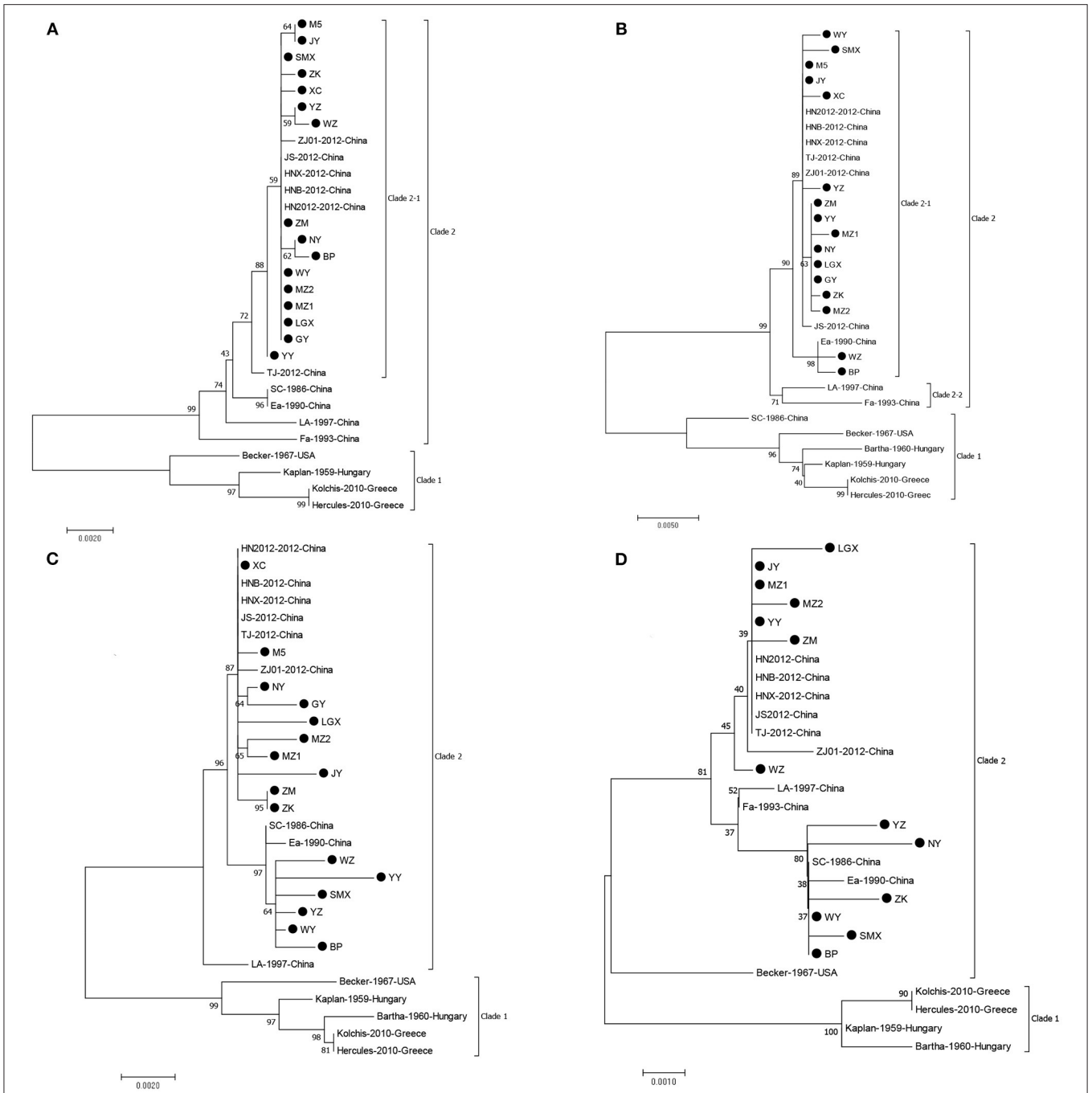

FIGURE 2 | Phylogenetic tree constructed by aligning nucleotide sequences of gE **(A)**, gC **(B)**, gB **(C)**, and gD **(D)** genes of the PRV isolates and reference strains using the NJ method. Bootstrapping with 1,000 replicates was performed to determine the percentage reliability for each internal node. Black circles indicate PRV field isolates in this study.

positive PRV gE antibodies were detected in only 3–5% of serum samples (32). Since 2012, severe PRV outbreaks have occurred on several swine farms and spread rapidly to most of China (6, 20, 27, 32). Although the PRV infection has recently decreased since the Chinese government proposed the eradication program based on PR in 2011, it remains not completely eradicated (14, 19, 20). Some research demonstrates that novel PR is caused by reemerging PRV strains (6, 13, 19, 20, 33), and this study further confirms reemerging PRV strains are prevalent in China. To control and prevent the PRV infection in swine herds, we should develop effective vaccines and combine them with other integrated control measures,

such as serological and virological monitoring, and biosafety procedures. In addition, the Chinese government should call on all relevant practitioners (farmers, veterinarians, scientists, vaccine manufacturers, officials, and communities) to join hands for fighting the disease and learn from many countries in South America, North America, and Europe that successfully eliminated PR for a long time. Facing the prevalence of PR, it is worth further study to evaluate whether the current immunization procedures and biosafety measures are reasonable and effective.

In conclusion, this study suggests that PR is not yet eradicated and still exists in central China, and the aas of gE, gC, gB, and gD of 16 PRV isolates from this study show mutations compared with the early Chinese PRV strains. Further, it can be speculated that these variations may be the cause of the reemergence of PR in China. The question of whether the genetic variations seen in complete gE, gC, gB, and gD genes of these PRV isolates affect the pathogenicity of PRV is currently under further investigation, and the complete genome sequencing of the isolates is also necessary.

DATA AVAILABILITY STATEMENT

The datasets presented in this study are deposited in the online repositories. The names of the repository/repositories and accession number(s) can be found in the article/**Supplementary Material**.

ETHICS STATEMENT

All experimental procedures were reviewed and approved by the Henan Agriculture University Animal Care and Use Committee (license number SCXK (Henan) 2013-0001).

AUTHOR CONTRIBUTIONS

H-HZ and H-YC have made substantial contributions to the conception, design of the work, the acquisition, and analysis. TX and Z-YW carried out interpretation of data. X-SL and L-LZ discussed and prepared the final report. H-HZ, H-YC, and Y-LB have drafted the work or substantively revised it. All authors have read and approved the final manuscript.

FUNDING

This work was supported by the Zhongyuan High Level Talents Special Support Plan (No. 204200510015), Program for Scientific and Technological Innovation Talents in Universities of Ministry of Education of Henan Province (No. 21HASTIT039), and Fang's family (Hong Kong) foundation.

SUPPLEMENTARY MATERIAL

The Supplementary Material for this article can be found online at: https://www.frontiersin.org/articles/10.3389/fvets.2021.764982/full#supplementary-material

REFERENCES

1. Muller T, Hahn EC, Tottewitz F, Kramer M, Klupp BG, Mettenleiter TC, et al. Pseudorabies virus in wild swine: a global perspective. *Arch Virol.* (2011) 156:1691–705. doi: 10.1007/s00705-011-1080-2
2. Pomeranz LE, Reynolds AE, Hengartner CJ. Molecular biology of pseudorabies virus: impact on neurovirology and veterinary medicine. *Microbiol Mol Biol Rev.* (2005) 69:462–500. doi: 10.1128/MMBR.69.3.462-500.2005
3. Gu J, Hu D, Peng T, Wang Y, Ma Z, Liu Z, et al. Epidemiological investigation of pseudorabies in Shandong Province from 2013 to 2016. *Transbound Emerg Dis.* (2018) 65:890–98. doi: 10.1111/tbed.12827
4. Ketusing N, Reeves A, Portacci K, Yano T, Olea-Popelka F, Keefe T, et al. Evaluation of strategies for the eradication of Pseudorabies virus (Aujeszky's disease) in commercial swine farms in Chiang-Mai and Lampoon Provinces, Thailand, using a simulation disease spread model. *Transbound Emerg Dis.* (2014) 61:169–76. doi: 10.1111/tbed.12017
5. Tong GZ, Chen HC. Pseudorabies epidemic status and control measures in China. *Chin J Vet Sci.* (1999) 19:4–5. doi: 10.3969/j.issn.1005-4545.1999.01.001
6. An TQ, Peng JM, Tian ZJ, Zhao HY, Li N, Liu YM, et al. Pseudorabies virus variant in Bartha-K61-vaccinated pigs, China, 2012. *Emerg Infect Dis.* (2013) 19:1749–55. doi: 10.3201/eid1911.130177
7. Klupp BG, Hengartner CJ, Mettenleiter TC, Enquist LW. Complete, annotated sequence of the pseudorabies virus genome. *J Virol.* (2004) 78:424–40. doi: 10.1128/JVI.78.4.2166.2004
8. Ober BT, Summerfield A, Mattlinger C, Wiesmüller KH, Jung G, Pfaff E, et al. Vaccine-induced, pseudorabies virus-specific, extrathymic CD4+CD8+ memory T-helper cells in swine. *J Virol.* (1998) 72:4866–73. doi: 10.1128/JVI.72.6.4866-4873.1998
9. Ober B, Teufel B, Wiesmüller K, Jung G, Pfaff E, Saalmüller A, et al. The porcine humoral immune response against pseudorabies virus specifically targets attachment sites on glycoprotein gC. *J Virol.* (2000) 74:1752–60. doi: 10.1128/JVI.74.4.1752-1760.2000
10. Wang X, Wu CX, Song XR, Chen HC, Liu ZF. Comparison of pseudorabies virus China reference strain with emerging variants reveals independent virus evolution within specific geographic regions. *Virology.* (2017) 506:92–8. doi: 10.1016/j.virol.2017.03.013
11. Schröter C, Vallbracht M, Altenschmidt J, Kargoll S, Fuchs W, Klupp B, et al. Mutations in pseudorabies virus glycoproteins gB, gD, and gH functionally compensate for the absence of gL. *J Virol.* (2015) 90:2264–72. doi: 10.1128/JVI.02739-15
12. Fonseca A, Camargos M, Sales M, Heinemann M, Leite R, Reis J. Pseudorabies virus can be classified into five genotypes using partial sequences of UL44. *Braz J Microbiol.* (2012) 43:1632–40. doi: 10.1590/S1517-838220120004 00048
13. Ye C, Zhang QZ, Tian ZJ, Zheng H, Zhao K, Liu F, et al. Genomic characterization of emergent pseudorabies virus in China reveals marked sequence divergence: evidence for the existence of two major genotypes. *Virology.* (2015) 483:32–43. doi: 10.1016/j.virol.2015.04.013
14. Wang Y, Qiao S, Li X, Xie W, Guo J, Li Q, et al. Molecular epidemiology of outbreak-associated pseudorabies virus (PRV) strains in central China. *Virus Genes.* (2015) 50:401–9. doi: 10.1007/s11262-015-1190-0
15. Kimman T, de Wind N, Oei-Lie N, Pol J, Berns A, Gielkens A. Contribution of single genes within the unique short region of Aujeszky's disease virus (suid herpesvirus type 1) to virulence, pathogenesis and immunogenicity. *J Gen Virol.* (1992) 73:243–51. doi: 10.1099/0022-1317-73-2-243
16. Wang M, Wang L, Zhao Q. Efficacy evaluation of two live virus vaccines against an emerging pseudorabies virus variant. *Pol J Vet Sci.* (2019) 22:639–45. doi: 10.24425/pjvs.2019.129975

17. He WT, Auclert LZ, Zhai XF, Wong G, Zhang C, Zhu HN, et al. Interspecies transmission, genetic diversity, and evolutionary dynamics of pseudorabies virus. *J Infect Dis.* (2019) 219:1705–15. doi: 10.1093/infdis/jiy731
18. Ma Z, Han Z, Liu Z, Meng F, Wang H, Cao L, et al. Epidemiological investigation of porcine pseudorabies virus and its coinfection rate in Shandong Province in China from 2015 to 2018. *J Vet Sci.* (2020) 21:e36. doi: 10.4142/jvs.2020.21.e36
19. Sun Y, Liang W, Liu Q, Zhao T, Zhu H, Hua L, et al. Epidemiological and genetic characteristics of swine pseudorabies virus in mainland China between 2012 and 2017. *PeerJ.* (2018) 6:e5785. doi: 10.7717/peerj.5785
20. Zhai XF, Zhao W, Li KM, Zhang C, Wang CC, Su S, et al. Genome characteristics and evolution of pseudorabies virus strains in Eastern China from 2017 to 2019. *Virol Sin.* (2019) 34:601–09. doi: 10.1007/s12250-019-00140-1
21. Zhao Y, Wang LQ, Zheng HH, Yang YR, Liu F, Zheng LL, et al. Construction and immunogenicity of a gE/gI/TK-deleted PRV based on porcine pseudorabies virus variant. *Mol Cell Probe.* (2020) 53:101605. doi: 10.1016/j.mcp.2020.101605
22. Binn L, Lazar E, Eddy G, Kajima M. Recovery and characterization of a minute virus of canines. *Infect Immun.* (1970) 1:503–8. doi: 10.1128/iai.1.5.503-508.1970
23. Reed LJ. A simple method of estimating fifty percent endpoints. *Am J Hyg.* (1938) 27:493–7. doi: 10.1093/oxfordjournals.aje.a118408
24. Kumar S, Stecher G, Tamura K. MEGA7: molecular evolutionary genetics analysis version 7.0 for bigger datasets. *Mol Biol Evol.* (2016) 33:1870–4. doi: 10.1093/molbev/msw054
25. Zheng HH, Wang LQ, Fu PF, Zheng LL, Chen HY, Liu F. Characterization of a recombinant pseudorabies virus expressing porcine parvovirus VP2 protein and porcine IL-6. *Virol J.* (2020) 17:19. doi: 10.1186/s12985-020-1292-8
26. Tian RB, Jin Y, Xu T, Zhao Y, Wang ZY, Chen HY. Development of a SYBR green I-based duplex real-time PCR assay for detection of pseudorabies virus and porcine circovirus 3. *Mol Cell Probe.* (2020) 53:101593. doi: 10.1016/j.mcp.2020.101593
27. Wu R, Bai CY, Sun JZ, Chang SK, Zhang XK. Emergence of virulent pseudorabies virus infection in northern China. *J Vet Sci.* (2013) 14:363–5. doi: 10.4142/jvs.2013.14.3.363
28. Laval K, Vernejoul J, Van Cleemput J, Koyuncu O, Enquist L. Virulent pseudorabies virus infection induces a specific and lethal systemic inflammatory response in mice. *J Virol.* (2018) 92:e01614-18. doi: 10.1128/JVI.01614-18
29. Zhu L, Yi Y, Xu Z, Cheng L, Tang S, Guo W. Growth, physicochemical properties, and morphogenesis of Chinese wild-type PRV Fa and its gene-deleted mutant strain PRV SA215. *Virol J.* (2011) 8:272. doi: 10.1186/1743-422X-8-272
30. Karger A, Schmidt J, Mettenleiter TC. Infectivity of a pseudorabies virus mutant lacking attachment glycoproteins C and D. *J Virol.* (1998) 72:7341–8. doi: 10.1128/JVI.72.9.7341-7348.1998
31. Lomniczi B, Watanabe S, Ben-Porat T, Kaplan A. Genome location and identification of functions defective in the Bartha vaccine strain of pseudorabies virus. *J Virol.* (1987) 61:796–801. doi: 10.1128/jvi.61.3.796-801.1987
32. Gu ZQ, Hou CC, Sun HF, Yang WP, Dong J, Bai J, et al. Emergence of highly virulent pseudorabies virus in southern China. *Can J Vet Res.* (2015) 79:221–8.
33. Hu RM, Zhou Q, Song WB, Sun EC, Zhang MM, He QG, et al. Novel pseudorabies virus variant with defects in TK, gE and gI protects growing pigs against lethal challenge. *Vaccine.* (2015) 33:5733–40. doi: 10.1016/j.vaccine.2015.09.066

Conflict of Interest: The authors declare that the research was conducted in the absence of any commercial or financial relationships that could be construed as a potential conflict of interest.

Publisher's Note: All claims expressed in this article are solely those of the authors and do not necessarily represent those of their affiliated organizations, or those of the publisher, the editors and the reviewers. Any product that may be evaluated in this article, or claim that may be made by its manufacturer, is not guaranteed or endorsed by the publisher.

frontiers in Veterinary Science

ORIGINAL RESEARCH
published: 24 November 2021
doi: 10.3389/fvets.2021.746129

Extension of Sylvatic Circulation of African Swine Fever Virus in Extralimital Warthogs in South Africa

Anthony F. Craig[1], Mathilde L. Schade-Weskott[1†], Henry J. Harris[2], Livio Heath[2], Gideon J. P. Kriel[3], Lin-Mari de Klerk-Lorist[4], Louis van Schalkwyk[1,4,5], Peter Buss[6], Jessie D. Trujillo[7], Jan E. Crafford[1], Juergen A. Richt[1,7] and Robert Swanepoel[1]*

[1] Vectors and Vector-Borne Diseases Research Programme, Department of Veterinary Tropical Diseases, Faculty of Veterinary Science, University of Pretoria, Pretoria, South Africa, [2] Agricultural Research Council-Onderstepoort Veterinary Research Transboundary Animal Diseases Laboratory, Pretoria, South Africa, [3] Provincial Veterinary Services, Department of Agriculture, Land Reform and Rural Development, Kimberley, South Africa, [4] Office of the State Veterinarian, Department of Agriculture, Land Reform and Rural Development, Kruger National Park, Skukuza, South Africa, [5] Department of Migration, Max Planck Institute of Animal Behavior, Radolfzell, Germany, [6] Veterinary Wildlife Services, South African National Parks, Kruger National Park, Skukuza, South Africa, [7] Diagnostic Medicine/Pathobiology, Center of Excellence for Emerging and Zoonotic Animal Diseases (CEEZAD), College of Veterinary Medicine, Kansas State University, Manhattan, KS, United States

Sylvatic circulation of African swine fever virus (ASFV) in warthogs and *Ornithodoros* ticks that live in warthog burrows historically occurred in northern South Africa. Outbreaks of the disease in domestic pigs originated in this region. A controlled area was declared in the north in 1935 and regulations were implemented to prevent transfer of potentially infected suids or products to the rest of the country. However, over the past six decades, warthogs have been widely translocated to the south where the extralimital animals have flourished to become an invasive species. Since 2016, there have been outbreaks of ASF in pigs outside the controlled area that cannot be linked to transfer of infected animals or products from the north. An investigation in 2008–2012 revealed that the presence of *Ornithodoros* ticks and ASFV in warthog burrows extended marginally across the boundary of the controlled area. We found serological evidence of ASFV circulation in extralimital warthogs further south in the central part of the country.

Keywords: African swine fever virus (ASFV), sylvatic circulation, extralimital warthogs, South Africa, serosurveilance

OPEN ACCESS

Edited by:
Levon Abrahamyan, Université de Montréal, Canada

Reviewed by:
Denis V. Kolbasov, Federal Research Center of Virology and Microbiology, Russia
Fedor Korennoy, Federal Center for Animal Health (FGBI ARRIAH), Russia
Klaus Depner, Friedrich-Loeffler-Institute, Germany

***Correspondence:**
Robert Swanepoel
bob.swanepoel@up.ac.za

†Present address:
Mathilde L. Schade-Weskott, 272 BIO Ltd., Woking, United Kingdom

Specialty section:
This article was submitted to Veterinary Epidemiology and Economics, a section of the journal Frontiers in Veterinary Science

Received: *06 September 2021*
Accepted: *20 October 2021*
Published: *24 November 2021*

Citation:
Craig AF, Schade-Weskott ML, Harris HJ, Heath L, Kriel GJP, de Klerk-Lorist L-M, van Schalkwyk L, Buss P, Trujillo JD, Crafford JE, Richt JA and Swanepoel R (2021) Extension of Sylvatic Circulation of African Swine Fever Virus in Extralimital Warthogs in South Africa. Front. Vet. Sci. 8:746129. doi: 10.3389/fvets.2021.746129

INTRODUCTION

African swine fever virus (ASFV) was first recognized in 1910 as the causative agent of a contagious and lethal disease of domestic pigs introduced into Kenya during the colonial era and farmed in proximity to wild suids (1). It subsequently emerged that the virus was maintained in the savannah areas of eastern and southern Africa through sylvatic circulation in the common warthog (*Phacochoerus africanus*) that does not become ill after infection and eyeless argasid ticks of the *Ornithodoros (Ornithodoros) moubata* complex that live in warthog burrows (2–5). More importantly, the virus can also be maintained through uncontrolled spread in populations of domestic pigs, and this has been facilitated in recent decades by widespread increase in small-scale pig farming in Africa that frequently involves free-ranging animals and informal trading in communal and peri-urban areas (6, 7).

In South Africa, the disease was first recognized in 1926 in pigs farmed in the northernmost Limpopo Province (LP) where warthogs were present (8, 9). Outbreaks of the disease either occurred in the north of the country or were initiated elsewhere through movement of infected pigs or pork products from the north, notably to farms in the environs of Johannesburg in Gauteng Province (GP) and from there to properties in Western Cape Province (WCP) (10). Consequently, an ASF controlled area was declared in 1935 to include the known distribution range of warthogs at that time (**Figure 1**) (10). Regulations were instituted to prevent movement of infected pigs or products from the controlled area, and to ensure that outbreaks were eradicated through slaughter of infected herds plus disinfection and quarantine of premises. Carcasses of hunted or culled wild suids could be transported under veterinary permit provided that the skin, head, hooves, and internal organs were removed (10).

The last outbreak in WCP was only eradicated in 1939. There were a few outbreaks of ASF in 1951 associated with the feeding of swill from five local abattoirs in GP, one of which is known to have received a consignment of infected pigs from Namibia (11). In 1996, isolated outbreaks occurred on three adjoining farms in northern GP close to the boundary of the controlled area (**Figure 2**) (12). Thereafter, the regulatory measures proved effective until 2012 when a series of outbreaks on smallholdings in adjacent areas of GP and Mpumalanga Province (MP) were traced to initial illegal movement of infected pigs from LP followed by local spread of infection involving sale of animals at auctions (12–14). The virus genotype involved, XXII, had previously been detected in the district of origin of the infected pigs in LP (15, 16). From 2016 onwards, there have been successive series of outbreaks of ASF in domestic pigs in GP, MP, North West Province (NWP), Northern Cape Province (NCP), and Free State Province (FSP) that cannot be linked to movement of infected pigs or products from the controlled area (**Figure 3**) (15, 18–20). A structured serosurvey found that the outbreaks of 2016 and 2017 had been eradicated effectively, with no evidence of persistence of infection in local pig populations (21).

Meanwhile, from 1963 onwards, there had been widespread translocation of warthogs to the south of the country associated with the growth of an extensive wildlife ranching and conservation industry, and the extralimital animals flourished to the extent that they are regarded as an invasive species (**Figure 3**) (17, 22–24). An investigation conducted in 2008–2012 on farms within 20 km of the boundary revealed the presence

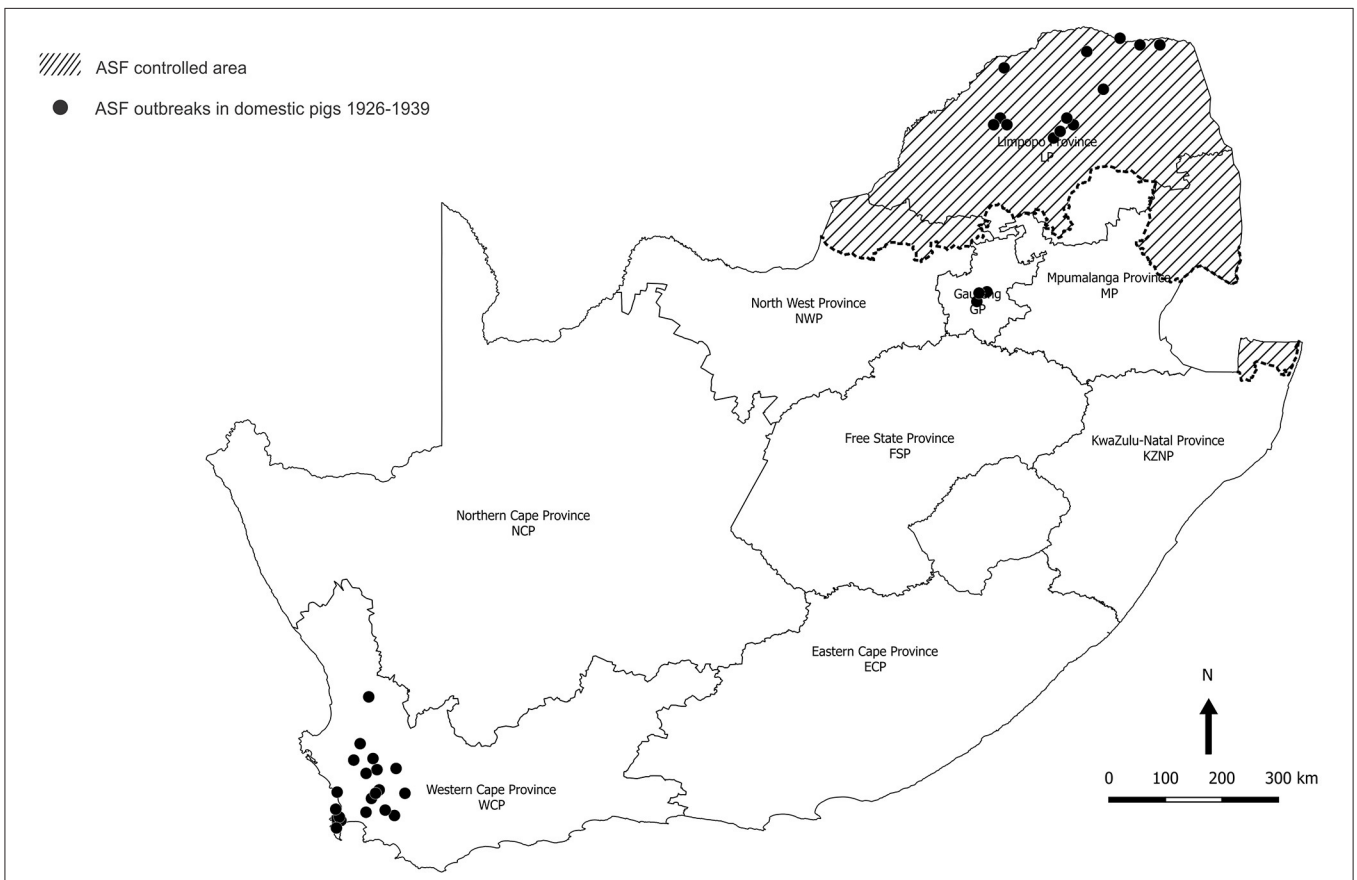

FIGURE 1 | Distribution of 37 outbreaks of African swine fever in South Africa, 1926–1939, for which approximate coordinates (correct to 0.1 degree) were derived from references cited in the text. The South African Protection of Personal Information Act 4 of 2013 precludes divulging names and accurate coordinates of private property.

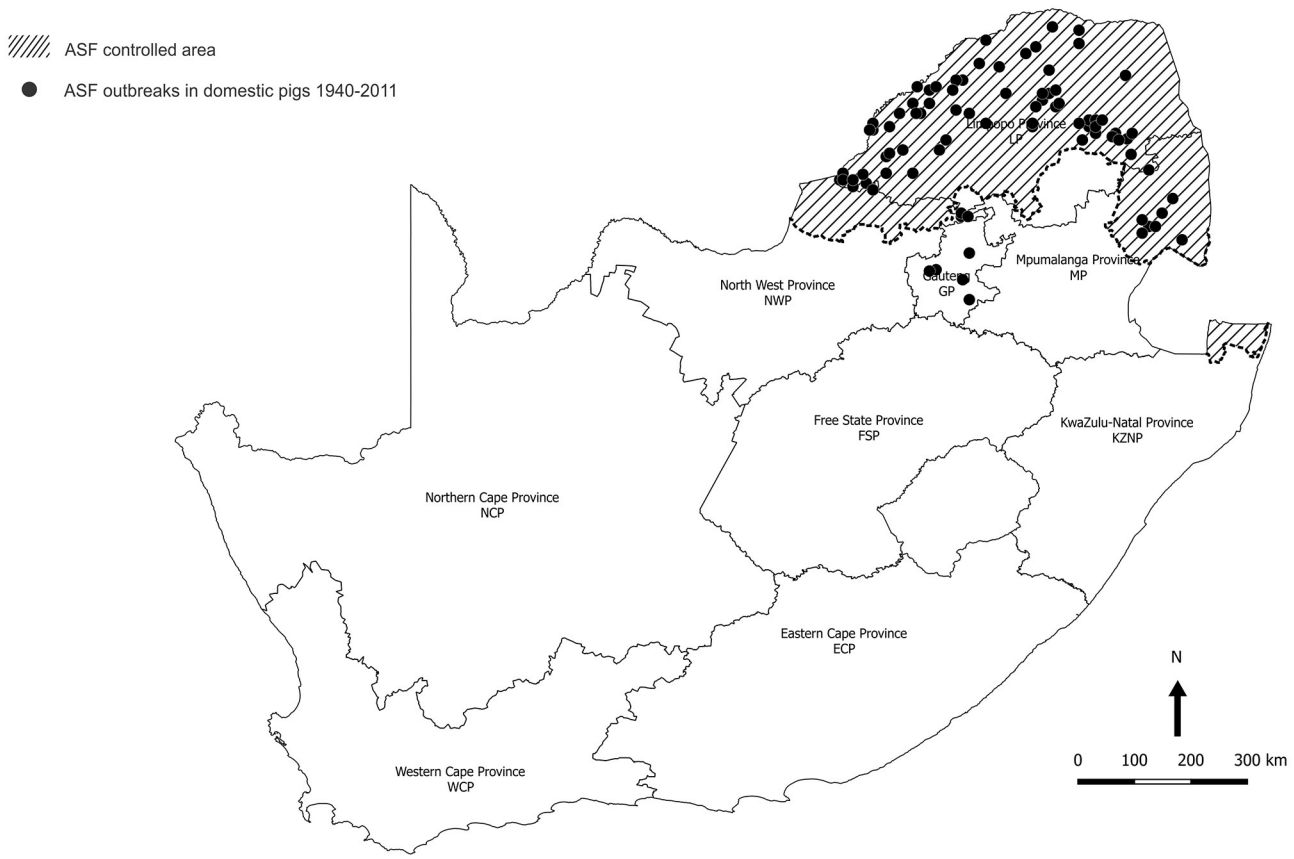

FIGURE 2 | Distribution of 89 outbreaks of African swine fever in South Africa, 1940–2011, for which approximate coordinates (correct to 0.1 degree) were derived from references cited in the text.

of *Ornithodoros* ticks in warthog burrows beyond the controlled area in NWP, GP, LP, and MP, with ASFV detected in one pool of ticks from MP (14). We were prompted to test warthog sera acquired opportunistically for evidence of sylvatic circulation of ASFV further south, and the findings are presented here.

MATERIALS AND METHODS

Study Sites

Baseline observations were made on serum samples obtained from warthogs in the Greater Kruger National Park (GKNP) that comprises the national park plus 20 adjoining private parks and lies within the controlled area where ASFV is known to be prevalent (**Figure 4**). For contrast, serum samples were collected in 2019 during a warthog culling operation in Addo Elephant National Park (Addo ENP) in ECP where ASF had never been recorded. Specific evidence of sylvatic circulation of ASFV beyond the controlled area was sought in the NCP by testing samples collected during a warthog culling operation in 2019 in Mokala National Park (Mokala NP), plus stored serum samples that had been collected earlier in the same park and in the provincial Rolfontein Nature Reserve (Rolfontein NR) that lies south of Mokala NP (**Figure 4**). In addition, blood samples from wild suids hunted or culled on private properties were sought through negotiation with organizations representing the wildlife industry, or collected in association with provincial veterinary officials in the vicinity of past outbreaks of ASF (**Figure 4**).

Samples

Altogether, 2,469 samples were collected from 546 warthogs in one provincial and three national nature reserves, including 783 duplicate tissue samples in formalin-fixative (**Table 1**).

Samples from GKNP consisted mainly of serum collected from warthogs translocated internally or culled for managerial purposes from 1999 to 2020 and stored at −80°C, but included a few blood samples and a number of lymph node and visceral organ samples collected from culled animals for an unrelated study (25) (**Table 1**).

Samples collected during the culling operations in Addo ENP and Mokala NP in 2019 comprised clotted blood for serum, whole blood collected with EDTA, mandibular, mediastinal, and mesenteric lymph nodes, plus spleen and bone marrow. Thymus and adrenal samples were collected from two fetuses encountered in Mokala NP. Samples other than blood or serum were collected mainly for a subsidiary study on distribution of ASFV in warthog tissues to be reported separately. A serial number was allocated to each warthog, and the date of sampling, gender, and age group estimated from size and dentition (26) were recorded.

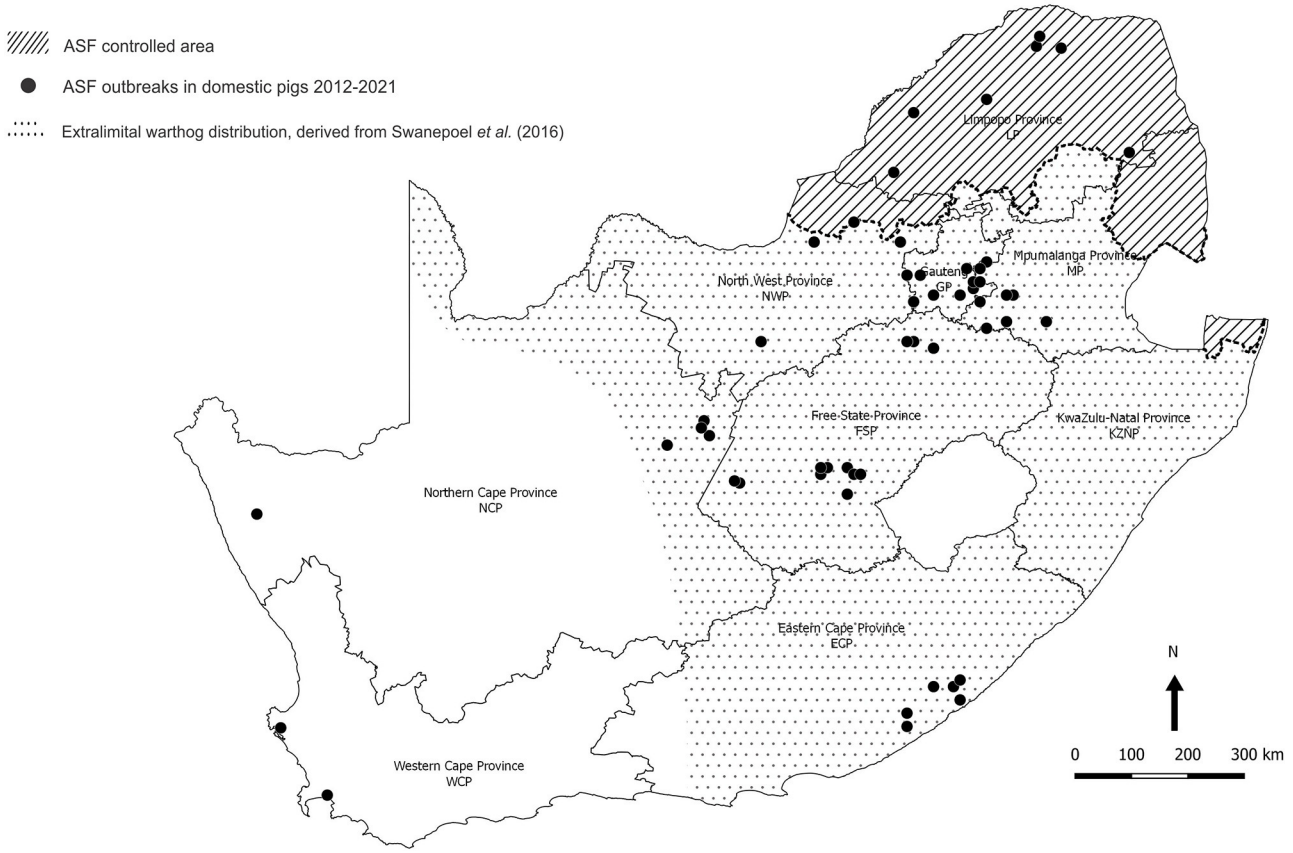

FIGURE 3 | Distribution of 85 outbreaks of African swine fever in South Africa, 2012–2020, for which approximate coordinates (correct to 0.1 degree) were derived from references cited in the text. The distribution of warthogs outside the controlled area was plotted with QGIS (Penn Libraries, Philadelphia, PA) using data from Swanepoel et al. (17).

Access was obtained retrospectively to 23 warthog sera that had been collected during a culling operation in 2017 in Mokala NP and stored at −80°C, plus 44 warthog sera collected in 2016 and stored at −20°C in the provincial Rolfontein NR situated approximately 100 km south of Mokala NP.

Blood samples from animals hunted or culled on private properties were intended to include any wild suids that may be encountered, not just warthogs. In the event, only 48 samples were received from 19 properties (farms or small nature reserves), 10 of which were situated inside the controlled area and 9 outside (**Table 2**). The samples comprised dried blood collected on Nobuto cellulose strips (NCS) (Advantec, Tokyo, Japan) or clotted blood from warthogs and Eurasian wild boars submitted by landowners and hunters from properties 1 to 17, plus clotted blood, mediastinal lymph node, and spleen samples from 4 warthogs collected in association with provincial veterinary officials during investigations on properties 18 and 19 in the vicinity of past ASF outbreaks in NCP (**Table 2**).

Detection of Antibody to ASFV

Tests for antibody to ASFV p72 protein in serum samples were performed with INgezim PPA Compac R.11.PPA.K3 blocking enzyme-linked immunosorbent assay (ELISA) kits (Eurofins Technologies Ingenasa, Madrid, Spain) used according to the manufacturer's instructions. Dried blood samples on NCS were eluted with kit buffer before testing (27).

Nucleic Acid Extraction, ASFV DNA Detection, and p72 Genotyping

Approximately 10% (w/v) suspensions of warthog tissues were prepared by homogenizing samples in phosphate-buffered saline, pH 7.2 (PBS). Automated nucleic acid extraction was performed with IndiMag Pathogen kits (Indical Bioscience, Leipzig, Germany) using slight modifications to the manufacturer's instructions. Briefly, 200 µl of tissue homogenate supernatant was added to 300 µl of ATL buffer (Qiagen, Dusseldorf, Germany) and 40 µl of proteinase K (Qiagen) and incubated at 56°C for 2 h before 200 µl of the lysed sample was added to 200 µl of AL buffer (Qiagen) and incubated at 70°C for 10 min. For whole blood samples, 200 µl was added directly to 200 µl of AL buffer and mixed well. For all samples, 200 µl of the AL lysate was added to the IndiMag buffer for extraction. Each extraction included known ASFV-positive controls. Eluates were stored at −80°C until further use.

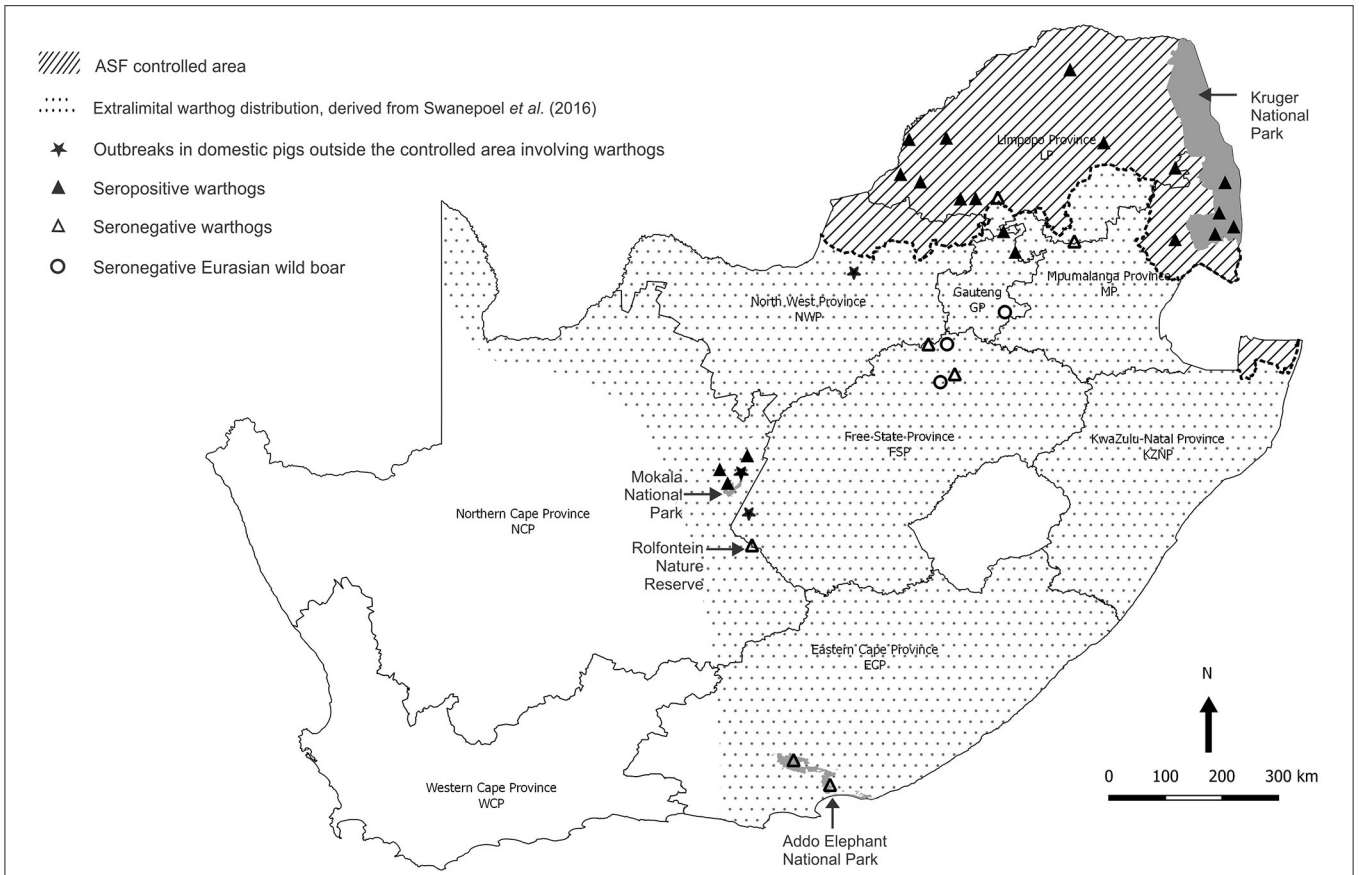

FIGURE 4 | Sites where samples from warthogs and Eurasian wild boars were obtained and tested for evidence of infection with African swine fever virus, and farms outside the controlled area where African swine fever outbreaks in domestic pigs were ascribed to contact with warthogs in 2017 and 2019.

TABLE 1 | Samples obtained from warthogs in four nature reserves in South Africa (abbreviations as given in the text).

	GKNP	Addo ENP	Mokala NP		Rolfontein NR
Years of sampling	**1999–2020**	**2019**	**2017**	**2019**	**2016**
Serum	207	116	23	77	44
EDTA blood	3	114	0	75	0
Spleen	11	36	0	82	0
Miscellaneous organs	14	0	0	0	0
Peripheral LN	95	137	0	82	0
Mediastinal LN	49	134	0	82	0
Mesenteric LN	41	14	0	81	0
Bone marrow	34	50	0	81	0
Fetal thymus	0	0	0	2	0
Fetal adrenal	0	0	0	2	0
Sub-total	454	601	23	564	44
Formalin-fixed duplicates	0	371	0	412	0
Total samples	454	972	999		44
Total warthogs sampled	241	154	107		44

Eluates were tested for ASFV nucleic acid using the real-time quantitative PCR (qPCR) assay of Zsak et al. (28) with modifications (29). Briefly, 5 µl of DNA was amplified in 20-µl reactions using 20 pmol of the published primers and 7 pmol of probe in Perfecta Fastmix II (Quanta Biosciences, Beverly, MA). Positive and no template controls (NTC) were included for each

TABLE 2 | Dried blood samples on Nobuto cellulose strips (Ncs) and clotted blood samples from warthogs or Eurasian wild boars received from hunters or landowners from 10 properties inside and 9 outside the African swine fever controlled area in South Africa during 2019 and 2020 (abbreviations as given in the text).

Property	Municipal area	Province	Species	Sample	No. of samples	ASF ELISA positive
Properties inside the ASF controlled area						
1	Makhado	LP	Warthog	Ncs	3	3
2	Lephalale	LP	Warthog	Ncs	4	4
3	Lephalale	LP	Warthog	Ncs	3	3
4	Thabazimbi	LP	Warthog	Ncs	4	4
5	Thabazimbi	LP	Warthog	Ncs	2	2
6	Thabazimbi	LP	Warthog	Ncs	3	3
7	Modimolle	LP	Warthog	Ncs	1	0
8	Bela Bela	LP	Warthog	Ncs	1	1
9	Bela Bela	LP	Warthog	Ncs	4	4
10	Mbombela	MP	Warthog	Ncs	4	2
Properties outside the ASF controlled area						
11	Bela Bela	LP	Warthog	Ncs	2	2
12	Elias Motsoaledi	LP	Warthog	Ncs	1	0
13	Tlokwe	NWP	Eu wild boar	Blood	1	0
13	Tlokwe	NWP	Warthog	Blood	1	0
14	Ekurhuleni	GP	Eu wild boar	Blood	1	0
15	Tshwane	GP	Warthog	Ncs	2	2
16	Ngwathe	FSP	Warthog	Ncs	2	0
17	Ngwathe	FSP	Eu wild boar	Ncs	1	0
18	Dikgatlong	NCP	Warthog	Blood*	2	2
19	Dikgatlong	NCP	Warthog	Blood*	2	2
					44	34

**Additionally, mediastinal lymph node and spleen samples were obtained from the same animals.*

PCR run. Samples with Cq mean values ≤38 (selected as the cutoff value based on the analytical sensitivity limits of the qPCR assay) were considered positive.

To confirm that ASFV was identified in warthog tissues from Mokala NP, nucleic acid from the qPCR-positive spleen sample with lowest Cq mean value was amplified using primers p72-D and p72-U and the cycling conditions of Bastos et al. (30). An appropriately sized band of amplification product was excised from the agarose electrophoresis gel, purified, and subjected to Sanger nucleotide sequencing. The sequence was viewed and maximum likelihood phylogenetic comparisons made with representative sequences of the 24 known ASFV p72 genotypes (31) using MEGA X software (32).

RESULTS

The results obtained in the ELISA for antibody to ASFV in warthog sera from the four nature reserves are presented in **Figures 4**, **5**. As expected, a high prevalence of antibody was found in the sera of warthogs from GKNP, 97.1% (201/207), with doubtful reactions recorded in a further two juveniles, while no antibody activity was detected in sera from Addo ENP in ECP where no ASF outbreaks had ever been recorded. In contrast, a high prevalence of antibody was detected in sera collected during the 2019 culling operation in Mokala NP, 98.7% (76/77), some 400 km south of the controlled area, and also in the sera collected there in 2017, 91.3% (21/23), while no antibody was detected in the 44 samples collected in Rolfontein NR in 2016.

A high prevalence of antibody, 26/29 (89.6%), was detected in dried warthog blood samples obtained from 9/10 private properties within the ASF controlled area (**Table 2** and **Figure 4**). Outside the controlled area, antibody was detected on only 4/9 properties. These included positive reactions in four warthog blood samples from properties 11 and 15 (a small nature reserve), that lie close to each other and to the three farms where ASF outbreaks occurred in 1996 within 40 km south of the boundary of the controlled area near Pretoria in northern GP, plus four warthog sera from properties 18 and 19 that are situated about 100 km north and west of Mokala NP in the vicinity of past outbreaks of ASF in pigs in NCP. The remaining samples tested negative despite the fact that two sera from properties 13 and 17 in NWP and FSP came from Eurasian wild boars shot as free-ranging animals in proximity to free-ranging warthogs. In the course of the investigations, histories were obtained to confirm that fresh warthog offal had been fed to pigs on one farm where an outbreak of ASF had occurred in NCP in 2017, and that free-roaming pigs had been in contact with warthogs, including carcasses, on a farm where an outbreak occurred in the adjacent eastern FSP in 2017, with both locations being over 100 km distant from Mokala NP (**Table 2** and **Figure 4**) (20). In addition, an outbreak of ASF in 2019 involved both pigs and Eurasian wild

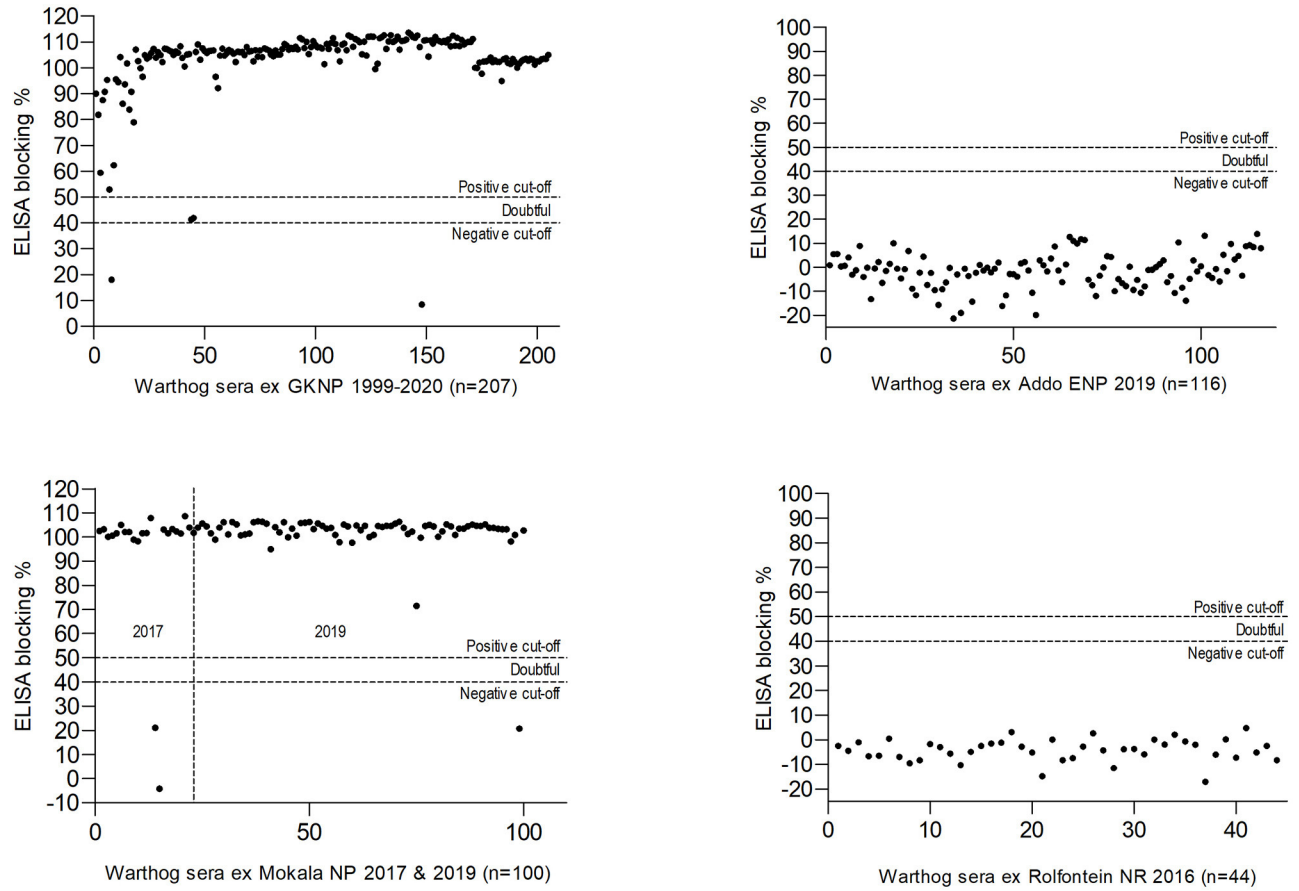

FIGURE 5 | Results of blocking enzyme-linked immunosorbent assays (ELISA) for antibody to African swine fever virus performed on warthog sera obtained from four nature reserves in South Africa (abbreviations as given in the text).

boars that had escaped their pens on a farm where warthogs were present 10 km south of the controlled area in NWP (**Table 2** and **Figure 4**) (20).

ELISA is not accredited for detection of ASF antibody in warthog sera, and in order to confirm the presumptive evidence for presence of the virus in Mokala NP, all 75 warthog EDTA blood samples and the 412 other tissue samples collected in Mokala NP in 2019 were tested for ASFV nucleic acid by qPCR (28, 29). All EDTA blood samples tested negative but 13 of the other samples from Mokala NP, including mandibular, mediastinal, and mesenteric lymph nodes plus spleen tested positive. The sample with the lowest Cq mean value, spleen from warthog Mokala NP 77, was selected for PCR with the Bastos et al. (30) p72 primers and the product determined to belong to the p72 genotype I of ASFV as had been identified in the disease outbreaks outside the controlled area in 2016 and subsequently in the same districts (15). The more recent outbreaks of ASF that occurred in ECP and WCP in 2020 and 2021 subsequent to the present sampling (**Figure 3**) were associated with genotype II virus, also detected in an outbreak in NWP in 2019 on the boundary of the controlled area, but otherwise associated with Mozambique, Madagascar, Mauritius, Tanzania, Zambia, and Zimbabwe (6, 7, 20, 30, 33–35).

DISCUSSION

Bushpigs (*Potamochoerus larvatus*) are the only indigenous wild suids present in South Africa apart from warthogs (36). They are widely distributed in wooded areas and sleep in lairs. Consequently, they do not have the same exposure to *Ornithodoros* ticks in burrows as warthogs. Bushpigs do not become ill following experimental inoculation with ASFV but develop viremic infection and can be transiently contagious for domestic pigs (37–40). Natural infection of bushpigs with ASFV, presumed to involve environmental contamination, has been reported in East Africa with some evidence of transmission of virus to domestic pigs (41–44).

In South Africa, bushpigs were stated to be less commonly infected with ASFV than warthogs and have never been implicated in outbreaks of the disease in domestic pigs, although on occasion warthogs and Eurasian wild boars have been misidentified as bushpigs (16, 45). They are less frequently hunted than warthogs and no samples from bushpigs were received for testing during the present study.

Feral domestic pigs and Eurasian wild boars, *Sus scrofa ferus*, are exotic to sub-Saharan Africa. They are susceptible to the disease and can be involved in spread of infection by contagion.

A recently discovered mechanism for maintenance of ASFV involves survival of infectivity in carcasses in the cold climate of northern Europe and scavenging by wild boars (7, 46).

Eurasian wild boars were introduced into South Africa to control pine tree moths in WCP where residual populations still exist, but apparently they did not adapt well to conditions in that region (47). Attempts were made to farm with Eurasian wild boars and cross-bred domestic pigs inside the controlled area in LP and MP, and to utilize them for hunting, but the animals succumbed to ASFV (16, 18, 20, 48). As mentioned in *Results*, an outbreak of ASFV involving domestic pigs and Eurasian wild boars occurred on a farm where warthogs were present in NWP in 2019, and three blood samples were received from wild boars in NWP, GP, and FSP for the present project (**Table 2** and **Figure 4**). Since Eurasian wild boars usually succumb to ASFV infection, it was to be expected that the three blood samples tested negative for antibody to the virus, but the presence of these animals in NWP, GP, and FSP suggests that there is need to monitor the distribution and growth of populations in South Africa, particularly since the species has proved to be a highly invasive elsewhere.

The present findings confirm that there is circulation of ASFV in warthogs beyond the controlled area in South Africa (**Table 2** and **Figures 4**, **5**), but the full extent of spread of infection and the mechanisms involved remain largely undetermined. Unbeknown to the present authors, aliquots of 91 of the same GKNP sera were included in an unrelated survey with similar ASFV findings (49), but this is immaterial since the samples were used in the current study mainly to confirm the validity of the antibody test for warthog sera. Samples from extralimital warthogs were of central interest.

Warthog piglets are infected by ticks while confined to burrows during early life and develop intense viremia that in turn facilitates infection of ticks (4). Low-intensity viremia and infection of lymphatic tissues may persist for months but warthogs are not contagious for domestic pigs or each other (1, 40). There is controversy about the infectivity of warthog offal for domestic pigs, but it has recently been confirmed that low doses of virus are infective for pigs by mouth (7, 50). The majority of outbreaks of ASF recorded within the controlled area in South Africa involved known contact between domestic pigs and live warthogs, carcasses, or offal (16).

Transmission of ASFV by ticks was discovered in Spain after introduction of the virus into Europe and involved domestic pigs and *Ornithodoros (Pavlovskyella) erraticus* ticks (51). Circulation of ASFV in domestic pigs and *O. (O.) moubata* complex ticks living in crevices of poorly constructed animal shelters was documented in Malawi and probably occurs elsewhere in Africa, but has not been reported in South Africa (7, 52). *Ornithodoros* ticks generally engorge blood meals in minutes to hours and detach while animals are at rest but can be conveyed passively on their hosts between burrows or to the environs of domestic pigs to transmit infection (53–56). Transport of *Ornithodoros* ticks on live warthogs or carcasses to the environs of piggeries has been observed in the controlled area (16).

The original warthog translocations in South Africa were undertaken by officials of national and provincial parks in order to replace the Cape warthog (*P. aethiopicus aethiopicus*), formerly present in the south of the country but extinct after the rinderpest epidemic of 1896 (57, 58). Warthogs were sourced from the Hluhluwe-iMfolozi Game Reserve in KwaZulu-Natal Province considered to be free of *Ornithodoros* ticks and ASFV at the time (7, 22). Translocations were made to the ECP in 1976–1977 and from there to Rolfontein NR in NCP in 1984. From 1991 onwards, Rolfontein NR served as the source for transfers to other reserves in NCP (24, 59). The lack of antibody to ASFV in warthog sera collected in Rolfontein NR in 2016 and Addo ENP in ECP in 2019 (**Figure 5**) implies that the virus was not disseminated during the original warthog translocations.

When Mokala NP was established in 2007, many animals were transferred from the former Vaalbos National Park in NCP, but warthogs were not included since they were already present on the farms incorporated into the new park (Mr. J. de Klerk, Manager, Mokala NP, personal communication, 2019). Hence, the high prevalence of antibody found in Mokala NP in 2017 and 2019 implies that the virus is endemic in the region, not just in the park. This is consistent with the detection of seropositive warthogs on farms 18 and 19 (**Table 2**) and the histories of contact of domestic pigs with warthog tissues in the outbreaks of ASF recorded on farms in NCP and adjacent FSP in 2017 (**Figure 4**).

Major nature reserves have not been implicated in triggering outbreaks of ASF in domestic pigs in South Africa, but the large populations of warthogs present on private land appear to play a direct role. To what extent multiple unrecorded translocations of warthogs that accompanied the burgeoning of game ranches and private nature reserves (24, 60) promoted dispersal of ticks and ASFV is less important than the potential threat posed by continued expansion of extralimital warthog populations and possible utilization without due regard to biosafety measures. The threat is greater for small-scale pig farmers who exercise little control on potential introduction of infection (6, 61, 62) than it is for commercial producers that apply strict compartmentalization procedures.

The taxonomy of Afrotropical *Ornithodoros* ticks was recently reviewed with description of new species and type localities, but little is known about ASFV vector competence and distribution ranges for some species (63). Observations on the occurrence of *Ornithodoros* tick species and their ASFV infection status in relation to a selection of the current study sites will be presented separately.

DATA AVAILABILITY STATEMENT

The original contributions presented in the study are included in the article/supplementary material, further inquiries can be directed to the corresponding author.

ETHICS STATEMENT

The animal study was reviewed and approved by University of Pretoria—Animal Ethics Committee. Written informed consent

was obtained from the owners for the participation of their animals in this study.

AUTHOR CONTRIBUTIONS

AC: planned and performed the study and prepared the manuscript under supervision as part of a Ph.D. project. MS-W: provided guidance in conducting laboratory procedures and provided field assistance. HH: provided guidance in conducting laboratory procedures. LH: provided guidance in conducting laboratory procedures and analysis and interpretation of data. GK: provided regional state veterinary supervision and assistance in conducting field studies. L-MK-L and LS: provided regional state veterinary supervision and assistance in conducting field studies. PB: provided guidance and access to biobanked warthog samples. JT: provided guidance in conducting laboratory procedures. JC: co-supervised the study and provided guidance in conducting field studies. JR: suggested conducting a research project on African swine fever in South Africa and raised the funds for the research contract. RS: supervised planning and performance of the study and preparation of the manuscript. All authors contributed to critical revision of the manuscript and approved the final version to be submitted for publication.

FUNDING

We acknowledge the support of NBAF Transition funds from the State of Kansas, the P20GM130448 under Award No. P20GM130448, and the Department of Homeland Security Center of Excellence for Emerging and Zoonotic Animal Diseases under Grant No. HSHQDC 16-A-B0006 to JR.

ACKNOWLEDGMENTS

We thank the South African Hunters and Game Conservation Association for arranging submission by their members of blood samples from hunted warthogs and Eurasian wild boars. We thank Dr. Angela Brüns of Veterinary Wildlife Services, South African National Parks, Kimberley, for samples collected during the 2017 culling operation in Mokala NP, and the ASF research team members of the Agricultural Research Council-Onderstepoort Veterinary Research, Transboundary Animal Diseases Laboratory (TADL) for technical assistance and guidance. The project was supported by a research contract from Kansas State University and a grant awarded by the South African Agricultural Sector Education and Training Authority (AgriSETA) to the Department of Veterinary Tropical Diseases, Faculty of Veterinary Science, University of Pretoria (UP).

REFERENCES

1. Montgomery RE. On a form of swine fever occurring in British East Africa Kenya Colony. *J Comp Pathol Ther.* (1921) 34:159–91. doi: 10.1016/S0368-1742(21)80031-4
2. Plowright W, Parker J, Peirce MA. African swine fever virus in ticks *Ornithodoros moubata*, murray collected from animal burrows in Tanzania. *Nature.* (1969) 2215185:1071–3. doi: 10.1038/2211071a0
3. Pini A. African swine fever: some observations and considerations. *S Afr J Sci.* (1977) 73:133–4.
4. Thomson GR. The epidemiology of African swine fever: the role of free-living hosts in Africa. *Onderstepoort J Vet Res.* (1985) 52:201–9.
5. Thomson GR, Gainaru M, Lewis A, Biggs H, Nevill E, Van der Pypekamp H, et al. The relationship between African swine fever virus, the warthog and Ornithodoros species in southern Africa. In: Wilkinson PJ, editor. *African Swine Fever*. Commission of the European Communities. EUR 8644 EN (1983). p. 85–100.
6. Penrith ML, Bastos AD, Etter EM, Beltrán -Alcrudo D. Epidemiology of African swine fever in Africa today: sylvatic cycle versus socio-economic imperatives. *Transbound Emerg Dis Animals.* (2019). 662:672–86. doi: 10.1111/tbed.13117
7. Penrith ML, Thomson GR, Bastos ADS, Etter, EMC. African swine fever. In: Coetzer JAW, Thomson GR, Maclachlan NJ, Penrith ML, editors. *Infectious Diseases of Livestock, Anipedia*. Cape Town: Oxford University Press (2019).
8. Steyn, D. Preliminary report on a South African virus disease amongst pigs. In: *13th and 14th Reports of the Director of Veterinary Education and Research*. Pretoria: Union of South Africa (1928). p. 415–28.
9. Steyn D. East African virus disease in pigs. In: *18th Report of the Director of Veterinary Services and Animal Industry*. Pretoria: Union of South Africa (1932). p. 99–109.
10. De Kock G, Robinson EM, Keppel JJ. Swine fever in South Africa. *Onderstepoort J. Vet Sci.* (1940) 14:31–93.
11. Neitz WO. *African Swine Fever. Emerging Diseases of Animals*. Rome: FAO Agricultural Studies (1963). p. 61.
12. Penrith ML, Vosloo W, Jori F, Bastos AD. African swine fever virus eradication in Africa. *Virus Res.* (2013) 1731:228–46. doi: 10.1016/j.virusres.10.011
13. Geertsma PJ, Mpofu D, Walters J. Investigation and control of an outbreak of African swine fever in the Gauteng Province in 2012. In: *Proceedings: 10th Annual Congress of the Southern African Society for Veterinary Epidemiology and Preventive Medicine.* (2012). p. 1–3.
14. Magadla NR, Vosloo W, Heath L, Gummow B. The African swine fever control zone in South Africa and its current relevance. *Onderstepoort J Vet Res.* (2016) 831:a1034. doi: 10.4102/ojvr.v83i1.1034
15. Janse van Rensburg L, Van Heerden J, Penrith ML, Heath LE, Rametse T, Etter EMC. Investigation of African swine fever outbreaks in pigs outside the controlled areas of South Africa, 2012-2017. *J S Afr Vet Assoc.* (2020) 910:e1–9. doi: 10.4102/jsava.v91i0.1997
16. Janse van Rensburg L, Etter E, Heath L, Penrith ML, Van Heerden J. Understanding African swine fever outbreaks in domestic pigs in a sylvatic endemic area: the case of the South African controlled area between 1977–2017. *Transbound Emerg Dis Animals*. (2020) 676:2753–69. doi: 10.1111/tbed.13632
17. Swanepoel M, Schulze E, Cumming DHM. A conservation assessment of *Phacochoerus africanus*. In: ChildMF, Roxburgh L, Do Linh San E, Raimondo D, Davies-Mostert HT editors. *The Red List of Mammals of South Africa, Swaziland and Lesotho*. Pretoria: South African National Biodiversity Institute and Endangered Wildlife Trust, South Africa (2016).
18. DALRRD. (Department of Agriculture, Land Reform and Rural Development). *Disease Database.* (1993-2019). Available online at: https://www.dalrrd.gov.za/Branches/Agricultural-Production-Health-Food-Safety/Animal-Health/Epidemiology/diseasedatabase (accessed 2021)
19. Mulumba-Mfumu LK, Saegerman C, Dixon LK, Madimba KC, Kazadi E, Mukalakata NT, et al. African swine fever: update on Eastern, Central and Southern Africa. *Transbound Emerg Dis Animals.* (2019) 664:1462–80. doi: 10.1111/tbed.13187
20. WAHIS. *Immediate Notifications and Follow-Ups.* (2005-2020). Available online at: http://www.oie.int/wahis2/public/wahid.php/Diseaseinformation/Immsummary

21. Van Rensburg LJ, Penrith ML, van Heerden J, Heath L, Eric ME. Investigation into eradication of African swine fever in domestic pigs from a previous outbreak (2016/17) area of South Africa. *Res Vet Sci.* (2020) 133:42–7. doi: 10.1016/j.rvsc.08.013
22. Penzhorn BL. A summary of the reintroduction of ungulates into South African National Parks (to 31 December 1970). *Koedoe.* (1971) 14:145–59. doi: 10.4102/koedoe.v14i1.725
23. Carruthers J. "Wilding the farm or farming the wild"? The evolution of scientific game ranching in South Africa from the 1960s to the present. Trans. R. Soc. S. Afr. (2008) 632:160–81. doi: 10.1080/00359190809519220
24. Swanepoel M. *Distribution, utilization and management of the extralimital common warthog Phacochoerus africanus in South Africa. Doctor of Philosophy, Conservation, Ecology, and Entomology Thesis, Stellenbosch University, Stellenbosch*. Available online at: https://scholar.sun.ac.za
25. Roos EO, Buss P, de Klerk-Lorist LM, Hewlett J, Hausler GA, Rossouw L. Test performance of three serological assays for the detection of *Mycobacterium bovis* infection in common warthogs (*Phacochoerus africanus*). *Vet Immunol Immunopathol*. (2016) 182:79–84. doi: 10.1016/j.vetimm.10.006
26. Mason DR. Dentition and age determination of the warthog *Phacochoerus aethiopicus* in Zululand, South Africa. *Koedoe.* (1984) 27:79–119. doi: 10.4102/koedoe.v27i1.553
27. Randriamparany T, Kouakou KV, Michaud V, Fernández-Pinero J, Gallardo C, Le Potier MF. et al. (2014). African swine fever diagnosis adapted to tropical conditions by the use of dried-blood filter papers. *Transbound. Emerg Dis Animals.* 63. doi: 10.1111./tbed.12295
28. Zsak L, Borca MV, Risatti GR, Zsak A, French RA, Lu Z, et al. Preclinical diagnosis of African swine fever in contact-exposed swine by a real-time PCR assay. *J Clin Microbiol.* (2005) 431:112–9. doi: 10.1128/JCM.43.1.112-119.2005
29. Sunwoo SY, Pérez-Núñez D, Morozov I, Sánchez EG, Gaudreault NN, Trujillo JD, et al. DNA-protein vaccination strategy does not protect from challenge with African swine fever virus Armenia 2007 strain. *Vaccines.* (2019) 7:12. doi: 10.3390/vaccines7010012
30. Bastos ADS, Penrith ML, Crucière C, Edrich JL, Hutchings G, Roger F, et al. Genotyping field strains of African swine fever virus by partial p72 gene characterization. *Arch Virol.* (2003) 148:693–706. doi: 10.1007/s00705-002-0946-8
31. Quembo CJ, Jori F, Vosloo W, Heath L. Genetic characterization of African swine fever virus isolates from soft ticks at the wildlife/domestic interface in Mozambique and identification of a novel genotype. *Transbound Emerg Dis Animals.* (2018) 652:420–31. doi: 10.1111/tbed.12700
32. Kumar S, Stecher G, Li M, Knyaz C, Tamura K. MEGA X: Molecular evolutionary genetics analysis across computing platforms. *Mol Biol Evol.* (2018) 356:1547–9. doi: 10.1093/molbev/msy096
33. Bastos AD, Penrith ML, Macome F, Pinto F, Thomson GR. Co-circulation of two genetically distinct viruses in an outbreak of African swine fever in Mozambique: no evidence for individual co-infection. *Vet Microbiol.* 1033:169–82. doi: 10.1016/j.vetmic.09.003
34. DALRRD (Department of Agriculture, Land Reform and Rural Development). *African Swine Fever Outbreak and Surveillance Update Report.* (2020). Available online at: http://nahf.co.za/wp-content/uploads/ASF-update-2020-05-19.pdf (accessed 2021)
35. DALRRD (Department of Agriculture, Land Reform and Rural Development). *African Swine Fever Outbreak Reported in the Western Cape for the First Time.* (2021). Available online at: https://www.drdlr.gov.za/sites/Internet/Latest%20News/Pages/African-swine-fever-outbreak-400reported-in-the-Western-Cape-for-the-first-time.aspx (accessed, 2021)
36. Venter J, Ehlers Smith Y, Seydack A. A conservation assessment of *Potamochoerus* larvatus. In: Child MF, Roxburgh L, Do Linh San E, Raimondo D, Davies-Mostert HT, editors. *The Red List of Mammals of South Africa, Swaziland and Lesotho. South African National Biodiversity Institute and Endangered Wildlife Trust, South Africa* (2016)
37. Anderson EC, Hutchings GH, Mukarati N, Wilkinson PJ. African swine fever virus infection of the bushpig *Potamochoerus porcus* and its significance in the epidemiology of the disease. *Vet Microbiol.* (1998) 621:1–15. doi: 10.1016/S0378-1135(98)00187-4
38. Oura CA, Powell PP, Anderson E, Parkhouse RM. The pathogenesis of African swine fever in the resistant bushpig. *J Gen Virol.* (1998) 79:1439–43. doi: 10.1099/0022-1317-79-6-1439
39. Salguero FJ. Comparative pathology and pathogenesis of African swine fever infection in swine. *Front Vet Sci.* (2020). 7:282. doi: 10.3389./fvets.2020.00282
40. Thomson GR, Gainaru MD, Van Dellen AF. Experimental infection of warthog *Phacochoerus aethiopicus* with African swine fever virus. *Onderstepoort J Vet Res.* (1980) 47:19–22.
41. Tray DE. African swine fever. *Adv Vet Sci.* (1963) 8:299–333.
42. Kukielka EA, Jori F, Martínez-López B, Chenais E, Masembe C, Chavernac D, et al. Wild and domestic pig interactions at the wildlife-livestock interface of Murchison Falls National Park, Uganda, and the potential association with African swine fever outbreaks. *Front Vet Sci.* (2016) 3:31. doi: 10.3389/fvets.2016.00031
43. Okoth E, Gallardo C, Macharia JM, Omore A, Pelayo V, Bulimo DW, et al. (2013). Comparison of African swine fever virus prevalence and risk in two contrasting pig-farming systems in South-west and Central Kenya. *Prev Vet Med*. (2012) 1102:198–205. doi: 10.1016/j.prevetmed.11.012
44. Ståhl K, Ogweng P, Okoth E, Tonny A, Muhangi D, Leblanc N, et al. Understanding the dynamics and spread of African swine fever virus at the wildlife-livestock interface: insights into the potential role of the bushpig, *Potamochoerus larvatus*. *Suiform Soundings*. (2014) 13:24–8.
45. Mansvelt PR. The incidence and control of African swine fever in the Republic of South Africa. *Bull Off Int Épizoot.* (1963) 60:889–94.
46. Chenais E, Ståhl K, Guberti V, Depner K. Identification of wild boar–habitat epidemiologic cycle in African swine fever epizootic. *Emerg Infect Dis.* (2018) 24:810–2. doi: 10.3201/eid2404.172127
47. Botha SA. Feral pigs in the Western Cape Province: failure of a potentially invasive species. *South Afr For J.* (1989) 1511:17–25. doi: 10.1080/00382167.1989.9630500
48. Penrith ML. *Experiences With ASF and African Wild Pigs OIE-CIC Joint International Meeting on Early Detection and Prevention of African Swine Fever (ASF) and Other Animal Health Issues at the Wildlife-Livestock-Human Interface OIE*. Paris: OIE (2014).
49. Neiffer D, Hewlett J, Buss P, Rossouw L, Hausler G, deKlerk-Lorist LM, et al. Antibody prevalence to African swine fever, *Mycobacterium bovis*, foot-and-mouth disease virus, Rift Valley fever virus, influenza A virus, and *Brucella* and *Leptospira* spp. *in free-ranging warthog Phacochoerus africanus populations in South Africa. J Wildl Dis.* (2021) 57:60–70. doi: 10.7589./JWD-D-20-00011
50. Niederwerder MC, Stoian AM, Rowland RR, Dritz SS, Petrovan V, Constance LA, et al. Infectious dose of African swine fever virus when consumed naturally in liquid or feed. *Emerg Infect Dis*. (2019) 25:891doi: 10.3201/eid2505.181495
51. Sanchez-Botija AC. Reservorios del virus de la peste porcina africana. Investigación del virus de la PPA en los artrópodos mediante la prueba de la hemoadsorción [Reservoirs of ASFV: a study of the ASFV in arthropods by means of the haemadsorption test]. *Bull Off Int Épizoot*. (1963) 60:895–9.
52. Haresnape J, Mamu FD. The distribution of ticks of the *Ornithodoros moubata* complex (*Ixodoidea: Argasidae*) in Malawi, and its relation to African swine fever epizootiology. *J Hyg.* (1986) 96:535–44. doi: 10.1017/S0022172400066341
53. Plowright W, Thomson GR, Neser JA. African swine fever. In: Coetzer JAW, Thomson GR,Tustin RC, editor. *Infectious Diseases of Livestock, With Special Reference to Southern Africa*. 1st edn. Cape Town: Oxford University Press (1994).
54. Horak IG, Biggs HC, Hanssen TS, Hanssen RE. The prevalence of helminth and arthropod parasites of warthog, *Phacochoerus aethiopicus*, in South West Africa/Namibia. *Onderstepoort J Vet Res.* (1983) 50:145–8.
55. Horak, I. G., Boomker, J., Vos, D., e., and Potgieter, V. (1988). Parasites of domestic and wild animals in South Africa. XXIII. Helminth and arthropod parasites of warthogs, *Phacochoerus aethiopicus*, in the eastern Transvaal Lowveld. *Onderstepoort J Vet Res.* (1988) 55:145–52.
56. Boomker J, Horak IG, Booyse DG, Meyer S. Parasites of South African wildlife. VIII Helminth and arthropod parasites of warthogs, Phacochoerus aethiopicus, in the eastern Transvaal Onderstepoort. *J Vet Res*. (1991) 58:195–202.

57. Grubb P. *The Afrotropical suids Phacochoerus, Hylochoerus, and Potamochoerus: Taxonorny and Description*. Gland, Switzerland: International Union for Conservation of Nature and Natural Resources (1993).
58. Vercammen P, Mason DR. *The Warthogs Phacochoerus Africanus and P. aethiopicus: Status and Action Plan Summary*. Gland, Switzerland: International Union for Conservation of Nature and Natural Resources (1993).
59. Somers M, Penzhorn B. Reproduction in a reintroduced warthog population in the Eastern Cape Province. *S. Afr J Wildl Res.* (1992) 22:57–60.
60. Maciejewski K, Kerley GIH. Understanding tourists' preference for mammal species in private protected areas: is there a case for extralimital species for ecotourism? *PLoS ONE.* (2014) 9:e88192. doi: 10.1371/journal.pone.0088192
61. Fasina FO, Mokoele JM, Spencer BT, Van Leengoed LA, Bevis Y, Booysen I. Spatio-temporal patterns and movement analysis of pigs from smallholder farms and implications for African swine fever spread, Limpopo province, South Africa. *Onderstepoort J Vet Res.* (2015) 82:11. doi: 10.4102/ojvr.v82i1.795
62. Etter EM, Mushagaluza Ciza A, Mapendere C, Ferguson W, Jori F and Penrith M (2019). Understanding ASF dynamic in South Africa: from spatio-temporal analysis at national level to fine special network analysis. *Front. Vet. Sci. Conference Abstract: GeoVet 2019. Novel spatio-temporal approaches in the era of Big Data*. doi: 10.3389/conf.fvets.05.00083
63. Bakkes DK, De Klerk D, Latif AA, Mans BJ. Integrative taxonomy of Afrotropical *Ornithodoros Acari: Ixodida: Argasidae*. *Ticks Tick Borne Dis.* (2018) 94:1006–37. doi: 10.1016/j.ttbdis.03.024

Conflict of Interest: The authors declare that the research was conducted in the absence of any commercial or financial relationships that could be construed as a potential conflict of interest.

frontiers in Veterinary Science

BRIEF RESEARCH REPORT
published: 09 December 2021
doi: 10.3389/fvets.2021.763859

Canine Leptospirosis Outbreak in Japan

Jun Saeki[1]* *and Aki Tanaka*[2]

[1] Department of Animal Sciences, Teikyo University of Science, Tokyo, Japan, [2] Department of Wildlife Medicine, Nippon Veterinary and Life Science University, Tokyo, Japan

Canine leptospirosis was suspected in 11 dogs in Osaka Prefecture, Japan and 9 dogs died within a month, from October 12 to November 10, 2017. Eight of the dogs had been taken on walks along the same riverbed and 4 dogs lived in the same town. Logistic regression analysis between a comparative group and the incident cases group showed that the odds of leptospirosis infection was 13.3 times higher ($p = 0.044$) in the dogs taken on walks along the riverbed than in the dogs not being walked along the riverbed. It is suggesting that these walks had been a risk factor. Microscopic agglutination tests showed that antibody titers against *Leptospira interrogans* serovar Australis were 1:2,560 and 1:10,240 in 2 dogs. Therefore, *L. interrogans* serovar Australis was suspected to be the causative agent, for which no canine vaccine is available in Japan. These results suggested that *L. interrogans* serovar Australis can cause local outbreaks. The development of a canine vaccine against various serotypes might help reduce local infections. Leptospirosis is an important infectious disease of dogs and it is also a zoonotic disease.

Keywords: leptospirosis, outbreak, Australis, dog, zoonosis

OPEN ACCESS

Edited by:
Lester J. Perez, University of Illinois at Urbana–Champaign, United States

Reviewed by:
Sara Savic, Scientific Veterinary Institute Novi Sad, Serbia
Leila Ullmann, São Paulo State University (UNESP), Brazil

***Correspondence:**
Jun Saeki
j-saeki@ntu.ac.jp

Specialty section:
This article was submitted to Veterinary Infectious Diseases, a section of the journal Frontiers in Veterinary Science

Received: *24 August 2021*
Accepted: *17 November 2021*
Published: *09 December 2021*

Citation:
Saeki J and Tanaka A (2021) Canine Leptospirosis Outbreak in Japan. Front. Vet. Sci. 8:763859. doi: 10.3389/fvets.2021.763859

INTRODUCTION

Leptospirosis is a common zoonotic disease caused by infection with the bacterium *Leptospira interrogans*, which has 24 serogroups and more than 250 known serovars (1–4). When infected with *L. interrogans*, animals may exhibit an acute course with symptoms such as jaundice, hemorrhage, and renal failure, or they might have few symptoms but continue shedding the bacteria (1–4). In some cases, animals shed the bacteria in their urine for several weeks to several years (2–4). Humans and dogs can be infected by direct or indirect contact with water and soil contaminated by the urine of wild rodents and other animals carrying the bacteria (2–4). In Japan, human infection with *L. interrogans* is categorized as a Class 4 infectious disease under the Act on the Prevention of Infectious Diseases and Medical Care for Patients with Infectious Diseases (the Infectious Diseases Control Law). In addition, the Act on Domestic Animal Infectious Diseases Control requires veterinarians to report dogs infected with *L. interrogans* serovars Pomona, Canicola, Icterohaemorrhagiae, Autumnalis, and Australis, *L. kirschneri* serovar Grippotyphosa, and *L. borgpetersenii* serovar Hardjo, as well as suspected cases. In October and November 2017, there was a series of notifications of suspected cases of canine leptospirosis based on the Act on Domestic Animal Infectious Diseases Control in Osaka Prefecture, Japan. An overview of these canine leptospirosis outbreak cases was previously reported (5). However, there have been few reports of community-acquired infections in dogs. Therefore, the aim of this study was to further analyze the outbreak and estimate the risk factors for infection.

METHODS

Cases Investigated

The study population included dogs with suspected canine leptospirosis and dogs that visited veterinary hospitals in the northern part of Osaka Prefecture from September to November 2017 for vaccinations or other symptoms not characteristic for leptospirosis, such as skin diseases. Medical records were retrospectively evaluated and reported suspected cases of canine leptospirosis were included for analysis. Obtained data included breed, sex, age, date of onset, symptoms, basis of diagnosis, prognosis, vaccination history, dog walking route, and outing history.

An observational study design was employed to evaluate factors associated with the suspected leptospirosis.

Statistical Analysis

The Shapiro–Wilk test was performed to evaluate the normality of the data. Logistic regression analysis was performed to evaluate the factors associated with suspected leptospirosis cases and breed, age, sex, vaccination history, type of vaccine, and history of walking along riverbeds. Stata/IC 16 (StataCorp LLC, College Station, Texas) was used for all analyses. For statistical inferences, two-sided hypothesis tests were used with a 5% significance level.

Microscopic Agglutination Test

Sera were obtained from six cases and were tested using the microscopic agglutination test (MAT) and a panel of seven reference serotypes, as indicated by the standard method described by the International Epizootic Office (OIE) Manual of Diagnostic Tests and Vaccines for Terrestrial Animals 2021 (6). Five serovars were used: *L. interrogans* serovars Canicola (*L*. Canicola), Australis (*L*. Austlasis), Copenhageni (*L*. Copenhageni), Autumnalis (*L*. Autaumnalis), and Hebdomadis (*L*. Hebdomadis). The antibody titers for *L. interrogans* serovar Copenhageni were considered as those for *L. interrogans* serovar Icterohaemorrhagiae (*L*. Icterohaemorrhagiae) because both of them belong to the same serogroup.

RESULTS

Statistical Analysis

Characteristics of the study population are presented in **Table 1**. The study included 19 dogs were reported by eight veterinarians in October to November 2017. Eleven dogs (case No. 4, 5, 7, 9, 10, 11, 12, 14, 16, 17, and 19) with suspected canine leptospirosis, another eight dogs (case No. 1, 2, 3, 6, 8, 13, 15, and 18) were included as a comparative group that were brought to the hospital for vaccination or other symptoms not characteristic for leptospirosis, such as skin diseases. Age ranged from 1 to 13 years, and seven Dogs were male and 12 Dogs were female. Of the 11 dogs suspected to be infected, five dogs were diagnosed as having leptospirosis based on clinical symptoms or clinical course (case No. 5, 7, 14, 16, and 17), four dogs were IgM antibody positive (case No. 9, 10, 11, and 12), and two had *Leptospira* spp. DNA detected in the blood (case No. 19) and urine (case No. 4) was analyzed by polymerase chain reaction (PCR). All six dogs that had been vaccinated with a combination of two or three *Leptospira* spp. antigens died (case No. 4, 5, 12, 14, 16, and 19), including 4 dogs that had been vaccinated within 1 year (case No. 4, 5, 14, and 19). Whereas, neither of two recovered cases had been vaccinated with *Leptospira s*pp. Antigens (case No. 7 and 11). Eight of the infected dogs lived in the same city (case No. 4, 5, 9, 11, 12, 16, 17, and 19) and four dogs lived within a 100-m radius of each other (case No. 9, 11, 12, and 17). In terms of outing history, seven of these eight dogs had been taken on walks along the same riverbed as their usual walking route (case No. 4, 5, 9, 11, 12, 16, and 19).

There were no significant associations of vaccination within 1 year, the presence of *Leptospira* spp. antigens in the vaccine, breed, age, or sex with the occurrence of suspected symptoms of leptospirosis. The odds of leptospirosis infection were 13.3 times higher in the dogs that had a history of being taken for walks along the riverbed than in the dogs not being walked along the riverbed ($p = 0.044$).

MAT

Antibody titers against *Leptospira s*pp. antigens in six cases are shown in **Table 2**. MAT was able to be performed on six cases in which the veterinarians cooperated in providing samples.

A titer of 1/100 is taken as a positive titer by the International Epizootic Office (OIE) Manual of Diagnostic Tests and Vaccines for Terrestrial Animals 2021 (6). The definitive diagnosis of infection was set at an antibody titers of 1:800 or higher (2, 11).

Notably, case No. 11 showed clinical signs of jaundice and hepatic failure, and the anti-*L*. Australis antibody titer was 1:10,240. Case No. 19 showed jaundice and renal failure, and the anti-*L*. Australis antibody titer was 1:2,560.

DISCUSSION

According to the Osaka Prefectural Livestock Hygiene Service Center, the number of canine leptospirosis cases reported in accordance with the law in Osaka Prefecture was five cases in 2014, five cases in 2015, and one case in 2016. The cases in the present study were considered to constitute an outbreak because the number of notifications was almost double that of previous years, with 11 cases reported within a month, from October 12 to November 10, 2017.

In dogs infected with *Leptospira* spp., bacteremia occurs within about 4 days of infection, and various clinical symptoms appear within about 7 days. After about 10 days of infection, antibody levels rise, and after about 2 weeks, the bacteria are excreted in the urine (4). Because the course of the disease depends on the antibody status of the individual (4), diagnoses in clinical cases should be made by selecting appropriate test methods, considering vaccination history and timing, and comprehensively evaluating clinical symptoms (2–4). In the present study, infection was confirmed in 7 cases by either MAT, PCR, or IgM antibody detection, but in three cases resulting in death due to acute progression, diagnosis was based on characteristic clinical symptoms. In another case, diagnosis was based on characteristic clinical symptoms and exclusion diagnosis.

TABLE 1 | Characteristics of the study population.

No.	Reported date	Breed	Age (years)/sex	Address[a]	Onset date	Symptoms Purpose of visit	Evidence of diagnosis	Prognosis Condition	Vaccination history[b] (year/month)	Walk to the riverbed	Death date	Visit date
1	–	Toy Poodle	4 y/F	4, K-cho, J-city	–	Panniculitis	–	Good	6 combination vaccine (2014)	Yes	–	9/22
2	–	Bichon Frise	1/M	2, K-town, J-city	–	Flea parasites	–	Good	5 combination vaccine (2017)	No	–	9/26
3	–	Shiba	6/F	4, K-town, J-city	–	Combination vaccination	–	Good	5 combination vaccine (2017)	Yes	–	9/26
4	10/16	Border Collie	3/F	1, K-town, J-city	9/Late	Jaundice, DIC	IgM (–) Urine PCR (+)	Death	8 Combination vaccine (2016)	Yes	Unknown	9/late
5	10/16	Border Collie	10/M	1, K-town, J-city	9/late	Jaundice, DIC	Clinical symptoms IgM (–) Urine PCR (–)	Death	8 Combination vaccine (2016)	Yes	Unknown	9/late
6	–	Shih Tzu	9/M	1, S-town, J-city	–	Dermatitis	–	Good	Unknown	No	–	10/3
7	10/18	German Shepherd	5/M	5, M-town, L-city	10/2	Jaundice, Hepatic failure Renal failure	Clinical symptoms Urine PCR (–)	Recovery	6 Combination vaccine (2017/5)	Yes	–	10/5
8	–	Papillon	1/F	3, K-town, J-city	–	Rabies vaccination	–	Good	6 Combination vaccine (2016)	No	–	10/6
9	10/15	Mongrel	4/F	1, N-town, J-city	10/8	Severe, Acute death	IgM (+)	Death	Unvaccinated	Yes	10/11	10/11
10	10/18	Bulldog	6/F	2, Q-town, P-city	10/8	Hepatic dysfunction	IgM (+) Urine PCR (–)	Death	Unvaccinated	No	Unknown	10/12
11	10/12	Mongrel	5/F	1, N-town, J-city	10/9	Jaundice, Hepatic failure	IgM (+) Urine PCR (–)	Recovery	5 Combination vaccine (2016/9)	Yes	–	10/11
12	10/19	Mongrel	13/F	1, N-town, J-city	10/10	Pyrexia, Jaundice, Renal failure	IgM (+)	Death	9 Combination vaccine (2015/12)	Yes	Unknown	10/13
13	–	Shiba	4/F	3, K-town, J-city	–	Rabies vaccination	–	Good	Unvaccinated	Unknown	–	10/14

(Continued)

TABLE 1 | Continued

No.	Reported date	Breed	Age (years)/sex	Address[a]	Onset date	Symptoms Purpose of visit	Evidence of diagnosis	Prognosis Condition	Vaccination history[b] (year/month)	Walk to the riverbed	Death date	Visit date
14	11/10	Miniature Schnauzer	8/M	2, S-town, T-ward, R-city	10/15	Severe, Acute death	Clinical progress	Death	8 Combination vaccine (2016/7)	Unknown	10/18	10/18
15	–	Miniature Dachshund	5/F	3, K-town, J-city	–	Combination vaccination	–	Good	6 Combination vaccine (2017)	No	–	10/18
16	10/29	Toy Poodle	10/M	1, K-town, J-city	10/18	Jaundice, Renal failure	Clinical symptoms Urine/Blood PCR (–)	Death	9 combination vaccine (2015/5)	Yes	10/23	10/20
17	10/26	Miniature Schnauzer	8/M	1, N-town, J-city	10/22	Hepatic failure Renal failure, thrombopenia	Clinical symptoms	Death	Unvaccinated	Unknown	10/23	10/23
18	–	Mongrel	11/F	1, N-town, J-city	-	Home visit (cohabitation dog)	–	Good	5 combination vaccine (2013)	Yes	–	10/23
19	11/9	Mix	11/F	1, R-town, J-city	11/1	Jaundice, Renal failure	Urine PCR (–) Blood PCR (+)	Death	9 combination vaccine (2016/9)	Yes	11/4	11/1

[a] *City and town names are not shown for privacy and anonymity.*

[b] *5 and 6 combination vaccines: did not contain Leptospira spp. antigens; 8 combination vaccine: including serovar Icterohaemorrhagiae and serovar Canicola antigens; 9 combination vaccine: including serovar Copenhageni, serovar Canicola, and serovar Hebdomadis antigens.*

DIC, disseminate intravascular coagulation; F, female; M, male; PCR, polymerase chain reaction.

TABLE 2 | Antibody titers against *Leptospira* spp. antigens in six dogs (Microscopic agglutination test).

No.	Antigens				
	L.c	**L.i**	**L.h**	**L.at**	**L.as**
11	<1:10	1:160	<1:10	<1:10	1:10,240
12	<1:10	1:40	<1:10	<1:10	<1:10
14	<1:10	1:320	<1:10	<1:10	<1:10
16	<1:10	1:40	<1:10	1:20	1:20
17	<1:10	<1:10	<1:10	<1:10	<1:10
19	<1;10	1:80	1:20	1:80	1:2,560

L.c, L.Canicola; L.i, L.Icterohaemorrhagiae; L.h, L.Hebdomadis; L.at, L.Autumnalis; L.as, L.Australis.

In diagnosis by MAT, paired sera are used immediately after and 10 to 14 days after disease onset, and if the antibody titer increases more than 4-fold, infection with the suspected serovar is diagnosed (2–4). However, in many cases in the present study, progress was acute and paired sera collection was difficult, so the diagnosis was made using a single serum sample. Many cases of acute leptospirosis die within 2–4 days after disease onset, before IgG antibodies rise (2–4), and diagnosis by MAT is limited. Because there is no canine vaccine containing *L.* Australis antigens that is currently sold or used in Japan, the high antibody titers of *L.* Australis in cases No. 11 and No. 19 might indicate infection with this serovar. In a single sample, it was assumed that a high MAT titer (≥800), accompanied by clinical signs of leptospirosis, is highly suggestive of active infection (2, 11). Even in the cases where the serovar could not be identified, *Leptospira* spp. DNA was detected in the urine of case No. 4, and IgM antibody was positive in cases No. 9, 10, 11, and 12. Although PCR is a useful method for proving the presence of trace amounts of bacteria in blood, urine, and tissues, it cannot identify serovars. In an experimental case of *L.* Canicola infection, *Leptospira* spp. DNA was detected in the blood by PCR on the fourth day after infection, but not thereafter; however, it was detected in the urine after 8 days (7). Also, treatment with antibacterial agents might return a false-negative result (4). The IgM antibody test can detect antibodies against *L.* Canicola, *L.* Autaumnalis, *L.* Australis, *L.* Icterohaemorrhagiae, and *L.* Hebdomadis, but, similar to PCR, it cannot identify serovars. It is suitable as a test in the early stage of infection because IgM antibodies increase within about 3–7 days after infection before decreasing (2–4). Of the 4 dogs that tested positive for IgM antibodies, cases No. 9, 11 and 12 lived in the same town and developed the disease over 3 days from October 8 to 10. This finding suggests that they might have been infected at about the same time by the same source. Of the 11 dogs with suspected infection, eight dogs lived in the same city and neighboring cities. Furthermore, seven of these eight dogs were taken on walks along the same riverbed as their usual walking route, and epidemiological analysis indicated that they were infected at this site. Recently, there has been an increase in the number of feral raccoons (*Procyon lotor*) in Japan because of abandonment of pet raccoons imported to Japan from North America (8). These animals have been implicated as a source of zoonotic pathogens, including *Leptospira* spp. (9). Raccoons living in the vicinity of the outbreak area are also known to have high antibody titers against *Leptospira* spp. (10) and are considered a possible source of infection. There have been few reports of outbreaks of infectious diseases in household dogs. Often the number of cases is also small, so conducting epidemiological studies is difficult. In the present study, factors associated with an outbreak of canine leptospirosis were evaluated.

L. Hebdomadis has been documented as the most common cause of canine leptospirosis in Japan, accounting for 53.3% of all reported cases (11). Although vaccination is reported to be effective in preventing onset and reducing the severity of canine leptospirosis (12), effectiveness is considered serovar-specific (13). Currently, the *Leptospira* spp. canine vaccine available in Japan contains only *L.* Canicola, *L.* Icterohaemorrhagiae, *L.* Hebdomadis, *L. interrogans* serovars Pomona and *L. kirschneri* serovar Grippotyphosa antigens, and does not contain the antigens of *L.* Australis detected in the present study. This might explain why some dogs died in this outbreak despite being vaccinated against *Leptospira* spp. There are known to be regional differences in the detected serovars (3, 14, 15). Because *L.* Australis has been reported to be the second-highest detected serovar (20.3%) after *L.* Hebdomadis in dogs in Japan (14), it is necessary to develop a vaccine containing antigens of this serovar. It is also desirable to develop vaccines in other countries and regions according to the outbreak situation.

Limitation of Study

Because this was a field survey of spontaneous cases, the number of cases was small and most of the dogs were not available for a long term follow up, some of the dogs died during the study period due to the illness. In addition, we were not able to obtain the complete information on the cases we evaluated.

DATA AVAILABILITY STATEMENT

The original contributions presented in the study are included in the article/supplementary material, further inquiries can be directed to the corresponding author.

AUTHOR CONTRIBUTIONS

JS was involved in the study design and data interpretation. AT was involved in the data analysis. Both authors critically revised the report, commented on drafts of the manuscript, and approved the final report.

ACKNOWLEDGMENTS

We would like to express our deepest gratitude to the Animal Protection and Livestock Division, Osaka Prefecture and to the veterinarians who cooperated in the interviews and in the epidemiological survey. We also thank Kyoto Biken Laboratories, Inc. for their cooperation in the testing.

REFERENCES

1. Levett PN. Leptospirosis. *Clin Microbiol Rev*. (2011) 14:296–326. doi: 10.1128/CMR.14.2.296-326.2001
2. Sykes JE, Hatmann K, Lunn KF, Moore GE, Stoddard RA, Goldstein RE. 2010 ACVIM small animal consensus statement on leptospirosis: diagnosis, epidemiology, treatment, and prevention. *J Vet Int Med*. (2011) 25:1–13. doi: 10.1111/j.1939-1676.2010.0654.x
3. Schuller S, Francey T, Hartmann K, Hugonnard M, Kohn B, Nally JE, et al. European consensus statement on leptospirosis in dogs and cats. *J Small Anim Pract*. (2015) 56:159–79. doi: 10.1111/jsap.12328
4. Green CE, Skyes JE, Moore GE, Goldstein RE, Schultz RD. Leptospirosis. In: Green CE, editor. *Infectious Diseases of the Dog and Cat*. 4th ed. Toronto, ON: Elsevier Inc. (2012). p. 431–47.
5. Saeki J, Kitahara C. Canine leptospirosis outbreak in Osaka. *J JpnVet Med Assoc*. (2019) 72:167–71. doi: 10.12935/jvma.72.167
6. International Epizootic Office Manual of Diagnostic Tests and Vaccines for Terrestrial Animalsd. *Chapter 3.1.12 Leptospirosis*. Paris: OIE (2021).
7. Branger C, Blanchard B, Fillonneau C, Suard I, Aviat F, Chevallier B, et al. Polymerase chain reaction assay specific for pathogenic Leptospira based on the gene hap1 encoding the hemolysis-associated protein-1. *FEMS Microbiol Lett*. (2005) 243:437–45. doi: 10.1016/j.femsle.2005.01.007
8. Ikeda T, Asano M, Matoba Y, Abe G. Present status of invasive alien raccoon and its impact in Japan. *Glob Environ Res*. (2004) 8:125–31.
9. Prescott J. Canine leptospirosis in Canada: a veterinarian's perspective. *Can Med Assoc J*. (2008) 178:397–8. doi: 10.1503/cmaj.071092
10. Saeki J, Nakanishi H, Masubuchi K, Matsubayashi M, Furuya M, Tani H, et al. A serological survey of *Leptospira* spp., antibodies in wild raccoons (*Procyon lotor*) in Osaka, Japan. Asian *J Anim Vet Adv*. (2016) 11:258–62. doi: 10.3923/ajava.2016.258.262
11. Koizumi N, Mizutani M, Akachi S, Okano S, Yamamoto S, Horikawa K, et al. Molecular and serological investigation of Leptospira and leptospirosis in dogs in Japan. *J Med Microbiol*. (2013) 62:630–6. doi: 10.1099/jmm.0.050039-0
12. Andre-Fontaine G, Triger L. MAT cross-reactions or vaccine cross-protection: retrospective study of 863 leptospirosis canine cases. *Heliyon*. (2018) 4:e00869. doi: 10.1016/j.heliyon.2018.e00869
13. Koizumi N, Watanabe H. Leptospirosis vaccines: past, present, and future. *J Postgrad Med*. (2005) 51:210–4.
14. Akuzawa M, Oishi A, Fushuku S, Deguchi E, Misumi K, Sakamoto H, et al. Survey of the Leptospira antibody from dogs in 6 regions of Japan. *J Jpn Vet Med Assoc*. (1999) 52:780–3. doi: 10.12935/jvma1951.52.780
15. Takeda M, Konishi M, Shiono M, Iida Y, Nagata H, Katsura S, et al. Prevalence of Leptospira antibodies among stray dogs in Osaka, Japan. *J Jpn Vet Med Assoc*. (2004) 57:809–12. doi: 10.12935/jvma1951.57.809

Conflict of Interest: The authors declare that the research was conducted in the absence of any commercial or financial relationships that could be construed as a potential conflict of interest.

Publisher's Note: All claims expressed in this article are solely those of the authors and do not necessarily represent those of their affiliated organizations, or those of the publisher, the editors and the reviewers. Any product that may be evaluated in this article, or claim that may be made by its manufacturer, is not guaranteed or endorsed by the publisher.

frontiers in Veterinary Science

ORIGINAL RESEARCH
published: 12 January 2022
doi: 10.3389/fvets.2021.715307

Experimental Susceptibility of North American Raccoons (*Procyon lotor*) and Striped Skunks (*Mephitis mephitis*) to SARS-CoV-2

Raquel Francisco[1,2]*, *Sonia M. Hernandez*[1,2]*, *Daniel G. Mead*[2], *Kayla G. Adcock*[2], *Sydney C. Burke*[1,2], *Nicole M. Nemeth*[2,3] and *Michael J. Yabsley*[1,2]

[1] Warnell School of Forestry and Natural Resources, University of Georgia, Athens, GA, United States, [2] Southeastern Cooperative Wildlife Disease Study, Department of Population Health, College of Veterinary Medicine, University of Georgia, Athens, GA, United States, [3] Department of Pathology, College of Veterinary Medicine, University of Georgia, Athens, GA, United States

OPEN ACCESS

Edited by:
Lester J. Perez,
University of Illinois at Urbana–Champaign, United States

Reviewed by:
Brianna R. Beechler,
Oregon State University, United States
Conrad Martin Freuling,
Friedrich-Loeffler-Institute, Germany

***Correspondence:**
Raquel Francisco
raquel.francisco@uga.edu
Sonia M. Hernandez
shernz@uga.edu

Specialty section:
This article was submitted to Veterinary Epidemiology and Economics, a section of the journal Frontiers in Veterinary Science

Received: 26 May 2021
Accepted: 20 December 2021
Published: 12 January 2022

Citation:
Francisco R, Hernandez SM, Mead DG, Adcock KG, Burke SC, Nemeth NM and Yabsley MJ (2022) Experimental Susceptibility of North American Raccoons (Procyon lotor) and Striped Skunks (Mephitis mephitis) to SARS-CoV-2. Front. Vet. Sci. 8:715307. doi: 10.3389/fvets.2021.715307

Recent spillback events of SARS-CoV-2 from humans to animals has raised concerns about it becoming endemic in wildlife. A sylvatic cycle of SARS-CoV-2 could present multiple opportunities for repeated spillback into human populations and other susceptible wildlife. Based on their taxonomy and natural history, two native North American wildlife species —the striped skunk (*Mephitis mephitis*) and the raccoon (*Procyon lotor*) —represent a high likelihood of susceptibility and ecological opportunity of becoming infected with SARS-CoV-2. Eight skunks and raccoons were each intranasally inoculated with one of two doses of the virus (10^3 PFU and 10^5 PFU) and housed in pairs. To evaluate direct transmission, a naïve animal was added to each inoculated pair 48 h post-inoculation. Four control animals of each species were handled like the experimental groups. At predetermined intervals, we collected nasal and rectal swabs to quantify virus shed via virus isolation and detect viral RNA via rRT-PCR and blood for serum neutralization. Lastly, animals were euthanized at staggered intervals to describe disease progression through histopathology and immunohistochemistry. No animals developed clinical disease. All intranasally inoculated animals seroconverted, suggesting both species are susceptible to SARS-CoV-2 infection. The highest titers in skunks and raccoons were 1:128 and 1:64, respectively. Low quantities of virus were isolated from 2/8 inoculated skunks for up to day 5 post-inoculation, however no virus was isolated from inoculated raccoons or direct contacts of either species. Neither species had gross lesions, but recovering mild chronic pneumonia consistent with viral insult was recorded histologically in 5/8 inoculated skunks. Unlike another SARS-CoV-2 infection trial in these species, we detected neutralizing antibodies in inoculated raccoons; thus, future wildlife serologic surveillance results must be interpreted with caution. Due to the inability to isolate virus from raccoons, the lack of evidence of direct transmission between both species, and low amount of virus shed by skunks, it seems unlikely

for SARS-CoV-2 to become established in raccoon and skunk populations and for virus to spillback into humans. Continued outbreaks in non-domestic species, wild and captive, highlight that additional research on the susceptibility of SARS-CoV-2 in wildlife, especially musteloidea, and of conservation concern, is needed.

Keywords: SARS-CoV-2, COVID-19, raccoons, skunks, Mephitidae, zoonoses, wildlife, One Health

INTRODUCTION

As severe acute respiratory syndrome coronavirus 2 (SARS-CoV-2) continues to circulate on a global scale, the need to identify potential animal reservoirs, especially among wildlife, has become a priority, spurring surveillance and susceptibility trials of numerous species (1–15). Indeed, the COVID-19 pandemic has highlighted the need for a global One Health approach to address its solution (16). Wildlife health assessments, pathogen surveillance, and experimental trials are intrinsic components of this approach which have been neglected until recent decades, but have been integral in understanding the epidemiology of other recent pandemics such as severe acute respiratory syndrome (SARS) and middle eastern respiratory syndrome (MERS) (17–19).

Ongoing spillover events from humans to pets (e.g., dogs and cats), commercial animals (e.g., mink), and captive wildlife (e.g., tigers, gorillas) have raised concerns about the ability of SARS-CoV-2 to become endemic in abundant native wildlife species (20–22). A sylvatic cycle of SARS-CoV-2 could present multiple opportunities for repeated spillback into human populations and susceptible wildlife species. While the role of free-living wildlife in the emergence of SARS-CoV-2 remains unclear, the susceptibility and potential of a wildlife species as a reservoir could hold substantiable implications, not just for public health, but for the management, research, rehabilitation, and conservation of other susceptible animal species (23). In North America, several members of the Musteloidea (Mustelidae, Mephitidae, and Procyonidae) families are both taxonomically and ecologically relevant and likely have a high probability of becoming exposed to, infected with, and developing clinical disease to SARS-CoV-2 (24–28). In fact, ferrets (*Mustela putorius furo*), close relatives to North American Musteloidea, are well-established animal models for SARS (29–32) and are highly susceptible to SARS-CoV-2 (8–10, 33–38). Another close relative, mink (*Neovison vison*), is also highly susceptible to SARS-CoV-2 in experimental inoculations trials, as well as natural infections in commercial farms (5, 39–43). Most recently, Asian small-clawed otters (*Aonyx cinereus*) in a zoological institution were infected with SARS-CoV-2 (44). Like ferrets, both mink and otters experienced varying levels of respiratory disease upon infection with SARS-CoV-2. Unlike ferrets, both species were first found to be susceptible after transmission from an infected human caretaker, highlighting the anthropozoonotic potential of this virus (45).

Two Musteloidea, striped skunks (*Mephitis mephitis,* Mephitidae) and raccoons (*Procyon lotor,* Procyonidae), range throughout much of North America, and are abundant, opportunistic, omnivorous generalists (46). Raccoons are also well established in regions of Europe and Asia (47). Both species have become habituated to seek food and shelter near human homes, resulting in frequent interactions with domestic animals, humans, and their waste. **Figure 1** depicts several hypothetical pathways from which SAR-CoV-2 can be transmitted from humans, both directly and indirectly, to species that have ample ecological opportunity, such as raccoons and skunks, justifying their importance as potential reservoirs. Skunks and raccoons are already notorious reservoirs of viruses that have substantial impacts on other wildlife and humans (i.e., rabies virus, canine distemper virus, protoparvoviruses) (48, 49). To determine their role in the epidemiology of SARS-CoV-2, this study evaluated the susceptibility to infection, seroconversion, transmission potential between conspecifics, tissue tropism, and pathology associated with SARS-CoV-2 in striped skunks and raccoons.

METHODS

Animals and Husbandry

Sixteen juvenile (∼10 week old), equal numbers of both sexes, captive-bred raccoons and skunks were obtained from a commercial, captive breeding animal facility in June and July 2020, respectively. Animals were either housed at the University of Georgia either in a Biosafety Level 2 (BSL-2) facility (control skunks) or in the Animal Health Research Center (AHRC; experimentally inoculated animals of both species and control raccoons) which is a high-security biocontainment facility. All of the experimental infection work was conducted under Biosafety Level 3 (BSL-3) protocols. All procedures involving the handling of animals and the SARS-CoV-2 virus were reviewed and approved by the University of Georgia's IACUC committee (A2020 04-016) and Office of Biosafety (2020 0048).

Animals were housed at ∼21°C and 50% humidity. Both species were fed daily with commercially available omnivore diet (Mazuri® Omnivore Diet, Purina Mills, LLC., USA) and offered water *ad libitum*. The diet was supplemented by various fresh greens and protein items such as boiled eggs. Animals were identified by purposely shaved patches of fur either on the left, right, or center of their rump. Prior to inoculations, nasal swabs, rectal swabs, and blood samples were collected and tested by microtitration serum neutralization (SN) and virus isolation (VI) to ensure animals were not currently or previously infected with SARS-CoV-2.

Experimental Design

Experimental animals ($n = 12$), excluding the control animals ($n = 4$) who were housed separately, were separated into 2

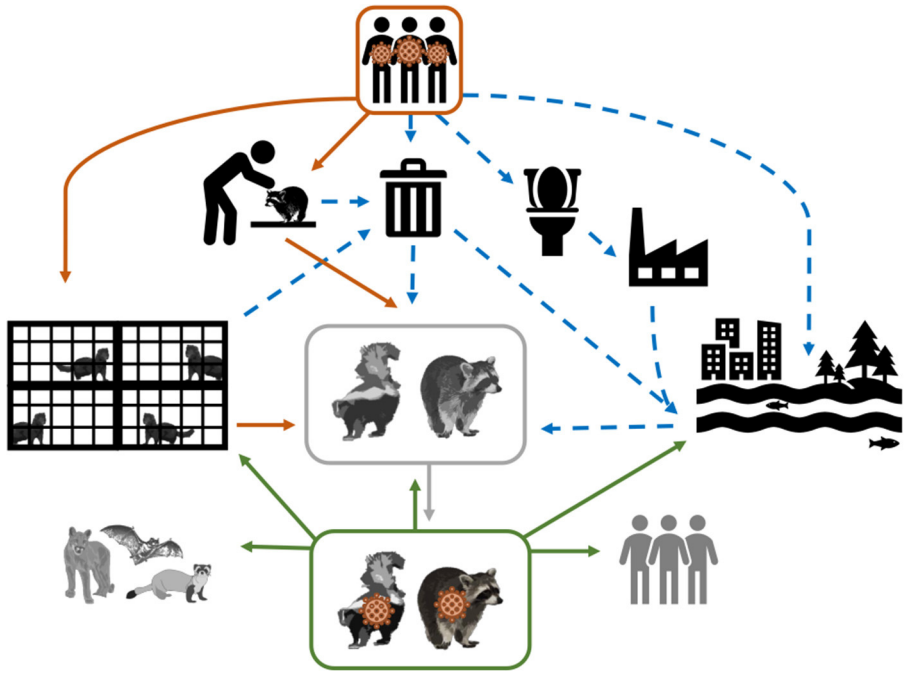

FIGURE 1 | Conceptual model of the mechanisms of SARS-CoV-2 transmission from infected humans (direct transmission = solid orange arrows; and indirect transmission = dashed blue arrows) to susceptible wildlife (represented in greyscale). As depicted, SARS-CoV-2 shed by humans can be directly transmitted through activities that require handling and close contact (e.g., research and wildlife rehabilitation), or commercial operations (e.g., fur farms); however virus shed by humans could make its way into the environment via garbage (i.e., medical waste and household waste) and sewage. The solid gray arrow represents the establishment of SARS-CoV-2 in a wildlife species. The hypothesized spillback from this SARS-CoV-2 wildlife reservoir to susceptible human populations and other wildlife species is demonstrated by the solid green arrows.

identical dosing groups with equal sexes per group. Each dose group consisted of four animals housed in pairs in two adjacent stainless-steel wire mesh cages (~1.5 x 1.5 x 2m). The high (H) and low (L) dose animals were intranasally inoculated with 10^3 PFU and 10^5 PFU of SARS-CoV-2 ($n = 4$ per dose, per species), respectively. The 10^5 PFU dose has produced infections in ferrets and other species (9, 10). The 10^3 PFU dose was used to mimic the amount of virus to which these species may be naturally exposed (e.g., through consuming human garbage or potentially animal-to-animal) and has also resulted in infections and clinical disease in ferrets (31, 37). Each animal was identified by a unique combination of numbers and letters that corresponded with their dosage group, their enclosure number, and the side where a section of their fur was shaved (i.e., raccoon H1L equated to high-dose raccoon from group 1 that shaved on the left side). All four experimental dose groups were housed in the same BSL-3 Agriculture (BSL-3Ag) room but were separated by approximately 6 meters and the directional air flow in the room flowed from the low to the high dose group (**Supplementary Figure 1**). The design of the BSL-3Ag facility does not allow for recirculated air, facilitating 13 to 15 air changes per hour, thus the likelihood of aerosol transmission between each group is negligible. To test for direct contact transmission, a single naïve conspecific was introduced to each pair of directly inoculated animals 48 h after inoculation. Control animals ($n = 4$) were housed in either a separate BSL-3Ag room (raccoons) or BSL-2 facility (skunks).

Virus and Inoculations

The SARS-CoV-2 isolate used was USA-WA1/2020 which was originally isolated from a middle-aged male in Washington, USA who traveled to Wuhan China in January 2020. Skunks and raccoons were inoculated with 5th passage virus. The virus was grown in vero-E6 cells (American Type Cell Culture [ATCC] Cat# CRL-1586, RRID:CVCL_0574) which were maintained in minimal essential medium (MEM, 5 L deionized water, 48 g of Minimal Essential Media Eagle (Sigma-Aldrich, Co., USA), 11.11 g bicarbonate) supplemented with 50 mL/L of iron fortified calf serum (Sigma-Aldrich, Co.) and 20 mL/L of Antibiotic Antimycotic Solution (10,000 units penicillin, 10 mg streptomycin, 25 μg amphotericin per mL). All cultures and microtitrations were incubated in a 5% CO_2 atmosphere and 37°C.

For procedures, such as inoculation and venipuncture, raccoons and skunks were anesthetized with a combination of dexmedetomidine (0.04 mg/kg) (Dexdomitor™, Orion Corporation, Finland) and butorphanol (0.2 mg/kg) (Torbugesic™, Zoetis Manufacturing and Research, Spain), intramuscularly (IM), and reversed with atipamezole (0.25

mg/kg) (Revertindine™, Modern Veterinary Therapeutics, Germany) and naloxone (0.02 mg/kg) (Wintac Limited, India) given IM to return them to pre-anesthetic function as rapidly as possible.

The intranasal inoculations were performed on anesthetized animals using a 21-gauge catheter attached to a 1 mL luer slip syringe (BD Syringe, Becton, Dickinson and Company, USA). Experimental animals that were intranasally inoculated with live virus ($n = 8$) will be referred to as the directly inoculated (DI) animals or groups. A single direct contact (DC) animal was introduced to each pair of DI animals 48 h post-inoculation to evaluate direct transmission.

Sampling

Animal health status (i.e., mentation, attitude, physical appearance, consumption of food) was evaluated twice daily. All animals were weighed at admission, and additional body weights were recorded for all animals on the days when they were fully anesthetized for venipuncture. Rectal temperatures were collected from all animals when anesthetized for venipuncture, normothermic was considered 37.2 to 39.2°C (99.0 to 102.5°F) for both species (50, 51). To collect serum, 2 mL of blood was drawn from the jugular vein and added to plain sterile vacutainer tubes (3 mL; Covidien™, USA).

For the collection of nasal and rectal swabs, animals were physically restrained and sedated with 30–45 mg/kg trazodone PO (Cadila Healthcare Ltd., India) suspended in either water or equal parts of ORA-Plus® Oral suspending vehicle and ORA-Sweet® (Perrigo, USA) in a syringe. The blood and swab collection scheme for both species is summarized in **Figure 2**. To evaluate environmental transmission, swabs of food and water bowls were obtained each sampling period prior to any animals being handled. Swabs and blood samples were also collected for all animals when euthanized.

Nasal swabs were obtained by swabbing both sides of the nasal passage using a single sterile polyester swab (Puritan, USA). Rectal swabs were obtained using sterile cotton swabs (Medline Industries, Inc., China). All swabs were placed in 1.5 mL cryovials (SealRite®) with 1 mL of Dulbecco's sterile phosphate-buffered saline (dPBS) (Sigma-Aldrich, Co.) for raccoons and 1 mL of sterile virus isolation medium composed of MEM for skunks. The blood samples and swabs were maintained in an insulated container with frozen gel packs until stored, and the whole blood was centrifuged within 1 h for the collection of serum. All swabs and serum were then stored at−80°C until processed.

Animals were anesthetized, euthanized, and necropsied at predetermined intervals to maximize the chance of detecting histopathologic changes during the course of infection. All animals were sampled as described above after humane euthanasia. Animals were anesthetized with dexmedetomidine (0.04 mg/kg) (Dexdomitor™), butorphanol (0.2 mg/kg) (Torbugesic™), and ketamine (5 mg/kg) (Zetamine™, OneVet, USA), and euthanized with an intracardiac dose of sodium pentobarbital (0.25 mL/kg) (Euthanasia Solution, Med-Pharmex Inc., USA). All animals were necropsied the day of euthanasia. Raccoons were euthanized on 9 dpi ($n = 5$; two DI from each dose group, and a control), on 11 dpi ($n = 3$; one DC one from each dose group, one control). The remaining experimental and control raccoons were euthanized and necropsied on 17 and 18 dpi, respectively. The experimental infection trials were performed first on raccoons. Due to the unremarkable nature of the raccoon gross necropsies, the necropsy interval was changed for skunk infection trials. Necropsies were performed earlier to capture early and subtle pathologic lesions such that skunks were euthanized on 4 dpi, ($n = 3$; two DI from each dose group, and a control), and on 8 dpi, ($n = 4$; two DI and two DC from each dose group) similar to Schlottau et al. and Freuling et al. (9, 52). A control skunk was euthanized on 7 dpi for comparison. The remaining control and experimental skunks were euthanized and necropsied on 14 and 15 dpi, respectively (**Figure 2**).

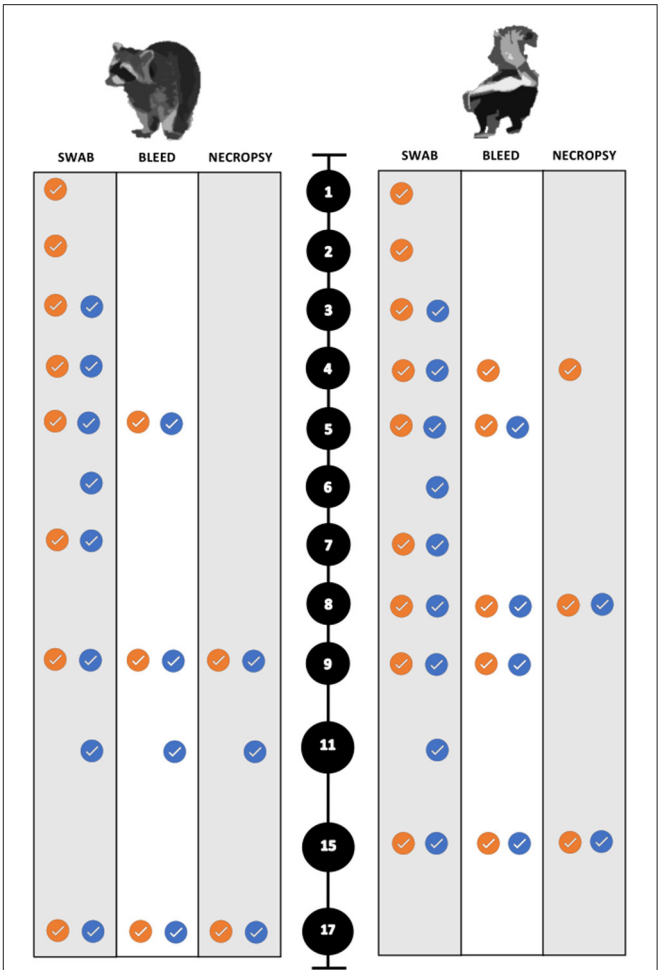

FIGURE 2 | Sampling scheme and timing for the experimental SARS-CoV-2 infection trials of both raccoons and striped skunks. The black circles represent days post inoculation (dpi). The orange circles indicate directly inoculated (DI) animals. The blue circles indicate the direct contact (DC) animals.

Sample Analysis

Virus Isolation and Molecular Testing

Swab samples were placed in individual microcentrifuge tubes containing 1 mL of viral media, vortexed, and then centrifuged

at 10,000 rpm for 10 min. Supernatant (100 μL) from each tube was inoculated into a separate well on a 12-well plate seeded with 3-to-4-day old Vero E6 cell culture monolayers. The plates were observed daily for cytopathic effect (CPE) for 10 days. If CPE was evident, the cell culture supernatant was collected and tested for the presence of SARS-CoV-2. Viral RNA (vRNA) was extracted from positive samples using the QIAamp Viral RNA Mini Kit (Qiagen Inc.), following the manufacturer's protocol. A validated real-time reverse transcription PCR (rRT-PCR) protocol was used for detection of SARS-CoV-2 (53, 54). Reactions were conducted on a Step OnePlus Real-Time PCR System (Applied Biosystems, Inc.).

The same rRT-PCR protocol was used as described above to evaluate tissues and nasal, fecal, and environmental swab samples for the presence of SARS-CoV-2 RNA. A positive rRT-PCR result was defined as the detection of both the N1 and N2 genes. Both the N1 and N2 primer/probe had to have a cycle threshold (Ct) of ≤ 35 to be considered positive for the presence of SARS-CoV-2 RNA. Samples evaluated that resulted in a Ct of >35 for both probes were considered negative and samples with a Ct of ≤35 for one probe and a Ct of >35 for the other probe were also considered negative as reported in Shriner et al. (41). Viral stock with a titer of 10^5 pfu/200 ul was used as a positive control.

Skunk tissues (nasal conchae, tracheobronchial lymph node, tonsil, mid-length trachea, right middle lobe lung, heart, kidney, and jejunum) and select raccoon tissues (tracheobronchial lymph node, tonsil, right middle lobe lung) samples were homogenized with gentleMACS™ C Tubes (Miltenyi Biotec Inc., Germany) using a gentleMACS™ Dissociator (Miltenyi Biotec Inc.). Tubes were then centrifuged at 3,220 rpm for 10 min at 22°C. Then, 100 μL of supernatant from each tube was inoculated into a separate well on a 12-well plate seeded with 3-to-4-day old Vero E6 cell culture monolayers. CPE was determined as discussed above. An additional 140 μL of supernatant from each tube was collected and tested for the presence of SARS-CoV-2 using the extraction protocol and rRT-PCR protocol listed above.

Plaque Assays to Quantify Virus

Cell culture supernatant (200 μL) from samples that were positive for SARS-CoV-2 via VI and rRT-PCR was diluted 10-fold (with the first well containing no dilution) for a series of 5 dilutions (10^{-1}, 10^{-2}, 10^{-3}, 10^{-4}, 10^{-5}), inoculated into a 6-well plate previously seeded with 4-day old Vero E6 cell culture monolayers, and incubated at 37°C and 5% CO_2 for 1 h. Each well was then overlaid with 4 mL of a gum tragacanth overlay solution (equal parts 2% gum tragacanth & 2XMEM, supplemented with 2 mL of Fetal Bovine Serum (FBS), 5 mL of Antibiotic Antimycotic Solution) and allowed to incubate as described above for 7 to 10 days. Once plaques were noted grossly, each cell culture was inactivated with 10% formalin and crystal violet solution and allowed to fix for 24 to 48 h. Once cells were fixed, SARS-CoV-2 titers ($\log_{10}$ PFU/mL) were evaluated in wells for which more than one plaque was present; no plaques were seen past 10^{-3} dilution on any sample. As previously determined, a ½ log is lost for each freeze thaw cycle, and all vials had been through 2 cycles, presumptively decreasing titers by 1 log (D.G. Mead and E.R. Lafortaine, unpublished data).

Microtitration Serum Neutralization

SARS-CoV-2 neutralizing antibodies were detected and quantified using serum microneutralization. Serum samples were heat-inactivated at 56°C for 30 min. Then, samples were 2-fold serially diluted in duplicates from 1:4 to 1:256 and incubated at 37°C and 5% CO_2 with 100 $TCID_{50}$ of the same strain of virus used in the inoculum in 96-well plates for 1 h. The wells were then overlaid with 150 μL of Vero E6 cells. The plates were incubated as described above and observed for CPE daily for 7 to 10 days, after which sample neutralization endpoint titers were determined.

Necropsy, Histology, and Immunohistochemistry

All inoculated and control animals were necropsied within 2 h of euthanasia. Approximately 0.5 cm^3 samples of nasal conchae, tracheobronchial lymph node, tonsil, mid-length trachea, right middle lobe lung, heart, kidney, and jejunum were placed in cryovials and stored at −80°C for subsequent laboratory analyses. Additional samples collected into 10% neutral buffered formalin for histopathologic evaluation included nasal sinus, trachea, left cranial and caudal lung lobes, right cranial and middle lung lobes, bronchus, lymph nodes (tracheobronchial, retropharyngeal, prescapular, and mesenteric), tonsil, tongue, esophagus, duodenum, jejunum, ileum, stomach, large intestine, left lateral liver lobe, gall bladder, pancreas, spleen, heart, kidney, thymus, thyroid gland, adrenal gland, gonad, skeletal muscle (biceps), urinary bladder, bone marrow, cerebrum, cerebellum, brainstem, and eye.

Once fixed, nasal sinus tissues were transferred to 12.5% neutral EDTA solution (250 g EDTA disodium salt (J.T. Baker Inc. USA), 1,750 mL distilled water, and 25 g sodium hydroxide) where they were allowed to decalcify for 14 to 21 days. Fixed tissues were routinely processed, embedded in paraffin wax, and 4 μm thick sections were stained with hematoxylin and eosin (HE). Duplicate slides with deep nasal sinus, mid-trachea, left cranial lung lobe, bronchus, tracheobronchial and prescapular lymph nodes, tonsil, and jejunum for all raccoons inoculated with low and high SARS-CoV-2 doses also underwent immunohistochemistry (IHC) for SARS-CoV-2 antigen. These same tissues, in addition to frontal nasal sinus, left caudal lung lobe, right cranial lung lobe, retropharyngeal lymph node, kidney and heart also underwent IHC for all skunks inoculated with low and high doses, as well as the two high dose direct contact skunks.

IHC was performed on an automated stainer (IntelliPATH, Biocare Medical, USA). A rabbit polyclonal antibody for SARS-CoV-2 (ThermoFisher, PA141098) at a dilution of 1:100 for 60 min was used. Antigen retrieval on tissue sections was achieved using Citrate Solution 10X (BioGenex, Fremont, USA) at a 1:10 dilution 10 for 15 min at 110°C. A biotinylated goat anti-rabbit antibody at a 1:100 dilution (Vector Laboratories, USA) was utilized to detect the target, and immunoreaction was visualized using Warp Red Chromogen (Biocare Medical) for 10 min and counterstained with hematoxylin. A cell pellet with

TABLE 1 | SARS-CoV-2 virus isolation data for two striped skunks (*Mephitis mephitis*) that shed virus after intranasal inoculation.

ID	Contact	Days post inoculation (dpi)				
Skunks*		**1**	**2**	**3**	**4**	**5**
H1-L	Directly inoculated	2	3.2			
H2-R	Directly inoculated			2.8	3.3	**0

*Values presented in plaque forming units (log_{10}/mL). *Both H1-L and H2-R were inoculated with a high dose [10^5 plaque forming units (PFU)] of SARS-CoV-2. No animals were found to shed virus after 5 dpi. **The culture for H2-R developed cytopathic effect (CPE) on 5 dpi, however, no plaques were seen after staining.*

infected cells was used as a positive control. All histology and immunohistochemistry were performed at the Athens Veterinary Diagnostic Laboratory at the University of Georgia and slides were read blindly by a board-certified veterinary pathologist.

RESULTS

None of the experimental animals of either species developed a fever (e.g., rectal temperature $>$ 39.2°C), lost weight, changed behavior or displayed any signs of clinical disease throughout the study. Viral shedding was only detected on nasal swabs by virus isolation from two high dose DI skunks (H2R on 3, 4, and 5 dpi and H1L on 1 and 2 dpi) (**Table 1**). The highest amount shed was 3.3 log_{10}/mL on 4 dpi. Virus was not isolated from any raccoon swabs, raccoon tissues, skunk rectal swabs, or skunk tissues.

All skunk and select raccoon samples were evaluated for the presence of vRNA using rRT-PCR (Ct of $\leq$35). SARS-CoV-2 RNA was detected in the nasal swabs of 3/8 DI raccoons (H1R, H2L, L2L) and 4/8 DI skunks (H1L, H1R, H2R, L2R); this includes two skunks, H1-L and H2-R, from which virus was isolated as displayed in **Table 2**. In addition, skunks H1-L and H2-R were the only animals in this study to have Ct values $\leq$ 28, a threshold that coincides with historic human data for obtaining culturable virus when evaluating the samples for the SARS-CoV-2 N gene via RT-PCR (**Supplementary Table 2**) (55). Viral RNA was also detected from one high dose DI skunk (H2R) nasal turbinate tissue sample from 8 dpi. No vRNA was detected from skunk or raccoon rectal swabs, skunk environmental swabs, or raccoon tissues. All directly inoculated animals of both species seroconverted—defined by a 4-fold increase in antibody titers—by the end of the study; however, no seroconversion occurred in any direct contact animals. The highest titer was 1:64 in raccoons and 1:128 in skunks, and the earliest seroconversion timepoint was on 9 dpi and 8 dpi, respectively (**Supplementary Table 1**).

The gross necropsies for all animals were unremarkable. No microscopic lesions or SARS-CoV-2 specific immunohistochemical labeling were evident in tissues from raccoons. The frontal and deep nasal conchae of three DI high dose skunks (H1R, H2R, H2L) and two DI low dose skunks (L1R, L2L) had mildly to moderately increased numbers of widely scattered lymphocytes and plasma cells in the superficial lamina propria vs. DC and control animals. At least one of four examined sections of lung, either the left cranial/caudal or right cranial/middle lung lobes, of DI high dose skunks (H1R, H2R, H1L) and DI low dose skunks (L2R, L2L) had mildly increased numbers of perivascular lymphocytes and plasma cells randomly scattered throughout the interstitium. There was no corresponding immunohistochemical labeling in these nor in any other tissues examined from skunks. Incidentally, all skunks had moderate to severe, diffuse hepatic lipidosis and one DI skunk (L1R) had focal, purulent rhinitis in the frontal nasal conchae. All skunks had robust lymphoid tissue in lymph nodes, spleen, bronchus-associated lymphoid tissue (BALT; lungs), and gastrointestinal-associated lymphoid tissue (GALT; intestine).

TABLE 2 | SARS-CoV-2 RNA detection in nasal swabs of intranasally direct inoculated (DI) and direct contact (DC) raccoons (*Procyon lotor*) and striped skunks (*Mephitis mephitis*) by real-time reverse transcriptase PCR (rRT-PCR).

DPI	Raccoon*		Skunk**	
Exposure	**Direct**	**Contact**	**Direct**	**Contact**
1	3/8		2/8	
2	0/8		4/8	
3	0/8	0/4	3/8	0/4
4	0/8	0/4	2/8	0/4
5	0/8	0/4	2/6	0/4
6		0/4		0/4
7	0/8	0/4	0/7	0/4
8			0/2	0/2
9	0/8	0/4	0/4	0/2
11		0/4		0/2
15			0/4	0/2
17	0/4	0/2		
Total seroconversion	8/8	0/4	8/8	0/4

*Of the rRT-PCR positive raccoons, 2/3 belonged to the DI high dose groups and 1/3 belonged to the DI low dose group. **Of the rRT-PCR positive skunks, 3/4 belonged to the DI high dose group and 1/4 belonged to the DI low dose group.*

DISCUSSION

A One Health approach to understand and mitigate the epidemiology and management of SARS-CoV-2 in a wide range of hosts calls for a collaborative effort between governmental agencies, academic and private institutions, and the public (56). Such efforts must include experimental trials, wildlife health assessments, and pathogen surveillance (57). In terms of the number of human infections and deaths and the currently known animal host range, the COVID-19 pandemic is one of the most important global emerging zoonoses to date, which will take a concerted multidisciplinary approach to manage.

Our findings demonstrate that while striped skunks and raccoons are susceptible to SARS-CoV-2 infection, it is unlikely that either species is likely to be a competent reservoir for SARS-CoV-2 in a natural setting. No animals experienced clinical disease during this study. Raccoons exhibited no pathology, and skunks had mild evidence of subclinical recovering cellular response to viral infection in the nasal conchae and lungs. The lack of virus isolation from raccoons, evidence of direct

transmission between both species, and low amount of virus shed by skunks would likely impede the virus's ability to establish in wild populations. Similar results of an experimental trial with skunks were reported by Bosco-Lauth et al. (7). Of 6 striped skunks that were intranasally inoculated with approximately 10^5 PFU of SARS-CoV-2, three shed virus up to 7 dpi, the highest amount of which was 2.3 $\log_{10}$ pfu/swab. They also isolated virus from the nasal turbinates of 2/3 skunks euthanized on 3 dpi, similar to the vRNA detected in a nasal turbinate tissue sample of a skunk euthanized on 8 dpi in our study. Also similar to our study, all inoculated skunks seroconverted. Bosco-Lauth et al. (7) also inoculated three raccoons, none of which were positive by VI or RT-PCR. In our study, all of our inoculated raccoons seroconverted whereas none of the raccoons in Bosco-Lauth et al. (7) seroconverted. The reason for this difference is unknown but could be due to the use of different serological assays. Another important difference between these two studies is that we included naïve contact animals to test cage-mate transmission, which provided data on the potential for SARS-CoV-2 to circulate in striped skunk and raccoon populations.

We describe viral RNA using presence/absence data similar to methods for SARS-CoV-2 animal reporting by the USDA (41, 58, 59). We also provide data on the detection of infectious virus (by plaque assay) to assist in assessing the potential for transmission of SARS-CoV-2 in nature. In some cases, virus quantification by PCR is used to estimate or determine virus quantities; however, this could lead to confusion as to how results translate to natural infections among wild and captive animals (55, 60, 61). In our study, virus was isolated from samples from two skunks (H1-L and H2-R) between 1 and 5 dpi; the corresponding Ct decreased notably between 3 and 4 dpi before steadily increasing (**Supplementary Table 2**). This trend may reflect diminished viral replication as Ct values increased. While rRT-PCR is a sensitive diagnostic tool to evaluate for the presence of SARS-CoV-2, it should be used in conjunction with additional assays such as virus isolation to strengthen inferences about transmission potential and other epidemiological factors in wildlife and others.

As with many susceptibility trials with wildlife, especially those that require high containment housing, availability, logistical challenges, and animal welfare considerations often limit sample size (62, 63). Given our studies small sample size and our animal sourcing, our findings may not readily translate into the susceptibility of wild populations due to factors such as senescence, immunocompetence (i.e., parasite burden, environmental conditions, gestation) and co-infections (e.g., canine distemper virus, parvovirus, etc.). Also, the rapid emergence of increasingly infectious SARS-CoV-2 variants in human populations presents new possibilities, such as increased transmissibility to previously marginally susceptible or unsusceptible species (64). Emerging variants of concern, B.1.1.7 and B.1.617.2, have been isolated from both companion animals (e.g., domestic dogs and cats) and captive wildlife (e.g., lions in a zoological institution), respectively (65–67). However, to date, no variants of concern have been isolated from free ranging wildlife, nor used in experimental infection trials of wildlife species, thus it is difficult to infer what impact these emerging variants will have on free-ranging raccoons and striped skunks. Despite evidence of poor transmission, care should be taken to avoid transmission of SARS-CoV-2 to skunks and raccoons in a captive setting (e.g., zoological institutions, rehabilitation centers) where close encounter with individuals shedding different strains and high viral loads may influence outcomes. In this study, all raccoons and skunks seroconverted after direct inoculation with SARS-CoV-2, however only a small subset of these animals shed detectable viral RNA ($n = 7$), and even less shed viable virus ($n = 2$). Moreover, these results suggest that seroprevalence studies may be the most sensitive large-scale approach for determining COVID-19 exposure in susceptible wildlife contrary to current PCR-based animal surveillance in the US (59). However, the lack of viral shedding in raccoons or select skunks highlight that future wildlife surveillance studies should interpret antibody presence with caution, as seroconversion is not indicative of an animal having a profound role in the epidemiology of SARS-CoV-2.

While it seems unlikely for SARS-CoV-2 to circulate in raccoon and skunk populations, other taxonomically related species, such as several species of mustelids including various otters, weasels, badgers, and martens; especially species of particular conservation concern, like black-footed ferrets (*Mustela nigripes*), European mink (*Mustela lutreola*), giant otters (*Pteronura brasiliensis*), and sea otters (*Enhydra lutris*) have yet to be studied. Infection of highly susceptible species held in captive breeding programs, could result in outbreaks, hampering reintroduction efforts. For example, these concerns, in part, led to the majority of the captive breeding population of black-footed ferrets at the National Black-Footed Ferret Conservation Center outside Fort Collins, Colorado to be immunized with an experimental vaccine early in the COVID-19 pandemic (68). Continued global outbreaks of SARS-CoV-2 in farmed mink (69), sporadic reports of infection in domestic animals (36, 70–72), and detected spillover into captive and free-living wildlife populations [e.g., wild and escaped mink in Utah; (41, 73), various species including tigers, gorilla, and otters in zoological collections; (44, 74, 75)] highlight that additional research including further exploration of the drivers, ecological pathways, and susceptibility of SARS-CoV-2 in wildlife, especially Musteloidea, are needed.

DATA AVAILABILITY STATEMENT

The original contributions presented in the study are included in the article/**Supplementary Material**, further inquiries can be directed to the corresponding authors.

ETHICS STATEMENT

The animal study was reviewed and approved by the University of Georgia's IACUC Committee (A2020 04-016) and Office of Biosafety (2020 0048).

AUTHOR CONTRIBUTIONS

SH, DM, NN, RF, and MY contributed to study design and implementation. SH, DM, SB, NN, MY, and RF participated

in the experimental trials and sampling. DM, KA, SB, and RF processed samples. NN, DM, KA, and RF interpreted the data. RF wrote the first draft of the manuscript. SH, MY, and NN both contributed large portions to the manuscript. All authors contributed to manuscript revision, read, and approved the submitted version.

FUNDING

Primary funding was provided by a National Science Foundation RAPID award (#2032044); graduate student assistantship support was additionally provided by an NSF EEID grant (#1518611). Additional support was provided by the member states wildlife management agencies of the Southeastern Cooperative Wildlife Disease Study through the Federal Aid to Wildlife Restoration Act (50 Stat. 917) and the Ecosystems Mission Area, United States Geological Survey, United States Department of Interior.

ACKNOWLEDGMENTS

We appreciate the technical assistance, excellent training, and animal care provided by the bioresources staff at the UGA Animal Health Research Center and animal care staff within Animal Resources in the UGA College of Veterinary Medicine. We also appreciate the technical expertise of the histotechnologists at the Athens Veterinary Diagnostic Laboratory. We thank Dr. Jeff Hogan, Department of Infectious Diseases, UGA for providing the SARS-CoV-2 isolate used in this study. This manuscript was previously made available by Biorxiv as a preprint (76): BioRxiv 2021.03.06.434226; doi: https://doi.org/10.1101/2021.03.06.434226.

SUPPLEMENTARY MATERIAL

The Supplementary Material for this article can be found online at: https://www.frontiersin.org/articles/10.3389/fvets.2021.715307/full#supplementary-material

REFERENCES

1. Zhao Y, Wang J, Kuang D, Xu J, Yang M, Ma C, et al. Susceptibility of tree shrew to SARS-CoV-2 infection. *Sci Rep.* (2020) 10:1–9. doi: 10.1038/s41598-020-72563-w
2. Wernike K, Aebischer A, Michelitsch A, Hoffmann D, Freuling C, Balkema-Buschmann A, et al. Multi-species ELISA for the detection of antibodies against SARS-CoV-2 in animals. *Transbound Emerg Dis.* (2020) 68:1779–85. doi: 10.1111/tbed.13926
3. Berhane Y, Suderman M, Babiuk S, Pickering B. Susceptibility of turkeys, chickens and chicken embryos to SARS-CoV-2. *Transbound Emerg Dis.* (2021) 68:3038–42. doi: 10.1111/tbed.13970
4. Bosco-Lauth AM, Hartwig AE, Porter SM, Gordy PW, Nehring M, Byas AD, et al. Experimental infection of domestic dogs and cats with SARS-CoV-2: Pathogenesis, transmission, and response to reexposure in cats. *Proc Natl Acad Sci U S A.* (2020) 117:26382–8. doi: 10.1073/pnas.2013102117
5. Shuai L, Zhong G, Yuan Q, Wen Z, Wang C, He X, et al. Replication, pathogenicity, and transmission of SARS-CoV-2 in minks. *Natl Sci Rev.* (2021) 8:nwaa291. doi: 10.1093/nsr/nwaa291
6. Ulrich L, Michelitsch A, Halwe N, Wernike K, Hoffmann D, Beer M. Experimental SARS-CoV-2 infection of bank voles. *Emerg Infect Dis.* (2021) 27:1193–5. doi: 10.3201/eid2704.204945
7. Bosco-Lauth AM, Root JJ, Porte SM, Walker AE, Guilbert L, Hawvermale D, et al. Survey of peridomestic mammal susceptibility to SARS-CoV-2 infection. *bioRxiv [Preprint].* (2021). doi: 10.1101/2021.01.21.427629
8. Kim Y-I, Kim S-G, Kim S-M, Kim E-H, Park S-J, Yu K-M, et al. Infection and rapid transmission of SARS-CoV-2 in ferrets. *Cell Host Microbe.* (2020) 27:704–9. doi: 10.1016/j.chom.2020.03.023
9. Schlottau K, Rissmann M, Graaf A, Schön J, Sehl J, Wylezich C, et al. SARS-CoV-2 in fruit bats, ferrets, pigs, and chickens: an experimental transmission study. *Lancet Microbe.* (2020) 19—20. doi: 10.2139/ssrn.3578792
10. Shi J, Wen Z, Zhong G, Yang H, Wang C, Huang B, et al. Susceptibility of ferrets, cats, dogs, and other domesticated animals to SARS–coronavirus 2. *Science.* (2020) 368:1016–20. doi: 10.1126/science.abb7015
11. Mykytyn AZ, Lamers MM, Okba NMA, Breugem TI, Schipper D, van den Doel PB, et al. Susceptibility of rabbits to SARS-CoV-2. *Emerg Microbes Infect.* (2021) 10:1–7. doi: 10.1080/22221751.2020.1868951
12. Ulrich L, Wernike K, Hoffmann D, Mettenleiter TC, Beer M. Experimental infection of cattle with SARS-CoV-2. *Emerg Infect Dis.* (2020) 26:2979–81. doi: 10.3201/eid2612.203799
13. Osterrieder N, Bertzbach LD, Dietert K, Abdelgawad A, Vladimirova D, Kunec D, et al. Age-dependent progression of SARS-CoV-2 infection in syrian hamsters. *Viruses.* (2020) 12:1–11. doi: 10.1101/2020.06.10.144188
14. Palmer MV, Martins M, Falkenberg S, Buckley A, Caserta LC, Mitchell PK, et al. Susceptibility of white-tailed deer (Odocoileus virginianus) to SARS-CoV-2. *J Virol.* (2021) 95. doi: 10.1128/JVI.00083-21
15. Pickering BS, Smith G, Pinette MM, Embury-Hyatt C, Moffat E, Marszal P, et al. Susceptibility of domestic swine to experimental infection with severe acute respiratory syndrome coronavirus 2. *Emerg Infect Dis.* (2021) 27:104–12. doi: 10.3201/eid2701.203399
16. El Zowalaty ME, Järhult JD. From SARS to COVID-19: a previously unknown SARS- related coronavirus (SARS-CoV-2) of pandemic potential infecting humans – Call for a One Health approach. One *Heal.* (2020) 9:100124. doi: 10.1016/j.onehlt.2020.100124
17. Guan Y, Zheng BJ, He YQ, Liu XL, Zhuang ZX, Cheung CL, et al. Isolation and characterization of viruses related to the SARS coronavirus from animals in Southern China. *Science.* (2003) 302:276–8. doi: 10.1126/science.1087139
18. Lau SKP, Wong ACP, Lau TCK, Woo PCY. Molecular evolution of MERS coronavirus: Dromedaries as a recent intermediate host or long-time animal reservoir? *Int J Mol Sci.* (2017) 18:2183. doi: 10.3390/ijms18102138
19. Dhama K, Patel SK, Sharun K, Pathak M, Tiwari R, Yatoo MI, et al. SARS-CoV-2 jumping the species barrier: Zoonotic lessons from SARS, MERS and recent advances to combat this pandemic virus. *Travel Med Infect Dis.* (2020) 37:101830. doi: 10.1016/j.tmaid.2020.101830
20. Franklin AB, Bevins SN. Spillover of SARS-CoV-2 into novel wild hosts in North America: a conceptual model for perpetuation of the pathogen. *Sci Total Environ.* (2020) 733:139358. doi: 10.1016/j.scitotenv.2020.139358
21. Gryseels S, De Bruyn L, Gyselings R, Calvignac-Spencer S, Leendertz FH, Leirs H. Risk of human-to-wildlife transmission of SARS-CoV-2. *Mamm Rev.* (2021) 51:272–92. doi: 10.1111/mam.12225
22. Olival KJ, Cryan PM, Amman BR, Baric RS, Blehert DS, Brook CE, et al. Possibility for reverse zoonotic transmission of sars-cov-2 to free-ranging wildlife: a case study of bats. *PLoS Pathog.* (2020) 16:1–19. doi: 10.1371/journal.ppat.1008758
23. Delahay RJ, de la Fuente J, Smith GC, Sharun K, Snary EL, Flores Girón L, et al. Assessing the risks of SARS-CoV-2 in wildlife. *One Health Outlook.* (2021) 3:7. doi: 10.1186/s42522-021-00039-6
24. Manes C, Gollakner R, Capua I. Could mustelids spur COVID-19 into a panzootic? *Vet Ital.* (2020) 56:65-6. doi: 10.12834/VetIt.2375.13627.1
25. Stout AE, Guo Q, Millet JK, de Matos R, Whittaker GR. Coronaviruses associated with the superfamily musteloidea. *MBio.* (2021) 12:1–14. doi: 10.1128/mBio.02873-20

26. Martínez-Hernández F, Isaak-Delgado AB, Alfonso-Toledo JA, Muñoz-García CI, Villalobos G, Aréchiga-Ceballos N, et al. Assessing the SARS-CoV-2 threat to wildlife: Potential risk to a broad range of mammals. *Perspect Ecol Conserv*. (2020) 18:223–34. doi: 10.1016/j.pecon.2020.09.008
27. Becker DJ, Albery GF, Sjodin AR, Poisot T, Dallas TA, Eskew EA, et al. Predicting wildlife hosts of betacoronaviruses for SARS-CoV-2 sampling prioritization. *bioRxiv [Preprint]*. (2020). doi: 10.1101/2020.05.22.111344
28. Zhao J, Cui W, Tian BP. The potential intermediate hosts for SARS-CoV-2. *Front Microbiol.* (2020) 11:1–11. doi: 10.3389/fmicb.2020.580137
29. Martina BEE, Haagmans BL, Kuiken T, Fouchier RAM, Rimmelzwaan GF, Van Amerongen G, et al. SARS virus infection of cats and ferrets. *Nature.* (2003) 425:915. doi: 10.1038/425915a
30. Van Den Brand JMA, Lhaagmans B, Leijten L, Van Riel D, Emartina BE, Osterhaus ADME, et al. Pathology of experimental SARS coronavirus infection in cats and ferrets. *Vet Pathol.* (2008) 45:551–62. doi: 10.1354/vp.45-4-551
31. Chu YK, Ali GD, Jia F, Li Q, Kelvin D, Couch RC, et al. The SARS-CoV ferret model in an infection-challenge study. *Virology.* (2008) 374:151–63. doi: 10.1016/j.virol.2007.12.032
32. ter Meulen J, Bakker AB, van den Brink EN, Weverling GJ, Martina BE, Haagmans BL, et al. Human monoclonal antibody as prophylaxis for SARS coronavirus infection in ferrets. *Lancet.* (2004) 363:2139–41. doi: 10.1016/S0140-6736(04)16506-9
33. Richard M, Kok A, de Meulder D, Bestebroer TM, Lamers MM, Okba NMA, et al. SARS-CoV-2 is transmitted via contact and via the air between ferrets. *Nat Commun.* (2020) 11:3496. doi: 10.1038/s41467-020-17367-2
34. Everett HE, Lean FZX, Byrne AMP, van Diemen PM, Rhodes S, James J, et al. Intranasal infection of ferrets with SARS-CoV-2 as a model for asymptomatic human infection. *Viruses.* (2021) 13:113. doi: 10.3390/v13010113
35. Marsh GA, McAuley AJ, Brown S, Pharo EA, Crameri S, Au GG, et al. In vitro characterisation of SARS-CoV-2 and susceptibility of domestic ferrets (Mustela putorius furo). *Transbound Emerg Dis.* (2021) 1−11. doi: 10.1111/tbed.13978
36. Gortázar C, Barroso-Arévalo S, Ferreras-Colino, Isla EJ, Fuente G de la, Rivera B, et al. Natural SARS-CoV-2 infection in kept ferrets, Spain. *bioRxiv*. (2021). doi: 10.1101/2021.01.14.426652
37. Monchatre-Leroy E, Lesellier S, Wasniewski M, Picard-Meyer E, Richomme C, Boué F, et al. Hamster and ferret experimental infection with intranasal low dose of a single strain of SARS-CoV-2. *J Gen Virol.* (2021) 102:001567. doi: 10.1099/jgv.0.001567
38. Kutter JS, de Meulder D, Bestebroer TM, Lexmond P, Mulders A, Richard M, et al. SARS-CoV and SARS-CoV-2 are transmitted through the air between ferrets over more than one meter distance. *Nat Commun.* (2021) 12:1653. doi: 10.1038/s41467-021-21918-6
39. Molenaar RJ, Vreman S, Hakze-van der Honing RW, Zwart R, de Rond J, Weesendorp E, et al. Clinical and pathological findings in SARS-CoV-2 disease outbreaks in farmed mink (Neovison vison). *Vet Pathol.* (2020) 57:653–7. doi: 10.1177/0300985820943535
40. Aguilo-Gisbert J. First description of natural SARS-CoV-2 infection in two wild American minks (Neovison vison). *Preprints.* (2021). doi: 10.20944/preprints202103.0647.v1
41. Shriner SA, Ellis JW, Root JJ, Roug A, Stopak SR, Wiscomb GW, et al. SARS-CoV-2 exposure in escaped mink, Utah, USA. *Emerg Infect Dis.* (2021) 27:988–90. doi: 10.3201/eid2703.204444
42. Oreshkova N, Moelnaar RJ, Vreman S, Harders F, Munnink BBO, Van Der Honin RWH, et al. SARS-CoV-2 infection in farmed minks, the. *Euro Surveill.* (2020) 25:1–7. doi: 10.2807/1560-7917.ES.2020.25.23.2001005
43. Oude Munnink BB, Sikkema RS, Nieuwenhuijse DF, Molenaar RJ, Munger E, Molenkamp R, et al. Transmission of SARS-CoV-2 on mink farms between humans and mink and back to humans. *Science.* (2020) 177:eabe5901. doi: 10.1126/science.abe5901
44. United States Department of Agriculture. *Confirmation of COVID-19 in Otters at an Aquarium in Georgia*. (2021). Available online at: https://www.aphis.usda.gov/aphis/newsroom/stakeholder-info/sa_by_date/sa-2021/sa-04/covid-georgia-otters#:$\sim$:text=Washington%2C%20D.C.%2C%20April%2021%2C,at%20an%20aquarium%20in%20Georgia.
45. Banerjee A, Mossman K, Baker ML. Zooanthroponotic potential of SARS-CoV-2 and implications of reintroduction into human populations. *Cell Host Microbe.* (2021) 29:160–4. doi: 10.1016/j.chom.2021.01.004
46. Zeveloff SI. *Raccoons: A Natural History.* Washington, DC: Smithsonian Institution Press (2002).
47. Louppe V, Leroy B, Herrel A, Veron G. Current and future climatic regions favourable for a globally introduced wild carnivore, the raccoon Procyon lotor. *Sci Rep*. (2019) 9:1–13. doi: 10.1038/s41598-019-45713-y
48. Charlton KM, Webster WA, Casey GA. Skunk rabies. In: Baer GM, editor. *The Natural History of Rabies*, 2nd ed. Boca Raton, FL; CRC Press (1991). p. 307–24.
49. Williams ES, Munson L. Morbilliviral Disease. In: Williams ES, Barker IK, editors. *Infectious Diseases of Wild Mammals*. 3rd ed. Ames, IA: Iowa State University Press (2001). p. 3–62.
50. Schott R. Natural history and medical management of procyonids. In: Hernandez SM, Barron HW, Miller EA, Aguilar RF, Yabsley MJ, editors. *Medical Management of Wildlife Species: A Guide for Practitioners*. Hoboken, NJ: Wiley(2019). p. 271–82. doi: 10.1002/9781119036708.ch21
51. Abou-Madi N. Natural History and Medical Management of Mustelids. In: Hernandez SM, Barron HW, Miller EA, Aguilar RF, Yabsley MJ, editors. *Medical Management of Wildlife Species: A Guide for Practitioners*. Hoboken, NJ: Wiley(2019) p. 283–96. doi: 10.1002/9781119036708.ch22
52. Freuling CM, Breithaupt A, Müller T, Sehl J, Balkema-Buschmann A, Rissmann M, et al. Susceptibility of raccoon dogs for experimental SARS-CoV-2 infection. *Emerg Infect Dis.* (2020) 26:2982–5. doi: 10.3201/eid2612.203733
53. Lu X, Wang L, Sakthivel SK, Whitaker B, Murray J, Kamili S, et al. US CDC real-time reverse transcription PCR panel for detection of severe acute respiratory syndrome Coronavirus 2. *Emerg Infect Dis.* (2020) 26:1654–65. doi: 10.3201/eid2608.201246
54. Centers for Disease Control and Prevention. *CDC 2019-Novel Coronavirus (2019-nCoV) Real-Time RT-PCR Diagnostic Panel*. (2020). Available online at: https://www.fda.gov/media/134922/download.
55. Kim M-C, Cui C, Shin K-R, Bae J-Y, Kweon O-J, Lee M-K, et al. Duration of culturable SARS-CoV-2 in hospitalized patients with Covid-19. *N Engl J Med.* (2021) 384:671–3. doi: 10.1056/NEJMc2027040
56. Karesh WB, Dobson A, Lloyd-Smith JO, Lubroth J, Dixon MA, Bennett M, et al. Ecology of zoonoses: natural and unnatural histories. *Lancet.* (2012) 380:1936–45. doi: 10.1016/S0140-6736(12)61678-X
57. Wood JLN, Leach M, Waldman L, MacGregor H, Fooks AR, Jones KE, et al. A framework for the study of zoonotic disease emergence and its drivers: spillover of bat pathogens as a case study. *Philos Trans R Soc B Biol Sci.* (2012) 367:2881–92. doi: 10.1098/rstb.2012.0228
58. Chandler JC, Bevins SN, Ellis JW, Linder TJ, Tell RM, Jenkins-Moore M, et al. SARS-CoV-2 exposure in wild white-tailed deer (Odocoileus virginianus). *bioRxiv [Preprint].* (2021) 118:e2114828118. doi: 10.1073/pnas.2114828118
59. U.S. Department of Agriculture. *Confirmed Cases of SARS-CoV-2 in Animals in the United States*. (2021). Available online at: https://www.aphis.usda.gov/aphis/dashboards/tableau/sars-dashboard
60. Badu K, Oyebola K, Zahouli JZB, Fagbamigbe AF, de Souza DK, Dukhi N, et al. SARS-CoV-2 Viral shedding and transmission dynamics: implications of WHO COVID-19 discharge guidelines. *Front Med.* (2021) 8:1–11. doi: 10.3389/fmed.2021.648660
61. Widders A, Broom A, Broom J. SARS-CoV-2: the viral shedding vs infectivity dilemma. *Infect Dis Heal.* (2020) 25:210–5. doi: 10.1016/j.idh.2020.05.002
62. Palmer MV, Cox RJ, Waters WR, Thacker TC, Whipple DL. Using white-tailed deer (odocoileus virginianus) in infectious disease research. *J Am Assoc Lab Anim Sci.* (2017) 56:350–60.
63. Olsen SC. Biosafety considerations for *in vivo* work with risk group 3 pathogens in large animals and wildlife in North America. *Anim Heal Res Rev*. (2013) 14:2–10. doi: 10.1017/S1466252312000217
64. Montagutelli X, Prot M, Levillayer L, Salazar EB, Jouvion G, Conquet L, et al. The B1.351 and P.1 variants extend SARS-CoV-2 host range to mice. *bioRxiv*. (2021). doi: 10.1101/2021.03.18.436013
65. Hamer SA, Ghai RR, Zecca IB, Auckland LD, Roundy CM, Davila E, et al. SARS-CoV-2 B.1.1.7 variant of concern detected in a pet dog and cat after exposure to a person with COVID-19, USA. *Transbound Emerg Dis.* (2021) 1–3. doi: 10.1111/tbed.14122

66. Grimm D. Major coronavirus variant found in pets for first time. *Science*. (2021). doi: 10.1126/science.abi6152
67. Sidharth M. *Chennai Zoo Lions Infected With Delta Variant of COVID-19, Reveals Genome Sequencing. WION*. (2021). Available online at: https://www.wionews.com/india-news/chennai-zoo-lions-infected-with-delta-variant-of-covid-19-reveals-genome-sequencing-392441
68. Neff EP. Keeping an eye on the human-animal interface. *Lab Anim*. (2021) 50:55–8. doi: 10.1038/s41684-021-00725-y
69. Sharun K, Tiwari R, Natesan S, Dhama K. SARS-CoV-2 infection in farmed minks, associated zoonotic concerns, and importance of the one health approach during the ongoing COVID-19 pandemic. *Vet Q*. (2021) 41:50–60. doi: 10.1080/01652176.2020.1867776
70. Deng J, Liu Y, Sun C, Bai J, Sun J, Hao L, et al. SARS-CoV-2 serological survey of cats in China before and after the pandemic. *Virol Sin*. (2020) 35:846–8. doi: 10.1007/s12250-020-00284-5
71. Hosie MJ, Hofmann-Lehmann R, Hartmann K, Egberink H, Truyen U, Addie DD, et al. Anthropogenic infection of cats during the 2020 COVID-19 pandemic. *Viruses*. (2021) 13:1–13. doi: 10.3390/v13020185
72. Sit THC, Brackman CJ, Ip SM, Tam KWS, Law PYT, To EMW, et al. Infection of dogs with SARS-CoV-2. *Nature*. (2020) 586:776–8. doi: 10.1038/s41586-020-2334-5
73. United States Department of Agriculture. *USDA Confirms SARS-CoV-2 in Mink in Utah*. (2020). Available online at: https://www.aphis.usda.gov/aphis/newsroom/stakeholder-info/sa_by_date/sa-2020/sa-08/sare-cov-2-mink#:~:text=Washington%2C%20D.C.%2C%20August%2017%2C,at%20two%20farms%20in%20Utah.
74. McAloose D, Laverack M, Wang L, Killian ML, Caserta LC, Yuan F, et al. From People to panthera : natural SARS-CoV-2 infection in tigers and lions at the bronx zoo. *MBio*. (2020) 11:085201. doi: 10.1128/mBio.02220-20
75. United States Department of Agriculture. *Confirmation of COVID-19 in Gorillas at a California Zoo Washington*. (2021). Available online at: https://www.aphis.usda.gov/aphis/newsroom/stakeholder-info/sa_by_date/sa-2021/sa-01/ca-gorillas-sars-cov-2.
76. Francisco R, Hernandez SM, Mead DG, Adcock KG, Burke SC, Nemeth NM, et al. Experimental susceptibility of North American raccoons (Procyon lotor) and striped skunks (Mephitis mephitis) to SARS-CoV-2. *bioRxiv [Preprint]*. (2021). doi: 10.1101/2021.03.06.434226

Conflict of Interest: The authors declare that the research was conducted in the absence of any commercial or financial relationships that could be construed as a potential conflict of interest.

frontiers in Veterinary Science

ORIGINAL RESEARCH
published: 31 January 2022
doi: 10.3389/fvets.2021.730424

Climate Conditions During a Rift Valley Fever Post-epizootic Period in Free State, South Africa, 2014–2019

Assaf Anyamba[1,2*†], *Richard Damoah*[2,3], *Alan Kemp*[4], *Jennifer L. Small*[2,5], *Melinda K. Rostal*[6], *Whitney Bagge*[6], *Claudia Cordel*[7], *Robert Brand*[8,9], *William B. Karesh*[8] *and Janusz T. Paweska*[4]

[1] *Universities Space Research Association, Columbia, MD, United States,* [2] *Biospheric Sciences Laboratory, NASA Goddard Space Flight Center, Greenbelt, MD, United States,* [3] *Physics Department and Goddard Earth Sciences Technology and Research, Morgan State University, Baltimore, MD, United States,* [4] *Center for Emerging and Zoonotic Diseases, Johannesburg, South Africa,* [5] *Science Systems and Applications, Inc., Lanham, MD, United States,* [6] *EcoHealth Alliance, New York, NY, United States,* [7] *Execuvet, Bloemfontein, South Africa,* [8] *Cuyahoga County Board of Health, Parma, OH, United States,* [9] *Department of Soil, Crop and Climate Sciences, University of the Free State, Bloemfontein, South Africa*

Rift Valley fever virus (RVFV) activity in Southern Africa tends to occur during periods of sustained elevated rainfall, cooler than normal conditions, and abundant vegetation cover creating ideal conditions for the increase and propagation of populations of RVFV mosquito vectors. These climatic and ecological conditions are modulated by large-scale tropical-wide *El Niño*–Southern Oscillation (ENSO) phenomena. The aim of this 5-year study was to investigate climatic conditions during Rift Valley fever "post-epizootic" period in Free State province of the Republic of South Africa, which historically experienced the largest RVF outbreaks in this country. We collected satellite-derived rainfall, land surface temperature (LST), and normalized difference vegetation index (NDVI) data since 2014 to understand broad environmental conditions in the years following a period of sustained and widespread large RVF outbreaks (2008–2011) in the region. We found this post-epizootic/interepizootic period to be characterized by below-normal rainfall (∼-500 mm), above LSTs (∼+12°C), depressed NDVI (60% below normal), and severe drought as manifested particularly during the 2015–2016 growing season. Such conditions reduce the patchwork of appropriate habitats available for emergence of RVFV vectors and diminish chances of RVFV activity. However, the 2016–2017 growing season saw a marked return to somewhat wetter conditions without any reported RVFV transmission. In general, the aggregate vector collections during this 5-year period follow patterns observed in climate measurements. During the 2017–2018 growing season, late and seasonally above average rainfall resulted in a focal RVF outbreak in one location in the study region. This unanticipated event is an indicator of cryptic RVF activity during post-epizootic period and may be a harbinger of RVFV activity in the coming years.

Keywords: climate variability, ENSO, post-epizootic, Rift Valley fever, mosquito vectors

OPEN ACCESS

Edited by:
Lester J. Perez, University of Illinois at Urbana–Champaign, United States

Reviewed by:
Amy Yomiko Vittor, University of Florida, United States
Henri Edouard Zefack Tonnang, International Centre of Insect Physiology and Ecology (ICIPE), Kenya

***Correspondence:**
Assaf Anyamba
assaf.anyamba@nasa.gov

***Present address:**
Goddard Earth Sciences Technology and Research, University of Maryland Baltimore Country, Baltimore, MD, United States

Specialty section:
This article was submitted to Veterinary Infectious Diseases, a section of the journal Frontiers in Veterinary Science

Received: *24 June 2021*
Accepted: *20 December 2021*
Published: *31 January 2022*

Citation:
Anyamba A, Damoah R, Kemp A, Small JL, Rostal MK, Bagge W, Cordel C, Brand R, Karesh WB and Paweska JT (2022) Climate Conditions During a Rift Valley Fever Post-epizootic Period in Free State, South Africa, 2014–2019. Front. Vet. Sci. 8:730424. doi: 10.3389/fvets.2021.730424

INTRODUCTION

Rift Valley fever (RVF) is an acute viral disease predominantly of domestic animals (cattle, buffalo, sheep, goats, and camels) and secondarily, of human populations. The endemic region of RVF covers most of sub-Saharan Africa, the Arabian Peninsula (Saudi Arabia and Yemen), and Madagascar (1, 2). Epicenters of epizootics and epidemics located in Eastern and Southern Africa are driven by persistent and above-normal rainfall associated with global scale *El Niño*-Southern Oscillation (ENSO) phenomena teleconnections (3, 4). Broadly, RVF outbreaks tend to occur in Eastern Africa during the positive phase of ENSO (*El Niño*) and in Southern Africa during the negative phase of ENSO (*La Niña*). The two phases describe the periods of persistent and above normal rainfall in each region leading to flooding of *pan/dambo* habitats. Flooding of these ecological niches where the various primary mosquito vectors of RVF-virus (RVFV) *Aedes* species and secondary *Culex* species emerge in massive numbers to trigger an outbreak. The impacts of an outbreak are varied and range from high rates of abortions and deaths in affected livestock to mild influenza-like illness and severe clinical symptoms in humans, including hemorrhagic manifestations, hepatitis, retinitis and encephalitis, and mortality in humans (∼1–35%) to abortions and mortality in affected livestock (∼80–100%) (1). The impacts on economies are pronounced, especially on livestock trade, and were estimated at $60M during the 2006–2007 outbreak in East Africa (5) and $12M (R203.4M) to the sheep farming sector alone during the 2010 outbreak in South Africa (6, 7). Due to its prominence as a cross-over pathogen, RVFV is listed as a biological agent by US government public health and defense agencies (Department of Defense, United States Department of Agriculture, Centers of Diseases Control and Prevention) and international public and animal health organizations (World Health Organization, Food Agricultural Organization, and the World Organization for Animal Health), requiring focused investigations in RVFV-endemic and neighboring regions.

One such investigation is *Understanding Rift Valley Fever in the Republic of South Africa* in which we are comprehensively studying an array of key facets influencing the RVF disease system using a One Health approach during the study period 2014–2019, which we refer to here as *post-epizootic* period. We interpreted this period to correspond to interepizootic/inter-epidemic period because of the likelihood of future RVF epizootics/epidemics. The One Health approach used is a collaborative, multisectoral, and transdisciplinary approach involving climate variable observations at regional level, vegetation, ecology and soil investigation, mosquito vector surveillance at local level, epidemiological investigations in livestock, wildlife, and human populations at farm level. The project therefore recognizes the interconnection between people, animals, plants, and their shared environment. The project is organized into eight work packages: 1. *Understanding the effects of climate and weather* (this study), 2. *Investigating vegetation ecology* (8), 3. *Investigating wetland soil properties* (9), 4. *Investigating ecological characteristics of RVFV vector mosquitoes*, 5. *Determining the seroprevalence of RVFV antibodies in farm workers* (10), 6. *Determining the seroprevalence of RVFV antibodies of farmed and free-ranging wild ruminants and domestic livestock* (11), 7. *Investigating changes in RVFV antibody levels in a sheep cohort*, and 8. *Comparison of cattle and buffalo serostatus in the Free State and Limpopo*. This paper reports on findings from *Understanding the Effects of Climate and Weather*, which has monitored and analyzed broad-scale satellite-derived climatic and environmental variables that influence RVFV mosquito vector populations. Among these variables are rainfall, considered the primary large-scale driver of RVFV activity, vegetation [normalized difference vegetation index (NDVI)], land surface temperature (LST), evapotranspiration, etc., which are proximate determinants of habitat conditions influencing survival and propagation of RVF vector populations (12–14). Climate variability characterized by year-to-year rainfall, vegetation, and land surface temperature are important broad scale drivers influencing the distribution in space and time of Rift Valley fever mosquito populations; therefore, understanding this component of the RVF disease system is critical to the implementation of various efforts to prevent, control, and mitigate potential outbreaks.

MATERIALS AND METHODS

Study Area

The project is being conducted in a ∼200 × 200 km area [28S−30.45S, 24E−26.65E] covering a large part of the Free State province and portions of both Eastern Cape and Northern Cape provinces. Significant epidemics were reported in these regions of South Africa in 1951, 1975, and 2010 with epizootics in 1951, 1975, 1984, 1999, 2008, and 2009, 2010, and 2011 (15, 16) with apparently quiescent inter-epidemic periods. Many of these epidemics had their epicenter in the Free State as can be observed from the recent epizootics as shown in **Figure 1**. Annual long-term rainfall in the region ranges between ∼200 mm to the west and southwest of the region and a maximum of ∼550 mm to the eastern and northeastern parts of the region. The climatological spatial patterns of land surface temperature with maximum values of ∼35°C in the west/southwest, and normalized difference vegetation index with maximum values of ∼0.45 in the east/northeastern parts of the region reflect the long-term annual mean patterns of rainfall. The combination of these climate metrics with the underlying geology has over time produced landcover patterns dominated by grasslands, savanna, and Nama-Karoo biomes (17), which includes fynbos elements, shrubs, and woodland species. Embedded in these three biomes are the azonal wetlands, which include the study area pan habitats, with vegetation distinct from the surrounding upland vegetation (8). Dryland agriculture that is heavily dependent on variable rainfall is practiced in the east, while locations in the drier west and southwest use irrigated agriculture to buffer against low and variable rainfall. The study area receives on average of ∼96% of rainfall between September and May and 4% between June and August, considering the southern hemisphere summer rainfall season. There is, however, high interannual variability in rainfall producing periods of above normal rainfall and floods and episodes of very low rainfall and

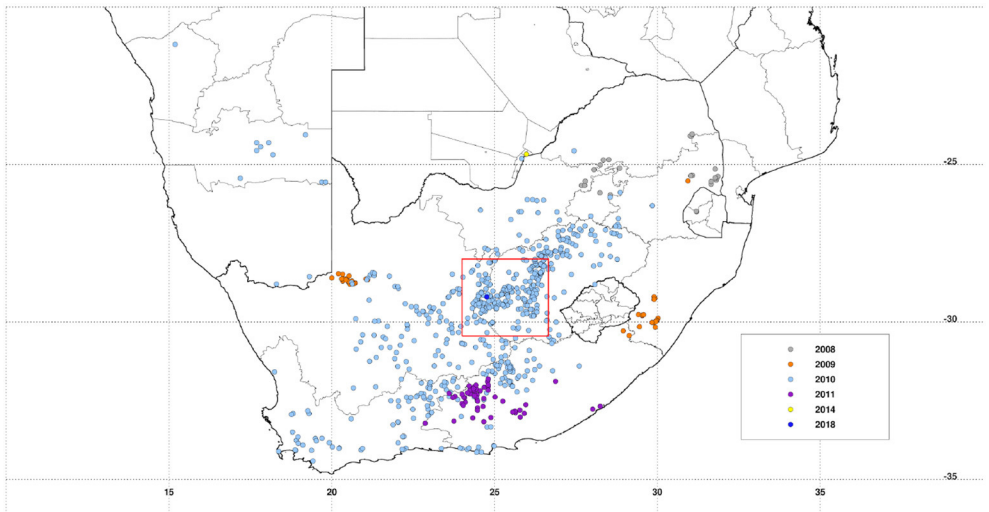

FIGURE 1 | Distribution of recent Rift Valley fever activity (2008–2018) over the southern Africa region. *Rift Valley fever in the Republic of South Africa* study region is marked by a red square outline [28S−30.45S, 24E−26.65E], centered on Free State and Northern Cape Province border, the epicenter of multiple epizootics. Data plotted were derived from the World Organization for Animal Health (OIE) World Animal Health Information System (WAHIS) database.

extreme drought. Periods of above-normal rainfall like 2009–2011 create conditions for outbreaks to occur and propagate. The study region thus has an approximately east–west ecological gradient from Bloemfontein to Mokala National Park (MNP) that can be observed in climate metrics and land cover patterns (**Figure 2**).

Data

Climate Data

Three satellite-derived climate data sets are used in evaluating the patterns of rainfall and land surface conditions over the region during the study period (2014–2019). The three data sets are (a) daily/monthly rainfall from the Africa Rainfall Climatology (ARC) data, (b) monthly normalized difference vegetation index, and (c) monthly land surface temperature. Details on these datasets are given below:

(a) African Rainfall Climatology (ARC) dataset is sourced from the National Oceanic and Atmospheric Administration (NOAA)—Climate Prediction Center (CPC) archives. ARC data are derived from several satellites and *in situ* sources, including the polar orbiting Special Sensor Microwave/Imager and Advanced Microwave Sounding Unit microwave sensors, infrared bands of the geostationary METEOSAT platforms, and rain gauge measurements from the Global Telecommunications System daily total rainfall product. The data are mapped to a spatial resolution of 0.1° × 0.1° over Africa and the Middle East. These data are available as a daily time series from 1983 to present (18).

(b) Normalized difference vegetation index (NDVI) data are derived from NASA's Earth Observing System Moderate Resolution Imaging Spectroradiometer (MODIS) instrument aboard the Terra (EOS AM-1) spacecraft. The NDVI and similar vegetation indices are widely used to infer the photosynthetic capacity of vegetation and are used as a land surface input in various weather, climate, biogeochemical, and hydrological models (19). Applications of normalized difference vegetation index are numerous and varied and include agricultural monitoring, famine early warning, ecological monitoring for habitats indicative of pest and arthropod vector emergence and survival, and determination of land use and land cover changes, among others (12, 20–22). The normalized difference vegetation index is simply the ratio of the difference between the near-infrared and red reflectance to their sum; since green leaves with dense chlorophyll are more reflective in the near-infrared wavelengths than in the visible, this ratio is higher (approaching one) for healthy green vegetation and lower (approaching zero) for stressed vegetation (23). MODIS normalized difference vegetation index data are derived from the red and near-infrared bands, centered at 648 nm and 848 nm, respectively. The reflectance data are atmospherically corrected and masked for cloud, cloud shadow, and aerosol contamination (24). In this study we use the global monthly Climate Modeling Grid (CMG) MOD13C2 product with a spatial resolution of 0.05° × 0.05° (∼5.5 × 5.5 km) aggregated from nominal 250 m MODIS NDVI.

(c) Land surface temperature (LST) was also derived from the MODIS instrument. Land surface temperature is a key parameter in land surface processes affecting climate and therefore influencing the biology, organisms, and ecosystems from local to global scales. Changes in land surface temperatures can induce convection at the boundary layer and influence air temperature, surface winds, cloudiness, and precipitation (25). All these variables influence habitat conditions of mosquito vectors. Land surface temperature

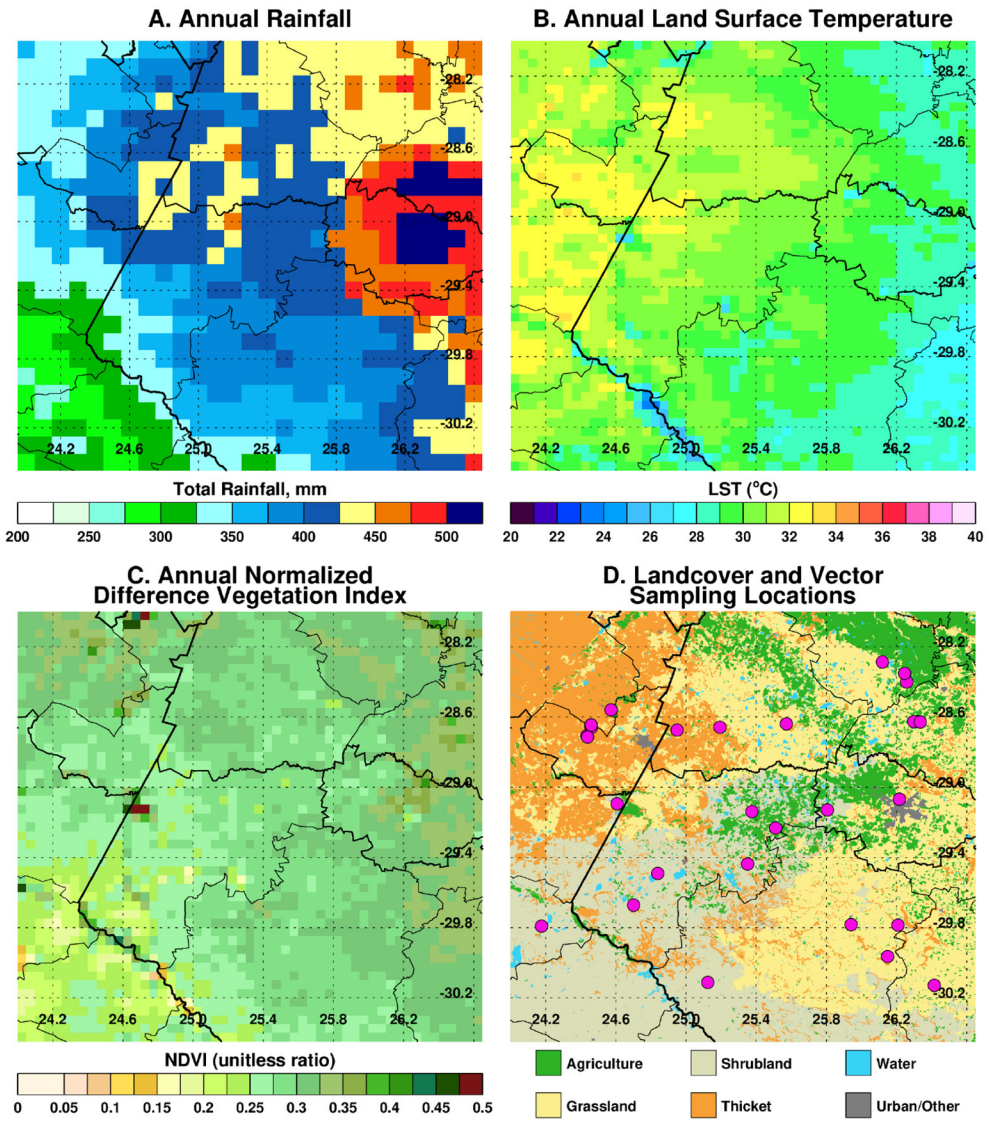

FIGURE 2 | Climate metrics and land cover characteristic of the study region. In **(A)** annual long-term rainfall (1983–2019), **(B)** annual long-term land surface temperature (2000–2019), **(C)** annual long-term normalized vegetation index (2000–2019), and **(D)** land cover classification. The spatial variations and patterning in **(B–D)** to a large extent reflect the patterns in long-term rainfall.

has proved useful for agricultural applications in estimating crop water demands and drought severity assessments (26). It is also an emerging variable in vector-borne disease applications (21). We used land surface temperature to infer temperature conditions on the land surface especially in vegetated areas, which serve as potential vector emergence sites during the study period. In this study, we use the global Climate Modeling Grid (CMG) product MOD11C3 at 0.05° spatial resolution. This data set is derived from daytime and nighttime thermal infrared measurements in bands 31 (10.8–11.3 nm) and 32 (11.8–12.3 nm) using the day/night land surface temperature algorithm. Cloud screening is performed using the MODIS cloud mask product (MOD35_L2), prior to the land surface temperature calculation.

Mosquito Vector Data

To complement the satellite-based climate observations, adult floodwater mosquito vectors were sampled by the vector ecology team at over 21 locations daily (shown in **Supplementary Figure 1**). Given the sampling strategy this amounts to every 2 weeks per site during the growing season (September–May). Sampling was performed using US Centers for Disease Control and Prevention (CDC) CO_2-baited traps placed at dusk to lure feeding adult female mosquitoes from diurnal resting locations. The sampling schedule was designed to be flexible to allow sampling all sites within the week. However, due to various issues at project startup, there was no regular sampling until the 2015–2016 season. In addition, significant weather events at times, including excessive rainfall or severe

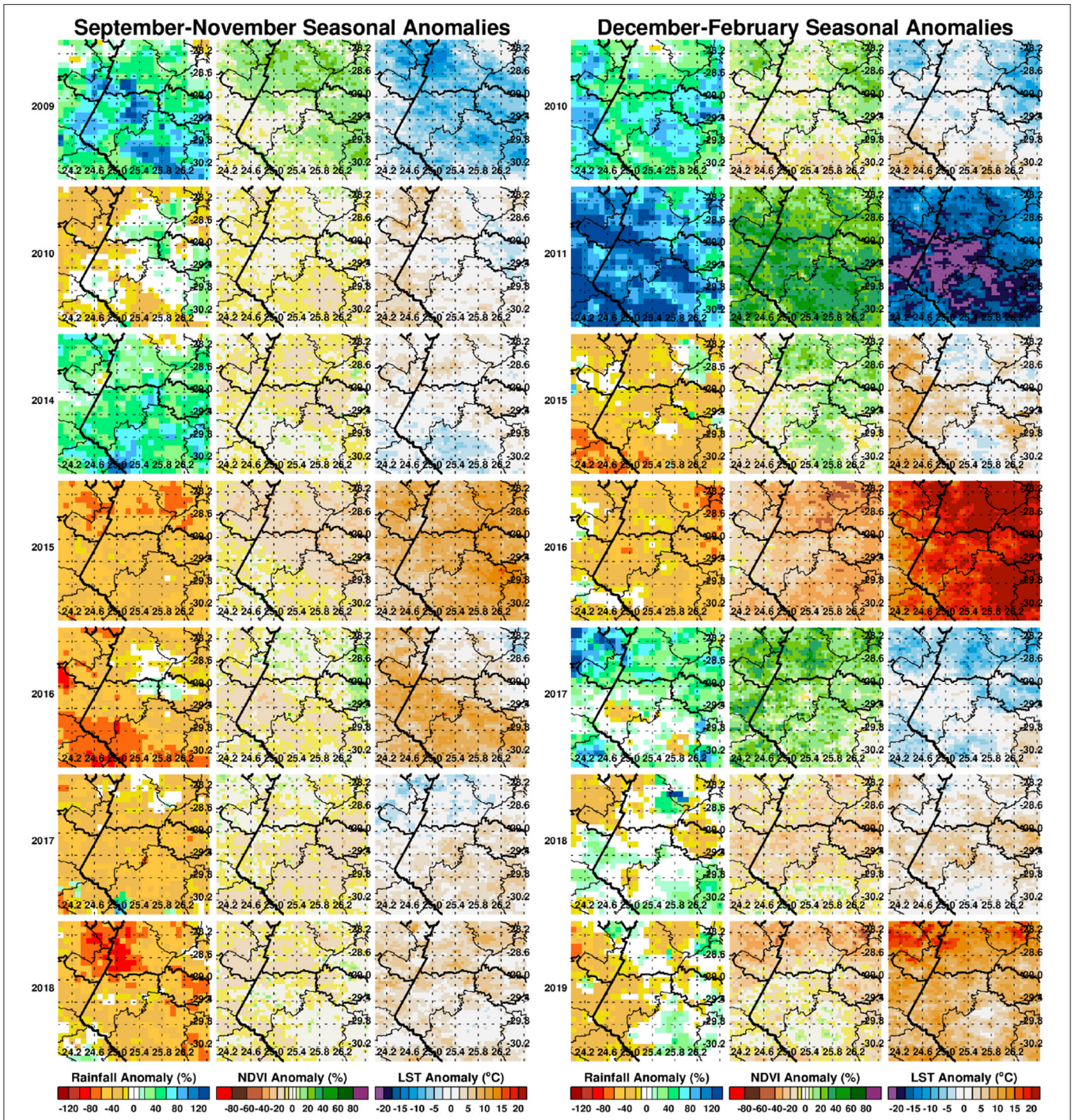

FIGURE 3 | Continued

winds, made it impossible to access some sites and set traps, forcing the team to trap at alternate sites. In this paper we use aggregated adult female mosquito population collection numbers sampled during the project period to compare to the 5-year variability in climate conditions. The vector data presented in this paper are adjusted for trap effort. Trap effort was summarized as the number of hours the trap was open multiplied by the number of traps that were set. For instances where the time the trap was open was not available, the median of all available data was used. Number of traps was available for all data. Thus, the adult female mosquito numbers were divided by this trap effort (hours trap was open multiplied by number of

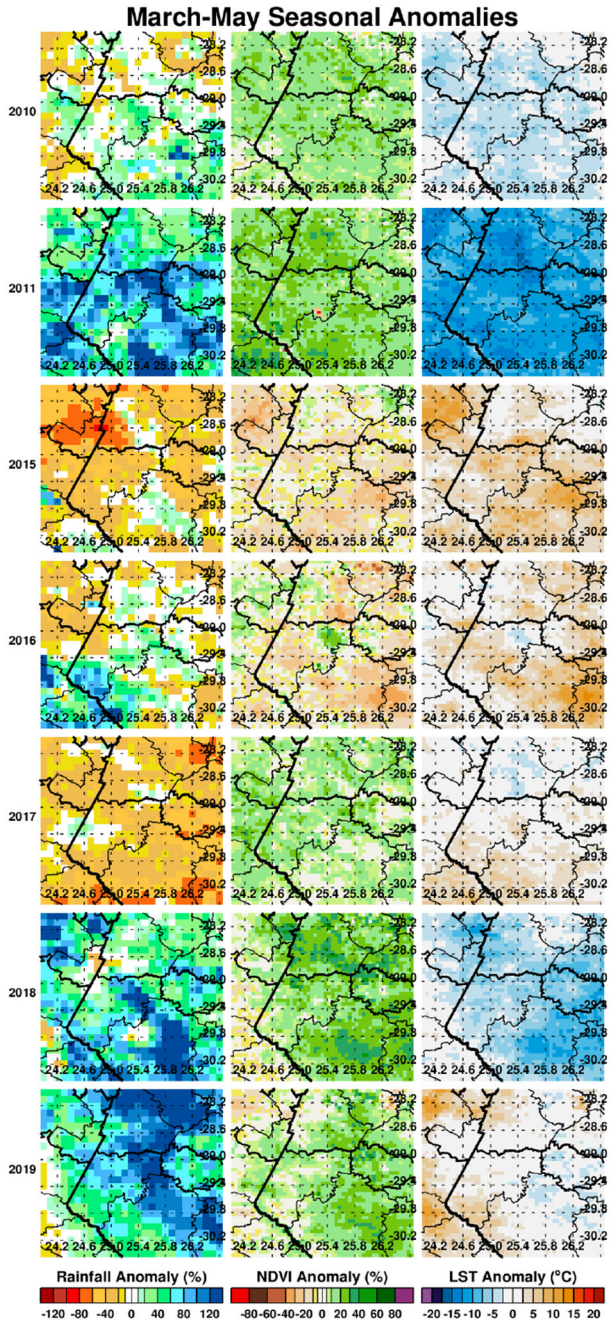

FIGURE 3 | Seasonal anomaly patterns of rainfall, normalized difference vegetation index, and land surface temperatures for epizootic seasons (2009/2010, 2010/2011) and study post-epizootic/interepizootic period seasons from 2014–2019. Seasons are defined by early (September–November: SON), mid (December–February: DJF), and end (March–May: MAM). Rainfall and normalized difference vegetation index anomalies are expressed as percentage departures while land surface temperatures are expressed as absolute departures from the respective seasonal long-term means.

trap sets) for summary numbers of adult female mosquitoes, and this trap effort was included as an offset in modeling the adult female mosquito number.

Data Analysis

Satellite Data Treatment

We processed, mapped, and subset all satellite rainfall, LST, and NDVI data within the study region extent (28S−30.45S, 24E−26.65E). For each climate variable, we computed both daily and monthly long-term means and corresponding absolute and standardized anomalies. We also examined the growing/rainfall season conditions by calculating seasonal anomalies. For the growing season we divided the season into early (September–November; SON), peak (December–February; DJF), and end (March–May; MAM) to examine the evolution of growing conditions, classified as below-normal, normal, and above-normal. For given vector sampling locations we tracked the seasonal growing conditions of the location using the seasonal rainfall cumulative metric by comparing the daily cumulative rainfall against the daily long-term mean. Daily cumulative rainfall values above the daily long-term mean values are a proxy for potential flooding of dambos/pans and therefore conducive to the emergence and propagation of vectors in general, but RVFV vectors in particular (27, 28). In all cases, at monthly or seasonal time scale we have calculated anomalies using two complementary methods as:

(a) Absolute anomalies $x' = x - \underline{x}$

(b) Standardized anomalies $z = \frac{x-\underline{x}}{s_x} = \frac{x'}{s_x}$

Where x' is the anomaly for a given month (e.g., January) or seasonal anomaly (DJF), x the absolute values of a given month or season, the respective long term means or climatology values of the respective month and season, z the standardized anomaly or z-scores for a given month or season, and s_x the corresponding standard deviation. The effect of standardization is to remove influences of local variability so we can compare the difference over space and over time from the different climate measurements (29). Results of absolute anomalies are presented in **Figure 3** and the standardized anomalies are given in the **Supplementary Figure 2**. For ease of interpretation by the reader, we have expressed absolute anomalies as percentage departures from the long-term mean for rainfall and normalized difference vegetation index metrics. Anomalies during the epizootic/period (2009–2010, 2010–2011) are included for reference purposes representing the most recent epidemic/epizootic period.

Vector and Climate Data Analysis

To investigate the relationship between vector populations and climate/environmental data, we employed a negative binomial regression model of the form,

$$M_f = \text{Rainfall} + \text{NDVI} + \text{LST} + \text{Offset}$$

where M_f is the number of adult female mosquitoes and Offset is the number of hours the traps were open (or median) * number of traps, to compare monthly rainfall, monthly normalized difference vegetation index, and monthly land surface temperature with total adult female vector populations sampled over the entire region. As the outcome measure, number of adult female mosquitoes, is a count variable, we employed

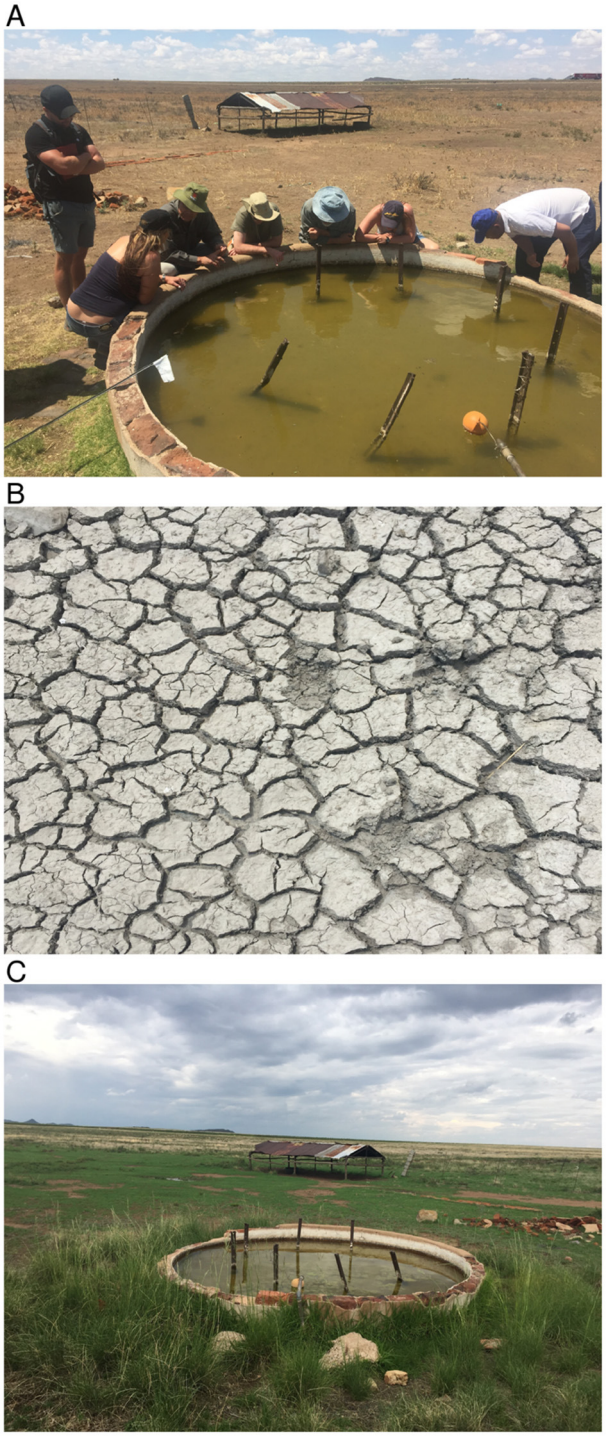

FIGURE 4 | Contrasting conditions in and around Meadows pan habitat (location shown in **Supplementary Figure 1**). [**(A)**-top] severe drought conditions in March 2016 at the peak of the growing season (rainfall total: ∼75.82 mm, long-term mean: 109.65 mm; normalized difference vegetation index: ∼0.28, long-term mean: 0.44; land surface temperature: 34.6°C, long-term mean: 31.9°C), [**(B)**-middle], desiccated dambo/plan floor during the same time period, and [**(C)**-bottom] March 2018: vegetation growth after sustained wet conditions (rainfall total: ∼182.80 mm, long-term mean: 109.65 mm; normalized difference vegetation index: ∼0.51, long-term mean: 0.44; land surface temperature: 28.04°C, long-term mean: 31.9°C).

a negative binomial regression approach with an offset for trap effort. The model structure maintains the data as count data with the negative binomial approach, and inclusion of the offset accounts for varying "rates" of mosquito capture—instances in the field data collection where number of traps or hours the trap was open might have varied from collection to collection based on field conditions—which would impact the number of mosquitoes caught at each collection time point. The offset employed in this model is a composite of both how long the trap was open and the number of traps that were set. For records in which the number of hours the trap was open was not present, we took the median of available data and multiplied that by the number of traps that were open during that collection time point. Complete data were available for number of traps set for all data collection time points.

RESULTS

Spatial and Temporal Patterns of Climate Anomalies

We first examined the spatial patterns in climate variable anomalies. In order to reduce the amount of data to examine we show the patterns by season: early season (September–November), mid-season (December–February), and end season (March–May). Geographic patterns of absolute anomalies for the study area are presented in **Figure 3** (see standardized anomalies in **Supplementary Figure 2** for reference). Anomalies during 2009–2010 and 2010–2011 are included for reference purposes, representing the recent epidemic/epizootic period. The patterns show that the epizootic period was dominated by an early start (2009–2010) to the season with favorable conditions for RVFV vectors during SON 2009 (widespread rainfall, above normal vegetation conditions and cooler than normal land surface temperature) that propagated into the mid-season (DJF) and further enhancement of these conditions in the last quarter of the season (MAM) for both vegetation and land surface temperature. The 2010–2011 epizootic period had a delayed start of the season but the rest of the season from December 2010 to May 2011 had enhanced and favorable conditions for the emergence of RVFV vectors and subsequent outbreaks as shown in **Figure 1**. During the study period 2014–2019, classified as post-epizootic/interepizootic period, the study region has been dominated by below normal rainfall, drier than normal vegetation conditions, and above normal land surface temperatures. The exceptions to this general pattern are: early-season during the 2014–15 season (SON2014), mid-season (DJF) in the 2016-2017 season, and late seasons in 2017–2018 (MAM2018) and 2018–2019 (MAM2019). The drier than normal conditions during this period reached a record low during the mid-season (DJF) 2015–2016 period with rainfall 60–80% below normal, normalized difference vegetation index ∼80% below normal, and land surface temperatures up to +20°C above normal over most of region (**Figure 3**). The contrasting patterns of land surface conditions during this post-epizootic period are best illustrated by field work evidence as shown in **Figure 4**. In drought years as shown in **Figures 4A,B**,

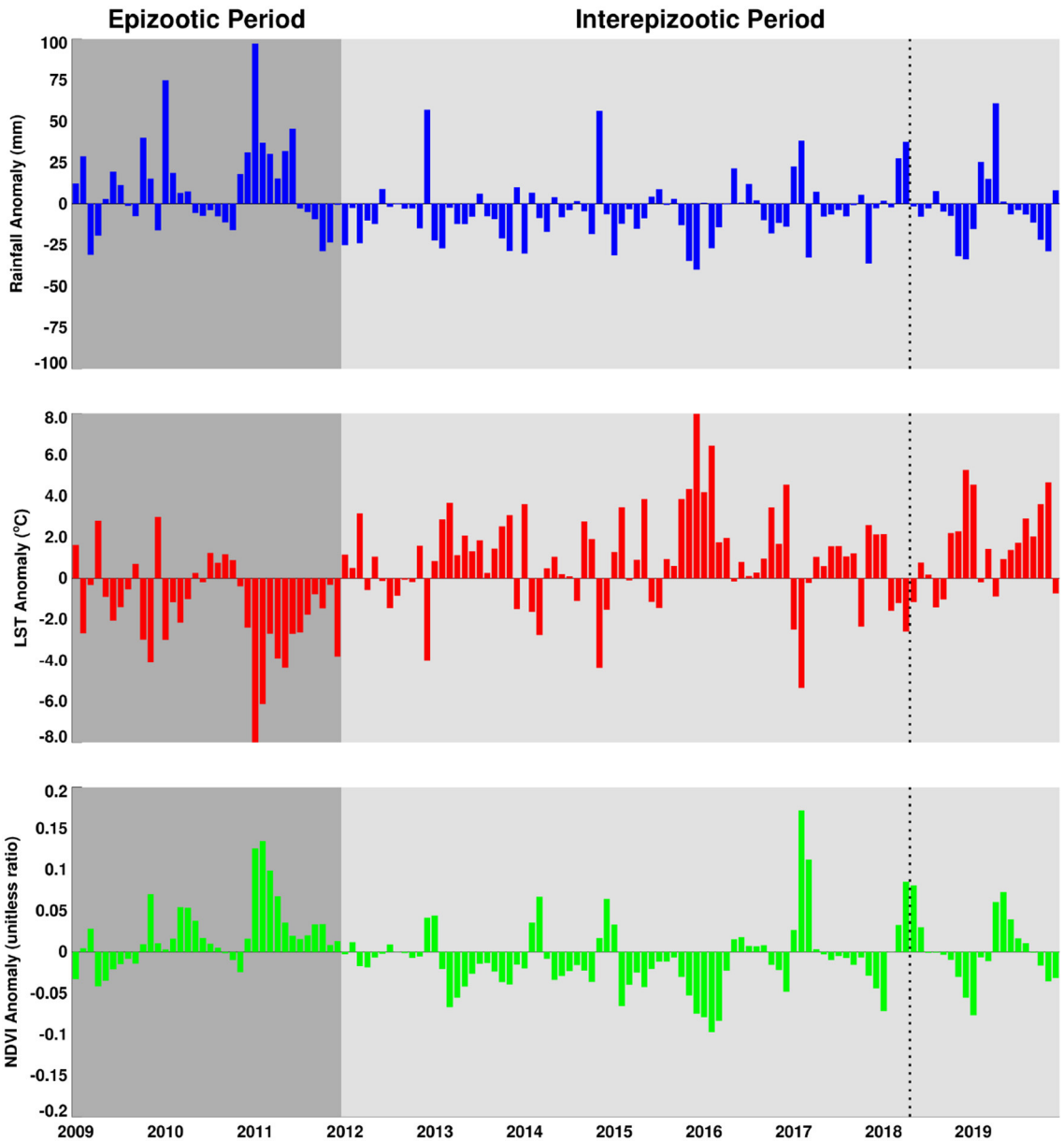

FIGURE 5 | Anomaly time series of rainfall, land surface temperature and normalized difference vegetation index for the period 2009–2019. The Rift Valley fever epizootic period (2009–2011) is shaded in dark grey and shows predominantly above normal rainfall, lower than normal land surface temperatures, and above normalized difference vegetation index and opposed to the interepizootic/post-epizootic period (2012–2019) with lower than normal rainfall and normalized difference vegetation index and persistence of higher than normal land surface temperatures marked by the extreme drought of 2015–2016. The dotted line shows the approximate timing of the isolated outbreak during 2017–2018 growing season.

due to excessive livestock herbivory, there is no vegetation cover outside wetlands, and even in certain pan habitats, all wetlands vegetation, which is generally considered impalatable, is totally grazed, which would result in NDVI of 0 or near 0 representing bare soil or scant vegetation cover. The amount of vegetation cover—density, and the type of vegetation—wetland species adapted to anaerobic conditions, are important as habitat for mosquito vectors. While NDVI is useful when correlated with rainfall, it is of specific importance for the mosquito vectors as they require wetland vegetation which, in the pans and palustrine habitats in the Free State, is embedded in the surrounding vegetation, and far more limited in extent. Because wetland vegetation is so limited in size in the Free State, green up in vegetation surrounding pan habitats is prominently detected from background by satellite measurements of vegetation photosynthetic capacity represented as high NDVI. **Figure 4C** illustrates this with the recovery and vegetation growth after sustained wet conditions in March

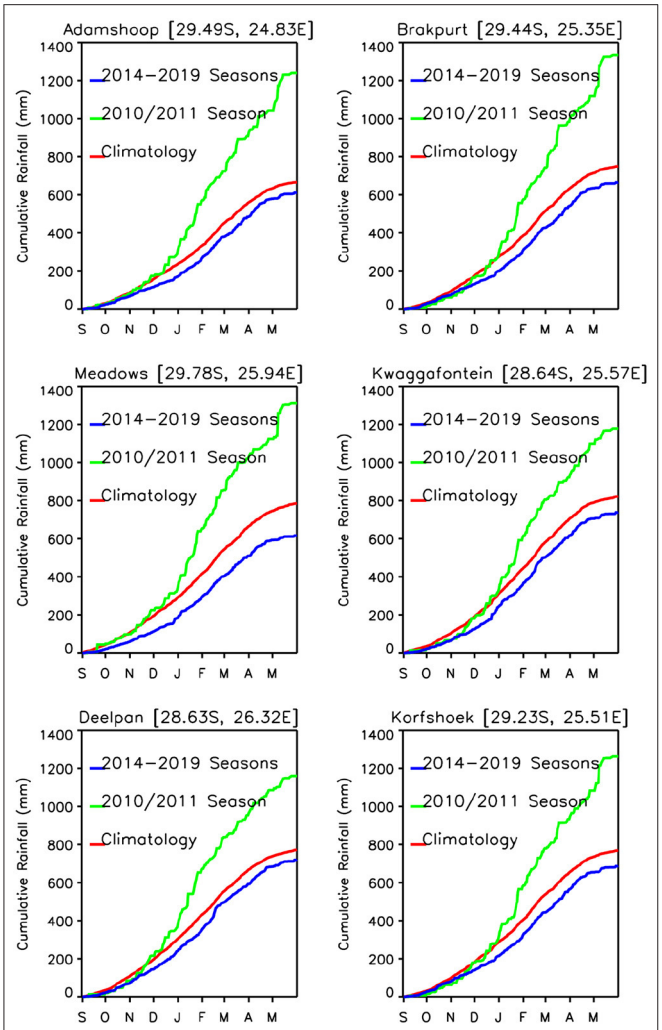

FIGURE 6 | Daily cumulative rainfall time series trajectories for epizootic period (2010/2011; green) and interepizootic period (average of 2014–2019; blue) compared to the daily long-term mean rainfall (red) for six selected study sites. The epizootic season (2010–2011) shown in green, was above the long-term mean, with a rainfall excess ranging between ∼200 and ∼600 mm across study sites by May. The study post-epizootic/interepizootic period shows persistently below normal rainfall with a shortfall of ∼100 mm by May across all study sites.

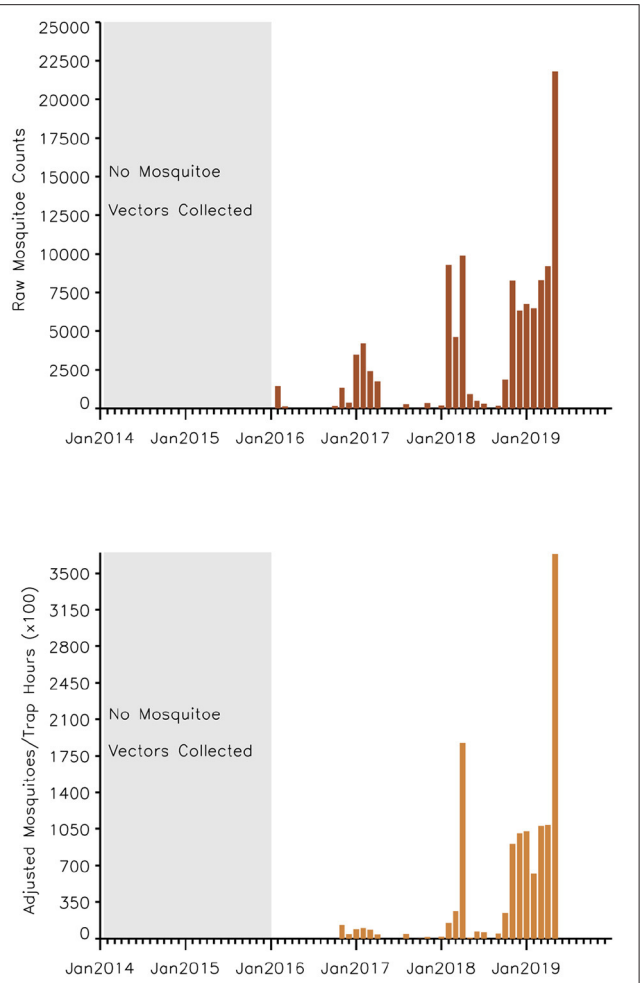

FIGURE 7 | Time series of aggregate mosquito vector counts (of various floodwater *Aedes spp*. and *Culex spp.*) for the study period September 2014–2019 (**top**) raw mosquito vector counts (**bottom**), adjusted mosquito vector counts accounting for trap effort during the study period. The number of vectors collected shows an increasing trend over time in concert in the increase in rainfall improving habitat conditions. Taking into consideration the trapping effort, 2014–2015 and 2015–2016 seasons had no vectors collected during this period of severe drought conditions.

2018 during the 2017–2018 growing season (**Figure 3**: March–May 2018).

The area averaged climate anomaly time series for the region shown in **Figure 5** illustrate that the post-epizootic period 2012–2019 (study period starts in 2014) has been dominated by below normal rainfall, above normal land surface temperatures, and below normal vegetation conditions. This is opposed to the epizootic period 2009–2011 which was characterized by above normal rainfall, below normal land surface temperatures, and above normal vegetation conditions. This figure also illustrates direct correlation between rainfall and NDVI but an inverse relationship between these two parameters and LST. It is clear that during the epizootic period (2009–2011), the intensity of the amplitudes and the spread of the base months starting early 2009 until later 2011 they are ∼18/23 months of above normal rainfall/NDVI and the inverse LST. When compared with successive periods in the following years, this pattern is not persistent enough in magnitude nor of the temporal range required for a large scale outbreak.

The area average growing season absolute rainfall for two seasons (2009/2010, 2010/2011) was 50.80 mm and for the 5 years of the study period was 39.4 mm. In terms of growing season cumulative rainfall anomalies, the epizootic period had excess rainfall on the order of ∼+367.50 mm compared to a deficit of ∼-266.25 mm for the entire post-epizootic growing seasons period (2012–2019). **Supplementary Table 1** shows the study area's average metrics for rainfall, normalized difference vegetation

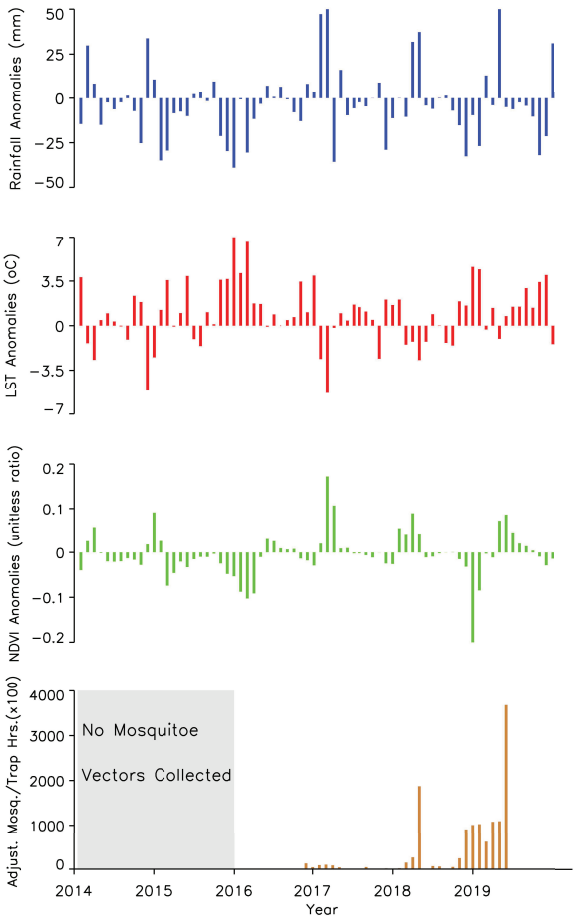

FIGURE 8 | Time series measurements of rainfall, land surface temperatures, normalized difference vegetation index anomalies, and adjusted mosquito vector collections during the study period. Vector collections only became prominent when rainfall and NDVI were trending toward above normal during the growing seasons from 2017–2019.

index, and land surface temperature for the entire period from 2012–2019. Examining cumulative rainfall trajectories for six selected study sites (**Supplementary Figure 3**), we find that only 2016/2017 and 2017/2018 are near normal and slightly above normal rainfall toward the end of the season. Other than that, none of the growing seasons during the study period exhibited persistent above normal rainfall that was sufficient enough to create ideal conditions to trigger an outbreak as was the case during the epizootic period in 2010/2011. In totality, the daily cumulative rainfall trajectories for the selected study sites indicate that there is a clear and contrasting difference between the epizootic (2010/2011) and study/post epizootic period (2014–2019) rainfall conditions (**Figure 6**) that is also reflected in other climate metrics.

TABLE 1 | Regression results of female adult vector populations and rainfall, normalized difference vegetation index (NDVI), and land surface temperature (LST).

Variable	Estimate	Std. Error	*p*-value
Rainfall	−0.00281	0.01419	0.843
NDVI	12.55334	5.53645	0.023*
LST	0.14202	0.05395	0.008*

** indicates a statistically significant result at the 0.05 level.*
Adjusted R-squared: 0.273.

Implications for Vector Populations

A time series of the total monthly mosquito vectors collected and the corrected for trap effort during the study period are shown in **Figure 7** and indicate an increasing trend over the 5-year period. Low numbers of vector populations were collected during the 2016–2017 seasons, with the lowest/none during the 2015–2016 period after adjustment for trap effort during the great desiccation period. However, since the 2016/2017 growing season there has been an increase in the number of vectors collected with the highest adjusted numbers during the 2018–2019 growing season. These patterns mirror the trends in climate variables shown in **Figures 5**, **8** especially for rainfall and as reflected in spatial patterns in **Figure 3**. A negative binomial regression analysis of climate variables averaged for the entire study region (rainfall, normalized difference vegetation index, land surface temperature as independent variables) and vector populations (dependent variable) for all growing seasons under study shows that, at the monthly time scale, both NDVI and LST are significantly positively correlated with vector populations, while rainfall is negatively, and not significantly, correlated (**Table 1**, adjusted R-squared 0.273). NDVI, LST and Rainfall were not collinear. To assess whether there was any seasonal time trend in the data, we incorporated a smooth function for season into the model of mosquito abundance using the mgcv package in R statistical software and compared the two models by AIC. The model without the smooth for season had the lower AIC and is thus the model we chose. Interestingly, the estimate for NDVI was substantially higher than the others in the model, indicating a strong positive relationship between NDVI and number of adult female mosquitoes. Since NDVI is a linear function of rainfall in semi-arid areas like the study area (30), it captures the memory of previous and present rainfall events including all surface conditions. It has been shown that environmental temperatures of 25°C−30°C are ideal for the propagation of Rift Valley fever and other disease vectors (31, 32). This is also reflected in land surface temperature shifts during the Rift Valley fever outbreaks (21). As can be noted in **Figure 9** as an example, comparing the aggregate climate variable conditions for land surface temperature between the epizootic (2011 January–March) and the interepizootic (2016 January–March) periods, temperature distribution shifts leftwards to ∼26°C–∼33°C during the epizootic period, while during the post-epizootic/interepizootic period, the distribution shifts right of climatology to ∼36°C−44°C. We performed a *t*-test to determine the significance of the differences in means between

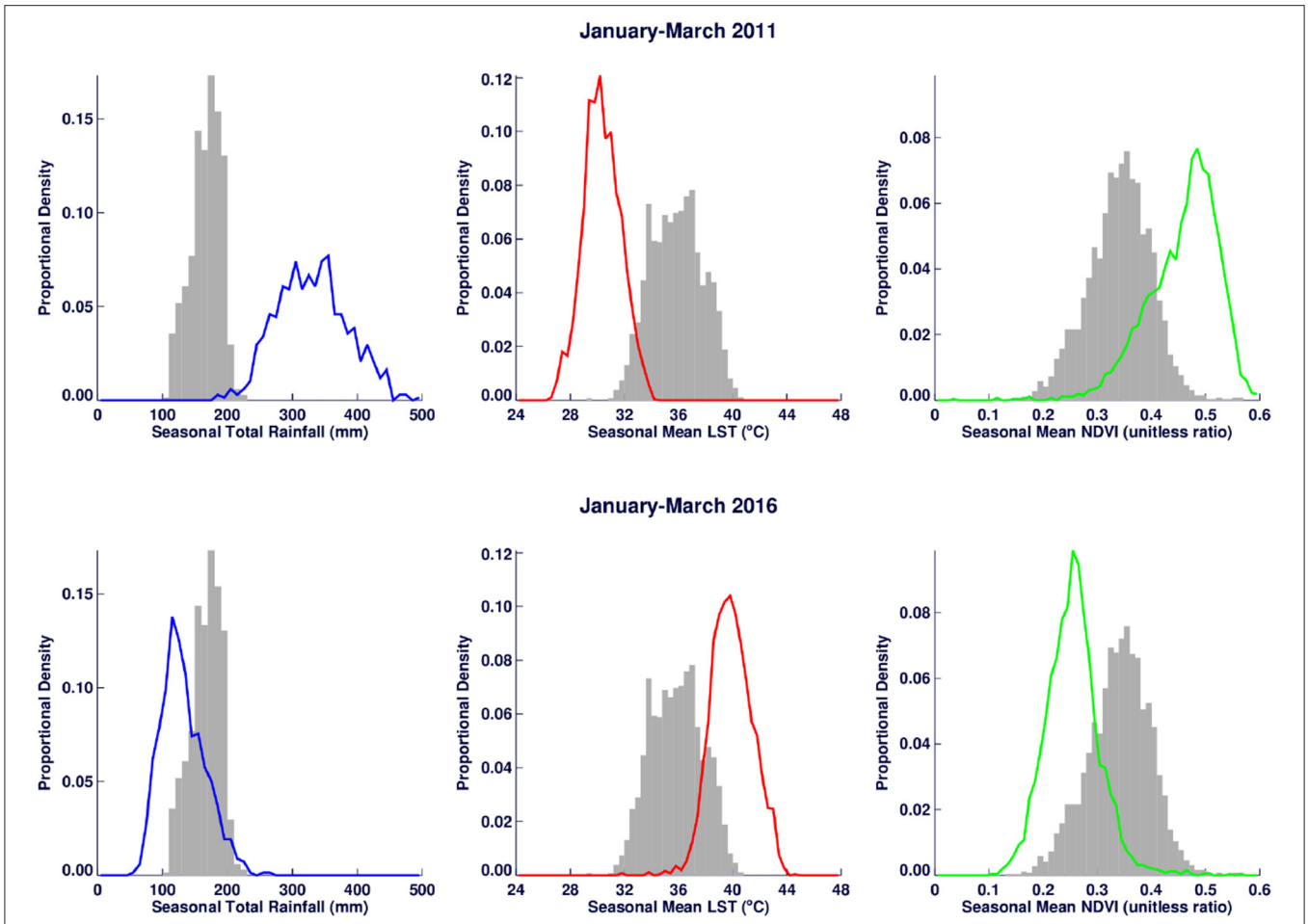

FIGURE 9 | Climate variable distribution comparisons between Rift Valley fever epizootic period (January–March 2011) (**top**) and post-epizootic period (January–March 2016) illustrates clear shift to the right of the long-term mean distribution (in rainfall and normalized difference vegetation index) and to left (land surface temperature) during the epizootic period. The distribution shifts are reversed during the interepizootic period. The gray bars represent the long-term mean distribution for each variable.

the peak seasons (January–March) of the two representative years for epizootic period against the interepizootic year (null hypothesis H0: means are the same, alternative HA: the means are different) for all the climate variables. Results indicate that we reject the null hypothesis, as indeed the means differ significantly between epizootic (2010, 2011) and post-epizootic/interepizootic year (2016) at 95% confidence level. The former conditions favor the emergence and propagation of large populations of Rift Valley fever vectors. **Supplementary Figure 4** also illustrates that for the entire study region, rainfall is consistently below or near the long-team mean during this post-epizootic period unlike the above normal rainfall conditions during the epizootic period. In addition, peak rainfall is shifted later into the season and has two peaks in February and April during the interepizootic period, which differs from the peak of January for both the climatology and the epizootic period. Accordingly, the normalized difference vegetation index is consistently below normal during the post-epizootic/interepizootic period and only approaches the long-term mean toward the end of the season in concert with rainfall. Land surface temperatures are correspondingly consistently above the long-term mean for most of the entire growing season, conditions only reach below 30°C in April and May, and it is therefore no surprise that the bulk of vectors collected throughout the entire study period are in May (**Supplementary Figure 5**). This shift in the combined climate and ecological conditions may explain the cryptic and localized outbreak that occurred during this interepizootic period in the southwest corner of the study region in May 2018 (**Figures 1**, **5**) (33, 35).

SUMMARY AND CONCLUSIONS

The post-epizootic period has been characterized to a large extent by below normal rainfall, poor vegetation conditions, and above normal land surface temperature during the growing/rainfall season (September–May). These conditions are dramatically exemplified by the nadir during the 2015/2016 growing season with low rainfall, depressed vegetation conditions, and abnormally high land surface temperatures. For the entire

study period, rainfall and normalized difference vegetation index have peaked later in the season in April; a month or two later than average. The conditions have implications for vector abundance both through space and time: a small population of vectors was collected in 2014–2016/17 seasons; only until later in the study period have we had an increased number of collections. Also given that conditions have been peaking later in the season, thermal conditions have not been favorable for propagation of large numbers of vectors with early and mid-season land surface temperatures measuring above 30°C. This aspect may partly account for the localized outbreak in April 2018 late in the growing season. As a whole; during the post-epizootic period, we can conclude that conditions have not been favorable for large scale regional Rift Valley fever activity.

Field observations have also shown us that the Free State region is a complex landscape, with numerous potential habitats—land of 10 000 pans (34)—both natural and artificial. In this respect, large-scale monitoring of drivers of climate variability such as ENSO and monitoring of proximate regional environmental indicators (rainfall, NDVI, soil moisture, etc.) to detect specific shifts in patterns can support targeted vector surveillance in high-risk areas and concurrent vaccination campaigns. This will be an effective method to prevent and control RVF and minimize the scale of costs and damage such as those during and after the 2009–2011 epizootic period. Under large-scale flood conditions, it would be impossible to manage or control an outbreak; most farmers will not be reached due to unnavigable road networks. Given the critical importance of agriculture and livestock farming, in particular to South Africa's economy and to rural livelihoods, it is imperative that the livestock agricultural industry, in partnership with the South African government, strategizes on a consistent farmer support plan of annual vaccination of the young animals using Smithburn vaccine (provided there are no cold chain issues). This will eliminate the chance of devastating outbreaks. If this were to become standard practice, it would improve and enhance the prospects of animal production to the advantage of South Africa's domestic and export markets and reduce the chance of a large-scale devastating outbreak event.

DATA AVAILABILITY STATEMENT

The original contributions presented in the study are included in the article/**Supplementary Material**, further inquiries can be directed to the corresponding author.

AUTHOR CONTRIBUTIONS

AA: conceptualization and writing—original draft. AA, RD, AK, JS, MKR, WB, RB, and CC: data collection and curation. AA and RD: formal analysis. WBK, MKR, and JTP: funding acquisition. AA, RD, JLS, WB, and MKR: methodology. RD, JLS, and WB: software. AA, RD, JLS, and WB: validation and visualization. All authors contributed to the article, writing-review and editing, and approved the submitted version.

FUNDING

Understanding Rift Valley Fever in the Republic of South Africa, PI: WK. Defense Threat Reduction Agency—Biological Threat Reduction Program (DTRA-BTRP)—Thrust Area 6, CC WMD (HDTRA-14-1-0029). The project was sponsored by the US Department of Defense, Defense Threat Reduction Agency.

ACKNOWLEDGMENTS

We would like to thank our One Health field team (Lara Van Staden and Albie Loots) from ExecuVet that assisted with field work and collected mosquito vector data used in this study. We would also like to acknowledge the contributions of Dr. Seth C. Britch (USDA-ARS-CMAVE) in reviewing early versions this manuscript and two anonymous reviewers for their critical comments that helped improve the manuscript.

SUPPLEMENTARY MATERIAL

The Supplementary Material for this article can be found online at: https://www.frontiersin.org/articles/10.3389/fvets.2021.730424/full#supplementary-material

REFERENCES

1. Meegan J, Bailey C. Rift Valley fever. In *Arboviruses: Epidemiology and Ecology*, vol. IV. Monath TP, ed. Boca Raton, FL: CRC Press Inc. (1989). p. 51–76. doi: 10.1201/9780429289170-4
2. Paweska JT, van Vuren PJ. Rift Valley Fever Virus: A Virus with Potential for Global Emergence. In: *The Role of Animals in Emerging Viral Diseases* (ed. Johnson, N.) Ch. 8. Academic Press. (2014) p.169–200. doi: 10.1016/B978-0-12-405191-1.00008-9
3. Anyamba A, Linthicum KJ, Small JS, Britch SC„ Pak E, de La Rocque S, et al. Prediction, assessment of the Rift Valley fever activity in East and Southern Africa 2006–2008 and possible vector control strategies. *Am J Trop Med Hyg.* (2010) 83:43–51. doi: 10.4269/ajtmh.2010.09-0289
4. Linthicum KJ, Anyamba A, Tucker CJ, Kelley PW, Myers MF, Peters CJ. Climate and satellite indicators to forecast rift valley fever epidemics in Kenya. *Science.* (1999) 285:397–400. doi: 10.1126/science.285.5426.397
5. Little PD. Hidden Value on the Hoof: Cross-Border Livestock Trade in Eastern Africa. Common Market for Eastern and Southern Africa Comprehensive African Agriculture Development Program, Policy Brief Number 2, February 2009. (2009). Available online at: http://www.nepad-caadp.net/pdf/COMESA%20CAADP%20Policy%20Brief%202%20Cross%20Border%20Livestock%20Trade%20(2).pdf
6. Mdlulwa Z, and Ngwane CB. Evaluating the impact of 2010 Rift Valley fever outbreaks on sheep numbers in three provinces of South Africa. *Afr J Agric Res.* (2016) 12:979–86, doi: 10.5897/AJAR2016.11130
7. Mdlulwa Z. (2015). *The socio-economic impact the of 2008–2010 Rift Valley fever outbreaks on livestock farmers in South Africa* (M.Sc. Thesis). Pretoria: University of Pretoria.
8. Brand RF, Rostal MK, Kemp A, Anyamba A, Zwiegers H, Van Huyssteen CW, et al. A phytosociological analysis and description of wetland vegetation and ecological factors associated with locations of high mortality for the 2010-11 Rift Valley fever outbreak in South Africa. *PLoS ONE.* (2018) 13:e0191585. doi: 10.1371/journal.pone.0191585

9. Verster A, Liang J, Rostal MK, Kemp A, Brand R, Anyamba A, et al. Selected wetland soil properties correlate to Rift Valley fever livestock mortalities reported in 2009-10 in central South Africa. *PLoS ONE.* (2020) 15:e0232481. doi: 10.1371/journal.pone.0232481
10. Msimang V, Thompson PN, Jansen van Vuren P, Tempia S, Cordel C, Kgaladi J, et al. Rift Valley fever virus exposure amongst farmers, farm workers, and veterinary professionals in central South Africa. *Viruses*. (2019) 11:140. doi: 10.3390/v11020140
11. Ngoshe YB, Avenant A, Rostal MK, Karesh WB, Paweska PT, van Vuren PJ, et al. Patterns of Rift Valley fever virus seropositivity in domestic ruminants in central South Africa four years after a large outbreak. *Sci Rep*. (2020) 10:5489. doi: 10.1038/s41598-020-62453-6
12. Linthicum KJ, Bailey CL, Davies FG, Tucker CJ. Detection of Rift Valley fever viral activity in Kenya by satellite remote sensing imagery. *Science.* (1987) 235:1656–9. doi: 10.1126/science.3823909
13. Anyamba A, Linthicum J, Mahoney R, Tucker CJ, Kelly PW. Mapping potential risk of rift valley fever outbreaks in african savannas using vegetation index time series data. *Photogrammetric Engineering Remote Sensing: Special Issue – Remote Sensing and Human Health.* (2002) 68:137–45. Available online at: https://www.scinapse.io/papers/1571759017
14. Mosomtai G, Evander M, Sandström P, Ahlm C, Sang R, Hassan OA, et al. Association of ecological factors with Rift Valley fever occurrence and mapping of risk zones in Kenya. *J Glob Infect Dis*. (2016) 46:49–55. doi: 10.1016/j.ijid.2016.03.013
15. Pienaar NJ, and Thompson PN. Temporal and spatial history of Rift Valley fever in South Africa: 1950 to 2011. *Onderstepoort J Vet Res*. (2013) 80:384. doi: 10.4102/ojvr.v80i1.384
16. Grobbelaar AA, Weyer J, Leman PA, Kemp A, Paweska JT, Swanepoel R. Molecular epidemiology of rift valley fever virus. *Emerg Infect Dis.* (2011) 17:2270–6. doi: 10.3201/eid1712.111035
17. Mucina L, and Rutherford MC. The vegetation of South Africa, Lesotho and Swaziland. Strelitzia 1. Pretoria: South African National Biodiversity Institute (2006). Available Online at: https://www.sanbi.org/wp-content/uploads/2018/05/Strelitzia-19.pdf
18. Novella NS, and Thiaw WM. African rainfall climatology version 2 for famine early warning systems. *J Appl Meteor Climatol*. (2013) 52:588–606, doi: 10.1175/JAMC-D-11-0238.1
19. Townshend JRG, Justice CO. Towards operational monitoring of terrestrial systems by moderate-resolution remote sensing. *Remote Sens Environ.* (2002) 83:351–9. doi: 10.1016/S0034-4257(02)00082-2
20. Tucker CJ. History of the Use of AVHRR Data for Land Applications. In: *Advances in the Use of NOAA AVHRR Data for Land Applications. Springer: Netherlands p.* (1996) 1–19. doi: 10.1007/978-94-009-0203-9_1
21. Anyamba A, Small JL, Britch SC, Tucker CJ, Pak EW, Reynolds CA, et al. Recent Weather Extremes and Impacts on Agricultural Production and Vector-Borne Disease Outbreak Patterns. *PLoS ONE*. (2014) 9:e92538. doi: 10.1371/journal.pone.0092538
22. Tucker CJ, Hielkema JU, and Roffey J. The potential of satellite remote sensing of ecological conditions for survey and forecasting desert-locust activity. *Int J Remote Sens*. (1985) 6:127–38. doi: 10.1080/01431168508948429
23. Tucker CJ. Red and photographic infrared linear combinations for monitoring vegetation. *Rem Sens Environ*. (1979) 8:127–150. doi: 10.1016/0034-4257(79)90013-0
24. Holben BN. Characteristics of maximum-value composite images from temporal AVHRR data. *Int J Remote Sens.* (1986) 7:1417–34. doi: 10.1080/01431168608948945
25. Wan Z, Zhang Y, Zhang Q, Li Z. Validation of the land-surface temperature products retrieved from Terra Moderate Resolution Imaging Spectroradiometer data. *Remote Sens Environ.* (2002) 83:163–80. doi: 10.1016/S0034-4257(02)00093-7
26. Karnieli A, Agam N, Pinker RT, Anderson,M., Imhoff ML, Gutman GG, et al. Use of NDVI and land surface temperature for drought assessment: merits and limitations. *J Clim*. (2010) 23:618–33. doi: 10.1175/2009JCLI2900.1
27. Davies FG, Linthicum KJ, James AD. Rainfall and epizootic Rift Valley Fever. *Bull World Health Organ.* (1985) 63:941–3.
28. Anyamba A, Chretien J, Small J, Tucker CJ, Formenty PB, Richardson JH, et al. Prediction of a Rift Valley fever outbreak. *Proc Nat Acad Sci.* (2009) 106:955–9. doi: 10.1073/pnas.0806490106
29. Wilks DS. *Statistical Methods in the Atmospheric Sciences*. Academic Press: San Diego, CA. (1995) p. 41–4.
30. Nicholson SE, Davenport, ML, Malo AR. A comparison of the vegetation response to rainfall in the Sahel and East Africa, using normalized difference vegetation index from NOAA AVHRR. *Climate Change*. (1990) 17:209–41. doi: 10.1007/BF00138369
31. Turell MJ. Effect of environmental temperature on the vector competence of Aedes fowleri for Rift Valley fever virus. *Res Virol.* (1989) 140:147–54. doi: 10.1016/S0923-2516(89)80092-5
32. Turell MJ. Effects of environmental temperature on the vector competence of *Aedes taeniorhynchus* for Rift Valley fever and Venezuelan equine encephalitis viruses. *Am J Trop Med Hyg.* (1993) 49:672–670. doi: 10.4269/ajtmh.1993.49.672
33. van Vuren PJ, Kgaladi J, Msimang V, Paweska JT. Rift Valley fever reemergence after 7 years of quiescence, South Africa, May 2018. *Emerg Infect Dis.* (2019) 25:338–41. doi: 10.3201/eid2502.181289
34. Geldenhuys JN. Classification of the Pans of the Western Orange Free State. *South African Journal of Wildlife Research.* (1982) 12.
35. van Vuren PJ, Kgaladi J, Patharoo,V., Ohaebosim P, Msimang,V., Nyokong B, et al. Human cases of Rift Valley fever in South Africa, 2018. *Vector Borne Zoonotic Dis*. (2018) 18:713–5. doi: 10.1089/vbz.2018.2357

Author Disclaimer: The content of the information does not necessarily reflect the position or the policy of the Federal government, and no official endorsement should be inferred.

Conflict of Interest: JS is employed by Science Systems and Applications, Inc.

The remaining authors declare that the research was conducted in the absence of any commercial or financial relationships that could be construed as a potential conflict of interest.

Publisher's Note: All claims expressed in this article are solely those of the authors and do not necessarily represent those of their affiliated organizations, or those of the publisher, the editors and the reviewers. Any product that may be evaluated in this article, or claim that may be made by its manufacturer, is not guaranteed or endorsed by the publisher.

frontiers in Veterinary Science

ORIGINAL RESEARCH
published: 08 March 2022
doi: 10.3389/fvets.2022.745934

High Occurrence Among Calves and Close Phylogenetic Relationships With Human Viruses Warrants Close Surveillance of Rotaviruses in Kuwaiti Dairy Farms

Mohammad A. Alotaibi[1], S. Al-Amad[1], Ali Chenari Bouket[2], H. Al-Aqeel[1], E. Haider[1], A. Bin Hijji[1], Lassaad Belbahri[3] and Faizah N. Alenezi[4]*

[1] Biotechnology Program, Environmental and Life Sciences and Research Center, Kuwait Institute for Scientific Research, Kuwait City, Kuwait, [2] East Azarbaijan Agricultural and Natural Resources Research and Education Center, Plant Protection Research Department, Agricultural Research, Education and Extension Organization (AREEO), Tabriz, Iran, [3] Laboratory of Soil Biology, University of Neuchatel, Neuchatel, Switzerland, [4] Jaber Al-Ahmad Armed Forces Hospital, Kuwait City, Kuwait

Rotavirus, one of the main pathogens causing morbidity and mortality in neonatal dairy calves worldwide, is responsible for 30–44% of cattle deaths. It is considered to be the most common etiologic agent of diarrhea in neonatal dairy calves and children, the dominant type being group A. Two hundred seventy animals from 27 farms from 2 regions of Kuwait were tested for the presence of Rotavirus serogroup A (RVA) using latex agglutination test (LAT) and reverse transcription–polymerase chain (RT-PCR) testing. RVA non-structural proteins NSP1-2, NSP4-5 and capsid protein genes VP1-7 were characterized by next generation sequencing. LAT was positive in 15.56% of the animals, and RT-PCR in 28.89%. Using RT-PCR as a reference method, LAT was 100% specific but only 83.33% sensitive. ANOVA analysis showed correlation only with the location of the farms but no significant correlation with the age and sex of the animals. Although there was a tendency of clustering of RVA positive animals, it did not reach statistical significance ($p = 0.035$ for LAT). The phylogenetic analysis showed that Kuwaiti isolates of group A rotavirus clustered with human rotaviruses. Taken together, it seems that rotavirus was present in most of the dairy farms in Kuwait. The high occurrence of the virus in calves in Kuwaiti dairy farms and the close phylogenetic affinity with human isolates warrants urgent action to minimize and control its spread between calves in farms.

Keywords: rotavirus, Kuwait, calves, RNA, phylogenetic RVA

OPEN ACCESS

Edited by:
Yashpal S. Malik, Indian Veterinary Research Institute (IVRI), India

Reviewed by:
Minakshi-Prasad, Lala Lajpat Rai University of Veterinary and Animal Sciences, India
Aman Ullah Khan, University of Veterinary and Animal Sciences, Pakistan
Himani Dhanze, Indian Veterinary Research Institute (IVRI), India

****Correspondence:***
Mohammad A. Alotaibi
maotaibi@kisr.edu.kw

Specialty section:
This article was submitted to Veterinary Infectious Diseases, a section of the journal Frontiers in Veterinary Science

Received: *22 July 2021*
Accepted: *01 February 2022*
Published: *08 March 2022*

Citation:
Alotaibi MA, Al-Amad S, Chenari Bouket A, Al-Aqeel H, Haider E, Hijji AB, Belbahri L and Alenezi FN (2022) High Occurrence Among Calves and Close Phylogenetic Relationships With Human Viruses Warrants Close Surveillance of Rotaviruses in Kuwaiti Dairy Farms. Front. Vet. Sci. 9:745934. doi: 10.3389/fvets.2022.745934

INTRODUCTION

Neonatal and young calve's diarrhea (NCD) is a common syndrome and major health issue in the livestock industry, worldwide, resulting in both short- and long-term economic consequences that stem from increased morbidity and mortality. Decreased growth rate, increased caring needs, prolonged calving time, and incidental death are the main causes of the substantial increase in the overall costs of treatment and present a serious obstacle for a sustainable livestock industry. Given that in many countries this industry is a major economic resource, the constant monitoring of livestock health is of paramount importance. Moreover, as the industry is constantly growing due to the high demand for cattle meat, milk, and milk products, the requirement for verified, consistently healthy animals is increasing.

The main etiological agent for bovine diarrhea is rotavirus A (RVA), a species of a double stranded RNA virus family, the *Reoviridae*, that acts and transmits through the gastrointestinal route. Full genomic classification has revealed a common origin for porcine, bovine and human rotavirus strains (1, 2). As with all zoonoses, the virus moves back and forth from the human caregivers to the animals and vice versa, creating a constant open pool of new infections (3). Furthermore, the transmission within the same farm imposes the immediate and timely sequestration of the infected animals, before creating viral outbreaks that affect the whole herd. Moreover, there is evidence of interspecies transmission, such as from goat to cattle (4).

RVA infections are a constant health issue across the cattle farming industry, worldwide. A decade-long study, in Brazil, revealed that the RVA cattle infection rate remains constant through the years, despite the progress in our understanding of health epidemiology, the worldwide compliance clauses and the rigorous animal testing (5). In Uruguay, a large dairy and beef producer, RVA infection occurrence in calves reaches 57%. Additionally, there was a statistically significant difference between dairy (59.5%) and beef calves (28.4%), while diarrhea was associated with higher viral load (6). In Northwest Argentina the reported occurrence was 63% in dairy farms, while in beef herds the occurrence was 40% (7). In Bangladesh, RVA RNA was detected in only 6.2% of all cattle tested (8), while in India the reported RT-PCR positivity was 10.19% (9).

In Kuwait, the Public Authority of Agriculture and Fisheries (PAAF), reports approximately 9,004 dairy cattle, with a production rate of 19.78 liters/cow (10). RVA infection has been constantly impacting severely the Kuwaiti livestock, with a mean calf mortality of almost 44% (11). Indeed, in previous RVA outbreaks, the mortality rate reached almost 90% in some farms (12, 13), with a cost of $252 per year per dead calf (14).

The present study aims to assess the current occurrence of rotavirus A infection in Kuwaiti cattle livestock, using the routine diagnostic tools that are used in real life situations (namely agglutination and RT-PCR), as well as novel next generation sequencing (NSG). We believe that this study will update the current situation of livestock in the country, help promote RVA surveillance and awareness campaigns and assist animal health authorities and policy makers draw up relevant guidelines and recommendations.

MATERIALS AND METHODS

Sampling

Fecal samples (triplicates) from 10 random calves, each <1-year old, were collected from 27 randomly selected farms from two regions, namely 25 from Sulaibiya (north) and 2 from Kabed, during a period of 12 months (January-December 2016), resulting in a total of 810 samples. Sulaibiya is a major livestock region, where 47 dairy farms and the Kuwait Cattle Research Centre of the Public Authority for Agricultural Affairs, and Fish Resources are located.

Samples of calve's feces were collected, randomly, regardless of the calf health condition or the presence/absence of any symptoms. The total number of calves in dairy farms was 852. Upon which the samples size was calculated to be around 265 and was rounded to 270 to test 10 calves from each farm so that we could achieve a statistical accuracy of 95% and a confidence interval of +/−3.45%, was calculated (15, 16).

Latex Agglutination

Approximately 10 g of calf feces was suspended in 5 ml of phosphate buffered saline solution, mixed by vortexing 30 sec, then 2 drops of fecal suspension were placed into a specific well, in order to perform latex agglutination (LAT) RVA detection, using the LTA kit Virotect-Rota, (Omega Diagnostics Ltd, UK), according to supplier instructions.

RNA Extraction

RNA was extracted using QIAamp Viral RNA Mini Kit (QIAamp Viral RNA Mini Kit, 52906, Qiagen, UK). Viral RNA extraction was performed according to the manufacturer and has been previously reported (17). The total extracted viral RNA was quantified spectrophotometrically by Nano-drop (18) to determine purity and concentration, then aliquoted and stored at−80°C, until further use.

RT-PCR

RT-PCR amplification was performed to detect RVA capsid VP7 RNA sequences, using the primers previously described. RT-PCR was first optimized to ensure the highest sensitivity (17). Briefly, 2 μl of RNA extract were reverse transcribed and amplified in a 25 μl one-step reaction for 35 cycles. The resulting amplicon was expected to be 257 bp, and it was visualized by gel electrophoresis, using 1.2% gel agarose with 0.05% ethidium bromide.

NGS of the RVA

For NGS, the non-structural proteins NSP1-2, NSP4-5 and capsid protein genes VP1-7 were selected. RNA sample concentration was adjusted to 100 ng. An RNA library was then generated using NEBNext® Ultra RNA Library Prep Kit for Illumina (New England Biolabs, UK) following manufacturer recommendations. After library quality assessment using a Bioanalyser (Agilent Technologies, UK), sequencing was carried out on a MiSeq sequencer (Illumina, UK). MiSeq reporter software (Illumina, UK) was then used to mine the generated data. Reads were aligned with the sequence of targeted rotavirus non-structural proteins NSP1-2, NSP4-5 and capsid protein genes VP1-7 and consensus sequences of the protein genes used

as reference sequences in CLC Genomics Workbench (CLC bio, UK). The assembled gene sequences were compared to reference rotavirus gene sequences using the ClustalW program within MEGA 5.05 package (19). Using PhyML version 3.0, phylogenetic trees were constructed (20) and p-distances were calculated in MEGA 5.05 to determine the similarities of the genes to reference strains in GenBank.

Statistical Analysis

Sensitivity, specificity, positive (PPV) and negative (NPV) predictive values were calculated as described at https://www.medcalc.org/calc/diagnostic_test.php.

The data were analyzed using the free access statistical software Jamovi 1.8.2.

RESULTS

Study Population

The characteristics of the participating animals are summarized in **Table 1**. The animal's ages ranged from 7 to 150 days with a mean of 45.03 days. Since these are dairy farms, most animals were female ($n = 209$) with only 61 males.

Presence of RVA Viral Infection

Out of the 270 animals 42 were positive for LAT (15.56%), almost double were positive for RT-PCR (28.89%). All LAT positive samples were RT-PCR positive, accounting for a strong correlation ($p < 0.001$), but the reverse does not apply. All triplicates showed the same result; thus, reproducibility of both LAT and PCR is 100%. **Figure 1** illustrates an example of RT-PCR for 12 samples.

Considering PCR as a reference method, the LAT sensitivity was 83.33% (73.62 to 90.58%) and specificity is 100.00% (97.97 to 100.00%). The PPV was 100.00%, while the NPV was 93.66%. Therefore, the accuracy of LAT was 95.19%.

Another observation from **Table 1** is that RVA positive cattle are clustered in specific farms at least as far as the LAT test is concerned. However, there seems to be no correlation with individual farms ($p = 0.035$ for LAT; $p = 0.264$ for RT-PCR), although it seems that the farm location is significant ($p < 0.001$ for both LAT and RT-PCR), with Kabed being associated with higher viral presence (**Table 2**). The small number of Kabed farms mandates that this correlation should be further tested and not be generalized. Moreover, sex is not correlated with RVA infection ($p = 0.027$ for LAT; $p = 0.446$ for RT-PCR). Age also does not correlate with RVA infection ($p = 0.129$ for LAT; $p = 0.133$ for RT-PCR).

Phylogenetic Analysis of Kuwaiti RVA Strains

All generated sequences have been submitted to GenBank (MH717372, MH717373, MH717374, MH717375, MH717366, MH717367, MH717368, MH717369, MH717370 and MH717371) (**Table 3**). Blast analysis of rotavirus non-structural proteins NSP1 clearly showed strong similarity with RVA NSP 1 sequences from Ireland (GQ428136), Turkey (KX212886), Thailand (LC367320) among numerous other matches.

TABLE 1 | RVA infection in male and female calves, by LTA and RT-PCR.

	Age (days)				
Farm no	Range	Mean	F/M Ratio	LTA (+)	RT-PCR (+)
1	25–90	42.0	8/2	0	3
2	30–90	51.0	8/2	0	3
3	20–120	51.0	8/2	0	0
4	20–90	54.5	8/2	1	5
5	10–150	57.0	10/0	2	4
6	20–150	72.0	10/0	1	3
7	20–25	22.0	10/0	7	10
8	8–60	25.5	5/5	10	10
9	20–60	32.0	9/1	0	1
10	20–60	34.5	9/1	0	2
11	20–75	37.0	7/3	0	0
12	7–75	36.7	7/3	0	1
13	20–75	35.5	6/4	0	0
14	15–69	44.6	6/4	1	1
15	15–75	55,0	8/2	0	0
16	7–150	38.8	9/1	0	0
17	30–120	68.0	6/4	0	0
18	20–50	37.0	10/0	0	0
19	30–90	68.0	10/0	0	0
20	30–75	54.5	10/0	0	0
21	15–30	23.7	3/7	0	0
22	15–45	25.5	9/1	0	0
23	15–90	53.5	7/3	0	0
24	25–45	36.0	6/4	0	6
25	10–30	21.5	8/2	4	8
26	20–150	61.5	8/2	9	10
27	30–120	77.5	4/6	7	10
Total			209/61	42	78

Phylogenetic analysis of Kuwaiti isolates of rotavirus group A gene sequences using either non-structural protein NSP4 or capsid protein genes VP4, 6 and 7 in single gene trees allowed confirmation that Kuwaiti isolates of rotavirus group A cluster with rotavirus group A isolates collected around the world. NSP4, VP4 and VP7 sequences showed close relationships with bovine isolates of the rotavirus, while NSP4, VP4, VP6 and VP7 additionally suggest close relationships with rotavirus isolates of simian, porcine, avian and human origins. Phylogenetic analysis using concatenated NSP4, VP4, VP6 and VP7 gene sequences unambiguously documented the close relationship of the Kuwaiti isolates with rotaviruses of human origin (**Figure 2**). The sequencing was performed for 10 samples from the 2 farms in Kabed and the 8 from the Saulibiya were sequenced, that covered all locations.

DISCUSSION

Rotavirus in calves in Kuwait represents a major challenge to dairy producers, since it is one of the contributing reasons that leads to a high rate of economic losses, e.g., in Kuwait $252

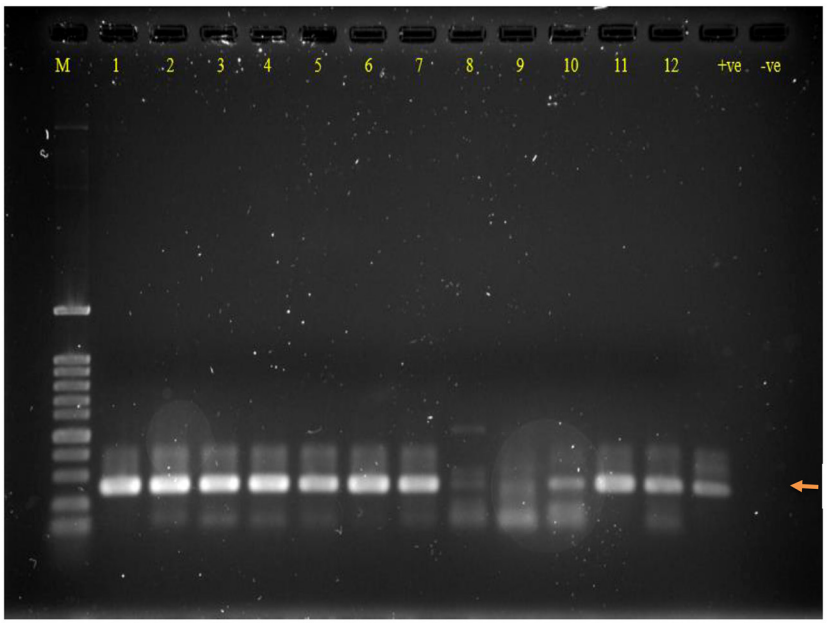

FIGURE 1 | Agarose gel electrophoresis of RT-PCR DNA product of calve's fecal samples following RNA extraction and controls. *Lane M: DNA ladder 100 bp, Lanes 1–12: samples; (+ve) RT-PCR RVA positive control; (−ve) RT-PCR negative control. RT-PCR dsDNA product size 257 bp.*

TABLE 2 | Non-parametric ANOVA correlation statistics (Kruskal-Wallis).

	LTA (+)		RT-PCR (+)	
	x^2	*p*-value	x^2	*p*-value
Age	2.30	0.129	2.261	0.133
Sex	4.88	0.027	0.581	0.446
Farm Code	4.45	0.035	1.245	0.264
Farm Site	68.04	<0.001	52.972	<0.001

per year per dead calf (14). The livestock industry is growing in Kuwait due to high domestic demand for cattle meat, milk and milk products. The annual production of milk is 4,500 l/cow and the total number of cattle in Kuwait is 27,000 (12). Calf mortality is one of the major limiting factors for the sustainable growth of livestock industry, and sometimes the mortality rate could reach up to 90% in some farms in Kuwait (12). Infectious diseases are a major cause of mortality. Rotavirus is a high-risk pathogen if not treated well in advance, and calf mean mortality in Kuwait was found to be 44% (11, 14).

In Kuwait, a study of calf mortality was performed in 2001 by Razzaque et al. (14) who reported high mean calf mortality rates as follows: 44% in preweaned calves, while in some improperly managed farms, the mortality rate reached 90%. The high mortality rate of calves, which led to a livestock and financial loss for the farmers, was shown to be due to pathogens, detected using immunological methods, causing diarrhea, pneumonia, and dehydration in calves. The detected pathogens included rotavirus as well as bacteria (*Salmonella*, *E. coli*, and *Pasteurella*). The calculated financial loss in Kuwait per dead calf was $252 (14). The study also indicated that the farmers do not provide proper protection for their calves, such as vaccination, or use biosecurity measures, such as the isolation of infected calves. The lack of these measures has led to a major problem in the management of cattle farms in Kuwait. If the infected calves recover from rotavirus infection, they will suffer from health problems, e.g., loss of weight and deficiency in providing milk (12). In addition to the significant losses through calves dying, the farmers lose even more by importing replacement heifers from outside Kuwait to compensate for their shortage (12).

The present study focuses on the presence of RVA in the dairy farms of Kuwait. The occurrence of RVA in cattle is an ongoing process, because of its paramount importance for the livelihood of the cattle industry. Our study was based on the random selection of the calves, regardless of symptoms, and therefore the observed occurrence is a screenshot of the actual virus occurrence in the country.

A recent study from India showed 20.34% of diarrhoeic cattle aged 0–3 months were RVA positive (21). In another Indian study, from a different area, the diarrhoeic animals showed an RVA occurrence of 13.11% (9). In the same study the percentages of LAT and RT-PCR are comparable, which is not the case in our study. Our results show an RVA occurrence of 15.56 and 28.89%, for LAT and RT-PCR testing, respectively. The discrepancy of these methods has been observed previously (22). Most studies report a higher percentage for the LAT test and the highest specificity for the RT-PCR (23), whilst in our study LAT positive results were all confirmed by viral genome detection, resulting in a very high specificity.

Despite the known shortcomings of LAT testing, it is a useful approach because of its convenience, low price, and possibility of

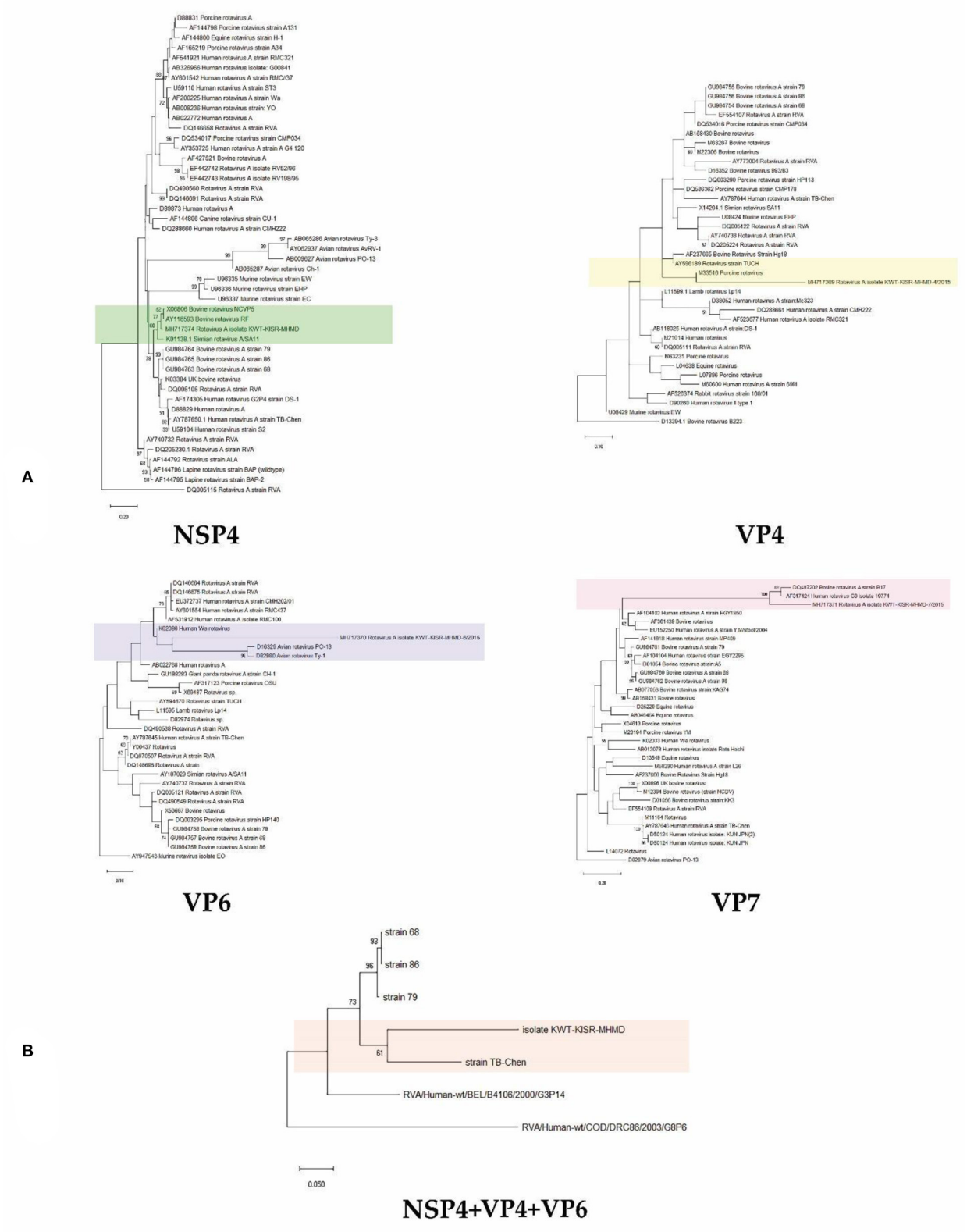

FIGURE 2 | Neighbour-joining phylogenomic tree of veterinary important viruses including KWT-KISR-MHMD isolate **(A)** using NSP4, VP4, VP6 and VP7 genes separately and **(B)** concatenated (NSP4+VP4+VP6) genes. DQ005115, D13394.1, AY947543, D82979 and RVA/Human-wt/BEL/B4106/2000/G3P14 were used as outgroups, respectively. Supports for branches were assessed by bootstrap resampling of the data set with 1000 replications.

TABLE 3 | Rotavirus group A Kuwaiti isolate gene sequences and their accession numbers.

GenBank accession number	Gene location
MH717372	NSP1 gene, partial cds
MH717373	NSP2-like gene, complete sequence
MH717374	NSP4-like gene, partial sequence
MH717375	NSP5-like gene, complete sequence
MH717366	VP1 capsid protein gene, partial cds
MH717367	VP2 capsid protein gene, partial cds
MH717368	VP3 capsid protein gene, partial cds
MH717369	VP4 capsid protein gene, partial cds
MH717370	VP6 capsid protein gene, partial cds
MH717371	VP7 capsid protein gene, partial cds

use in the field by non-specialized personnel (24). Nevertheless, our results showed a lot of missed animals, and thus reveal potential sources of viral spread and farm contamination. ELISA is another alternative with a good correlation to RT-PCR testing (25), but requires a laboratory setting to be conducted.

Another observation of our study was that if one animal is found positive with either technique, the possibility of having more infected animals within the same herd is quite large. It was obvious from our results that there were clusters of infection, while very few farms were virus free. We also found that one region had significantly higher occurrence of the virus than the other, however, the under-representation of the second region might account for skewed results. Overall, the detected RVA presence within our farms is quite high and further measures to contain the viral spread should be implemented (17). Vaccination of cattle has been proven to be beneficial against RVAG6 as this genotype does not appear in calves born by vaccinated mothers. Additionally, it is known that vaccination against RVA reduces the incidence of diarrhea independent of infection genotype (26). Current research has demonstrated a possible way of passive immunization of cattle with anti-bovine RVA immunoglobulin yolks (IgYs) from hens immunized with the two RVAs with different genotypes [G6P (5) and G10P (11)]. If it is confirmed, it will provide another tool against RVAs (27).

Phylogenetic analysis using concatenated NSP4, VP4, VP6 and VP7 gene sequences showed that they were all clustering within the RVA strains, having a 94% nucleotide sequence similarity. The presence of only one strain may be explained by the small size of the country and the relatively small cattle population, compared to bigger exporters and breeders worldwide. Moreover, there was a sequence affiliation with rotaviruses of human origin, suggesting a zoonotic transmission. Rotaviruses are known to have wide host range, infecting many animal species as well as humans. RVA groups A to C have been shown to infect both humans and animals. A study in Iran also highlighted the possibility of mixed rotavirus infections, in a percentage as high as 30.4% (28). A study in India, using human rotavirus specific primers, found that 2 / 230 sheep, goats and neonatal lamps fecal samples were positive for group A rotavirus (29). Given that the region with the highest occurrence in our study is known for sheep farming, we cannot exclude interspecies transmission. In Turkey, 55.33% of sheep have tested positive for RVA (30), while a similar study in Spain showed 42.6 % to harbor a mixed infection (31). The most commonly detected strains in both human and animals are G2, G3, G4, and G9, P (3).

Whilst we made sure to have a statistical validation of our sampling, nevertheless we were not able to collect samples from all dairy farms of Kuwait. Therefore, we cannot generalize our findings to the whole country. However, our results provide enough proof that rigorous preventive screening of cattle, nationwide, is imperative. Another limitation is that Kuwait is a rather small country, thus the livestock population is also limited. Big studies are therefore limited by the size of the state. The proximity of Kuwait to other large international cattle producers (e.g., India) makes our findings valuable, as trans-border infections are possible.

The present study provides baseline data for occurrence of group A rotavirus in calves under 1 year of age in Kuwait. Further in-depth studies are required to determine any correlation of the calve's viral strain with the human viral strain.

CONCLUSION AND RECOMMENDATIONS

Rotavirus is highly present all the year in calves regardless of the animal's location in Kuwait, and the virus should be included in detection and control programs by farmers and Public Authority of Agriculture and Fisheries Resources (PAAFR).

LAT could be used by farmers because of its simplicity, rapidity, and low cost when compared with molecular techniques.

Since there are advantages of LAT, it is recommended to use it for initial screening of rotavirus in dairy farms, and if there is a positive sample(s) in a farm, extend the detection using RT-PCR in all calves in the same farm to determine the precise number of calves infected with the virus.

Rotavirus screening is recommended to be in the list of pathogens by PAAFR for all dairy farms in Kuwait.

DATA AVAILABILITY STATEMENT

The datasets presented in this study can be found in online repositories. The names of the repository/repositories and accession number(s) can be found in the article/**Supplementary Material**.

ETHICS STATEMENT

The animal study was reviewed and approved by Kuwait Agricultural and Fisheries Agency. Written informed consent for participation was not obtained from the owners because the authorization was taken from the Governmental Agency.

AUTHOR CONTRIBUTIONS

MA: project leader. AH: samples collection. SA-A, HA-A, and EH: RNA extraction, quantification, PCR amplification, gel electrophoresis, and documentation. AC, LB, and FA: performed dissemination, genetic analysis, and interpretation for viral genome. Genetic sequencing was completed in University of Leicester, UK. All authors contributed to the article and approved the submitted version.

FUNDING

This research was completely funded and supported by Kuwait Institute for Scientific Research (Kuwait).

ACKNOWLEDGMENTS

We thank the Public Authority for Agriculture Affairs and Fisheries Resources for their support. We also extend our thanks to Dr. Abdulrahman Alkandary, Ms Hanadi Bastaki and all the staff in Sulaibiyah, Kabd and the other PAAFR farms for fecal calves sampling permission and collection.

SUPPLEMENTARY MATERIAL

The Supplementary Material for this article can be found online at: https://www.frontiersin.org/articles/10.3389/fvets.2022.745934/full#supplementary-material

REFERENCES

1. Matthijnssens J, Ciarlet M, Heiman E, Arijs I, Delbeke T, McDonald SM, et al. Full genome-based classification of rotaviruses reveals a common origin between human Wa-Like and porcine rotavirus strains and human DS-1-like and bovine rotavirus strains. *J Virol.* (2008) 82:3204–19. doi: 10.1128/JVI.02257-07
2. Tacharoenmuang R, Komoto S, Guntapong R, Ide T, Sinchai P, Upachai S, et al. Full genome characterization of novel DS-1-Like G8P[8] rotavirus strains that have emerged in thailand: reassortment of bovine and human rotavirus gene segments in emerging DS-1-like intergenogroup reassortant strains. *PLoS ONE.* (2016) 11:e0165826. doi: 10.1371/journal.pone.0165826
3. Geletu US, Usmael MA, Bari FD. Rotavirus in calves and its zoonotic importance. *Vet Med Int.* (2021) 2021:6639701. doi: 10.1155/2021/6639701
4. Alaoui Amine S, Melloul M, El Alaoui MA, Boulahyaoui H, Loutfi C, Touil N, et al. Evidence for zoonotic transmission of species a rotavirus from goat and cattle in nomadic herds in Morocco, 2012-2014. *Virus Genes.* (2020) 56:582–93. doi: 10.1007/s11262-020-01778-w
5. Medeiros TNS, Lorenzetti E, Massi RP, Alfieri AF, Alfieri AA, Medeiros TNS, et al. Neonatal diarrhea and rotavirus A infection in beef and dairy calves, Brazil, 2006-2015. *Pesqui Vet Bras.* (2020) 40:7–11. doi: 10.1590/1678-5150-pvb-5919
6. Castells M, Caffarena RD, Casaux ML, Schild C, Miño S, Castells F, et al. Phylogenetic analyses of rotavirus A from cattle in uruguay reveal the circulation of common and uncommon genotypes and suggest interspecies transmission. *Pathogens.* (2020) 9:570. doi: 10.3390/pathogens9070570
7. Bertoni E, Aduriz M, Bok M, Vega C, Saif L, Aguirre D, et al. First report of group A rotavirus and bovine coronavirus associated with neonatal calf diarrhea in the northwest of Argentina. *Trop Anim Health Prod.* (2020) 52:2761–8. doi: 10.1007/s11250-020-02293-8
8. Hossain MB, Rahman MdS, Watson OJ, Islam A, Rahman S, et al. Epidemiology and genotypes of group A rotaviruses in cattle and goats of Bangladesh, 2009-2010. *Infect Genet Evol.* (2020) 79:104170. doi: 10.1016/j.meegid.2020.104170
9. Makwana PM, Kalyani I, Desai D, Patel J, Solanki J, Patel D, et al. Detection of bovine rotavirus (BRV) infection in neonatal calves of in and around Navsari district of South Gujarat, India. *J Entomol Zool Stud.* (2020) 8:1092–7.
10. Public Authority of Agriculture Affairs and Fish Resources. *Annual Statistical Bulletin 2019-2020.* (2019). Available online at: http://www.paaf.gov.kw/
11. Majeed QAH, Al-Batel MK, Abdou N-EMI, El-Azazy OME, Sami AM, El-Said H. Infectious causes of neonatal diarrhea in cattle in Kuwait with special reference to cryptosporidiosis. *J Anim Vet Adv J.* (2011) 10:2282–6. doi: 10.3923/javaa.2011.2282.2286
12. Razzaque M, Bedair M, Al-Mutawa S. Economic impact of calf mortality on dairy farms in Kuwait. *Pakistan Vet J.* (2009) 29:97–101.
13. Razzaque MA, Al-Mutawa T, Abbas S, Bedair M. Performance of pre-weaned dairy calves under hot arid environment: effects of immunoglobulins and age on diseases and mortality. *Am J Appl Sci.* (2009) 6:1885–91. doi: 10.3844/ajassp.2009.1885.1891
14. Razzaque MA, Sharp D, Al-Mutawa T, Al-Muhanna M, Abbas S, Shalaby AR, et al. *Field and laboratory investigation of calf mortality in Kuwait and its economic impact on dairy production*. (No. KISR6004). Kuwait Institute for Scientific Research (2001). Available online at: https://krc.kuwaitresearch.com/1/264
15. Del Siegle. *Neag School of Education – University of Connecticut*. (2020). Availablibe online at: https://researchbasics.education.uconn.edu/sample-size/# (accessed June 2021).
16. Creative Research Systems. *Sample Size Calculator—Confidence Level, Confidence Interval, Sample Size, Population Size, Relevant Population* - (2012). Available online at: https://www.surveysystem.com/sscalc.html
17. Alotaibi MA. Internalisation of enteric viruses by acanthamoeba castellanii, via ingestion of virus-infected mammalian cells. *Food Environ Virol.* (2011) 3:109–14. doi: 10.1007/s12560-011-9067-4
18. Hayasaka D, Aoki K, Kouichi M. Development of simple and rapid assay to detect viral RNA of tick-borne encephalitis virus by reverse transcription-loop-mediated isothermal amplification. *Virol J.* (2013) 10:1–10. doi: 10.1186/1743-422X-10-68
19. Tamura K, Peterson D, Peterson N, Stecher G, Nei M, Kumar S. MEGA5: molecular evolutionary genetics analysis using maximum likelihood, evolutionary distance, and maximum parsimony methods. *Mol Biol Evol.* (2011) 28:2731–9. doi: 10.1093/molbev/msr121
20. Guindon S, Dufayard J-F, Lefort V, Anisimova M, Hordijk W, Gascuel O. New algorithms and methods to estimate maximum-likelihood phylogenies: assessing the performance of PhyML 3.0. *Syst Biol.* (2010) 59:307–21. doi: 10.1093/sysbio/syq010
21. Sruthy S, Tumlam U, Warke S, Ingle V, Bhojane G, Hedau M. VP6 gene based RT-PCR for detection of rotavirus associated with diarrhea in bovine calves. *J Entomol Zool Stud.* (2019) 7:373–6.
22. Soltan MA, Tsai Y-L, Lee P-YA, Tsai C-F, Chang H-FG, Wang H-TT, et al. Comparison of electron microscopy, ELISA, real time RT-PCR and insulated isothermal RT-PCR for the detection of Rotavirus group A (RVA) in feces of different animal species. *J Virol Methods.* (2016) 235:99–104. doi: 10.1016/j.jviromet.2016.05.006
23. Hamzavi H, Azaran A, Makvandi M, Karami S, Ardakani MR, Nejad ASM. Performance of latex agglutination, ELISA and RT-PCR for diagnosis of Rotavirus infection. *J Biol Res.* (2017) 90:2. doi: 10.4081/jbr.2017.6522
24. Cho Y, Yoon K-J. An overview of calf diarrhea—infectious etiology, diagnosis, and intervention. *J Vet Sci.* (2014) 15:1–17. doi: 10.4142/jvs.2014.15.1.1
25. Abouelyazeed EA, Hassanien RT, Afify AF. Cross Sectional Study for Evaluation of Rapid Test and RT-PCR in Detection of BRV in Fecal Samples of Diarrhetic Calves in Egypt. *Adv Anim Vet Sci.* (2020) 9:387–92. doi: 10.17582/journal.aavs/2021/9.3.387.392
26. Fritzen JTT, Oliveira MV, Lorenzetti E, Miyabe FM, Viziack MP, Rodrigues CA, et al. Longitudinal surveillance of rotavirus A genotypes circulating

in a high milk yield dairy cattle herd after the introduction of a rotavirus vaccine. *Vet Microbiol.* (2019) 230:260–4. doi: 10.1016/j.vetmic.2019.02.022

27. Odagiri K, Yoshizawa N, Sakihara H, Umeda K, Rahman S, Nguyen SV, et al. Development of genotype-specific anti-bovine rotavirus A immunoglobulin yolk based on a current molecular epidemiological analysis of bovine rotaviruses A collected in Japan during 2017–2020. *Viruses.* (2020) 12:1386. doi: 10.3390/v12121386
28. Lorestani N, Moradi A, Teimoori A, Masodi M, Khanizadeh S, Hassanpour M, et al. Molecular and serologic characterization of rotavirus from children with acute gastroenteritis in northern Iran, Gorgan. *BMC Gastroenterol.* (2019) 19:100. doi: 10.1186/s12876-019-1025-x
29. Choudhary P, Minakshi P, Ranjan K, Basanti B. Zooanthroponotic transmission of rotavirus in Haryana State of Northern India. *Acta Virol.* (2017) 61:77–85. doi: 10.4149/av_2017_01_77
30. Yilmaz V, Timurkan MO, coşkun N, Yildirim Y. Investigation of Rotavirus infection in sheep using serological and molecular techniques. *Indian J Anim Res.* (2017) 51:525–30. doi: 10.18805/ijar.11463
31. Benito AA, Monteagudo LV, Arnal JL, Baselga C, Quílez J. Occurrence and genetic diversity of rotavirus A in faeces of diarrheic calves submitted to a veterinary laboratory in Spain. *Prev Vet Med.* (2020) 185:105196. doi: 10.1016/j.prevetmed.2020.105196

Conflict of Interest: The authors declare that the research was conducted in the absence of any commercial or financial relationships that could be construed as a potential conflict of interest.

Publisher's Note: All claims expressed in this article are solely those of the authors and do not necessarily represent those of their affiliated organizations, or those of the publisher, the editors and the reviewers. Any product that may be evaluated in this article, or claim that may be made by its manufacturer, is not guaranteed or endorsed by the publisher.

frontiers | Frontiers in Veterinary Science

TYPE Original Research
PUBLISHED 28 July 2022
DOI 10.3389/fvets.2022.754255

OPEN ACCESS

EDITED BY
Levon Abrahamyan,
Université de Montréal, Canada

REVIEWED BY
Mark Wilber,
University of Tennessee, Knoxville, United States
Ahmed Ragab Elbestawy,
Damanhour University, Egypt

*CORRESPONDENCE
Kimihito Ito
itok@czc.hokudai.ac.jp

SPECIALTY SECTION
This article was submitted to Veterinary Epidemiology and Economics, a section of the journal Frontiers in Veterinary Science

RECEIVED 06 August 2021
ACCEPTED 30 June 2022
PUBLISHED 28 July 2022

CITATION
Kim K and Ito K (2022) Targeted sampling reduces the uncertainty in force of infection estimates from serological surveillance. *Front. Vet. Sci.* 9:754255. doi: 10.3389/fvets.2022.754255

Targeted sampling reduces the uncertainty in force of infection estimates from serological surveillance

Kiyeon Kim and Kimihito Ito*

Division of Bioinformatics, International Institute for Zoonosis Control, Hokkaido University, Sapporo, Japan

Age bins are frequently used in serological studies of infectious diseases in wildlife to deal with uncertainty in the age of sampled animals. This study analyzed how age binning and targeted sampling in serological surveillance affect the width of the 95% confidence interval (CI) of the estimated force of infection (FOI) of infectious diseases. We indicate that the optimal target population with the narrowest 95% CI differs depending on the expected FOI using computer simulations and mathematical models. In addition, our findings show that we can substantially reduce the number of animals required to infer transmission risk by tailoring targeted, age-based sampling to specific epidemiological situations.

KEYWORDS

serological surveillance, wildlife, catalytic model, force of infection, confidence intervals, targeted sampling

Introduction

Serological surveillance monitors how fractions of individuals in a population have been infected with a specific infectious disease in the past or present. Serological tests analyze the level of pathogen-specific antibodies in the serum of individuals. Seroprevalence, the relative frequency of seropositive individuals in the population, helps us understand the epidemiology of the infectious disease, especially when the disease is asymptomatic or mildly symptomatic (1, 2). The data from serological surveillance are used to study the epidemiology of infectious diseases in humans (3), livestock (4), pet animals (5), and wildlife (6).

With mathematical models, seroprevalence data are analyzed to make an epidemiological inference. The basic reproduction number (R_0) is one of the most vital epidemiological quantities, defined as the average number of secondary cases arising from a single infectious individual when it is exposed to a susceptible population (7). The force of infection (FOI) is another key epidemiological quantity, defined as the per capita rate at which susceptible individuals acquire infection (7). Various approaches have been applied to evaluate the FOI of endemic infectious diseases. Examples include the catalytic model assuming constant FOI within a homogeneously mixed population (8) and linear

infection model with FOI changing linearly with age (9), the polynomial infection model that generalizes the linear infection model (10), and the exponentially damped linear model assuming an initially increasing FOI and an exponentially damping FOI with age (11). Using these models, the calculation of FOI requires the numbers of seropositive and seronegative individuals coupled with their age.

Currently, the age of domestic animals can be obtained in most countries. In contrast, the age of animals is inferred from age-dependent characteristics. For example, the age can be estimated by assessing animals' teeth (12–16). These approaches are applied after anesthetizing or killing the animals, and it is challenging to apply them to endangered animal species for their conservation. Some of their ages were obtained by tracking the animals from birth (17). Furthermore, measurement of size, weight, gum line recession, wear of a tooth, and tail length (18, 19) can be used to estimate the age of animals. Some studies have inferred animal age using the length of telomere (20) or the percentage of methylated DNA in specific genes (21).

Age binning is used in epidemiological studies of wildlife. It can be considered stratified sampling, which divides the population into homogeneous groups called stratum and collects samples from the strata (22). It is known that the variances of estimated quantities from stratified sampling are smaller than that from random sampling, especially when each stratum becomes homogeneous concerning the quantities under study. D' Amato et al. indicated that stratified sampling could reduce uncertainty in the mortality projections under a log bilinear Poisson Lee-Carter model (23). Age groups in wildlife studies are designed so that animals in the same age group share the same characteristics, such as physiology, behavior, and feeding, which affect disease transmission. The stratification of animals using their age may reduce the uncertainty in FOI since animals in the same bin are expected to have the same seroprevalence. Many studies use stratified sampling across animal ages for serological surveillance (24–27). Nevertheless, there is no preceding theoretical work studying the effect of stratified sampling on the confidence interval of FOI in serological surveillance.

This study analyzed how age binning and targeted sampling in serological surveillance affect the width of 95% CIs of the FOI of infectious diseases. We optimized the age group from which samples were drawn to minimize the width of 95% CI of the FOI. We assumed a situation where the exact ages of sampled animals are unknown and/or the age group from which sampling is allowed is limited. We show that using computer simulations and mathematical models, the optimal target population with the narrowest CI differs depending on the FOI. Moreover, we concluded by discussing the situations where surveillance targeting a specific age group is most beneficial.

Materials and methods

Model of seroprevalence

This study used a simple catalytic curve to model the seroprevalence of infectious diseases under endemic equilibrium (28). The catalytic model may not be common in the serological study of wildlife infection. Since our purpose is to investigate the effect of age binning on the CI of estimated FOI, we used this model to keep our mathematical model simple. The model assumes that (1) the population is homogeneously mixed, (2) FOI λ is constant over all age groups, and (3) infected individuals acquire a lifelong immunity (28). The proportion of seropositive individuals at age a, $p(a)$, is approximated by a simple catalytic curve,

$$p(a) \approx 1 - \exp(-\lambda a). \quad (1)$$

Let L be the lifespan of the target animal under surveillance. An age group of animals can be represented by $G(qL, rL)$, where qL and rL are the lower and upper bound ages of the age group, such that $0 \leq q \leq r \leq 1$. We set lifespan L to 150 weeks for the simulations and numerical analysis in this study. We assumed that all infected animals recover from their infections and none of them die of the infection. We also assumed that all animals die at an expected lifespan, called the Type 1 survival model. Therefore, the ages of animals in the population are uniformly distributed from 0 to L. Although these assumptions do not hold for wildlife populations, this simple model provided an analytically tractable means to evaluate the effect of targeted sampling on the CIs of estimated FOI.

Simulation of serological surveillance

Serological surveillance focusing on an age group $G(qL, rL)$ was simulated using samples made up of N animals whose ages were randomly chosen from a uniform real distribution ranging from qL to rL. Animal i at age a_i was set to be positive with probability $p(a_i)$ and negative with probability $1 - p(a_i)$ according to Eq. (1). We assume no error in diagnosis, that is, there is no false-positive or false-negative detection of pathogen-specific antibodies.

Estimation of λL

From the ages of seropositive and seronegative animals, FOI λ can be estimated by maximizing the following likelihood function,

$$L(\lambda; a_1, \ldots, a_k, a_{k+1}, \ldots, a_N) = \prod_{i=1}^{k} p(a_i) \prod_{i=k+1}^{N} (1 - p(a_i)) \quad (2)$$

where $a_1, \ldots, a_k$ are ages of seropositive animals and $a_{k+1}, \ldots a_N$ are ages of seronegative animals.

Let $p\,(qL, rL)$ be the probability that an animal in $G\,(qL, rL)$ is seropositive. From the uniform assumption on the age distribution, $p\,(qL,\ rL)$ is given by

$$p\left(qL, rL\right) = \frac{\int_{qL}^{rL} p\,(t)\,dt}{\left(r-q\right)L} = 1 + \frac{\exp\left(-r\lambda L\right) - \exp\left(-q\lambda L\right)}{\left(r-q\right)\lambda L}. \quad (3)$$

Let k be the number of seropositive samples among a total of N samples. The FOI λ can be estimated by maximizing the likelihood function of λ given by

$$L\left(\lambda\,;N,k\right) = \binom{N}{k}\left(p\left(qL,rL\right)\right)^k\left(1-p\left(qL,rL\right)\right)^{N-k}. \quad (4)$$

In the case we draw samples from m age groups, the likelihood function is represented as a product of Eq. (4) as follows:

$$L\left(\lambda\,;N_1,\ldots,N_m,k_1,\ldots,k_m\right) = \prod_{i=1}^{m}\binom{N_i}{k_i}\left(p_{pos}\left(q_iL,r_iL\right)\right)^{k_i}\left(1-p_{pos}\left(q_iL,r_iL\right)\right)^{N_i-k_i} \quad (5)$$

where, q_i and r_i are the ratios of the lower and upper bound ages of the ith age group to L.

When we assume that all samples are collected at the age of lifespan L, Eq. (1) can be used instead of Eq. (3), and we get

$$p\,(L,L) = 1 - \exp\left(-\lambda L\right). \quad (6)$$

The likelihood function is represented by Eq. (4).

Note that the basic reproduction number, R_0, can be calculated from the estimate of λ according to the formula given by Anderson and May (7) as follows:

$$R_0 = \frac{\lambda L}{1-\exp\left(-\lambda L\right)}. \quad (7)$$

If λL is large enough, Eq. (7) can be reduced to $R_0 = \lambda L$.

Sampling strategies

To investigate how age binning and targeted sampling affect the width of 95% CIs of FOI in serological surveillance, we compared CIs of λ estimated under seven different sampling strategies (Table 1). We assume that the ages of animals in the target population do not affect the probability of animals being sampled for each strategy. Strategies 0, 1, and 2 collect samples randomly from the entire population, and q and r are set to zero and one. Strategy 0 represents the ideal surveillance, under which the exact age of each sampled animal is provided. Since the likelihood function in Eq. (2) needs the result of the serological test of animals coupled with their ages, Eq. (2) can be used to estimate λ from samples only for Strategy 0. In strategies 1 and 2, samples are drawn from the entire population, but the results of serological tests of sampled animals are summed up in the age group they belong. Strategy 1 divides the population into two groups at half of their lifespan. This strategy can be considered the standard approach using two age bins adopted for serological surveillance in wildlife. The likelihood function in Eq. (5) gives the likelihood function for Strategy 1 because it collects samples from two age groups. Strategy 2 treats the entire population as a single age group and does not provide age information for the animals sampled. Equation (4) with $q = 0$ and $r = 1$ gives the likelihood function for Strategy 2.

Strategies 3, 4, 5, and 6 collect samples only from animals with a specific age or a specific age group. Strategy 3 samples only animals with an age range from zero to $0.5L$. Strategy 4 samples only animals at the age of $0.5L$. Strategy 5 samples only animals whose age ranges from $0.5L$ to L. Strategy 6 samples only animals at the age of L, animals that are dying. Values of q and r for each strategy are shown in Table 1. Equation (5) with $q = 0$ and $r = 0.5$ gives the likelihood function for Strategy 3, and Eq. (5) with $q = 0.5$ and $r = 1$ gives that for Strategy 5. Equation (2) with $a_k = 0.5$ for $1 \leq k \leq N$ gives the likelihood function for Strategy 4 and Eq. (2) with $a_k = 1$ for $1 \leq k \leq N$ gives that for Strategy 6.

For each strategy, 1,000 simulations of serological surveillance were conducted for $\lambda L = 1.5$, 3.0, and 6.0. Values of λL at 1.5, 3.0, and 6.0 are selected to represent a slightly transmissible infectious disease, for example, hepatitis E virus (29), moderately transmissible one, for example, African swine fever (30), and a highly transmissible one, for example, Bovine herpes virus 1 (31). The value of λL and its 95% CI was estimated from the numbers of seropositive and seronegative samples drawn from target age groups. The estimates of λL were calculated by maximizing the likelihood, and their CIs were calculated using profile likelihood method (32). More precisely, we calculated the intervals by finding λL of which profile likelihood is $\log\left(\textit{maximum likelihood}\right) - (\chi^2(1 - 0.05))/2$ where the degrees of freedom of χ^2 statistic is one. The width of CI was calculated by subtracting the lower bound of CI from the upper bound of CI. The width of 95% CI can be infinity and CI width of infinity were excluded from the calculation of average. We used three values for λ, 0.01, 0.02, and 0.04, of which λL were 1.5, 3, and 6, respectively, to investigate the effect of λ on CI width of estimation.

Effects of the target age group on estimation

We simulated serological tests using different values of q and r to examine the effect of q and r on the estimation of λ. We changed q from zero to one and r on q to one by a step of 0.02,

TABLE 1 Seven sampling strategy models.

Strategy	q^*	$r^\dagger$	Age category	N	Sampling target and age information
0	0	1	∞	100	Animals of all ages, exact age provided
1	0	1	2	100	Animals of all ages, two age bins, no exact age provided
2	0	1	1	100	Animals of all ages, no exact age provided
3	0	0.5	1	100	Young animals, no exact age provided
4	0.5	0.5	1	100	Animals whose age is half of the lifespan
5	0.5	1	1	100	Old animals, no exact age provided
6	1	1	1	100	Animals at dying

*q, ratio of lower boundary age of the sampled age group to lifespan.
†r, ratio of upper boundary age of the sampled age group to lifespan.

TABLE 2 Three constraints for calculating the expected width of 95% CI of λL.

Constraint	Minimum sampling age	Maximum sampling age
Constraint 1	qL	qL
Constraint 2	0	rL
Constraint 3	qL	L

where $0 \leq q \leq r \leq 1$. Estimates of λL and their 95% CI width were estimated from samples and averaged over the 1,000 simulations. The upper and lower bounds of the 95% CI of λL are calculated using the profile likelihood technique. The average width of the 95% CI was set to be undefined when more than 5% of 95% CI contained infinity.

Age group that minimizes the expected width of 95% CI of λL

Parameter q or r was modified under the three constraints in Table 2 to evaluate the link between λL and the target age group that minimizes the breadth of the 95% CI. The first constraint restricts the age of the target population to the animal at a specific age by $q = r$ and changes $q(= r)$. The second constraint fixes the lower bound q at zero and changes the upper bound r. The third constraint changes lower bound q under fixed upper bound r. Under constraints 1 and 3, we looked for the value of q having the narrowest width of 95% CI of λL for $0 \leq \lambda L \leq 10$. Under constraint 2, we looked for the value of r having the narrowest width of 95% CI. N is the number of animals sampled, and it is set to 50, 100, or 200.

Analytical approach to the expected width of 95% CI

Under the three constraints in Table 2, we can calculate the expected values of the 95% CI width of estimated λL using the normal approximation of the binomial distribution. Suppose the number of seropositive animal observations follows a binomial distribution with sample size N and seroprevalence p. Assuming that N is the number of samples and large enough, the number of seropositive animals, k, can be approximated by a normal distribution with a mean of Np and variance of $Np\ (1-p)$. In total, 95% of k will be within the following range:

$$Np - 1.96\sqrt{Np\left(1-p\right)} \leq k \leq Np + 1.96\sqrt{Np\left(1-p\right)}. \quad (8)$$

Let $\hat{p} = k/N$ be empirical seroprevalence estimated from samples, and then we obtain the following relationship:

$$p - 1.96\sqrt{p\left(1-p\right)/N} \leq \hat{p} \leq p + 1.96\sqrt{p\left(1-p\right)/N}. \quad (9)$$

If Inequality (9) is rearranged for p, we obtain the following relationship:

$$\hat{p} - 1.96\sqrt{\frac{\hat{p}\left(1-\hat{p}\right)}{N}} \leq p \leq \hat{p} + 1.96\sqrt{\frac{\hat{p}\left(1-\hat{p}\right)}{N}}. \quad (10)$$

The seroprevalence, p, at a specific age (an age group under Constraint 1) is calculated from Eq. (1). The estimated value of λL can be calculated as follows:

$$\lambda L = -\frac{\ln\left(1-p\right)}{q}. \quad (11)$$

From Inequality (10) and Eq. (11), we get the following relationship:

$$-\frac{1}{q}\ln\left(1-\hat{p}+1.96\sqrt{\frac{\hat{p}\left(1-\hat{p}\right)}{N}}\right) \leq \lambda L \leq -\frac{1}{q}\ln\left(1-\hat{p}-1.96\sqrt{\frac{\hat{p}\left(1-\hat{p}\right)}{N}}\right). \quad (12)$$

TABLE 3 Estimated values of λL and their 95% CIs for seven sampling strategies.

λL	Strategy	$q^{\star}$	$r^{\dagger}$	Age category	Estimated λL (95% CI)	CI width
1.5	0	0	1	∞	1.512 (1.112, 2.007)	0.895
	1	0	1	2	1.510 (1.102, 2.026)	0.924
	2	0	1	1	1.514 (1.078, 2.105)	1.027
	3	0	0.5	1	1.512 (1.009, 2.191)	1.182
	4	0.5	0.5	1	1.512 (1.136, 1.973)	0.837
	5	0.5	1	1	1.512 (1.159, 1.942)	0.784
	6	1	1	1	1.525 (1.186, 1.936)	0.751
3.0	0	0	1	∞	3.049 (2.300, 3.994)	1.694
	1	0	1	2	3.082 (2.288, 4.136)	1.848
	2	0	1	1	3.054 (2.174, 4.378)	2.204
	3	0	0.5	1	3.026 (2.154, 4.206)	2.052
	4	0.5	0.5	1	3.048 (2.370, 3.871)	1.500
	5	0.5	1	1	3.050 (2.334, 3.979)	1.645
	6	1	1	1	3.096 (2.310, 4.229)	1.920
6.0	0	0	1	∞	6.194 (4.477, 8.610)	4.133
	1	0	1	2	6.270 (4.328, 9.717)	5.389
	2	0	1	1	6.334 (4.116, 10.724)	6.609
	3	0	0.5	1	6.173 (4.390, 8.862)	4.472
	4	0.5	0.5	1	6.149 (4.592, 8.388)	3.796
	5	0.5	1	1	5.850 (4.030, 9.231)§	5.200
	6	1	1	1	4.548 (3.112, 7.319)✠	4.207

Simulations were repeated 1,000 times for each sampling strategy, and the estimated values, their 95% CIs, and the width of 95% CIs were averaged over repeated simulations.
$^{\star}q$: ratio of the minimum boundary age of the sampled age group to lifespan.
†r: ratio of the maximum boundary age of the sampled age group to lifespan.
§The estimation of 95% CI was averaged only for 767 successful simulations out of 1,000.
✠The estimation of 95% CI was averaged only for 201 successful simulations out of 1,000.

The width of 95% CI of λL can be estimated by subtracting the lower boundary of 95% CI of λL from the upper boundary of 95% CI of λL below:

$$\frac{1}{q}\left(\ln\left(\frac{1-\hat{p}+1.96\sqrt{\hat{p}\left(1-\hat{p}\right)/N}}{1-\hat{p}-1.96\sqrt{\hat{p}\left(1-\hat{p}\right)/N}}\right)\right). \quad (13)$$

Since the expected value of $\hat{p}$ is p, then the expected value of 95% CI width of λL is as follows:

$$\frac{1}{q}\left(\ln\left(\frac{1-p+1.96\sqrt{p\left(1-p\right)/N}}{1-p-1.96\sqrt{p\left(1-p\right)/N}}\right)\right). \quad (14)$$

Substituting p with $1-\exp\left(-\lambda Lq\right)$ the expected width of 95% CI is represented as

$$\frac{1}{q}\left(\ln\left(\frac{\exp\left(-\lambda Lq\right)+1.96\sqrt{\left(1-\exp\left(-\lambda Lq\right)\right)\exp\left(-\lambda Lq\right)/N}}{\exp\left(-\lambda Lq\right)-1.96\sqrt{\left(1-\exp\left(-\lambda Lq\right)\right)\exp\left(-\lambda Lq\right)/N}}\right)\right). \quad (15)$$

The seroprevalence, p, at a specific age group under constraints 2 and 3 is calculated from Eq. (3). However, the analytical derivation of an explicit form of λL from Eq. (3) is complicated, and we get λL using numerical analysis of Eq. (3). The expected width of 95% CI of λL was estimated using Eq. (10) in the same way as Constraint 1.

Results

Estimation by different strategies

Table 3 displays estimates of over 1,000 repeats of serological surveillance simulations, estimations of λL with 95% CIs, and the width of 95% CIs. When λL is 1.5, all strategies estimated λL close to the true value of 1.5. However, the average width of their CI showed variations among strategies. Strategies 0, 1, and 2, all sampled from the entire population, had different CI widths. This difference is attributed to the difference in information given to each strategy. Strategy 0, given the complete age information of samples, had the narrowest CI width among the three. Strategy 2, given no age information of samples, had the widest CI width. Strategy 1 was given incomplete age information, whether each animal was younger (or older) than half of their lifespan, and ranked the second of the three.

Among all strategies, Strategy 6, which takes samples only from animals at the age of death, had the narrowest 95% CI of 0.751. The second narrowest value was 0.784 with Strategy 5, which takes samples only from animals whose ages are older than half of their lifespan. These results are counter-intuitive because CI estimated from a subpopulation was narrower than Strategy 0; random sampling from the entire population with complete age information resulted in a width of 0.895. The maximum average width of CI of λL was 1.182 with Strategy 3, which takes samples only from animals whose ages are younger than half of their lifespan. When $\lambda L = 3.0$, the seven tested strategies estimated λL close to the true value of 3.0. Again, the average widths of their CI were different depending on strategies (Table 3), but the tendency was different from when $\lambda L = 1.5$. Among strategies, Strategy 4, which takes samples only from the animal at the age of half of the lifespan, had the narrowest 95% CI of 1.500. The second narrowest is Strategy 5, which takes samples only from old animals older than half of their lifespan. Again, these findings are counter-intuitive because the CIs are narrower than those of Strategy 0. In sampling Strategy 2, the largest average width of CI of λL was 2.204.

When $\lambda L = 6.0$, all strategies except Strategy 6 estimated λL close to the true value of 6.0 (Table 3). Among all strategies, Strategy 4, which takes samples only from the animal at half of the lifespan, again had the narrowest 95% CI of 3.796. The second narrowest is Strategy 0, which takes samples from animals at any age with complete age information. Seroprevalence in the old population is close to one, and the information from animals in the old population becomes uninformative. For this reason, the FOI estimated by Strategy 6 became inaccurate. Moreover, the width of CI of λL of the Strategies 5 and 6 was not available for some simulations because λL is estimated to be infinity when only seropositive animals are sampled.

Effect of target age group on estimation

Figure 1 shows the estimates and widths of 95% CI of λL estimated from samples drawn from different age groups in serological surveillance simulations. The top left corner, where $q = 0$ and $r = 1$ in each panel, represents Strategy 2 in Table 1. The point at the middle of the left edge, where $q = 0$ and $r = 0.5$, represents Strategy 3, and the point at the center of the top edge, where $q = 0.5$ and $r = 1$, represents Strategy 5. The top right corner, where $q = 1$ and $r = 1$, represents Strategy 6, and the point in the center of the panel, where $q = 0.5$ and $r = 0.5$, represents Strategy 4.

Figures 1A,B indicates that the estimates have the narrowest 95% CI in the area around the top right corner when λL is 1.5. This indicates that sampling from an old population is reliable when λL is 1.5. The reliable area changes when λL is 3.0 or 6.0. Estimates have the narrowest 95% CI in the area around the center of the diagonal line when λL is 3.0 (Figures 1C,D). The reliable area shifts to the lower left when λL is 6.0 (Figures 1E,F). The width of 95% CI became large for some combinations of q and r (black cells in Figures 1B,D,F. The widths of 95% CI were not available for other combinations (white cells in Figures 1B,D,F). These points are addressed in the discussion.

Table 4 shows the combination of q and r, which resulted in the minimum width of 95% CI of λL when λL is 1.5 or 3.0 or 6.0 in serological surveillance simulations. These results suggested that the narrowest 95% CI can be achieved by surveillance targeting the old population when λL is small and surveillance targeting the young population when λL is large. Estimations and 95% CI for combinations of q and r when λL were 1.5, 3.0, and 6.0 are provided in Supplementary Tables 1–3, respectively.

Figure 2 shows the relationship between λL and the sampling age parameter that resulted in the narrowest 95% CI. We call such a parameter value an optimum age parameter value. The optimum age parameter values for all three Constraints were one when λL is small (Figures 2A–C). The range of λL at the height of one indicates that the inclusion of the oldest members of the population is needed to minimize the width of 95% CI of λL when λL is small. For all Constraints in Table 2, the optimum age parameter values decreased as λL increased (Figures 2A–C). Table 5 shows the values of λL and their widths of 95% CI when the optimum age parameter value is 0.5 for each Constraint. The optimum age parameter value for each Constraint is older than half of the lifespan if λL is less than the value indicated in Table 5 and *vice versa*.

Figure 3 shows the relationship between λL and the narrowest width of 95% CI of estimated λL. The narrowest 95% CI of λL monotonically increases as λL increases for all Constraints regardless of the sample number N (Figure 3). Among the three constraints, Constraint 1 (solid line) has the narrowest width of 95% CI for all λL regardless of N. Comparing Constraints 2 (dashed line) and 3 (dotted line), Constraint 2 has a narrower width of 95% CI than Constraint 3 when $\lambda L \leq 3.43$, $\lambda L \leq 4.05$, and $\lambda L \leq 4.52$ for $N = 50$, 100, and 200, respectively. Constraint 3 has a narrower width of 95% CI than Constraint 2 when $\lambda L > 3.43$, $\lambda L > 4.05$, and $\lambda L > 4.52$ for $N = 50$, 100, and 200, respectively. The slope of the curve of Constraint 3 increases by a large amount compared with that of constraints 1 and 2. This result indicates that Constraint 3, where $r = 1$, should be carefully selected to estimate λL when $\lambda L > 3.43$, $\lambda L > 4.05$, and $\lambda L > 4.52$ for $N = 50$, 100, and 200, respectively.

Supplementary Figure 1 shows the relationship between the age parameter q [panels (A–C) and (G), (H), and (I)]or r [panels (D), (E), and (F)] and the expected width of 95% CI of λL. The narrowest width of 95% CI of λL decreases as λL decreases. Supplementary Figure 1 shows how the sample number affects the width of 95% CI of λL. The expected width of 95% CI of estimated λL decreased as the number of samples increased.

Discussion

This study analyzed how age binning and targeted sampling affected the accuracy of the estimation of the FOI, λ. Assuming that infectious diseases are endemic in a homogeneously mixed population with constant λ over age under lifelong immunity, we found that the age group that minimizes the width of 95% CI of λL was different depending on the value of λ and the number of samples N.

Using simulations of serological surveillance, we found that surveillance targeting a specific age or age group resulted in a narrower 95% CI of estimated λL than the standard age-binned sampling from the entire population (Strategy 1) in particular situations (Table 3). Surveillance targeting animals older than half of their lifespan (Strategy 5) had a narrower 95% CIs than not only a standard wildlife surveillance approach targeted the entire population using two age bins (Strategy 1) but also well-informed surveillance that targeted the entire population with precise age (Strategy 0) and when $\lambda L = 1.5$ (Table 3). Surveillance targeted animals younger than half of their lifespan (Strategy 3) had a narrower 95% CIs than Strategy

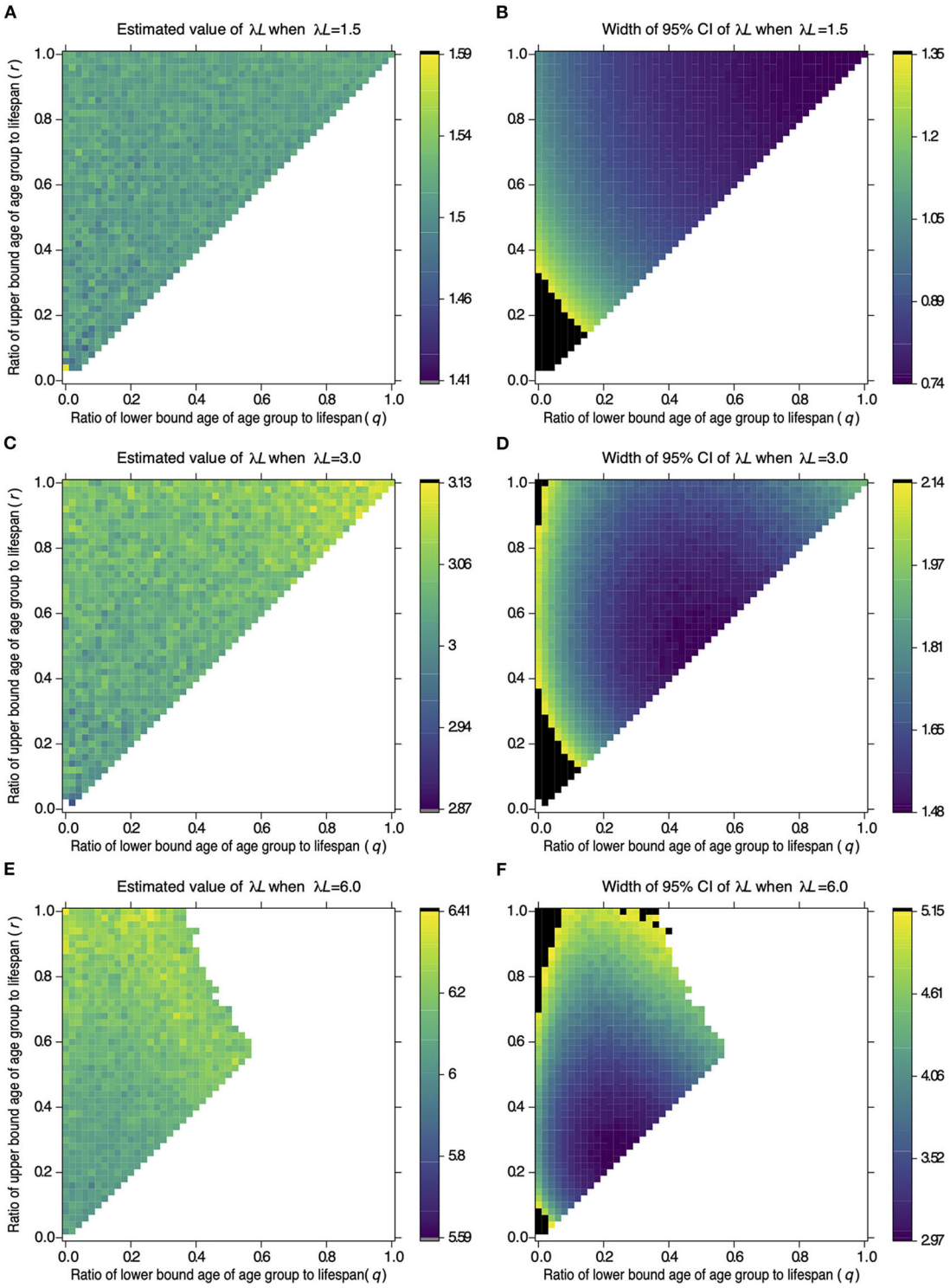

FIGURE 1
Effect of the target age group on the estimate of λL and its 95% CI width. The color of a cell in **(A,C,E)** represents the value of λL estimated from samples of the target age group defined by age parameters q and r on the x- and y-axis. A cell in **(B,D,F)** represents the width of 95% CI of λL estimated from the samples as **(A,C,E)**, respectively. Values of λL and 95% CI width were estimated from 100 samples drawn from the target population. Serological surveillance was simulated 1,000 times under settings where $\lambda L = 1.5$ **(A,B)**, $\lambda L = 3.0$ **(C,D)**, and $\lambda L = 6.0$ **(E,F)**. The color of a cell represents the averaged value in 1,000 repetitions, and the color key next to each panel shows colors associated with the values. The black cells in **(B,D,F)** represent widths above the 95th percentile of all widths of CI. The white cells represent the combination of sampling age parameters. The results are not available to estimate 95% CI of λL by the profile likelihood method in more than 5% of repetitions.

TABLE 4 Combinations of q and r resulted in the narrowest 95% CI of λL.

λL	q	r	Width of 95% CI of λL
1.5	0.98	0.98	0.741
3.0	0.48	0.48	1.485
6.0	0.22	0.26	2.974

1 when $\lambda L = 6.0$ (Table 3). These results indicated a chance to narrow down the 95% CI by serological surveillance targeting a particular age group.

Even when animals' actual ages were provided (Strategy 0), surveillance targeting the entire population did not always guarantee the calculation of the narrowest width of the 95% CI of λL (Table 3). These results are related to the properties of stratified sampling. Targeted serological surveillance sampling can be considered a special case of stratified sampling. Stratified sampling can reduce uncertainty compared with a random sampling of the entire population (22). Seroprevalence in the young population is mostly zero, and seroprevalence in the old population is more informative than that in the young population when FOI is small. When FOI is large, on the other hand, the seroprevalence in the old population is close to one, and the seroprevalence in the young population is more informative than that in the old population. Therefore, more samples from the old population can be used by Strategies 5 and 6 than by Strategy 0 or 1. This is why, when FOI is modest, tailored sampling outperforms fully informed sampling from the entire population.

Constraint 1, surveillance targeting animals at a given age, was found to have the smallest 95% CI of λL regardless of λL and three tested N among the three constraints in Table 2. Nevertheless, it is difficult to conduct surveillance targeting only animals of a specific age in wildlife. When Constraint 2, surveillance targeting animals younger than specific age, and Constraint 3, surveillance targeting animals older than specific age, are compared, the choice between Constraints 2 and 3 depends on the value of λL. For example, when the sample number $N = 100$, surveillance based on Constraints 2 and 3 intersects at $\lambda L = 4.05$. Constraint 3 has a narrower 95% CI than Constraint 2 when λL is less than the intersection and *vice versa*. Moreover, note that the width of the narrowest 95% CI of Constraint 3 is much wider than that of Constraint 2 in the right area of Figure 3B. These findings showed that surveillance targeting animals older than a specified age (Constraint 3) is a good choice when the value of λL is less than the intersection point. Still, it is not a good decision when the value of λL is greater than the intersection point.

Extremely broad confidence intervals, including ones with infinite breadth, are produced by some combinations of λL and target age groups. The estimate of λL becomes infinity when

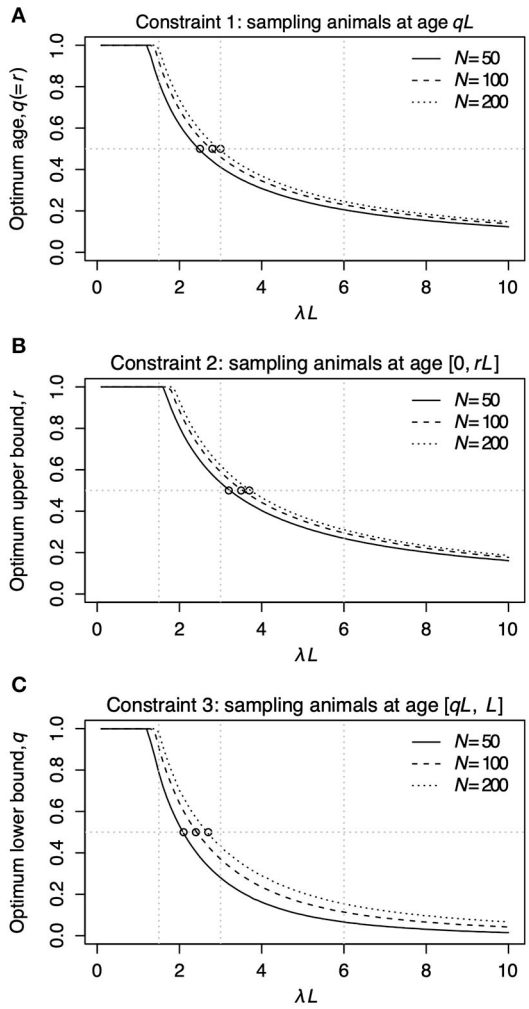

FIGURE 2
The relationship between λL and the optimum age parameter value for Constraints 1 **(A)**, 2 **(B)**, and 3 **(C)**. In each panel, the solid line represents $N = 50$, the dashed line represents $N = 100$, and the dotted line represents $N = 200$. The horizontal line in **(A)** represents $r = q = 0.5$ for Constraint 1. The horizontal line in **(A)** represents $r = 0.5$ for Constraint 2. The horizontal line in **(A)** represents $q = 0.5$ for Constraint 3. The open circles in **(A–C)** denote the points where the optimum sampling age parameters are 0.5. Vertical panel lines **(A–C)** are drawn at $\lambda L = 1.5$, $\lambda L = 3.0$, and $\lambda L = 6.0$, which are the values used in the sampling simulation in Table 3.

all samples are seropositive in a surveillance simulation. As a result, the 95% CI of estimated λL can have an infinite width. This phenomenon was observed as white cells in the upper right corner in Figure 1F, where old animals were sampled when $\lambda L = 6.0$. Alternatively, most samples can be seronegative when λL is small and surveillance targets the young age group. As a result, the 95% CI of estimated λL becomes wide. The confidence interval can also be wide; this phenomenon was observed as black cells at the lower left corner in Figures 1B,D, where young

TABLE 5 The value of λL and the width of 95% CI of estimated λL when the optimum age parameter values are 0.5.

Constraints	N	λL	Width of 95% CI
Constraint 1 ($q = 0.5,\ r = 0.5$)	50	2.46	1.846
	100	2.76	1.408
	200	2.95	1.041
Constraint 2 ($q = 0, r = 0.5$)	50	3.22	3.183
	100	3.54	2.397
	200	3.73	1.756
Constraint 3 ($q = 0.5, r = 1$)	50	2.08	1.649
	100	2.43	1.320
	200	2.67	1.008

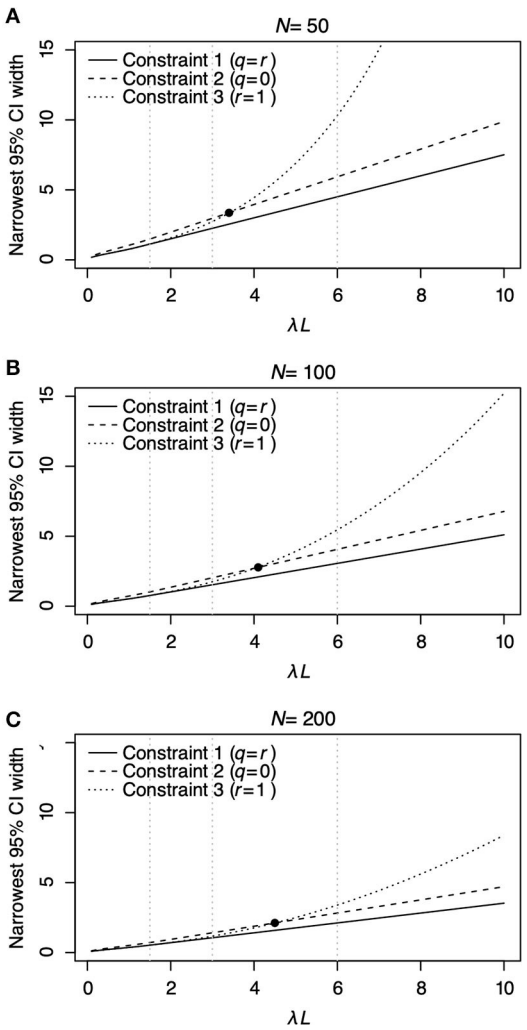

FIGURE 3
The relationship between λL and the narrowest 95% CI of λL for each constraint is shown in Table 2 under different $N = 50$ **(A)**, $N = 100$ **(B)**, and $N = 200$ **(C)**. In each panel, the solid line represents Constraint 1, where $q = r$; the dashed line represents Constraint 2, where $q = 0$; and the dotted line represents Constraint 3, where $r = 1$. The filled circles in **(A–C)** denote the point where the narrowest 95% CI of λL under Constraints 2 and 3 has the same value. Vertical panel lines **(A–C)** are drawn at $\lambda L = 1.5$, $\lambda L = 3.0$, and $\lambda L = 6.0$, which are the values used in the surveillance simulations in Table 3.

animals were sampled when $\lambda L = 1.5$ or $\lambda L = 3.0$. These phenomena can also be observed in Supplementary Figure 1.

Generally, the width of 95% CI of λL can be narrowed down by increasing the number of samples. However, collecting serum samples from wildlife is limited, particularly for endangered species. Our results indicated that the width of the 95% CI of FOI can be narrowed down by increasing the number of samples in specific age ranges. Setting the age group to be sampled at the design step of surveillance can reduce the number of sampled animals in particular situations. For example, the standard sampling strategy using two age bins from the entire population (Strategy 1) with 100 serum samples had a 95% CI width of λL of 0.924 on average under $\lambda L = 1.5$ (Table 3). Surveillance only from animals older than half their lifespan (Strategy 5) with 73 samples resulted in a 95% CI of 0.924 (Supplementary Figure 2). Switching the sampling strategy from strategies 1 to 5 can decrease the number of sampled animals in this situation.

In this study, we assumed that the age distribution in the population was uniform, which is rarely true for wild animals. A non-uniform age distribution can affect Eq. (3) and its subsequent derivations. However, we think the uniform age assumption does not affect our main results, as long as the seroprevalence remains similar. In addition, we assumed that all animals recovered from the infectious disease without dying of infection. The model can be used to analyze infectious diseases in which the lethality is limited if the seroprevalence is not affected by fatal infections. This non-fatal assumption may be critical if a fatal infectious disease is analyzed because the seroprevalence of old animals does not increase in the same way as a non-fatal infectious disease. This is a common difficulty in analyzing seroprevalence data of a fatal infectious disease, and our presented method does not apply to serological surveillance of fatal infectious diseases.

We used the simplest model of seroprevalence called the catalytic model, which assumes that FOI is constant over age in a homogeneously mixed population acquiring lifelong immunity (8). However, several models assume that the FOI can depend on age. Among them are the catalytic linear infection model (11), the catalytic polynomial infection model (10), and the exponentially damped linear model (9). Furthermore, FOI could be represented using the Who Acquires Infection From Whom matrix, which represents transmissibility among age groups (7, 33, 34). Optimizing targeted sampling in serological surveillance under these models remains our future work.

The results in this study are based on computer simulations of serological surveillance. Justifying our method using real datasets of serological surveillance is another direction of our future work. When applying our technique to real datasets, the number of samples, sampling times, and types of pathogens, such as bacteria and viruses, are all significant considerations.

In the serological surveillance of endemic disease, we discovered that tailored sampling could lower the width of the 95% CI of FOI. To take full advantage of the targeted sampling, however, it is necessary to know the expected value of FOI of the target infectious disease in advance. Estimating FOI itself is the purpose of serological surveillance, and it is difficult to know the expected value of FOI. One realistic solution to this problem is to apply targeted sampling after estimating FOI using preliminary serological surveillance with few samples. FOI estimated from previous research can be used for deciding the target range of samples for current surveillance. This approach can be considered adaptive surveillance (35), where surveillance is designed based on the results of previous modeling studies. Annual serological surveillance of infectious diseases would take advantage of the targeted sampling if we can assume that the FOI of target diseases remains similar over time.

To summarize, the optimal target population with the narrowest 95% CI differs depending on the expected FOI. Therefore, sampling should be targeted at the younger age groups to minimize the 95% CI in estimating large FOI. However, sampling should be targeted at the old age groups in estimating small FOI. Our future study will be to justify our strategy using an actual dataset of serological surveillance.

Data availability statement

The original contributions presented in the study are included in the article/Supplementary material, further inquiries can be directed to the corresponding author.

Author contributions

KK conducted simulations and the analysis of data. KK and KI wrote the manuscript. All authors contributed to the article and approved the submitted version.

Funding

This work was supported by the Japan Agency for Medical Research and Development (grant number JP21wm0125008) and Japan Society for the Promotion of Science (grant number 21H03490).

Conflict of interest

The authors declare that the research was conducted in the absence of any commercial or financial relationships that could be construed as a potential conflict of interest.

Publisher's note

Supplementary material

The Supplementary Material for this article can be found online at: https://www.frontiersin.org/articles/10.3389/fvets.2022.754255/full#supplementary-material

References

1. Stagno S, Reynolds DW, Tsiantos A, Fuccillo DA, Long W, Alford CA. Comparative serial virologic and serologic studies of symptomatic and subclinical congenitally and natally acquired cytomegalovirus infections. *J Infect Dis.* (1975) 132:568–77. doi: 10.1093/infdis/132.5.568

2. Leung NH, Xu C, Ip DK, Cowling BJ. The fraction of influenza virus infections that are asymptomatic: a systematic review and meta-analysis. *Epidemiology.* (2015) 26:862–72. doi: 10.1097/EDE.0000000000000340

3. Morgan-Capner P, Wright J, Miller CL, Miller E. Surveillance of antibody to measles, mumps, and rubella by age. *BMJ.* (1988) 297:770–2. doi: 10.1136/bmj.297.6651.770

4. Remond M, Kaiser C, Lebreton F. Diagnosis and screening of foot-and-mouth disease. *Comp Immunol Microbiol Infect Dis.* (2002) 25:309–20. doi: 10.1016/S0147-9571(02)00028-0

5. Carman PS, Povey RC. The seroprevalence of canine parvovirus-2 in a selected sample of the canine population in ontario. *Can Vet J.* (1984) 25:259–62.

6. Gilbert AT, Fooks AR, Hayman DT, Horton DL, Muller T, Plowright R, et al. Deciphering serology to understand the ecology of infectious diseases in wildlife. *Ecohealth.* (2013) 10:298–313. doi: 10.1007/s10393-013-0856-0

7. Anderson RM, May RM. *Infectious diseases of humans: dynamics and control.* Oxford: Oxford university press. (1992).

8. Muench H. Derivation of rates from summation data by the catalytic curve. *J Am Stat Assoc.* (1934) 29:25–38. doi: 10.1080/01621459.1934.10502684

9. Griffiths DA. A catalytic model of infection for measles. *J R Stat Soc Ser C Appl Stat.* (1974) 23:330–9. doi: 10.2307/2347126

10. Grenfell BT, Anderson RM. The estimation of age-related rates of infection from case notifications and serological data. *J Hyg (Lond).* (1985) 95:419–36. doi: 10.1017/S0022172400062859

11. Farrington CP. Modelling forces of infection for measles, mumps and rubella. *Stat Med.* (1990) 9:953–67. doi: 10.1002/sim.4780090811

12. Brown WAB, Chapman NG. The dentition of red deer (Cervus elaphus): a scoring scheme to assess age from wear of the permanent molariform teeth. *J Zool.* (1991) 224:519–36. doi: 10.1111/j.1469-7998.1991.tb03783.x

13. Landon DB, Waite CA, Peterson RO, Mech LD. Evaluation of age determination techniques for gray wolves. *J Wildl Manage.* (1998) 62:674–82. doi: 10.2307/3802343

14. Gipson PS, Ballard WB, Nowak RM, Mech LD. Accuracy and precision of estimating age of gray wolves by tooth wear. *J Wildl Manage.* (2000) 64:752–8. doi: 10.2307/3802745

15. Marti I, Ryser-Degiorgis M-P. A tooth wear scoring scheme for age estimation of the Eurasian lynx (Lynx lynx) under field conditions. *Eur J Wildl Res.* (2018) 64:1–13. doi: 10.1007/s10344-018-1198-6

16. Herrman JM, Morey JS, Takeshita R, De Guise S, Wells RS, McFee W, et al. Age determination of common bottlenose dolphins (Tursiops truncatus) using dental radiography pulp:tooth area ratio measurements. *PLoS One.* (2020) 15:e0242273. doi: 10.1371/journal.pone.0242273

17. Reynolds JJH, Carver S, Cunningham MW, Logan KA, Vickers W, Crooks KR, et al. Feline immunodeficiency virus in puma: estimation of force of infection reveals insights into transmission. *Ecol Evol.* (2019) 9:11010–24. doi: 10.1002/ece3.5584

18. Ashman DL, Christensen GC, Hess ML, Tsukamoto GK, Wichersham MS. *The mountain lion in Nevada*. Reno (NV): Nevada, Department of Wildlife 1983. p. 75.

19. Laundré JW, Hernández L, Streubel D, Altendorf K, González CL. Aging mountain lions using gum-line recession. *Wildl Soc Bull.* (2000) 28:963–6. doi: 10.2307/3783855

20. Olsen MT, Robbins J, Bérubé M, Rew MB, Palsbøll PJ. Utility of telomere length measurements for age determination of humpback whales. *NAMMCO Sci Pub*. (2018) 10. doi: 10.7557/3.3194

21. Wright PGR, Mathews F, Schofield H, Morris C, Burrage J, Smith A, et al. Application of a novel molecular method to age free-living wild Bechstein's bats. *Mol Ecol Resour.* (2018) 18:1374–80. doi: 10.1111/1755-0998.12925

22. Deaton A. The analysis of household surveys: a microeconometric approach to development policy. Washington, DC: World Bank Group (2018). ISBN: 97814648 13313.

23. D'Amato V, Haberman S, Russolillo M. The stratified sampling bootstrap for measuring the uncertainty in mortality forecasts. *Methodol Comput Appl Probab.* (2012) 14:135–48. doi: 10.1007/s11009-011-9225-z

24. Bondo KJ, Pearl DL, Janecko N, Boerlin P, Reid-Smith RJ, Parmley J, et al. Epidemiology of Salmonella on the paws and in the faeces of free-ranging raccoons (Procyon Lotor) in Southern Ontario, Canada. *Zoonoses Public Health.* (2016) 63:303–10. doi: 10.1111/zph.12232

25. Fakour S, Naserabadi S, Ahmadi E. The first positive serological study on rift valley fever in ruminants of Iran. *J Vector Borne Dis.* (2017) 54:348–52. doi: 10.4103/0972-9062.225840

26. Moreira TR, Sarturi C, Stelmachtchuk FN, Andersson E, Norlander E, de Oliveira FLC, et al. Prevalence of antibodies against Toxoplasma gondii and Neospora spp. *in equids of Western Para, Brazil Acta Trop.* (2019) 189:39–45. doi: 10.1016/j.actatropica.2018.09.023

27. Loi F, Cappai S, Laddomada A, Feliziani F, Oggiano A, Franzoni G, et al. Mathematical approach to estimating the main epidemiological parameters of African swine fever in wild boar. *Vaccines (Basel).* (2020) 8:521. doi: 10.3390/vaccines8030521

28. Dietz K. Transmission and control of arbovirus diseases. *Epidemiology.* (1975) 104:104–21.

29. Andraud M, Dumarest M, Cariolet R, Aylaj B, Barnaud E, Eono F, et al. Direct contact and environmental contaminations are responsible for HEV transmission in pigs. *Vet Res.* (2013) 44:102. doi: 10.1186/1297-9716-44-102

30. Guinat C, Gubbins S, Vergne T, Gonzales JL, Dixon L, Pfeiffer DU. Experimental pig-to-pig transmission dynamics for African swine fever virus, Georgia 2007/1 strain. *Epidemiol Infect.* (2016) 144:25–34. doi: 10.1017/S0950268815000862

31. Hage JJ, Schukken YH, Barkema HW, Benedictus G, Rijsewijk FA, Wentink GH. Population dynamics of bovine herpesvirus 1 infection in a dairy herd. *Vet Microbiol.* (1996) 53:169–80. doi: 10.1016/S0378-1135(96)01245-X

32. Venzon DJ, Moolgavkar SH, A. method for computing profile-likelihood-based confidence-intervals. *J R Stat Soc Ser C Appl Stat.* (1988) 37:87–94. doi: 10.2307/2347496

33. Diekmann O, Heesterbeek JA, Metz JA. On the definition and the computation of the basic reproduction ratio R0 in models for infectious diseases in heterogeneous populations. *J Math Biol.* (1990) 28:365–82. doi: 10.1007/BF00178324

34. Farrington CP, Kanaan MN, Gay NJ. Estimation of the basic reproduction number for infectious diseases from age-stratified serological survey data. *J R Stat Soc Ser C Appl Stat.* (2001) 50:251–92. doi: 10.1111/1467-9876.00233

35. Miller RS, Pepin KM. Prospects for improving management of animal disease introductions using disease-dynamic models. *J Anim Sci.* (2019) 97:2291–307. doi: 10.1093/jas/skz125

Frontiers in Veterinary Science

Transforms how we investigate and improve animal health

The third most-cited veterinary science journal, bridging animal and human health with a comparative approach to medical challenges. It explores innovative biotechnology and therapy for improved health outcomes.

Discover the latest Research Topics

See more →

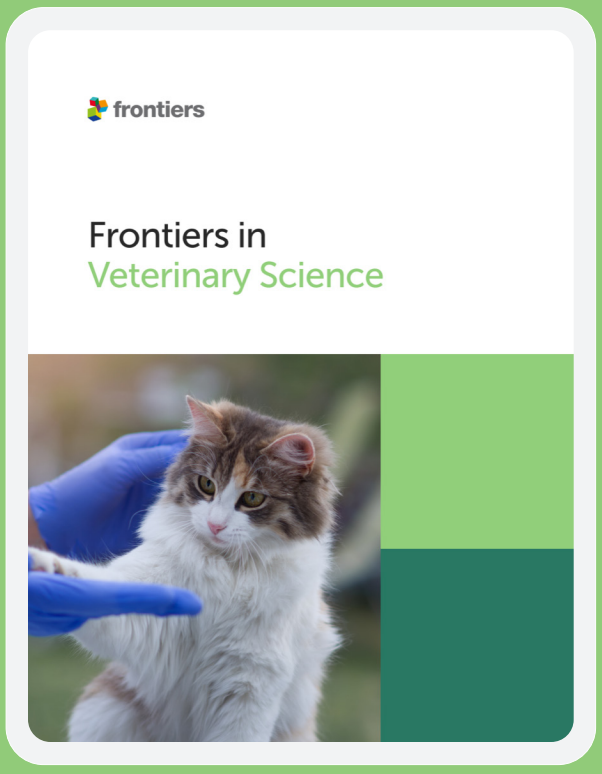

Frontiers

Avenue du Tribunal-Fédéral 34
1005 Lausanne, Switzerland
frontiersin.org

Contact us

+41 (0)21 510 17 00
frontiersin.org/about/contact